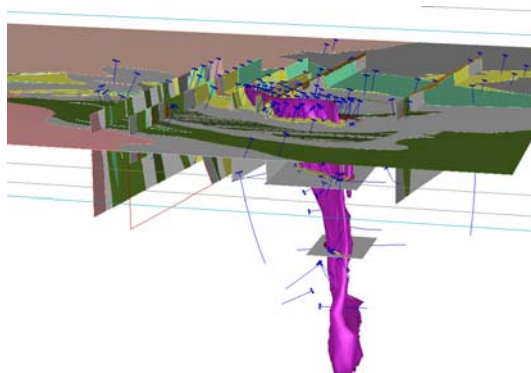


Technical Report



PYHÄSALMI MODELING PROJECT

13.5.1997-12.5.1999

Outokumpu Mining Oy



Geological Survey of Finland



TABLE OF CONTENTS

TABLE OF CONTENTS

SUMMARY	1
INTRODUCTION	3
PROJECT OBJECTIVES	3
ORGANIZATION AND FUNDING	3
RESPONSIBILITIES	5
PROGRAMME	5
WORK DESCRIPTIONS AND RESULTS	6

SECTION A, DATA MANAGEMENT

A DATA MANAGEMENT	1
A1 PREVIOUS EXPLORATION DATA COLLECTION AND DATA TRANSFERS	1
A2 DRILL HOLE RELOGGING AND SAMPLING FOR X-RAY ASSAYING	3
A3 NEW ASSAYS AND OLD DATA VALIDATION	4

SECTION B, GEOLOGY

B GEOLOGY	1
B1 DATA MANAGEMENT	1
B2 FIELD GEOLOGY	1
B2.1 REGIONAL GEOLOGY	2
B2.2 PYHÄSALMI VOLCANIC COMPLEX	5
B2.2.1 Ruotanen formation	5
B2.2.2 Mullikkoräme formation	11
B2.2.3 Pyhäsalmi complex intrusions	16
B2.2.4 Dike rocks	18
B2.2.5 Unclassified intrusives	19
B2.2.6 Unclassified felsic and mafic gneisses	19
B2.2.7 Mica gneisses	19
B3 SECTION AND PLAN RECONSTRUCTIONS	19
B4 STRUCTURAL AND DEFORMATION MODELING AND METAMORPHISM	19
B4.1 REGIONAL STRUCTURES	22
B4.2 STRUCTURES IN THE PYHÄSALMI AREA	23
B4.2.1 Structure of the Pyhäsalmi mine area	23
B4.2.2 Deformation history	25
B4.3 STRUCTURE OF THE MULLIKKORÄME MINE	29
B4.4 3D MODELING AND THE SHAPE OF THE PYHÄSALMI DEPOSIT	30
B4.4.1 Methods	32
B4.4.2 Results and interpretations	33
B4.4.2.1 General assumptions	33
B4.4.2.1 Evolution of the shape of the Pyhäsalmi ore deposit	35
B4.4.2.3 3d-lithology and 3d-structures in the Ruotanen area	35
B4.4.3 Conclusions	37
B4.5 METAMORPHIC EVOLUTION IN THE RUOTANEN AREA	38
B4.5.1 Previous studies	38
B4.5.2 Sampling and investigation methods	38
B4.5.3 Lithologies	39
B4.5.3.1 Metapelites around Lake Pyhäjärvi	39
B4.5.3.2 Ruotanen formation	39
B4.5.4 PT-conditions	39
B4.5.4.1 Metapelites around Lake Pyhäjärvi	40
B4.5.4.2 Rocks adjacent to Pyhäsalmi mine	40
B4.5.5 Geo-Path program	42
B4.5.6 Summary of PT-path	42
B4.5.7 Conclusions	44
B5 PALEOVOLCANOLOGY	45

B5.1 PALEOVOLCANOLOGICAL FIELD OBSERVATIONS	45
B5.1.1 Ruotanen formation Mukurinperä member	45
B5.1.2 Mullikkoräme formation Riitavuori member	47
B5.1.3 Mullikkoräme formation Tetrinmäki member	48
B5.2 TRACE ELEMENT AND REE GEOCHEMISTRY IN THE PYHÄSALMI VOLCANIC COMPLEX	49
B5.2.1 Ruotanen formation	50
B5.2.1 Mullikkoräme formation	55
B5.3 STRATIGRAPHY AND TIMING	61
B REFERENCES	63

SECTION C, LITHOGEOCHEMISTRY

C INTRODUCTION	1
C1 SAMPLES AND ANALYTICAL TECHNIQUES	1
C1.1 OLD SAMPLES AND ANALYSES	1
C1.2 NEW SAMPLES AND ANALYSES	4
C1.3 DATA PREPARATION	9
C1.3.1 Comparison of old and new data	9
C1.3.2 Calibration of old analyses	11
C1.3.3 Analysis method comparisons	11
C2 LITHOGEOCHEMICAL CHARACTERIZATION	15
C2.1 GEOCHEMISTRY OF PRIMARY ROCKS	15
C2.2 GEOCHEMICAL ALTERATION	23
C2.2.1 General characteristics	23
C2.2.2 Alteration mineralogy of volcanites	33
C2.2.3 Alteration categories and element enrichment/ depletion	35
C2.2.4 Lithogeochemical indices	38
C2.2.5 Protoliths of altered volcanites	41
C2.2.6 Mass transfer during alteration	43
C2.2.7 Best pathfinders	44
C3 LITHOGEOCHEMICAL MODELING	50
C CONCLUSIONS AND RECOMMENDATIONS	54
C REFERENCES	55

SECTION D, GEOPHYSICS

D GEOPHYSICS	1
D1 DATA TRANSFER AND MANAGEMENT	1
D2 PETROPHYSICS	2
D2.1 GENERAL	2
D2.2 SUSCEPTIBILITY VALUES OF DIFFERENT ROCK TYPES	2
D2.3 DENSITY VALUES OF DIFFERENT ROCK TYPES	3
D2.4 RESISTIVITY VALUES OF DIFFERENT ROCK TYPES	5
D2.5 CONDUCTIVITY VALUES OF DIFFERENT ROCK TYPES	5
D2.6 PETROPHYSICAL PROPERTIES OF ALTERED AND UNALTERED FELSIC VOLCANITES	6
D2.7 PETROPHYSICAL PROPERTIES OF ALTERED AND UNALTERED MAFIC VOLCANITES	8
D3 AIRBORNE AND GROUND GEOPHYSICS	10
D4 DOWNHOLE GEOPHYSICS	11
D5 GEOPHYSICAL MODELING	12
D5.1 GRAVITY AND MAGNETIC INTERPRETATIONS IN THE RUOTANEN AREA	12
D5.2 GEFINEX 400S INTERPRETATIONS IN THE RUOTANEN AREA	20
D5.3 DOWNHOLE EM INTERPRETATIONS IN THE RUOTANEN AREA	22
D5.4 GRAVITY INTERPRETATIONS IN THE MULLIKKORÄME AREA	23
D5.5 GEFINEX 400S INTERPRETATIONS IN THE MULLIKKORÄME AREA	26
D5.6 DOWNHOLE EM INTERPRETATIONS IN THE MULLIKKORÄME AREA	29

D CONCLUSIONS AND RECOMMENDATIONS	31
-----------------------------------	----

SECTION E, STATISTICS AND 3D MODELING

E STATISTICS AND 3D MODELING	1
E1 DATA MANAGEMENT	1
E2 DATA STRUCTURE ANALYSIS	1
E2.1 METHODS	1
E2.1.1 Multivariate data structure	1
E2.1.2 Spatial data structure	1
E2.1.3 The association of the contents in lithochemical assays with distance to ore	1
E2.2 RESULTS	2
E3 STATISTICAL CLASSIFICATION OF LITHOLOGICAL SAMPLES	9
E3.1 METHOD	9
E3.1.1 Bayes decision rule	9
E3.1.2 Estimating prior probabilities	11
E3.1.3 Estimating the conditional densities	11
E3.1.4 Estimating the performance of the classifier	12
E3.2 DATA SET AND CLASSIFICATION SETTINGS	12
E3.3 RESULTS FROM THE FIRST CLASSIFICATION	13
E3.4 RESULTS FROM THE SECOND CLASSIFICATION	14
E4 3D MODELING	18
E4 SUMMARY	18
E4.1 INTRODUCTION	18
E4.1.1 Objectives	18
E4.1.2 Material	18
E4.1.3 Methods	19
E4.2 SPATIAL STATISTICS	20
E4.2.1 Pyhäsalmi district and subareas, classical statistics	20
E4.2.2 Pyhäsalmi district geostatistics	25
E4.2.3 Spatial grade anisotropy	27
E4.2.4 Mullikkoräme special features	36
E4.3 SPATIAL MODELING	38
E4.3.1 Grade value interpolation on planes	38
E4.3.2 Mineralization type delineation on planes	38
E4.3.3 3D solid modeling	39
E4.3.4 "Hot spots" and metal zoning	39
E4.4 CONCLUSIONS AND RECOMMENDATIONS	41
E4 Explanation for figures E4.17-28	42
E4 Figures 17-28	44
E REFERENCES	57

SECTION F, EXPLORATION MODEL

F EXPLORATION MODEL	1
F1 PYHÄSALMI EXPLORATION MODEL	1
F1.1 Deposit environments at Pyhäsalmi and Mullikkoräme	2
F1.2 Genetic model	2
F1.3 Geological characteristics	3
F1.4 Lithochemical characteristics	4
F1.5 Geophysical characteristics	5
F1.6 Geomathematics	6
F CONCLUSIONS AND RECOMMENDATIONS	7
F REFERENCES	7

SECTION G, TEST DRILLING

G TEST DRILLING	1
G1 DRILLING CAMPAIGN	1
G2 TEST DRILL HOLES	3
G2.1 PYS-107 CONTINUATION	3
G2.2 PYS-116	3
G2.3 PYS-117	3
G2.4 PYS-118	4
G2.5 PYS-119	5
G2.6 PYS-119A	6
G2.7 MU-152	6
G2.8 DIRECTIONAL DRILLING	7
G2.8.1 Steering in hole PYS-119a	8
G2.8.2 Conclusions on directional drilling	9

APPENDICES (Separate Volume)

APPENDIX 1 (Project categories, objectives and reporting responsibilities: in Finnish)
APPENDIX A1 (Gemcom's *.mdb drill hole workspace notes)
APPENDIX A2 (List of all relogged, new and test drill holes)
APPENDIX B1 (List of digitized plans and sections)
APPENDIX C1 (List of all sampled drill holes)
APPENDIX C2 (Regression equations)
APPENDIX C3 (Subgroup classification criteria for volcanites and statistics)
APPENDIX D1 (Map of Pyhäsalmi-Kettuperä area co-ordinate systematics)
APPENDIX E1 (Statistics and geostatistics of drill hole data for 3D modeling purposes: In Finnish)

ATTACHMENT

CD-ROM discs (one including everything and the other one including GTK's GIS-data base) including the report in digital format (*.doc and *.pdf) and all related data sets, software projects/sessions, images and metadata descriptions.

SUMMARY

PROJECT OVERVIEW

Heikki Puustjärvi (ed.)

8.11.2006

Confidential

SUMMARY

The purpose of the Pyhäsalmi Modeling Project was to create an exploration model for the Pyhäsalmi type of volcanogenic massive sulphide (VMS) deposits, including the areally and genetically closely related Mullikkoräme deposit. Targets for further exploration in the area would be generated applying the geomodel thus generated. An important phase in the project programme was the testing of the model by deep drilling, especially directional drilling, technology rather new for Finland.

Because the project was of multi-aspect nature and targeted to create products applicable to generic exploration for ore deposits of the VMS type, it was found practical to establish a joint project between Outokumpu Mining Oy (OM) and the Geological Survey of Finland (GTK). Thus was brought together top knowledge on VMS deposits in Finland.

The Pyhäsalmi Modeling Project spread over two years (13.5.1997-12.5.1999). It was structured to function as two parallel subprojects, OM and GTK having own budgets and programmes but sharing common objectives. OM was the manager of the joint project. The Project Manager was the only full-time employee for the project; research capacities in OM and GTK were utilised to carry out expert work. Two outside consultants were used: the University of Turku for structural geology and TA Consulting for geophysics.

The main objectives of the project were the following. 1: To create an exploration model for the Pyhäsalmi type of VMS deposits – a model applicable in analogous geological environments, 2: To introduce new directional drilling technology, previously untested in Finland, and 3: To discover new ore in the Pyhäsalmi-Mullikkoräme area. The project's budget totalled FIM 6.9 million (OM 4.5, GTK 2.4); it was support-funded by Technology Development Centre, Finland (TEKES): 30% for OM, 50% for GTK.

The work programme was divided into seven categories: data management, geology, litho-geochemistry, geophysics, three-dimensional modeling and statistics, exploration model, and test drilling. The project was initiated by acquiring and analysing all exploration data available for the Pyhäsalmi-Mullikkoräme area. Thereafter, based on the said data, the partners conducted their shares of work independently according to the project programme and schedule agreed on in advance. The work resulted in organised data sets that were archived as CD-ROM files, consequently the partners can use and import/export project data as necessary.

In the modeling phase, the results were combined and formulated to an exploration model – path of exploration procedures. It is applicable to exploration in the Pyhäsalmi area as well as analogous geological successions elsewhere. The model, based on data processing and geophysical measurements, indicated ore-potential targets that were tested by drilling. Such locations existed at Mine Village, Pyhäsalmi east contact zone, Lehto altered felsic volcanite zone, and on the continuation of the Mullikkoräme deep orebody. An indication for VMS-type ore was

Heikki Puustjärvi (ed.)

8.11.2006

Confidential

intersected at Kettuperä, north of the Pyhäsalmi mine; however, economic discovery was not made.

The test drilling was contracted to Suomen Malmi Oy. During the drilling, Swedish Liw-In-Stone directional drilling technology was tested; however, a conclusion was drawn that the method requires further development to become applicable in routine exploration. This means that acute need for proper directional drilling method still exists to lower costs in testing deep-seated targets and facilitate drilling in areas of heavy infrastructure as well as close-space drilling in mines.

Despite specific areas of exploration know-how, the partners obtained general knowledge on the use of different geo-software in exploration data handling and three-dimensional modeling. The fact that the results and working practices of the Pyhäsalmi Modeling Project can be applied to exploration for ore deposits of the VMS type worldwide is emphasised.

INTRODUCTION

Heikki Puustjärvi (ed.)

8.11.2006

Confidential

Discussions concerning ore reserves and exploration potential in the Pyhäsalmi-Mullikkoräme area in summer 1996 led to a memorandum by the Pyhäsalmi mine chief geologist. This included a proposal for an exploration programme in the Pyhäsalmi mining camp. With regard to the needs of the Finnish mining and metals industry as a whole and due to the foreseeable exploration future it was decided to prepare a proposal for a joint programme between Outokumpu Mining Oy (OM) and the Geological Survey of Finland (GTK). Because of the need to develop new exploration technologies in the project, the role of TEKES (Development Center of Technology) as a third party was seen necessary. Two separate project proposals (OM and GTK) for TEKES participation as a funding party into the 2-year joint project were filed 20.12.1996. The proposals were approved in the beginning of April 1997 but the project start-up was filed as of 01.03.1997.

PROJECT OBJECTIVES

The first priority was to obtain indications for possible new ore in the Pyhäsalmi-Mullikkoräme area so to make a discovery hole. Due to the twofold nature of the project other demands were set to serve both research and technical aspects of exploration work. The second objective was to create an exploration model for the Pyhäsalmi type of ore deposit – a model that could be applied to analogous lithological sequences worldwide. The third objective was to bring into country a previously untested directional drilling method.

ORGANIZATION AND FUNDING

The project organisation is composed of two parallel subprojects (OM and GTK) both of which have their own leaders but operations are managed by a project manager, the only full time project employee (Fig.1). A project management committee supervises project operations. TEKES as a co-funder is informed of operations through term reporting.

Management committee:

Markku Isohanni	senior VP-Exploration	OM
Markku Mäkelä	director	GTK
Eljas Ekdahl	program director	GTK
Heikki Papunen	professor	Turku University
Teuvo Jurvansuu	mine manager	Pyhäsalmi

Project and subproject leaders:

Kaarlo Mäkelä	exploration manager	OM
Pekka Nurmi	research manager	GTK

Project personnel :

1. project manager (24)	Heikki Puustjärvi	OM
-------------------------	-------------------	----

Heikki Puustjärvi (ed.)

8.11.2006

Confidential

2. geochemist (12)	Kalevi Rasilainen	GTK
3. geophysicist (12)	Turo Ahokas	GX-consulting
4. structural geologist (10)	Jouni Luukas	GTK
5. structural geologist (5)	Timo Kilpeläinen	Turku University
6. volcanologist (2)	Jukka Kousa	GTK
7. geomathematician (4)	Jyrki Parkkinen	GTK
8. statistician (4)	Nils Gustavsson	GTK
9. statistician (1)	Ilkka Suppala	GTK
10. student (6)	AP Tapio	Turku University
11. logistics	Timo Mäki	Pyhäsalmi mine

The figures in parentheses refer to manmonths involved in the project.

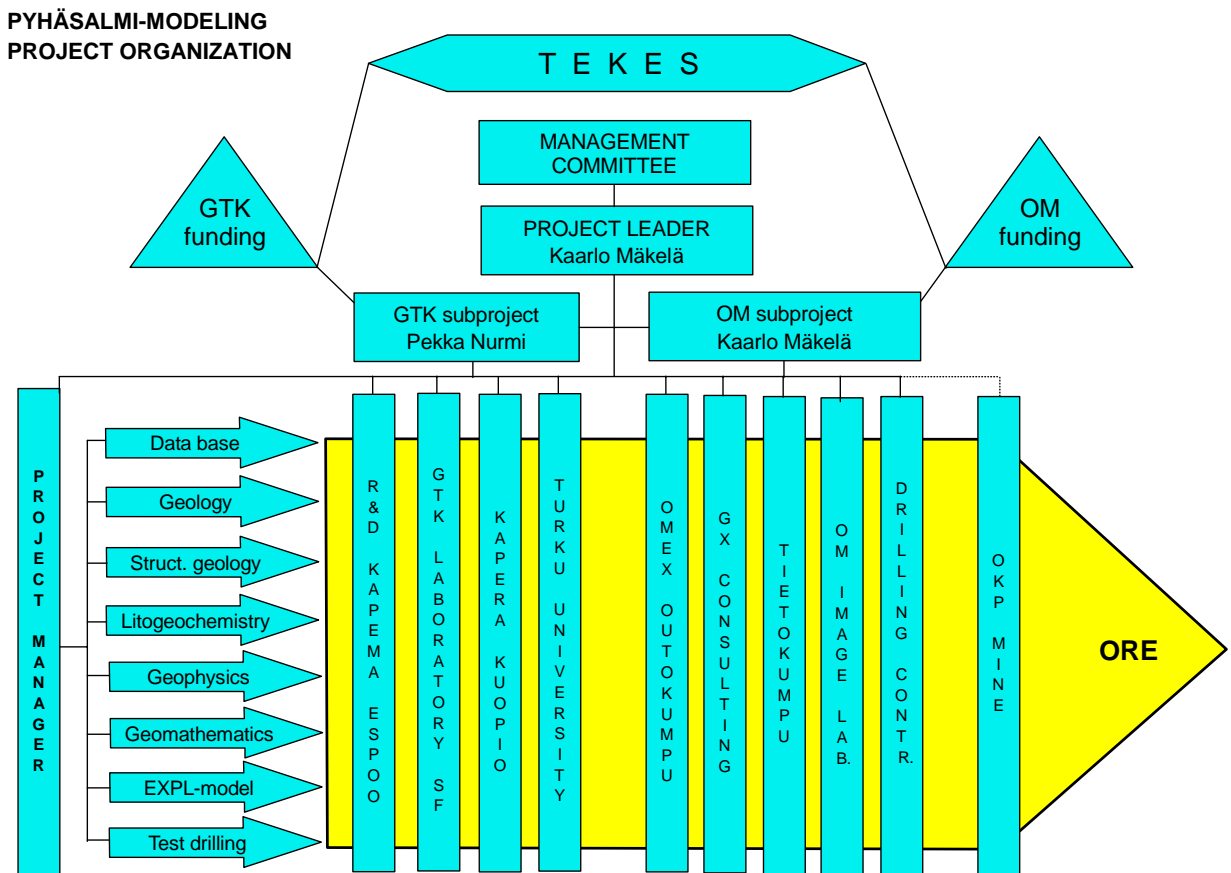


Figure 1. Pyhäsalmi Modeling Project organization

Total budget for the two-year joint project was originally 6886 TFIM of which OM's subproject totalled 4481 TFIM and GTK's respectively 2405 TFIM. TEKES committed to fund 30% of OM's and 50% of GTK's approved costs.

Heikki Puustjärvi (ed.)

8.11.2006

Confidential

RESPONSIBILITIES

Working responsibilities within the whole project were divided between the two subprojects as follows. Project management, data management, drill core relogging, sampling, geophysics and test drilling were the main responsibilities of OM. GTK has been responsible for assays, structural geology, litho geochemistry, statistics and 3D-modeling. Integration of results and reporting has been duties of the project manager.

PROGRAMME

The original project proposals included categorized work phases for budgeting purposes. A more detailed programme and a schedule were done after the project start up in June '97 (Table 1, Appendix 1, in Finnish).

Table 1. Pyhäsalmi Modeling Project schedule

PROJECT SCHEDULE	1 9 9 7						1 9 9 8						99										
	t	k	e	s	l	m	j	t	h	m	h	t	k	e	s	l	m	j	t	h	m	h	t
A. Data management																							
A1. Previous expl. data collection	x	xx	xx	xx																			
A2. DDH logging and sampling		xx	xx	xx	xx																		
A3. Assaying and old data validation		x	xx	xx	xx	xx	xx	xx	xx	xx	xx												
B. Geology																							
B1. Data transfers and management	x	xx	x																				
B2. Surface geology, mappings, trenching		xx	xx	xx	xx	xx	xx	xx	xx	xx	xx												
B3. Section and plan constructions				xx	xx	xx	xx	xx	xx	xx	xx												
B4. Structural geology and metamorphosis			xx						xx	xx	xx	xx	xx	xx	xx	xx							
B5. Paleovolcanology			xx	xx								xx	xx										
C. Litho geochemistry																							
C1. Data transfers and management		xx			xx	xx	xx	xx	xx	xx													
C2. Litho geochemical characterization					xx	xx	xx	xx	xx	xx	xx	xx	xx	xx	xx								
C3. Litho geochemical modeling									xx	xx	xx	xx	xx	xx	xx								
D. Geophysics																							
D1. Data transfers and management	x	xx	xx	xx	xx																		
D2. Petrophysics	x	xx	xx																				
D3. Airborne and ground geophysics			xx	xx	xx	xx	xx																
D4. Down hole geophysics							xx	xx	xx	xx	xx												
D5. Geophysical modeling									xx	xx	xx	xx	xx	xx	xx								
E. 3D-modeling and statistics																							
E1. Data transfers and management					xx	xx	xx	xx	xx	xx	xx												
E2. Data structures characterization									xx	xx	xx												
E3. Statistics										xx	xx	xx	xx	xx	xx								
E4. 3D-modeling											xx	xx	xx	xx	xx								
F. Exploration model																							
F1. Integration of parallel projects															xx	xx							
F2. Test drilling planning																xx							
G. Test Drilling																xx	xx	xx	xx	xx	xx	xx	xx
H. Reporting						x						x					x					xx	xx

WORK DESCRIPTIONS AND RESULTS

The following sections of the report are written by researchers involved and comprises a description of all work accomplished and results following the schedule categories (A-G).

SECTION A

DATA MANAGEMENT

Heikki Puustjärvi (ed.)

8.11.2006

Confidential

A DATA MANAGEMENT (H. Puustjärvi)

A 1 PREVIOUS EXPLORATION DATA COLLECTION AND DATA TRANSFERS

The collection of previous drilling data mainly comprised data transfer from the Tietokumpu (OM exploration data manager) Ingres database and from the Pyhäsalmi mine Minenet database (Appendix A1). The ASCII-format data files transferred were transformed into the Finnish KKJ3-zone national coordinate system. First all collected drillhole lithological data had to be equalized by coding all original litho-abbreviations in the logs according to a chosen system (protolith indexed as a numeric code and three consecutive capital letter columns for alteration mineralogy). XRF assay results and a common knowledge of the meaning of lithological abbreviations were used when interpreting the original old data. Manipulated data files (in Excel) were then imported into Gem4Win, ArcView, Systat and other statistical programs for further use in GTK and OM. An example of the log-script and used lithological coding keys are seen in Table 2. Data was delivered via e-mail and occasionally via an established ftp-route between OM and GTK.

Geological maps were not previously in a GIS-compatible format, consequently all geological base data were collected as archived maps in OM/Outokumpu exploration office and Pyhäsalmi mine and digitized into the ArcView as GIS applicable regional and target packages.

Geophysical data consisted airborne magnetic+electromagnetic, ground gravity+magnetic+induced polarity data. They were extracted from the Tietokumpu Ingres database, transferred to GX-consulting for further use in various geophysical software (Excel, Oasis Montaj, Em-Vision and Model-Vision) and to OM image processing services to produce GIS-compatible airborne and ground data compilations for use as reference bases in geological interpretations. Gefinex-em soundings, downhole-em data, downhole in situ loggings for susceptibility+resistivity and specific gravity measurements (from core samples) were collected from separate 3.5" HD-discs archived in the OM/Outokumpu exploration office. Data files were transferred by e-mail.

All data used are arranged into separate data files and referred to as project data CD-discs attached to this report.

Heikki Puustjärvi (ed.)

8.11.2006

Confidential

Table 2. An example of a logg-script of a coded DDH lithology and used rockcodes

HOLE-ID	FROM	TO	ROCKTYPE	CODE	ALTA	ALTB	ALTC
PYO-50	0	5.66	MAATA	0			
PYO-50	5.66	13.8	HVULK	1	F		
PYO-50	13.8	20.2	HJ KVMSPF	61			
PYO-50	20.2	24	HVULK	1	C	S	
PYO-50	24	24.42	EJ	63			
PYO-50	24.42	29.13	HVULK	1	S	C	
PYO-50	29.13	32.35	KRDKLOSER	3	X	C	K
PYO-50	32.35	36.82	KLOFLOSERL	3	K	F	X
PYO-50	36.82	40.7	FLOKLOSERL	3	F	K	X
PYO-50	40.7	43.25	KRDFLOKLOL	3	X	C	F
PYO-50	43.25	48.05	HVULK	1	C	S	F
PYO-50	48.05	53.57	HVULK	1	C	S	F
PYO-50	53.57	58.45	HVULK	1	C	S	F
PYO-50	58.45	65.65	HVULK	1	F	S	C
PYO-50	65.65	70.05	HVULK	1	C	F	S
PYO-50	70.05	73	HVULK	1	S	C	

ROCKCODES USED IN THE PYHASALMI-MODELING PROJECT:

0	OVERBURDEN
1	FELSIC VOLCANICS
2	INTERMEDIATE VOLCANICS
21	MICA SCHIST
22	BLACK SCHIST (GRAPHITIC)
3	MAFIC VOLCANICS
4	MINERALIZED
51	FELSIC INTRUSIVE
52	INTERMEDIATE INTRUSIVE
53	MAFIC INTRUSIVE
61	FELSIC DIKE
62	INTERM. DIKE
63	MAFIC DIKE
7	SHEAR/ FAULT/ BROKEN
8	PLAGIOCLASE-URALITE-PORPHYRY
9	UNCLASSIFIED
10	TALC-CARBONATE BEARING ROCKS AND SKARN
11	REVERSE DRILLING
A	AMPHIBOLE
B	BRECCIA
C	CORDIERITE
E	EPIDOTE
F	FLOGOPITE
G	GARNET
K	CHLORITE
M	MAGNETITE
S	SERISITE
X	SULPHIDES
T	TALC
Q	SILICIFIED
E.G.	A CODE OF 1SCX MEANS A FELSIC VOLCANIC ROCK WITH SERICITE AND CORDIERITE ALTERATION AND SOME SULPHIDES

Heikki Puustjärvi (ed.)

8.11.2006

Confidential

A 2 DRILL HOLE RELOGGING AND SAMPLING FOR X-RAY ASSAYING

For interpretation and modelling of structural geology, litho-geochemistry and geophysics around the immediate Pyhäsalmi and Mullikkoräme deposit surroundings, it was necessary to broaden the previous assay (XRF+AAS) database and to categorize all lithologies and alterations. This task was accomplished by selecting a number of old drillholes for relogging and sampling. Additionally to this the project benefited from a new superficial drilling campaign conducted by the Pyhäsalmi and Mullikkoräme mine geological departments.

The following drillhole sets were chosen for relogging. Pyhäsalmi: 22 surface and 20 underground holes completed with the new fall '97 drilling campaign that created availability to six more underground holes and seven surface holes, all together adding up to 13387.3m in 55 drillholes. Mullikkoräme: 16 underground holes and respectively one new underground and five new surface holes totalling 4996.5 m in 22 drillholes (Appendix A2 and Fig. A1).

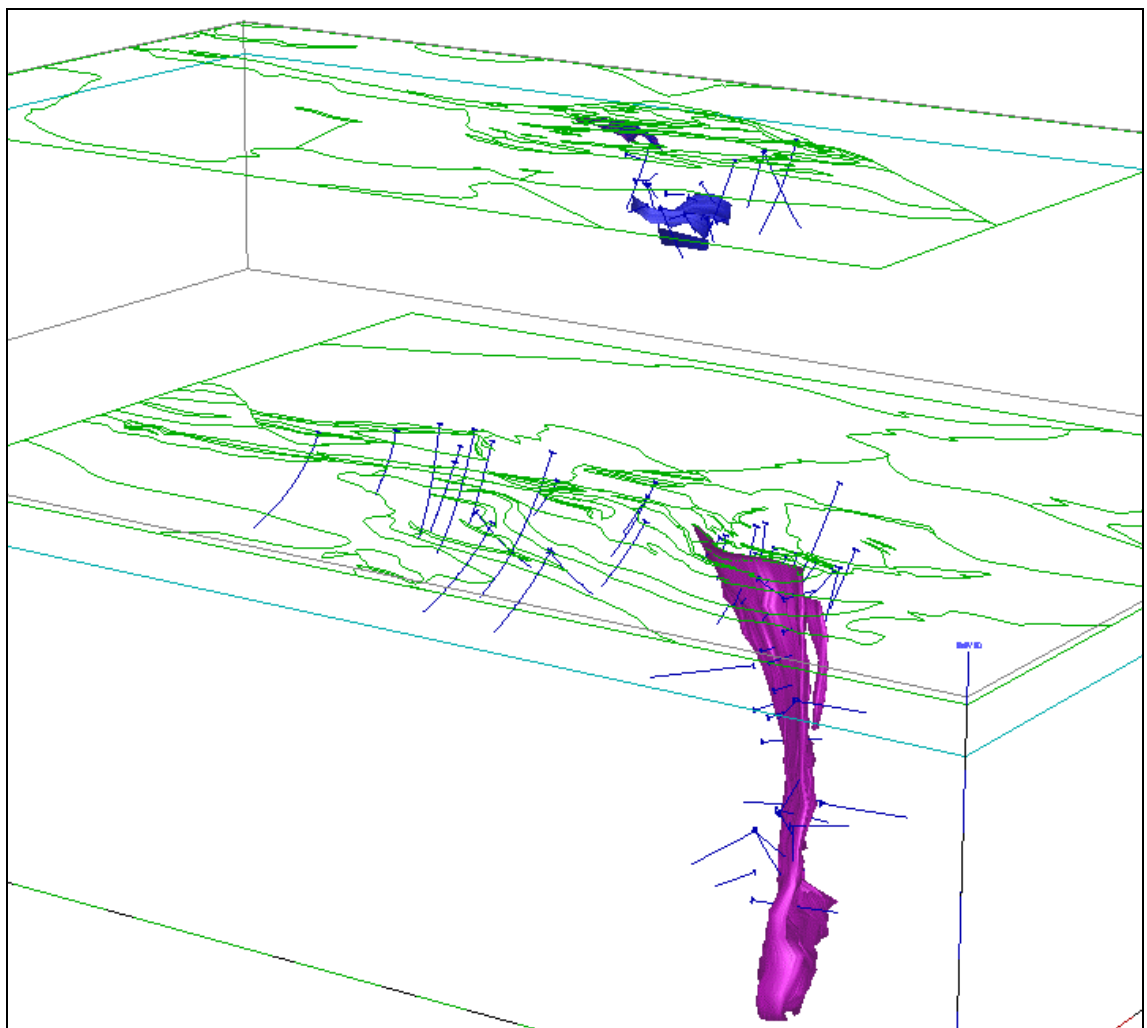


Figure A 1. 3D-composite sketch (looking from SW +30 degr.) of reglogged Dhole locations in relation to surface geology polygons (green lines) and ore bodies (magenta and blue).

Heikki Puustjärvi (ed.)

8.11.2006

Confidential

Drillhole logging was done by recording all lithological changes - rock composition, structure, alteration mineralogy, mineralization - and applying a specific way of lithogeochemical sampling. This was done by sampling strictly according to the changing lithological properties and taking a 10-cm-long core sample per every meter. Composite samples were made at intervals not exceeding five meters. Clearly base metal bearing and pervasively pyritised samples were split for their whole lengths (<5 m). This method produced 2517 samples for Pyhäsalmi relogged and new holes to be assayed by the chosen XRF-method. For Mullikkoräme the sample amount added up to 1048.

Drill hole logs were first written manually at the time of the physical logging and sampling procedure in field camp and in the Outokumpu exploration office premises then input as Excel files and imported into the geological Gem4Win software, which produces Access format data files of all imported data. This allows an easy later extraction of project data files that are stored in the Gem4Win Gcdbmp.mdb file.

Core sampling for new XRF assays took place coeval with the lithological logging. Samples were collected continuously as described above, numbered, bagged and collected into wooden boxes for shipment to the GTK laboratory in Espoo. All relogged cores are stored in the Pyhäsalmi mine. The rest of the pulverised XRF samples are stored in OM at Outokumpu.

A 3 NEW ASSAYS AND OLD DATA VALIDATION (K.Rasilainen)

See section C 1 for descriptions of assay methods and old and new data comparisons.

SECTION B

GEOLOGY

Heikki Puustjärvi (ed.)

8.11.2006

Confidential

B GEOLOGY (J.Luukas, H.Puustjärvi, J.Kousa)

The subproject "Geology" consists of five parallel categories: data management, field geology, section and plan reconstructions, structural and deformation modelling including chapters for metamorphism and paleovolcanology. The objectives of this subproject are rather wide-ranged in trying to explain the overall geological evolution and its genetic link to ore formation of the VMS type. All parallel categories are referred independently and summarized in chapter Paleovolcanology.

B 1 DATA MANAGEMENT

During the late spring of 1997 the first thing was to evaluate all existing geological surface data. Previous field notes and maps (E. Marttila/GTK, J. Pitkänen/OM, K. Ruotanen/OM, J. Luukas/OM) were checked and all relevant locations and lithological data were saved into project files. Existing field maps (1:10 000) from the Pyhäsalmi mine and the Liittoperä-Torvela area made by J. Luukas (OM) in the beginning of 1990's were digitized. The surrounding areas were compiled from the data captured from 1:100 000 geological bedrock maps (3321, 3322, 3323) by E. Marttila (GTK). J. Luukas then compiled a preliminary surface bedrock map with ArcView GIS-program. At this stage airborne geophysical data (magnetic and electromagnetic) were processed and used as background TIF-images in ArcView. The ground geophysical data (magnetic, electromagnetic and gravity) were processed later in the same way.

After the field works period a new updated surface geological map was drawn using also numerated lithological data obtained from exploration drillholes around the mines. The surface map is available in ArcView (*.shp) and MapInfo (*.tab) formats including all mapping in different scales. There are separate files for polygons, lithological boundary lines and overprinting lines. Codes related to these files are reported in the metadata file of the attached CD-ROM disc. DXF-files made by ArcView DXF-script are also available.

Additionally to the surface geological map a map showing different formations, lithodemes and rock sequences was compiled for stratigraphical and descriptive use and is available as well in the before-mentioned formats.

B 2 FIELD GEOLOGY

Remapping of volcanites around the Pyhäsalmi and Mullikkoräme mines was carried out during the summer of 1997. A-P. Tapio, an assisting field geologist, mapped 101 outcrops within the project area during the summer. At the same time J. Luukas mapped 88 outcrops studying especially structural features around the mines. J. Kousa made notes from 40 localities studying paleovolcanological features on key outcrops.

Ten lithologically and structurally interesting outcrops around the Pyhäsalmi mine were cleaned by tractor excavator during the 1997 field season. These outcrops

Heikki Puustjärvi (ed.)

8.11.2006

Confidential

were then washed and mapped in detail (1:100) by A-P. Tapio. Later on the drawings were digitized for use in GIS-software. Additionally two trenches were excavated at the Riitavuori area east of the Mullikkoräme mine and also an old trench at Parviaisaho north of the Mullikkoräme mine, still in a fairly good condition, was studied in detail.

B 2.1 REGIONAL GEOLOGY

The bedrock of the Pyhäsalmi area is a part of the Svecofennian domain between the Archaean Basement Complex in the east and the Central Finland Granitoid Complex in the southwest. Lithologically this area belongs to the NW-trending Savo Schist Belt (SSB) (e.g. Lundqvist et al.1997). Structurally this area belongs to a crossing zone of the NW-trending Raahe-Ladoga Zone (RLZ) and the SE-trending Oulujärvi Shear Zone (OSZ), where crustal scale tectonic blocks of separate metamorphic and lithological characteristics are defined (Fig. B1).

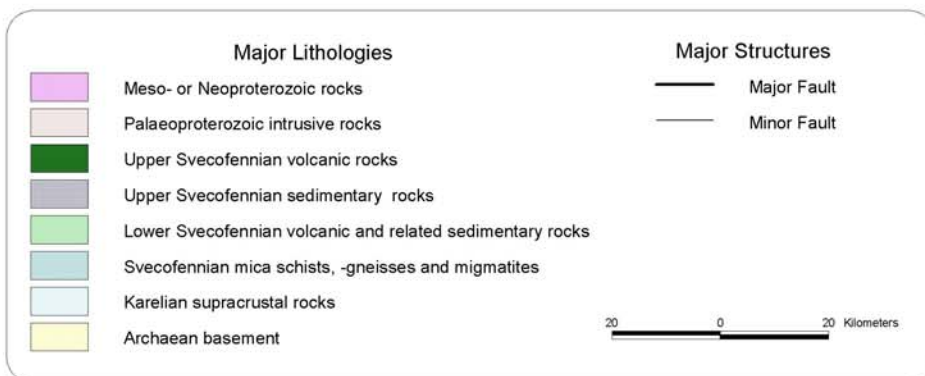
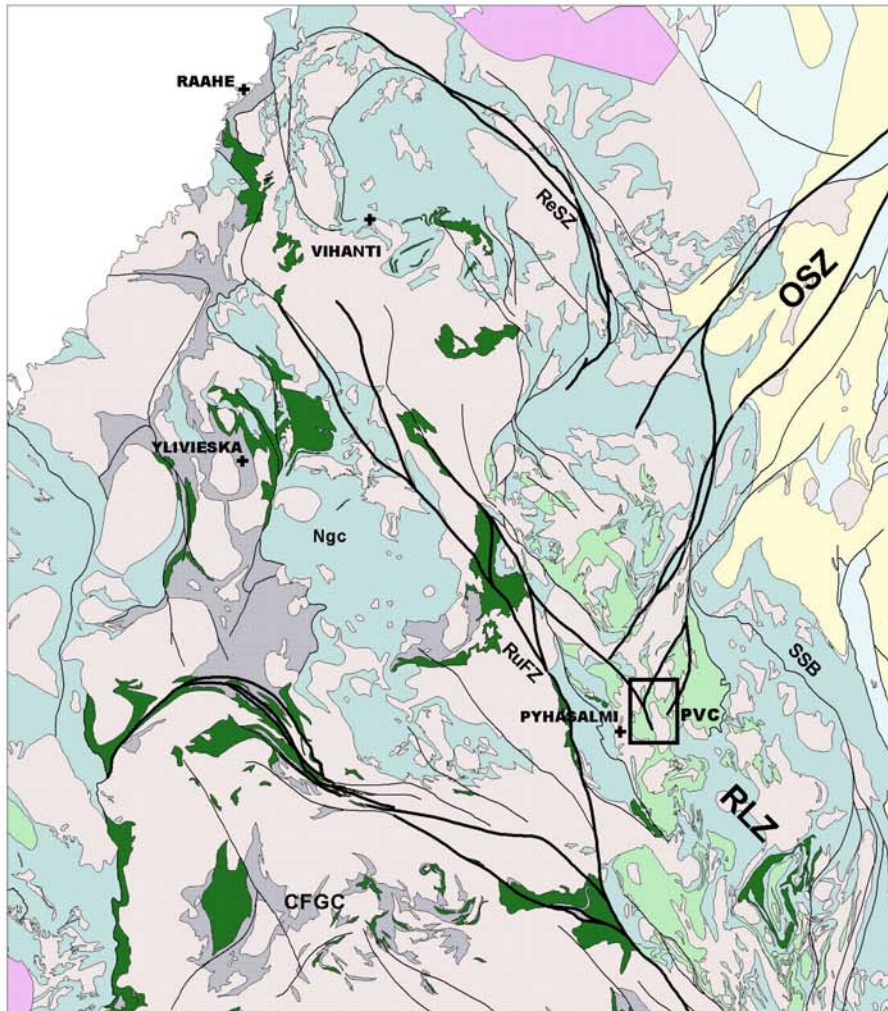


Fig. B1. Generalised lithological map of Ostrobothnia. The map is based on the Bedrock map of Central Fennoscandia (Lundqvist et al. 1996). The study area (PVC) is shown by a rectangle. Abbreviations as in the text.

Heikki Puustjärvi (ed.)

8.11.2006

Confidential

Because of numerous VHMS deposits and Ni-bearing mafic intrusions, Kahma (1973) called this zone the Main Sulphide Ore Belt. The idea, that the rocks of the Svecofennian Domain are closely related to the 2.0-1.8 Ga old Paleoproterozoic island arcs, was first described by Hietanen (1975). Since then this idea is widely accepted by many authors (e.g. Gaál 1986, Park 1991, Ekdahl 1993, Lahtinen 1994, Kousa et al. 1994).

The SSB consists mainly moderately to highly metamorphosed migmatitic mica gneisses, which are originally turbiditic metasedimentary rocks. Graphite-bearing schists, black schists and carbonate beds are common intercalations in these rocks. Volcanic rocks exist as narrow discontinuous belts or limited occurrences among both metasedimentary rocks and intrusive complexes. Metavolcanic rocks in central Ostrobothnia represent two different age groups, which also display distinct chemical characteristics (Weihed & Mäki 1997).

Besides supracrustal rocks numerous plutonic rocks exist in the Svecofennian domain forming large intrusive complexes (e.g. the Central Finland Granitoid Complex, CFGC) or separate intrusions along the Raahe-Ladoga Zone. These intrusive rocks are mainly quartzdioritic to granitic in composition, while mafic and ultramafic intrusions are subordinate. Isotope studies (e.g. Huhma 1986, Lahtinen 1994) show that these Paleoproterozoic intrusive rocks are purely mantle-derived with no sign of Archaean components.

In the northern Ostrobothnia metavolcanites can be classified into two different age groups which also have distinct chemical characteristics. By these criteria two major stratigraphic groups have been suggested by Kousa (1990). As presented in Weihed & Mäki (1997) the younger volcanic rocks exist mainly around the Nivala gneiss complex (NgC). This complex is separated from the Pyhäsalmi area by a major fault system called the Ruhaperä Fault Zone (RuFZ). It is suggested that metavolcanic formations (Kuusaa fm, Kangas fm, Sievi fm) are probably emplaced stratigraphically above the migmatitic mica gneisses of the NgC. Also the Pihtipudas Formation south of Pyhäsalmi can be classified into this group. Well-preserved primary structures in these volcanic formations indicate subareal or shallow water depositional environment for the calc-alkaline metavolcanites. The metavolcanic rocks vary from basalts to potassium rhyolites in composition and have a mature island arc affinity. This volcanism is closely related to early, syntectonic magmatism of the Central Finland Granitoid Complex, c. 1890-1875 Ma in age. This magmatism is also related with peak regional metamorphism in the area.

The rocks of the older volcanic group are situated in separate belts or complexes along the RLZ. In the Pyhäsalmi area these volcanic rocks are situated in a moderately to highly metamorphosed area between the Archaean basement to the east and the Nivala gneiss complex to the west. Migmatitic mica gneisses whose turbidite origin can still be recognised in places dominate this area. The mica gneisses are intercalated with minor quartz feldspar gneisses, black schists, skarn beds and some amphibolites of volcanic origin. The metavolcanic rocks form roughly an ovoid (10x20 km²) volcanic complex (called the Pyhäsalmi volcanic

Heikki Puustjärvi (ed.)

8.11.2006

Confidential

complex, Pvc) within the migmatitic mica gneisses and plutonic rocks. Massive sulphide deposits (Pyhäsalmi and Mullikkoräme) are closely related to this older volcanic environment. Most of the felsic rocks of the Pyhäsalmi area can be classified as calc-alkaline, low-K rhyolites, derived from the melting of an unknown Paleoproterozoic sialic crust (Weihered & Mäki, 1997). The felsic volcanic rocks are considered cogenetic (Kousa 1990, Lahtinen 1994) with the oldest known rock, the Kettuperä gneiss, dated at 1930±15 Ma (Helovuori 1979). At the eastern side of the complex a U-Pb zircon age of 1921±2 Ma from the quartz porphyritic rhyolite is correlated to the Kettuperä gneiss. The mafic metavolcanites are sub-alkalic, low-K tholeiitic basalts to basaltic andesites with primitive IAT affinity (Kousa et al. 1994).

B 2.2 PYHÄSALMI VOLCANIC COMPLEX

The Pyhäsalmi volcanic complex (Fig. B2.) (formerly known as Ruotanen schist belt in Helovuori 1979) can be divided into the **Ruotanen formation** (Ruf) in the west and the **Mullikkoräme formation** (Muf) in the east (Fig. B3.). Syntectonic plutonic rocks separate these formations: Kokkokangas granodiorite and Jusko diorite. The Ruotanen formation is N-S trending, 9 km long and 0,5-4 km wide volcanic formation with the Pyhäsalmi mine at its centre. The Mullikkoräme formation is N-S trending, 2 km wide and 12 km long volcanic entity whose northern part (Liittoperä-Torvela area) is not considered in this study. Both formations are poorly exposed and the lithological map is at many places based on drillholes, airborne geophysical data and ground geophysics. For example the northernmost part (Särkisalo member) of the Ruotanen formation is heavily interpreted.

The lowermost part of the Pyhäsalmi volcanic complex consists of silicic volcanites (tuffaceous and pyroclastic lavas) with minor mafic intercalations. Towards the top mafic pyroclastics, pillow lavas, and pillow breccias become more abundant. The metavolcanites in the Pyhäsalmi area are locally well preserved, but most of the rocks have been strongly altered by hydrothermal processes and deformed by later tectonic events (Weihered & Mäki 1997).

The poorly exposed and known central part of the Pyhäsalmi volcanic complex was previously interpreted partly as a basement for the Ruotanen and Mullikkoräme Formations (Kettuperä gneiss) and partly as younger intrusive rocks (Weihered & Mäki 1997). In the more detailed interpretations done by this project the central area is considered mainly as intrusive rocks and, according to drillcore relogging and XRF-assays, the Kettuperä gneiss is interpreted as a separate and lowermost member (Kettuperä member) of the Ruotanen Formation.

B 2.2.1 Ruotanen formation

The Ruotanen formation has been interpreted to consist of seven separate members according to drilling data, field geology and geophysical interpretations.

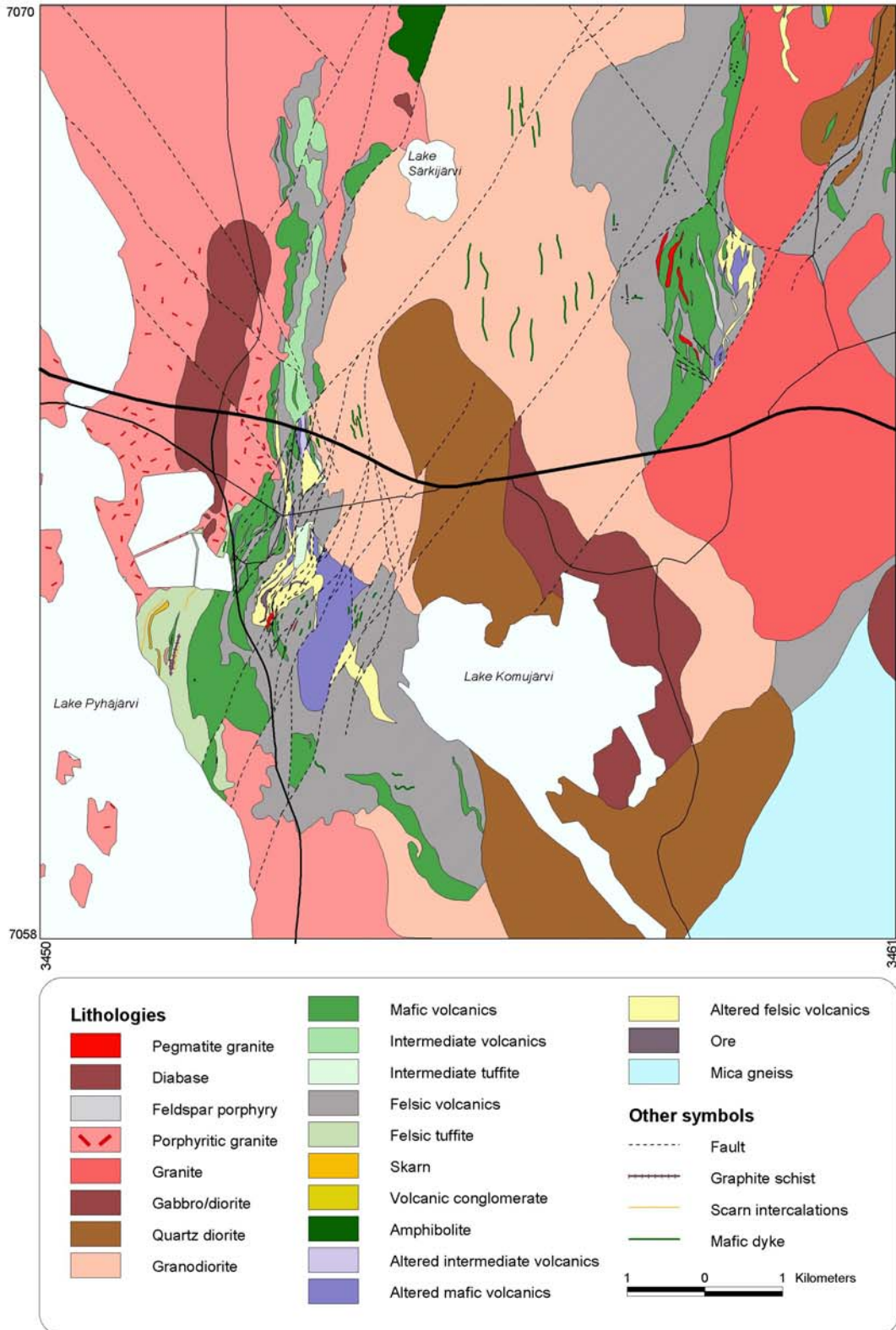


Fig. B2. Lithological map of the Pyhäsalmi volcanic complex.

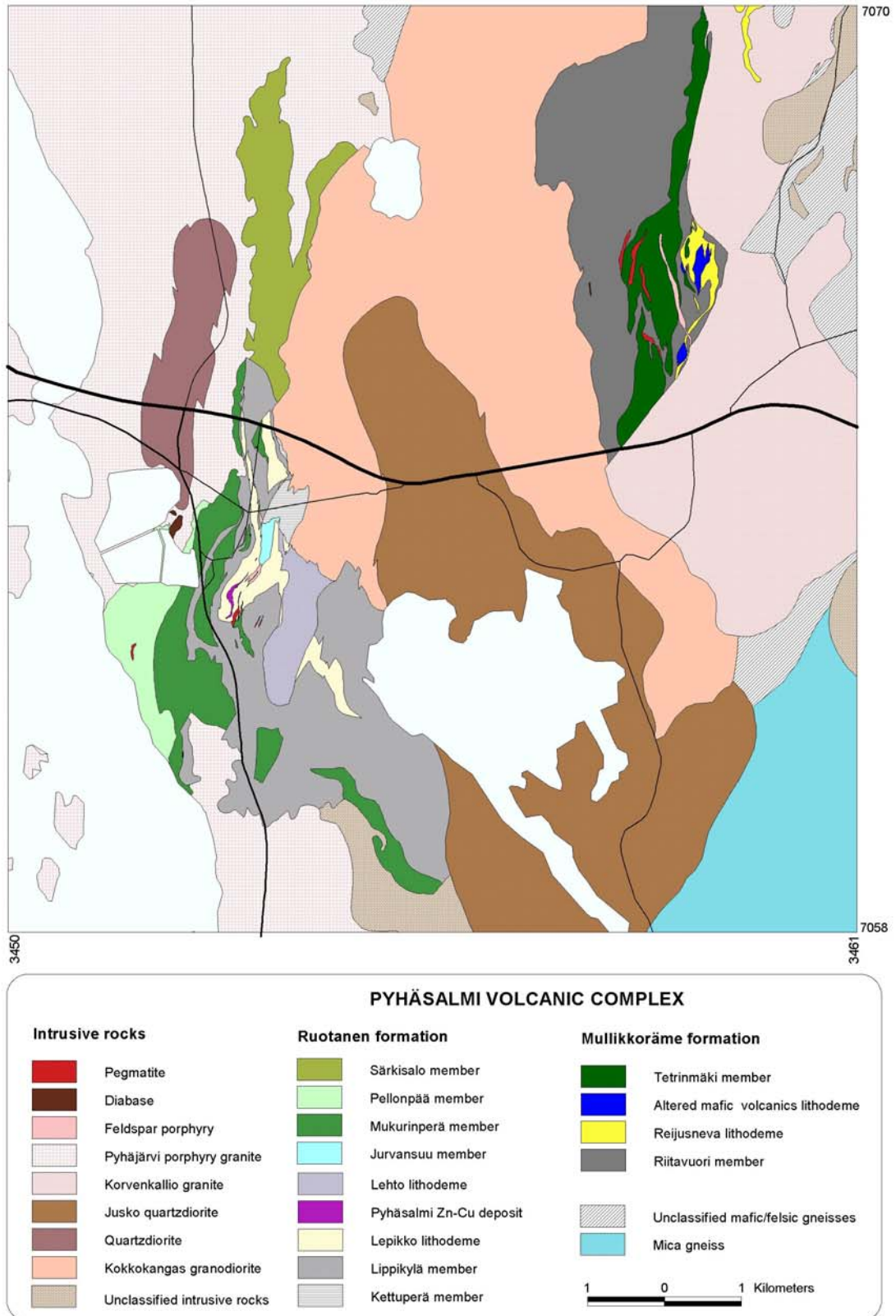


Fig. B3. Major stratigraphic units of the Pyhäsalmi volcanic complex.

Heikki Puustjärvi (ed.)

8.11.2006

Confidential

Kettuperä member - The lowermost member is named according to Kettuperä map locality 2.5 km north of the mine. Because of the lack of outcrops the appearance of this member is based solely on drillhole data. It is seen in drillholes that pinkish-grey volcanites (Fig. B5) are intruded by medium-grained granodioritic gneiss wedges (Kokkokangas granodiorite) which form part of the central area of the Pyhäsalmi volcanic complex. The pinkish-grey sodium-rich felsic metavolcanite has been dated using three samples from the drillhole PYS-27 giving a Zr-Pb age of 1930 ± 15 Ma. The same samples gave $^{143}\text{Nd}/^{147}\text{Nd}$ values of $2.6 \pm 0.9 > 3.2 \pm 0.4$.

The pinkish-grey felsic gneiss has been interpreted to represent a coherent silicic lava/synvolcanic cryptodome. The rock is composed of sparsely occurring plagioclase-quartz phenocrysts within a homogenous fine-grained groundmass, which has evenly spaced green mineral clusters (obscure and cloudy 2mm-1cm) of epidote (+Qtz-Gar-Bt-Chl-Fehdx). The amount and cluster size seems to increase towards the contact with grey Qtz-fsp-phyric volcanites (Lippikylä member). Epidote clusters may indicate dry high-level magma emplacement having miarolitic cavities filled with late magmatic volatile components or being just an indication of a magma contamination most effectively shown now along its contacts (Galley 1998).

Lippikylä member - The Kettuperä member felsic metavolcanites are overlain by fairly diverse group of grey felsic metavolcanites. The contact between the Kettuperä member and the overlaying metavolcanites is usually obscured by shearing, faulting and intrusion of mafic dikes and granodioritic gneiss wedges. In places (hole PYS-113) it is proposed that the contact is gradational. This regional major member has been named as the Lippikylä member (according to a mapsite 1.3 km SSE of the mine) and it includes practically all unaltered felsic metavolcanites outside the Pyhäsalmi VMS-deposit and its alteration zone. Many outcrops belong to this member in the Topiskonrämpe area (3 km SW of the mine) as well as at the mine vicinity and especially around the open pit. The waste rock open pit (for mine backfill) is blasted into this member.

The member mainly consists of grey-pinkish sodium-rich quartz-plagioclase-phyric rhyolitic metavolcanites and abundant mafic dikes of variable thickness (Fig. B5). Additionally, mafic sills and thin mafic metavolcanite interlayers were interpreted to occur in it. There are several textural variations besides the Qtz-fsp-phyric main type, such as grey, massive, fine-grained and banded (due to strong foliation) fragmental (lava/pumice clasts), spotty grey-creamy in color. At Kettuperä, the northern part of the area, there is a compositionally intermediate bed of this member evidently representing a lateral resedimented facies of the member metavolcanites.

The felsic metavolcanites of this member have been interpreted to represent mainly a package of lavas, cryptodomes and their autoclastic facies with subordinate pyroclastites.

Lepikko lithodeme - The Lippikylä member is overlain by moderately and pervasively altered felsic and mafic volcanites appearing now as pale greenish-

Heikki Puustjärvi (ed.)

8.11.2006

Confidential

yellow sericite-cordierite schists/rocks called here as Lepikko lithodeme due to its uncertain protolithological nature. The Pyhäsalmi massive sulphide ore is included within this member as an essential part. The name for this member has been adopted according to the company guesthouse located 400 m north of the mine. Contacts between the Lippikylä member and the Lepikko lithodeme are often tectonic (in drill cores), however in places a gradual change is seen between these members (e.g. at the NW-cliff of the waste rock open-pit, Fig. B5).

The distribution of altered rocks has been delineated into five separate domains. The main one is the large area of sericite-cordierite schists with some cordierite-antophyllite layers hosting the Pyhäsalmi VMS-deposit (Fig. B5). This continues further north into two zones - the western Kettuperä sericite-cordierite schist and the main Kettuperä alteration zone. There is still one area dominated by sericitic alteration further SE of the mine area at Tuomiaho. Besides these alteration zones dominated by felsic volcanites there is a large area of altered mafic volcanites east of the mine called **Lehto lithodeme**. It is composed of coarse antophyllite-cordierite-bearing gneisses and rocks (originally mafic lavas and pyroclastites) with a large amount of amphibole-mica-garnet-magnetite-bearing heterogeneous varieties including amphibolitic and uralite-phyric dikes. Due to strong deformation (transposing, pinching/swelling and faulting) it is difficult to reconstruct the nature of the alteration zones, but it is likely that all sericite-cordierite-altered volcanites form stratigraphically a more or less (due to original stratal/cross-stratal permeabilities) uniform strata enclosing the VMS-deposit. The Lehto alteration zone in mafic volcanites would be a stratigraphically lower/lateral component belonging to the contact zone of Lepikko and Lippikylä members.

Textures seen in the felsic altered volcanites are usually quartz-phyric and brecciated (alteration surrounding clasts) indicating the same kind of nature of volcanites as for the Lippikylä member. It is possible that the proportion of more permeable autoclastic breccias and pyroclastics is larger being the reason for the large amount of altered rocks.

The increase of pyrite (disseminated, clusters, stripes, layers) is a prominent feature within the altered rocks when approaching the VMS-deposit. Further outside of the alteration zone there is also a lesser amount of pyrrhotite and magnetite. The Lehto alteration zone is typically pyrrhotite- and magnetite-bearing.

Pyhäsalmi Zn-Cu deposit - is a typical massive sulphide deposit surrounded by volcanites and an alteration halo. The surficial S-shaped form of the orebody has been moulded by to polyphase deformation into a conical form at deeper levels. The N-S length of the outcropping part is about 650 m and at its maximum width about 80 m. The ore extends from surface down to 1400 m in depth. Alteration around the ore is pervasive showing strong sericitization and a lot of yellowish brown and dark pinitized cordierite. Pyrite banding and heavy dissemination is usual within the ore contact zones. At deeper levels the ore has been squeezed out of its alteration zone due to strong deformation. This phenomenon has led to a peculiar situation where the ore is within a very siliceous felsic volcanite possessing hardly any signs for closeness to ore. Practically all of the ore/waste contacts are

Heikki Puustjärvi (ed.)

8.11.2006

Confidential

clearly cutting at the deeper levels. Marks of alteration exist only within ore as sericite-cordierite-talc-bearing schists.

The Pyhäsalmi deposit is made of massive ore with 70% medium- to coarse-grained sulphides (pyrite-sphalerite-chalcopyrite-pyrrhotite). The sphalerite-rich ore is in places finely banded and thin porphyritic bands are common. Round pyrite phenocrysts occur in the fine-grained sphalerite matrix of the porphyry ore. A pyrite dissemination, which in places displays breccia structure, exists around the massive ore. Pyrrhotite has replaced pyrite at the southern end of the ore. Pyrrhotite replacement seems to be related to the intrusion of pegmatites and is common in strongly deformed (D₄) areas.

Jurvansuu member – occupies a small area mainly composed of reworked felsic-intermediate volcanites few hundred meters northeast from the Pyhäsalmi open pit. The main sericitic alteration zone is interpreted to be overlain by these intermediate volcanogenic schists which now form a small local synform. There are no outcrops of this member; the nature of the rocks is seen only in few drill holes. The rocks are quite variable being usually fine- to medium-grained, micaceous (flogopitic biotite) schists sometimes having abundant garnet as well as felsic and some amphibole bearing mafic layers. In drillhole PYS-75 the basal part of the synform is composed of a fairly coarse volcanic breccia/conglomerate (felsic fragments in an intermediate/mafic groundmass).

This member has been interpreted to represent eroded and rapidly resedimented volcanites during a short-lived instability period prior to the deposition of the Mukurinperä member mafic volcanites.

Mukurinperä member - Mafic unaltered volcanic rocks located mainly in the western and southeastern parts of the Ruotanen formation belong to this member. Stratigraphically, this member is interpreted to overlie the aforementioned members according to the facts that felsic volcanites are the only fragments found in these mafics and in the Lippikylä and Lepikko felsic volcanic members there are a lot of mafic dykes and sills. There are also westerly way-up observations of pillow lavas at Mukurinperä and Vanhainkoti, which fact is in concordance with the stratigraphic conclusions. Most of the outcrops observed are in the mine area, at Topiskonrämpe and at Mukurinperä, the latter being the type locality for this member about 1km SW of the mine. The extent of the member has been largely interpreted according to the airborne and ground geophysics.

The mafic volcanites of this member contain pyroclastic breccia and pillow lava structures. Some felsic interlayers and altered horizons have been identified in drillholes W-NW of the mine. Pyroclastic breccias have been identified mainly on both sides of the mine containing fragments of slightly altered quartz-phyric felsic volcanites even up to 5 meters in diameter e.g. near the southern edge of the open pit (Fig. B6). In the Kettuperä area similar pyroclastic breccias have been identified in drillhole PYS-114. Pillow structures have been identified in metalava at Mukurinperä.

Heikki Puustjärvi (ed.)

8.11.2006

Confidential

Pellonpää member - is the westernmost member of the Ruotanen formation. It mainly consists of skarn-banded felsic volcanites (qtz-phyric breccias, tufts, tuffites, Fig. B6), pure skarn rocks and intermediate tuffites with minor graphite- and pyrrhotite-bearing beds. This member has been delineated mainly according to ground- and airborne geophysics as well as drillhole data. Outcrops of this member are very scarce. This member has been understood to represent mixed lithologies of volcanites, epiclastites and carbonate sediments succeeding the extrusion of the Mukurinperä mafic volcanites.

Särkisalo member - is the northernmost part of the Ruotanen formation. This N-S trending member is narrow and surrounded by intrusive rocks. There are no outcrops in this area and the lithological data is gathered from few scattered drillholes. The main lithologies are unaltered felsic, intermediate and mafic volcanites with abundant mafic and granitic dykes. The stratigraphic position of this member is not clear, but most probably it can be correlated to the lower part of the Ruotanen formation.

B 2.2.2 Mullikkoräme formation

The Mullikkoräme formation is divided into four major members (Figs. B3 and B7) of which the northernmost Purola member is not included in this report due to location outside the project area.

Riitavuori member - The lowermost member is located in the western part of the formation. A small hill called Riitavuori, west of the Mullikkoräme mine, represents the type locality of this member. The main lithology on this hill is pale greyish fine-grained sodium-rich felsic volcanite showing sparse primary structures (e.g. quartz-phyric and volcanic breccia structures). The pyroclastic material contains intercalations of lava-like rhyolitic quartz porphyry and rhyodacitic volcanic breccia. The phenocrysts of the quartz porphyry are 1-2 mm in size. Beside quartz, the other main mineral is albite-oligoclase, occurring as 3 mm grains, which sometimes seem patchy because of their microcline contents. Hornblende and biotite are also encountered as main constituents. Accessory minerals include epidote, titanite, muscovite and carbonate. N-S trending mafic dykes abound. At the southwestern side of the hill the Kokkokangas granodiorite has intruded into felsic volcanites. A quartz-porphyritic rhyolite has been dated yielding a U-Pb zircon age of 1921±2 Ma corresponding to the age of the Kettuperä member.

Northwards from the Riitavuori felsic volcanites are mostly pale reddish-grey fine-grained rocks lacking primary structures. Such rock is usually difficult to distinguish from fine-grained granite gneiss. The only exception is at Heikinaho, 2 km north of Riitavuori, where coarse volcanic breccia structures are seen (Fig. B8).

Heikki Puustjärvi (ed.)

8.11.2006

Confidential

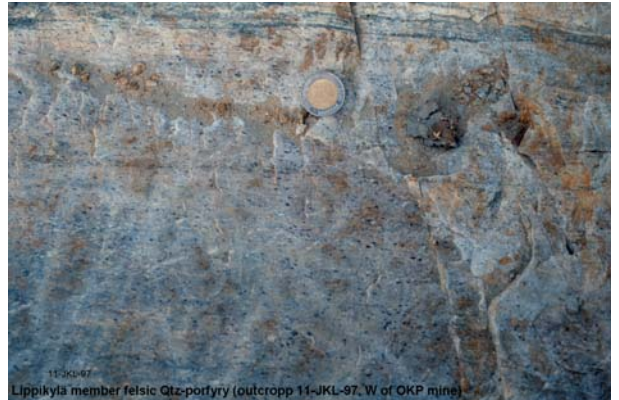


Figure B5. Unaltered and altered felsic volcanites of the Ruotanen formation at Pyhäsalmi.

Heikki Puustjärvi (ed.)

8.11.2006

Confidential

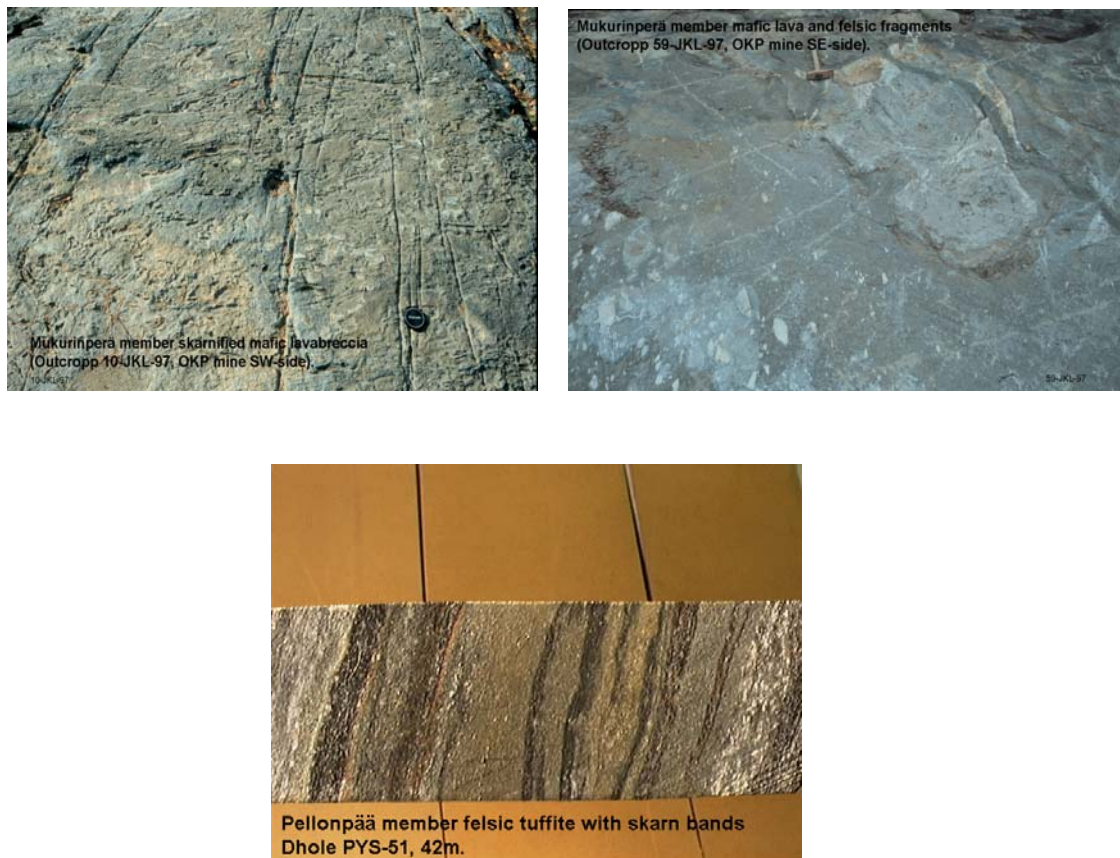


Figure B6. Mafic volcanites of the Mukurinperä member and a skarn bearing felsic tuffite of the Pellonpää member, all near by the Pyhäsalmi mine.

In general, this member seems to be a mixture of felsic volcanites displaying quartz-phyric and breccia structures. These have been interpreted to represent lavas, sills, dykes and subvolcanic domes (cryptodomes) but rarely tuffaceous or reworked beds.

Reijusneva lithodeme - is composed of altered felsic and mafic volcanites and includes mineralisations of VMS type. The use of a lithodeme nomination for these lithologies is a practical choice to distinguish altered ore-potential volcanites from their unaltered variants belonging possibly to both the Riitavuori member felsic volcanites and an indistinguishable Reijusneva 'member'. In general, alteration is not as strong as within the Lippikylä member of Ruotanen formation.

Altered felsic volcanites are sericitic, phlogopitic and chloritic in variable proportions. Cordierite is also found in all varieties (Figs. B8 and B9).

Contacts between unaltered and altered felsic volcanites are often gradational but also appearing as sharp tectonic contacts (Ser-schists) and stringer- or dyke-like

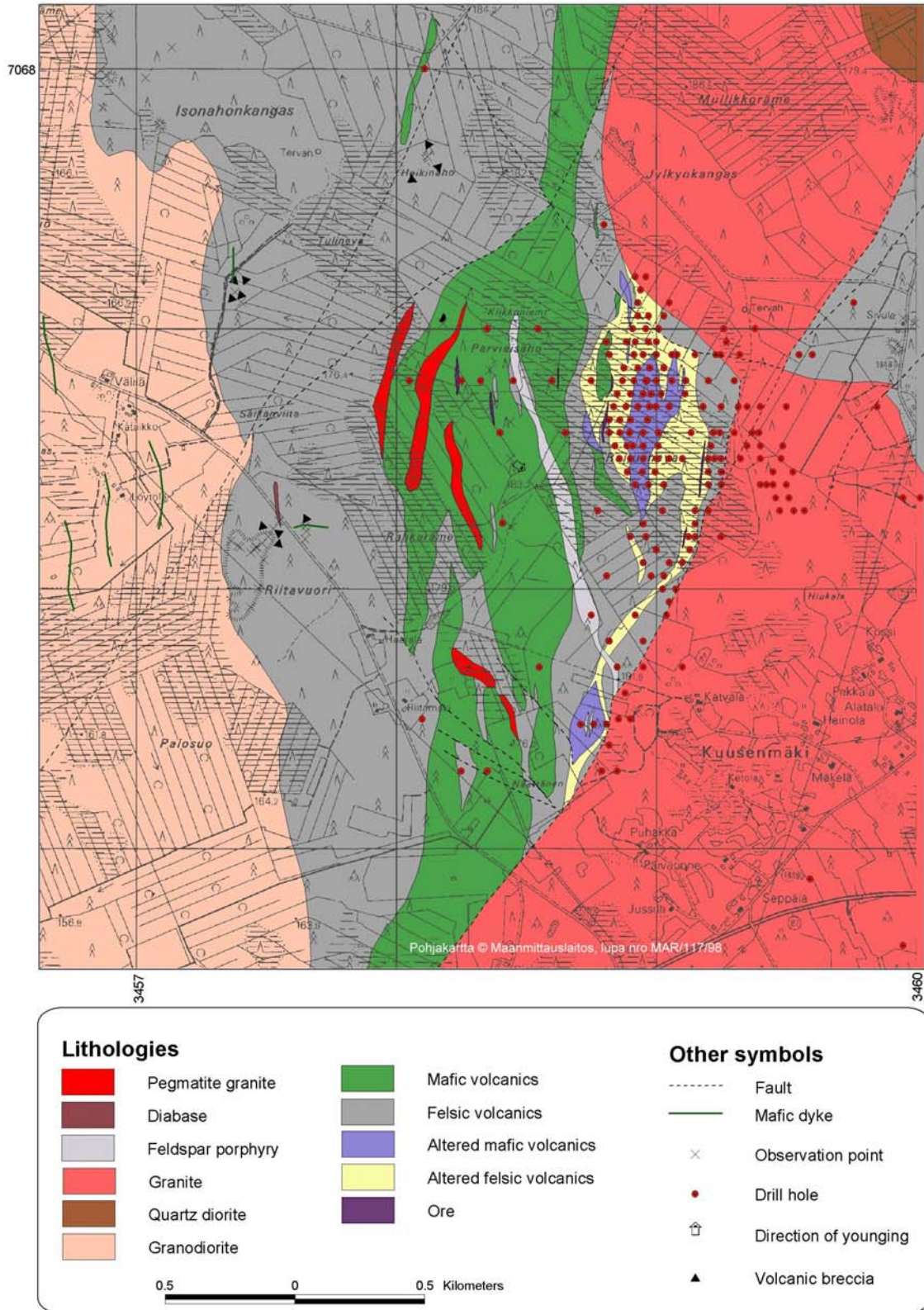


Fig.B7. Lithological map of the Mullikkoräme mine area

Heikki Puustjärvi (ed.)

8.11.2006

Confidential

networks (Chlo+Phlo-dominant alterations). Pyrite dissemination and semimassive bands are always present.

Differentiation between mafic unaltered and altered volcanites is clearer. Altered mafic volcanites are chloritic (phlogopitic) amphibole-cordierite gneisses depending on the degree of original hydrothermal alteration and later metamorphic effects (retrogression). Contacts between mafic and felsic volcanites are often characterized by a more intermediate lithology composed of plagioclase, cummingtonite-tremolite, quartz and carbonate. Pyrrhotite and pyrite dissemination (often fairly coarse-grained) is abundant.

Mullikkoräme mineralizations – outcrop in 3 separate N-S trending narrow lenses (A, B and C) overlain by the Reijusneva swamp area (Fig. B7). Only the westernmost lens cluster (A) had minable ore. The lenses in deep orebody are located below the outcropping B lens from +425-level down to +675-level. The partly mined westernmost “A-strata” was composed of three lenses dipping c. 55 degrees east and having a total N-S extension of 200 m and down-dip height of 100-150 m. Thicknesses of individual lenses were highly variable (1-10 m). All other lenses (B, C and deep ore lenses) are almost vertical and also highly variable in thickness. The largest of the deep ore lens cluster is the Siperia lens extending 300 m in N-S direction and having the height of 100-150 m. There are four additional ore lenses and some undelineated indications.

Mineralized horizons in the upper body at Mullikkoräme are mainly composed of massive sphalerite-pyrite-banded ore with subordinate magnetite, galena and chalcopyrite. Gangue minerals are quartz, carbonate, FeMg-silicates and baryte. The deep ore lenses are banded semimassive-disseminated sphalerite-galena-chalcopyrite-pyrite mineralizations with variable magnetite content. Gangue minerals are more carbonate-talc-dominated compared to ones in the upper ore. The texture in ore is more fine-grained than that at Pyhäsalmi. The only ore-related marker lithology is the baryte horizon, which is very local and discontinuous.

Strong small-scale block tectonics and strong NE-SW shearing along the volcanites/granite contact cause rapid variations in ore lens continuities. The Zn-mineralisation at Mullikkoräme totals c. 2 Mt at 6% Zn, of which c. 1 Mt have been mined.

Tetrimäki member - is an upper stratigraphic member of mafic volcanites. It forms a 5 km long, N-S trending and about 100-700 m thick easterly dipping synformal sequence of dark green fine-grained mafic volcanites. The contact between this and the underlying Riitavuori member can be interpreted on two outcrops as depositional although a slight schistosity makes the definite determination a bit uncertain. In both cases the lowest bed of the Tetrimäki member consists of massive mafic lava with few felsic blocks 10-50 cm in diameter originating from the Riitavuori member. Outcrops of this member are sparse, thus continuations of individual beds or flows are impossible to trace. On outcrops pillow lava, lava breccia and hyaloclastitic features can be seen indicating a subaqueous

Heikki Puustjärvi (ed.)

8.11.2006

Confidential

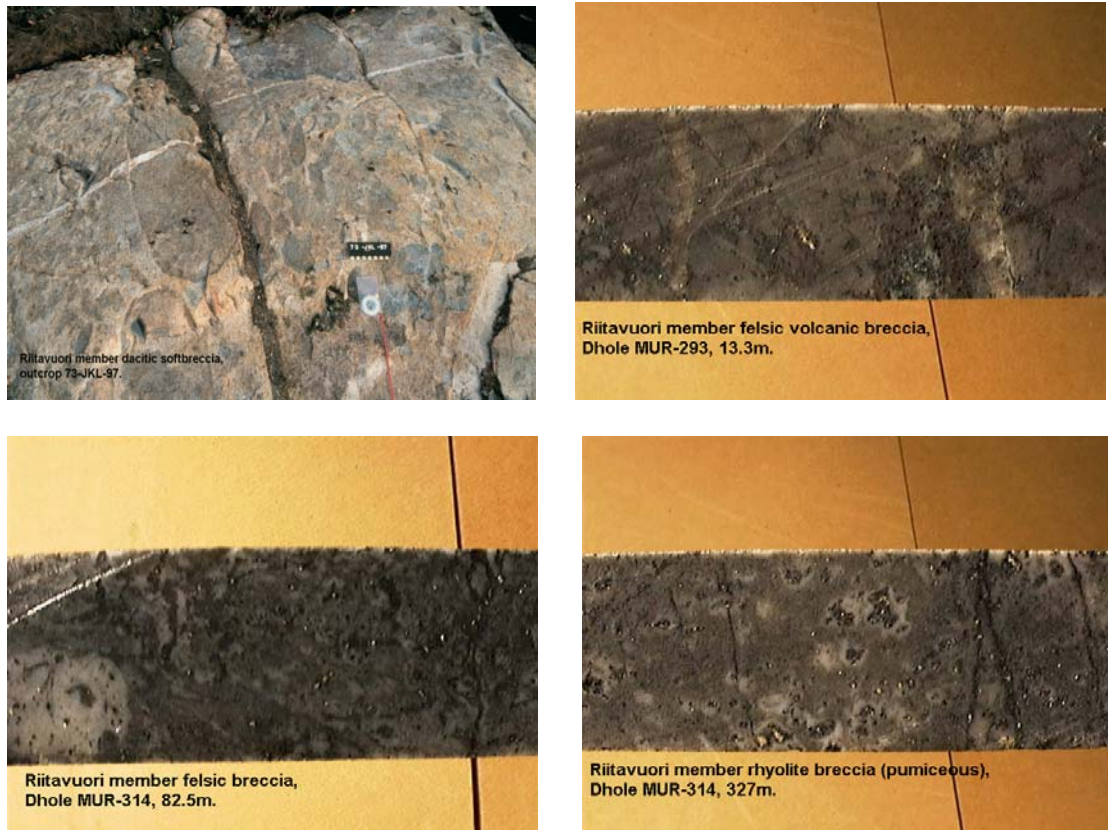


Figure B8. Riitavuori member unaltered felsic volcanites.

origin for the lava flow complex (Fig. B9). Mafic plagioclase and/or uraltite porphyritic and massive dykes are numerous. Hydrothermal and retrogressive alteration has affected the volcanites causing growth of chlorite, orto/clino-amphibole, epidote and magnetite. Some horizons are pyrrhotite-bearing and cause easily-detectable EM anomalies.

B 2.2.3 Pyhäsalmi complex intrusives

Kokkokangas granodiorite - A dominant rock type besides the Jusko quartzdiorite in the centre of the Pyhäsalmi volcanic complex is pale grey, medium-grained and mostly slightly or moderately foliated granodiorite. It is called the Kokkokangas granodiorite after a well-exposed area east of Lake Särkijärvi. Mafic dykes similar to ones in the adjacent felsic volcanites are abundant in this rock type.

Quartzdiorites and diorites - Around Lake Komujärvi there is a quartzdiorite-diorite intrusion, about 20 km² in size, inside the Pyhäsalmi volcanic complex. This intrusion has been called as Jusko or Komujärvi quartzdiorite/diorite (Marttila 1993). Dioritic rocks are exposed on the east shore of Komujärvi while quartzdiorite is present at the southern side of the lake. Some outcrops exist also at the northern part of the intrusion. This rock is usually slightly oriented or unoriented medium-grained intrusive. The zircon U-Pb age from the quartzdiorite yielded 1893±3 Ma.

Heikki Puustjärvi (ed.)

8.11.2006

Confidential

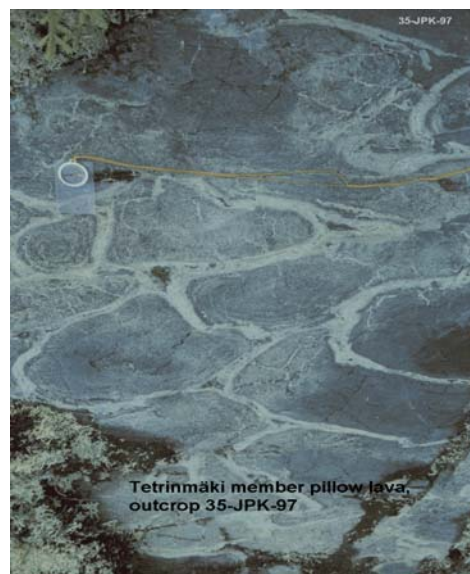


Figure B9. Reijusneva lithodeme altered felsic volcanites and Tetrinmäki member pillow lavas.

There is a gravimetric anomaly inside the porphyry granites west of the Ruotanen formation. This area has been interpreted as quartzdiorite by one outcrop.

Granites - The Pyhäsalmi volcanic complex is surrounded by voluminous granitic intrusives. The westernmost part of the area consists of coarse-grained porphyry

Heikki Puustjärvi (ed.)

8.11.2006

Confidential

granite. Outcrops (around dumps) show that the granite intruded into volcanites. This granite type yielded a U-Pb age of 1883 ± 25 from Vuotomäki. At the western side of the volcanic complex a medium-grained red-coloured granite called Korvenkallio granite has intruded into the volcanites of the Mullikkoräme formation. This intrusion is split into two major parts by D₄-fault.

B 2.2.4 Dike rocks

Feldspar porphyries - There are two types of feldspar porphyries. Immediately N-NE of the Pyhäsalmi deposit a pinkish-grey fine-grained feldspar porphyry is outcropping and has been followed in drillholes on few sections. It forms a sill or mini-laccolite body intruded into the Lepikko lithodeme altered felsic volcanites. Another more voluminous set of vertical, NW-trending coarser-grained and more granitic feldspar porphyry dikes intrude the Tetrinmäki and Riitavuori member volcanites in the Mullikkoräme area.

Diabases - There are several indications of feldspar ophitic diabase dikes within the whole of Pyhäsalmi volcanic complex. Best outcrops are seen on the eastern margin of the mine dumps where coarse-grained ophitic diabases outcrop. There they are cut by coarse-grained pink pegmatites.

Pegmatites - There are numerous coarse-grained pink/pinkish-grey pegmatite dikes cutting the whole range of the Pyhäsalmi volcanic complex rocks. Intrusion of one set of dikes of variable thickness is connected to the NE-SW trending D₄-phase sinistral deformation zones immediately at the eastern contact of the Pyhäsalmi ore deposit and further on other analogous parallels east of the mine site. At Mullikkoräme there are same type of pegmatites intruding into the western mafic volcanites (Tetrinmäki member) in two directional sets and additionally at the contact zone of the Korvenkallio granite with the Riitavuori member and Reijusneva lithodeme felsic volcanites. Especially the pegmatite having cutting contact relationship with the Pyhäsalmi deposit is important in predicting the possible continuation of the northern part of the Pyhäsalmi deposit at deeper (<+400) levels.

Mafic and felsic dikes - The whole bimodal volcanic sequence of the Pyhäsalmi complex has numerous mafic and felsic dikes, which are often difficult to distinguish from the compositionally corresponding extrusives. In general it can be said that uralite and/or plagioclase porphyries within mafic volcanites are dikes and narrow massive amphibolitic layers within felsic volcanites are likewise dikes/sills. Aplitic fine-grained massive dikes within mafics are sparse but numerous within felsics and they are sometimes difficult to distinguish from massive pinkish-grey felsic volcanites. There are still rhyodacitic feldspar-phyrlic dikes within the felsic volcanites especially in the Mullikkoräme area.

Heikki Puustjärvi (ed.)

8.11.2006

Confidential

B 2.2.5 Unclassified intrusives

These rocks outcrop as small segments within the project map area in the south and east comprising gabbroidic gneisses and granodioritic gneisses analogous to those at Kokkokangas.

B 2.2.6 Unclassified felsic and mafic gneisses

These rocks occupy unclassified segments in the north and east of the project map area consisting of amphibolitic gneisses (mafic volcanites) and fine-medium-grained felsic migmatitic gneisses (felsic volcanites).

B 2.2.7 Mica gneisses

In the SE-corner (Salmelanperä) of the project map there is a fairly large area of heterogeneous rocks composed of highly metamorphosed granite-veined mica gneisses including into quartz-feldspar gneiss, amphibolite and graphite-bearing layers.

B 3 SECTION AND PLAN RECONSTRUCTIONS (J. Luukas, H.Puustjärvi)

Geological vertical sections and subsurface plans were compiled using mainly exploration drillhole data. Mine maps were also used, especially in the Pyhäsalmi area, as well as data from underground mine drillings to enveloping country rock. Examples of constructed vertical sections and horizontal plans are shown in Figures B10 and B11. J. Luukas digitized the sections and plans with ArcView software. There are separate files for polygons, lithological lines and overprinting lines in the same manner as for the surface geological map. The polygon data is converted also into MapInfo (*.tab) and AutoCad formats (*.dxf). The DXF-conversions were done using ArcView script. The plans and vertical sections are also imported into the Gem4Win (Gemcom) software polygon workspace. The names used for the digitized plans and vertical sections are shown in Appendix B1.

B 4 STRUCTURAL AND DEFORMATION MODELING AND METAMORPHISM (J. Luukas, T. Kilpeläinen, A-P Tapio)

The aim of subproject B4 was to study local structural and metamorphic evolution around the Pyhäsalmi and Mullikkoräme mines and to correlate structures with regional ones. J. Luukas, in cooperation with T Kilpeläinen, carried out the detailed structural mapping and large-scale structural modelling. The 3D-modelling of the Pyhäsalmi mine was done by T. Kilpeläinen. A-P. Tapio and T. Kilpeläinen carried out the metamorphic studies. A brief description of the regional structures, as well as the results of the structural and metamorphic studies, are presented in the following chapters adapted from a text by J. Luukas (in Weihed and Mäki eds., 1997).

Heikki Puustjärvi (ed.)

8.11.2006

Confidential

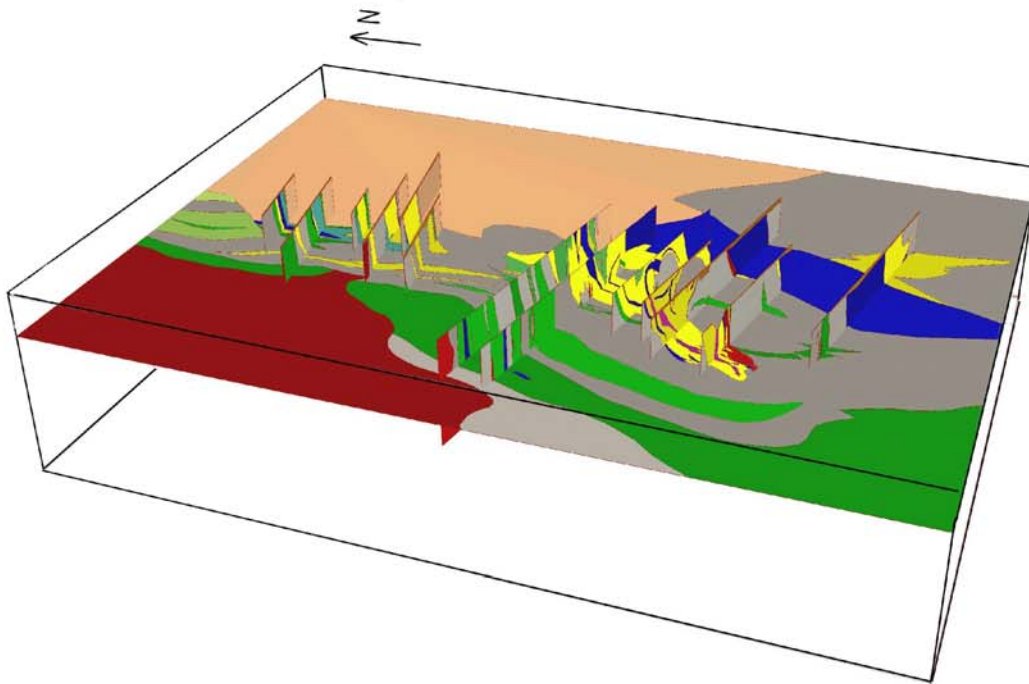


Fig. B10. A 3D picture of the Pyhäsalmi mine area showing digitized vertical sections and +210 horizontal plane.

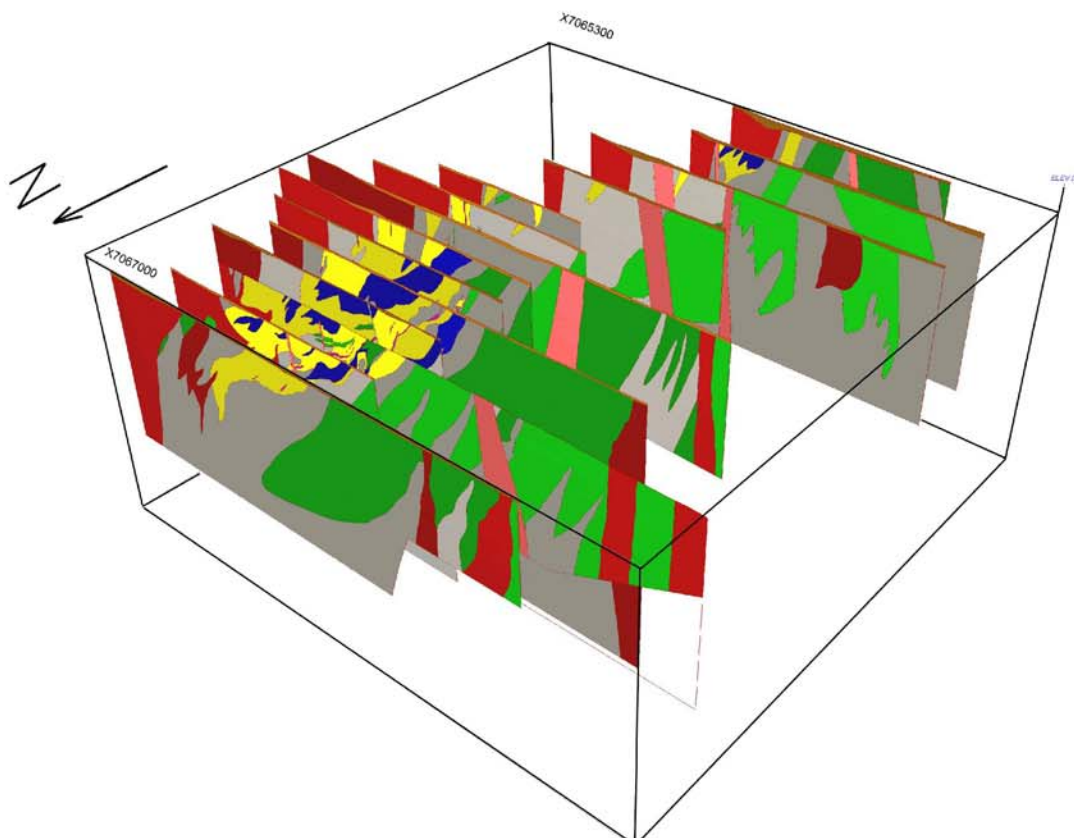


Fig. 11. A 3D picture of the Mulliköräme mine showing the digitized vertical sections.

Heikki Puustjärvi (ed.)

8.11.2006

Confidential

B 4.1 REGIONAL STRUCTURE

The palaeoproterozoic formations along the Raahe-Ladoga Zone have been affected by multiphase deformation, which is now manifested by fault-bounded blocks with internally different structural and metamorphic histories. Along the RLZ, the deformation history can be divided into an early phase of thrusting towards the craton and a younger phase of shearing, which produced the major vertical shear zones of the central Fennoscandian Shield.

In central Ostrobothnia isoclinal and tight F₁ folds (Luukas 1991) marked the earliest compression. They were identified from well-preserved mica gneisses near the border of the Archaean craton. This rarely identified structural stage has been considered to coeval with the nappe emplacements and recumbent folds described from eastern Finland by Koistinen (1981). During the D₂ stage, the D₁ structures were openly refolded reflecting progressive deformation in the same compressional regime. The D₁-D₂ tectono-metamorphic stage caused nappe emplacement towards east or northeast with considerable crustal thickening as a result.

The D₃ phase caused intense F₃ folding, which refolded the earlier flat-lying structures into upright position along the RLZ. Contemporaneous magmatism produced large volumes of tonalite and tonalitic migmatite related to high temperature, low pressure metamorphism at 670-800 °C and 5 kb (Korja et al. 1994). The emplacement of pyroxene-bearing granitoids at 1884 Ma ago, characteristic of the RLZ, is related to this stage. At the later stages of D₃ the deformation style changed gradually from folding to ductile shearing causing large-scale dextral SE-trending strike-slip faults along the RLZ thus initiating a major fragmentation in the crust. At the north-western end of the RLZ the dextral Ruhaperä Fault Zone (RuFZ) and Revonneva Shear Zone (ReSZ, Fig. B1) are examples of these shear zones. West of the RLZ the D₃ was not so penetrative and more open F₃ structures were generated. SE- and N-trending F₃ fold structures are the most conspicuous mesoscopic and macroscopic structures in central Ostrobothnia. The SE-trending structures in the RLZ and on the northern Ostrobothnia Schist Belt, east of Oulu, indicate that the compressional field was directed SE-NW during D₃ (Kärki et al. 1993).

After the D₃ event, folds and ductile shear zones were formed during D₄ stage. The E-trending axial planes of F₄ folds can be seen in many places in Ostrobothnia indicating that the compression field was shifted from SW-NE to N-S at this stage. The most conspicuous structural feature of D₄ stage is the crustal-scale sinistral SW-trending Oulujärvi Shear Zone (OSZ, Fig. B1), which transects the Kainuu Schist Belt and Archaean craton. The sinistral movement on the OSZ has caused a separation of the Vihanti-Pyhäsalmi belt into two separate blocks: the Vihanti and Pyhäsalmi belts, respectively. At this stage the Revonneva and Ruhaperä shear zones, formed during the D₃ stage, were reactivated with significant movement as exemplified around the Vihanti block. This block, characterized by a gravity-high anomaly and high metamorphic grade, is surrounded by major D₄ shear zones and nicely displays the fault-controlled nature of metamorphic blocks in the RLZ (Korsman et al. 1988). The south-western-most faults in the OSZ extend to the

Heikki Puustjärvi (ed.)

8.11.2006

Confidential

Pyhäsalmi area and display a strong structural influence on the Pyhäsalmi and Mullikkoräme deposits. Granitic partial melts, seen as potassium-rich neosomes, abundant pegmatites along the shear zones were generated during this deformation stage in the Oulujärvi region. Age data presented for the OSZ by Kärki et al. (1995) show that granitic intrusions were emplaced 1860-1800 Ma ago. This magmatism can be related to the 1830-1810 Ma tectonometamorphic event in the south-eastern part of the RLZ (Korsman et al. 1984, Korsman et al. 1988). Kärki and Laajoki (1995) pointed out that the role of D₄ event is more important than yet realized in the crustal deformation history of Finland.

B 4.2 STRUCTURES IN THE PYHÄSALMI AREA

B 4.2.1 Structure of the Pyhäsalmi mine area

The structural evolution of the Pyhäsalmi mine area has been studied in the 1980's by Koistinen (1983, 1984) and 1990's by Luukas (1992, 1994). These studies revealed the complexity of the structural evolution around the mine, however detailed metamorphic studies were not included in them. In the Koistinen's works, a 5-stage deformational history was suggested while the works of Luukas suggested four main deformation stages. In the both works the earliest deformation stage (D₁) was interpreted as flat-lying isoclinal folding which thickened the ore. D₂ stage in the both works refoled D₁ structures into upright position forming a major synform at the mine area. After these folding stages the deformation style changed (at D₃ -D₅ by Koistinen and D₄ by Luukas) into a zonal shear tectonism forming fault-bounded block structures. Luukas suggested D₃ as a new folding stage before the shear tectonism.

During this project these structural events were re-evaluated and a new model, which points out the importance of the late stage shear tectonism, is suggested. The structural mapping of the outcrops around the mine formed a base for the structural modelling of the area. Despite sparse outcrop, often in poor condition, the basic structural elements (D₃ and D₄) were identified with some accuracy. Underground geological maps prepared by mine geologists were studied in detail to recognize structures at the deeper levels. Also drillhole data, especially in the Lehto and Kettuperä areas, were used to achieve 3D-picture for these areas. Lithologies such as narrow cordierite-antophyllite rocks inside sericite schists were used as key horizons. Geophysical maps were useful in identifying late stage faults but their importance in identifying fold structures was minimal. Geophysical interpretations done during this project have been taken into consideration during the modelling.

From the structural studies point of view some remarks are made concerning the physical and chemical properties of rocks. The lithologies of the mine area can be divided into incompetent mica-rich altered rocks and competent quartz-feldspar-rich unaltered rocks. Because of difference in competence the

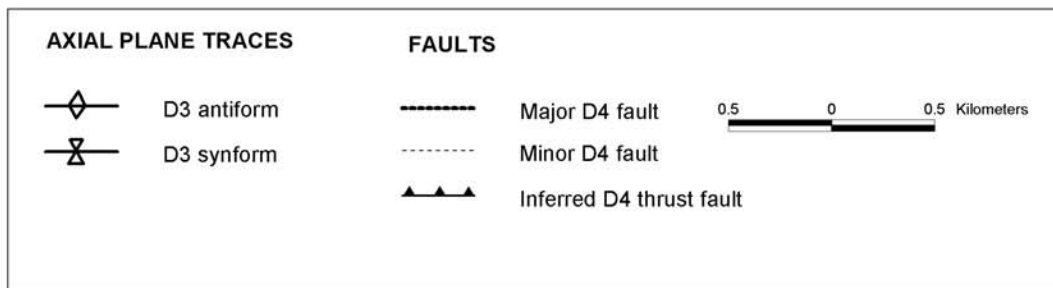
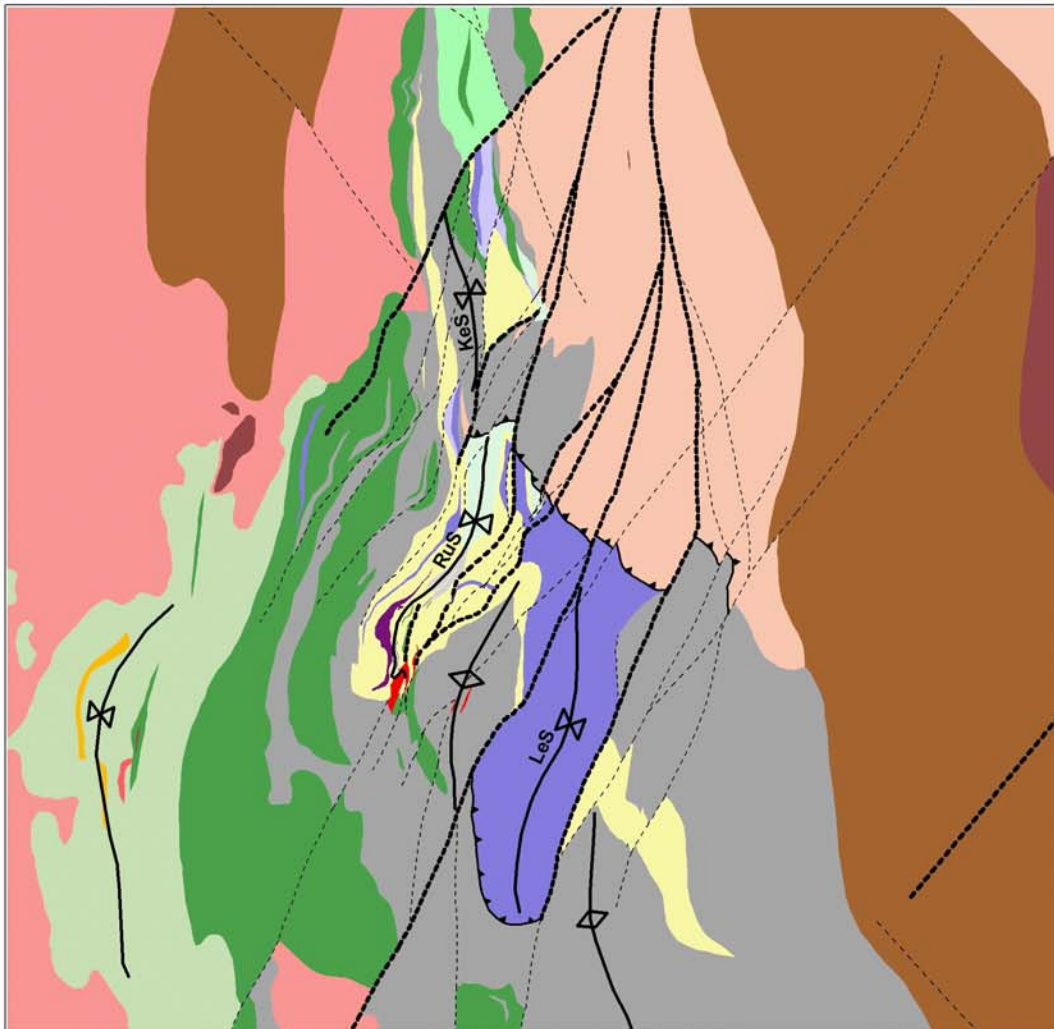


Fig. B12. Major structures of the Ruotanen area. LeS= Lehto synform, RuS= Ruotanen synform, KeS= Kettuperä synform. Lithologies as in Fig. B2.

Heikki Puustjärvi (ed.)

8.11.2006

Confidential

maximum strain has been directed towards incompetent lithologies while the competent rocks avoided the highest strains. As a result, the unaltered volcanites usually are less deformed showing even primary structures in many places. On the other hand the mica-rich altered felsic volcanites have absorbed the highest strain causing intense deformation in those lithologies. For that reason the sericite schists and the ore are situated in a tight and highly sheared fold structure while the felsic volcanites are folded more openly.

B 4.2.2 Deformation history

Primary planar structures (S_0), such as bedding in sedimentary and volcanogenic rocks, around the Pyhäsalmi mine are rather common. However, their importance remains minimal while configuring the earliest fold structures because they usually exist at separate outcrops that can't be connected. Anyhow they are informative in building paleovolcanological models. Primary bedding has been identified from some mafic pyroclastic breccias and pillow lavas. Felsic metavolcanites display a distinct banding but it is not certain if it represent primary bedding or metamorphic banding. S_0 structures in the tuffaceous sedimentary rocks (eg. Pellonpää area) have been identified from drillholes. Contrary to the earlier investigations, primary compositional zoning in the ore is strongly considered as a metamorphic feature.

Earliest deformational structures in the mine area are difficult to identify due strong and destructive later deformation. Koistinen (1983) identified an early-stage metamorphic S_1 schistosity in the vicinity of the ore deposit. F_1 fold structures were not identified from the surface but tight tongue-like parts and waste rock inclusions in the massive ore at the deeper levels of the mine were suggested to indicate D_1 deformation. Similar assumptions concerning the ore were suggested by Luukas (1992). In both of the studies F_1 structures were proposed to be formed in flat-lying position; later they were refolded to upright position. Tight-isoclinal D_1 structures were suggested to play an important role in thickening the original ore beds into thicker and economic layers. Such basic ideas on the effect of early-stage deformation remained during this project. The only exception are the tight tongue-like folds which were re-evaluated to be formed during D_4 shear.

Earlier, D_2 was considered as a major deformation stage which produced major synform-antiform structures in the mine area. On outcrops there are tight F_2 folds in which F_2 fold axis plunges south at 40-60° angle. A good example of F_2 is the fold structure in the pyroclastic breccia beside the laundry; there S_0 has been folded and felsic breccia fragments have been strongly flattened indicating S_2 schistosity. A distinct S_2 schistosity has been considered a typical feature for D_2 structures indicating a major regional-scale metamorphic event (prograde stage). For that reason, a strong schistosity parallel to the (metamorphic/primary?) banding in unaltered felsic volcanites has been considered as S_2 schistosity and a key structure in this area.

In former studies a major D_2 synform, in which the isoclinally folded (F_1) ore formed an important part, was suggested for the mine area. According to the latest interpretation this is a D_2 - D_3 interference structure strongly sheared during D_4 .

Heikki Puustjärvi (ed.)

8.11.2006

Confidential

Large-scale D_2 folds were not identified in the mine area but narrow down-plunging lithological bodies may indicate the existence of this sort of structures.

After D_2 folding the lithologies in the mine area were refolded in a more open manner forming D_3 synforms and antiforms. In meso-scale F_3 forms tight-open asymmetrical folds whose fold axis gently dips NNE in the wasterock open pit area and in the Topiskonräme area south of the former. The F_3 folds indicate that S_2 has been folded and no distinct S_3 axial plane schistosity developed; however, in the mine area a strong crenulation cleavage (S_3) developed at this stage in mica-rich lithologies. The axial plane of F_3 folds is generally upright.

Based on outcrop and drillhole data, large-scale D_3 synform-antiform structures can be modelled for the Ruotanen area (Fig. B12). Unaltered felsic volcanites form cores of two antiforms surrounded by deep D_3 synforms (the Ruotanen and Lehto synforms). The D_3 antiform, in the waste rock open pit area, is a gently NNE-plunging structure which acted as a competent block during later shearing events. The eastern Lehto synform mainly consists of cordierite-antophyllite rocks. Based on drillhole data it forms an at least 500 m deep structure. It is suggested, yet not proven, that there exists a sericite schist layer below this cordierite-antophyllite rock.

The western Ruotanen synform is a structure similar to that at Lehto. It mainly consists of altered felsic volcanites and massive ore. Knowledge of this structure is better because of intense drilling and mining operations. The Ruotanen synform is a tight structure the central part of which forms a local culmination from which the fold axes plunge south and north. South of this culmination point the synform is highly affected by D_4 -stage shearing that has caused complicated interference structures in the mine. North of the culmination point the synform becomes deeper and certain lithological units (eg. unaltered intermediate tuffaceous volcanoclastic sediments and a narrow cordierite-antophyllite rock layer) have been interpreted to form an upward-opening structure. A plausible explanation is that this synform extends to the Kettuperä area where a third synform (the Kettuperä synform) is suggested to exist. This synform consist of altered felsic volcanites on the sides and an unaltered felsic volcanite in the middle. The eastern alteration zone extends rather deep (600 m) as is the case at the Pyhäslmi mine.

As a whole, D_3 seems to be an open folding stage preceding major shearing. In regional scale, this stage can be correlated with the SE-NW-trending D_3 structures that strike along the RLZ. In the mine area, the identification of D_3 antiform revealed the existence of flat lying structures at the hinge zones. The new fold model suggests that the structures, formerly thought to be more or less vertical, can in fact be horizontal at many places. Such flat-lying structures can be modelled for the Pellonpää and Topiskonräme areas.

A structural feature conspicuous of the Ruotanen area is the intense shearing and fragmentation that occurred after D_3 folding. In the Ruotanen area, this D_4 stage (D_5 after Koistinen) seems to be a dominant deformation stage forming numerous sinistral strike slip faults, vertical shear folds and obvious thrust faults as well. The

Heikki Puustjärvi (ed.)

8.11.2006

Confidential

final mobilization of ore and the emplacement of voluminous pegmatites in the mine area are related to this stage. In lack of the suitable indicators the kinematics of this NNE-SSW-trending shearing is difficult to determine; however, the shearing is interpreted to be sinistral as based on major mainly sinistral shear folds and geophysical data. Possibly related vertical displacement is more difficult to identify. Metamorphic studies by A.-P. Tapio and T. Kilpeläinen reveal that noticeable metamorphic reactions took place during this stage.

F₄ shear folds in various scales are conspicuous of the mine. A major shear fold structure is located at the southern end of the D₂-D₃ synform. There a steeply SW-plunging (subvertical) sinistral fold can be traced at least to 1200 m depth. In sericite schists the effect of shear is seen as minor crenulated folds. The forementioned tongue-like parts in the ore are thought to have formed during this stage.

After the sinistral F₄ folding was over, deformation style changed to vertical-subvertical strike slip faulting, which can be correlated with the intense D₄ faulting along the OSZ. The geological surface map shows that numerous NNE-SSW-trending sinistral D₄ faults split the Ruotanen area into blocks. Such structures clearly preferred low-competence lithologies and approximately NNE-trending older structures. Specifically the contacts between altered and unaltered lithologies became highly sheared. Also less abundant SE-trending dextral faults have been interpreted for this area. They form a system conjugate to the NE-trending faults. Locations for these faults were inferred from drillholes, geophysical maps and geophysical interpretations.

It is plausible that thrust faults are related to these vertical strike slip faults. The most obvious place for such a thrust fault is the Ruotanen mine village area where the stratigraphically lowermost felsic volcanites (Kettuperä member) are in contact with tuffaceous sediments (Jurvansuu member) at intense NE-trending faults. Another case is that at the southern end of the Lehto synform where a D₄ thrust fault is suggested to exist.

In the mine area, voluminous pegmatite granites are related to the D₄ faulting in a manner typical for the OSZ. Such coarse-grained pegmatites are usually unsheared giving an impression that they intruded in tensional fractures after the main shearing stage was over. Voluminous fluid activity and high-grade metamorphic conditions are suggested by T. Kilpeläinen and A.-P. Tapio for this stage resulting in the formation of highly schistosed quartz-sericite schist.

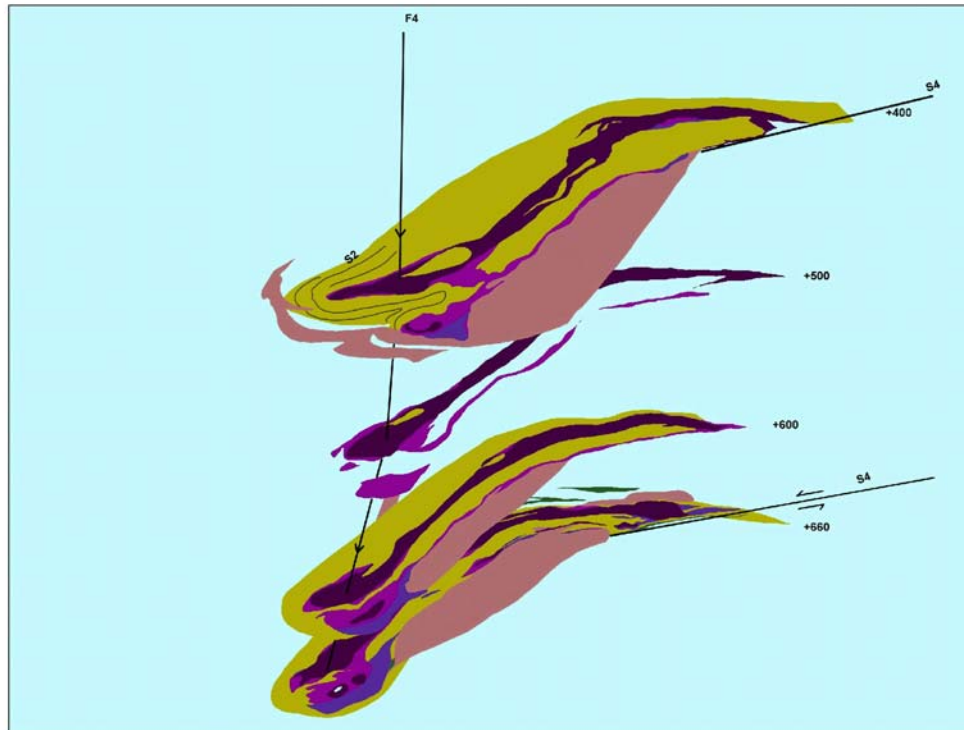


Fig. B13. A 3-D picture of the Pyhäsalmi mine (planes +400 - +660). A subvertical F4 fold axis is shown by a black arrow. A inferred sinistral D4 fault is also shown.

Such conditions are responsible for the final remobilization and recrystallization of the sulphide ore. Mine plans (+400-+660, Fig. B13) give the following impressions: On the east side of the ore there exists a D₄ fault trending NNE; the remobilization of ore forms a narrow “side ore” on the fault plane; pegmatite was emplaced at the fault plane; metamorphic alteration, caused by the thermal effect of pegmatite, transformed pyrite ore to pyrrhotite ore.

There are no age determinations for D₄, however estimations can be expressed. It is obvious that D₄ represents a retrogressive metamorphic stage that occurred after the peak of regional metamorphism 1890-1875 Ma ago. Age data for the OSZ (Kärki et al. 1995) show that granitic intrusions were emplaced 1860-1800 Ma ago thus providing broad limits for the age of D₄. There are two age determinations for titanite in the mine area; they give ages of 1830-1800 Ma. These ages can be interpreted as the metamorphic ages of D₄ stage.

It is concluded that the massive ore underwent four major deformation stages. The effect of D₁ and D₂ is difficult to estimate due to strong overprinting by D₄, however they can be considered as tight-isoclinal folding stages which greatly affected the ore. D₃ formed major synform-antiform structures in the area and refolded the massive ore into upright position. The ore got its final shape during intense D₄

Heikki Puustjärvi (ed.)

8.11.2006

Confidential

shearing. Also the remobilization of the ore, and the squeezing of the mobile ore into open spaces (eg. the deep ore), are due to D_4 shearing.

B 4.3 STRUCTURE OF THE MULLIKKORÄME MINE

Knowledge of structural features at the Mullikkoräme mine is radically smaller than that for the Pyhäsalmi mine. Detailed structural mapping has not been done at the Mullikkoräme mine. Also the structural information from surface is minimal in lack of outcrop in the vicinity of the mine. 3D-modelling for the Mullikkoräme area was done by inferring lithological boundaries adapted from drillhole data and lithological mapping in the mine. The resulting model was adjusted to the regional structural model with the few structural features seen in the mine. The 3D-model is visualized by vertical profiles (Fig. B11).

The Mullikkoräme mine is situated in a N-S-trending D_3 synform (the Mullikkoräme synform, Fig. B14) between the Kokkokangas granodiorite and the Korvenkallio granite. It can be divided into two structurally different parts. The western part of the altered volcanite zone represents a gently ($30-40^\circ$) east dipping limb of the D_3 synform. The eastern part of the altered zone, in the vicinity of the Korvenkallio granite, represents a vertical part of this synform, highly sheared during D_4 . This two-fold structure is displayed on vertical profiles X7066800 and X7066400 (Fig. B15).

Primary structures as well as the earliest deformational structures (D_1 and D_2) are sparse and difficult to interpret in the Mullikkoräme area. Younging direction can be determined from pillow lavas at Tetrinmäki and from a basic lava near the mine. The former indicates younging towards east and the latter towards southeast, however it is questionable if few observations have structural value in a polyphasically-deformed area. Down-directed tongue-like mafic volcanic lobes can be interpreted as F_2 fold structures (Fig. B15). It must be remembered that such lobes have been modelled only on the basis of drillholes. It is suggested that a strong S_2 schistosity developed at the axial planes of these folds; it is correlated with regional S_2 schistosity.

Even mesoscopic D_3 structures are sparse in the mine area. On the wall of the decline there is an observation of gently south-plunging dextral F_3 fold. There is also banded ore folded during D_3 (Fig. B16). A distinct schistosity developed at the axial plane of this fold. F_3 folds were not identified on surface.

Once D_3 folding was over, intense D_4 shearing played an important role in orienting and transposing lithologies especially in the deeper parts of the mine. Such is the case in the Pyhäsalmi mine, as well. The highest deformation concentrated at the contact between the Korvenkallio granite and the felsic volcanites that form a major D_4 fault in the mine. This fault represents the southernmost end of the Pyhäntä Fault, one of the major faults in the OSZ. This fault created highly sheared mylonitic rocks crushed into brittle pieces during later (post- D_4) movements.

Heikki Puustjärvi (ed.)

8.11.2006

Confidential

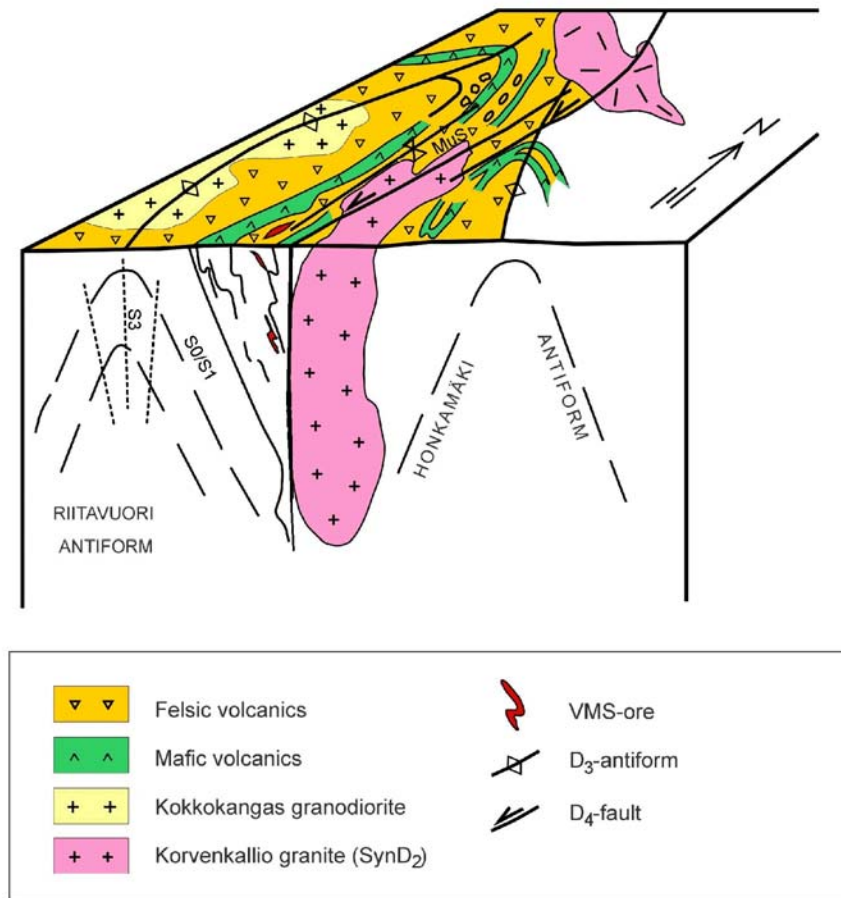


Fig. B14. The general structure of the Mullikkoräme mine area. MuS= Mullikkoräme synform.

The fault is considered to represent sinistral strike slip faults. Its western side is uplifted in relation to the eastern side. Also dextral conjugate faults exist in the area but their importance is smaller.

D_4 shearing transposed earlier structures to the direction of the major fault plane. For that reason lithologies, especially in the deeper parts of the mine, parallel the fault plane. The ore lenses (Siperia, Kharon etc.) in the deep parts of the mine are fault-controlled, their contacts are tectonic. It is possible that these small orebodies once formed a uniform body that was cut to pieces during D_4 shearing. Several minor faults are identified also in the upper parts of the mine (Fig. B15) indicating intense fault movements all over the area.

B 4.4 3D MODELING AND THE SHAPE OF THE PYHÄSALMI DEPOSIT (T.Kilpeläinen)

The objective of this part of project was to investigate structural and metamorphic patterns in the vicinity of the Ruotanen mine. The main purpose was to explain the

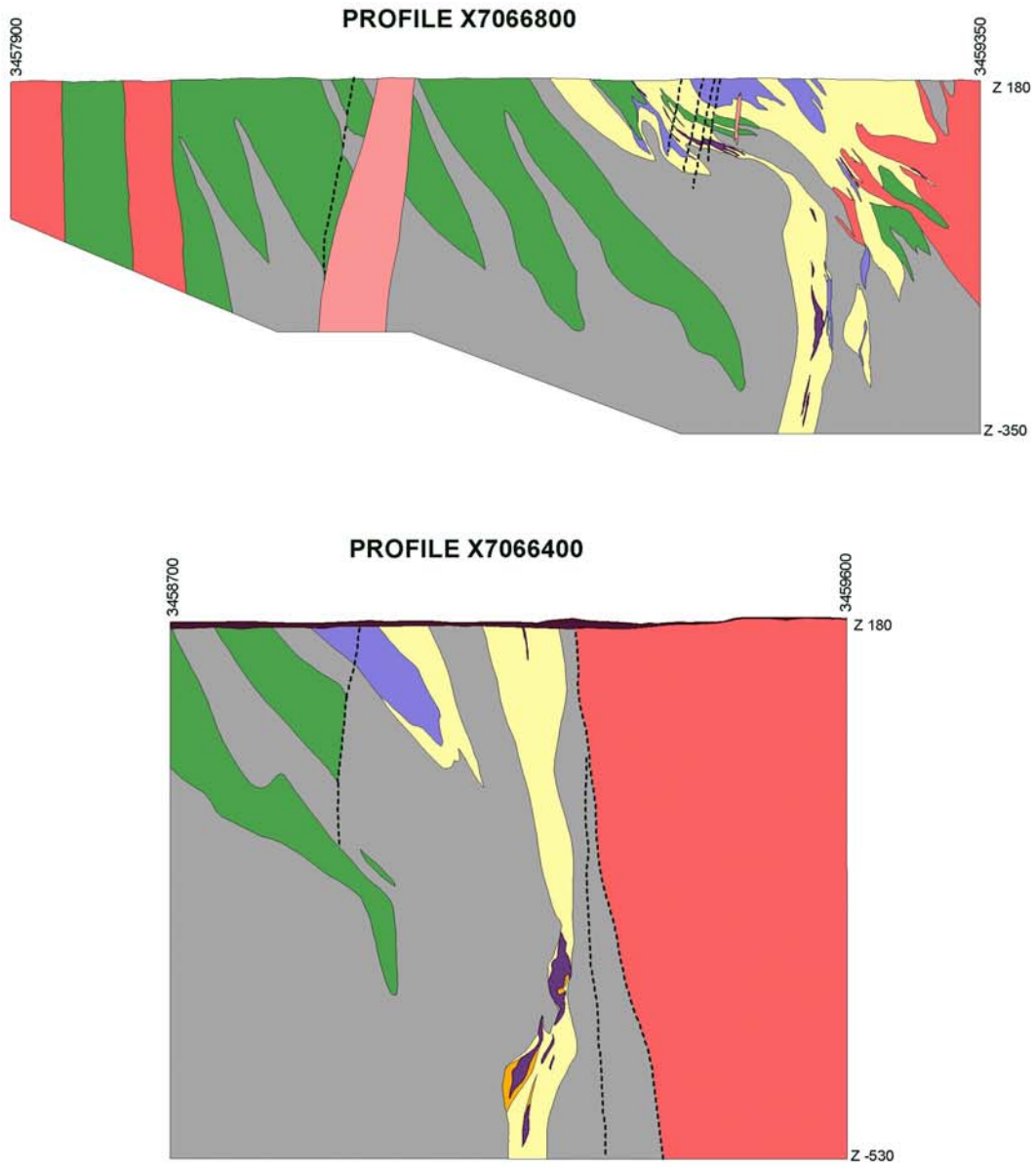


Fig. B15. Vertical profiles X7066800 and X7066400 from the Mullikkoräme mine area.

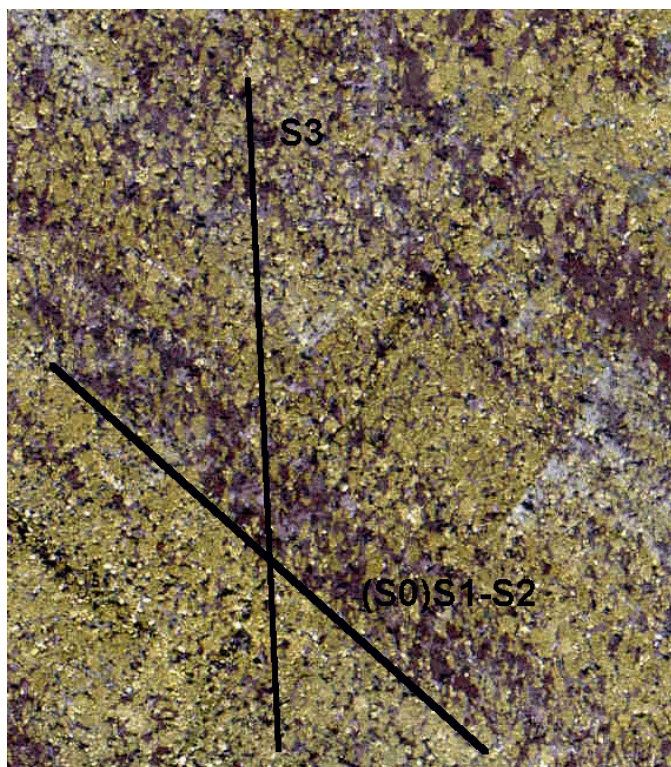


Figure B16. Mullikoräme banded sphalerite-pyrite ore looking at a vertically cut E-W sample showing a transformal S3 pyrite orientation (picture lower edge 4cm).

evolution of the current three-dimensional geometry of the Ruotanen orebody taking into account structures visible in country rocks and the metamorphic reactions connected to tectonic events.

The structural evolution of the project area is described by J. Luukas. Only the structures connected with the current topic are considered in the following. Also metamorphism is gently treated since detailed studies are reported by A-P Tapio.

B 4.4.1 Methods

The work was started with field observations in the vicinity of the Ruotanen mine, specifically at the open pit. Regional structural studies by J. Luukas and the resulting tectonic maps helped in the identification of various deformation features and the classification of structures in detail.

The 3D-modelling of the orebody was carried out by first digitizing the lithological contacts between 0-+1000 m levels in the Ruotanen mine (at 30-100 m intervals). AutoCAD software was used to connect the 3D face contacts of different levels. To simplify the 3D model, lithological contacts in the above-mentioned maps were smoothed and only the contacts between massive ore and "host rock" are shown (Fig. B17).

Heikki Puustjärvi (ed.)

8.11.2006

Confidential

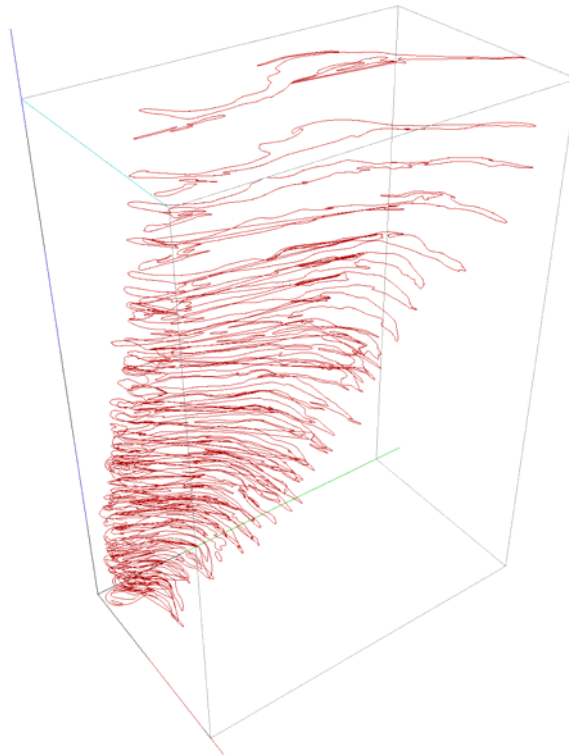


Figure B17. Pyhäsalmi ore and country rock boundary feature lines digitized for 3D-modeling on 0-1050 levels.

Similar procedure was used when constructing a regional 3D lithological map. Digitized maps used were the +0, +100, +150, +210 and +300 level lithological maps constructed by J. Luukas. The interpreted lithologies were based on mapping of outcrops, data from drillholes, and interpretations of geophysical maps. Also in such cases lithologies were simplified.

Based on the results of the above-mentioned studies an evolutionary model was constructed to explain the 3D geometry of the Ruotanen orebody. The basic idea was to compose a simplest-possible evolutionary model, which would at least explain the main structural and metamorphic features observed in the Ruotanen mine and on the outcrops nearby. One of the criteria was also that the model should be in harmony with the regional structural interpretations by J. Luukas.

B 4.4.2 Results and interpretations

B 4.4.2.1 General assumptions

It became evident that the primary structures (particularly bedding) in metavolcanites were badly destroyed by early alteration and later tectonic events. In most cases lithological contacts were tectonically disturbed. Penetrative schistosity, classified as S_4 by J. Luukas, was the dominant tectonic pattern.

The Ruotanen area is located at the central part of a broad, NNE-SSW-trending shear zone (D_4). In lack of suitable indicators the kinematics of this shearing is

Heikki Puustjärvi (ed.)

8.11.2006

Confidential

difficult to determine on outcrop. In broader scale the shearing seems to be sinistral as based on the interpretation of geophysical maps. Vertical displacement is more difficult to identify. Since the shearing is interpreted to be postmetamorphic (regional metamorphism, J. Luukas), remarkable changes in metamorphic temperature/pressure or P/T-paths (A-P. Tapio) have not been observed in the Ruotanen area. It follows that displacement can be interpreted to be horizontal at the scale of this study.

The D₄ shearing bears significance to the relative age of metamorphic reactions and S₄ schistosity (A-P. Tapio). The age of the peak metamorphism and D₄ are unclear, however most of the metamorphic reactions detected in the Ruotanen area took place during D₄. All of these reactions indicate decreasing pressure (maybe also temperature) and intense fluid activity during the shear.

Although the peak conditions of metamorphism appear high, no indications of partial melting have been found in the vicinity of the Ruotanen mine. The recognizable PT path starts at c. 600-700°C and 6-8 kb and can be follow to c. 600-650°C and 3-4 kb (A-P. Tapio). The main reactions took place syntectonically to penetrative S₄ schistosity, however some metamorphic minerals overgrow this schistosity. In other words, the main schistosity in the Ruotanen area developed under decreasing temperature/pressure and during intense fluid activity connected to D₄ shearing. Rock types generated during D₄ are exemplified by a cataclastic quartz-sericite-schist that surrounds the main part of the Ruotanen orebody.

The ages of regional metamorphism and metamorphic reactions syntectonic to D₄ are unclear. The northern part of the Svecofennian domain was largely stabilized at about 1880 Ma ago (e.g. Korsman et. al 1988), which may be the minimum age of regional metamorphism in the Ruotanen area. D₄ shearing crosscuts synkinematic intrusions 1880 Ma old. Granites or pegmatites have intruded into D₄ shear zones, but they have not been dated yet.

Seafloor alteration in the Ruotanen metavolcanites is widespread and remarkable, but the second-stage alteration discussed above is limited to separate shear zones. The reason for strong shearing can, at least partly, exist in "mechanically weak" altered volcanites themselves, however rocks that have suffered primary alteration are not always strongly sheared.

Although D₄ destroyed almost totally earlier structures (both tectonic and metamorphic), and since the current shape of the orebody is possible to explain with D₄-tectonics (this text), there's no need to explain D₁-D₃ structures and to take them into account when constructing the above-mentioned evolutionary model.

B 4.4.2.2 Evolution of the shape of the Pyhäsalmi ore deposit

Heikki Puustjärvi (ed.)

8.11.2006

Confidential

The Ruotanen orebody was strongly mobilized during D_4 shearing as evidenced by quartz-sericite schist inclusions in massive ore. Another piece of evidence is that the deepest parts of massive ore exist in unaltered hostrock.

The evolutionary model to explain the current 3D shape of Ruotanen ore body is based on the observed sinistral vergence of D_4 shearing and on the patterns indicating strong mobilization as an ore-forming process. Mobilization (enrichment) to low pressure tension gashes (en echelon) should cause an S-shaped body with long axis (on XY plane) at low angle to the direction of shear zone. Wavy arrows in Figure B18 indicate the mobilization both towards the shear zones and the opening fissure.

The pegmate pipe on the SE side of orebody was interpreted to have similar evolution and approximately the same age as the orebody.

If the model is correct, the thickest parts of the orebody should represent the oldest parts of mobilized sulphides. There should also be difference in age between the central parts of the body (older) and the zone close contacts with country rocks (younger).

The rotation axis of the S-shaped body plunges steeply SW (Fig. B13) indicating almost horizontal shearing during D_4 . This is in consistence with the interpretation based on metamorphic studies. The amount of horizontal displacement is unclear, but since the orebody still exists close to altered metavolcanites, the flow of sulphides seems to have happened mainly in local scale.

B 4.4.2.3 3D-lithology and 3D-structures in the Ruotanen area

The three-dimensional visualisation of lithology and structural patterns started with mapping of outcrops and continued with data collecting from drillholes. The continuation of lithologies below erosion level was interpreted also from geophysical maps. This part of work was made by J. Luukas.

Small amounts of data compel one to simplify lithology and structures. Data decrease fast downwards, and the precision with which the maps were drawn reflects data available between +0 and +300 m levels.

The techniques used for the interpretation of lithologies from level to level allowed one to connect lithological contacts with 3D faces in the final modelling stage. Shears observed on outcrops and in drillcore were impossible to connect between levels. It follows that shears were presented separately on each level in the 3D map. The shears appear as vertical, 40 m high "fences". The way of presentation is not absolutely correct, however it gives an impression of a complex shear system, which is in harmony with outcrop observations related interpretation (Fig. B19).

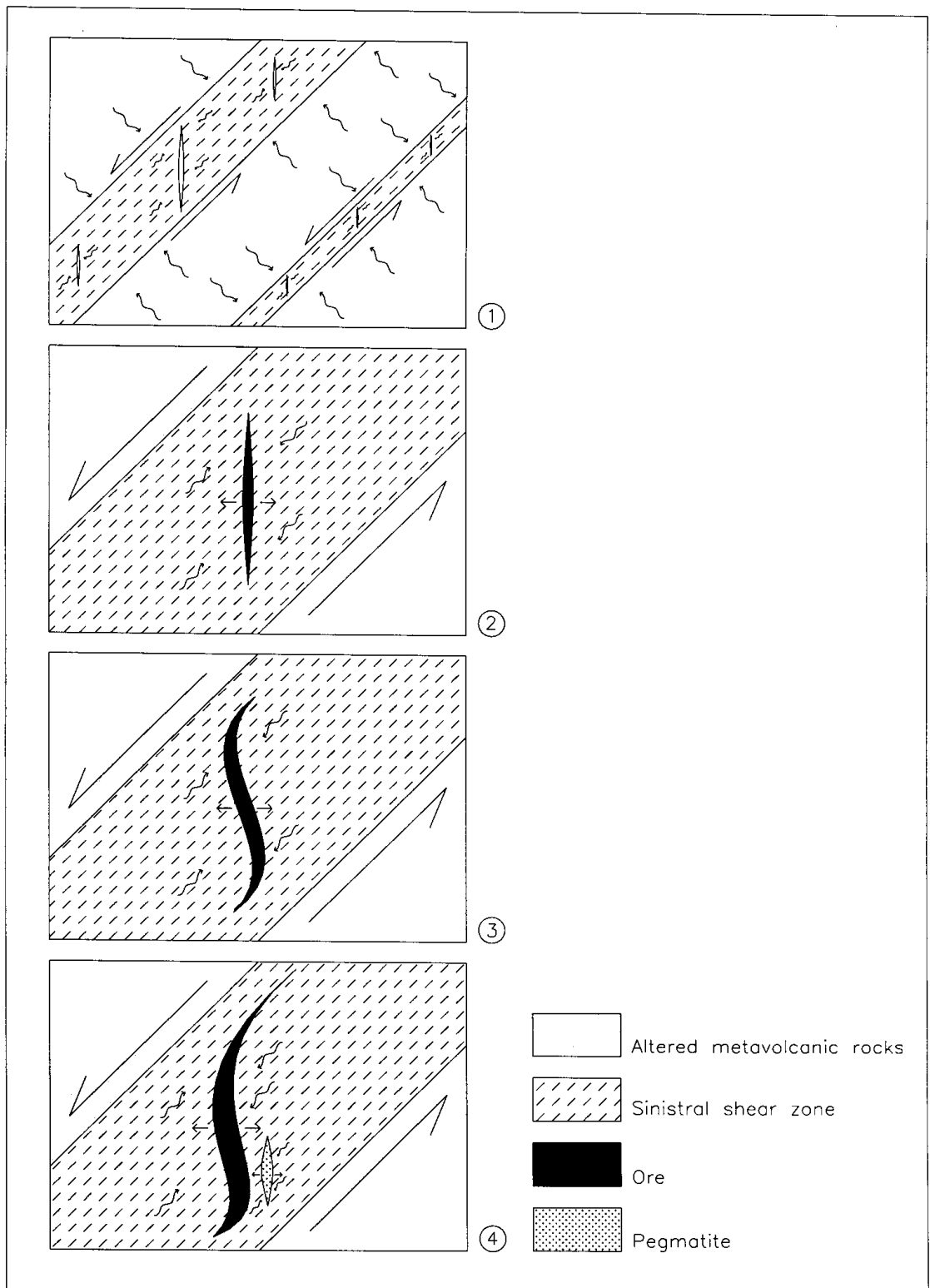


Figure B18. Tectonic evolution model of the Pyhäsalmi ore and the mine pegmatite intrusion during the sinistral D4-shearing.

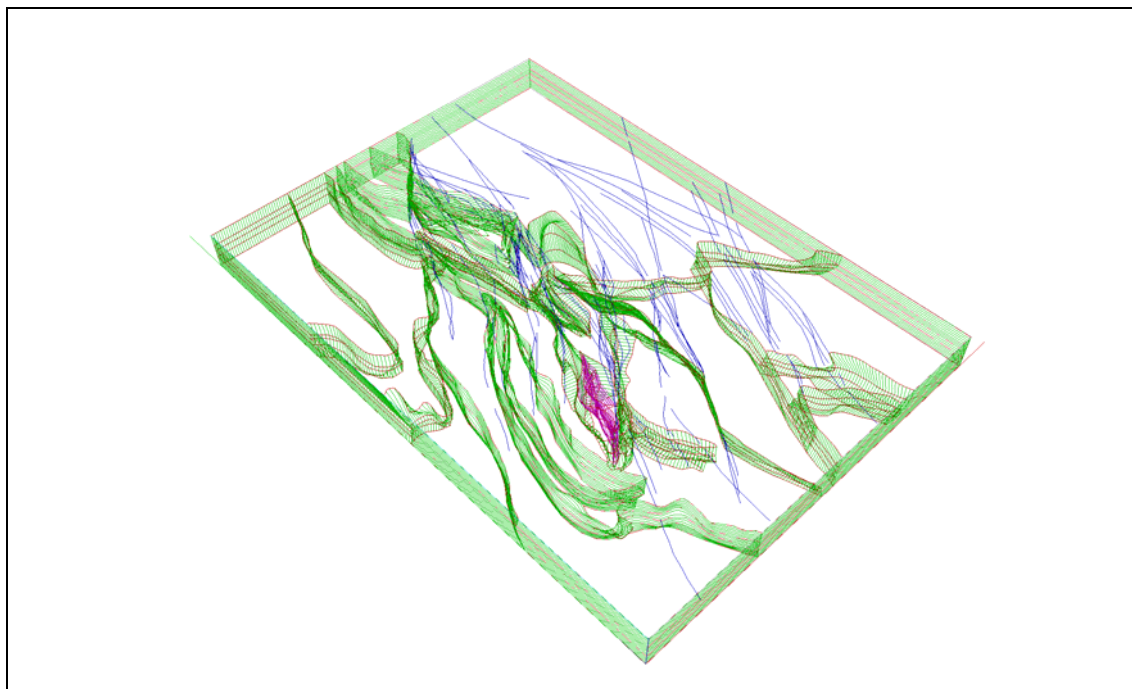


Figure B19. 3D-wire model (looking from +45 degr. SW) of 0-300 plan lithological boundaries (green) in relation to the Pyhäsalmi ore deposit (magenta) and D4-shears (blue).

The sense of shears (e.g. displacement of lithological contacts) was presented on the 3D map only in places. It is not possible to determine movement directions from unoriented drillcore and outcrops lacking kinematic indicators. As a whole, the shearings marked on the 3D map must be read as a sinistral, complex shear system, where local movement directions can vary.

B 4.4.3 Conclusions

The evolution of the Ruotanen orebody was interpreted to be syn-D₄-mobilized. However, the deposit is still located close to altered metavolcanite host. It means that the distance of mobilization was relatively short. From the structural point of view it is impossible to conclude whether the ore was massive or disseminated before the latest mobilization.

The evolution of the Ruotanen orebody resembles that of the Hallaperä deposit (Matti Pajunen, unpublished). In both of the cases mobilization continued during decreasing temperature and pressure, but the conditions during peak metamorphism were possibly different. Rocks surrounding the Hallaperä deposit are migmatized garnet-cordierite-sillimanite gneisses, while no evidence of partial melting was found at Ruotanen.

Enough structural data do not exist to allow the modelling of evolution for the Mullikkoräme deposit. Lithologically, the Ruotanen and Mullikkoräme deposits resemble each other, but the grade of regional metamorphism was possibly lower at Mullikkoräme. There temperature did not reached the mobility area of sulphides, consequently no enrichment took place during the retrograde stage.

Heikki Puustjärvi (ed.)

8.11.2006

Confidential

The exploration of similar shear-related, mobilized sulphides should contain careful primary structural and metamorphic studies. The D₄ shearing discussed here represents only a minor part of the huge shear system described by J. Luukas. Such late- to postmetamorphic shears divide the Svecofennian Savo Schist Belt to separate blocks. Each of the blocks display metamorphic characteristics of their own. Some of them contain minor ore deposits, which have not been studied from metamorphic and structural point of view. It may be possible to find similarities or rules that connect such deposits and at the same time provide ideas on how to classify areas critical for "tectonometamorphic, mobilized ores".

B 4.5 METAMORPHIC EVOLUTION IN THE RUOTANEN AREA (A-P. Tapio)

This study had the following purposes: to define the pressure-temperature evolution of the host rocks of Pyhäsalmi mine (the Ruotanen schist belt), to compare the P-T conditions within mica schists further away, to find out whether the entire research area (the Korppinen block) has a similar metamorphic history - or were the rocks in the Ruotanen schist belt metamorphosed under different conditions (Hölttä 1988, Marttila 1993). The study also aimed to test a new empirical hornblende geothermobarometer developed by T. Gerya (1997).

B 4.5.1 Previous studies

Pressure-temperature conditions in the Korppinen block, which also includes the Pyhäsalmi 1:100,000 map sheet, were previously studied by Hölttä (1988). Using the garnet-biotite geothermometer, garnet-cordierite-sillimanite-quartz geothermobarometer and garnet-plagioclase-sillimanite-quartz geobarometer in mica schists and gneisses, pressures of 5-6 kbars and temperatures of 650-700 °C were obtained for the culmination of metamorphism. Metamorphic conditions adjacent to the mine were not previously studied.

B 4.5.2 Sampling and investigation methods

Samples were collected from garnet and cordierite-sillimanite-bearing migmatized mica schists around Lake Pyhäjärvi and from amphibolites (mafic volcanites), cordierite-sillimanite mica schists (altered acid volcanites) and (garnet-)cordierite-orthoamphibole rocks (altered mafic volcanites) adjacent to the Pyhäsalmi S-Cu-Zn mine. Samples from mica schists around Lake Pyhäjärvi were collected from outcrops using a minidrill. Samples close to the mine originate from Outokumpu Mining Oy's older diamond drill cores.

Polished thin sections were prepared from all the new samples (60 thin sections in all) and also used were some 250 thin sections previously prepared at Pyhäsalmi mine. 40 whole rock samples were analysed with XRF at GTK in Espoo and 445 electron microprobe analyses on selected minerals were also carried out at GTK.

Heikki Puustjärvi (ed.)

8.11.2006

Confidential

B 4.5.3 Lithologies

B 4.5.3.1 Metapelites around Lake Pyhäjärvi

Samples from migmatized mica schists around Lake Pyhäjärvi contain either sillimanite and cordierite porphyroblasts in a biotite-quartz-plagioclase-K-feldspar matrix or garnet porphyroblasts in a biotite-quartz-plagioclase matrix. There are some accessory opaque minerals and apatite, chlorite (secondary after biotite) and sericite (after plagioclase) in both rock types. Some of the garnet-bearing rocks contain substantial amounts of hornblende.

B 4.5.3.2 The Ruotanen formation

Quartz-rich quartz-feldspar porphyries have been considered to represent unaltered acid volcanites in the Pyhäsalmi area. They mainly consist of fine-grained quartz and feldspars, larger rounded quartz phenocrysts and more angular feldspar phenocrysts. There are some sulphides in these rocks, but almost no micas.

The alteration in these is considered to be due to great amounts of fluid going through the rock. Sulphides probably precipitated from the fluids on an ancient sea floor. These fluids metasomatized the volcanites and changed their composition by leaching CaO and Na₂O from the rock and by adding MgO and K₂O. The altered acid volcanites are schistose quartz-rich rocks, which contain large amounts of muscovite and/or biotite, some albitic plagioclase and varying amounts of sulphides. Many of the rocks also contain cordierite and/or fibrolitic sillimanite. The effect of fluids is evident when comparing the mineralogies of unaltered and altered acid volcanites. Amphibolites (Fig. B20/2) in this study are considered to represent the "unaltered" mafic volcanites of the study area. They consist mainly of hornblende and plagioclase with some quartz, secondary biotite after hornblende, and locally epidote.

Altered mafic volcanites are usually quite coarse-grained orthoamphibole-biotite-, biotite-orthoamphibole-cordierite-, biotite-orthoamphibole-garnet-, biotite-cordierite-garnet- and sillimanite-cordierite-orthoamphibole-rocks with varying amounts of plagioclase, some sulphides and sometimes quartz in the matrix with biotite.

B 4.5.4 P-T-conditions

All thin sections were properly studied and metamorphic mineral reactions were recognized. Subsequently selected minerals were analysed with an electron microprobe and using all these data, with the help of Bermans (1988, 1990, 1991) TWEEQU-program v. 2.0 and Geryas (1997) GeoPath-program v. 1.2, it was possible to construct part of the pressure-temperature-path for rocks adjacent to the mine. For the mica schists surrounding the mine area it was not possible to construct a P-T-path because of the lack of adequate index minerals.

B 4.5.4.1 Metapelites around Lake Pyhäjärvi

Heikki Puustjärvi (ed.)

8.11.2006

Confidential

The old estimate of pressure and temperature by Hölttä (1988) is 5-6 kbars and 650-700 °C. There has been partial melting (migmatized pelites) and sillimanite is stable. Garnet-biotite geothermometer gives temperatures from 560 to 730 °C but new pressure estimate was not obtained.

B 4.5.4.2 Rocks adjacent to Pyhäsalmi mine

Reactions in altered acid volcanites:

- $\text{Phl} + \text{Q} + \text{St} = \text{S} + \text{Cd} + \text{Ann} + \text{V}$ (Fig. B20/3)
- inclusions in cordierite: staurolite (has quartz inclusions), quartz
- $\text{Bt} + \text{S} + \text{Q} + \text{V} = \text{Cd} + \text{Ms}$ (Fig. B20/4)
- inclusions in cordierite: biotite, quartz and sillimanite
- muscovite porphyroblasts overgrowing fibrolite aggregates
- Growth of Zn-spinel (gahnite)
- gahnite inclusions exist in cordierite but gahnite probably was not a reacting phase

Reactions in altered mafic volcanites:

- $\text{Oam} + \text{S} + \text{Q} = \text{Cd} + \text{V}$ (Fig. B20/5)
- anthophyllite and fibrolite inclusions in cordierite
- $\text{Oam} + \text{St} + \text{Q} = \text{Cd} + \text{V}$ (Fig. B20/6) and $\text{Oam} + \text{St} + \text{Q} = \text{Cd} + \text{Gt} + \text{V}$ (Fig. B20/7)
- garnet and cordierite porphyroblasts in biotite-plagioclase matrix,
- inclusions in cordierite: quartz, biotite, orthoamphibole and staurolite
- inclusions in garnet: quartz, biotite and staurolite
- $\text{Gt} + \text{Q} + \text{V} = \text{Cd} + \text{Oam}$ (Fig. B20/8)
- inclusions in cordierite: biotite, quartz and garnet
- orthoamphibole growing at the margins of cordierite and on the matrix
- cordierite pseudomorphs after garnet
- Growth of Zn-spinel (gahnite)
- there are some gahnite inclusions in cordierite, but gahnite probably

Heikki Puustjärvi (ed.)

8.11.2006

Confidential



Fig. 2. Hornblende rich amphibolite (the width of the photograph approx. 3.3 mm).

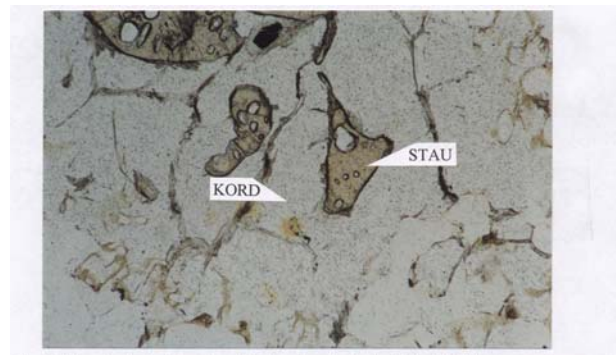


Fig. 3. Zincian staurolite inclusions in cordierite in an altered acid volcanic (the width of the photograph approx. 1.3 mm).

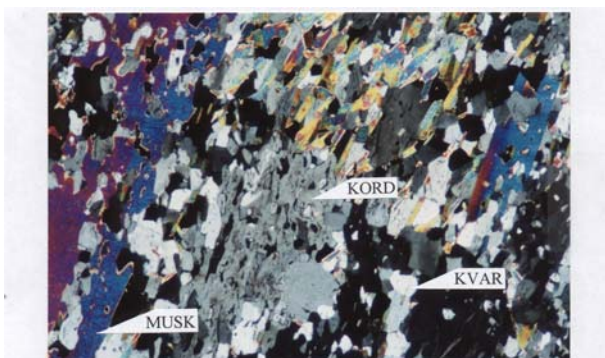


Fig. 4. Cordierite bearing altered acid volcanic. Muscovite porphyroblasts and fibrolitic sillimanite inclusions in cordierite (the width of the photograph approx. 3.3 mm).

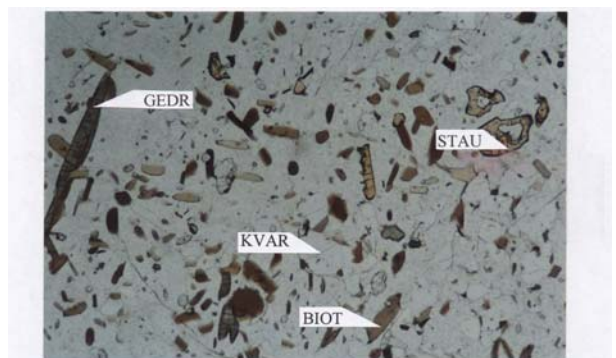


Fig. 5. Anthophyllite and fibrolite inclusions in cordierite porphyroblast (the width of the photograph approx. 3.3 mm).

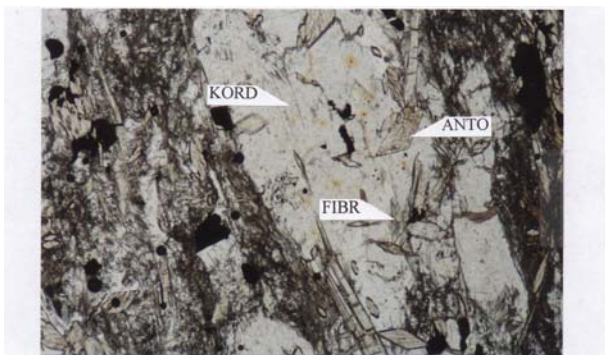


Fig. 6. Quartz, biotite, staurolite and gedrite inclusions in cordierite porphyroblast (the width of the photograph approx. 3.3 mm).

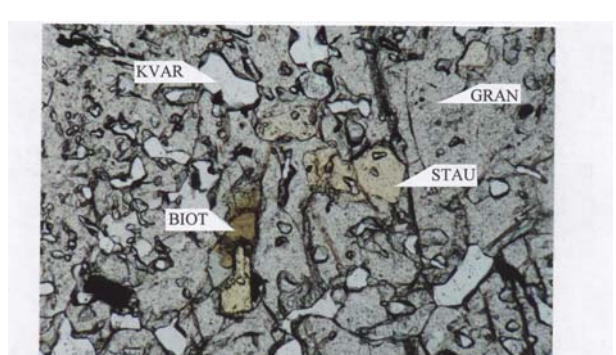


Fig. 7. Quartz, staurolite and biotite inclusions in almandine garnet (the width of the photograph approx. 1.3 mm).

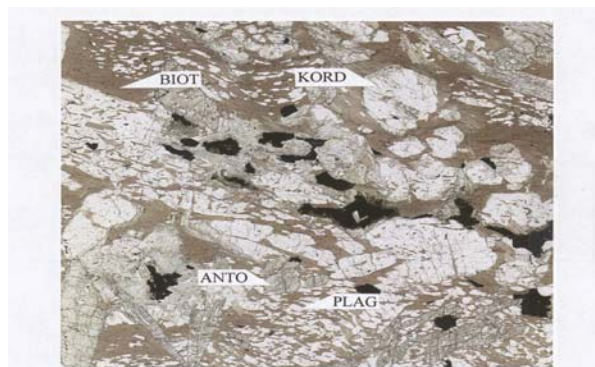


Fig. 8. Cordierite pseudomorphs after garnet in a cordierite - anthophyllite rock (the width of the photograph approx. 15 mm).

Figure B20. Series of thin section mineral paragenesis examples of metamorphic reactions from Pyhäsalmi.

Heikki Puustjärvi (ed.)

8.11.2006

Confidential

B 4.5.5 GeoPath-program

T. Geryas (1997) developed an empirical geothermobarometer for rocks mainly consisting of hornblende and plagioclase (+quartz). Using GEOPATH-program v.2.01 with amphibolites the thermobarometer gives a nice trend from approximately 4.3 kbars and 620°C to 2.5 kbar and 530°C, which is very reasonable compared with the other results (Fig. B21).

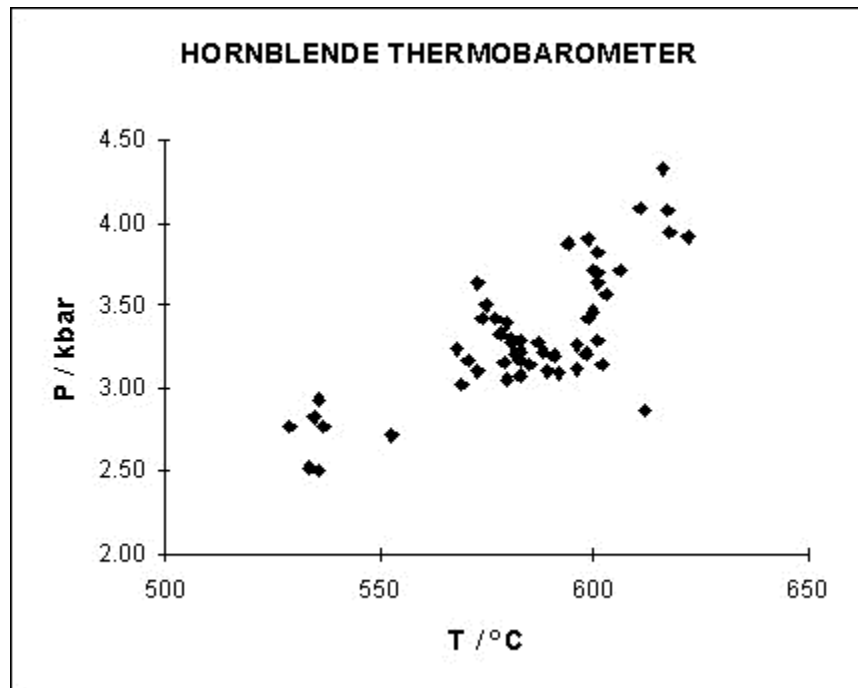


Figure B21. Diagram of the Geryas hornblende thermobarometer results from Pyhäsalmi samples.

B 4.5.6 Summary of P-T-path

In the Pyhäsalmi mine area, the highest metamorphic conditions obtained are around 600-700°C and 5-7 kbar (the assemblage Oam+S+Q in the altered acid volcanites) and the lowest P-T conditions around 530°C and 2.5 kbar (the hornblende geothermobarometer). There is no evidence of higher metamorphic grade, no partial melting or evidence of crossing the $Ms+Q = Kfs+Al_2SiO_5+V$ isograd (higher temperature) nor any relics of kyanite grains (higher pressure, Fig. B22).

There is significant partial melting in the mica schist of Korppinen block (metamorphic block enclosing Pyhäsalmi) and the pressure and temperature of the culmination of metamorphism are 5-6 kbars and 650-700°C.

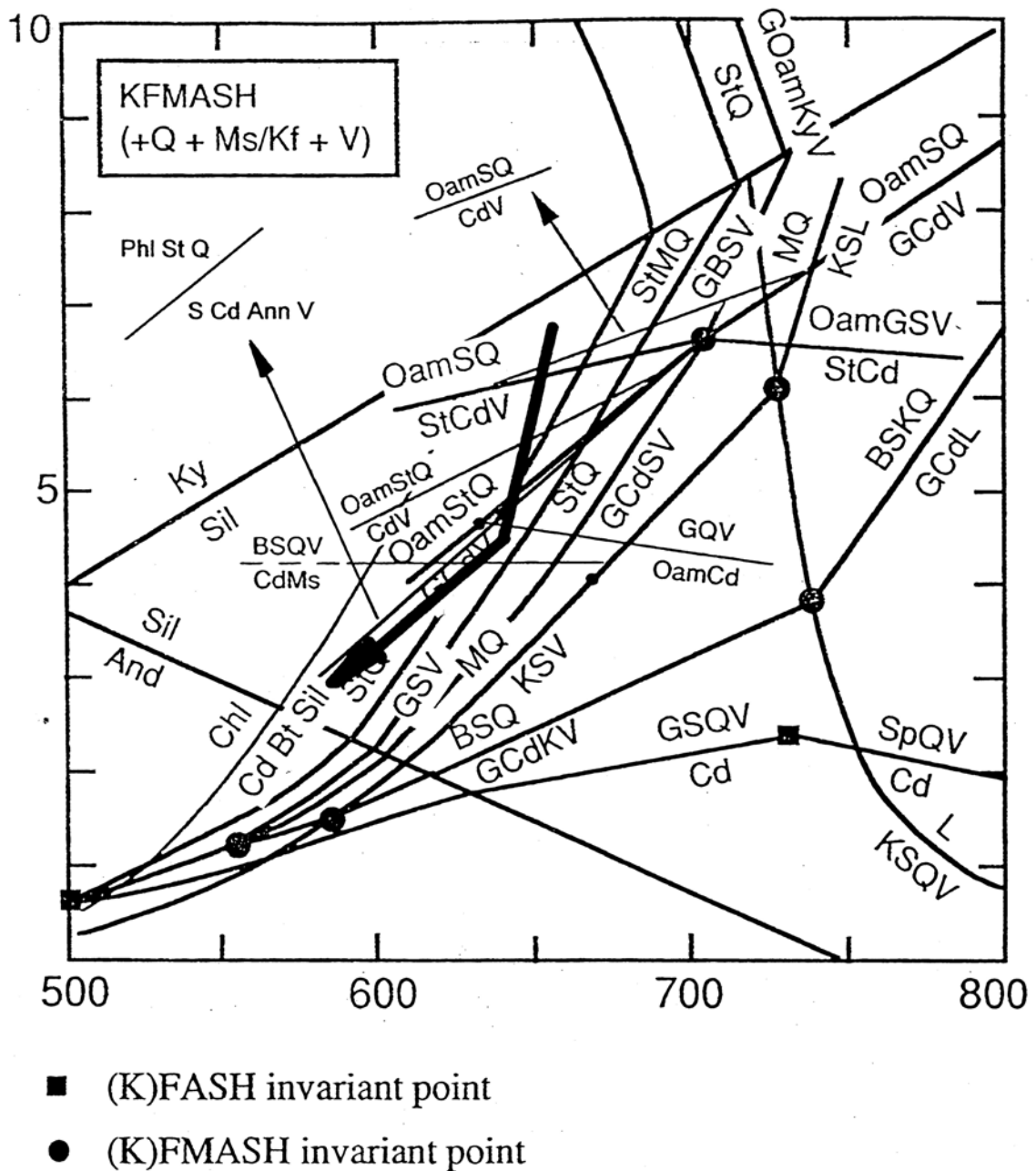


Figure B22. KFMASH-system phase diagram showing the recognized metamorphic reactions and the discovered part of the P-T path (modified after Spear 1995).

B 4.5.7 Conclusions

Geryas hornblende geothermobarometer seems to give reasonable results in this area. In the future it would be useful to try this method with amphibolites at Mullikkoräme, the satellite ore deposit 7 km NE of Pyhäsalmi mine, where the metamorphic conditions have been estimated to be lower than in Pyhäsalmi but no comprehensive metamorphic studies have yet been carried out.

Heikki Puustjärvi (ed.)

8.11.2006

Confidential

There is probably a difference between the peak metamorphic conditions in the Pyhäsalmi mine area (Ruotanen schist belt) and the surrounding mica schists (Korppinen block). Mica schists have been migmatized but in the mine area there is no evidence for partial melting, so the temperature in the surroundings seems to have exceeded that in the mine area. The peak pressure conditions are similar. One explanation is that the peak conditions have been the same in the whole area, but that there has been a very pervasive flux of fluids going through the rocks in the mine area after the peak conditions. This could have totally destroyed all the features of higher-grade metamorphism. Other possibility is that the mine represents a lower-T domain, which could be explained by tectonic movements post-dating metamorphism (Kriegsman, personal communication, March 1999).

Heikki Puustjärvi (ed.)

8.11.2006

Confidential

Fieldwork for the paleovolcanological part was done during four weeks in September 1997. The author has also worked in the same area for about two weeks 12 years earlier and visited the area during several excursions after that. In the field season 1997 at Ruotanen area there were several outcrops cleaned and mapped in detail by A-P Tapio and Jouni Luukas. These and also a selected number of other interesting outcrops around Ruotanen and Mullikkoräme were reviewed (see B2.2 and B5.1).

A total of 91 samples was collected. Sample size was about 0.5 to 1 kg. They were taken in most cases by minidrill. Hammer was used in places where it was possible to take a fresh and homogenous piece of rock. The idea of sampling was to take as unaltered pieces as possible from outcrops where the rock shows real volcanic character or structure. 85 samples were selected for analyses. Each sample was analysed at the chemistry laboratory of GTK, Espoo, using both whole-rock XRF and ICP-MS techniques. The XRF analyses were made by using both powder brickets and melted prepreparates to check if there is any difference of the results between these two methods. 42 samples were selected for the thin section study made by the author. The summary of the original observations from the outcrops, thin sections and the results of the chemical analyses are all presented in one Excel workbook, each in a unique table (MS Excel 5 format). The analytical data was handled and the plots printed by using the Minpet for Windows Version 2.02 software.

On the course of the modelling project six rock samples were also collected for age determination, four of them from the Pyhäsalmi mine area and two from the Mullikkoräme mine. The analyses were made by the laboratory of isotope geology at GTK, Espoo.

B 5.1 PALEOVOLCANOLOGICAL FIELD OBSERVATIONS

B 5.1.1 Ruotanen formation Mukurinperä member

All of the mafic metavolcanites in the Ruotanen area are considered here to belong into a single unit, the Mukurinperä member, although in practice there must be much more eruption events indicating more complicated nature and history for the Ruotanen formation. Outcrops are sparse and the composition of mafic metavolcanites do not display remarkable differences to allow more detailed conclusion about them.

About 1 km SW from the Pyhäsalmi mine, at Mukurinperä, there occur weakly deformed pillow lavas belonging to the heterogeneous Ruotanen schist zone. They are basaltic andesites by composition. The pillows are 10-50 cm in diameter and their 1-2 cm thick chilled margins can be readily discerned in spite of metamorphism. The interstices between pillows and often the pillow centers are pale green and corroded. The interstitial material contains some disseminated pyrite.

Heikki Puustjärvi (ed.)

8.11.2006

Confidential

Best-preserved pillow lavas of the Mukurinperä member are exposed on the shoreline of Lake Pyhäjärvi (Vanhainkoti) about 2 km SW of the mine. These lavas are highly vesicular and slightly flattened in N-S direction but still indicate nicely younging direction westwards like also the Mukurinperä pillow lava. Vesicles in the Vanhainkoti pillow lavas are concentrically oriented and filled with carbonate which differs these lavas from the other pillow lavas of both Ruotanen and Mullikkoräme formations.

A basaltic lava in a railroad cut c. 300 m N of the Pyhäsalmi open pit reflects also some weak features of pillow structures with albite-filled small amygdules. The pillows are highly deformed into long ribbons or lenses, and metamorphosed to amphibolite with oligoclasic plagioclase and hornblende as the main constituents and minor kummingtonite, biotite and quartz. The origin of an other amphibolite outcrop (Pesulankallio) c. 200 m N of the previous with highly deformed fragmentary structure has been an object of discussions for a long time. In common it has been proposed to be a pyroclastic breccia, but the other explanation could be an isolated pillow breccia resembling those structures observed in Tetrinmäki member lavas. This could explain the monotonous composition of those felsic fragments that in this case should represent deformed remnants of the original inter-pillow altered hyaloclastic matrix. Further, if we connect this with the former railroad cut pillow lava, it is possible to think these breccias as stratigraphically upper part of pillow lava flow indicating younging direction to northwest.

One depositional contact between felsic quartz porphyry of the Lippikylä member and mafic lava of the Mukurinperä member has been observed in an outcrop c. 300 m west of the open pit in a road cut. The contact between these two units is sharp and seems to be only very slightly affected by deformation. The mafic metalava here is massive but show some flow bottom breccia and westwards curving interflow lobe contacts probably indicating younging direction of this flow.

Other mafic metavolcanites included to the Mukurinperä member have been found only in few places about 2 to 3 km south and southeast of the Pyhäsalmi mine at Saapaskoski and Soidinmäki areas. These mafics are slightly schistose but show also sometimes elongated pillow-like forms indicated from epidotised rims or cavity fills. One polymictic pyroclastic or redeposited volcanic breccia outcrop has also been found among the Saapaskoski mafics.

In the close vicinity of the ore south of the Pyhäsalmi open pit there exists a definite type volcanic breccia of pyroclastic origin ("the hyppykuppakivi"), also included to the Mukurinperä member. In spite of high deformation and folding there can still be observed a diffuse roughly east-west-trending layering but no sign of younging direction. The rock is matrix-supported having mainly rounded felsic quartz porphyry fragments of lapilli to block size up c. 30 cm. The matrix has basaltic-andesitic composition with oligoclasic plagioclase, hornblende and biotite as the main constituents. Felsic fragments have the same composition than quartz porphyritic rhyolites of the Lippikylä member giving the idea that these mafic layer, and thus the Mukurinperä member, is younger than the Lippikylä member.

Heikki Puustjärvi (ed.)

8.11.2006

Confidential

B 5.1.2 Mullikkoräme formation Riitavuori member

Felsic volcanoclastic rocks are exposed on few outcrops west of the Tetrinmäki mafic lava member. The rhyolitic and rhyodacitic metavolcanites of the Riitavuori member (Figs. B3 and B7) are separated by a sharp, slightly deformed contact (seen only at two outcrops) from the eastern mafic lavas of the Tetrinmäki member. The pyroclastic material contains intercalations of lava-like rhyolitic quartz porphyry and rhyodasitic volcanic breccia.

At least four different types of felsic metavolcanites can be identified in the Riitavuori member based mainly on their chemical composition and also on some primary structural features observed from outcrops (Plate B7). At the hill Riitavuori all of these can be observed although the contacts remain covered by overburden. The layering in the Riitavuori area is proposed to be in N-S direction. The westernmost layer is obviously few tens of meters thick, a high-silica, quartz-porphyrific, sodium-rich rhyolite, which has been dated as 1921 Ma (Kousa et al. 1994). The phenocrysts of the quartz porphyry are 1-2 mm in size. Main constituents of the matrix are albitic plagioclase, quartz and biotite. Especially near the contact of the Kokkokangas granodiorite plagioclase becomes coarser and patchy because of its microcline content. This type of quartz porphyric metavolcanite has also been observed on one outcrop in Tetrinmäki, northern part of the study area, near the contact of Tetrinmäki member mafic lavas.

The second major unit in Riitavuori is c. 20-30 m thick rhyodasitic breccia east of the quartz porphyry. The mineral composition is albitic/oligoclastic plagioclase and quartz with minor hornblende and biotite. Accessory constituents are epidote, titanite, muscovite and carbonate. This breccia has its counterpart around Tulineva c. 1 km N of Riitavuori (Fig. B7). Felsic metavolcanites on the west side of Tulineva differ from those of Riitavuori having clear matrix-supported breccia structure with some remarkable big elongated and rounded clasts of the same rhyodacitic mineralogical and chemical composition than the matrix. The main constituents of this rocktype are oligoclastic plagioclase, quartz and biotite with some hornblende and potassium feldspar.

The third felsic unit in the Riitavuori member was observed in an outcrop made by tractor excavator on the NE side of the hill Riitavuori. It can be traced further at least 1.5 km NE to Heikinaho. This unit is indicated in Heikinaho by coarse breccia fragments in slightly quartz- and plagioclase-phyric felsic matrix. In Riitavuori the rock is more homogenous without any breccia structure. The main reason to include the rocks of these separate outcrops rather far away with each other into the same unit is their rather similar chemistry (Plates B8 and B1).

The fourth felsic unit in the Riitavuori member is seen only in a small excavated outcrop NE of the hill Riitavuori. This rhyolitic or even trachyandesitic (Plate B8, Mf4) rock has rather high Zr content and thus resembles the rhyolite (drillhole Pyo/Mu-116) on the eastern side of the felsic formation near the Mullikkoräme mine.

Heikki Puustjärvi (ed.)

8.11.2006

Confidential

Numerous N-S-orientated uralite and plagioclase porphyrite veins and amphibolitic dikes cut the rock and exhibit sharp contacts.

B 5.1.3 Mullikkoräme formation Tetrinmäki member

The Tetrinmäki member is composed of mafic lavas and lava breccias with occasionally well-preserved pillow structures. Such is the case especially in the northern part of the map area of this about 5 km long and up to 700 m wide N-S-striking zone (Fig. B7 and Plate B8). Outcrops belonging to this member are sparse and thus the continuation of an individual bed or flow is impossible to reconstruct. The contact between the Tetrinmäki and Riitavuori members can be seen only in two outcrops - one in the N part of Tetrinmäki and the other at Parviaisaho few hundred meters north of the Mullikkoräme mine. The contact in both cases can be proposed as depositional although a slight schistosity makes the definite determination uncertain. In both cases the lowest bed of the Tetrinmäki member consists of massive mafic lava with few felsic blocks 10 to appr. 50 cm in diameter originating from the Riitavuori member.

At Tetrinmäki the pillow lava is well exposed only in a rather small area where it makes a single flow unit with maximum thickness up to 50 m. This pillow lava bed is both underlain and covered by lava breccia layers consisting mostly of pillow fragments. High vesicularity of both pillow lava and lava breccia is evident indicating rapid or explosive gas escaping from the lava. These vesicles are now filled with epidote and frequently albite. Concentric and sometimes also radial cooling joints can still be recognised in many individual pillows as rims rich in epidote. In the lava bed pillows are rather tightly packed while the pillow breccias are hyaloclastite matrix-supported where the matrix is composed mainly of epidote and albite. The well-preserved pillows indicate younging direction of the lava bed clearly eastwards.

On the N part of the pillowed bed pillows are large and well-defined of about 20 cm to 2 m in diameter. Their size decreases eastwards and southwards and pillow breccias become more common. The breccias contain abundant yellowish-green fragments rich in epidote and the interstices are filled by hyaloclastic material. In the S part of the zone the lavas are dark green and massive, containing yellowish-green epidote segregations and amygdules. The Tetrinmäki pillow lavas are basalts and basaltic andesites. The main minerals are hornblende, epidote and variable amounts of plagioclase, which is clearly less abundant than the other two. Titanite and locally sulphides are the common accessory minerals.

Both the pillows and the breccias are cut by a dense swarm of mafic and intermediate dykes (Koivula, 1987). Their contact to the lavas is sharp, very often dark, fine-grained and massive. The strike of the dykes varies from N-S to NNW-SSE.

Southern part of the Tetrinmäki member can be observed in a few separate outcrops in the Mullikkoräme mine area and north of it around Parviaisaho. In an

Heikki Puustjärvi (ed.)

8.11.2006

Confidential

excavated outcrop there is seen a c. 100 m long east west trending section from the Riitavuori member rhyolite to obviously lower mafic metalavas of the Tetrinmäki member. At least six mafic flow units can be distinguished. Within the westernmost lava bed at the contact with the rhyolite there is a block-size rounded quartz porphyry fragment originating from the Riitavuori member. In this case younging direction can be proposed to be southeastwards. The three lowest lava beds about 10 to 30 m in thickness observed here have a massive bottom and pillowed top part.

The other outcrops in the Parvaisaho area display mainly massive mafic metalavas with in places well-preserved flow breccia and amygdaloidal structures. Epidotization and chloritization are very typical features in Parvaisaho mafics indicating at least quite low metamorphic grade or even primary alteration event. The mafic massive lava outcrop around the entrance tunnel of the Mullikkoräme mine has an amygdaloidal structure. This lava also displays large tube or pillow-like structures few metres in diameter indicating quite proximal nature of this flow.

B 5. 2 TRACE ELEMENT AND REE GEOCHEMISTRY IN THE PYHÄSALMI VOLCANIC COMPLEX

The paleovolcanological studies were based on field observations and lithogeochemical analyse data. The results of such investigations, discussed in this chapter, provide an areal view for the trace element and REE geochemistry in the Pyhäsalmi volcanic complex.

Data for the Ruotanen formation originate from the Lippikylä, Mukurinperä and Pellonpää members. The interpretation of the Mullikkoräme formation is based on the Riitavuori and Tetrinmäki members. The unexposed Kettuperä, Särkiperä and Jurvansuu members, and the altered lithodemes described in Chapter B2, are not included in this part of the study.

Despite sparsely exposed landscape the data presented herein are believed to verify the earlier picture of the Pyhäsalmi volcanic complex as a true bimodal entity (e.g., Mäki 1986, Kousa et al. 1994), a feature obvious in both major and trace element cases. Silica contents exceeding 80% SiO₂ in many of the felsic samples from the Ruotanen and Mullikkoräme formations would indicate rhyolitic compositions; however, this is a secondary feature caused by alteration. To avoid such alteration effect, rock classification presented in the following chapters is based simply on the trace element diagram (Zr/TiO₂*0.0001 vs. Nb/Y) by Winchester and Floyd (1977). According to the said formula the mafic metavolcanites of the Pyhäsalmi volcanic complex can be classified as subalkaline basalts and basaltic andesites while the felsic volcanites display rhyodacitic to rhyolitic character.

The REE distribution diagrams presented below demonstrate differences or similarities in the proposed individual eruption events within stratigraphic members. The REE data are normalised after the analytical data of the C1 Chondrite (Sun and McDonough 1989).

Heikki Puustjärvi (ed.)

8.11.2006

Confidential

The tectonomagmatic classification of felsic metavolcanites is based on granite discrimination diagrams, i.e. Nb vs. Y and Rb vs. Y+Nb (Pearce et al. 1984). The mafic metavolcanites are classified using the following diagrams: Zr-Ti/100-Sr/2 (Pearce 1973), Zr/4-Nb*2-Y (Meschede 1986), Th-Hf/3-Ta (Wood 1980) and V vs. Ti/1000 (Shervais 1982).

B 5.2.1 Ruotanen formation

Studies on the samples for paleovolcanological investigations indicate that at least six separate groups exist within the felsic metavolcanites of the Ruotanen formation (see Figs. B5 and ?). This points to differences in composition between eruption stages. Four of these groups are included in the Lippikylä member and two in the Pellonpää member. Despite slight overlapping this may be a true feature that supports the stratigraphic interpretation. Based on geochemical features, it is obvious that the quartz porphyries around the Pyhäsalmi deposit represent the same type of rhyolites to which also the felsic rocks at Piilola, c. 2 km south of the mine, are correlated. A surprising feature is the andesitic trace element composition in samples taken from the bottom of the backfill pit as well as in those from Topiskonräme. Both of the areas represent the Lippikylä member. The rather high silica contents indicate rhyodacitic composition for these rocks.

The REE distribution pattern in felsic volcanites (Plate B1) shows moderate to high enrichment in LREE, flat HREE patterns and slight to moderate Eu minima. An interesting feature is noticed in the REE patterns: they are identical for andesites of "the Topiskonräme - backfill pit bottom" type and the quartz-plagioclase-porphyrific rhyodacite west of the Pyhäsalmi deposit.

Among the mafic metavolcanites of the Mukurinperä member at least five types can be recognised. They include subalkaline and andesitic basalts. Their REE distribution (Plate B2) shows slight LREE enrichment probably indicating a similar source.

The tectonomagmatic character of the Ruotanen formation (Plate B3), as identified in almost any trace element combination, suggests a volcanic arc affinity for the felsic and mafic metavolcanites.

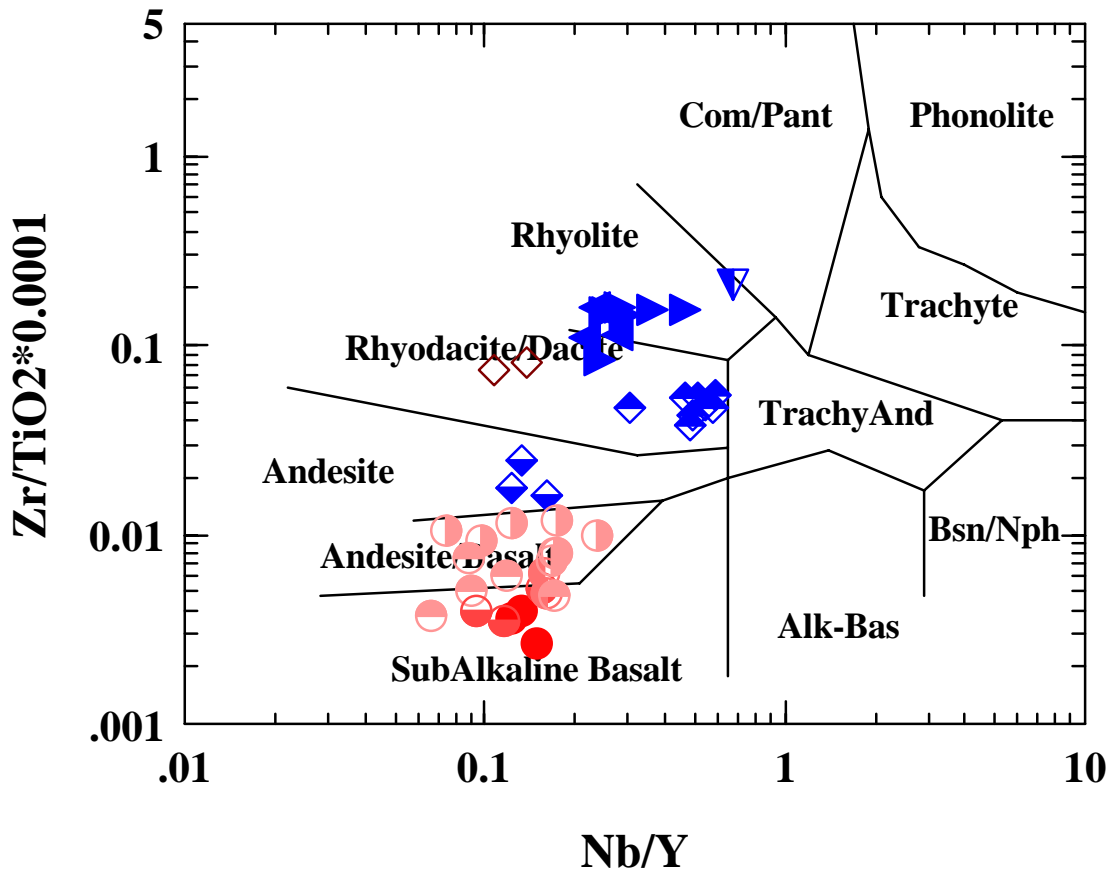


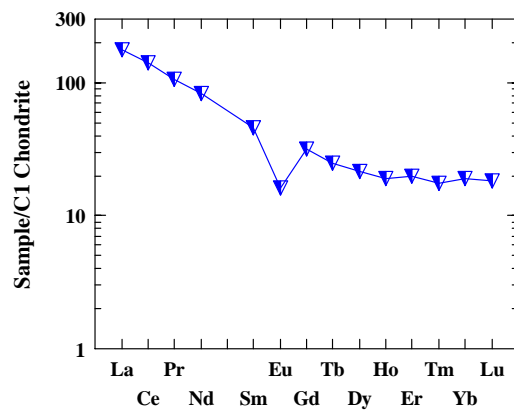
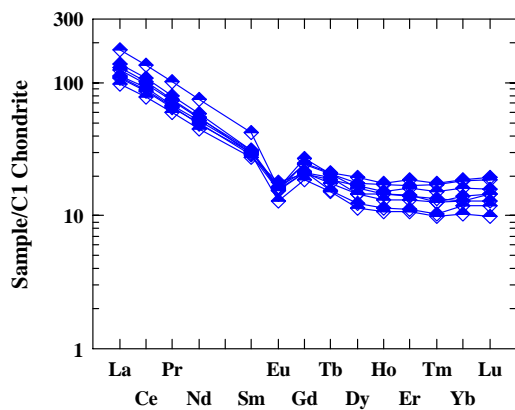
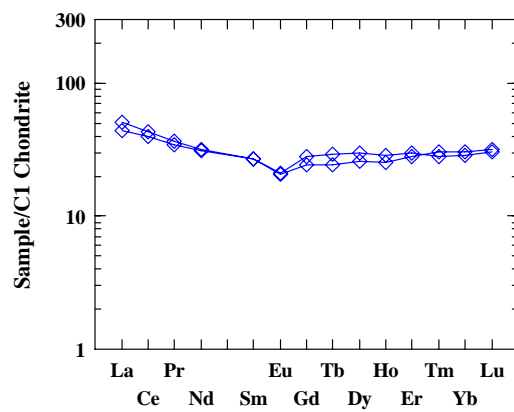
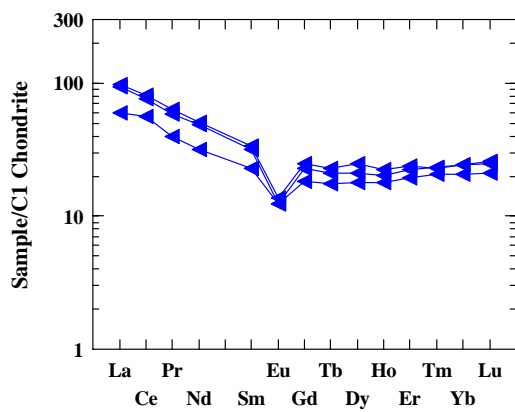
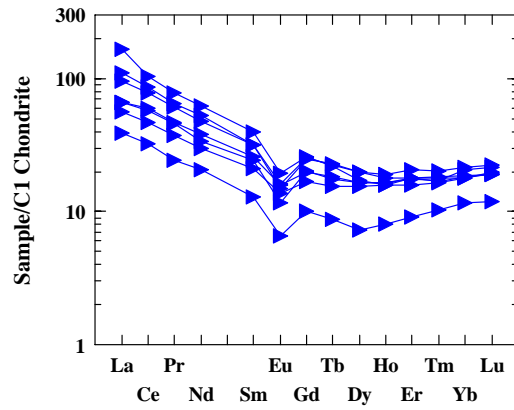
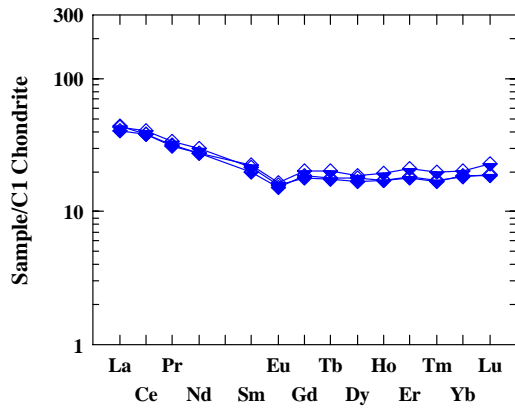
Figure B23. Geochemical classification of metavolcanites in the Ruotanen formation. See plates B1, B2 and B7 for symbol explanations.

Heikki Puustjärvi (ed.)

8.11.2006

Confidential

Plate B1. REE distribution diagrams for felsic metavolcanites in the Ruotanen formation. Sample sets Rf1-Rf6 refer to the plate B7 legend. Sample sets ordered as from Rf1 to Rf6 from upper left to lower right.

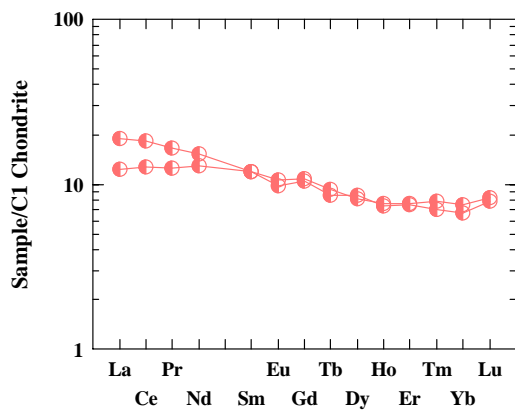
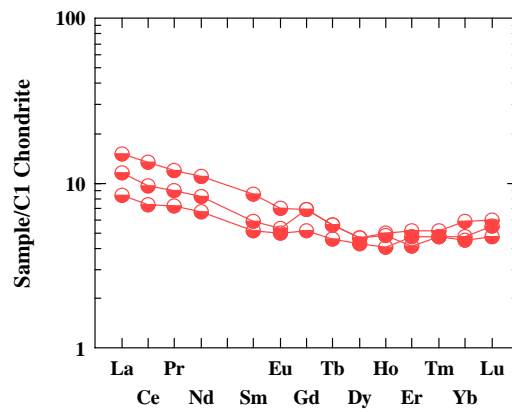
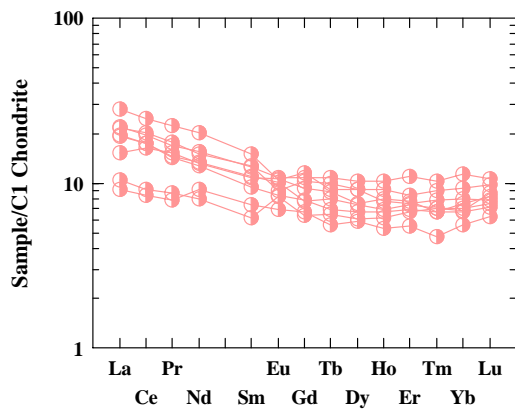
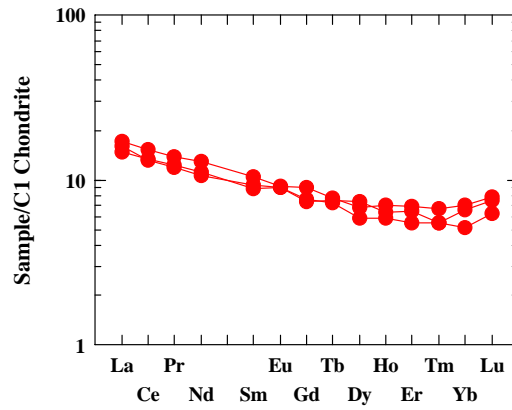
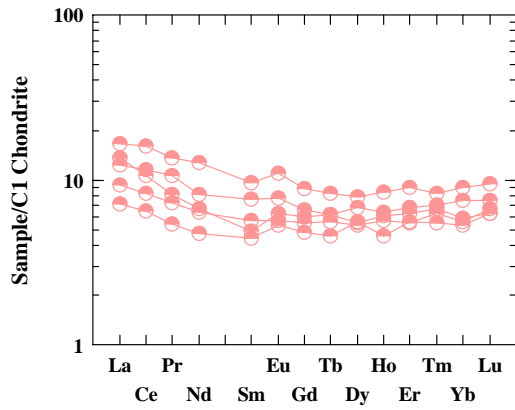


Heikki Puustjärvi (ed.)

8.11.2006

Confidential

Plate B2. REE distribution diagrams for mafic metavolcanites in the Ruotanen formation. Sample sets Rm1-Rm5 refer to the plate B7 legend. Sample sets ordered as from Rm1 to Rm5 from upper left to lower left.

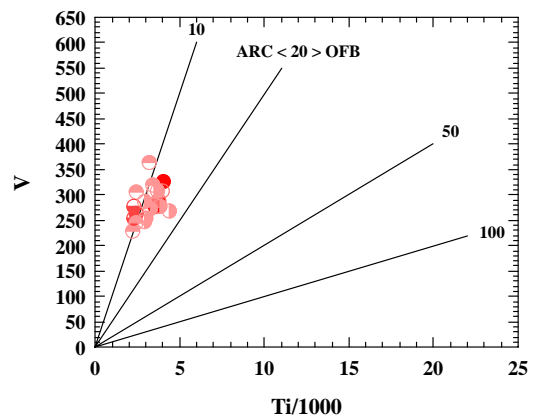
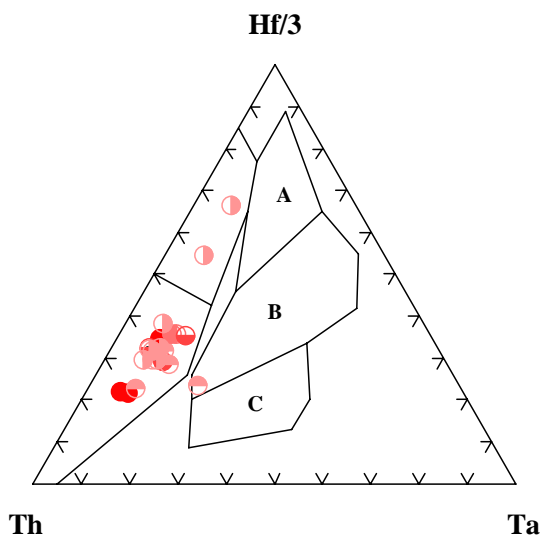
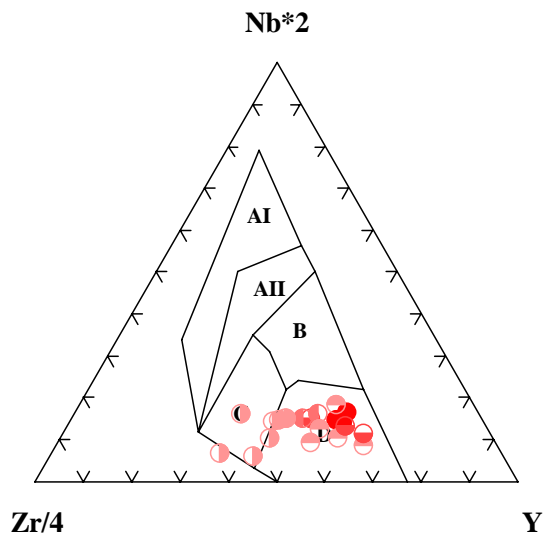
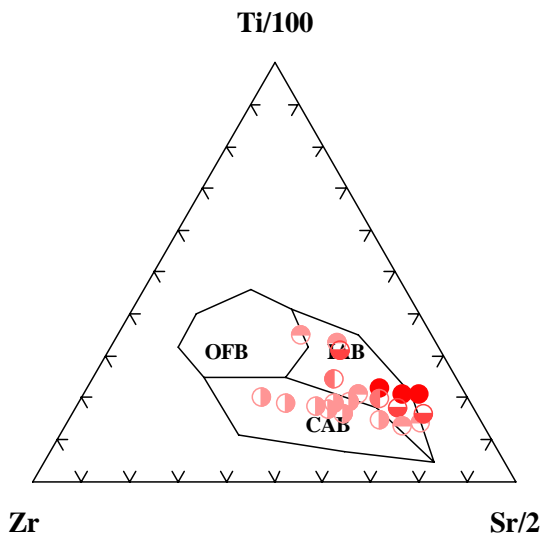
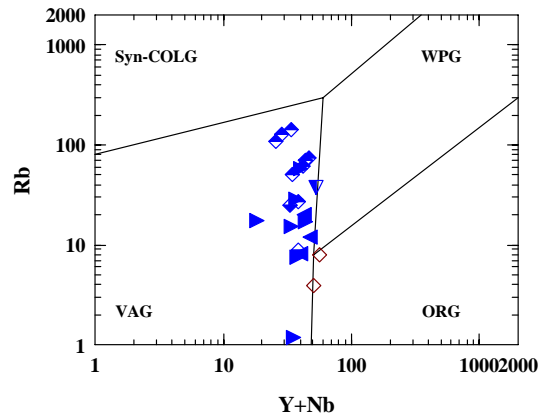
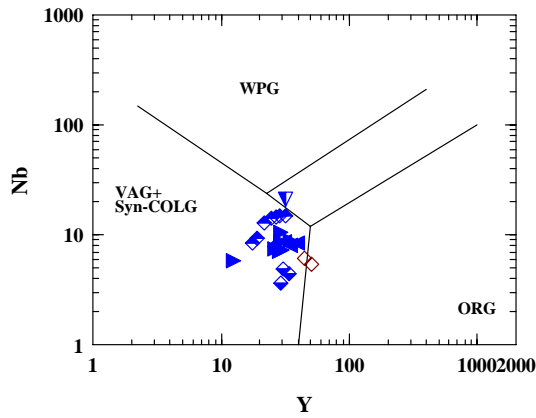


Heikki Puustjärvi (ed.)

8.11.2006

Confidential

Plate B3. Tectonomagmatic discrimination diagrams for metavolcanites in the Ruotanen formation. Sample set groups same as in plates B1 and B2.



B 5.2.2 Mullikkoräme formation

The Mullikkoräme formation displays rather similar geochemical features than does the Ruotanen formation. However, rocks seen in outcrops show differences described in earlier chapters. Geochemical bimodality is evident also in the Mullikkoräme formation.

Compositions in the felsic metavolcanites range from dacites to rhyolites and those in the mafic ones from subalkaline basalts to andesitic basalts (Fig. B24). In the field, the felsic rocks can be divided into four different types each of them showing distinct character. Compositions in the mafic rocks overlap.

Plate B4 demonstrates REE distribution in the four felsic rock types. The quartz porphyries, lowermost in stratigraphy, deviate in their LREE contents but have similar Eu minima and HREE distribution. The mafic rocks show moderate LREE enrichment (Plate B5); in few cases the patterns are rather flat.

The tectonomagmatic discrimination points to volcanic arc environment, as is the case with the Ruotanen formation. Only one type of lava, that at Parviaisaho, probably the lowest in stratigraphy, displays a slightly primitive character.

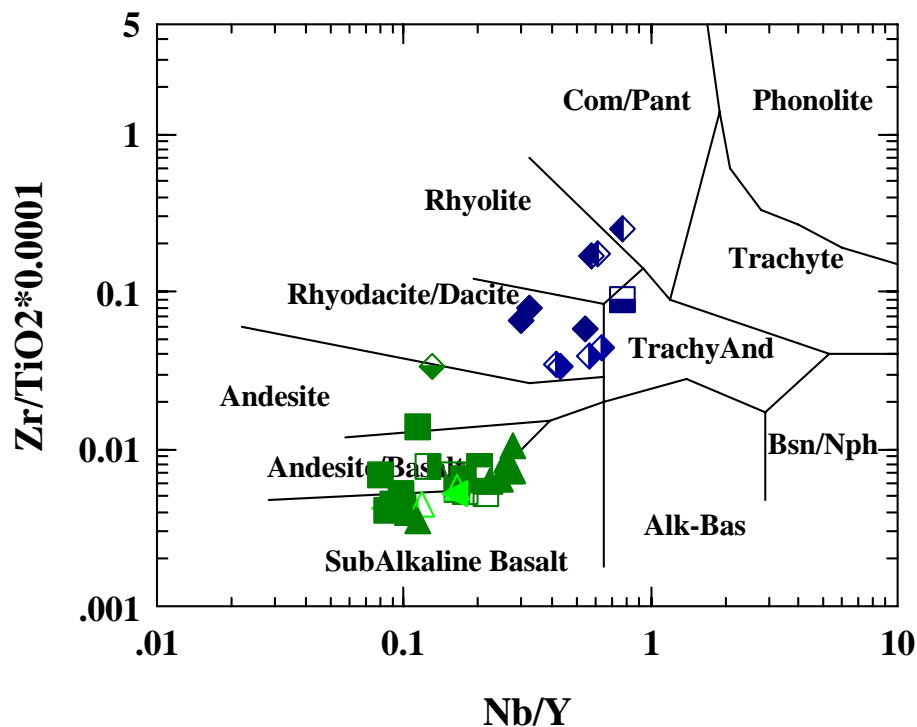


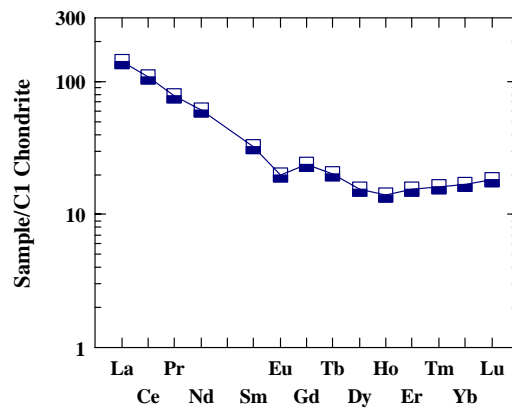
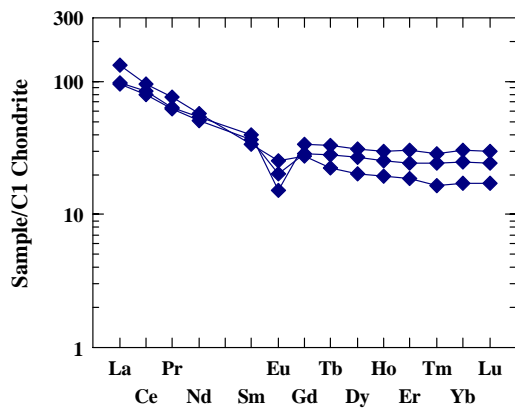
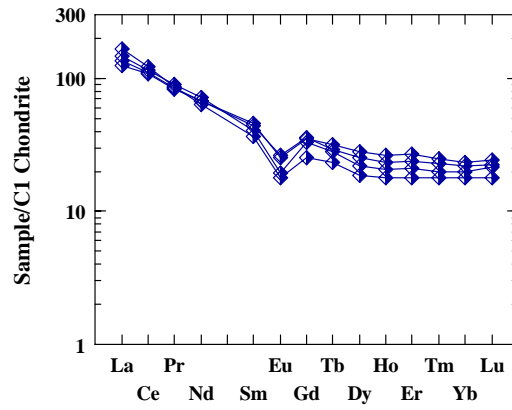
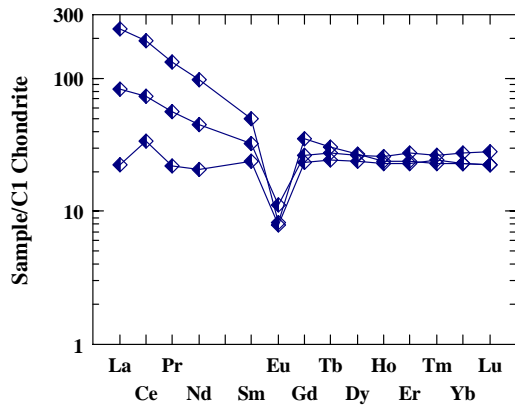
Figure B24. Classification of metavolcanites in the Mullikkoräme formation. See plates B4, B5 and B8 for symbol explanations.

Heikki Puustjärvi (ed.)

8.11.2006

Confidential

Plate B4. REE distribution diagrams for felsic metavolcanites in the Mullikkoräme formation. Sample sets refer to the Plate B8 legend. Sample sets are ordered as from Mf1 to Mf4 from upper left to lower right.



Heikki Puustjärvi (ed.)

8.11.2006

Confidential

Plate B5. REE distribution diagrams for mafic metavolcanites in the Mullikkoräme formation. Sample sets Mm1-Mm8 refer to the Plate B8 legend. Sample sets are ordered as from Mm1 to Mm4 from upper left to middle right and as Mm6 at lower left and as Mm5 (low shaded diamond), Mm7 (open triangle) and Mm8 (right shaded square).

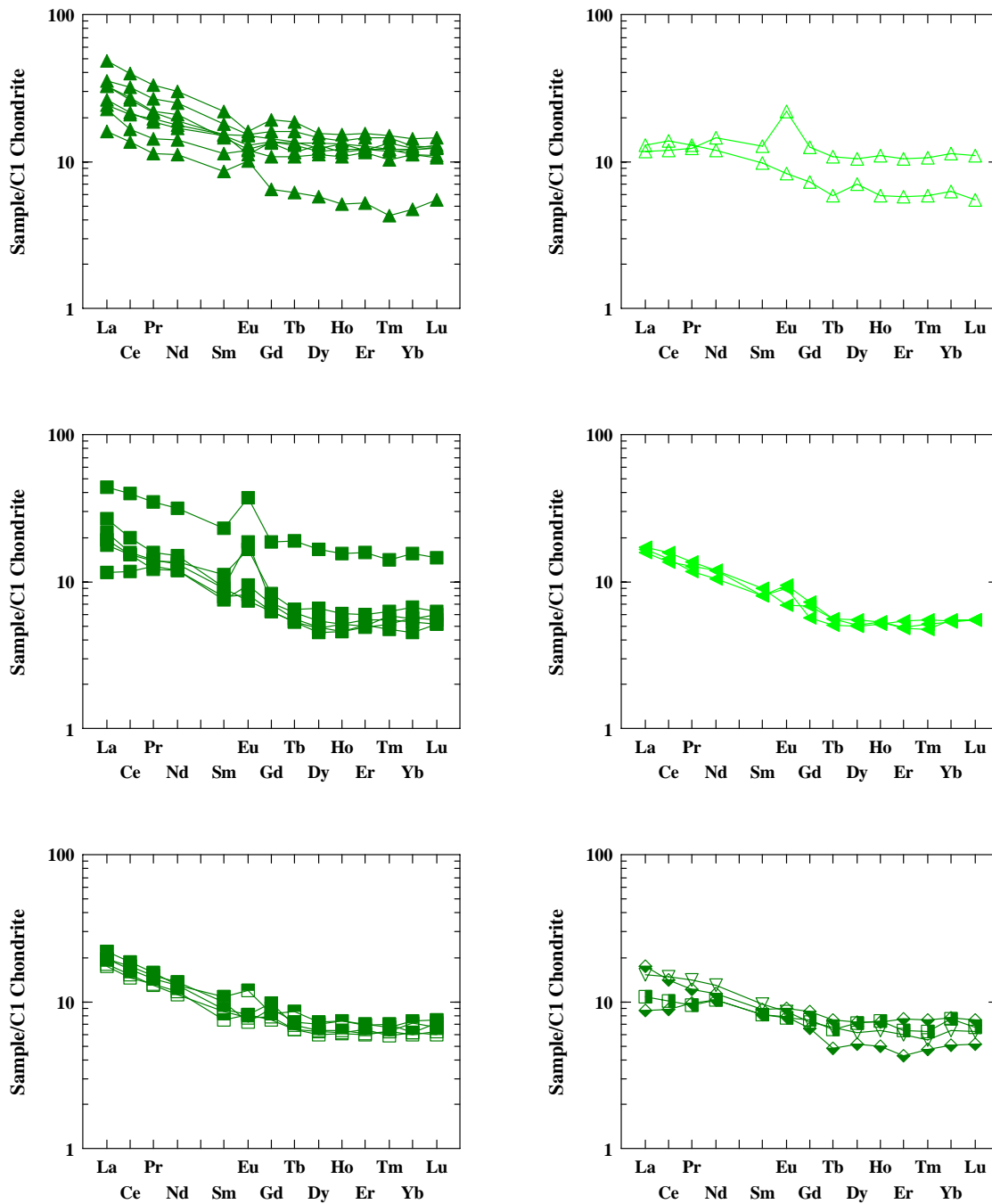


Plate B6. Tectonomagmatic discrimination diagrams for felsic and mafic metavolcanites in the Mullikkoräme formation. Sample set groups same as in Plates B4 and B5.

Heikki Puustjärvi (ed.)

8.11.2006

Confidential

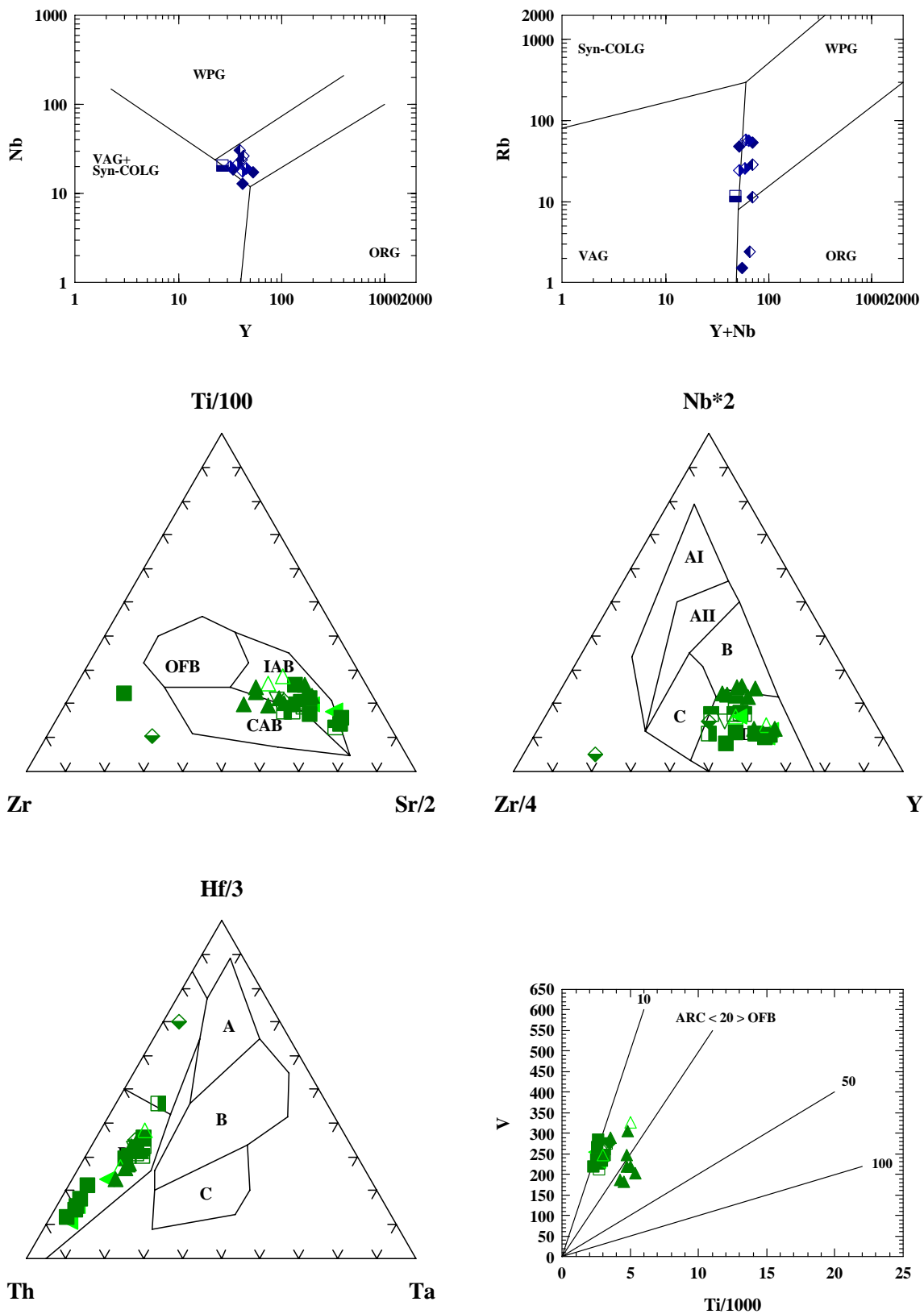


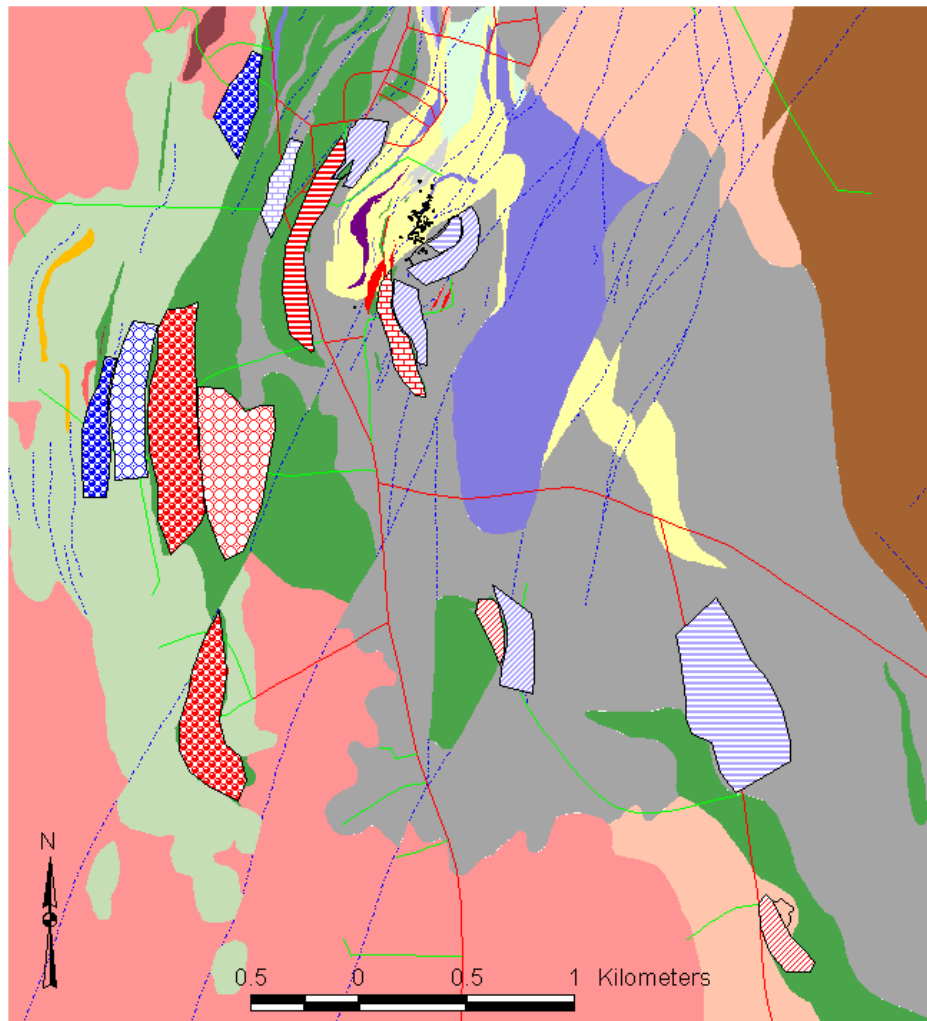
Figure B25. Distribution of ten different volcanic rock types observed in the Lippikylä, Mukurinperä and Pellonpää members of the Ruotanen formation. This greatly simplified model gives an idea of the westwards younging

Heikki Puustjärvi (ed.)

8.11.2006

Confidential

volcanic succession. More dense sampling and more excavated new outcrops are needed in future to get an accurate picture of this tectonically complicated formation.










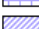


-  (Rm4) Mafic pillow lavas (Mukurinperä, Vanhainkoti)
-  (Rm5) Mafic massive lavas (Mukurinperä)
-  (Rm3) Mafic pyroclastic and tuffaceous rocks (south of the mine)
-  (Rm2) Mafic lavas (south and southeast of mine, Piilola and Soidinmäki)
-  (Rm1) Mafic lavas (west and north of the mine)
-  (Rf5) Felsic massive and tuffaceous layers west of the mine
-  (Rf5 and Mf1) Quartz porphyries of the lowest Pellonpää and Riitavuori member
-  (Rf4) Quartz plagioclase porphyry (on the road side west of the mine)
-  (Rf2 and Rf3) Quartz porphyry (around the Pyhäsalmi mine and in Piilola south of mine)
-  (Rf1) Rhyodacitic volcanite (Topiskonrämpe and back fill open pit bottom)

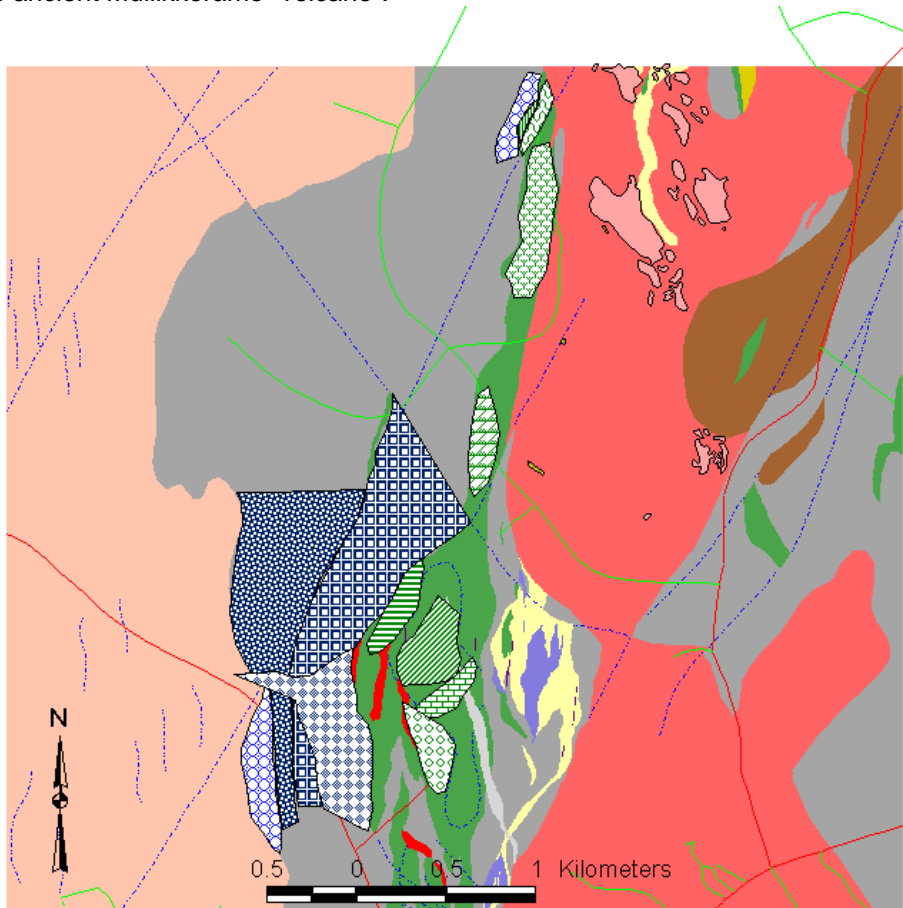
Figure B26. Distribution of different rock types of the Riitavuori and Tetrinmäki members of the Mullikkoräme formation. Sparse outcrops in the Mullikkoräme area makes it very difficult to connect especially the mafic rocks













Heikki Puustjärvi (ed.)

8.11.2006

Confidential

from an outcrop to another. Anyway, the Mullikkoräme formation seems to form an eastwards younging volcanic succession, which is obviously slightly younger and better preserved, less deformed and metamorphosed than the Ruotanen formation. By rotating the figure 90 degrees to the left, the reader may get a schematic sectional impression of the ancient Mullikkoräme "volcano".



-  (Mm6) Mafic pillow lavas (Tetrinmäki)
-  (Mm7) Deformed mafic pillow lava (north of Tetrinmäki)
-  (Mm5) Deformed mafic lava (pillowed?, Jylkynkangas)
-  (Mm4) Massive amygloidal mafic lavas, in part pillowed (Mullikkoräme mine area)
-  (Mm8) Massive mafic lava (on the top of quartz porphyry, Tetrinmäki)
-  (Mm3) Massive mafic lavas and lava breccias (north of the Mullikkoräme mine)
-  (Mm2) Massive mafic lavas (Parviaisaho)
-  (Mm1) Mafic in part pillowed lavas (Parviaisaho)
-  (Mf4) Massive high Zr rhyolite (Riitavuori northeast)
-  (Mf3) Felsic volcanic breccia (Heikinaho type)
-  (Mf2) Felsic rhyodacitic breccia (Riitavuori type soft breccia)
-  (Rf6 and Mf1) Quartz porphyries of the lowest Pellonpää and Riitavuori member

B 5.3 STRATIGRAPHY AND TIMING

Heikki Puustjärvi (ed.)

8.11.2006

Confidential

Sample	Lab. no	Map sheet	x-coord.	y-coord.	Location	Rock type
11-JKL-97	A1561	3321 12A	7062494	3452516	Pyhäsalmi mine area, road side 300 m, W of open pit	Rhyolite, plagioclase quartz porf.
17-JPK-97	A1562	3321 12A	7062165	3453179	Pyhäsalmi mine, backfill quarry, S-side	Rhyolite, quartz porf.
13-JPK-97	A1583	3321 12A	7062394	3453328	Pyhäsalmi mine, backfill quarry, N-side	Rhyodasite, quartz porf.
Kharon	A1584	3321 12D	7066730	3459100	Mullikkoräme mine	Rhyolite
R-2139/87-98m	A1597	3321 12A	7061937	3452733	Pyhäsalmi mine, z-coord. +1080m	Pegmatite granite
PyO/Mu-116/ 562,4-598,8m	A1598	3321 12D	7066500	3459480	Mullikkoräme mine, z-coord. +185m	Rhyolite, quartz porf, K- feldspar bearing

Again the stratigraphic interpretation of the Pyhäsalmi volcanic complex has to be done indirectly combining the earlier isotopic evidence available with the new outcrop observations and geochemical conclusions of this modelling project (see B2).

Now we can be sure that at least the earlier-mentioned Kettuperä gneiss is the lowermost felsic volcanic member of the Ruotanen formation having the age of c.1930 Ma. Any basement complex to this has never been reached. The Kettuperä member is followed by quartz porphyric rhyolites of the Lippikylä member. The contact between these is tectonic and thus the real stratigraphic position remains obscure. The altered rocks named as Lepikko (felsic protholith) and Lehto (mafic protholith) lithodemes including the Pyhäsalmi ore deposit have their stratigraphic position between the Lippikylä and Mukurinperä members. In one outcrop (10-JKL-97) the contact between these seems to be sharp but depositional. The few lava breccia and pillow structures observed among the Mukurinperä mafics confirm the idea of their position on top of the Lippikylä member. Also pyroclastic breccias with Lippikylä-type quartz porphyric fragments are interpreted to belong to the Mukurinperä member again indicating the position of it. These pyroclastic breccias may have a close connection to the Jurvansuu member reworked volcanics at the top of the sericite-altered Lepikko lithodeme. The poorly outcropped and drilled Pellonpää and Särkisalo members are more difficult to put in any definite place of the stratigraphic column but at least the former can be assumed to be directly on the top of the Mukurinperä member and thus being the uppermost part of the Ruotanen formation.

The Mullikkoräme formation is build up of felsic and mafic metavolcanites named as the Riitavuori and Tetrinmäki members, respectively. And again, analogous to the Ruotanen formation, stratigraphically between these two are the altered felsic (Reijusneva) and mafic lithodemes where the former is the host for the massive sulphide ore. As described in previous chapters of this text the Mullikkoräme formation starts by quartz porphyric rhyolites having the zircon U-Pb age of 1921 Ma. The contact between Riitavuori and Tetrinmäki members observed in two separate outcrops show clearly that the latter is on the top of the Riitavuori member. Also inside the Tetrinmäki member, lava and pillow lava structures observed show clear eastward to southeastward younging direction for this.

Heikki Puustjärvi (ed.)

8.11.2006

Confidential

As a conclusion of the former description it can be said that the Riitavuori member is slightly younger than the Kettuperä member. Their overlapping eNd values about from 2.6 to 3.4 (Lahtinen and Huhma 1996) may indicate same source for the magmas. The bimodal nature of both the Ruotanen and Mullikkoräme formations reflect the same kind of geotectonic environment and eruption conditions for these. Although there is great overlapping of chemical composition of the same type of rocks in these formations the slight but obvious difference between them may indicate directly some evolution of the magma reservoirs during time span about 10 Ma. Again the same kind chemical composition of the lowest bed of the Riitavuori member, the dated quartz porphyry, and the proposed lowest rhyolite bed of the Pellonperä member could serve as the key to connect the Ruotanen and the Mullikkoräme formations. Thus it is proposed here that the Mullikkoräme formation and Pellonpää member of the Ruotanen formation have the same time-stratigraphic position on the top, and the rest of the Ruotanen formation represents the oldest volcanic stage of the Pyhäsalmi volcanic complex.

B REFERENCES

Meschede M., 1986. A method of discriminating between different types of mid-ocean ridge basalts and continental tholeiites with the Nb-Zr-Y diagram. *Chemical Geology*, 56, 207-218.

Pearce J.A. and Cann J.R., 1973. Tectonic setting of basic volcanic rocks determined using trace element analyses. *Earth and Planetary Science Letters*, 19, 290-300.

Pearce J.A., Harris N.B.W., and Tindle, A.G., 1984. Trace element discrimination diagrams for the tectonic interpretation of granitic rocks. *Journal of Petrology*, 25, 956-983.

Shervais J.W., 1982. Ti-V plots and the petrogenesis of modern and ophiolitic lavas. *Earth and Planetary Science Letters*, 59, 101-118.

Sun S.S. and McDonough, W.F., 1989. Chemical and isotopic systematics of oceanic basalts: implications for mantle composition and processes. in *Magmatism in the ocean basins*. Geological Society, Special Publication, 42, 313-345.

Winchester J.A. and Floyd P.A., 1977. Geochemical discrimination of different magma series and their differentiation products using immobile elements. *Chemical Geology*, 20, 325-343.

Wood D.A., 1980. The application of Th-Hf-Ta diagram to problems of tectonomagmatic classification and to establishing the nature of crustal contamination of basaltic lavas of British Tertiary volcanic province. *Earth and Planetary Science Letters*, 50, 11-30.

Heikki Puustjärvi (ed.)

8.11.2006

Confidential

Ekdahl, E. 1993. Early Proterozoic Karelian and Svecofennian formations and the Evolution of the Raahe-Ladoga Ore Zone, based on the Pielavesi area, central Finland: Geol. Surv. Finland Bull. 373, 137p.

Ekdahl et al. in prep. GGT/SVEKA Pamphlet.

Helovuori, O. 1979. Geology of the Pyhäsalmi Ore Deposit, Finland. Economic Geology 74, 1084-1101.

Hietanen, A. 1975. Generation of potassium poor magmas in the northern Sierra Nevada and the Svecofennian of Finland. J. Res. U.S. Geol. Survey, Vol. 3, 631-645.

Huhma, H. 1986. Sm-Nd, U-Pb and Pb-Pb isotopic evidence for the origin of the early Proterozoic Svecokarelian crust in Finland. Geol. Surv. Finland Bull. 337: 1-48.

Kahma, A. 1973. The main metallogenic features in Finland. Geol. Surv. Finland Bull. 265, 29p.

Kärki, A., Laajoki, K. & Luukas, J. 1993. Major Paleoproterozoic shear zones of the central Fennoscandian Shield. Precambrian Research 64, 207-223.

Kärki, A. Laajoki, K. & Vaasjoki, M. 1995. Tectonic settings and isotopic dating of the late Archean and Paleoproterozoic granitoids in the central Fennoscandian Shield, Finland. Res Terrae, Ser. A 10.

Koistinen, T. J. 1981. Structural evolution of an early Proterozoic strata-bound Cu-Co-Zn deposit, Outokumpu, Finland. Transactions Royal Society of Edinburgh: Earth Sciences, 72, 115-158.

Koistinen, T. J. 1983. Pyhäsalmen geologiset tutkimukset I, Malmin ja sivukiven rakennegeologiaa. Report 020/3321 12/TJK/1983.

Koistinen, T. J. 1984. Pyhäsalmen geologiset tutkimukset II, Malmin lähiympäristön rakennegeologiaa. Report 020/3321 12/TJK/1984.

Korja, T., Luosto, U., Korsman, K. & Pajunen, M. 1994. Geophysical and metamorphic features of Paleoproterozoic Svecofennian orogeny and Paleoproterozoic overprinting on Archean crust. In Pajunen M. (ed.) High temperature-low pressure metamorphism and deep crustal structures. Geol. Surv. Finland, Guide 37, 11-20.

Korsman, K., Niemelä, R. & Wasenius, P. 1988. Multistage evolution of the Proterozoic crust in the Savo schist belt, eastern Finland. In Korsman, K. (ed.) Tectono-metamorphic evolution of the Raahe-Ladoga zone. Geol. Surv. Finland Bull. 343, 89-96.

Heikki Puustjärvi (ed.)

8.11.2006

Confidential

Korsman, K., Hölttä, P., Hautala, T. & Wasenius, P. 1984. Metamorphism as an indicator of evolution and structure of the crust in eastern Finland. Geol. Surv. Finland Bull. 328. 40p.

Kousa, J. 1990. Paleoproterozoic metavolcanic rocks in the boarder zone of Savo and Pohjanmaa, Central Finland. In Kähkönen, Y. (ed.) IGCP Project 217 Proterozoic Geochemistry. National Working Group in Finland. Symposium, Proterozoic Geochemistry, Helsinki 90. Abstracts, 29-30.

Kousa, J., Marttila, E. & Vaasjoki, M. 1994. Petrology, geochemistry and dating of Paleoproterozoic metavolcanic rocks in the Pyhäjärvi area, central Finland. Geol. Surv. Finland, Spec. Paper 19, 7-27.

Lahtinen, R. 1994. Crustal evolution of the Svecofennian and Karelian domains during 2.1-1.79 Ga, with special emphasis on the geochemistry and origin of 1.93-1.91 Ga gneissic tonalites and associated supracrustal rocks in the Rautalampi area, central Finland. Geol. Surv. Finland, Bull. 378, 128p.

Lundqvist, T., Bøe, R., Kousa, J., Lukkarinen, H., Lutro, O., Roberts, D., Solli, A., Stephens, M., & Weihed, P., 1996. Bedrock map of Central Fennoscandia. Scale 1:1 000 000. Geological Surveys of Finland (Espoo), Norway (Trondheim) and Sweden (Uppsala).

Luukas, J. 1991. Salahmin-Pyhännän alueen stratigrafia ja rakennegeologia. Res Terrae, Ser. B 16, (English abstract). 131p.

Luukas, J. 1992. Ruotasen alueen rakennetulkinta. internal report. Outokumpu Finnmines Oy. (in Finnish).

Marttila, E. 1993. Pyhäjärven kartta-alueen kallioperä. Summary: Pre-Quaternary rocks of the Pyhäjärvi map-sheet area. Geological map of Finland 1:100 000, Sheet 3321. Geological Survey of Finland. 64p.

Park, A.F. 1991. Continental growth by accretion: A tectonostratigraphic terrane analysis of the evolution of the western and central Baltic Shield, 2.50 to 1.75 Ga. Geol. Soc. America, Bull., Vol. 103, 522-537.

Berman, R. G. 1991. Thermobarometry using multiequilibrium calculations: a new technique with petrologic applications. Canadian Mineralogist, v. 29. 833-855.

Berman, R. G. 1990. Mixing properties of Ca-Mg-Fe-Mn garnets. The American Mineralogist, 75. 328-344.

Berman, R. G. 1988. Internally-consistent thermodynamic data for stoichiometric minerals in the system Na₂O-K₂O-CaO-MgO-FeO-Fe₂O₃-Al₂O₃-SiO₂-TiO₂-H₂O-CO₂. Journal of Petrology, 29. 445-522.

Heikki Puustjärvi (ed.)

8.11.2006

Confidential

Gerya, T. 1997. Amphibole geothermobarometer, a new empirical calibration. In: Mineral equilibria and databases. Meeting of the Mineral Equilibria Working Group of the International Mineralogical Association (IMA). Abstract. Geological Survey of Finland, Guide 46. 28-29.

Hölttä, P. 1988. Metamorphic zones and the evolution of granulite grade metamorphism in the early Proterozoic Pielavesi area, central Finland. Geological Survey of Finland, Bulletin 344. 50 p.

Kähkönen, Y. 1998. Svekofenniset liuskealueet - merestä peruskallioksi. In: Lehtinen, M., Nurmi, P. & Rämö, T. (toim.) 3000 vuosimiljoonaa Suomen Kallioperä. Helsinki: Suomen geologinen seura, 199-228.

Marttila, E. 1993. Pyhäjärven kartta-alueen kallioperä. Summary: Pre-Quaternary rocks of the Pyhäjärvi map-sheet area. Geological map of Finland 1 : 100 000. Explanation to the Maps of Pre-Quaternary Rocks, Sheet 3321 Pyhäjärvi. Geological Survey of Finland. 64 s.

Spear, F. S. 1995. Metamorphic Phase Equilibria and Pressure-Temperature-Time Paths. Washington: Mineralogical Society of America. 799p.

SECTION C

LITHOGEOCHEMISTRY

H. Puustjärvi (ed.)

08.11.06

Confidential

C INTRODUCTION (K. Rasilainen)

This section contains the results of the lithogeochemical subproject for the Pyhäsalmi Modeling Project. The main goals of the subproject were to characterize the nature of hydrothermal alteration around the Pyhäsalmi and Mullikkoräme VMS deposits, and to find the best pathfinders for exploration in the area. To achieve the goals, the geochemical nature of the least-altered volcanites was also briefly covered. However, the primary geochemical characteristics of the volcanites are dealt with in more detail in the report of the paleovolcanologic subproject.

This work is based on XRF analyses of drillcore samples. Hence, many elements that would be useful, either as pathfinders or for characterizing the nature of host rock volcanites, were not available. This limitation is important to bear in mind while evaluating and possibly applying the results described here.

C 1 SAMPLES AND ANALYTICAL TECHNIQUES

The material used in the geochemical study consists of 13108 drillcore samples from 421 diamond drillholes (Figs. C1-7, Table C1). Most of these (9575) are samples that were taken and analyzed by Outokumpu Mining Oy (OM) between 1958 and 1995. During this project, 3820 new drillcore samples were taken and analyzed. H. Puustjärvi selected all the drillcore samples. Lists of all sampled drillholes are given in Appendix C1.

Table C1. Number and average length of drillcore samples for each subarea.

	Pyhäsalmi	Kettuperä	Mullikkoräme
Number of drillholes	130	41	250
Number of samples	5466	1954	5688
Sample length, median (m)	2.8	5	3
Sample length, minimum (m)	0.09	0.1	0.05
Sample length, maximum (m)	24.96	10.85	66.6
Sample length, standard deviation (m)	1.94	1.48	2.38

C 1.1 OLD SAMPLES AND ANALYSES

The drillcore samples total 9575. Sample lengths vary from 0.05 m to 66.6 m; the median length is 2.9 m. The samples were analyzed by OM between 1958 and 1995 using XRF for the major and minor elements and AAS for Cu, Zn, Pb, Ni, Co, Ag and Au (Table C2).

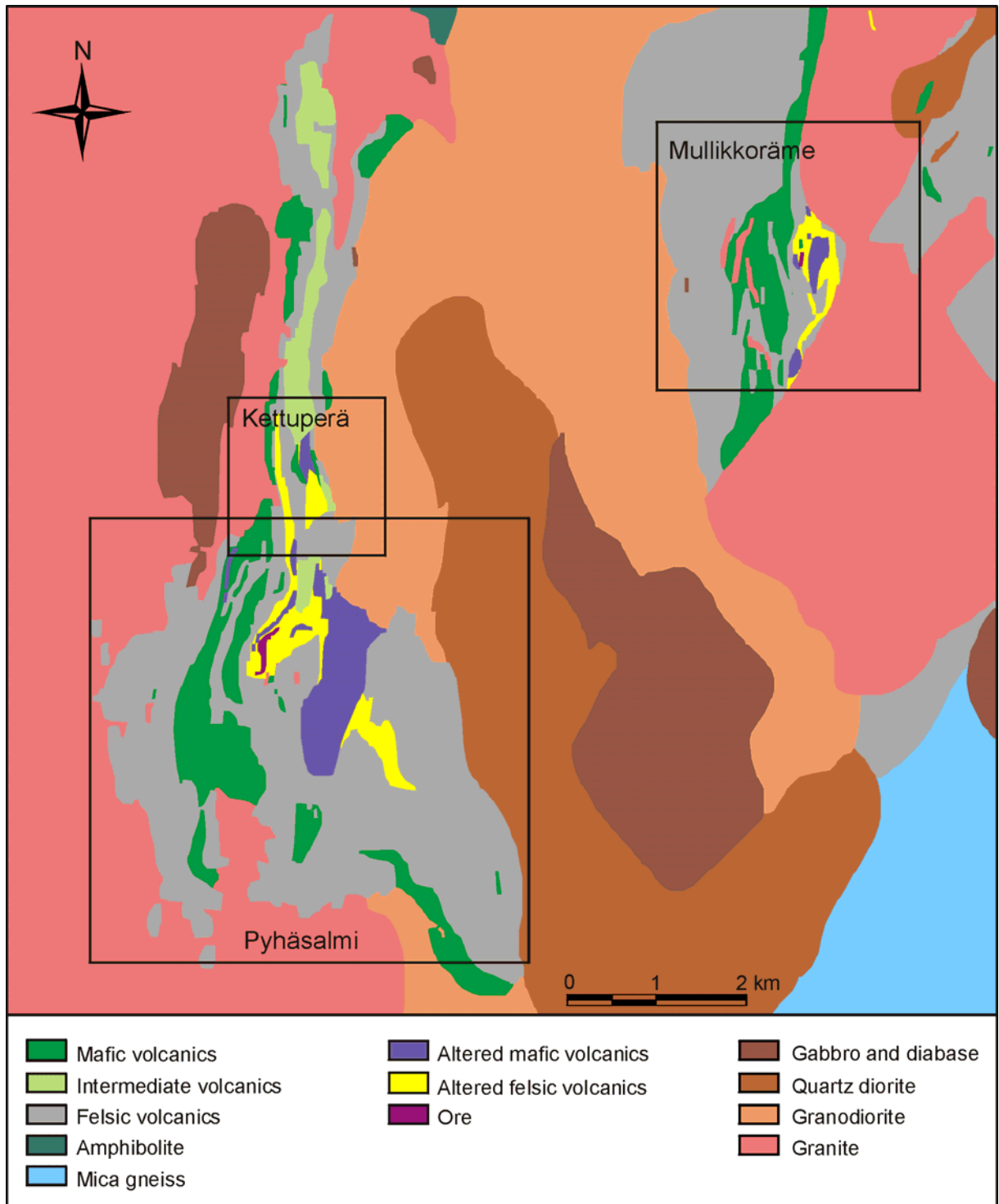


Figure C1. Geology of the Pyhäsalmi-Mullikkoräme area. Simplified from the map produced by J. Luukas for the Pyhäsalmi modeling project. The areas of Figs. 2, 4 and 6 are shown as rectangles.

H. Puustjärvi (ed.)

08.11.06

Confidential

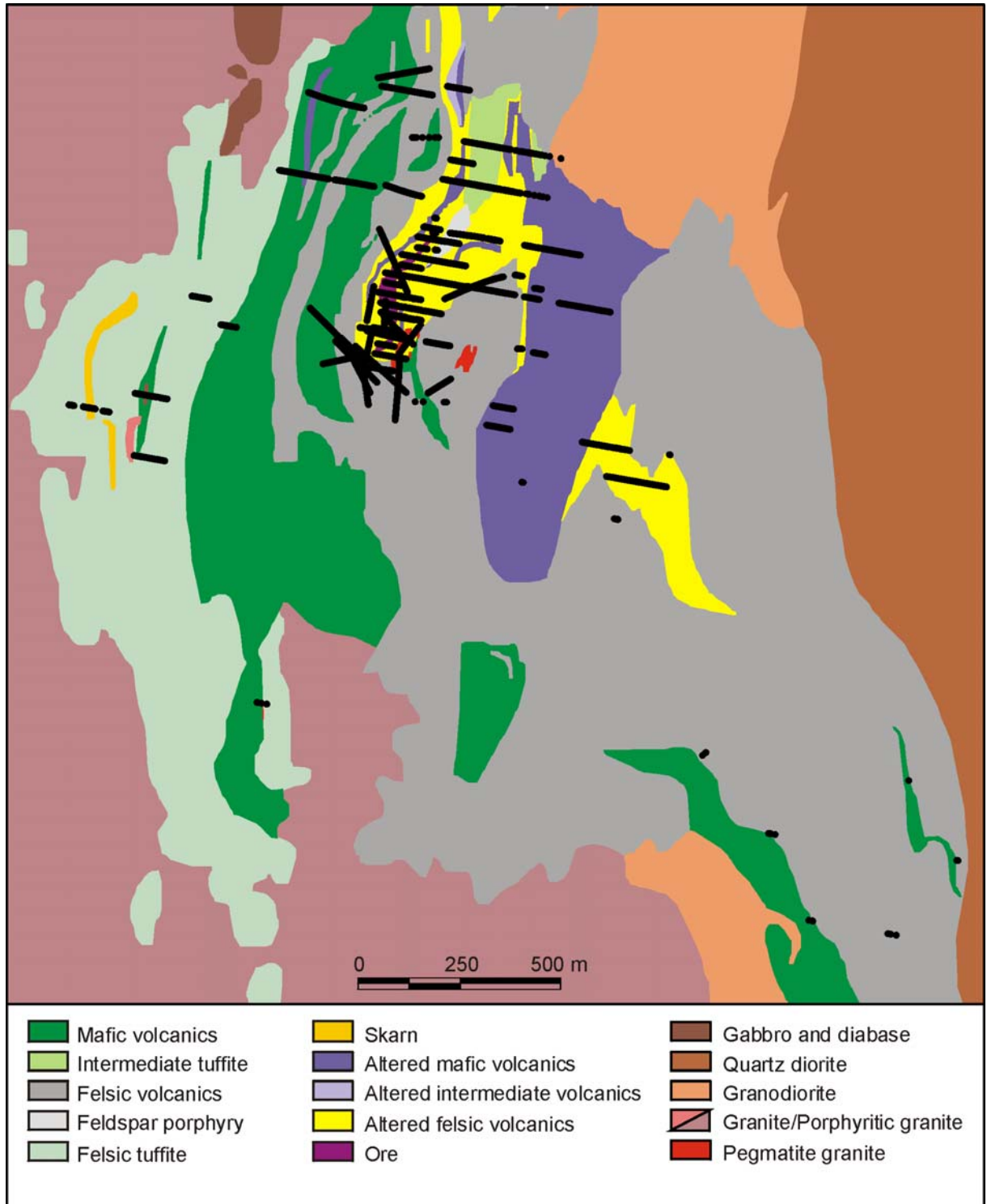


Figure C2. Geology of the Pyhäsalmi area. Simplified from the map produced by J. Luukas for the Pyhäsalmi modeling project. Projections of the drill core samples on the surface are shown as black dots.

H. Puustjärvi (ed.)

08.11.06

Confidential

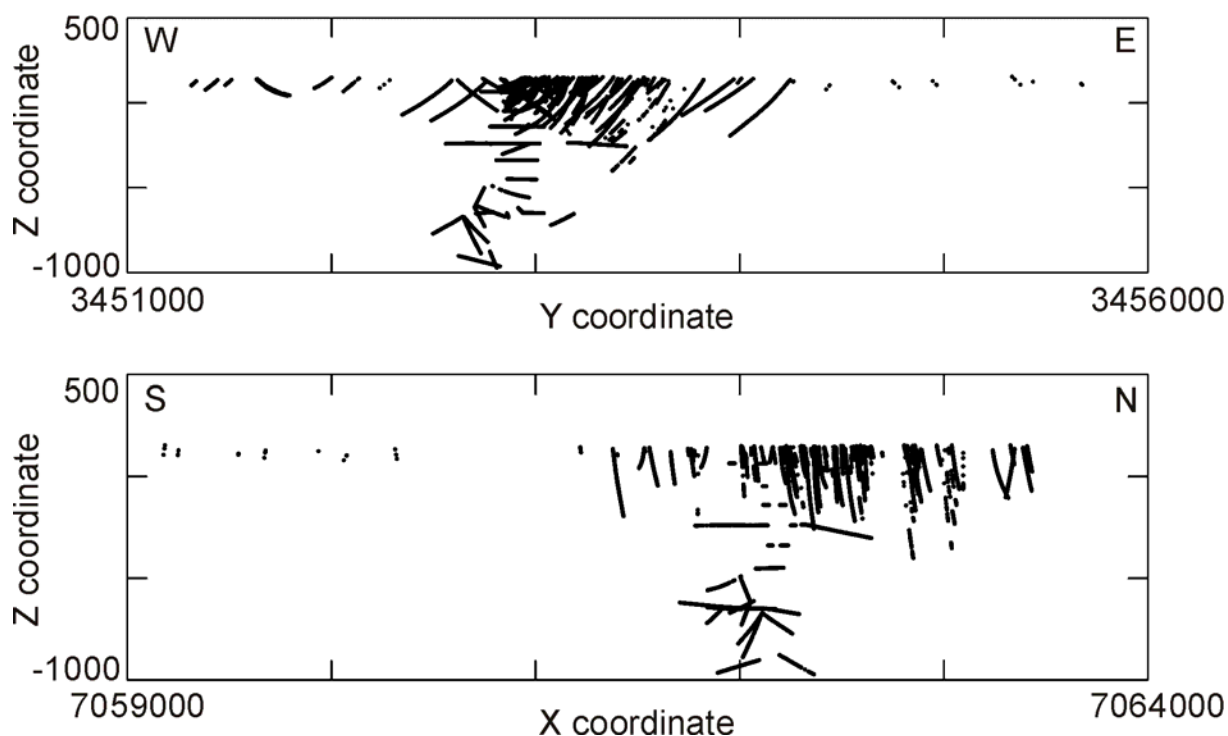


Figure C3. Diamond drill core samples at Pyhäsalmi projected on W-E and N-S vertical profiles.

C 1.2 NEW SAMPLES AND ANALYSES

The drillcore samples analyzed for the geochemistry subproject total 3820. Of these, 233 are powders of old OM samples that were reanalyzed for analysis comparison purposes. Sample lengths vary from 0.15 m to 15.3 m; the median length is 3.7 m. The samples were analyzed by XRF, 3157 of them at the chemical laboratory of GTK in Espoo and 663 at the chemical laboratory of the Technical Research Centre of Finland (VTT) in Outokumpu (Table C2).

Table C2. Summary of analytical techniques. Method: analytical method, N: number of samples, DL: detection limit (- means that no values are below the detection limit), Substituted: number substituted for values below detection limit, GRAV: gravimetric determination, LECO: carbon analyzer. Zr, Cr, V, Rb, Sr, Ba were calculated from oxide % values received from OM.

Element	OM analysis			GTK analysis			VTT analysis			Substituted
	Method	N	DL	Method	N	DL	Method	N	DL	
SiO ₂ %	XRF	7232	0.01	XRF	3103	0.02	XRF	650	0.01	-
TiO ₂ %	XRF	7232	0.002	XRF	3103	0.005	XRF	650	0.002	0.001
Al ₂ O ₃ %	XRF	7232	0.01	XRF	3103	0.02	XRF	650	0.01	0.005
Fe ₂ O ₃ %	XRF	7217	0.01	XRF	3103	0.03	XRF	650	0.01	-
MnO %	XRF	7232	0.002	XRF	3103	0.005	XRF	650	0.002	0.001
MgO %	XRF	7232	0.02	XRF	3103	0.03	XRF	650	0.02	0.01
CaO %	XRF	7232	0.01	XRF	3103	0.004	XRF	650	0.004	0.002
Na ₂ O %	XRF	7232	0.06	XRF	3103	0.06	XRF	650	0.06	0.03
K ₂ O %	XRF	7232	0.002	XRF	3103	0.004	XRF	650	0.002	0.001

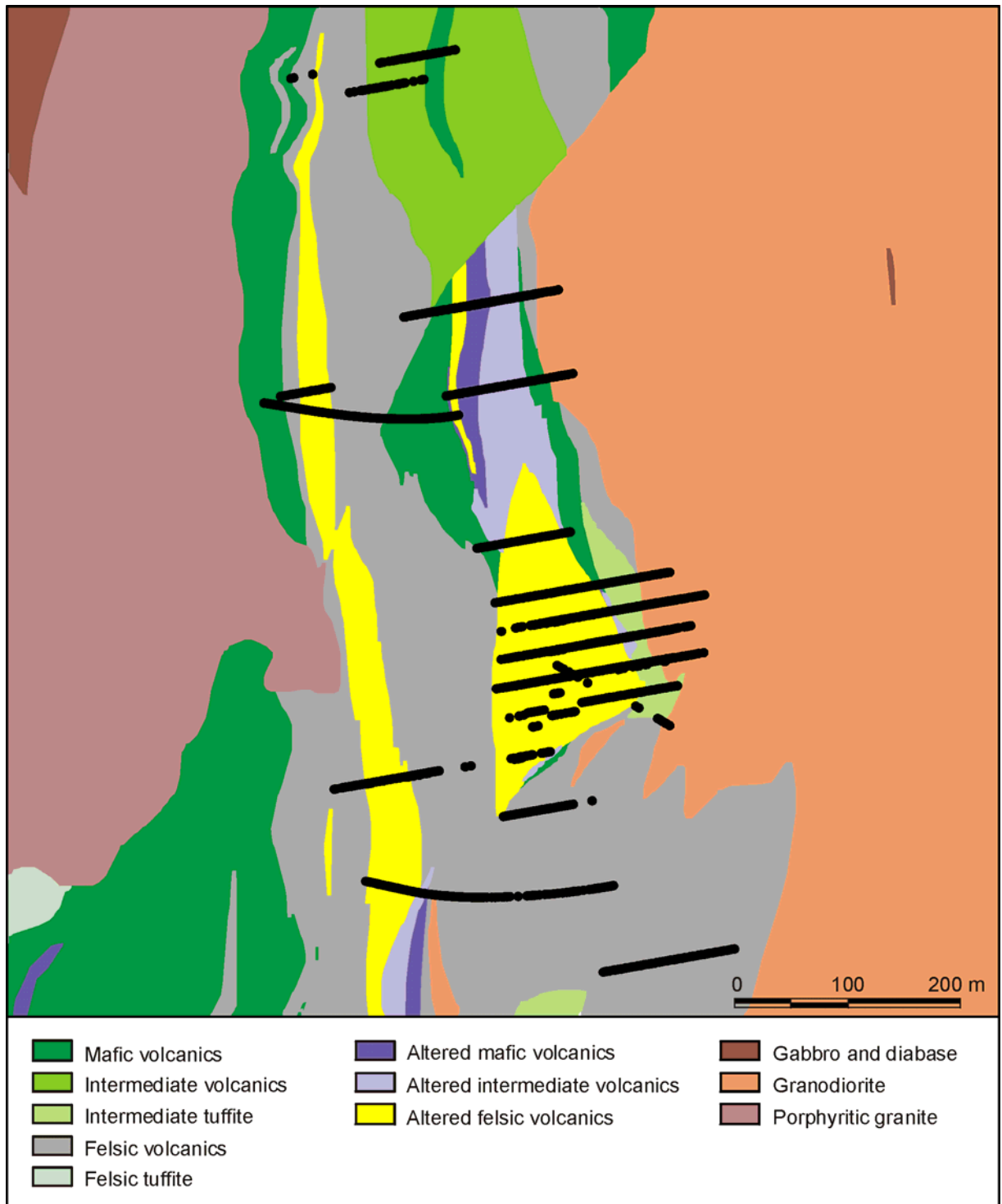


Figure C4. Geology of the Kettuperä area. Simplified from the map produced by J. Luukas for the Pyhäsalmi modeling project. Projections of the drill core samples on the surface are shown as black dots.

H. Puustjärvi (ed.)

08.11.06

Confidential

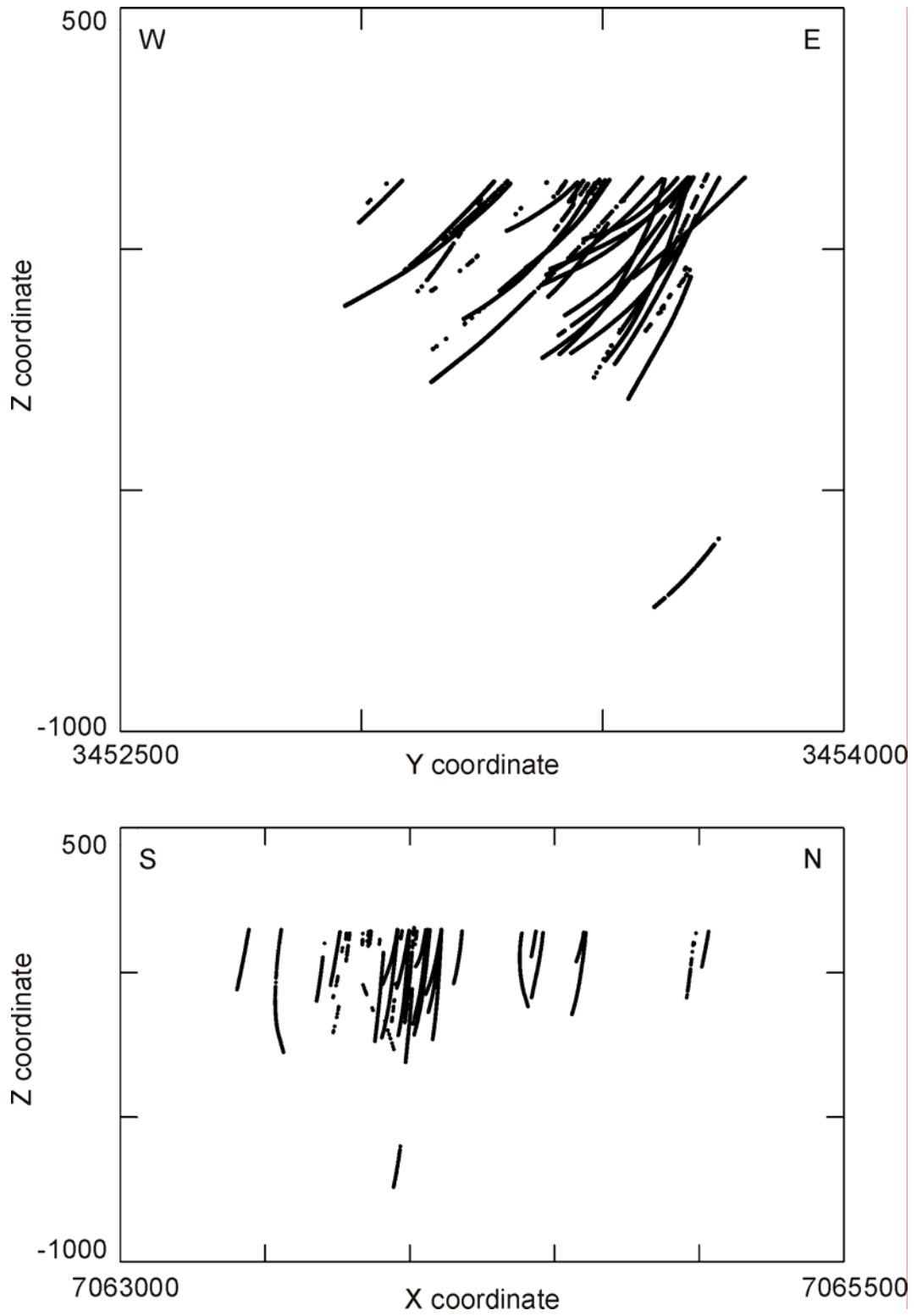


Figure C5. Diamond drill core samples at Kettuperä projected on W-E and N-S vertical profiles.

H. Puustjärvi (ed.)

08.11.06

Confidential

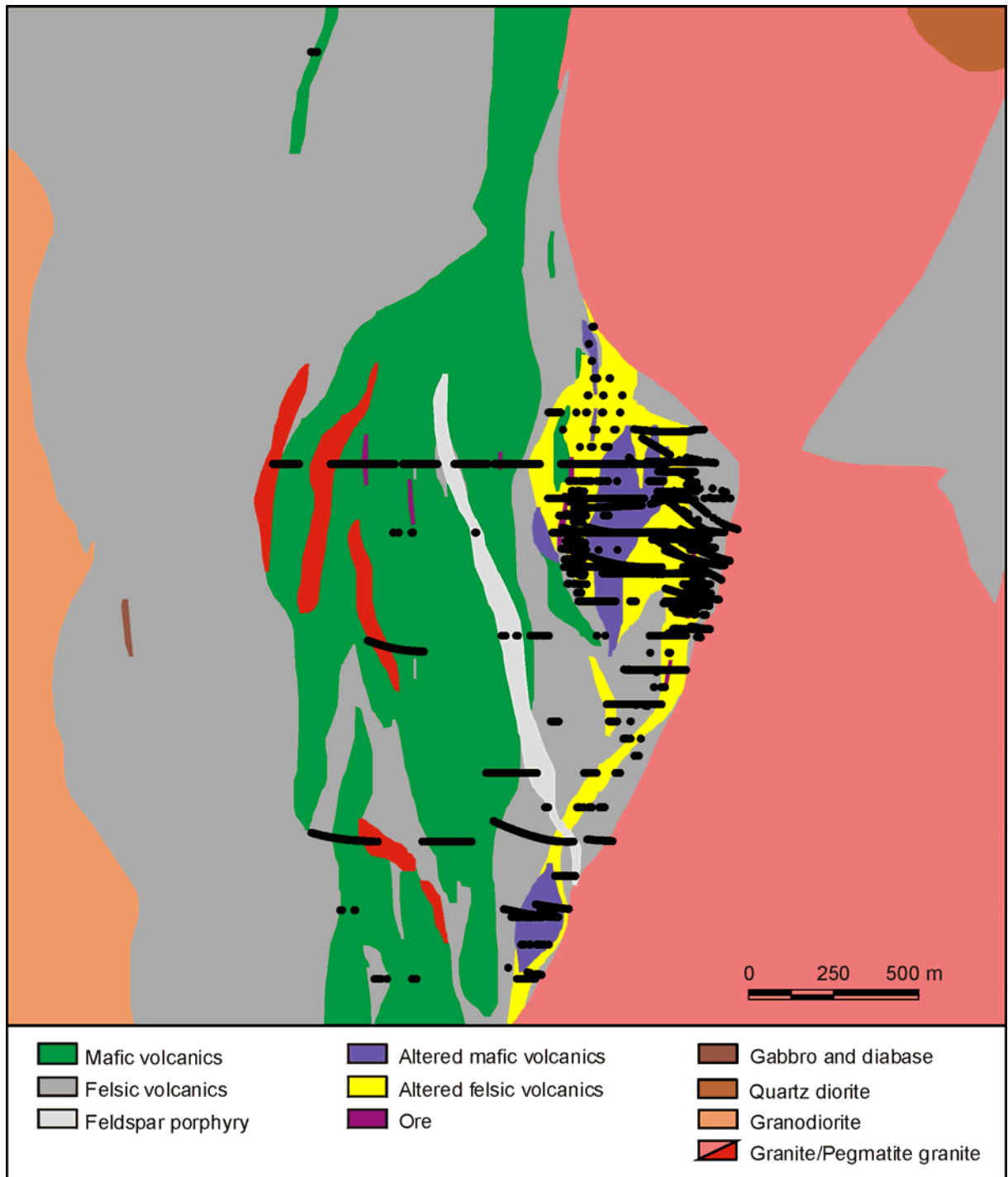


Figure C6. Geology of the Mullikkoräme area. Simplified from the map produced by J. Luukas for the Pyhäsalmi modeling project. Projections of the drill core samples on the surface are shown as black dots.

H. Puustjärvi (ed.)

08.11.06

Confidential

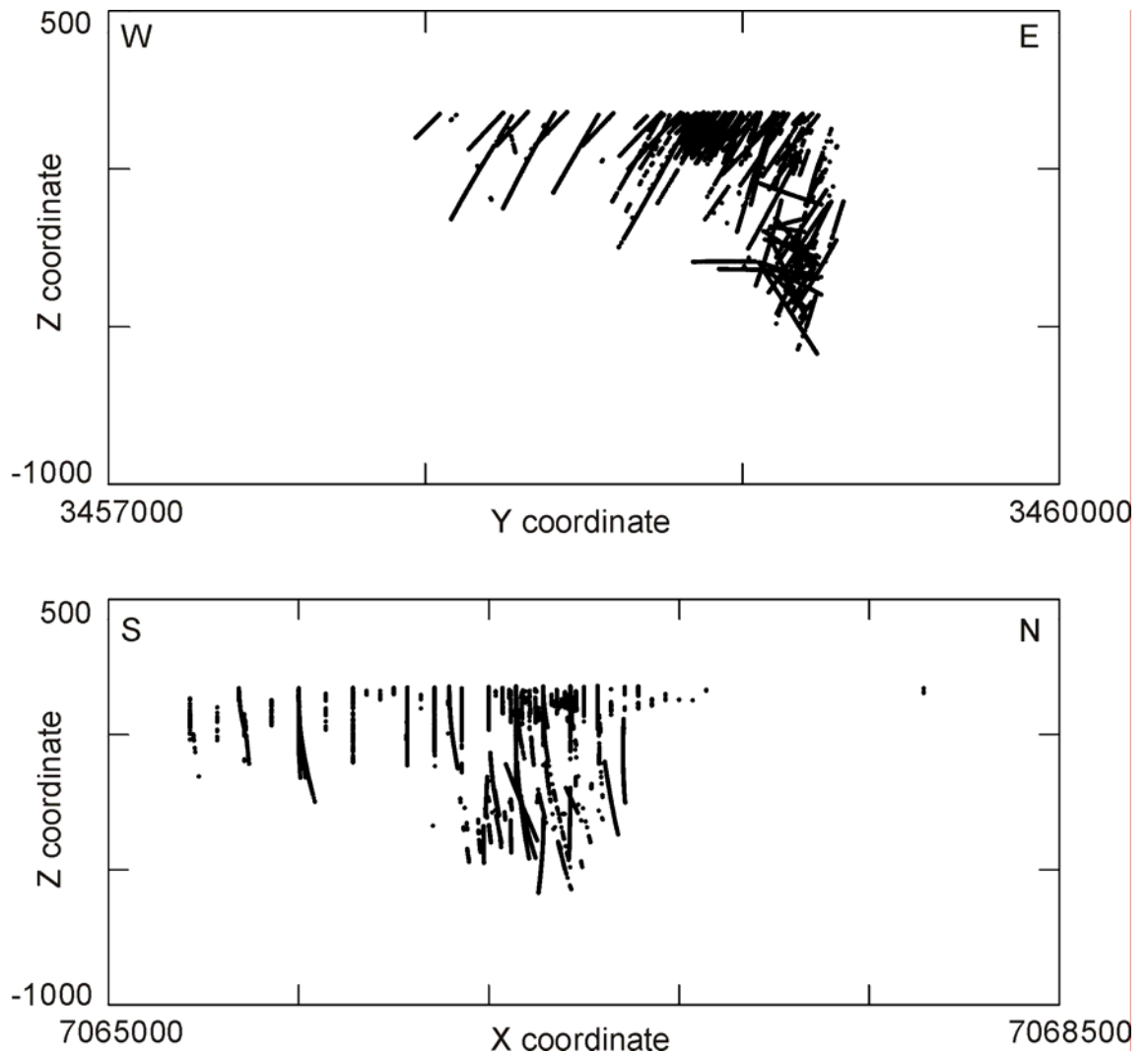


Figure C7. Diamond drill core samples at Mullikkoräme projected on W-E and N-S vertical profiles.

C 1.3 DATA PREPARATION

Before the chemical data could be used, it had to be included into an internally consistent database containing lithological, mineralogical and geographic information on the samples. To achieve internal consistency, the old and new analysis results were compared and calibrated. The resulting database was used to study the geochemical characteristic of the volcanites at the Pyhäsalmi and Mullikkoräme mines and their surroundings.

C 1.3.1 Comparison of old and new analyses

Before it was possible to use the old and new analysis results together, they were compared for possible biases and differences in level. The 233 samples that were analyzed at both OM and GTK were used for the comparisons. The sample set spans compositions from felsic (148 samples) through intermediate (19 samples) to mafic (62 samples), and from least altered to strongly altered.

H. Puustjärvi (ed.)

08.11.06

Confidential

Element	OKU analysis			GTK analysis	VTT analysis	Substituted
Au ppm	AAS	1962	0.001			0.0005

Most elements analyzed have differing detection limits for the various analysis sets (OM, GTK, VTT, see Table C2). To unify the database, a single value that is lower than the lowest detection limit for the element in question was substituted for every value below the detection limit. Sc, As, Nb, Mo, Sb, La, Bi, Th, U and W were not used in further work due to their poor analytical quality (too high detection limits).

Comparison of the old and new analyses showed that overall correspondence between the old and new analyses is acceptable. However, for some elements (e.g. Al, Zr) there are marked differences in analytical quality according to the year when the analysis was made, the early years before 1987 usually being the most unreliable. There are no noticeable differences in analytical quality between various rock types. Correlation between the old and new analyses in the test sample set is shown for selected elements in Figure C8.

C 1.3.2 Calibration of old analyses

To get an internally consistent database, the old OM analyses were calibrated to correspond to the new GTK and VTT analyses using linear regression for each element. When necessary, the old samples for each year were regressed separately. There are no new reference analyses for years 1979, 1992 and 1994. Consequently, old analyses for these years were not calibrated. Values below detection limit were not calibrated. In cases where the difference between the regressed and original values of an element was less than 5% of the original value, the original value was used instead of the regressed one. The regression equations used are given in Appendix C2.

C 1.3.3 Analysis method comparisons

All the XRF analyses used in the geochemical subproject are performed on pressed powder pellets. There was some uncertainty on how well the method works on highly altered rocks with high mica and chlorite contents. To clarify the issue, 124 samples were analyzed using both pressed pellets and glass disks. The samples represent compositions from unaltered to highly altered and from felsic to mafic. Comparisons showed that the pressed powder XRF analysis as performed in the chemical laboratory of the GTK is reliable for both the unaltered and altered felsic and mafic volcanites of the study area. The largest differences between the fused disc and pressed powder results are for SiO₂ in very silica-rich felsic volcanites (SiO₂ > 70%), and even these are relatively small (Fig. C9).

H. Puustjärvi (ed.)

08.11.06

Confidential

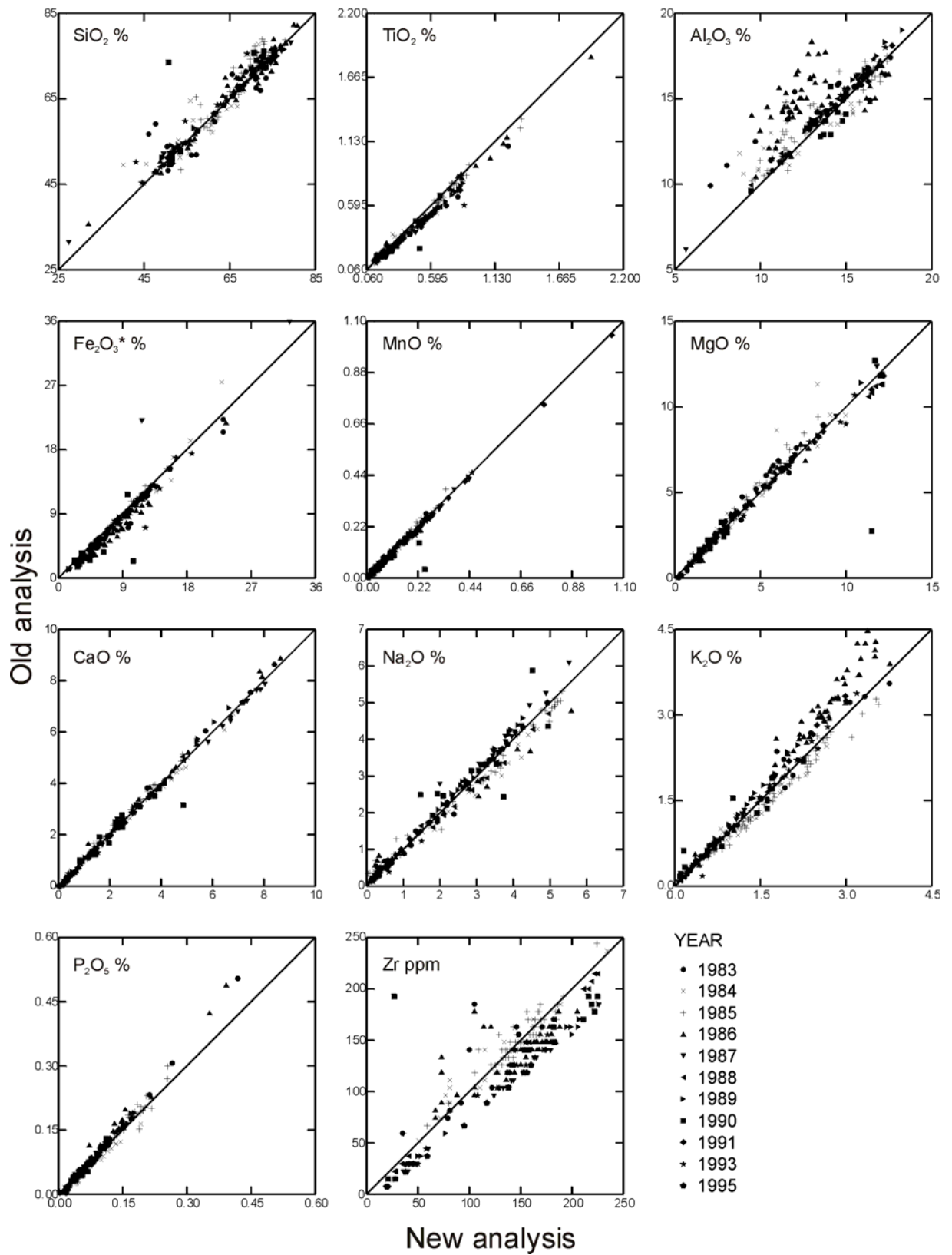


Figure C8a. Comparison of the old analyses made by Outokumpu Mining (OKU) with the new analyses made by the Geological Survey of Finland (GTK) for this project. All elements in the diagram were analyzed by XRF.

H. Puustjärvi (ed.)

08.11.06

Confidential

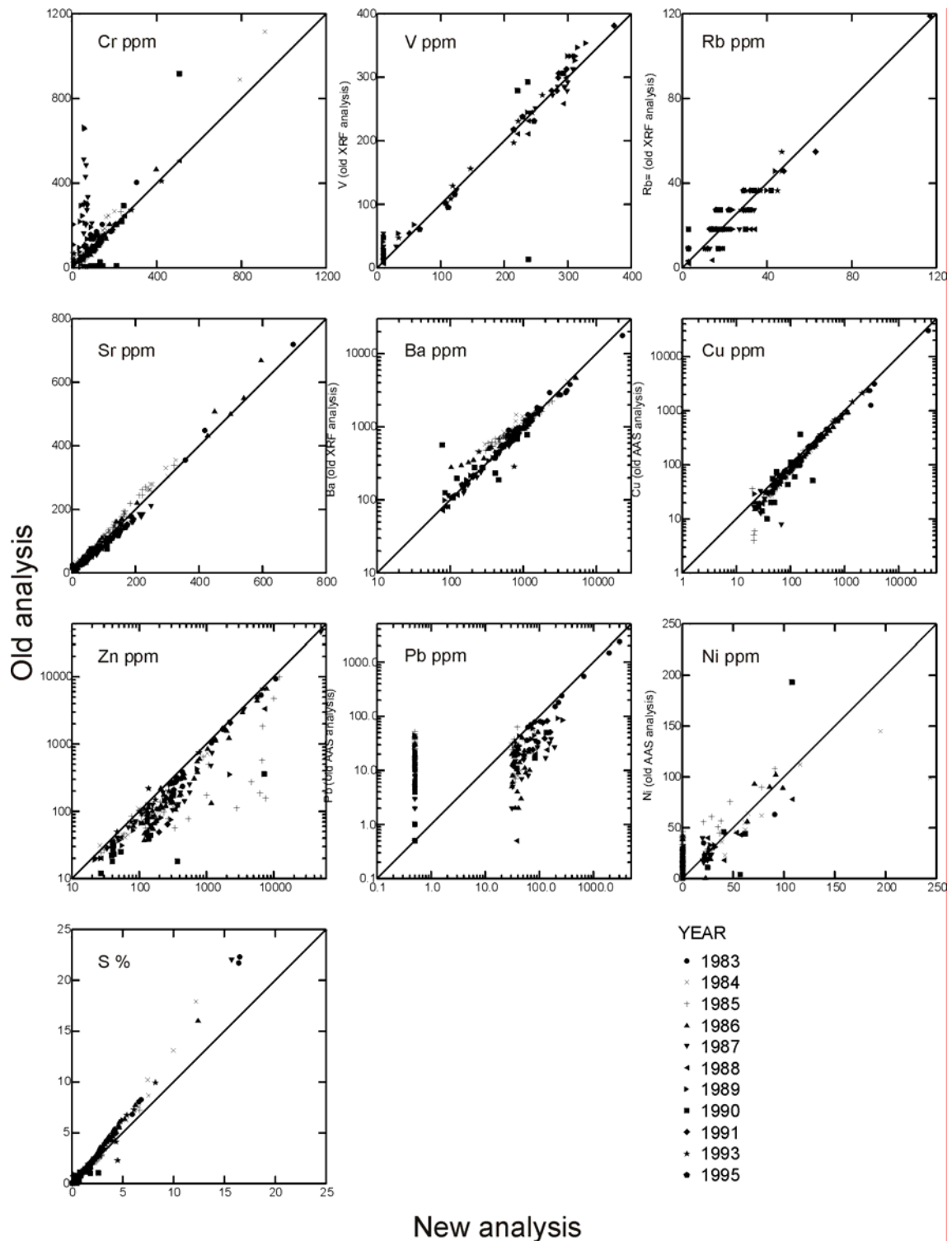


Figure C8b. Comparison of the old analyses made by OKU with the new analyses made by the GTK for this project. Cu, Zn, Pb and Ni were analyzed using AAS by OKU and using XRF by the GTK. The other elements were analyzed by XRF.

H. Puustjärvi (ed.)

08.11.06

Confidential

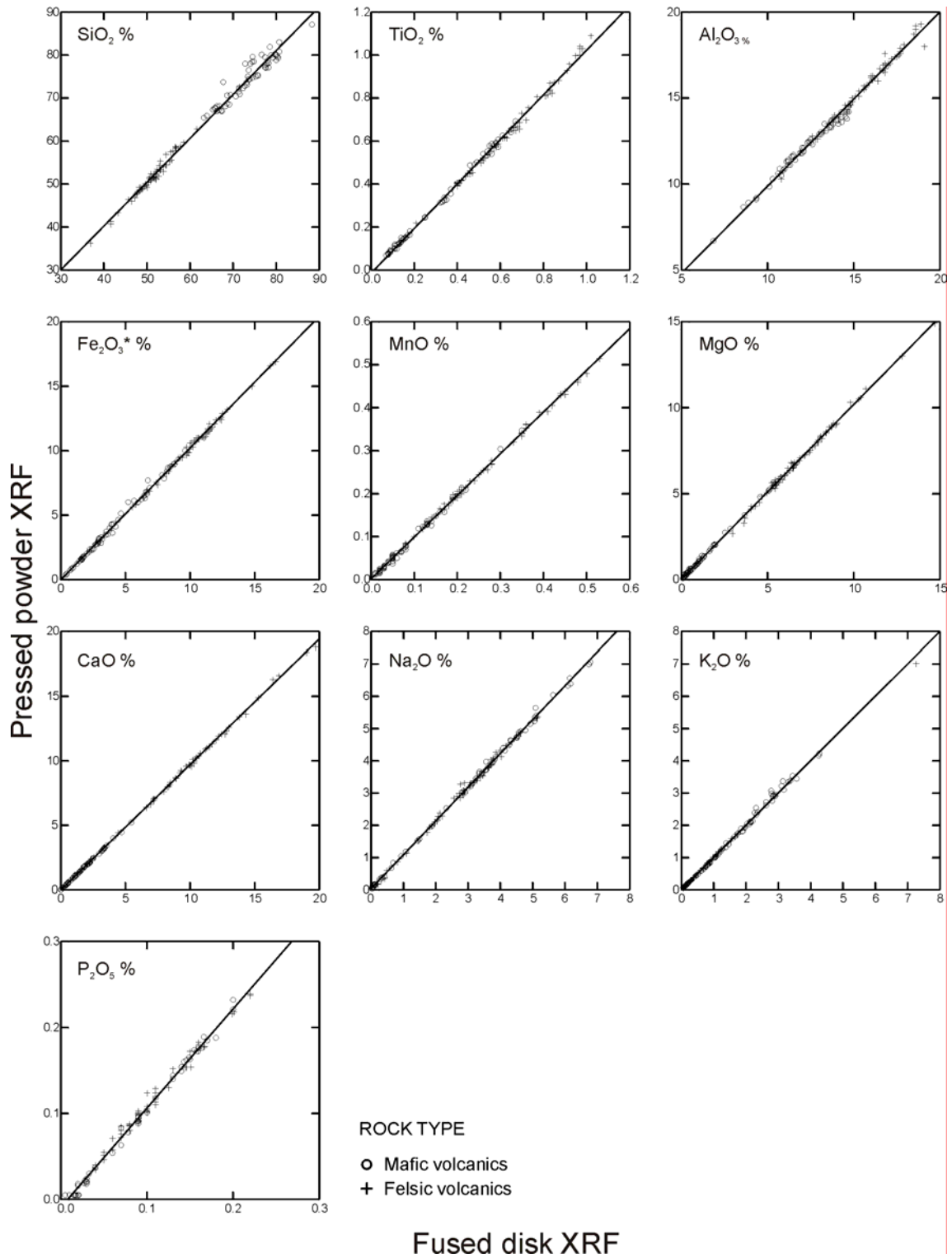


Figure C9. Comparison between pressed powder XRF and fused disk XRF results.

H. Puustjärvi (ed.)

08.11.06

Confidential

C 2 LITHOGEOCHEMICAL CHARACTERIZATION

C 2.1 GEOCHEMISTRY OF PRIMARY ROCKS

In addition to felsic, intermediate and mafic volcanites, the database includes analytical data on 11 rock types, including massive sulfide ore and many types of dikes and plutonic rocks. Only the volcanic rocks are considered in this report, because they dominate the area. The dikes and plutonic rocks have restricted occurrence, and at least some of them postdate ore formation. Most emphasis is placed on the felsic volcanic rocks, because they form the largest part of the volcanic succession and host ore at both Pyhäsalmi and Mullikkoräme. Mafic volcanites are also covered.

A large proportion of the samples used in the geochemistry subproject are altered and do not necessarily reliably depict the primary character of volcanism in the area. Hence, only the least-altered samples are used to characterize the primary geochemistry of the volcanites. Although it is logical to first describe the primary geochemistry of the volcanites and then proceed to characterize the alteration, it must be realized that the selection of the least-altered samples is based on studying the alteration, described later in this report. The least-altered felsic volcanic samples were defined with the following criteria:

- 1) Hashimoto index < 50 (see definition below)
- 2) S # 0.5 %
- 3) Cu # 50 ppm
- 4) Zn # 200 ppm
- 5) Pb # 100 ppm
- 6) Ba # 1000 ppm
- 7) No K enrichment in a $K_2O+Na_2O - K_2O/(K_2O+Na_2O)$ diagram
- 8) No reported alteration minerals.

For the least-altered mafic volcanites the criteria were:

- 1) Hashimoto index < 40
- 2) S # 0.5 %
- 3) Cu # 200 ppm
- 4) Zn # 200 ppm
- 5) Pb # 100 ppm
- 6) Ba # 1000 ppm
- 7) No K enrichment in a $K_2O+Na_2O - K_2O/(K_2O+Na_2O)$ diagram
- 8) No reported alteration minerals.

The Hashimoto index above is defined as follows (see chapter C 2.2.1):

$$100x(MgO+K_2O)/(MgO+CaO+Na_2O+K_2O).$$

The above criteria were selected after studying the geochemistry of the samples that were selected from as far from the ore as possible and that did not contain reported

H. Puustjärvi (ed.)

08.11.06

Confidential

alteration minerals. The least-altered samples were used to get a general idea of the primary geochemical character of the volcanites in the area and to derive estimates of background compositions to be used in mass transfer calculations.

In a Jensen (Al-Fe_{tot}+Ti-Mg) plot the felsic volcanites plot mostly in the tholeiitic rhyolite to dacite fields (Fig. C10). The Mullikkoräme felsic volcanites are slightly more Mg-rich and have a larger (but still small) proportion of the samples plotting in the calc-alkaline field than the Pyhäsalmi-Kettuperä volcanites. The mafic volcanites plot almost entirely in the high-Fe tholeiitic basalt field, with a few samples in the tholeiitic andesite field. According to their Zr/Y values, most of the least-altered felsic volcanites from both Pyhäsalmi-Kettuperä and Mullikkoräme are of transitional affinity and a small proportion of calc-alkaline affinity (Fig. C11). The mafic volcanites are mostly of tholeiitic affinity, but a small proportion of them shows a transitional to calc-alkaline affinity. In a SiO₂-Zr/TiO₂ diagram the least-altered felsic volcanites again plot mostly in the rhyolite and rhyodacite-dacite fields, whereas the least altered mafic volcanites trend from sub-alkaline basalt to andesite, with some samples in the alkali basalt field (Fig. C12). The felsic volcanites have several clusters of Zr/TiO₂ values, which can most clearly be seen when studying only the new chemical analyses made for this project (Fig. C13). For the new analyses, the average Zr/TiO₂ value for the Pyhäsalmi-Kettuperä felsic volcanites is higher (0.086) than for the Mullikkoräme felsic volcanites (0.052). For the mafic volcanites, there are no clear differences between the areas, nor are there clear clusters of Zr/TiO₂ values. The volcanic rocks were divided into subgroups based on the Zr/TiO₂ values. Nine subgroups were defined for the felsic volcanites, based on natural clustering of the Zr/TiO₂ values. For the mafic volcanites, two subgroups were defined. In addition, rocks that were reported as mafic volcanites but had Zr/TiO₂ values greater than 0.02 were discarded as probably altered felsic volcanites. For each subgroup, background composition was determined using the least-altered samples. The background compositions and subgroup classification criteria are given in Appendix C3.

There is a rough pattern in the areal distribution of the Zr/TiO₂ values. The lowest values generally occur furthest away from the massive sulfides for both the felsic and mafic volcanites, and the highest values occur near to the ore zones (Fig. C14). In the immediate altered wall rocks the Zr/TiO₂ values are again low. The drop to lower values of Zr/TiO₂ when approaching the ore at Pyhäsalmi corresponds fairly well to the beginning of visually detectable alteration. The Zr/TiO₂ levels are considered a primary feature since they are present in the least altered rocks. Hence, the correspondence between the drop to lower Zr/TiO₂ levels and the beginning of visual alteration can indicate a primary rock type control on the alteration process.

H. Puustjärvi (ed.)

08.11.06

Confidential

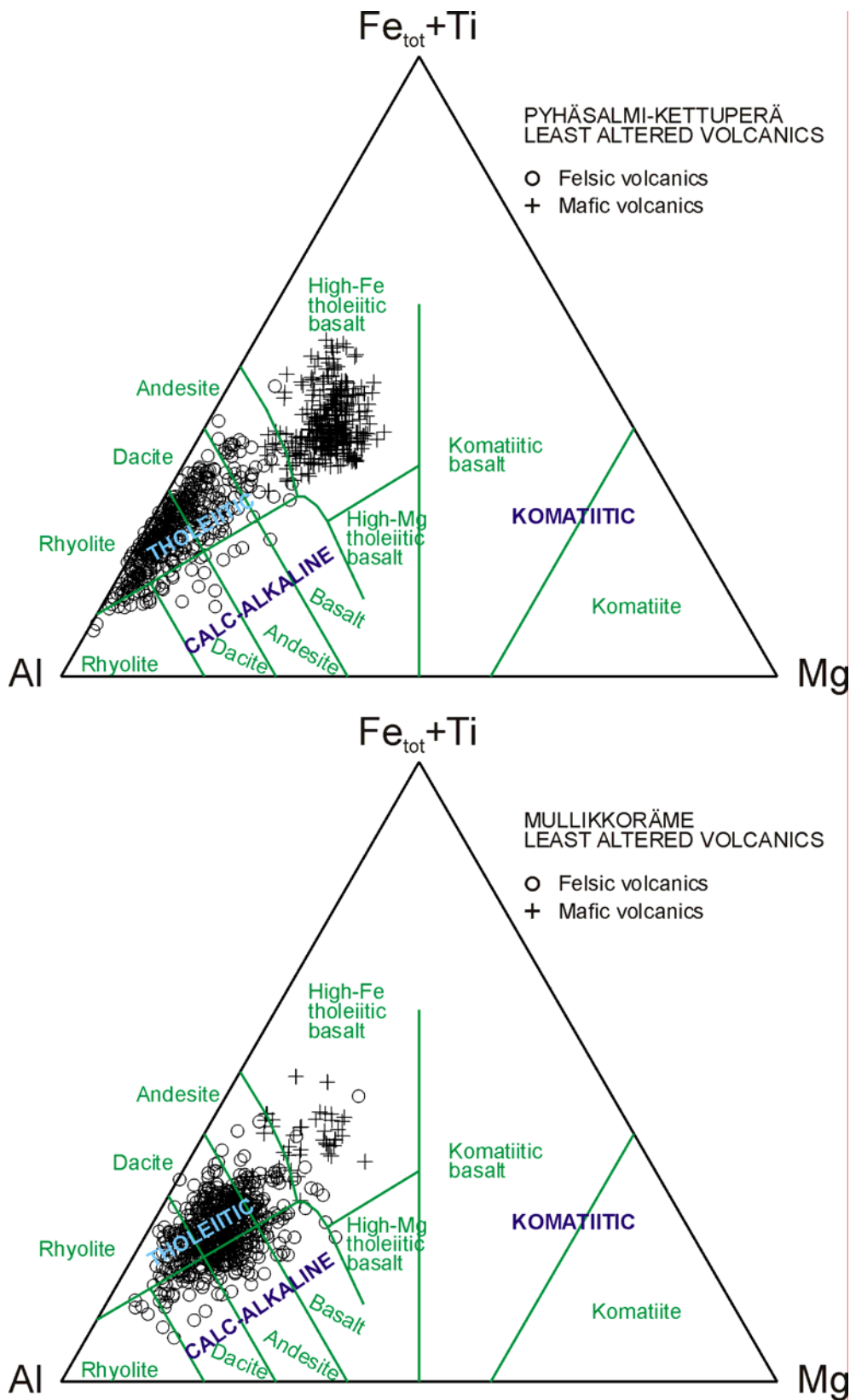


Figure C10. Jensen diagrams (Jensen 1976) for the least altered felsic and mafic volcanic rocks.

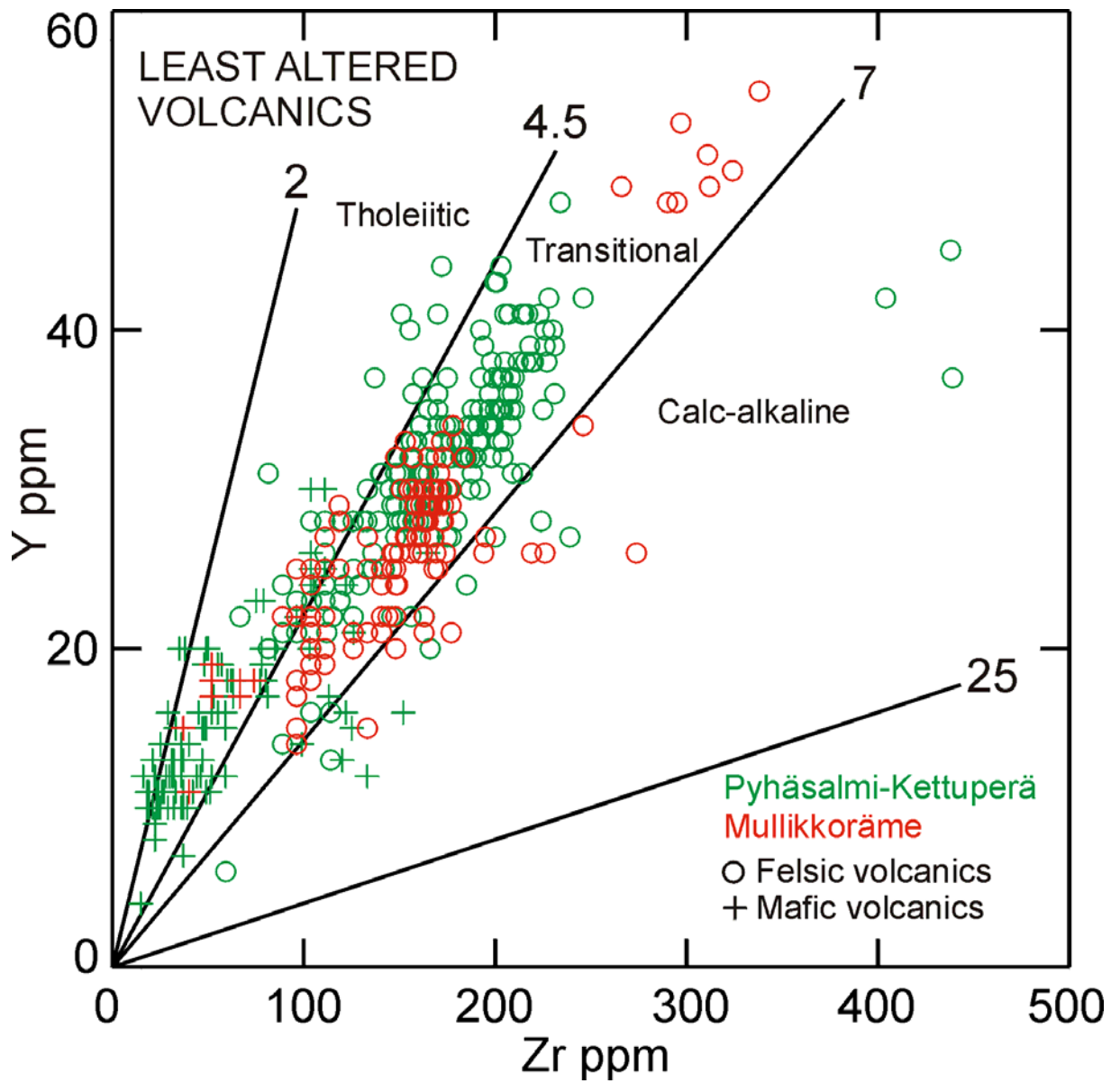


Figure C11. Chemical affinities of volcanites. The field boundaries are from Barrett and MacLean (1994).

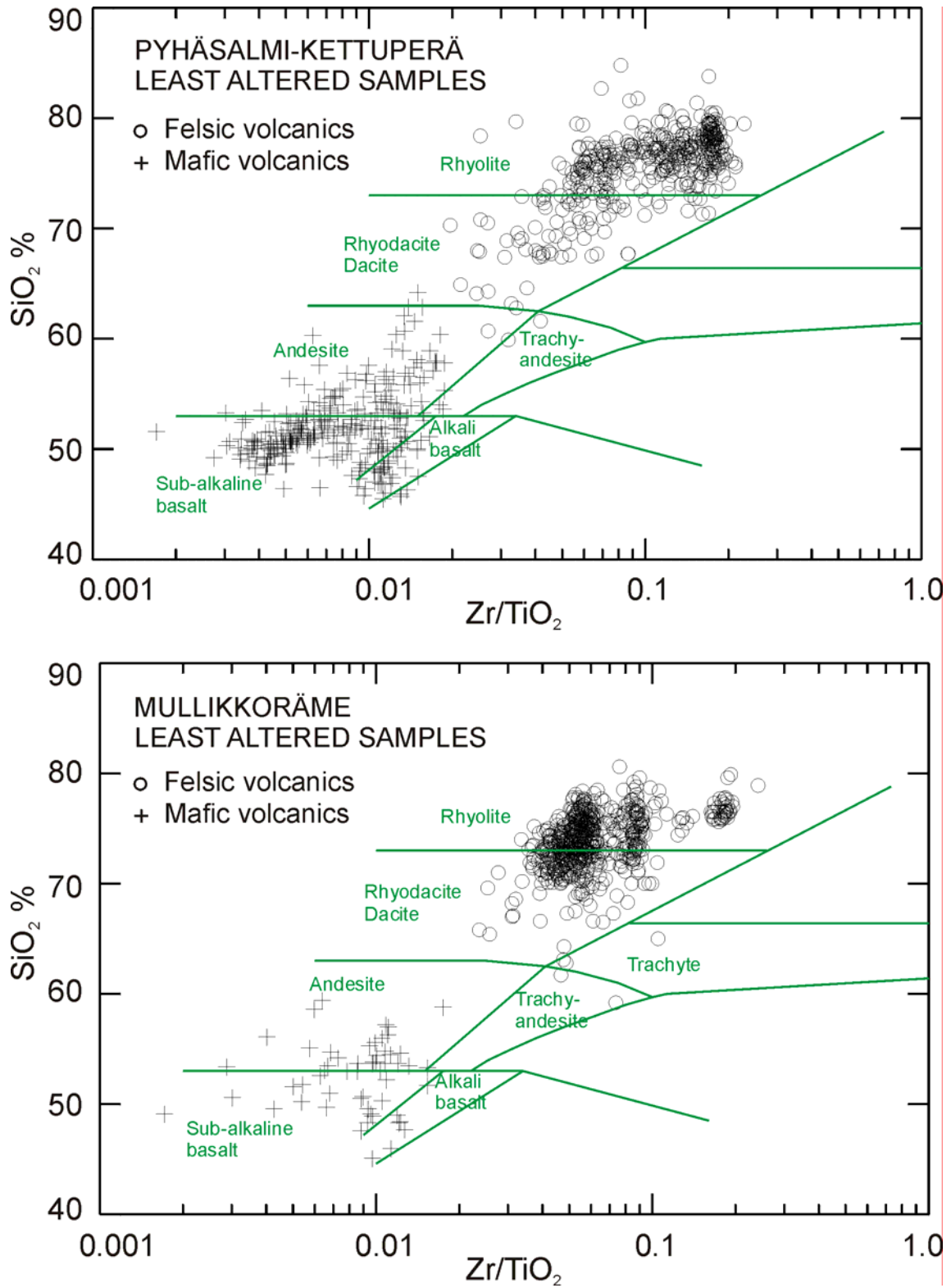


Figure C12. Zr/TiO₂ diagrams for the least altered volcanic rocks. The fields are from Winchester and Floyd (1977).

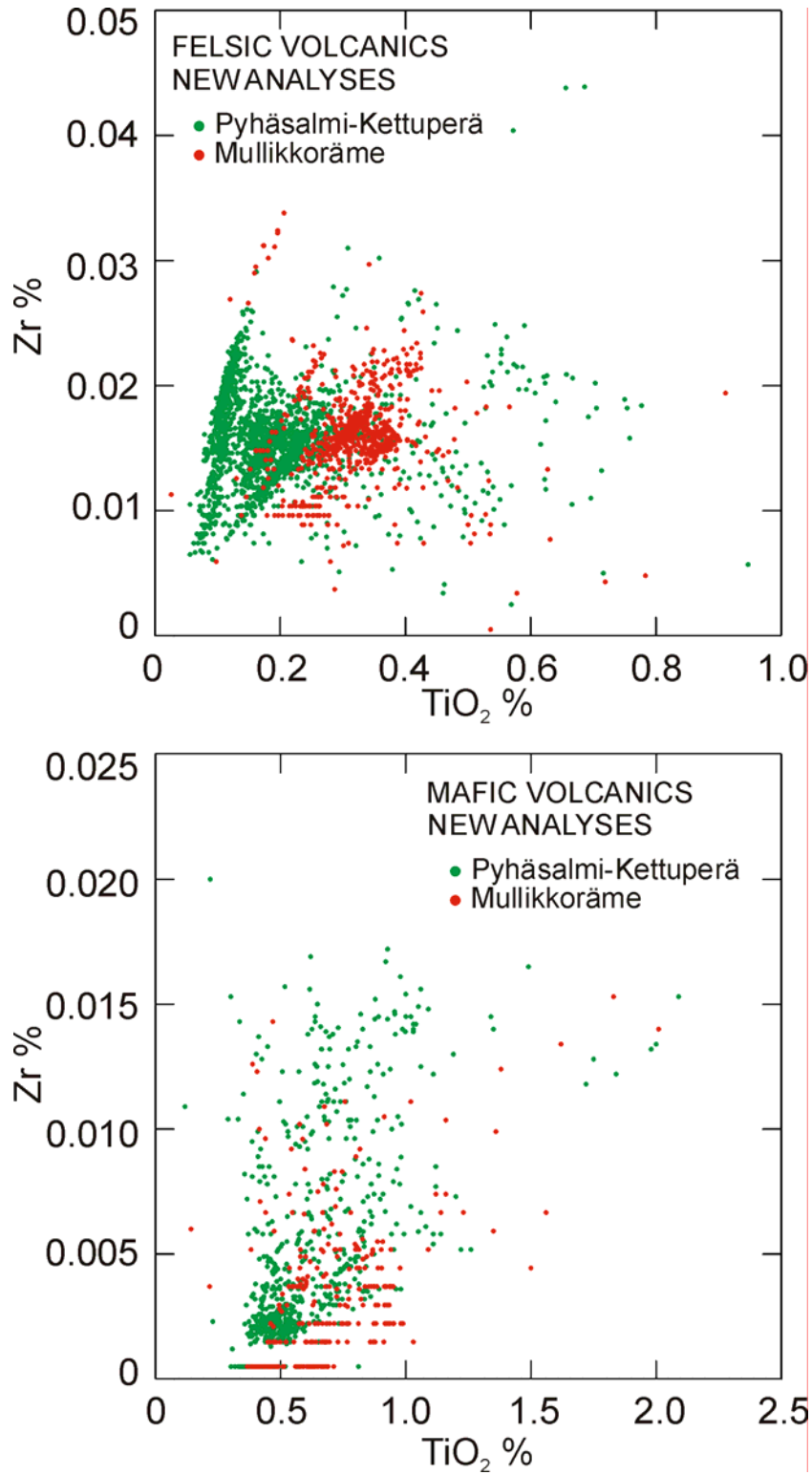


Figure C13. Variation of Zr/TiO₂ values for the volcanic rocks.

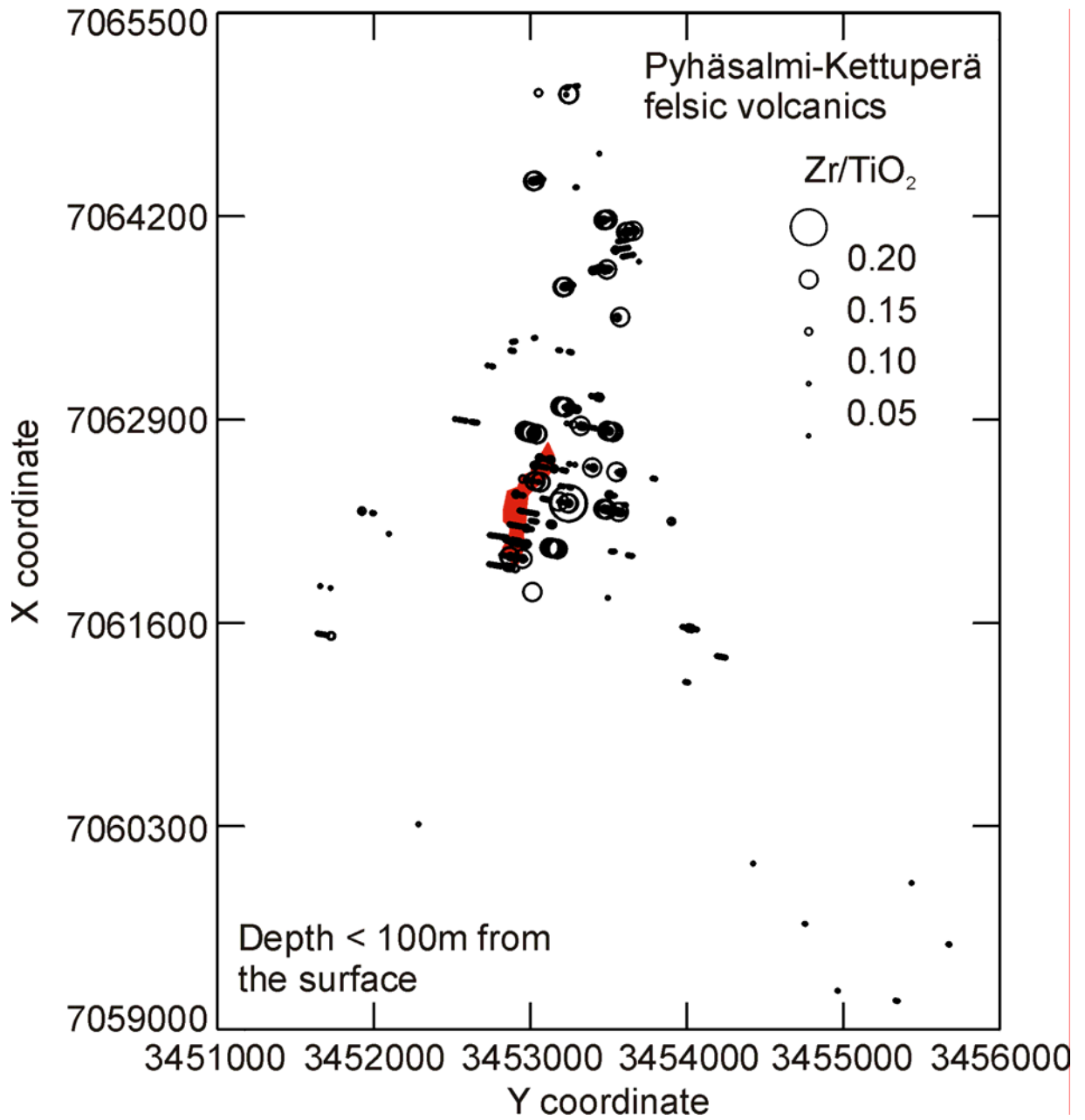


Figure C14a. Spatial distribution of the Zr/TiO₂ values at Pyhäsalmi-Kettuperä. For clarity, only samples less than 100 m below the surface have been used. The projection of the Pyhäsalmi orebody on the surface is shown in red.

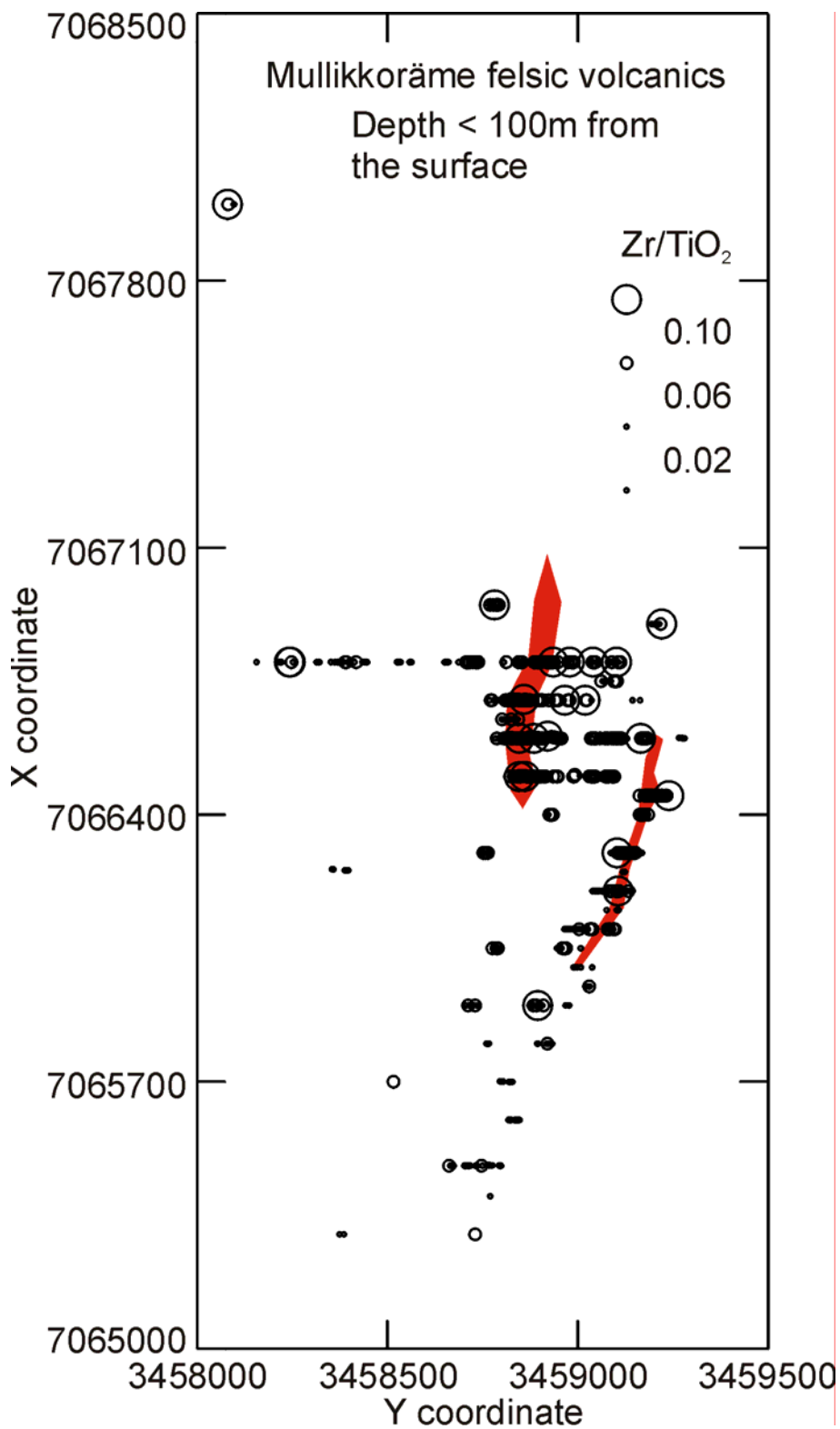


Figure C14b. Spatial distribution of the Zr/TiO₂ values at Mullikkoräme. For clarity, only samples less than 100 m below the surface have been used. The projections of the Mullikkoräme orebodies on the surface are shown in red.

H. Puustjärvi (ed.)

08.11.06

Confidential

C 2.2 GEOCHEMICAL ALTERATION

C 2.2.1 General characteristics

The most ubiquitous alteration minerals in the samples used in this study are sericite, cordierite, chlorite, phlogopite and sulphide minerals. This suggests that chemical alteration is characterized by alkali gains and losses, sulphur and ore metal gains, and possibly Mg and Fe gains. On the scale of the whole data set, proximity to ore is reflected as larger variance and heightened concentrations of Fe, Mn, Mg, K (especially in mafic volcanites), LOI, S, Ba, Rb (especially in mafic volcanites), Cu, Zn, Pb, Co and Ag, and lowered concentrations of Ca, Na and Sr. However, the behavior of individual elements is irregular. A more reliable indicator of alteration is an index that contains more than one element. Here, the Hashimoto index (Franklin 1997, Ishikawa et al. 1976),

$$100x(\text{MgO}+\text{K}_2\text{O})/(\text{MgO}+\text{CaO}+\text{Na}_2\text{O}+\text{K}_2\text{O}),$$

is used to describe the intensity of alteration. This index is sensitive to the most important mineralogical changes observed at Pyhäsalmi and Mullikkoräme. For the whole data set, the values of the index have a rough positive correlation with Fe, Mg, K, LOI, Rb, Ba, S, Cu, Zn and Ag and a negative correlation with Ca, Na and Sr (Fig. C15). The high values of the index are most strongly due to strong depletion of Na and Ca, and to lesser degree to the enrichment of K and Mg.

In the Pyhäsalmi felsic volcanites, the index values over 50 define an at the surface approximately 125-250 m broad NE trending anomaly that quite accurately coincides the mapped distribution of visually observable alteration (Fig. C16). The width of the anomaly diminishes downward to 0-3 m at the depth of 1000 m. At Kettuperä, the index defines two N trending anomalies, approximately 50 m and 50-125 m wide, which accurately coincide visually defined altered zones. The eastern anomaly continues at least to the depth of 870 m. At Mullikkoräme, the high values of the index coincide the zones of visually altered felsic volcanites, but the chemical anomaly is narrower and not as continuous as in the Pyhäsalmi-Kettuperä area.

In a $\text{K}_2\text{O}+\text{Na}_2\text{O} - \text{K}_2\text{O}/(\text{K}_2\text{O}+\text{Na}_2\text{O})$ diagram (Fig. C17), the volcanites show both relative K and Na enrichment. Positive correlation of S with the $\text{K}_2\text{O}/(\text{K}_2\text{O}+\text{Na}_2\text{O})$ values indicates that mineralization was related to K enrichment and Na depletion. The diminishing of the total alkali contents with the increase of the $\text{K}_2\text{O}/(\text{K}_2\text{O}+\text{Na}_2\text{O})$ values for the felsic volcanites again stresses the relatively greater importance of Na depletion. The Na enrichment that is most strong for the least-altered samples is considered to predate mineralization.

Some kind of primary rock type control on alteration is suggested by the occurrence of continuous zones of weakly altered felsic volcanites with high Zr/TiO₂ values within areas of more strongly altered felsic volcanites with lower Zr/TiO₂ values in many drillhole profiles at Pyhäsalmi (Fig. C18).

H. Puustjärvi (ed.)

08.11.06

Confidential

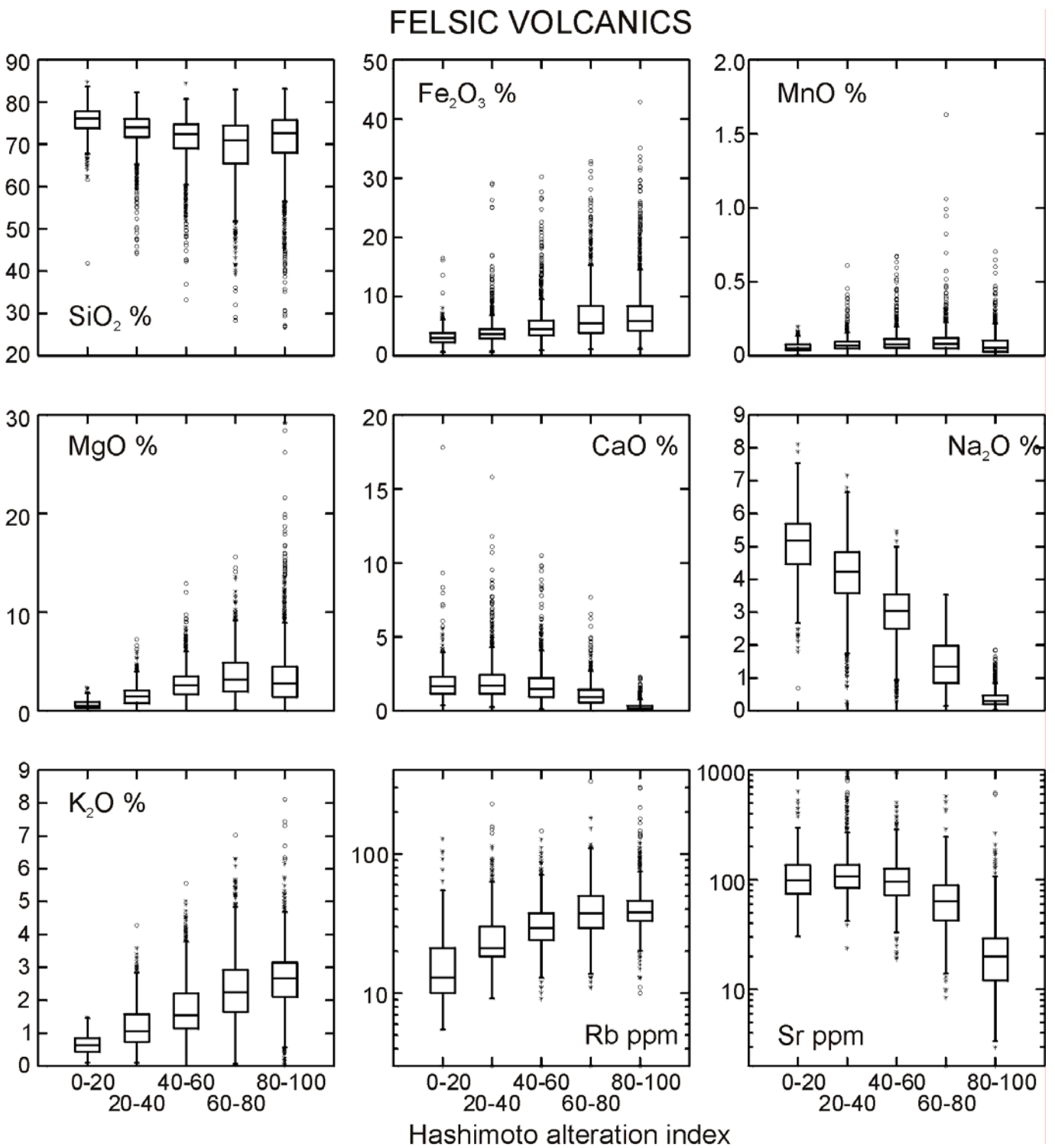


Figure C15a. Variation of element concentrations with the values of the Hashimoto alteration index for the felsic volcanic rocks.

H. Puustjärvi (ed.)

08.11.06

Confidential

FELSIC VOLCANICS

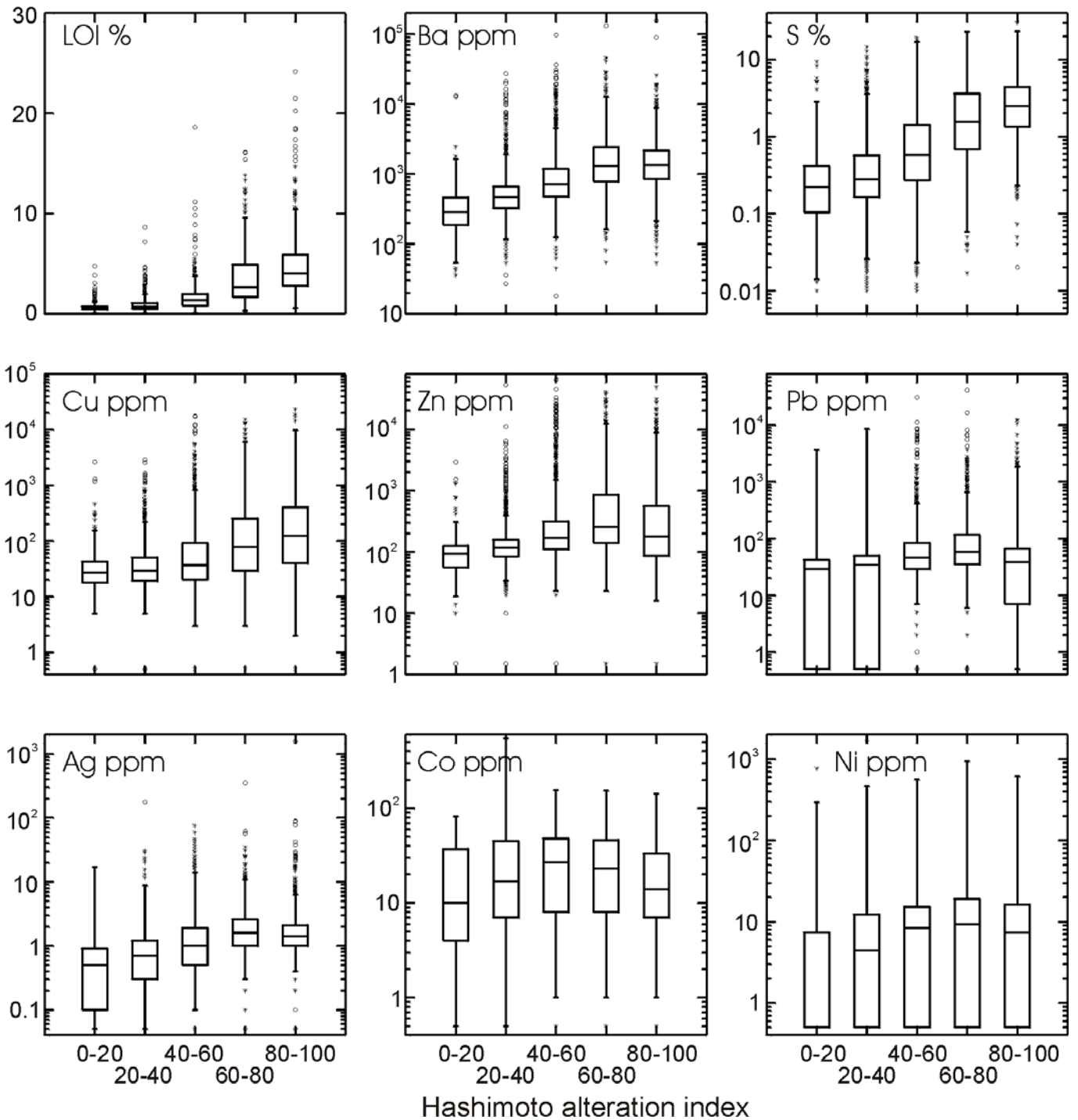


Figure C15b. Variation of element concentrations with the values of the Hashimoto alteration index for the felsic volcanic rocks.

H. Puustjärvi (ed.)

08.11.06

Confidential

MAFIC VOLCANICS

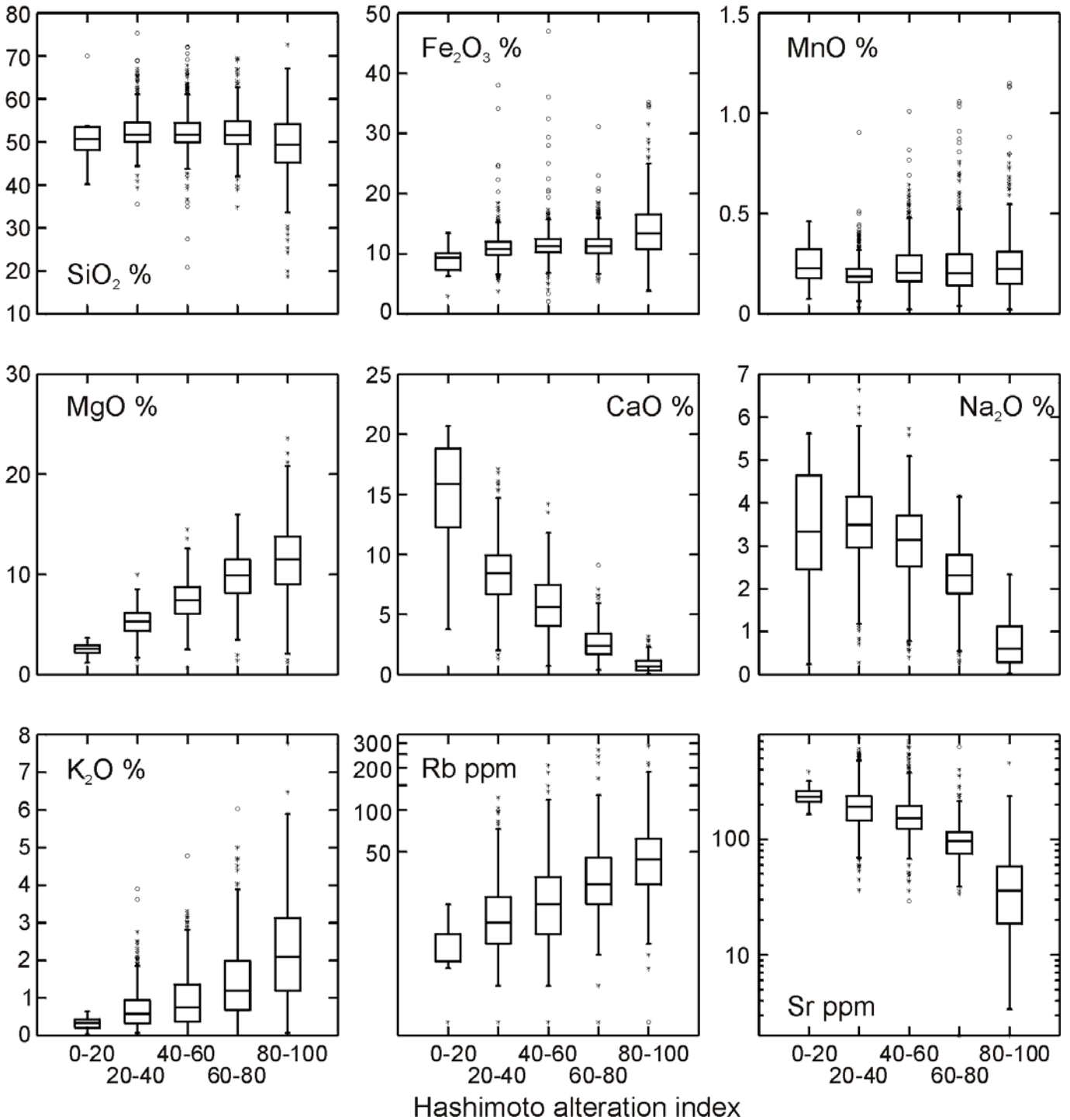


Figure C15c. Variation of element concentrations with the values of the Hashimoto alteration index for the mafic volcanic rocks.

H. Puustjärvi (ed.)

08.11.06

Confidential

MAFIC VOLCANICS

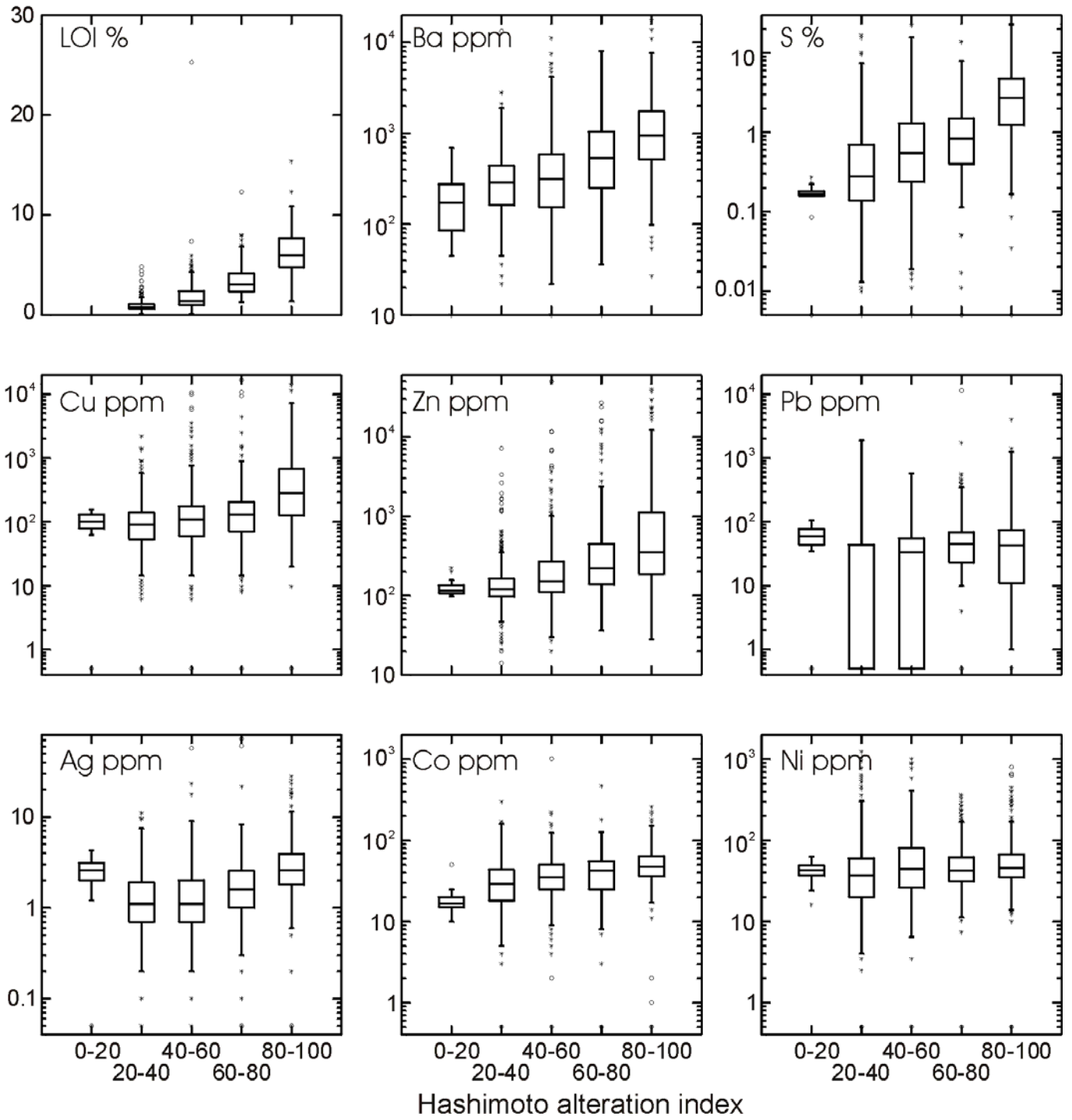


Figure C15d. Variation of element concentrations with the values of the Hashimoto alteration index for the mafic volcanic rocks.

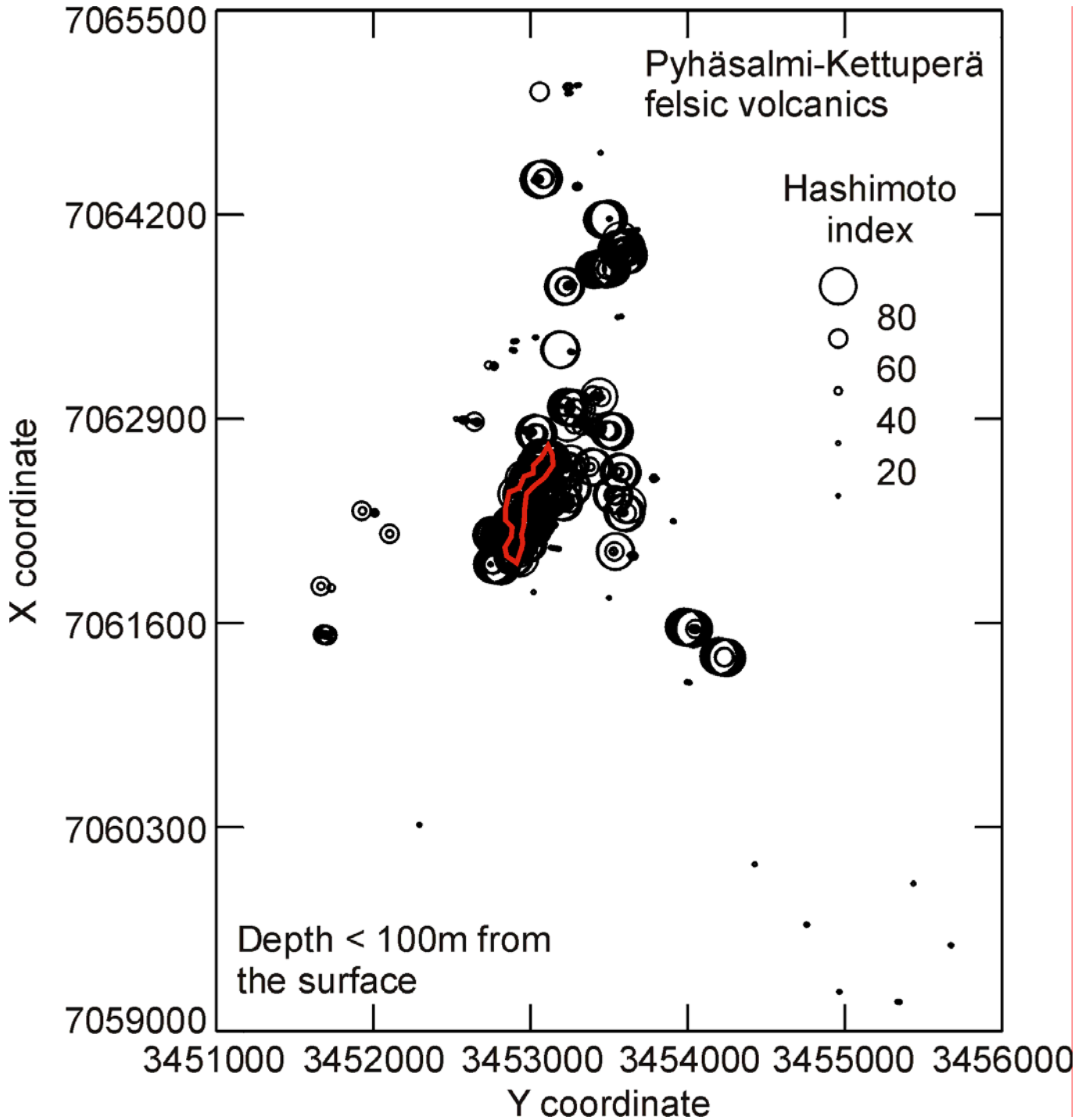


Figure C16a. Spatial distribution of the values of the Hashimoto alteration index at Pyhäsalmi-Kettuperä. For clarity, only samples less than 100 m below the surface have been used. The projection of the Pyhäsalmi orebody on the surface is shown in red.

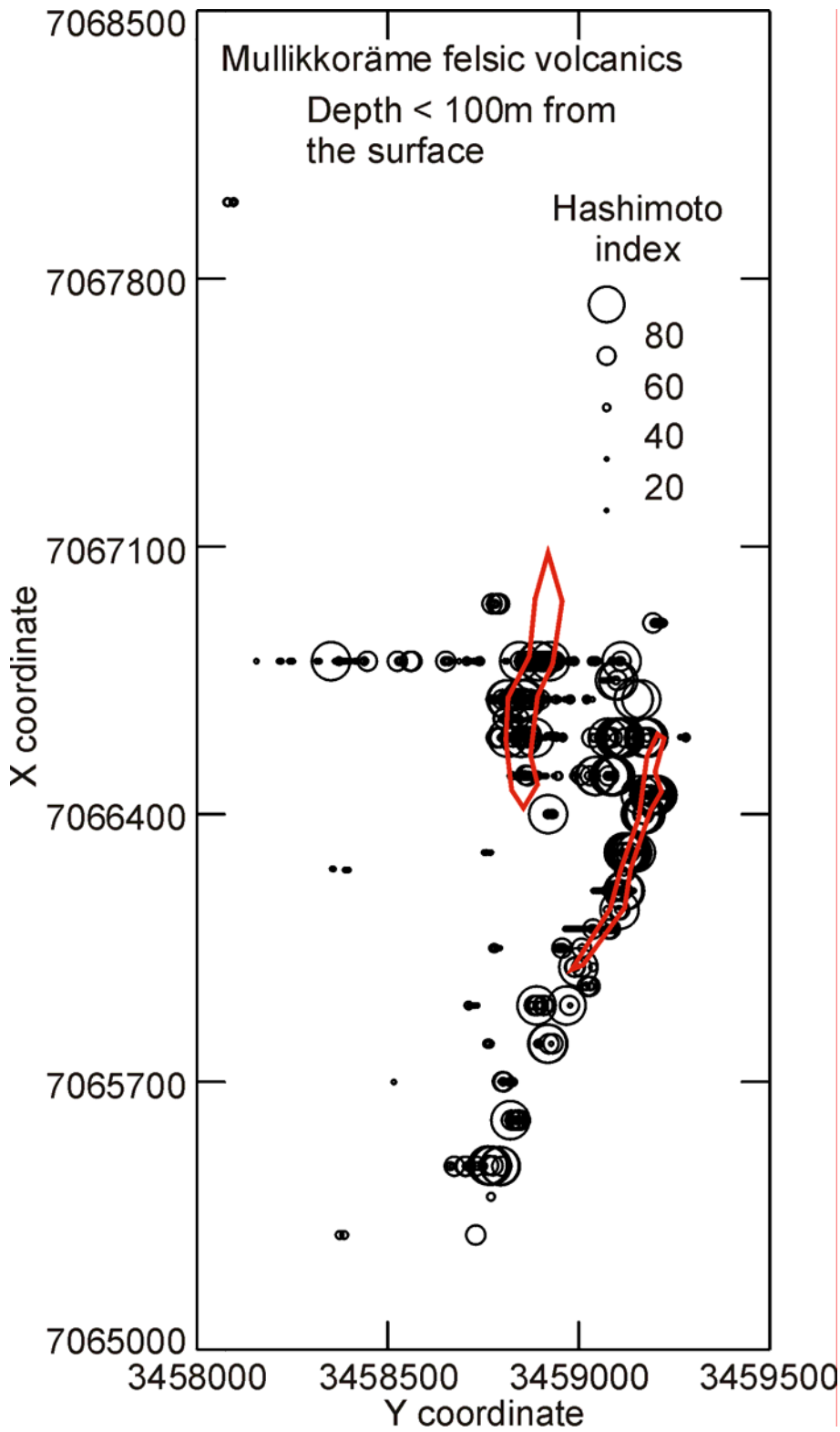


Figure C16b. Spatial distribution of the values of the Hashimoto alteration index at Mullikkoräme. For clarity, only samples less than 100 m below the surface have been used. The projections of the Mullikkoräme orebodies on the surface are shown in red.

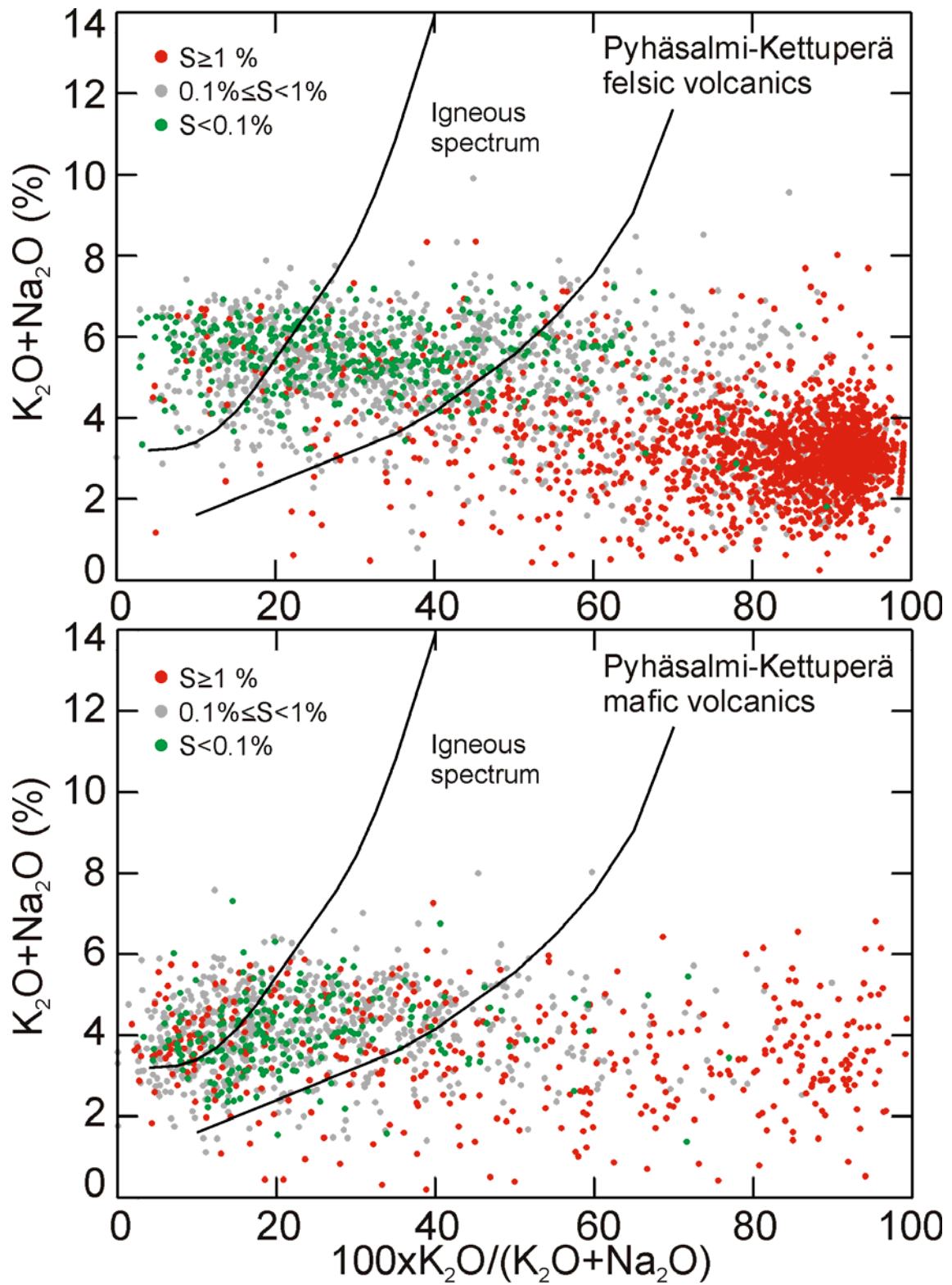


Figure C17a. The relation between alkali enrichments and depletions and sulphur concentrations at Pyhäsalmi-Kettuperä. The boundaries of the igneous spectrum are from Hughes (1973).

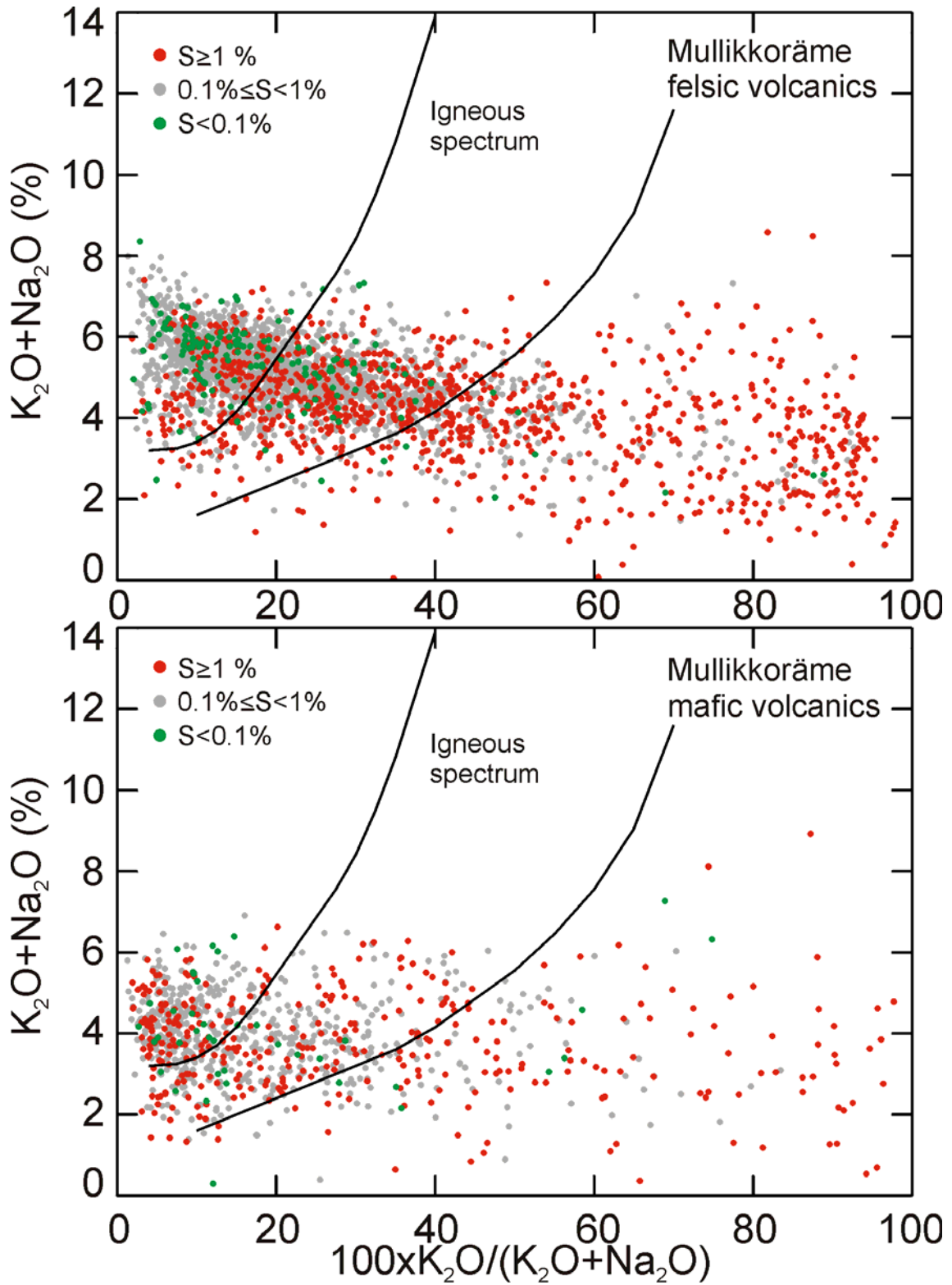


Figure C17a. The relation between alkali enrichments and depletions and sulphur concentrations at Pyhäsalmi-Kettuperä. The boundaries of the igneous spectrum are from Hughes (1973).

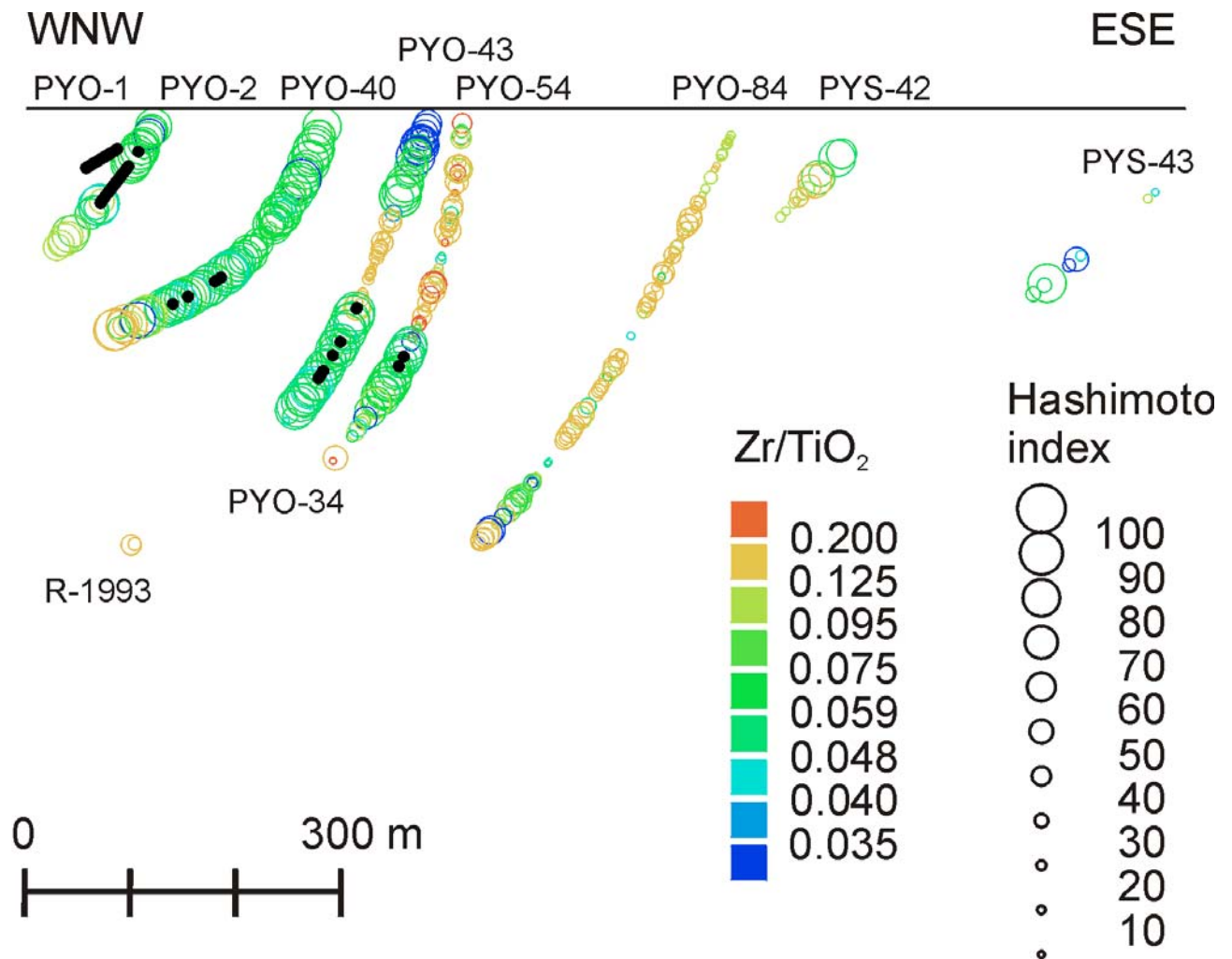


Figure C18. An example of the relation between the Zr/TiO₂ values and intensity of alteration in a WNW-ESE vertical profile at Pyhäsalmi. The black dots represent ore samples.

C 2.2.2 Alteration mineralogy of volcanites (H. Puustjärvi)

H. Puustjärvi (ed.)

08.11.06

Confidential

Lithologies of all relogged and new drillholes were categorized according to three identifiable minerals (Alt A, -B, -C). A standard procedure was used for coding lithologies in the old drillhole data, at least when it was possible to do so according to mineralogical rock names or as based on assays (see Table A1).

Mineralogical features in volcanites were compared with their alteration classification. The Hashimoto alteration index was used.

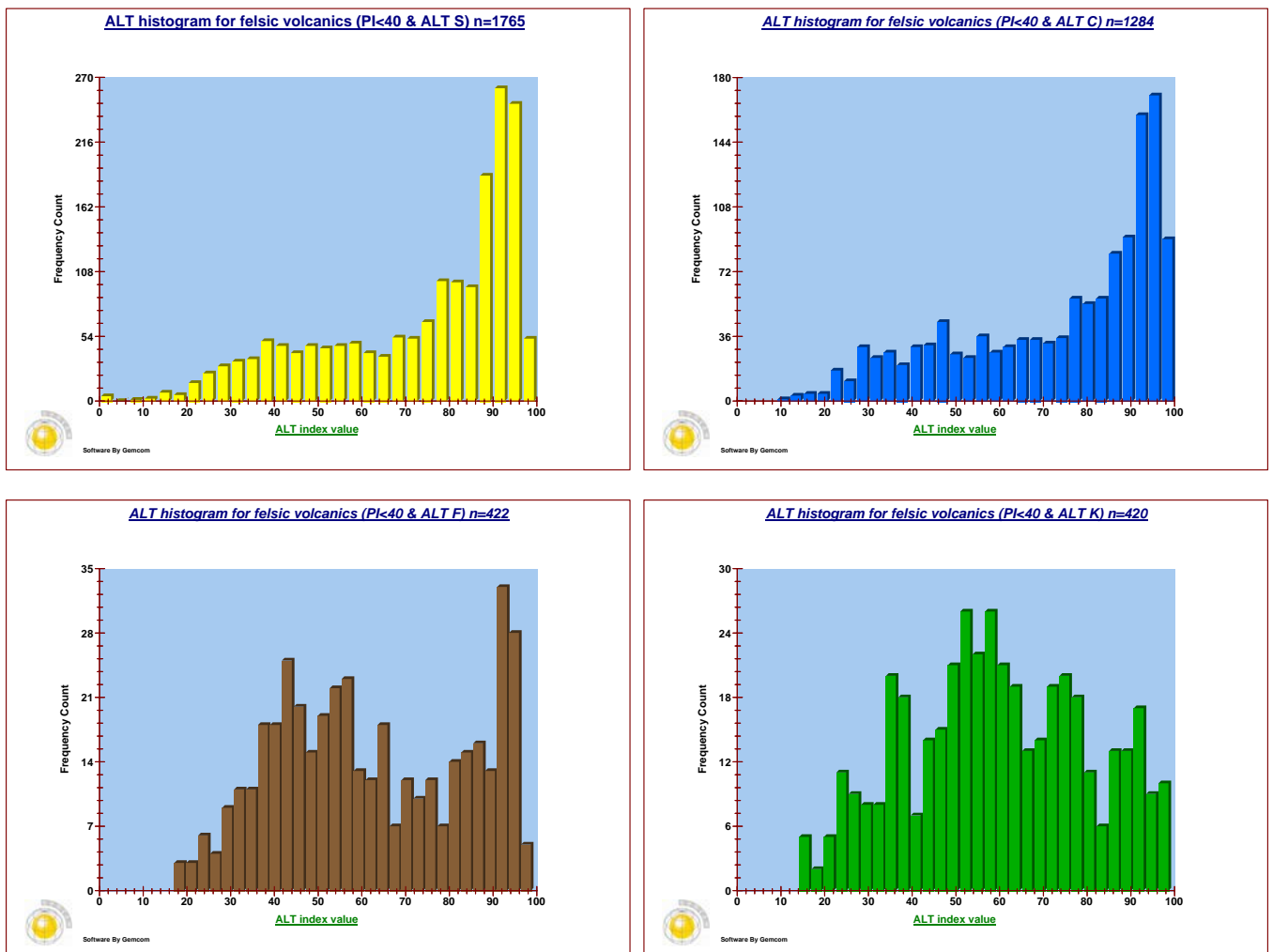


Figure C19. Frequency distribution diagrams of alteration mineralogy for logged felsic volcanites in different alteration index categories. PI count is the protolith index (TiO₂/ZrO₂) used to classify volcanites (see C 2.2.4). ALT S, C, F and K refer to the most important identified alteration minerals (sericite, cordierite, phlogopite, chlorite). ALT index values are calculated as $100(K_2O+MgO)/(K_2O+MgO+Na_2O+CaO)$.

H. Puustjärvi (ed.)

08.11.06

Confidential

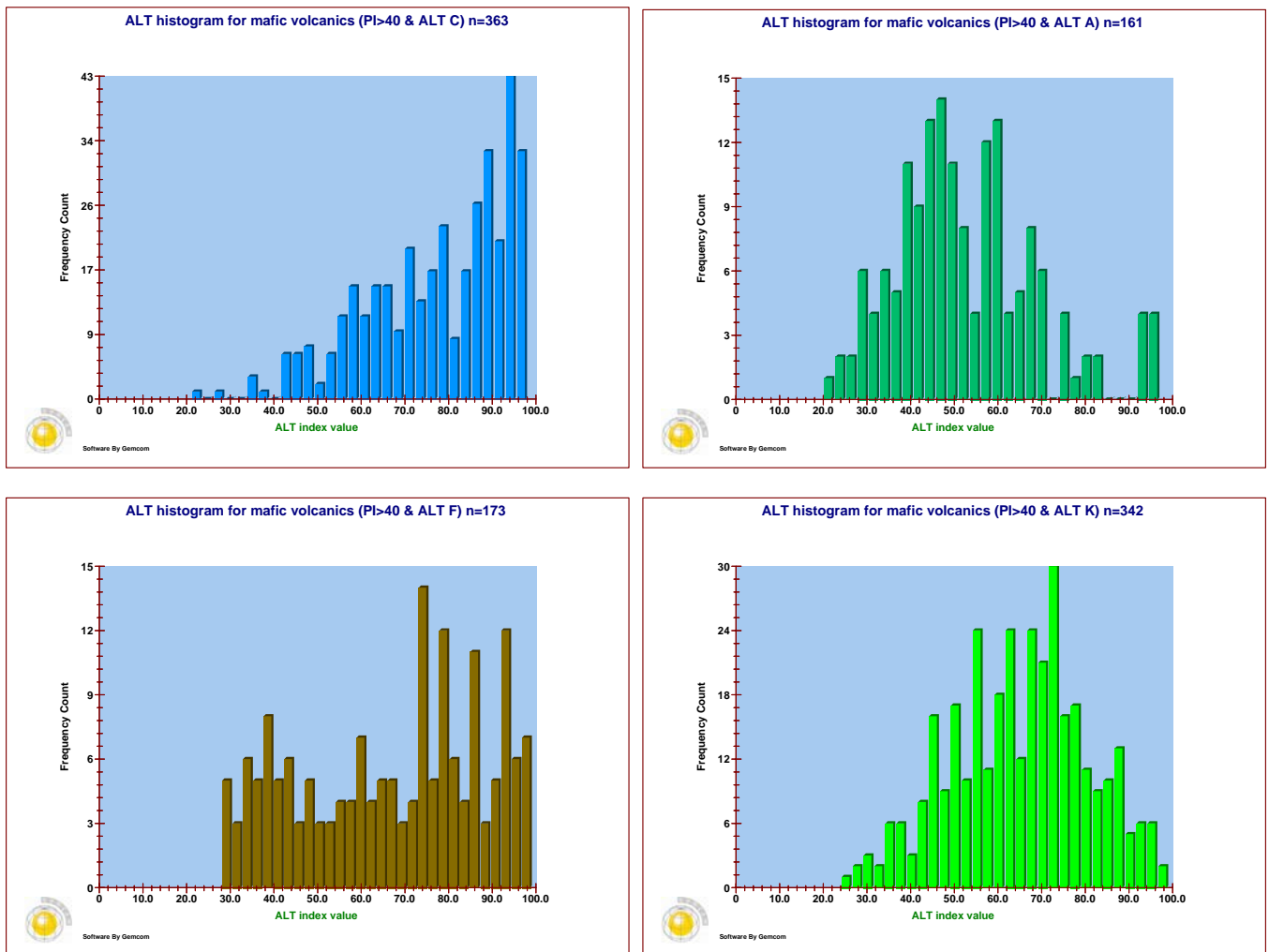


Figure C20. Frequency distribution diagrams of alteration mineralogy for logged mafic volcanites in different alteration index categories. PI count is the protolith index ($\text{TiO}_2/\text{ZrO}_2$) used to classify volcanites (see C 2.2.4). ALT C, A, F and K refer to the most important identified alteration minerals (cordierite, amphibole, phlogopite, chlorite). ALT index values are calculated as $100(\text{K}_2\text{O}+\text{MgO})/(\text{K}_2\text{O}+\text{MgO}+\text{Na}_2\text{O}+\text{CaO})$.

Figure C19 shows that, in the Pyhäsalmi–Mullikkoräme area, the intensity of VMS-style K- and Mg-enrichment in felsic volcanites correlates with quantities of sericite and cordierite and that the appearance of phlogopite and chlorite possibly indicates a broader and lower-intensity alteration event. The latter could be related to an earlier process predating the one that produced the sericite-cordierite alteration enveloping VMS mineralisation. High phlogopite frequencies indicate intense alteration and are typical for Mullikkoräme where phlogopite+/-chlorite occurs as stringers and veinlets.

Figure C20 displays corresponding diagrams for mafic volcanites. The amount of cordierite, followed by chlorite and amphibole (mostly orthoamphibole) is the best indicator for alteration intensity. Phlogopite seems to be present in every alteration category.

The above-presented correlations are a straightforward approach, yet practical in drillcore logging for exploration purposes. Complexities into this are due to the protolith

H. Puustjärvi (ed.)

08.11.06

Confidential

nature of volcanites (pure-re-sedimented-mixed) and progressive or retrograde metamorphism (see section B 4.5 by A-P Tapio).

C 2.2.3 Alteration categories and element enrichment/depletion (H. Puustjärvi)

To study compositions of altered lithologies the project Gemcom database assay data were grouped according to protolith index ($PI = TiO_2/ZrO_2$) and evenly (at 20% classes) categorised ALT index values ($ALT = 100(K_2O+MgO)/(K_2O+MgO+Na_2O+CaO)$) separately for Pyhäsalmi and Mullikkoräme. Felsic volcanites display PI below 40, mafic ones over 40 (Table C3 and CD-ROM Excel files stahv.xls and staev.xls).

Alteration class means for felsic and mafic volcanites were compared with the mean compositions of the least-altered samples. It should be noted that the least-altered class for mafic volcanites in the Pyhäsalmi area has an ALT index value of 33 representing weakly altered rocks. Assayed means were compared between the 'mother' and 'daughter' products using the Minpet 2.02 software Hildreth style diagram plotting, which allowed the calculation and graphical presentation of element enrichment and depletion between the least-altered normalised compositions (unaltered O2 category) and progressive alteration products (Fig.C21 and CD-ROM files lithogeochemistry\enrichdeplet*.PRZ and *.wmf).

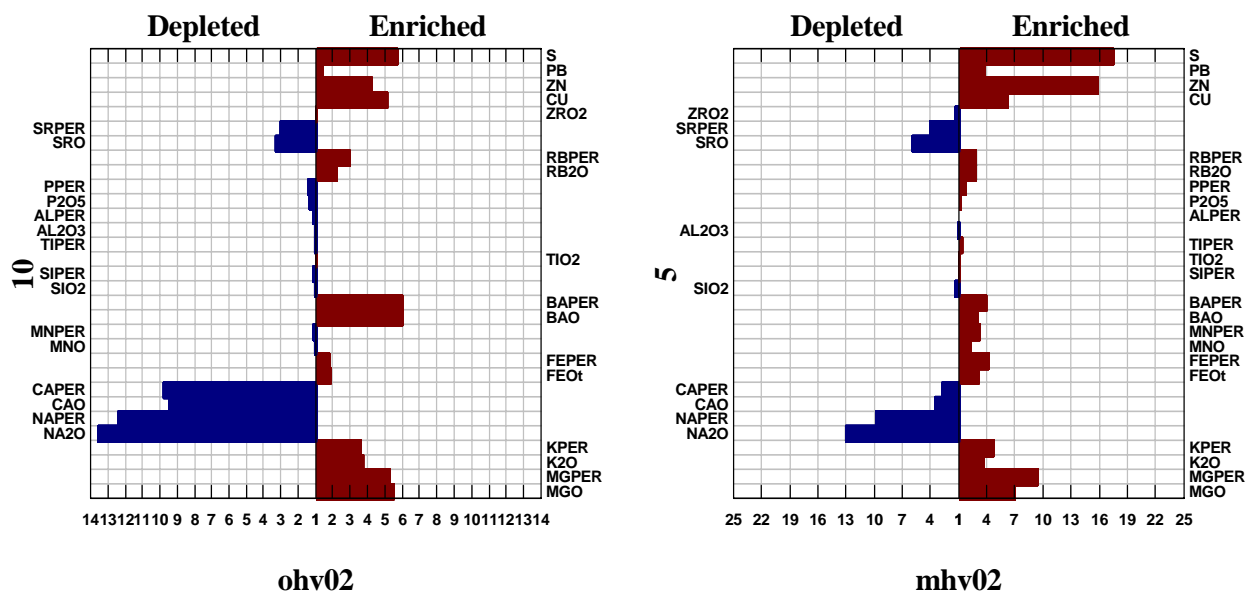


Figure C21. Diagrams exemplifying enrichment and depletion in most-altered felsic volcanites compared to least-altered ones at Pyhäsalmi and Mullikkoräme. ohv02 = OKP least altered felsics, mhv02 = OKMU least altered felsics. See text for *PER value explanations.

H. Puustjärvi (ed.)

08.11.06

Confidential

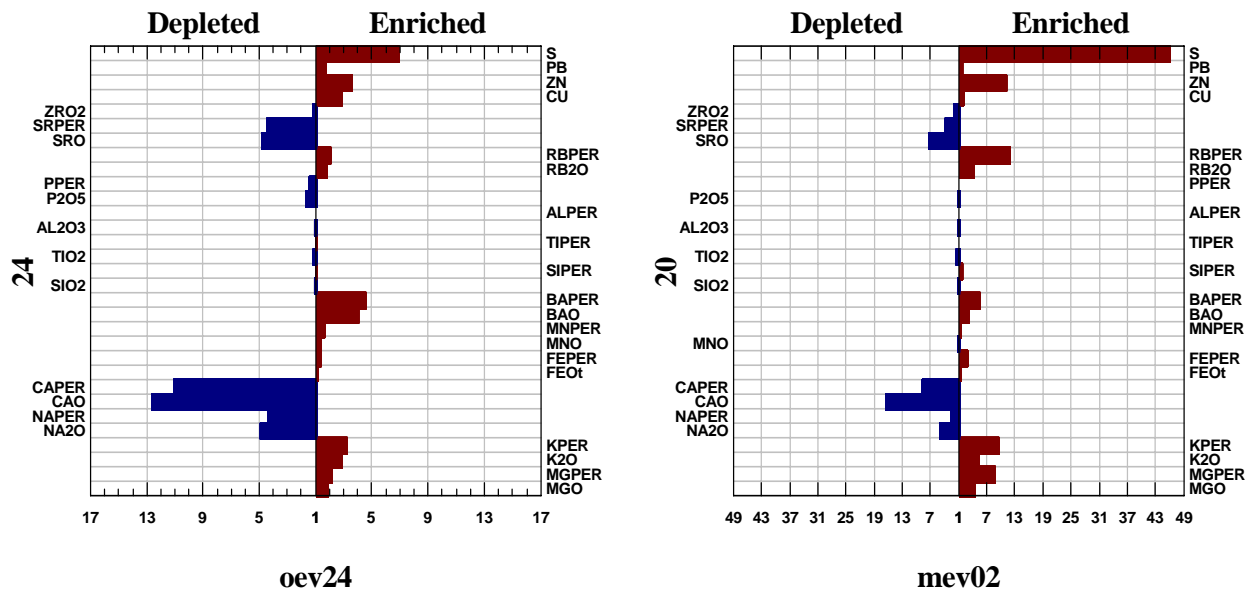


Figure C22. Diagrams exemplifying enrichment and depletion in most-altered mafic volcanites compared to the least-altered ones at Pyhäsalmi and Mullikkoräme. oev24 = OKP least altered mafics, mev02 = OKMU least altered mafics. See text for *PER value explanations.

Table C3.

Pyhäsalmi and Mullikkoräme volcanite mean (geometric) compositions (XRF%) for least altered and progressively altered classes.

SAMPLE	N	SIO ₂	TIO ₂	AL ₂ O ₃	FEO _t	MNO	MGO	CAO	RB ₂ O	SRO	BAO
hvm 02	143	68.57	0.225	11.56	2.59	0.049	0.92	1.37	0.0012	0.0123	0.03
hvm 24	979	69.94	0.271	12.52	3.28	0.071	1.83	1.55	0.0020	0.0123	0.05
hvm 46	846	63.68	0.260	11.48	4.74	0.091	3.16	1.51	0.0028	0.0105	0.11
hvm 68	432	54.55	0.229	9.79	8.15	0.116	5.11	1.27	0.0032	0.0067	0.16
hvm 81	313	52.98	0.241	10.18	8.45	0.120	6.57	0.39	0.0035	0.0021	0.09
hvo02	14	74.17	0.170	12.06	2.77	0.056	0.43	2.09	0.0021	0.0090	0.02
hvo24	88	69.73	0.257	13.13	3.83	0.076	1.29	2.70	0.0035	0.0158	0.08
hvo46	112	68.86	0.271	12.77	4.70	0.089	2.26	2.12	0.0041	0.0117	0.10
hvo68	216	69.44	0.204	11.49	5.14	0.071	2.21	0.98	0.0048	0.0066	0.17
hvo81	307	70.67	0.174	11.57	5.31	0.054	2.39	0.22	0.0048	0.0027	0.16
SAMPLE	N	SIO ₂	TIO ₂	AL ₂ O ₃	FEO _t	MNO	MGO	CAO	RB ₂ O	SRO	BAO
evm 02	20	51.68	0.688	17.47	7.02	0.246	2.63	12.95	0.0009	0.0242	0.01
evm 24	219	53.86	0.656	16.53	9.18	0.230	4.91	6.10	0.0013	0.0207	0.02
evm 46	396	50.93	0.574	15.40	10.17	0.244	7.75	5.13	0.0017	0.0151	0.02
evm 68	222	50.82	0.544	15.24	10.17	0.203	10.45	2.47	0.0027	0.0094	0.04
evm 81	66	49.18	0.499	13.93	11.12	0.225	12.23	0.79	0.0038	0.0033	0.06
evo24	76	53.32	0.576	16.29	9.40	0.177	4.75	7.84	0.0028	0.0199	0.03
evo46	71	52.49	0.638	16.32	9.86	0.191	6.61	5.73	0.0031	0.0215	0.08
evo68	101	53.49	0.624	15.83	10.11	0.211	8.13	2.05	0.0039	0.0096	0.09
evo81	76	50.87	0.509	15.90	11.39	0.253	9.15	0.62	0.0051	0.0041	0.12
SAMPLE	N	NA ₂ O	K ₂ O	ZRO ₂	P ₂ O ₅	CU	ZN	PB	S	PI	ALT
hvm 02	143	5.46	0.41	0.0175	0.055	0.0025	0.0059	0.0014	0.23	12	1
hvm 24	979	4.34	0.80	0.0189	0.066	0.0031	0.0086	0.0017	0.30	14	3
hvm 46	846	2.82	1.18	0.0176	0.068	0.0066	0.0303	0.0054	0.89	14	4
hvm 68	432	1.44	1.27	0.0135	0.076	0.0224	0.1311	0.0119	2.81	16	6
hvm 81	313	0.42	1.53	0.0133	0.077	0.0158	0.0936	0.0055	4.02	17	9
hvo02	14	4.22	0.73	0.0177	0.034	0.0030	0.0069	0.0040	0.51	9	1
hvo24	88	3.21	1.51	0.0194	0.056	0.0061	0.0157	0.0062	0.41	11	3
hvo46	112	2.14	2.08	0.0197	0.056	0.0089	0.0166	0.0060	0.64	12	5
hvo68	216	0.91	2.62	0.0182	0.036	0.0132	0.0349	0.0076	2.04	10	7
hvo81	307	0.31	2.76	0.0186	0.025	0.0156	0.0298	0.0060	2.92	8	8
SAMPLE	N	NA ₂ O	K ₂ O	ZRO ₂	P ₂ O ₅	CU	ZN	PB	S	PI	ALT
evm 02	20	3.99	0.25	0.0073	0.140	0.0069	0.0044	0.0019	0.03	94	1
evm 24	219	3.87	0.36	0.0051	0.141	0.0089	0.0114	0.0019	0.52	127	3
evm 46	396	3.08	0.53	0.0039	0.121	0.0104	0.0136	0.0020	0.54	147	4
evm 68	222	2.24	0.87	0.0034	0.115	0.0127	0.0211	0.0022	0.63	158	6
evm 81	66	0.82	1.33	0.0039	0.110	0.0152	0.0502	0.0038	1.54	127	8
evo24	76	3.00	0.83	0.0038	0.156	0.0082	0.0134	0.0019	0.43	145	3
evo46	71	2.08	1.31	0.0048	0.136	0.0150	0.0155	0.0029	0.72	120	4
evo68	101	1.81	1.90	0.0052	0.118	0.0109	0.0210	0.0036	1.20	111	7
evo81	76	0.61	2.44	0.0034	0.095	0.0240	0.0484	0.0034	2.99	141	8

Notes!

hv = felsic volcanite m = Mullikkoräme o = Pyhäsalmi
ev = mafic volcanite
02, 24, 46, 81 are ALT index categories as every 20% intervals.
All grades in %.

H. Puustjärvi (ed.)

08.11.06

Confidential

Table C4. Calculated enrichment and depletion for different alteration categories compared to the least-altered samples. E.g. the sample okp81 (an average of the most-altered felsic volcanites in the Pyhäsalmi area) displays a 6-fold enrichment in Ba content (Enriched column 1 Ba6) and a 12.5-fold depletion in Na content (Depleted column 1 Na12.5).

Alteration in Pyhäsalmi and Mullikkoräme

Felsic volcanics

Enriched

alt intens	1	2	3	4	5	6
okp24	Ba3	Mg<3	Zn>2	Cu	K	Rb
okp46	Mg<5	Ba3.5	Cu3	Rb	K	Zn
okp68	Ba6	Zn5	Mg5	Cu	S	K
okp81	Ba6	S<6	Mg5.5	Cu	Zn	K

Depleted

alt intens	1	2	3	4
okp24	Na1.5	Si	S	
okp46	Na2	Si		
okp68	Na4.5	Ca2	Sr	
okp81	Na12.5	Ca9.5	Sr3	P

alt intens	1	2	3	4	5	6
mu24	Mg<2	K<2	Ba1.5	Mn<1.5	Zn<1.5	Rb
mu46	Zn>5	Pb<4	S<4	Mg3.5	Ba3.5	K<3
mu68	Zn22	S12	Cu8.5	Pb7.5	Mg7	Ba<7
mu81	S17.5	Zn16	Mg9	Cu6.5	K4	Ba<4

alt intens	1	2	3	4
mu24	Na<1.5			
mu46	Na2	Sr		
mu68	Na3.5	Sr		
mu81	Na11.5	Ca3	Sr5	

Mafic volcanics

alt intens	1	2	3	4	5	6
okp46	Ba	Cu	S	Pb	K	Mg
okp68	S	Ba	Pb	K	Zn	Cu
okp81	S7	Ba4.5	Zn<4	K3	Cu3	Mg2

alt intens	1	2	3	4
okp46	Ca	Na	P	Si
okp68	Ca	Sr	Na	P
okp81	Ca12	Sr<5	Na4.5	P1.5

alt intens	1	2	3	4	5	6
mu24	S	Rb	Zn	Mg	K	Fe
mu46	S	Mg	Rb	K	Zn	Fe
mu68	S	Rb	Mg	K	Ba	Fe
mu81	S45	Zn11.5	Rb8	K7	Mg6	Ba3.5

alt intens	1	2	3	4
mu24	Ca			
mu46	Ca			
mu68	Ca	Sr		
mu81	Ca13	Sr5	Na3.5	

Table C5. An example of enrichment and depletion (elements in order of importance) in unaltered felsic volcanites (ohv02 = OKP mean and mhv02 = OKMU mean felsic volcanite) compared to different altered felsic volcanites. Mineralogical classification basis: S = sericite, C = cordierite, F = phlogopite, K = chlorite.

Alteration in Pyhäsalmi and Mullikkoräme

Felsic volcanics

+ ohv02	1	2	3	4	5	6
S	Ba	Mg	Zn	S	K	Cu
C	Mg	Ba	Zn	S	K	Rb
F	Mg	Zn	Ba	Cu	Rb	K
K	Mg	Zn	Cu	Ba	P	Fe

- ohv02	1	2	3	4
S	Ca	Na	Sr	
C	Na	Ca	Sr	
F	Na	Ca	Si	Sr
K	Na	Ca	Si	Sr

+ mhv02	1	2	3	4	5	6
S	S	K	Ba	Zn	Pb	Cu
C	S	K	Mg	Zn	Ba	Cu
F	Zn	Cu	Pb	S	K	Mg
K	Mg	Zn	S	Cu	Pb	K

- mhv02	1	2	3	4
S	Na	Ca	Sr	P
C	Na	Sr	Ca	
F	Na	Sr	Ca	Si
K	Na	Sr	Ca	Si

Figures C21 and C22 show that the most important elements, enriched in both felsic and mafic altered volcanites at Pyhäsalmi and Mullikkoräme, are Ba, Mg, base metals, sulphur and K. Generally, enrichment factors at Mullikkoräme are higher than those at Pyhäsalmi.

H. Puustjärvi (ed.)

08.11.06

Confidential

The impact of analytical closure effect was tested for the samples by calculating PER-ratio values for all major and some trace elements. This was done after Stanley, C.R. & Madeisky, H. E. (1993) by calculating the molar element/Zr ratios (e.g. $BaPER = (BaO \text{ wt}\% * 1 / BaO \text{ formula weight}) / (ZrO_2 \text{ wt}\% * 1 / ZrO_2 \text{ formula weight})$). The calculated values are stored in the Gemcom database (CD-ROM GCDBMP.mdb and as lithogeochemistry\enrichdeplet\sta_hvev_altmin.xls).

Figs. C21 and C22 show that big differences do not exist between element enrichment/depletion for the oxide wt% and PER-ratio values in altered felsic volcanites. Altered mafic volcanites show some differences, especially at Pyhäsalmi. This matter was not studied in detail but could be worth further work.

Table C4 displays element (in order of importance) enrichment/depletion factors for the progressive alteration process. The least-altered felsic and mafic volcanites in the Pyhäsalmi and Mulliköräme areas were compared with altered ones. The nature of alteration connected with mineralizations of the VMS type in the project area is clearly demonstrated. Enrichment in Ba, Mg, S, base metals (Cu+Zn+Pb) and K seems to be the order of importance in felsic volcanites at Pyhäsalmi. The corresponding order at Mulliköräme is Mg, S, base metals, K and Ba. For mafic volcanites, S is the most important enriched element followed by Ba, base metals, Mg (at Mulliköräme) and K (at Pyhäsalmi). Element depletion is clearly due to destruction process of feldspar displayed by the strong depletion of Na in felsic volcanites and Ca in mafic ones.

Table C5 displays same kind of element enrichment/depletion comparison for the least-altered felsic volcanites and their alteration mineralogies (the most important alteration mineral being classifier) at Pyhäsalmi and Mulliköräme. At Mulliköräme, sericite, cordierite or phlogopite alteration in felsic volcanites is clearly connected with hydrothermal mineralising processes.

C 2.2.4 Lithogeochemical indices (H. Puustjärvi)

Felsic volcanites often host sulphide deposits of the VMS type. At Pyhäsalmi and Mulliköräme they play a major role when planning lithogeochemical exploration, however the importance of mafic volcanites, part of the bimodal sequence, should not be underestimated. This was the starting point when practical applications were looked for in lithogeochemical indices. As a result, lithogeochemical indices can be presented as a list of element ratios, composites and direct analytical values (Table C6).

Protolith index PI, TiO_2/ZrO_2 , classifies most of the unaltered and altered lithologies to protolithic classes. In the Pyhäsalmi and Mulliköräme areas most of the felsic volcanites have $PI < 40$, mafic ones > 80 . Certain samples (reworked volcanites and mixed tuffs) display intermediate values.

Affinity index AFF, Zr/Y , classifies volcanites into tholeiitic, transitional and calc-alkaline series (thol < 4.5 , > 7 calcalk).

H. Puustjärvi (ed.)

08.11.06

Confidential

Rhyolite type index RT, Zr/TiO_2 , frames rhyolites as arc-related, transitional and rift-related ones (arc $0.04 <$ transitional > 0.12 rift).

ALT is the widely-used Hashimoto index, $100 * (K_2O + MgO) / (K_2O + MgO + Na_2O + CaO)$, which is an indicator applicable to gross alteration (0-20 unaltered, 20-40 weak, 40-60 medium, 60-80 strong, 80-100 pervasive alteration).

Sericite index SI equals $100 * K_2O / (K_2O + MgO)$. Values > 60 are clearly sericite-dominated. Phlogopite, biotite and possibly K-feldspar make interpretation complex.

Cordierite index CI, $100 * MgO / (MgO + K_2O)$, is the opposite of SI. It indicates deep discharge areas (and partly recharge areas) or immediate ore contact (talc-cordierite-rich rocks in disrupted seawater-infiltrated sequences).

PD is the proximity/distality index, FeO/MnO . High values (> 100) indicate proximity to hydrothermal event.

BaO anomalies ($BaO > 0.1\%$) effectively indicate hydrothermal discharge zones.

BN ($100 * BaO / (BaO + Na_2O)$) is an index for exhalite horizons. Values > 25 indicate exhalite precipitation.

BM combines base metal values, $Cu + Zn + Pb$. Values > 150 ppm are anomalous.

S is the analysed sulphur content (XRF%), $S > 0.3\%$ is anomalous.

CUR is the so-called copper ratio, $100 * Cu / (Cu + Zn)$, which indicates locations of hot discharge.

Table C6. Alteration indices along a drillhole (PYS-113, 351.05-606.9 m). The hole intersected variably altered and mineralized felsic volcanites at Kettuperä (south sector, mine village). Blank lines are mafic dikes (not sampled).

H. Puustjärvi (ed.)

08.11.06

Confidential

PI	AFF	RT	ALT	SI	CI	PD	BaO%	BN	BM	Sppm	CUR
11	5.7	0.066	45	32	65	27	0.075	3	200	590	0.00
10	6.1	0.075	52	51	35	26	0.131	4	90	770	0.00
14	4.1	0.053	61	54	41	34	0.073	3	80	860	0.25
10	5.0	0.074	46	45	45	33	0.052	2	310	1320	0.85
10	4.4	0.073	22	20	36	25	0.073	2	60	970	0.33
11	4.6	0.069	30	29	34	28	0.086	2	90	1010	0.40
10	3.9	0.076	33	32	37	26	0.108	3	90	1450	0.00
10	4.1	0.075	34	35	32	34	0.108	3	220	2130	0.00
10	4.1	0.074	24	24	37	28	0.092	2	110	2550	0.14
11	3.7	0.066	28	26	33	41	0.081	2	80	610	0.00
10	4.2	0.074	25	27	15	39	0.092	2	70	980	0.00
11	4.0	0.067	20	20	24	72	0.037	1	270	9780	0.09
11	3.1	0.066	21	31	63	26	0.03	1	1020	6360	0.01
12	4.8	0.060	37	43	29	30	0.071	2	100	990	0.00
10	3.8	0.072	34	39	39	30	0.058	2	90	470	0.00
7	3.8	0.113	46	50	24	23	0.12	4	120	310	0.00
7	3.7	0.111	47	54	16	29	0.07	3	70	250	0.00
8	4.1	0.088	32	34	41	36	0.109	4	120	320	0.13
7	4.2	0.103	41	45	19	33	0.092	2	70	360	0.00
28	4.6	0.027	39	38	46	50	0.051	1	150	1590	0.18
10	4.3	0.077	21	22	23	42	0.039	1	70	970	0.00
6	4.6	0.115	27	27	22	37	0.069	1	80	450	0.00
8	3.0	0.088	17	15	53	23	0.037	1	60	3070	0.00
7	4.3	0.111	62	63	18	24	0.155	5	210	3950	0.00
5	4.3	0.144	85	88	10	43	0.485	40	1800	10800	0.05
11	3.3	0.068	71	80	34	19	0.279	22	980	9850	0.08
6	4.0	0.119	84	86	42	17	0.119	19	260	11700	0.07
7	4.0	0.108	87	84	57	45	0.09	14	410	28900	0.38
10	6.5	0.076	97	96	47	143	0.119	40	530	45700	0.43
16	6.8	0.047	90	92	31	627	0.117	31	1610	119000	0.67
7	4.3	0.100	96	95	18	350	0.138	48	1460	32400	0.14
6	2.7	0.119	95	94	25	422	0.097	34	8620	69900	0.62
6	4.2	0.117	79	81	34	81	0.077	10	690	23800	0.10
13	3.9	0.058	70	68	51	56	0.072	5	810	13900	0.03
34	4.0	0.022	79	86	49	52	0.121	16	350	15500	0.34
7	5.0	0.104	84	85	25	102	0.152	22	1230	21100	0.13
5	7.7	0.154	54	62	19	100	0.858	26	1310	24200	0.16
5	5.4	0.142	89	91	16	68	0.357	38	1360	12600	0.04
8	5.8	0.098	75	81	21	111	0.204	22	8700	32000	0.01
6	6.7	0.129	71	79	18	627	0.303	25	8780	52400	0.03
5	5.6	0.139	91	93	19	80	0.166	34	1110	26800	0.03
5	4.9	0.141	83	86	19	29	0.112	16	190	21600	0.00
11	5.9	0.069	48	56	18	44	0.091	4	80	410	0.00
5	4.6	0.149	62	66	23	40	0.182	10	110	13800	0.00
5	4.5	0.145	20	22	25	40	0.069	2		7600	0.14
5	4.7	0.146	40	43	13	54	0.223	4	180	6990	0.00
5	4.4	0.142	42	51	11	34	0.071	3	100	500	0.00
5	4.9	0.145	33	39	8	38	0.085	2	110	2630	0.00
5	5.2	0.142	49	57	6	43	0.126	4	120	5430	0.00
5	4.7	0.141	38	44	7	50	0.106	3	110	10400	0.00
5	5.0	0.143	17	18	18	65	0.059	1	130	14500	0.00
6	4.5	0.123	28	35	18	34	0.094	3	80	640	0.00
5	4.0	0.139	14	14	44	21	0.023	1	100	1610	0.00
5	5.2	0.154	30	33	15	42	0.102	2	100	720	0.00
5	4.7	0.149	47	56	22	30	0.186	6	130	2870	0.13
6	5.4	0.134	58	64	22	43	0.102	4	120	6560	0.11
5	5.4	0.144	40	37	27	49	0.107	2	130	5810	0.00
5	5.2	0.147	39	43	10	45	0.834	18	110	6170	0.00
5	5.0	0.143	46	52	12	42	0.184	6	180	5220	0.00
6	4.8	0.125	25	27	19	38	0.063	2	100	5090	0.00
5	4.4	0.141	58	62	12	82	0.131	4	130	15200	0.11
5	4.4	0.140	35	45	7	41	0.126	4	110	2270	0.00
10	4.8	0.074	19	21	27	60	0.048	1	110	10300	0.00
5	4.5	0.138	21	26	11	43	0.032	1	100	1800	0.00
5	4.4	0.148	27	32	13	31	0.045	1	110	1470	0.14
12	4.4	0.060	37	49	20	36	0.071	2	120	8460	0.09

Table C6 displays heterogeneity in felsic volcanites and their relation to the best-mineralized section (BM and S). BaO anomalies spread wide within altered felsic volcanites, and the best-mineralized section is closely tied to precipitate horizons (BN).

H. Puustjärvi (ed.)

08.11.06

Confidential

The other (deeper) pyritic horizon seems to be more distal in nature (low PD, CI, CUR). It is not known whether such mineralized sections are stacked or brought into contact by folding or faulting.

Section F is referred for further discussion on the importance of felsic volcanites.

C 2.2.5 Protoliths of altered volcanites (H. Puustjärvi)

At the time of paleovolcanological sampling (from Pyhäsalmi and Mullikkoräme areas) it was decided to analyze the samples of the metamorphic study identically (MS-ICP and XRF) with the paleovolcanological sample set to make it possible to compare the similarities and differences of both sets and to make assumptions of the origin of the pervasively altered lithologies (cordierite, sericite, antophyllite and garnet bearing altered mafics and felsics) (see also section B 4.).

40 samples collected by A-P Tapio from the Pyhäsalmi mine alteration zone drill holes (Apmatm.xls in CD-ROM Excel directory) included 20 altered felsic volcanites, 17 altered mafic volcanites and as a reference three sedimentary gneisses (porphyroblastic mica gneisses) outside of the bimodal volcanic complex.

As seen in the Fig. C23 altered samples group within the same clusters of unaltered felsic and mafic volcanites. The stretch of altered felsics down to lower SiO₂ grades is due to abundant sulphides in the samples. REE and trace element spider graphs indicate clearly that grade distributions of the elements seen in the diagrams are equal to the ones of unaltered volcanites.

REE distributions of mafic volcanites and altered mafics does not seem to overlap completely and that could be an indication of HREE mobility during alteration or later metamorphic processes. Altered felsics show consistently higher Ba, Rb, Th and K grades than the unaltered felsic volcanites. This feature is typical for VMS-type alteration environments.

According to the above features it is quite justified to conclude that even during a pervasive alteration the REE and trace element contents indicate well the protolith compositions. In this case it is clear that protoliths of the collected altered samples have been chemically identical to the unaltered volcanites of the paleo-volcanological sample set.

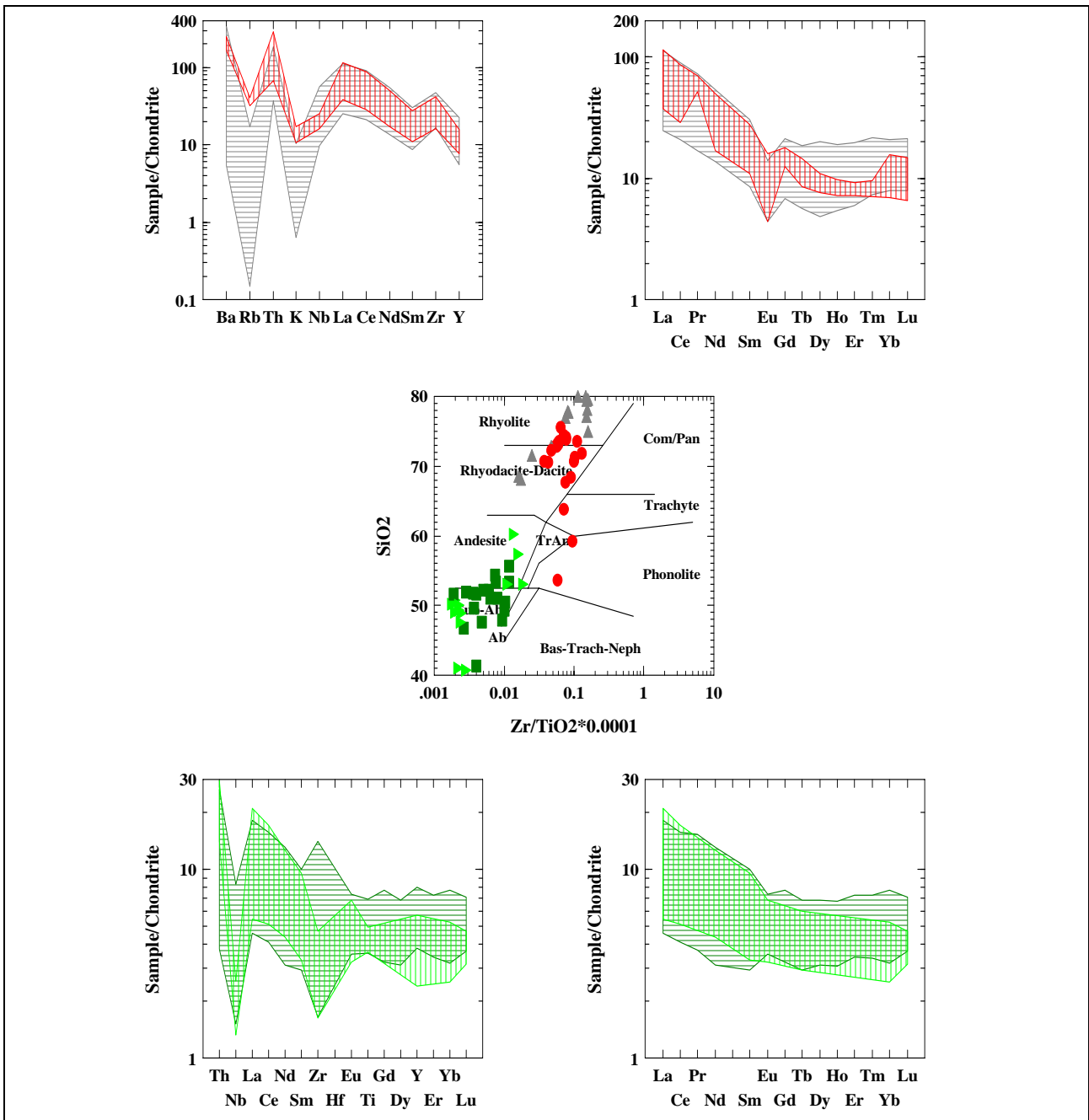


Figure C23. Unaltered and altered felsic and mafic volcanite samples from Pyhäsalmi Ruotanen formation plotted on Winchester-Floyd discrimination diagram in the middle and trace element spider and REE distribution diagrams at the top (felsic volcanites) and at the bottom (mafic volcanites). Grey triangle = felsic volcanites, green square = mafic volcanites, red dots = altered felsic volcanites, light green triangles = altered mafic volcanites. Hatch pattern colours on the diagrams are the same as for symbols. Limit for altered lithologies has been a value higher than 40 of the calculated Hashimoto index, $100(K_2O+MgO)/(K_2O+MgO+Na_2O+CaO)$.

H. Puustjärvi (ed.)

08.11.06

Confidential

C 2.2.6 Mass transfer during alteration

Mass transfer calculation is essentially a comparison of the concentration of a component in an altered rock with its concentration in an unaltered precursor rock using the change in the mass of the rock as a normalizing factor. It can be shown that this normalizing factor equals the ratio of the concentration of any immobile element in the precursor rock to its concentration in the altered rock (e.g. Grant 1986). Many studies have shown that Ti, Zr, Hf, Th, Nb, Ta, REE (except La) and Al are usually insensitive to alteration (e.g., Kerrich and Wyman 1996). Of these potentially immobile elements, only Ti, Al and Zr have been analyzed for the whole data set.

Mass transfer calculation was performed separately for the felsic and mafic volcanites and it included two phases. First, isocon diagrams were constructed using average concentrations of TiO_2 , Al_2O_3 and Zr in five groups of variously altered volcanites. These alteration groups were defined using the values 0-20, 20-40, 40-60, 60-80 and 80-100 of the Hashimoto alteration index. An isocon diagram was constructed for every Zr/ TiO_2 class in every alteration group. These diagrams indicated that mass transfer can be calculated for every volcanic sample using the median of $\text{Al}_2\text{O}_3^o/\text{Al}_2\text{O}_3$, $\text{TiO}_2^o/\text{TiO}_2$ and Zr^o/Zr values as the normalizing factor. The superscript o refers to the original background concentration given in Appendix 3. The calculation indicates that the average mass change associated with host rock alteration is moderate to small (Table C7).

A summary of average gains and losses of selected elements in altered volcanites is given in Fig. C24. Alteration is generally similar for both the felsic and mafic volcanites, and for both the Pyhäsalmi-Kettuperä and Mullikkoräme areas, and is characterized by strong leaching of Ca, Na and Sr, and strong to moderate enrichment of Au, S, LOI, Ba, Cu, Zn, Ag, K, Rb, Mg, Ni, Co and Pb. Iron shows moderate enrichment in the felsic volcanites, and V is strongly enriched in the felsic volcanites at Pyhäsalmi-Kettuperä. For Ca, Na, Sr, S, Ba, Cu, Ag and LOI, the enrichment or depletion tends to be stronger at Pyhäsalmi-Kettuperä than at Mullikkoräme, whereas the opposite is true for Zn, Pb, Co, K and Rb. The apparent depletion of Au in the mafic volcanites at Mullikkoräme is likely artificial. Six of the only 11 available concentrations are below the detection limit of 0.001 ppm and were given the value of 0.0005 ppm. This causes an apparent depletion in the mass transfer calculation for these samples. Using only the samples, which have Au concentrations above the detection limit, Au is enriched by a factor of 31 in the altered mafic volcanites at Mullikkoräme.

Table C7. Average mass change as % of original mass for moderately altered (60#Hashimoto index<80) and strongly altered (Hashimoto index≥80) volcanites. For the definition of the Hashimoto index, see chapter C ?

H. Puustjärvi (ed.)

08.11.06

Confidential

	Mass change in felsic volcanites		Mass change in mafic volcanites	
	Moderately altered	Strongly altered	Moderately altered	Strongly altered
Pyhäsalmi	N=427	N=883	N=154	N=134
Minimum	-46	-45	-64	-54
Maximum	165	306	56	130
Median	10	10	-12	-4
Kettuperä	N=154	N=696	N=16	N=49
Minimum	-46	-49	-51	-45
Maximum	282	237	29	91
Median	20	23	-17	6
Mullikkoräme	N=365	N=244	N=207	N=70
Minimum	-36	-45	-52	-37
Maximum	150	275	100	114
Median	2	2	14	13

C 2.2.7 Best pathfinders

A good pathfinder element or index can be defined as having a large anomaly around the ore deposit, showing consistently increasing or decreasing values toward the ore and preferably being insensitive to rock type variation. Candidates for well performing pathfinders are those components that show large gains or losses during alteration: Au, S, LOI, Ba, Cu, Zn, Ag, K, Rb, Mg, Pb, Ca, Na and Sr (Fig. C25) or their combinations. The areally most extensive anomalies are those of S, Zn, Cu and Ag, which practically cover the whole study areas at both Pyhäsalmi-Kettuperä and Mullikkoräme (Fig. C26). The rest of the above-mentioned elements, as well as the Hashimoto alteration index, show anomalies that approximately cover the areas of visually altered felsic volcanites (Fig. C16). The extent of Au and LOI anomalies could not be evaluated due to the restricted areal distribution of samples for which these components were analyzed.

Within individual drillholes, the concentrations of S, Cu, Zn, Pb, Ag, Ba and LOI most consistently define positive anomalies around the orebodies. The anomalies of Ba and S are often the largest (up to 350 m from ore) and those of Pb are usually the narrowest (Fig. C27). The major element concentrations, as well as the Hashimoto alteration index values, behave very irregularly at the drillhole scale.

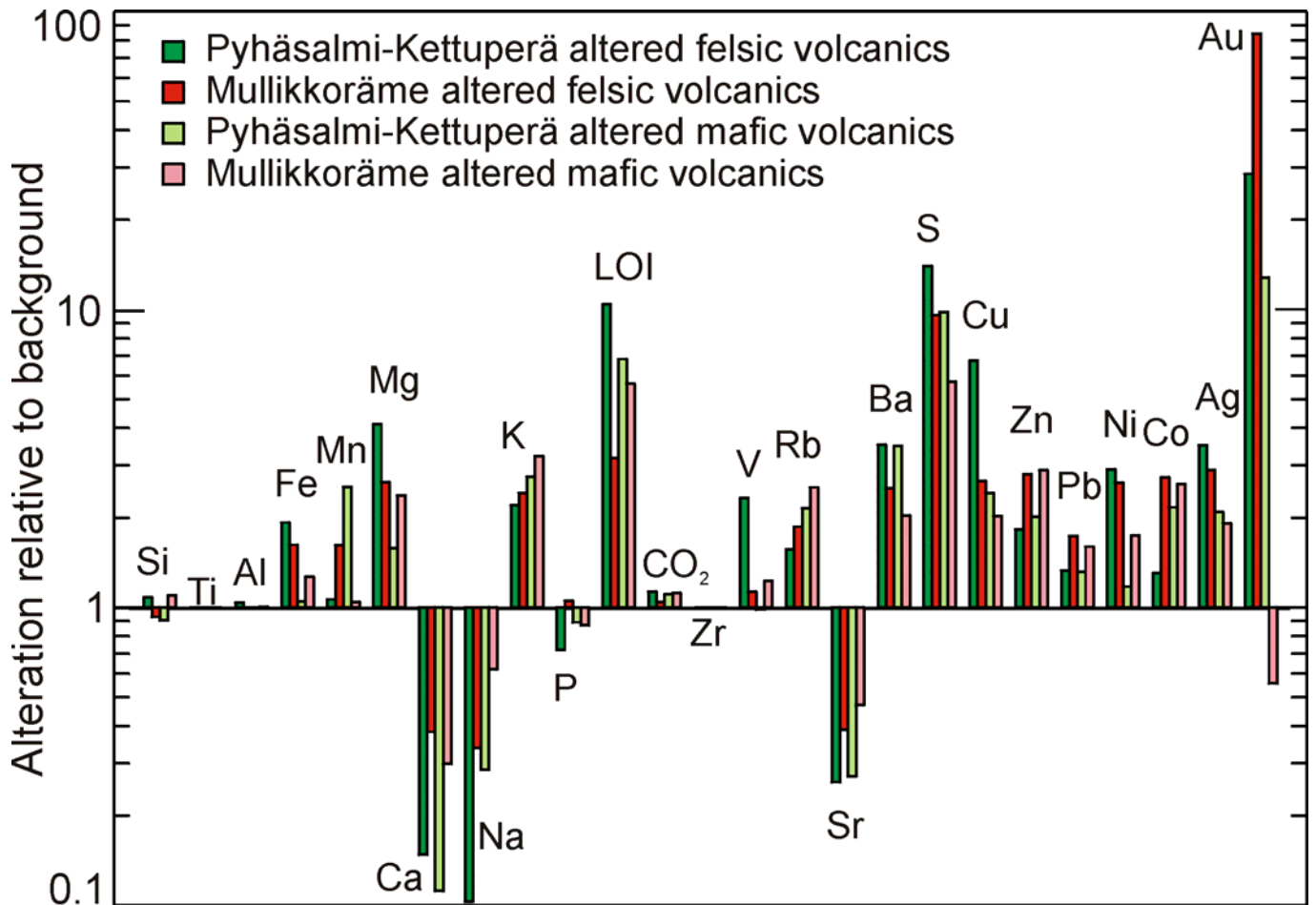


Figure C24. A summary of average gains and losses of selected elements for the altered volcanic rocks. Only samples for which the value of the Hashimoto alteration index is more than 60 are used.

The behavior of the pathfinder elements in the vertical direction was studied for the felsic volcanites at the southern end of the Pyhäsalmi orebody, where samples are available from the surface down to the depth of 1100 m. The width of the alteration zone there narrows from about 125 m at the surface to 0-3 m at the depth of 1000 m. When using all the available samples, including the weakly altered to unaltered ones, no systematic variation is detectable in the vertical direction. When only the most strongly altered samples with the Hashimoto alteration index equal or more than 80 are used, rough trends in the concentration of certain elements become apparent (Fig. C27). The concentrations of S, Ba and Pb tend to increase from the surface downward, and Zn concentration first decreases to the depth of about 450 m and then increases downward.

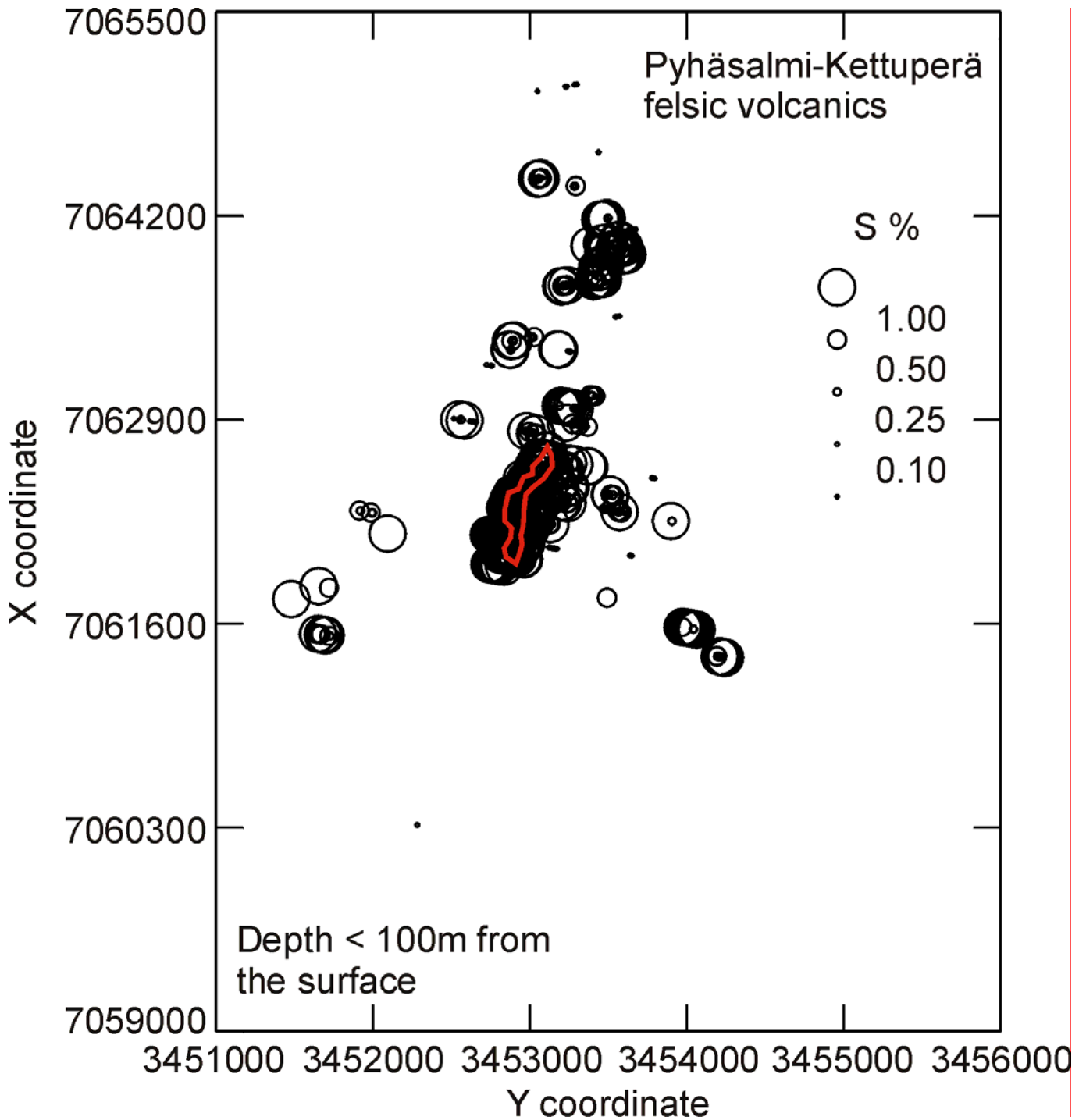


Figure C25a. Spatial distribution of sulphur concentration at Pyhäsalmi-Kettuperä. For clarity, only samples less than 100 m below the surface have been used. The projection of the Pyhäsalmi orebody on the surface is shown in red.

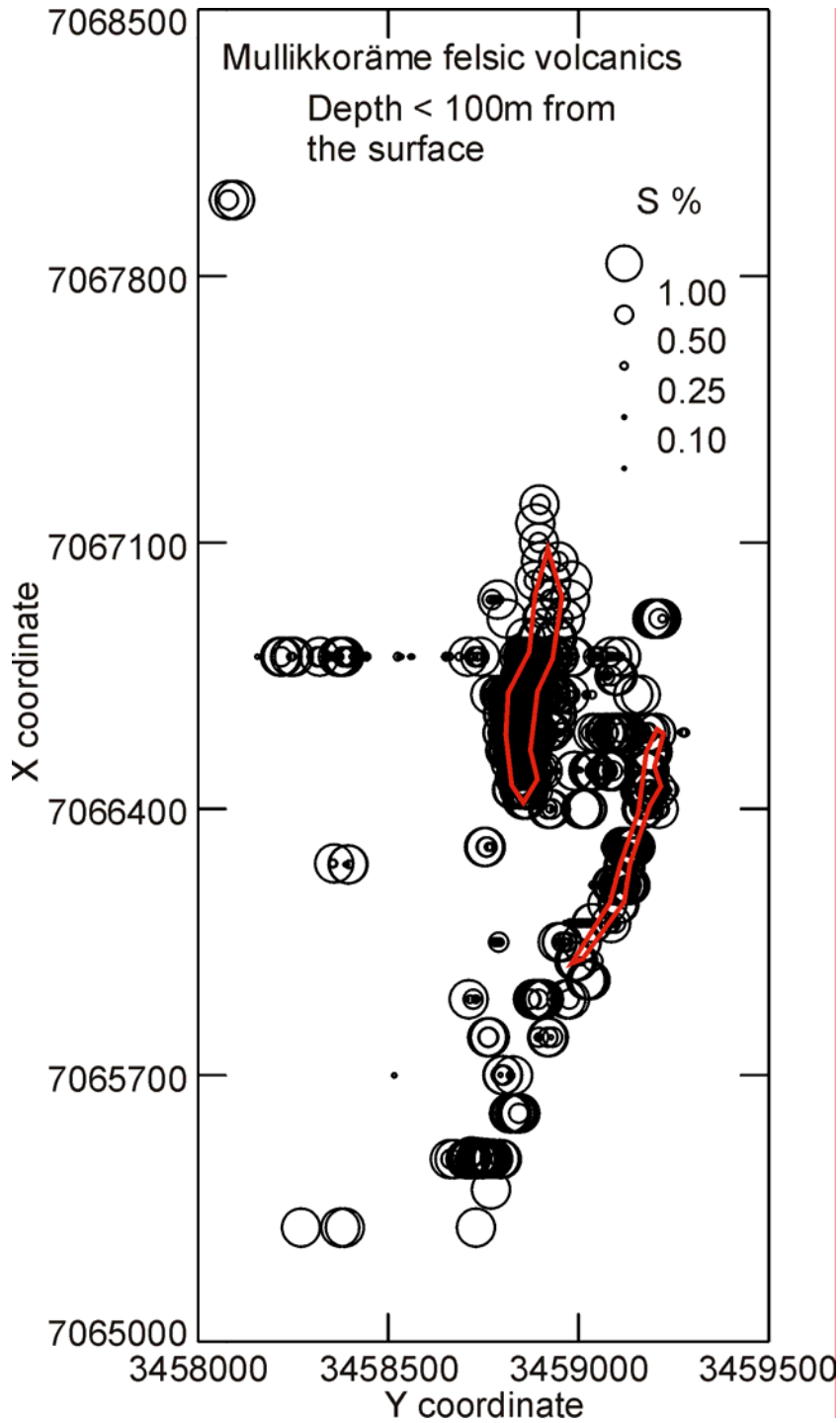


Figure C25b. Spatial distribution of sulphur concentration at Mullikkoräme. For clarity, only samples less than 100 m below the surface have been used. The projections of the Mullikkoräme orebodies on the surface are shown in red.

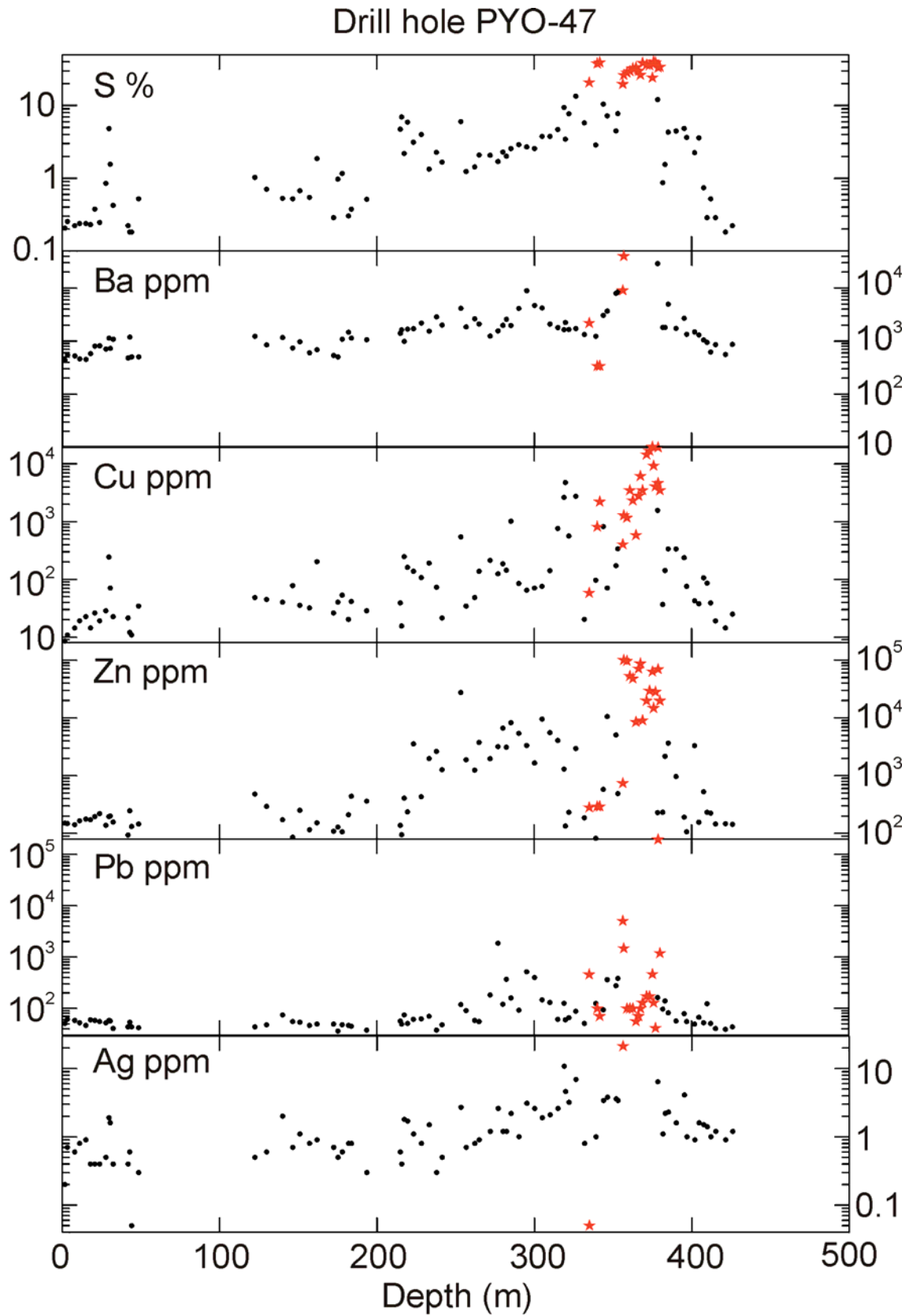


Figure C26. Variation of the concentrations of selected elements with depth along the diamond drill hole PYO-47 at Pyhäsalmi. The red stars represent ore samples.

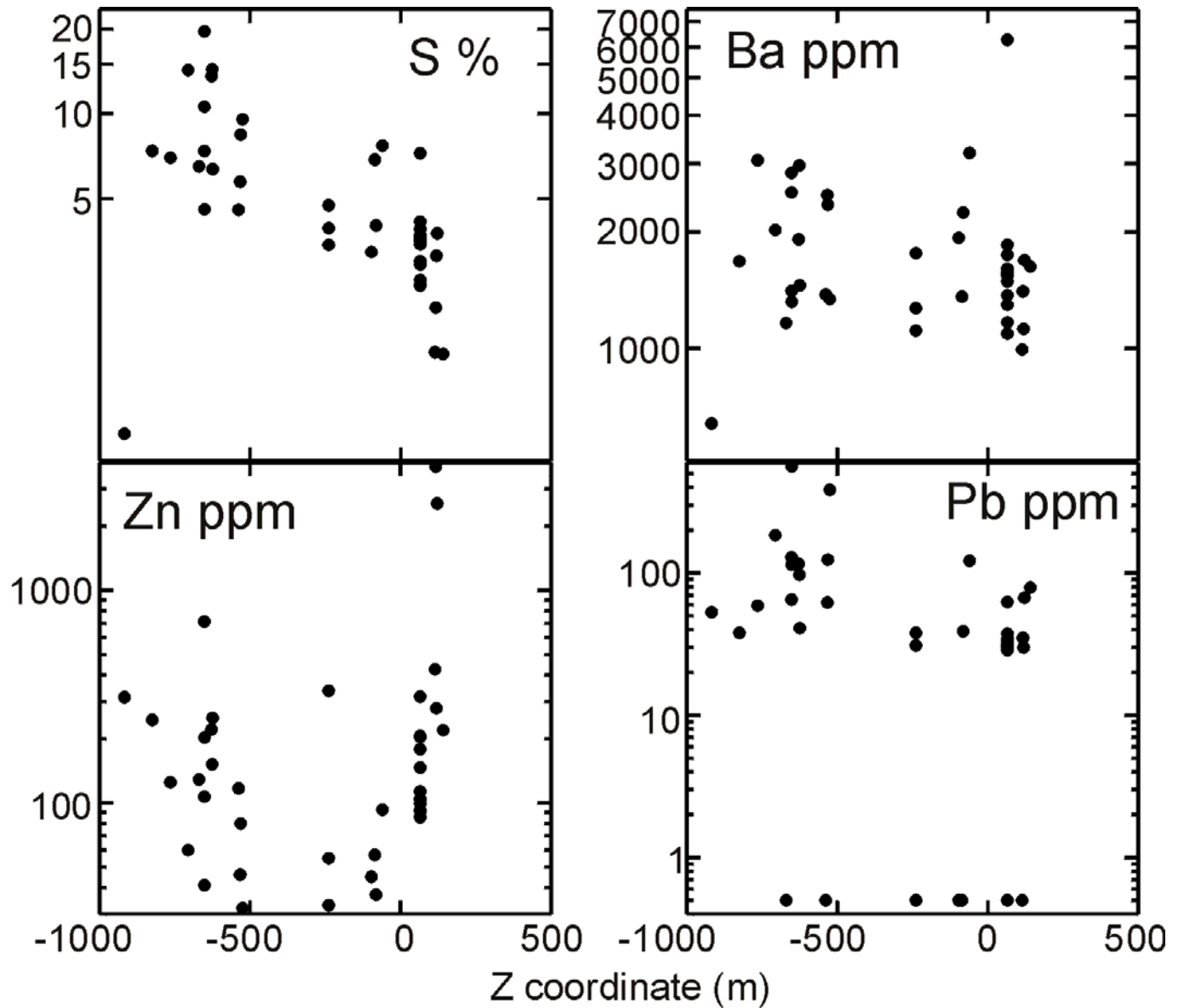


Figure C27. Variation of the concentrations of selected elements with depth along the southern vertical margin of the Pyhäsalmi orebody. Only strongly altered host rock samples for which the value of the Hashimoto alteration index is over 80 are used.

C 3 LITHOGEOCHEMICAL MODELING (H. Puustjärvi)

Lithochemical modeling is a path of the whole evaluation process of lithochemical data. So being, the previous chapters already have presented the basic characteristics and the explorational elements and indices to be used in search for VMS deposits of the Pyhäsalmi type.

Lithochemical data and indices used as exploration criteria have to be in such a format that they can be easily visualized. All lithochemical data of this project are stored as spreadsheet files (*.xls) and as Access format (*.mdb) data set in the Gemcom project Gcdbmp.mdb file. This allows many different ways of data inspection (all, categories, drillholes, etc.) as spreadsheets, graphs, point symbol maps, drillhole sections/plans, element grid/contour maps and as 3D views (Gemcom and ArcView 3D-mode).

The advantage of coeval 2D/3D data visualization is in outlining elemental variable grade/intensity variations in space and in solid modeling. In addition to those figures and tables already seen in previous chapters the following ones are examples of how lithochemical data has been manipulated and evaluated in this project.

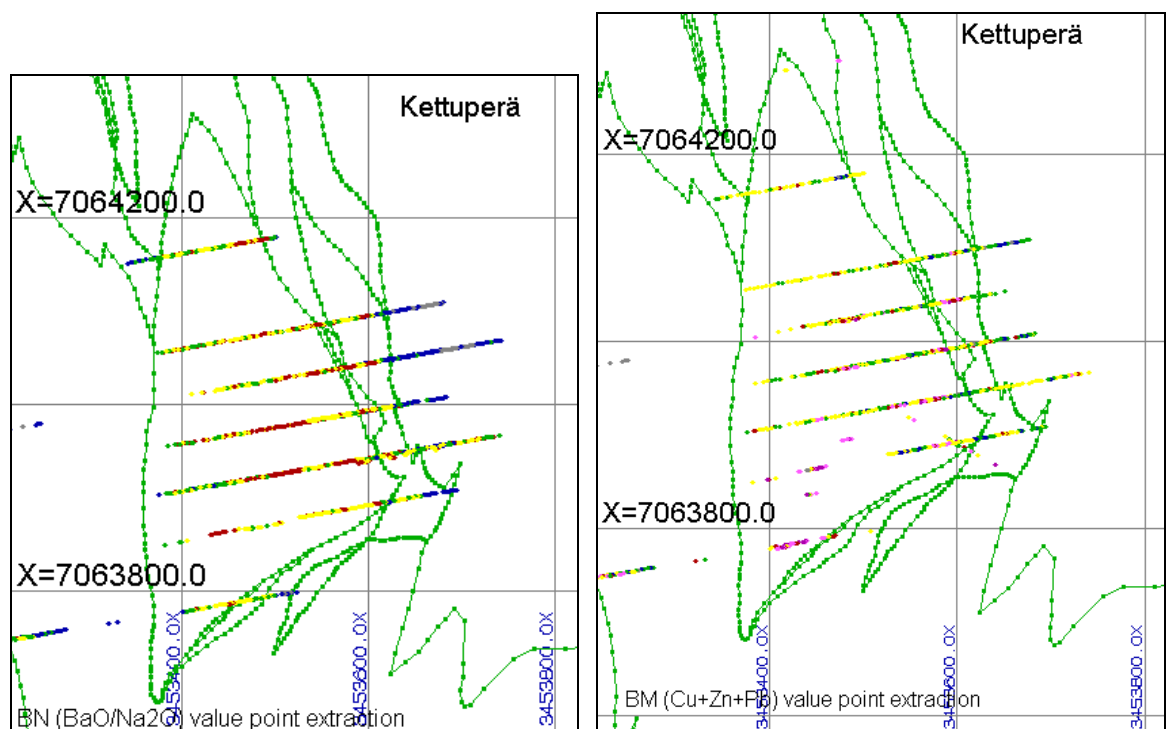


Figure C28. An example of surface plan projections from the Kettuperä area N of the Pyhäsalmi mine. Green dot lines are rock boundaries. Left figure illustrates two clear BN (strong precipitate) horizons (red-magenta dots) and the right one illustrates coincident BM (combined base metals) anomalies (red-light magenta-magenta) within the same sequence. Produced in Gemcom software.

Figure C28 is a lithochemical data base (Gemcom) variable extraction plot coloured

H. Puustjärvi (ed.)

08.11.06

Confidential

according to preset (frequency distribution based) anomaly categories. This form of data handling (point format) allows also 3D visualization. In case of sufficient drillhole or some other data points on sections or plans, it is possible to create multiple polygons and tie them together forming a 3D solid model of, for example, BM anomalies. This is what has been done especially in section E4.

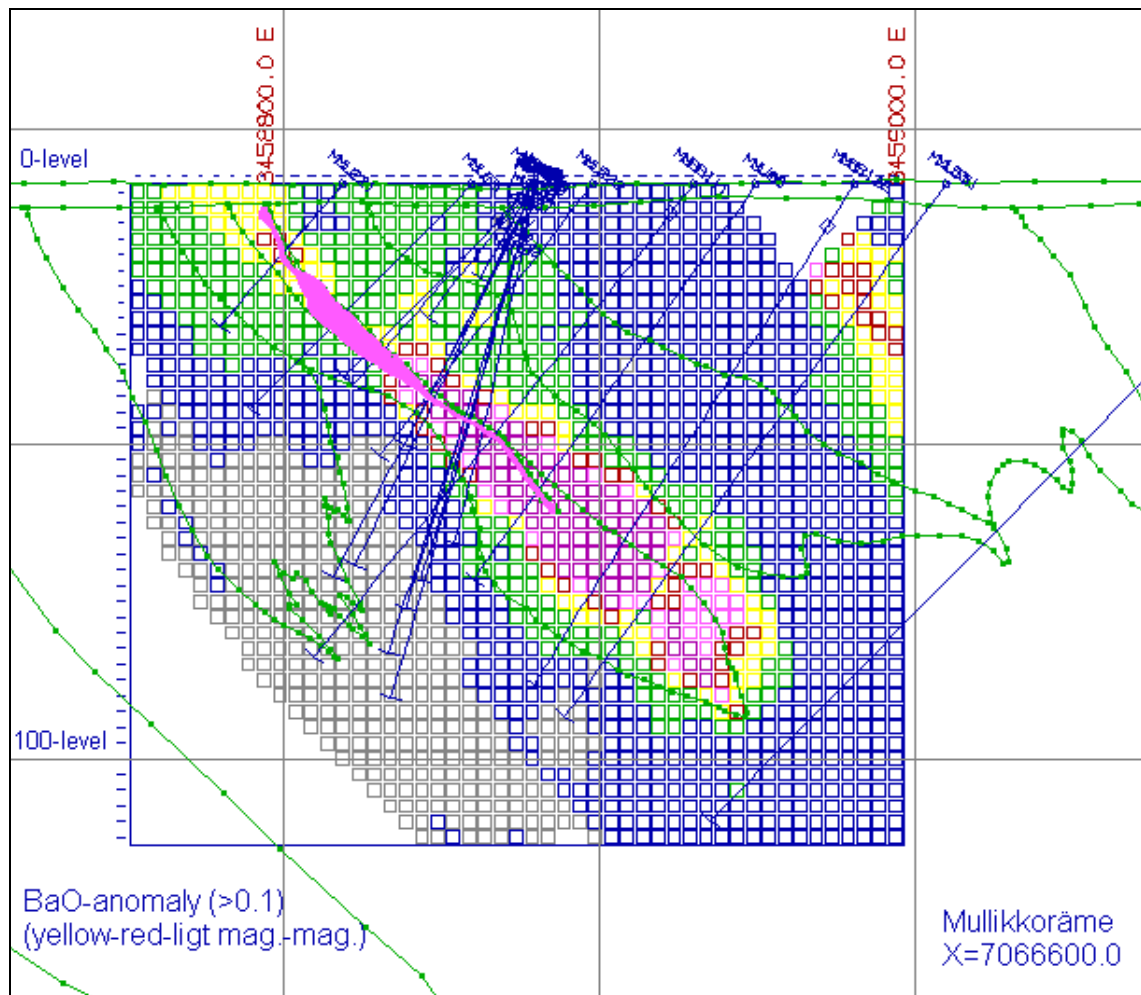


Figure C29. Mullikkoräme section X=66600, an example of Ba distribution in relation to rock boundaries (green dotlines) and near-surface A orebody (solid magenta). Ba anomalies (>0.1% BaO) yellow-red-light magenta-magenta.

Figure C29 is a BaO% point extraction grid map (gridded by using anisotropic XYZ inverse distance method) on the Mullikkoräme section X=66600 which illustrates a good correlation for Zn-ore and Ba-anomaly. The distribution of barium might be an indication of some distal/proximal polarity in relation to the ore.

H. Puustjärvi (ed.)

08.11.06

Confidential

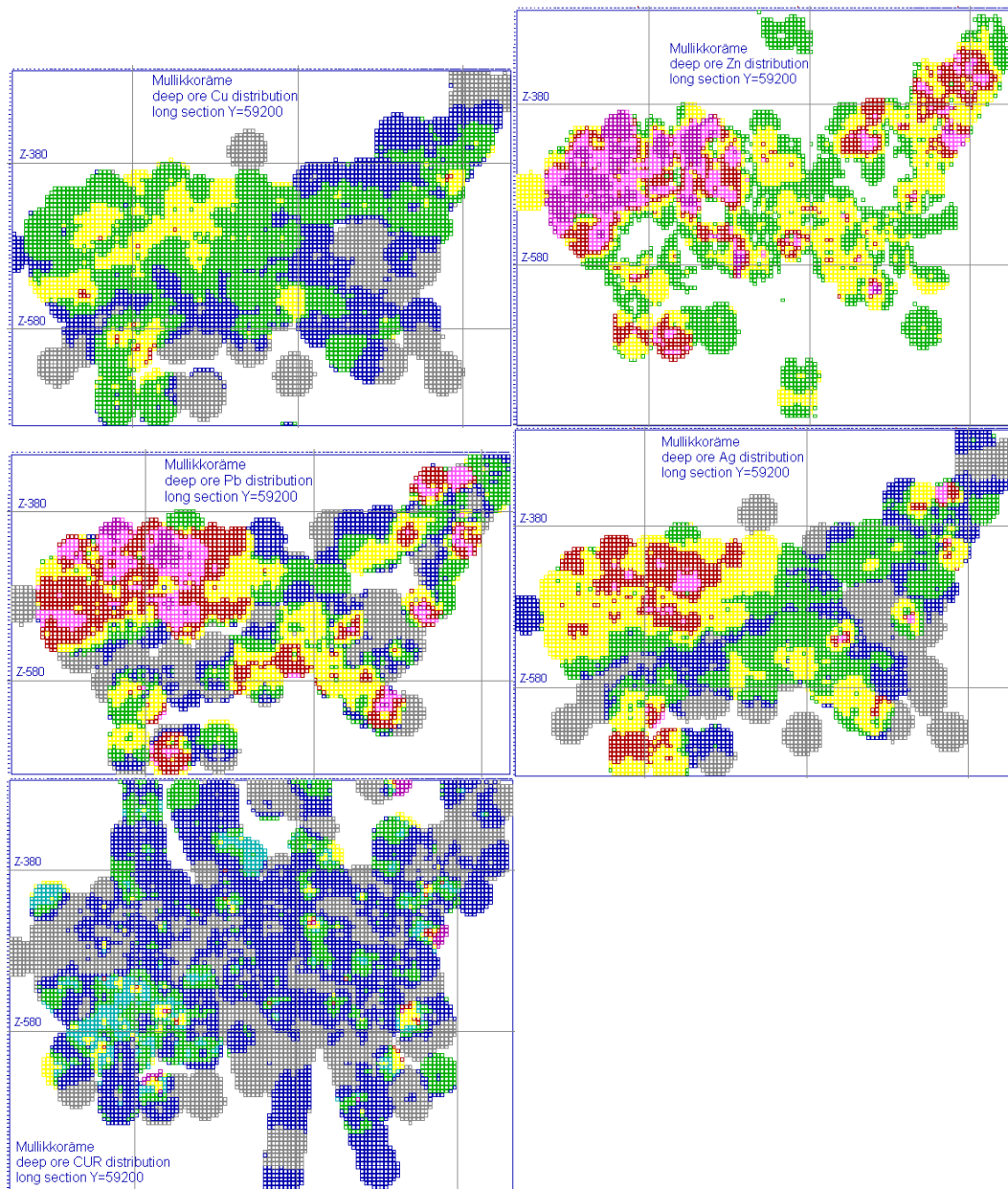


Figure C30. Mullikkoräme deep ore (Siperia) Cu, Zn, Pb, Ag and CUR (copper ratio, see lithochemical indices) distribution grid maps. Siperia ore lens is shown in the upper left part of the subfigures. Metal distributions within the Siperia show zonations and areas of different ore types. Pb and Ag distributions in the deeper levels possibly indicate new ore zones (distal rims of Cu-Zn lenses?). CUR anomalies indicate weak “hot ore fluid discharge areas”. Yellow-red-light magenta-magenta grid colours indicate increasing anomalies.

Figure C30 represents an example of base metals grade and copper-ratio value grid maps to evaluate potential exploration directions for new ore lenses at the depth continuation of the deep ore lens (Siperia) area.

H. Puustjärvi (ed.)

08.11.06

Confidential

Lithogeochemistry has been used in 3D solid modeling as mentioned in the base metals distribution and ore type modeling (section E) and in constructing alteration zone models (Fig. C31).

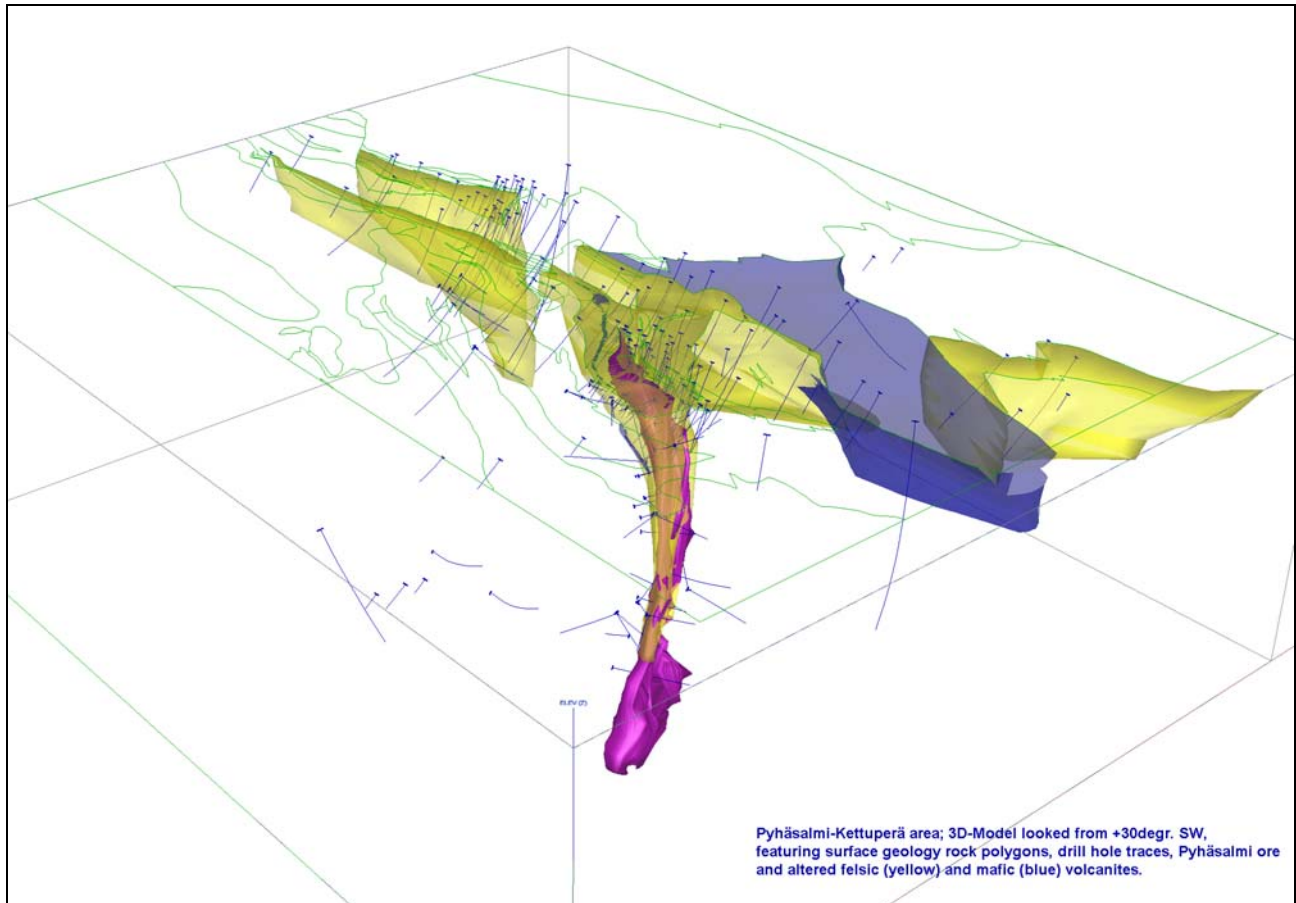


Figure C31. Pyhäsalmi-Kettuperä area 3D-Model of ore (magenta), altered felsic (yellow) and mafic (blue) volcanites. This figure shows clearly how the ore has been “squeezed” out of it’s original alteration halo to it’s present deep levels below the +1050m. Altered volcanites seem to form tight isoclinal synforms (see section B4).

All lithological sections, plans and 3D solid models are based on the coded drillcores and old/new assays. The original delineation of geological boundaries was done on plotted drillhole + analytical data sections/plans (Fig. C32), then digitized and manipulated in GIS (MapInfo, ArcView) and 3D (Gemcom) powered software.

Geological and especially lithogeochemical 3D modeling was done more or less preliminarily, but now knowing how and with what kind of a data to do that. Further studies should be done in the Pyhäsalmi-Mullikkoräme area and also during future exploration campaigns.

H. Puustjärvi (ed.)

08.11.06

Confidential

Zr/TiO₂ value for the felsic volcanites is higher at Pyhäsalmi than at Mullikkoräme. Systematic variation of the Zr/TiO₂ values suggests a primary rock type control for the hydrothermal alteration on the host rocks.

The rocks have suffered variable degrees of Na metasomatism that most likely preceded mineralization. Host rock alteration is characterized by strong leaching of Na, Ca and Sr, and strong to moderate enrichment of Au, S, LOI, Ba, Cu, Zn, Ag, K, Rb, Mg, Ni, Co and Pb. At the areal scale, S, Zn, Cu and Ag form anomalies that cover practically the whole study areas, whereas LOI, Ba, K, Rb, Mg, Ca, Na and Sr form anomalies that approximately coincide with or are more restricted than the visually detectable alteration. At a more detailed scale, the concentrations of S, Cu, Zn, Pb, Ag, Ba and LOI define up to 350-m wide positive anomalies across stratigraphy around the orebodies. Within the strongly altered felsic volcanic host rocks at the southern end of the Pyhäsalmi orebody, concentrations of S, Ba and Pb increase from the surface, and Zn concentration increases from the depth of 450 m, downward to at least the depth of 1000 m.

The characteristics of geochemical alteration, including the best pathfinders to ore have been covered by this report. However, understanding the controls of mineralization and the nature of volcanism and the paleohydrothermal system is of crucial importance for successful exploration in the whole Pyhäsalmi-Pielavesi area. To these ends, a restricted study of oxygen isotopes could be useful to define the upflow and downflow zones of the hydrothermal system. Also, a restricted study utilizing good quality trace (and major) element analysis could shed more light on the possible change in the nature of volcanism that could define the favorable stratigraphic horizon for mineralization. Also, the relation between the structure and geochemistry in the area could possibly be clarified by detailed studies.

C REFERENCES

Franklin, J.M. 1997. Lithogeochemical and Mineralogical Methods for Base Metal and Gold Exploration. In: Gubins, A.G. (editor) Proceedings of Exploration 97: Fourth Decennial International Conference on Mineral Exploration, GEO F/X, 191-208.

Galley, A., 1998. Characteristics of composite subvolcanic intrusive complexes associated with Precambrian VMS Districts. In: Camiro Project 94E07 third annual report, September 1998, pp. 1-40. The use of regional-scale alteration zones and subvolcanic intrusions in the exploration for volcanic-associated massive sulphide deposits.

Grant, J. A., 1986. The isocon diagram - A simple solution to Gresens= equation for metasomatic alteration. Economic Geology 81, 1976-1982.

Ishikawa, Y., Sawaguchi, T., Iwaya, S. and Horiochi, M. 1976. Delineation of prospecting targets for Kuroko deposits based on models on volcanism of underlying dacite and alteration halos. Mining Geology 26, 105-117.

H. Puustjärvi (ed.)

08.11.06

Confidential

Kerrich, R. and Wyman, D.A. 1996. The Trace Element Systematics of Igneous Rocks in Mineral Exploration: An Overview. In: Wyman, D.A. (editor) Trace Element Geochemistry of Volcanic Rocks: Applications for Massive Sulphide Exploration. Geological Association of Canada, Short Course Notes, Vol 12, 1-50.

Stanley, C.R. and Madeisky, H.E. 1993. Pearce Element Ratio Analysis: Applications in Lithochemical Exploration. The University of British Columbia MDRU Short Course Notes SC-13, 1-542.

SECTION D
GEOPHYSICS

Heikki Puustjärvi (ed.)

01.05.1999

Confidential

D GEOPHYSICS (T. Ahokas)

The objective of the geophysical modeling was to identify the critical parameters and parameter combinations, which best characterize ores, mineralized zones and immediate country rocks. An additional aspect was that they should be identifiable with interpretations within the complexly deformed and heterogeneously altered volcanites of the Pyhäsalmi type.

Geophysical surveys have been carried out in the Pyhasalmi area since 1950's and various methods have been used both on ground and in drillholes.

Prior to this project, Outokumpu Mining Oy (OM) saved the measured data mainly in digital format.

Low-altitude geophysical surveys, carried out by the Geological Survey of Finland, resulted in aeromagnetic and aero-EM data used in the modeling.

D 1 DATA TRANSFER AND MANAGEMENT

Geophysical airborne, ground survey and petrophysical data from drillholes were gathered from OM's Ingres database and office files. Such data were edited and saved in proper format (software applicable formats and *xls) for closer examination (plotting maps, interpretations, and statistics).

An automatic data gathering from the Ingres database of OM's Exploration department was used for systematic magnetic, gravity, HLEM (Slingram) and IP ground survey data. The data were edited (older values removed and newer ones accepted), sorted according to the line co-ordinates for interpretations and saved in Geosoft *.xyz file format on diskettes.

National co-ordinates were calculated for the ground geophysical data to facilitate comparison between different data.

Various tif-format grid maps were imported into ArcView GIS-system; they were produced of the gathered data to help geological mapping.

Gefinex 400S is EM equipment designed in the Outokumpu Group. The original survey data were saved only in office diskettes during last ten years. All of the data found on such diskettes were edited (incorrect values removed), sorted according to the line and station co-ordinates and saved in various formats for plotting and interpretations. Because of a great number of measured stations the editing of the Gefinex 400S data was the most time-consuming part of the editing work carried out during this project.

Petrophysical data were copied from OM office files into diskettes and all errors and incorrect values were removed. The data comprises more than 500 000 measured values. After editing such data were saved as Excel files for statistical examination.

Heikki Puustjärvi (ed.)

01.05.1999

Confidential

Some old downhole-EM data were re-processed and saved in Amira format for interpretations.

D 2 PETROPHYSICS

D 2.1 GENERAL

Petrophysical data originate from 104 holes drilled in the project area and consist susceptibility, resistivity, density and conductivity measurements at 0.1 m spacing. Most of the data were from the Mullikkoräme area. The list of the measured petrophysical parameters and surveyed drillholes is presented as a ddhpetro.xls file in geophysics directory on the attached CD-ROM.

Since different petrophysical loggings were carried out separately, the locations of the measured stations along the holes were not exactly equal. However, because of large amount of data, this didn't cause notable errors in the calculated average values.

Due to calibration problems the quality of the logged density values were not acceptable for statistical analysis. Fortunately, plenty of density determinations were done of drillcore samples, as well. Such core sample measurements were carried out at one-meter spacing. Therefore, also the other petrophysical parameters were drawn from the data files using the same one-meter spacing. All of the petrophysical one-meter-spacing parameters were linked to the drillcore geological coding and filed as drillhole-identifiable Excel files.

After this procedure there still were enough data to examine differences between petrophysical parameters in various rock types. The created data files include 28775 susceptibility, 9879 density, 28000 resistivity and 1430 conductivity values.

Distribution histograms of different petrophysical parameters were produced and average values were calculated. The data and the distribution histograms are presented as Excel files in the geophysics directory on the CD-ROM attached to this report.

Table D1 shows the average values of different petrophysical properties for each rock type examined. Such values are closer discussed in the following chapters.

D 2.2 SUSCEPTIBILITY VALUES OF DIFFERENT ROCK TYPES

Figure D1 shows the calculated average susceptibility values for six of the most common rock types. The vertical lines that cross the average values show variations of the values (90% of all values in the line area).

The average susceptibility values of mafic volcanites, mineralisation, talc-carbonate-bearing rocks, and skarns are slightly higher than those for the other rocks.

Heikki Puustjärvi (ed.)

01.05.1999

Confidential

Especially in the Mullikkoräme area, the mineralisation is in part highly magnetized. There is a large variation in values within rock types; consequently it is difficult to separate various rock types from each other.

Table D1

Pyhäsalmi area				
Average values of petrophysical parameters of different rock types				
Rock type	Susceptibility 10⁻⁵ SI	Density g/cm³	Resistivity ohm	Conductivity mV
Felsic volcanite				
all	366	2.72	9019	1.29
unaltered	403	2.71	12901	1.14
altered (no sulphides)	311	2.76	4938	1.39
sulphides	192	2.84	3656	2.82
Mafic volcanite				
all	815	2.92	5082	2.86
unaltered	587	2.94	6440	4.70
altered (no sulphides)	1026	2.85	4007	0.76
sulphides	1853	3.14	1161	0.78
Mineralisation	5431	3.49	37	3.10
Felsic intrusive	180	2.68	9921	1.16
Plagioclase-uralite-porphyrite	377	2.80	19170	2.44
Talc-carb. bearing rock and skarn	2327	3.18	94	2.53

Ground magnetic measurements indicate that parts of the mafic volcanites can be detected by magnetic surveying.

It is noted that the intensity of measured anomalies is higher than what can be caused by the measured susceptibility values, therefore volcanites must possess remanent magnetism.

D 2.3 DENSITY VALUES OF DIFFERENT ROCK TYPES

In the Mullikkoräme area, density values were measured only from drillcore samples; therefore it was not possible to compare rock densities between the Ruotanen and Mullikkoräme areas.

Average densities of different rock types show that mineralisation clearly display higher density value than the other rocks (Fig. D2).

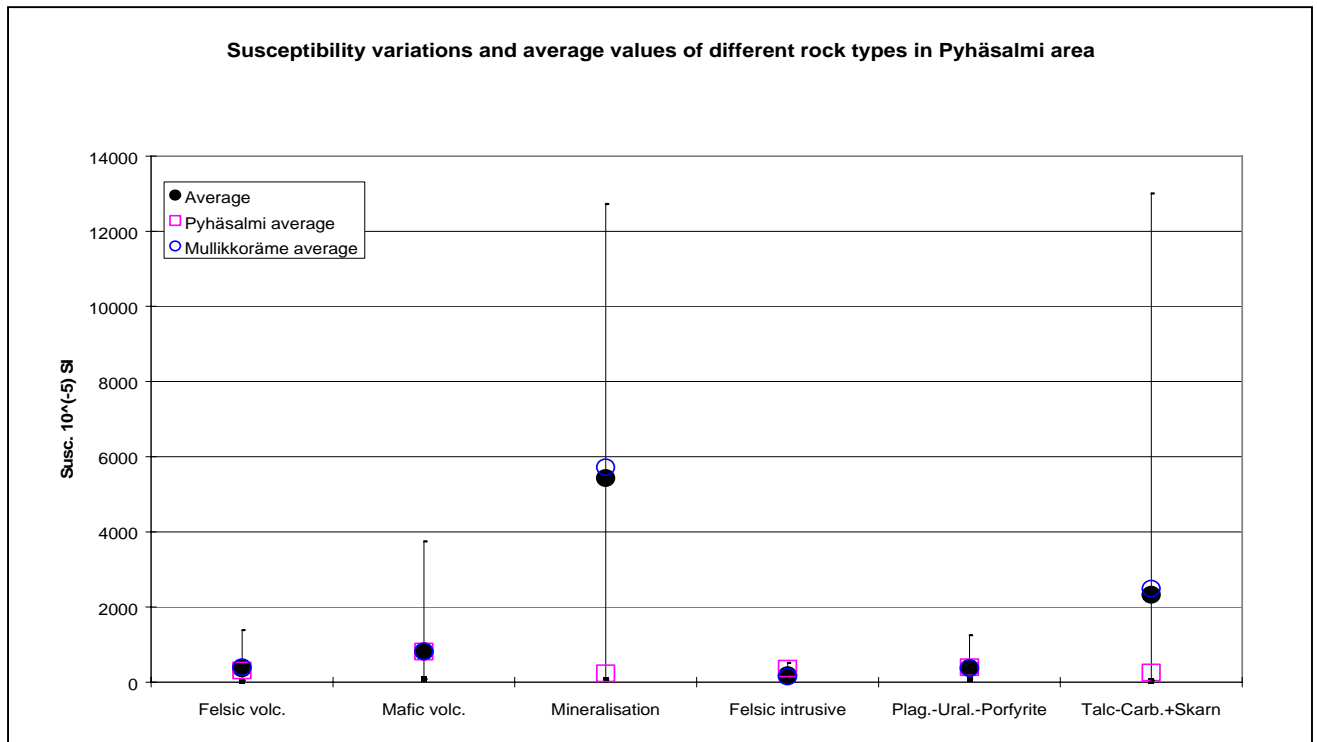


Figure D1.

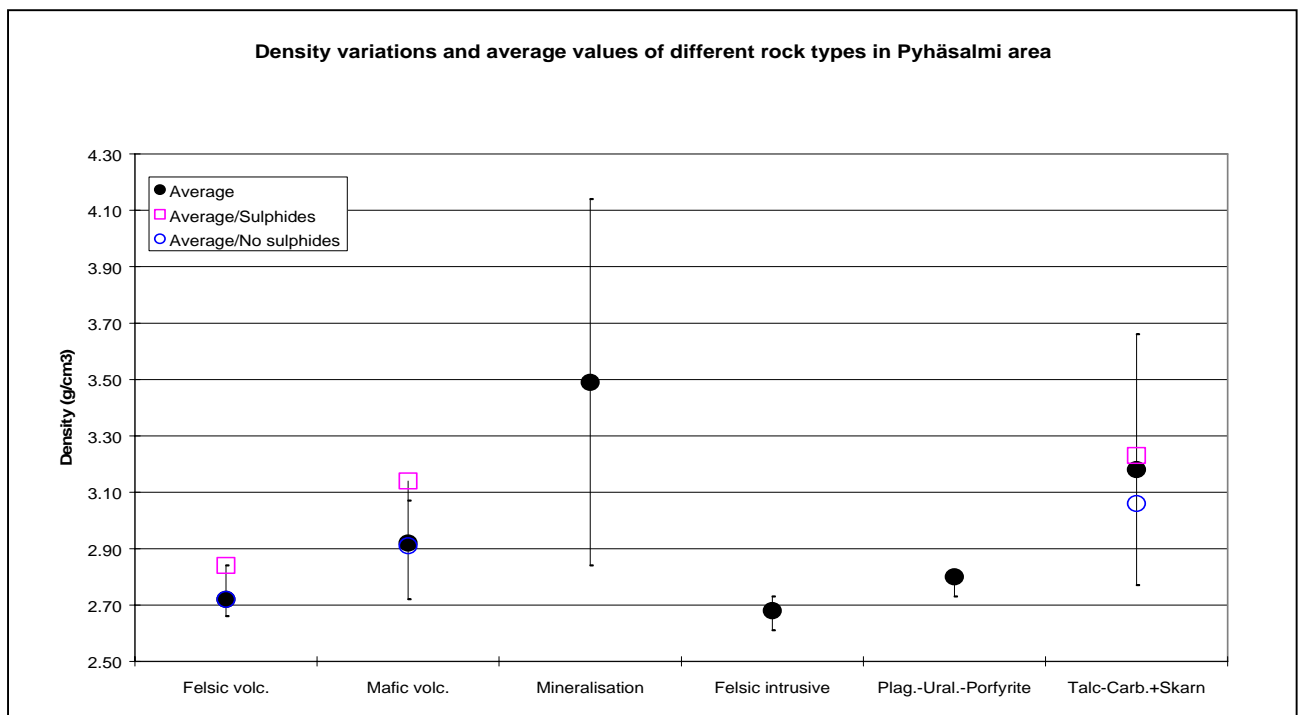


Figure D2.

Heikki Puustjärvi (ed.)

01.05.1999

Confidential

The results of the density determinations indicate that large mineralisations can be detected by gravity surveying, as shown by that in the Ruotanen area. In many cases the dimensions of mineralisations are so small (or the mineralisations are deep-seated) that it is very difficult to get reliable gravity anomalies of them.

According to the density values, it seems possible to separate at least felsic intrusives and mafic volcanites from felsic volcanites, and to interpret roughly geological structures.

D 2.4 RESISTIVITY VALUE S OF DIFFERENT ROCK TYPES

Mineralisation is the only good conductor in the Pyhäsalmi area. Some talc-carbonate-bearing rocks and skarns also display low resistivity values, but only when they include sulphides (Fig. D3).

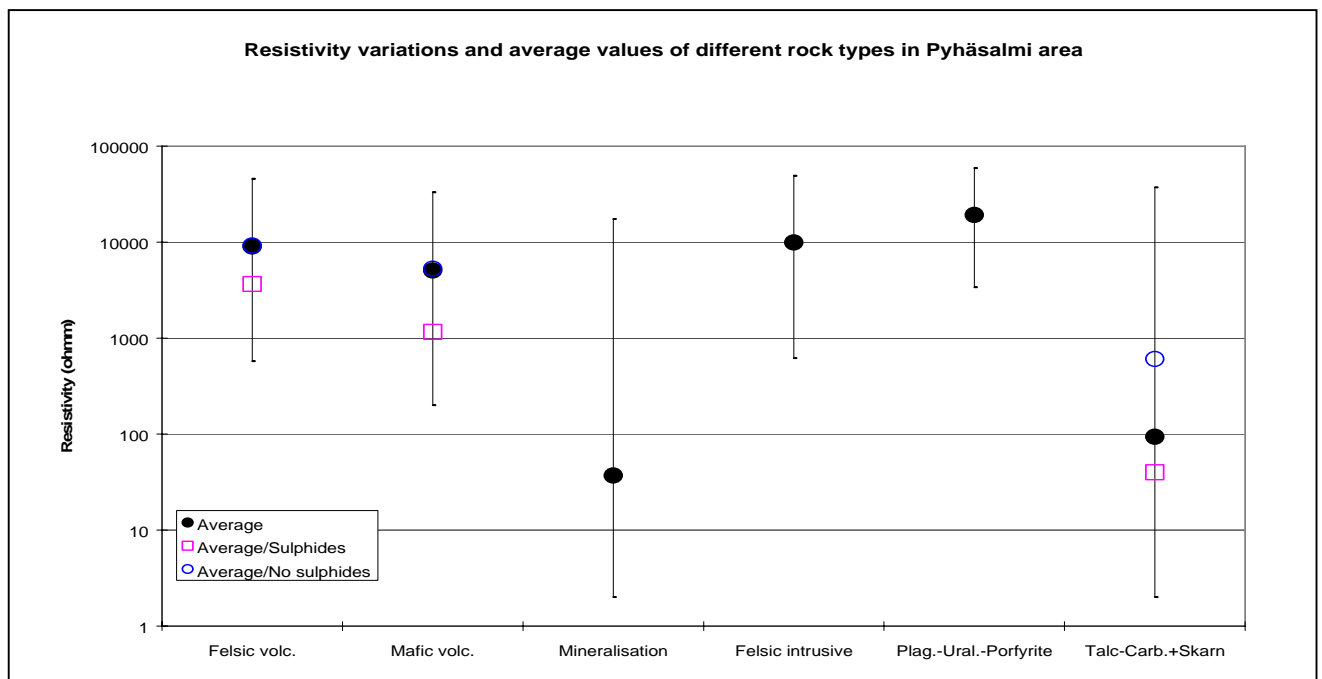


Figure D3.

Comparison between the resistivity values of different rock types shows that electrical and EM methods are good tools for exploration in the Pyhäsalmi area. For instance, the Pyhäsalmi ore deposit caused a big HLEM (Slingram) anomaly as seen on the HLEM survey map filed in the CD-ROM attached.

D 2.5 CONDUCTIVITY VALUES OF DIFFERENT ROCK TYPES

All of the conductivity values measured are mostly rather low, and different rock types cannot be separated from each other by these values (Fig. D4).

It is noted that the number of conductivity values measured was small and, for instance, only 19 mafic volcanite samples were measured (2 of them contained sulphides). Therefore the values presented in Figure D5 are not quite representative.

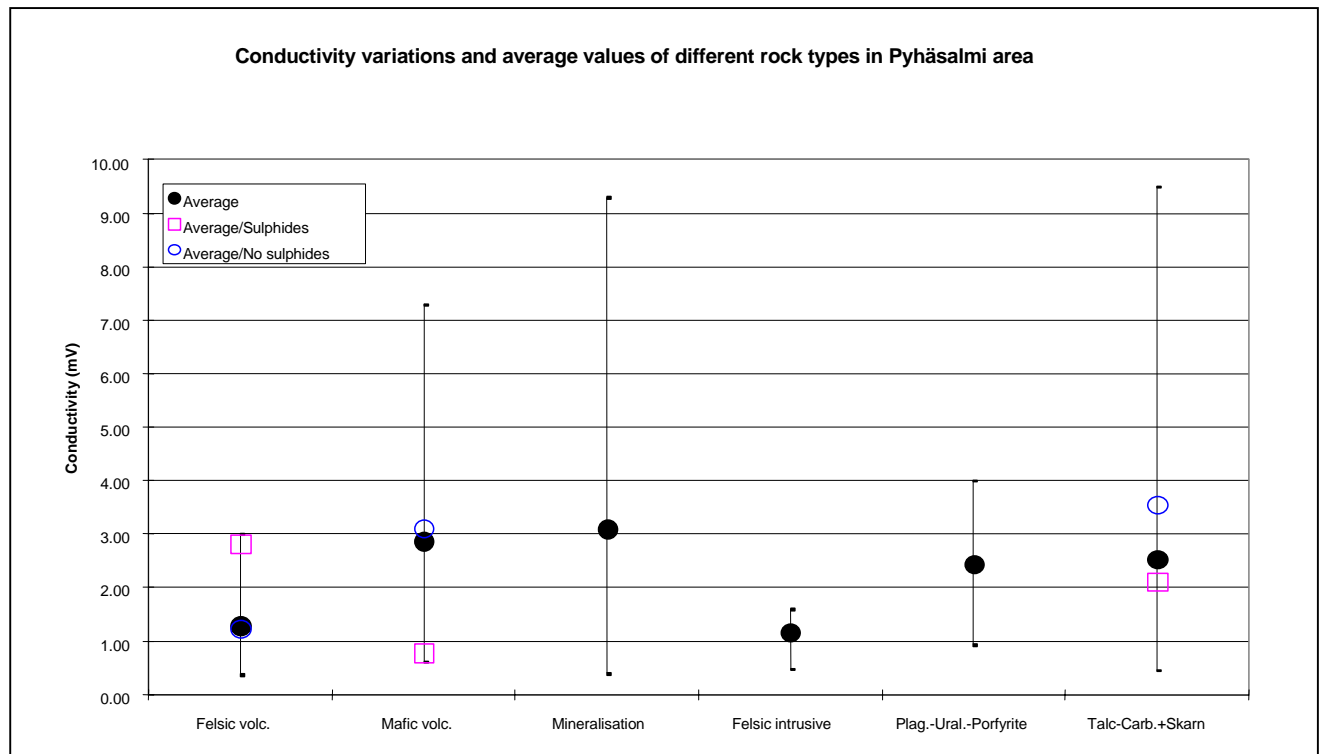


Figure D5.

D 2.6 PETROPHYSICAL PROPERTIES OF ALTERED AND UNALTERED FELSIC VOLCANITES

Detailed examination of petrophysical parameters in felsic volcanites was carried out to see whether there exist differences between unaltered and altered rocks.

Figure D6 shows that the density values of altered felsic volcanites are higher than those in unaltered ones. Sulphide-bearing felsic volcanites specifically display high density values.

Figure D6 also shows that the susceptibility values of both unaltered and altered felsic volcanites are rather low. Clear differences cannot be seen between these rock types.

Resistivity values in the altered felsic volcanites are lower than those in unaltered ones (Fig. D7). Difference between the resistivity values of the two groups is so small that it is difficult to separate the groups with geophysical methods. Sulphide-bearing felsic volcanites are more conductive than the other felsic volcanites, yet all of these rocks are poor conductors (Figure D8).

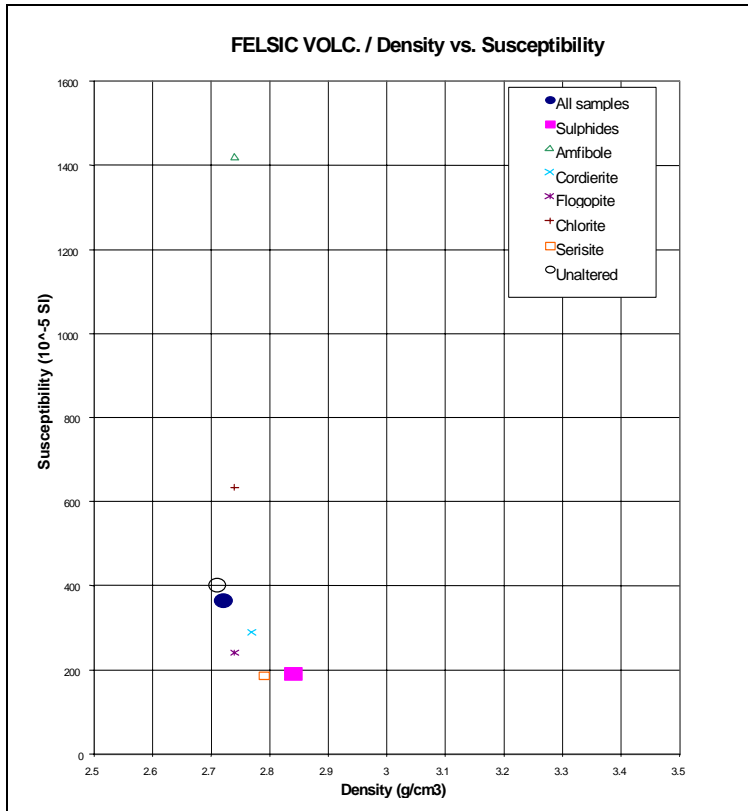


Figure D6

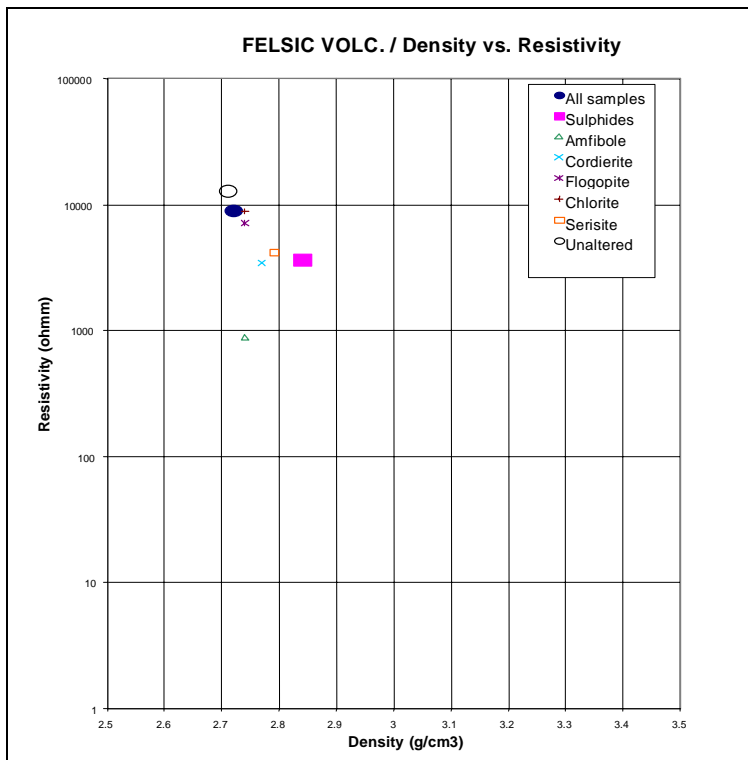


Figure D7.

Heikki Puustjärvi (ed.)

01.05.1999

Confidential

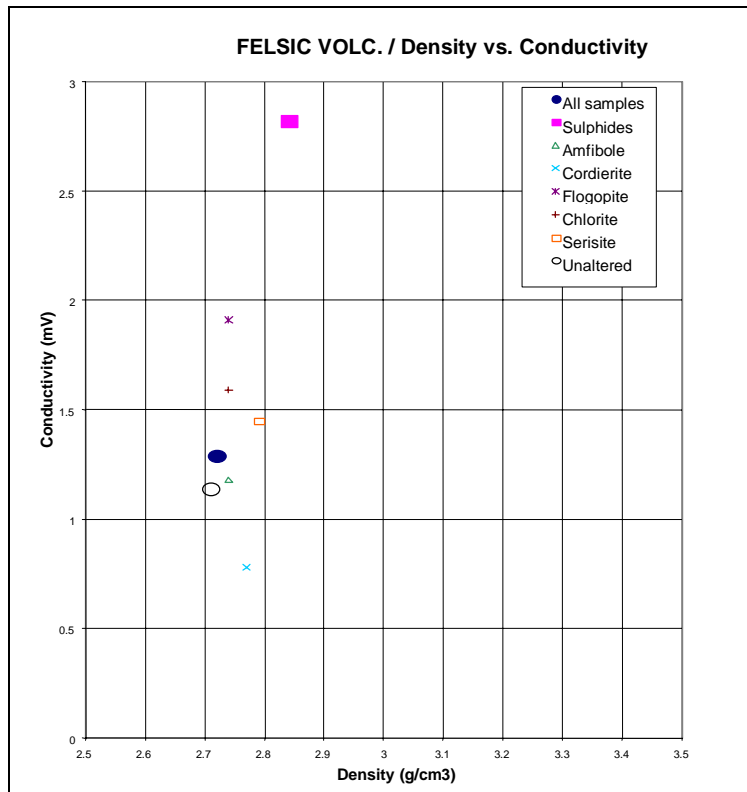


Figure D8.

D 2.7 PETROPHYSICAL PROPERTIES OF ALTERED AND UNALTERED MAFIC VOLCANITES

Petrophysical parameters in mafic volcanites were examined closer to see possible differences between unaltered and altered rocks.

Density determinations indicate that the density values of altered mafic volcanites are lower than those in unaltered ones, except for the sulphide-bearing samples, which display high densities (Fig. D9).

The susceptibility values of altered mafic volcanites are higher than those in unaltered ones; especially the sulphide-bearing samples have high susceptibilities.

The resistivity values of both unaltered and altered mafic volcanites are rather high and clear differences cannot be noticed between these rocks (Fig. D10).

Unaltered mafic volcanites seem to have higher conductivity values than altered ones (Fig. D11). However, because of the small number of samples, this result is not very reliable.

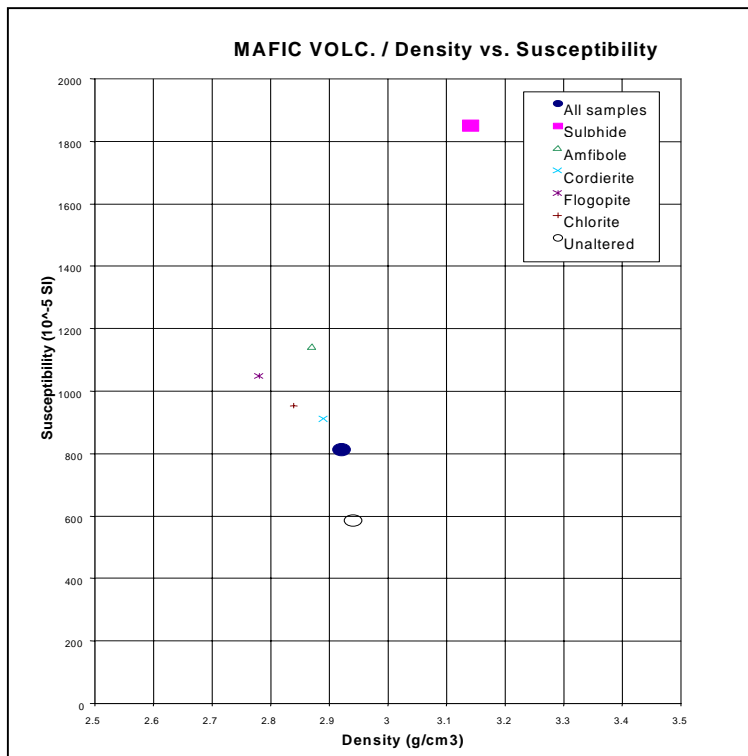


Figure D9.

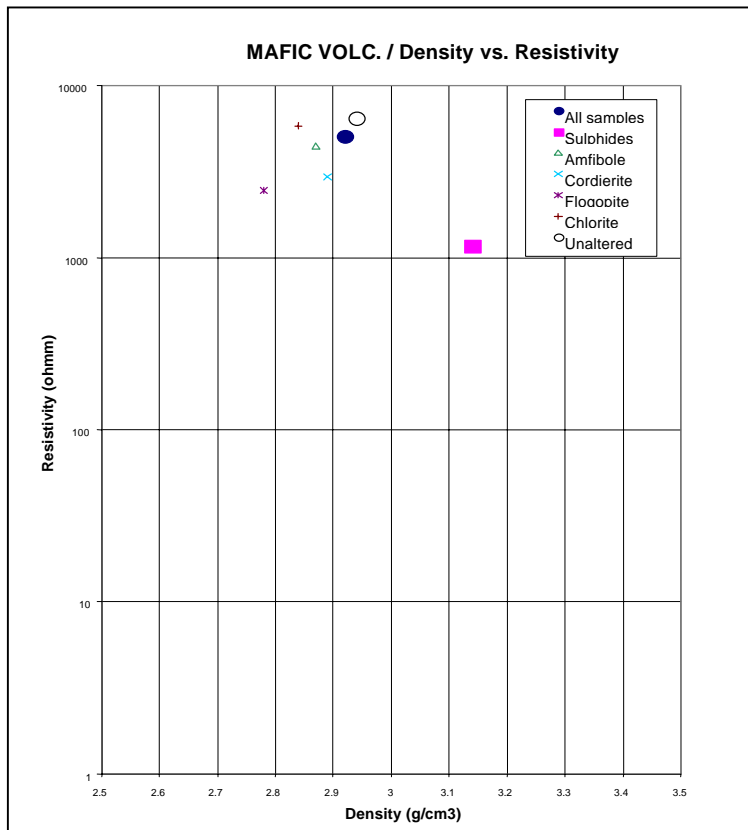


Figure D10.

Heikki Puustjärvi (ed.)

01.05.1999

Confidential

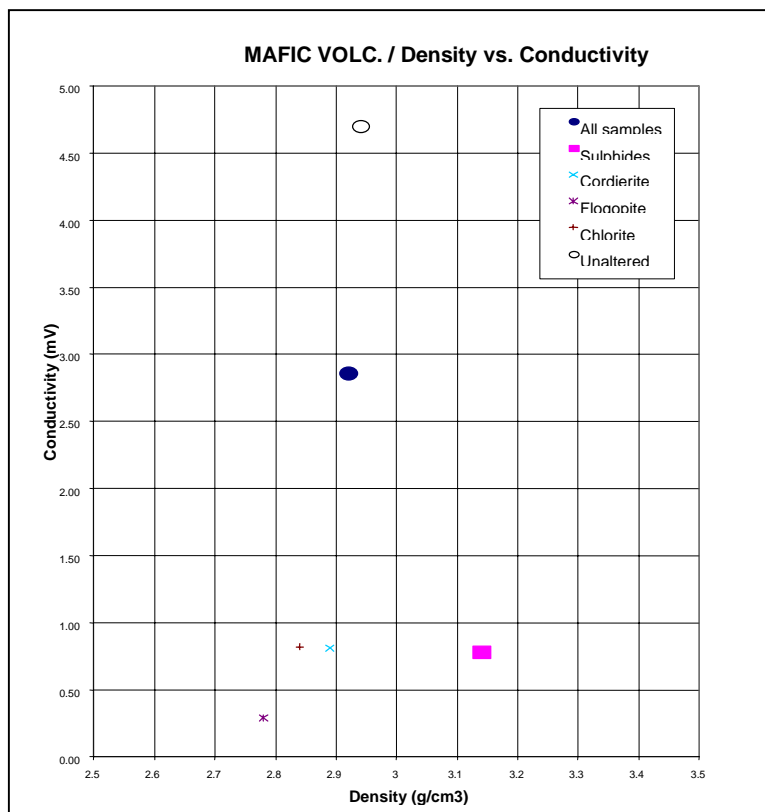


Figure D11.

D 3 AIRBORNE AND GROUND GEOPHYSICS

Low-altitude aeromagnetic and aero-EM surveys were carried out by the Geological Survey of Finland (GTK) in the Pyhäsalmi area. The resulting data were used in various map formats to trace geological units outside the ground survey areas. No interpretations were done on such data.

Several map formats were created of the geophysical ground survey data. The data and maps are presented in the geophysics directory of the attached CD-ROM.

Magnetic anomalies seem to be mostly caused by mafic volcanites. However, as the magnetic map indicates, it is not possible to exactly follow contacts because of the uneven distribution of magnetized sequences within these rocks. Also the ground magnetic data quality in the Ruotanen area was rather poor causing problems in creating maps and in interpretations.

HLEM (Slingram) anomalies are caused by mineralized formations located close to ground. IP anomalies show features similar to fracture zones, partly in areas of altered volcanites. Some of the HLEM anomalies are caused by overburden.

Because of a strong gradient it is difficult to see detailed information on gravity maps as exemplified by the Bouguer map of the Ruotanen area (Fig. D12a).

Heikki Puustjärvi (ed.)

01.05.1999

Confidential

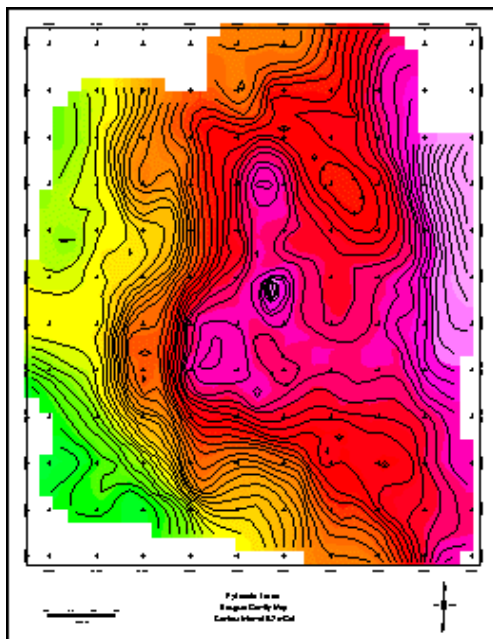


Figure D12a.

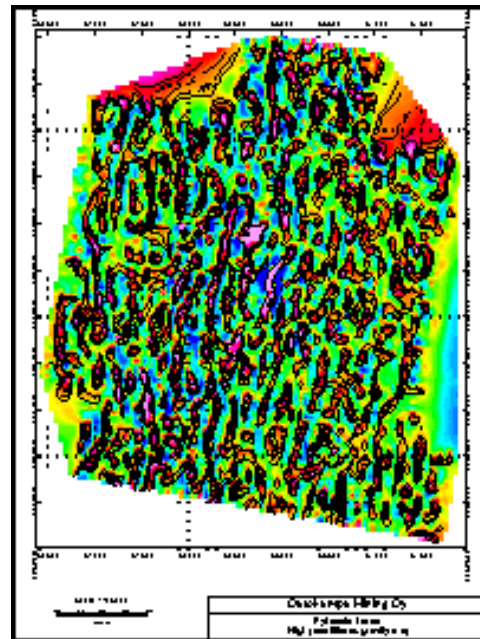


Figure D12b.

A high pass-filtered gravity map (Fig. D12b) shows more details. Best information of the gravity data can be achieved by the interpretation of 3D block models.

The Gefinex 400S survey data were interpreted using a layer model, and the results were presented as cross sections. The Gefinex 400S (also known as Sampo) system, designed in the Outokumpu Group, is a wide-band electromagnetic sounding method for inductively determining the electrical resistivity of ground at different depths using a fixed transmitter-receiver separation and changing frequency to obtain variable penetration.

During the project, new Gefinex 400S surveys were carried out to get more and better information on certain interesting targets: the Lehto area SE of the Pyhäsalmi mine, the Kettuperä area located within the mine village, and in-fill lines at Mullikkoräme.

D 4 DOWNHOLE GEOPHYSICS

Only few of the downhole EM surveys measured prior to the project were examined in the most interesting target areas.

New Protem surveys were carried out during the project to find out the locations of possible conductors in the vicinities of drillholes (all of them were test holes, see section G).

Drill hole PYS-118, located southeast of the Pyhäsalmi mine, was tested with a 3-component magnetometer but the results were not very promising (nearby

Heikki Puustjärvi (ed.)

01.05.1999

Confidential

magnetized bodies were not detected).

D 5 GEOPHYSICAL MODELING

Three-dimensional interpretations were carried out of gravity data in the Pyhäsalmi mine and the Mullikkoräme areas. Test interpretations were done of the magnetic data. ModelVision software (Encom Technology Pty. Ltd., Australia) was used in magnetic and gravity modeling.

The Gefinex 400S EM data profile interpretations were plotted as cross sections. The results were examined together with gravity interpretations and geological cross sections. The interpretations were carried out with special Gefinex 400S data processing and interpretation software.

All of the Protem downhole EM data were interpreted with EMVision software (Encom Technology Pty. Ltd., Australia).

D 5.1 GRAVITY AND MAGNETIC INTERPRETATIONS IN THE RUOTANEN AREA

The gravity interpretations were started on profiles where geology was well known because of previous drilling. Three-dimensional tabular (dipping prism) bodies were created using the geological and petrophysical information available on selected "model profiles". When a reasonable fit between the measured and calculated values was achieved the interpretations were extended over the survey area. A 200-meter spacing was mostly used between interpreted lines.

In the Ruotanen area, lines X=15500 (geol. section 2700), X=16000 (geol. section 3200), X=16200 (geol. section 3400), A=3900 and A=4200 were selected as primary profiles (geol. section names according to the Pyhäsalmi mine xy-coordinate practice).

Figures D13 – D17 show the interpretations of the five profiles. It is noted that, because of the models used, the interpretations are rather rough, however they reasonable approximate geological structures and show the dimensions of different geological units.

The gravity values on lines A=3900 and A=4200 were picked up from a Bouguer contour map and thus include only few measured values. Distance co-ordinates along the lines are absolute distance values starting from co-ordinate B=9000.

As earlier mentioned, the interpreted 3D structures cannot be noticed if examined only on maps produced with data processing methods without interpretations.

Heikki Puustjärvi (ed.)

01.05.1999

Confidential

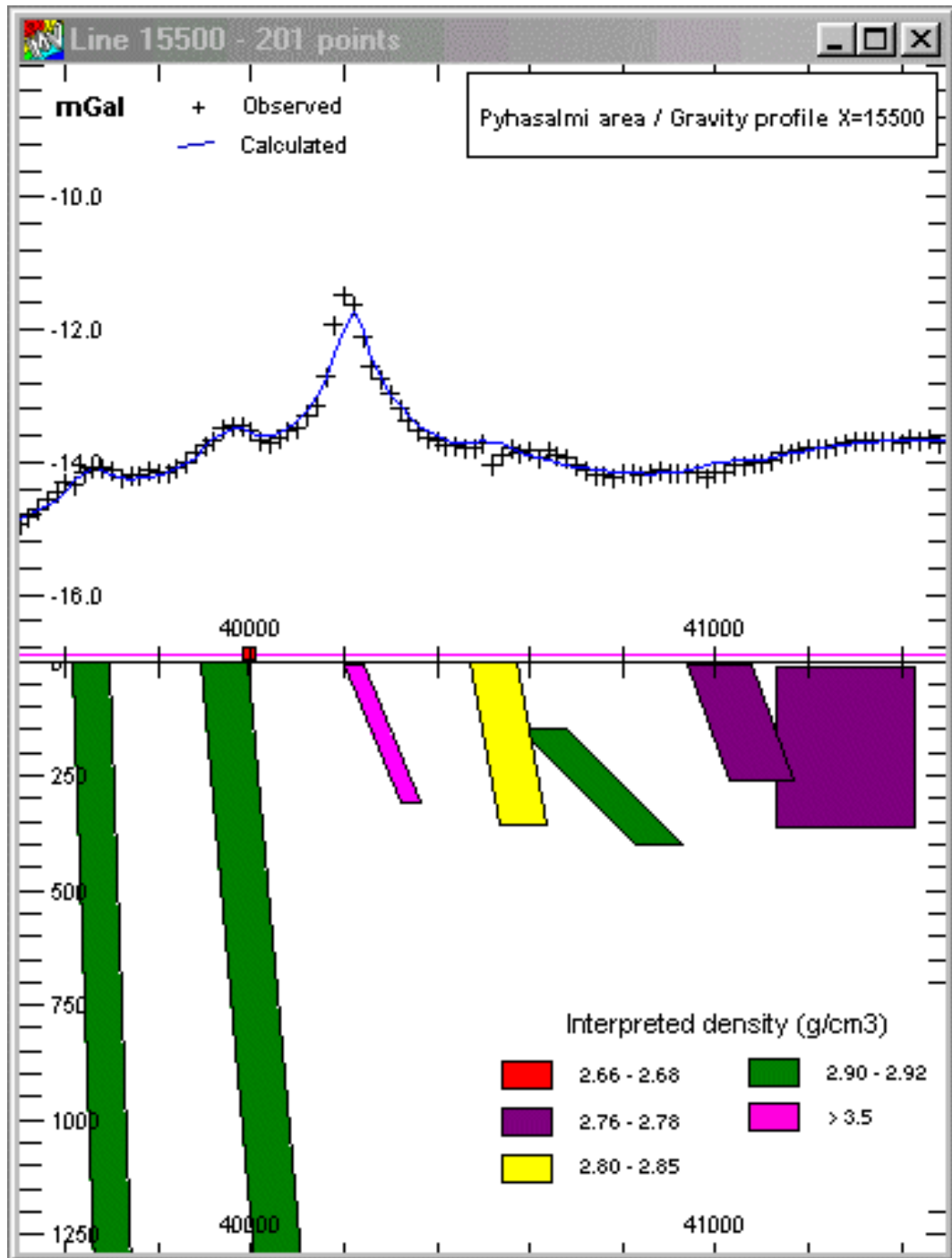


Figure D13.

Heikki Puustjärvi (ed.)

01.05.1999

Confidential

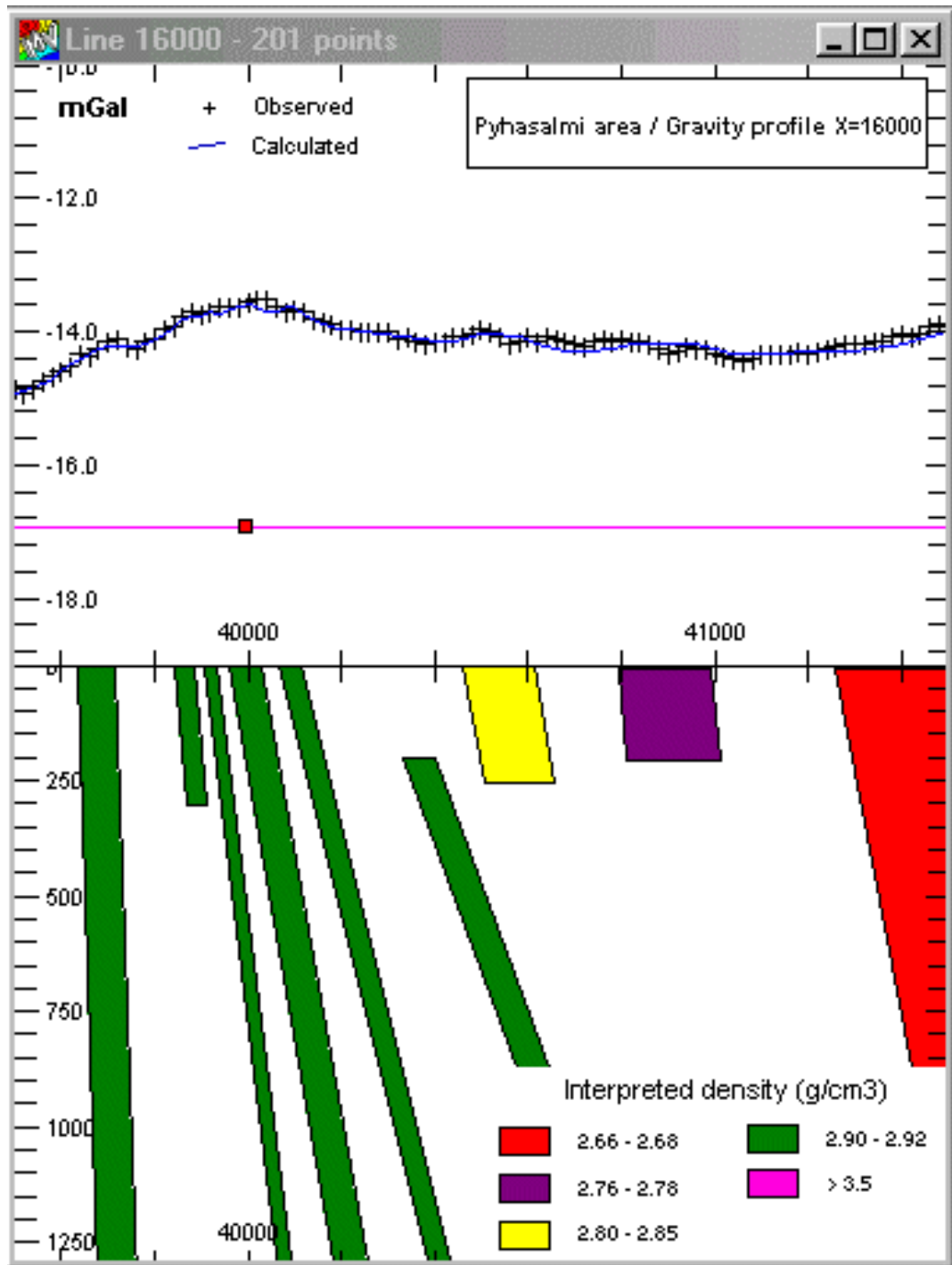


Figure D14.

Heikki Puustjärvi (ed.)

01.05.1999

Confidential

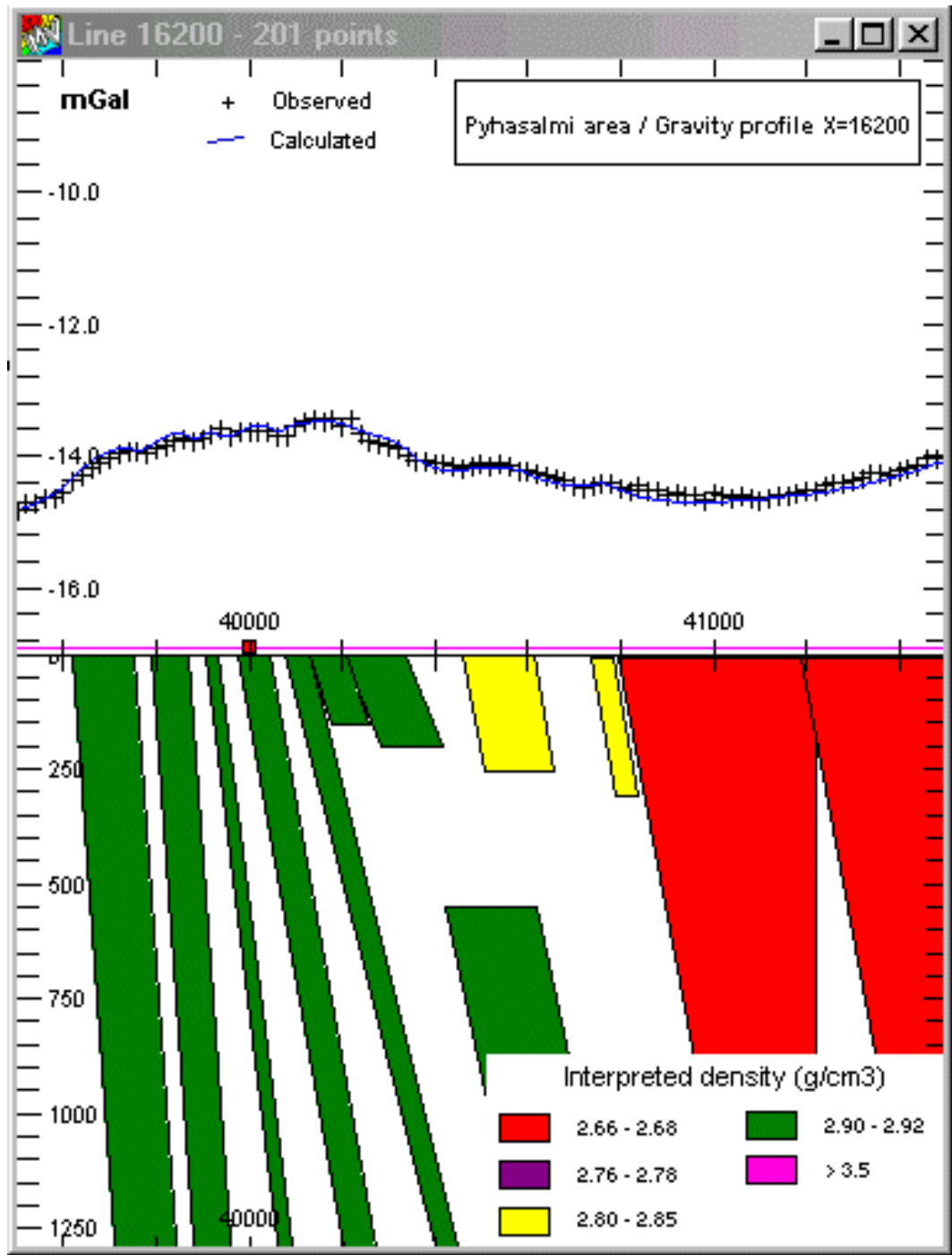


Figure D15.

Heikki Puustjärvi (ed.)

01.05.1999

Confidential

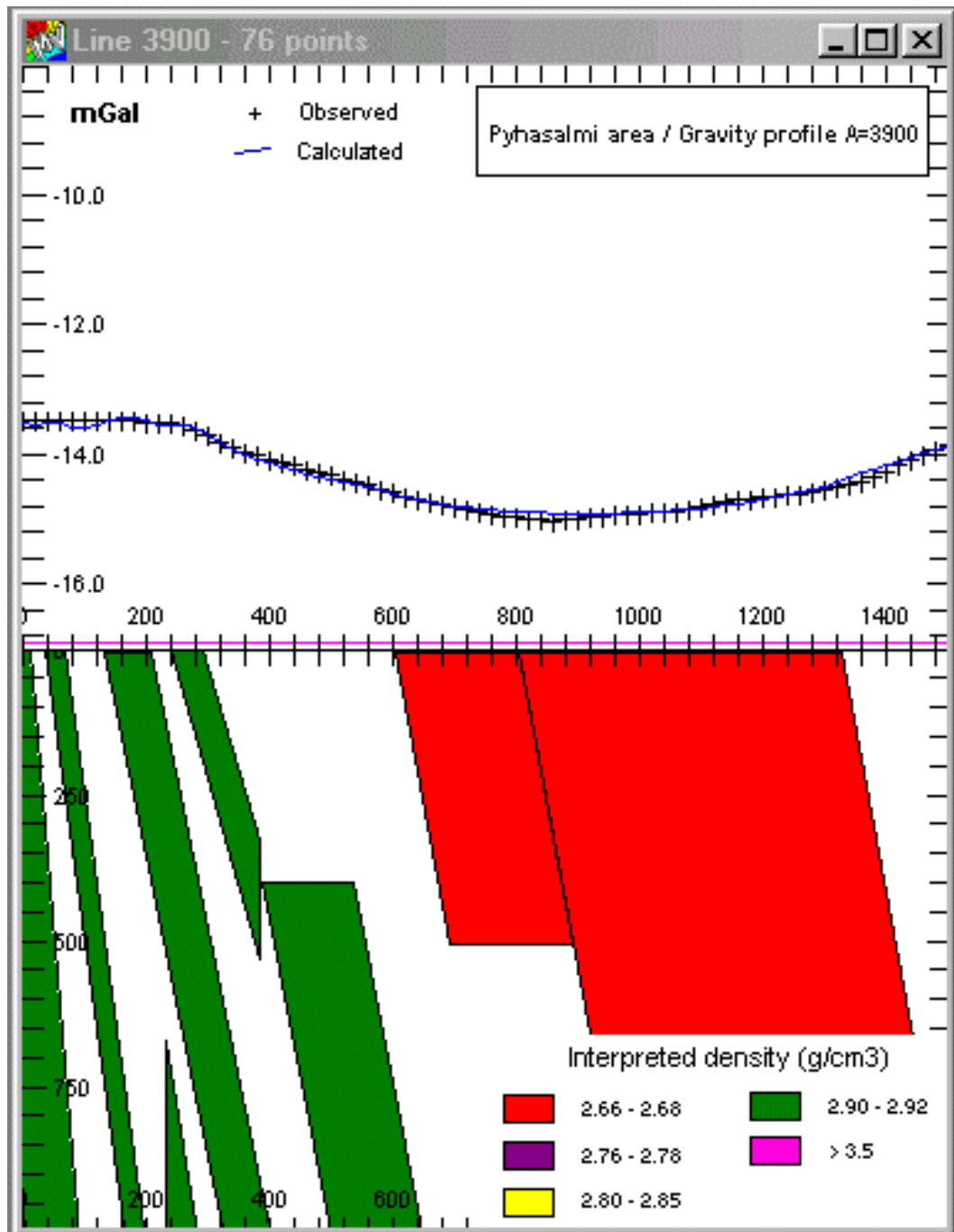


Figure D16.

Heikki Puustjärvi (ed.)

01.05.1999

Confidential

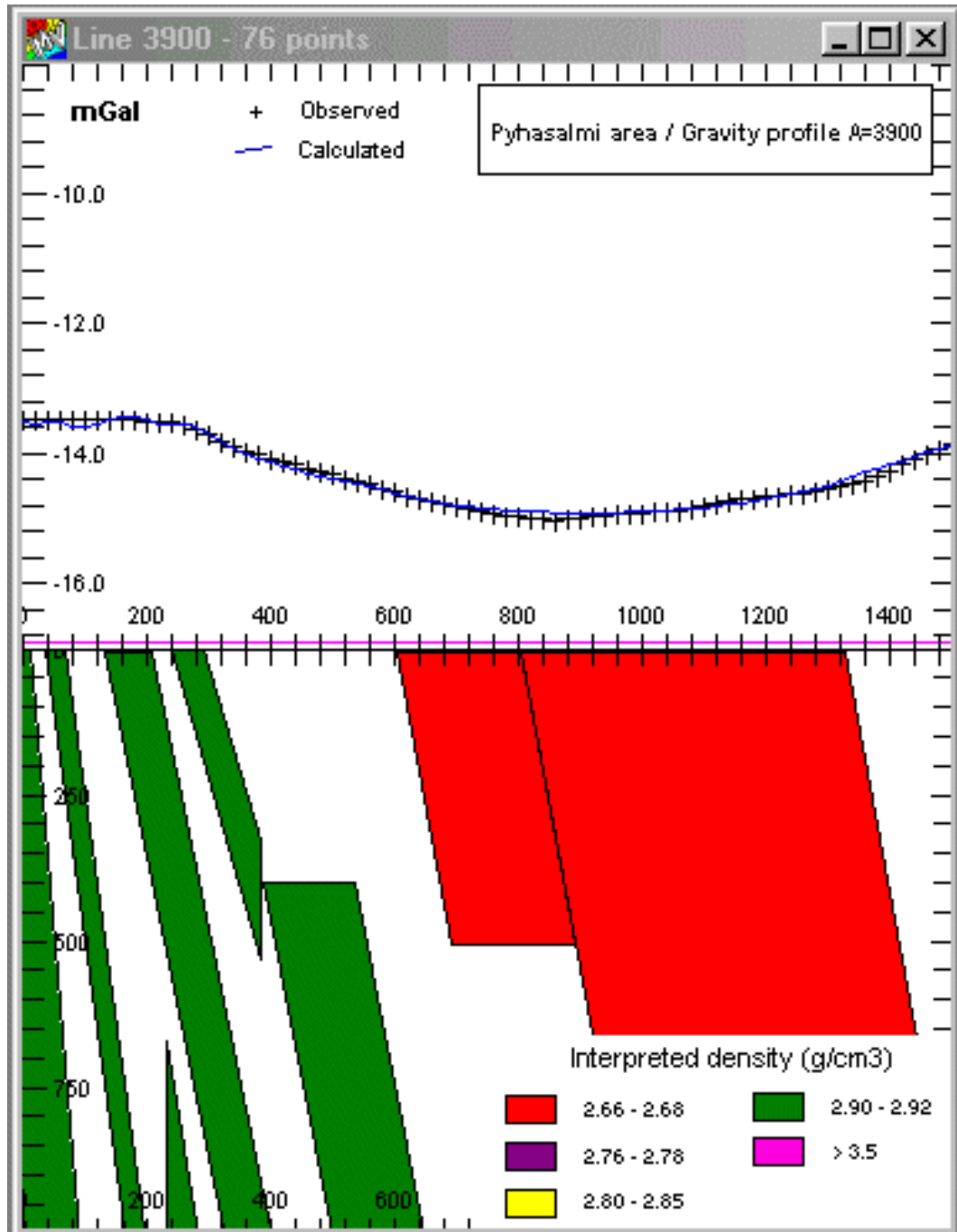


Figure D17.

Ground surface projections of the interpreted bodies in the Ruotanen area are presented in Fig. D18.

Heikki Puustjärvi (ed.)

01.05.1999

Confidential

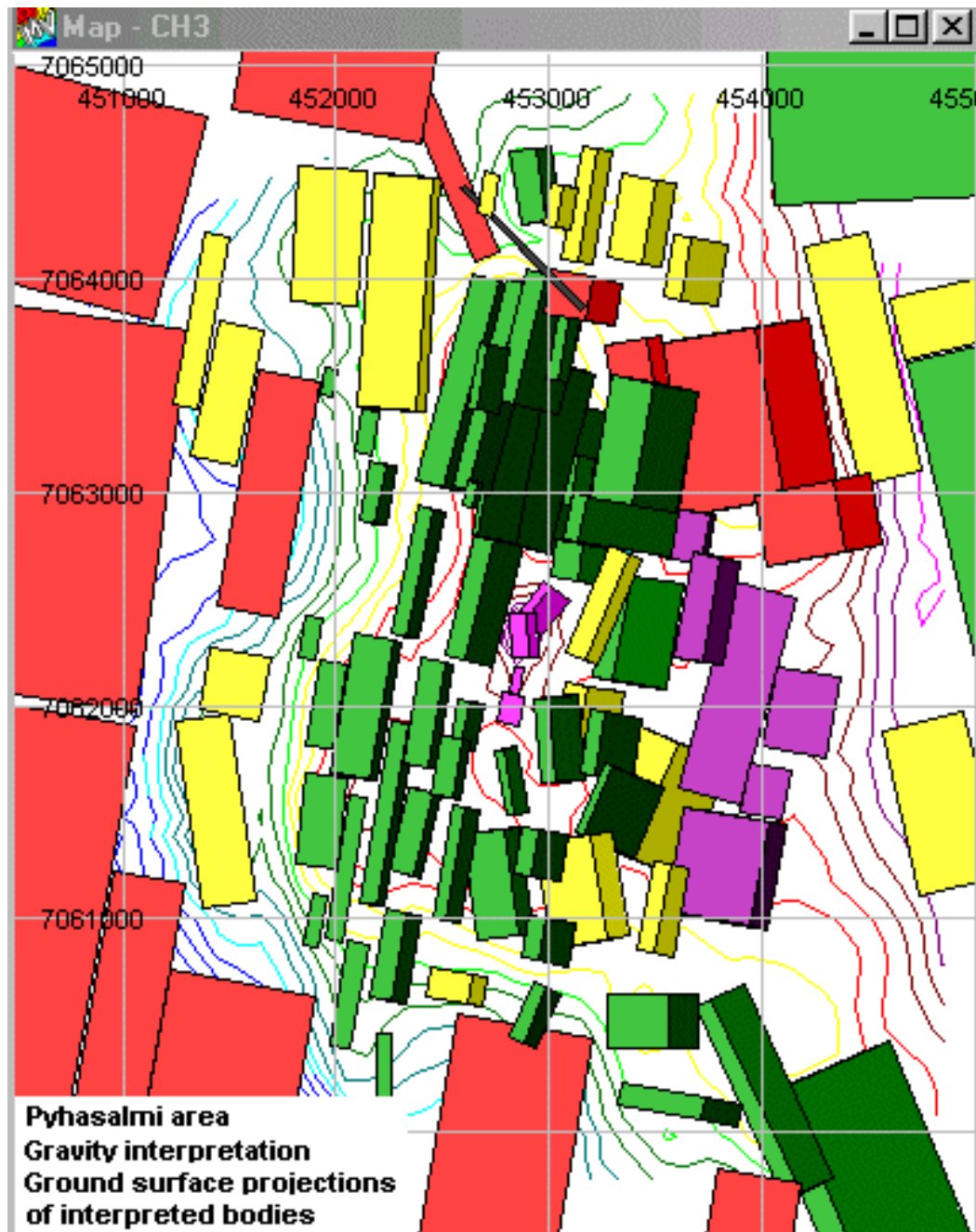


Figure D18.

The interpretation model includes more than 100 bodies. It is saved together with the measured profiles in ModelVision session format (CD-ROM) for possible follow-up work.

Figure D19 shows a rough interpretation of the magnetic data on Profile A=4200. Interpretation was done using the bodies used in the gravity interpretation added with new magnetized only bodies. The interpretation shows heterogeneous magnetization in mafic volcanites and that also granites are partly magnetized.

Heikki Puustjärvi (ed.)

01.05.1999

Confidential

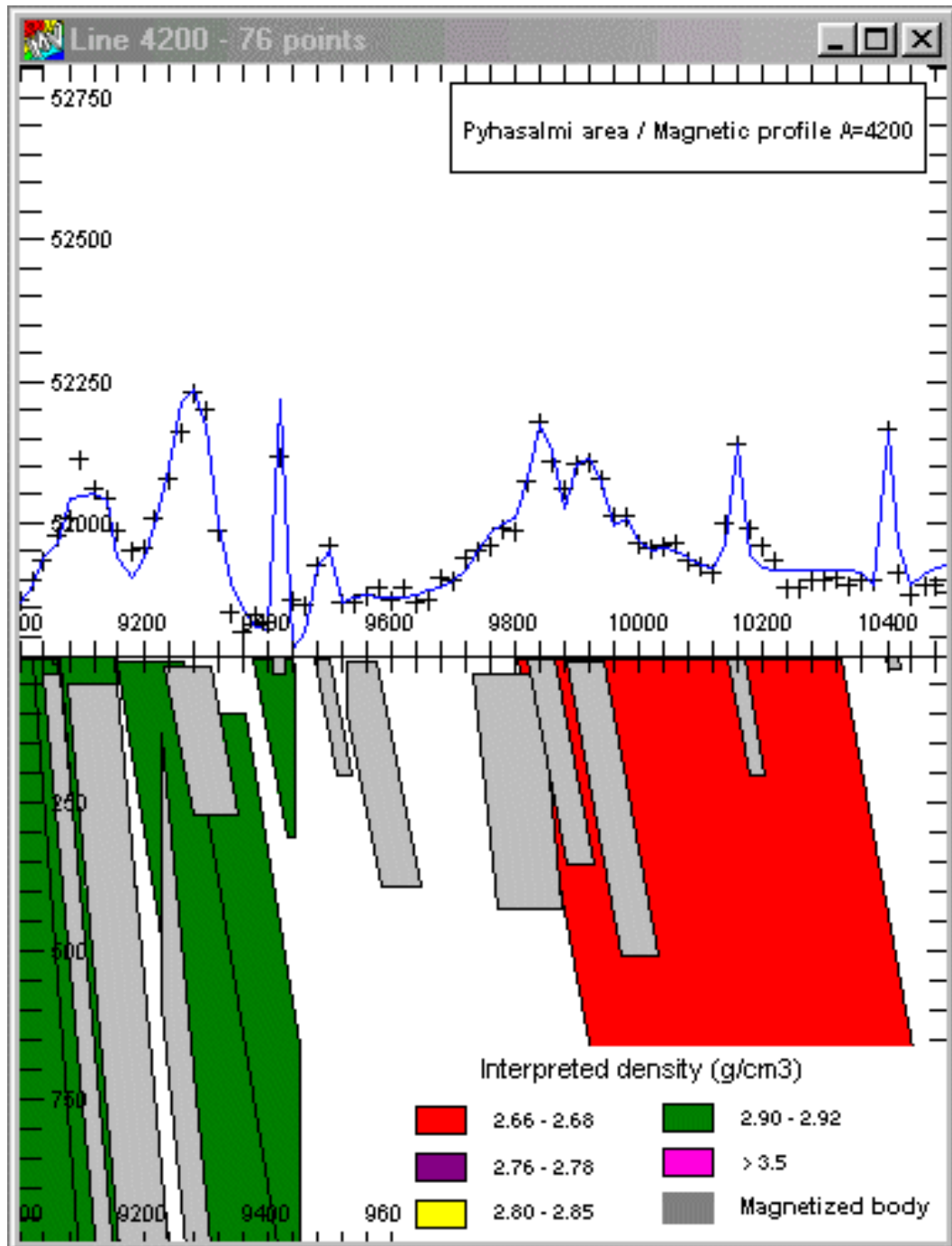


Figure D19.

Profile A=4200 shows that it is impossible to find contacts of different rock types by magnetic interpretation, therefore no three-dimensional modeling was done of the magnetic data in the survey area.

D 5.2 GEFINEX 400S INTERPRETATIONS IN THE RUOTANEN AREA

Gefinex 400S interpretations were carried out on 16 profiles measured prior to this

Heikki Puustjärvi (ed.)

01.05.1999

Confidential

project (coil separation 100-400 m), on 9 profiles measured in 1998 (coil separation 800 m) and on 7 profiles measured in 1999 (coil separation 600 m).

In the interpretations of the older profiles, three interesting anomalous areas were detected: The so-called Lehto area southeast of the Pyhäsalmi mine (line X=14850), an area west of the mine (line X=15000), and an area south of the Kettuperä area (line A=4200).

In the Lehto area, on line X=14850, a good conductor was detected at 500-600 m depth. To obtain better information of this deep-seated conductor the area was measured again using the coil separation of 800 meters. Figure D20 shows the interpretation result of this profile (X=14850). In spite of drillings (a new hole drilled and an old one continued) the source of the interpreted conductor remained unknown. Probably the conductor consists of several small conductive lenses. Conductive fractured zones may also exist in the same area.

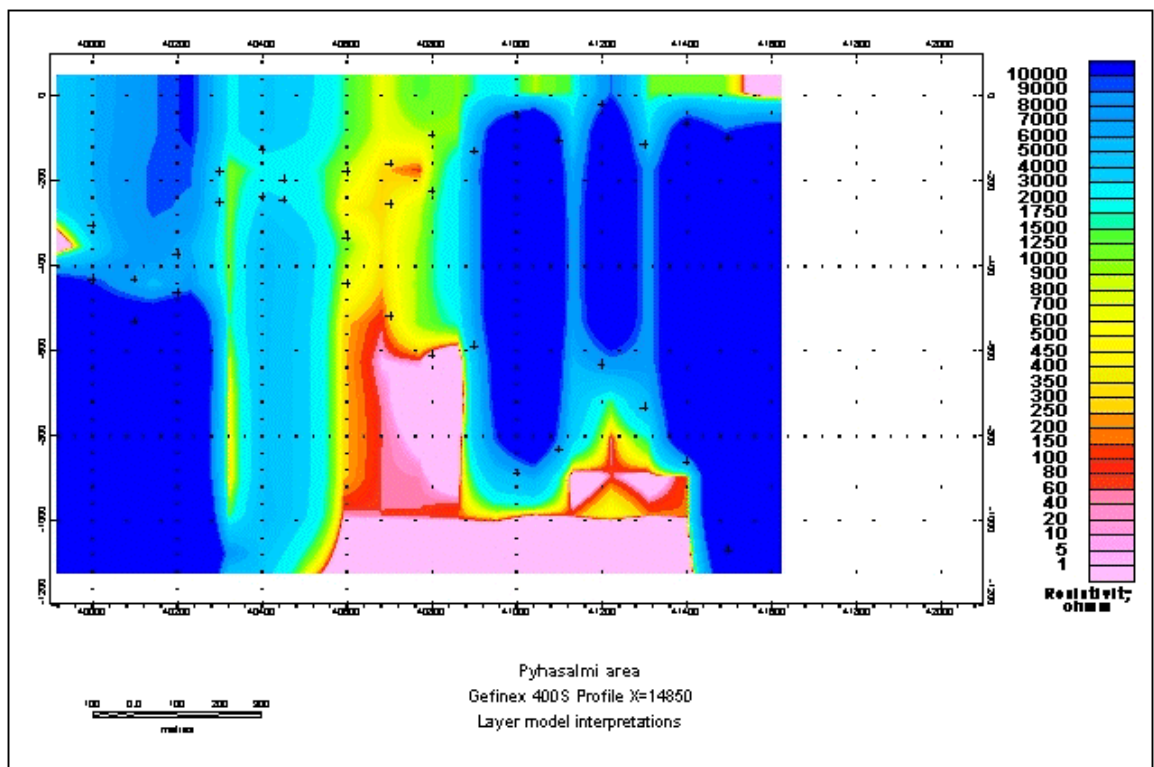


Figure D20.

West of the Pyhäsalmi mine, at the western end of Profile X=15000, there exists a good conductor at 250-400 m depth. It dips gently to the west as shown by the Gefinex 400S interpretation section in Fig. D21.

According to drilling results this Gefinex 400S anomaly is caused by graphite- and pyrrhotite-bearing zones (test drillhole PYS-117, see section G).

In the area between Kettuperä and the Pyhäsalmi orebody a deep-seated conductor

Heikki Puustjärvi (ed.)

01.05.1999

Confidential

was detected in the Gefinex 400S interpretations (Fig. D22). Since there was a gap in the earlier surveys, seven new profiles were measured at the beginning of 1999 to get more information for this area.

The new measurements detected conductors also to the south of profile A=4200 (possibly a deep-seated mineralisation is located in this area).

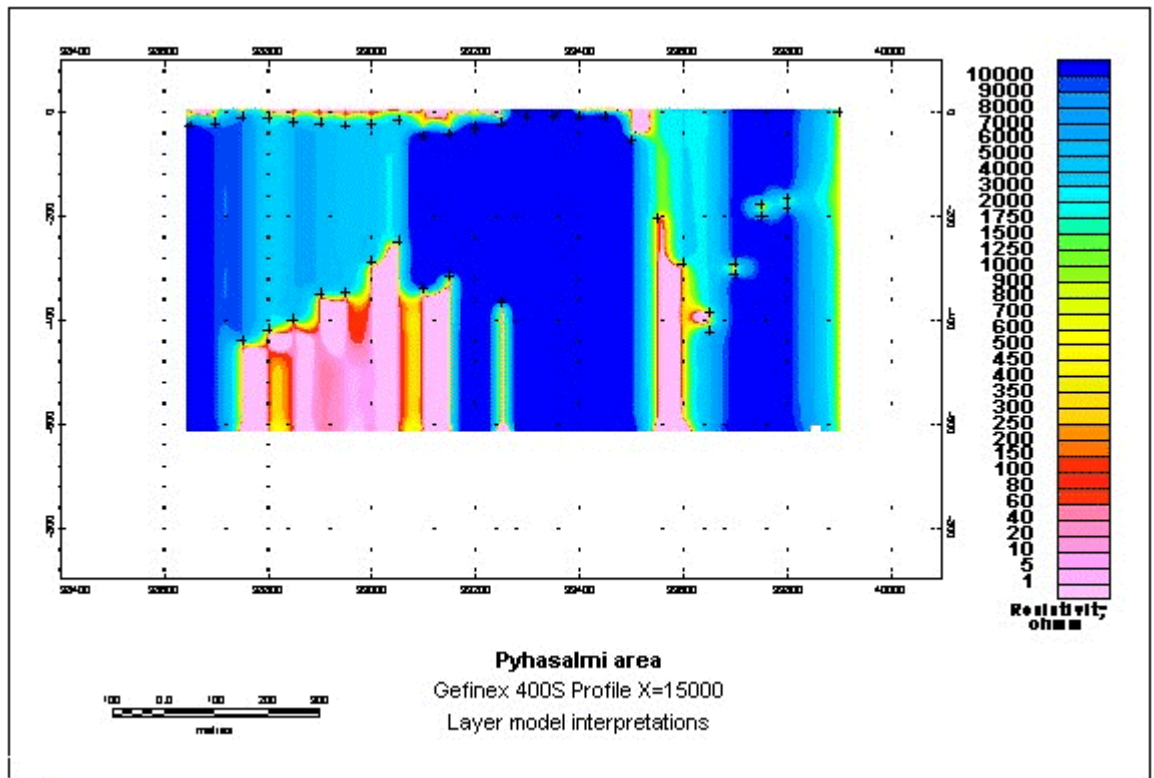


Figure D21.

Heikki Puustjärvi (ed.)

01.05.1999

Confidential

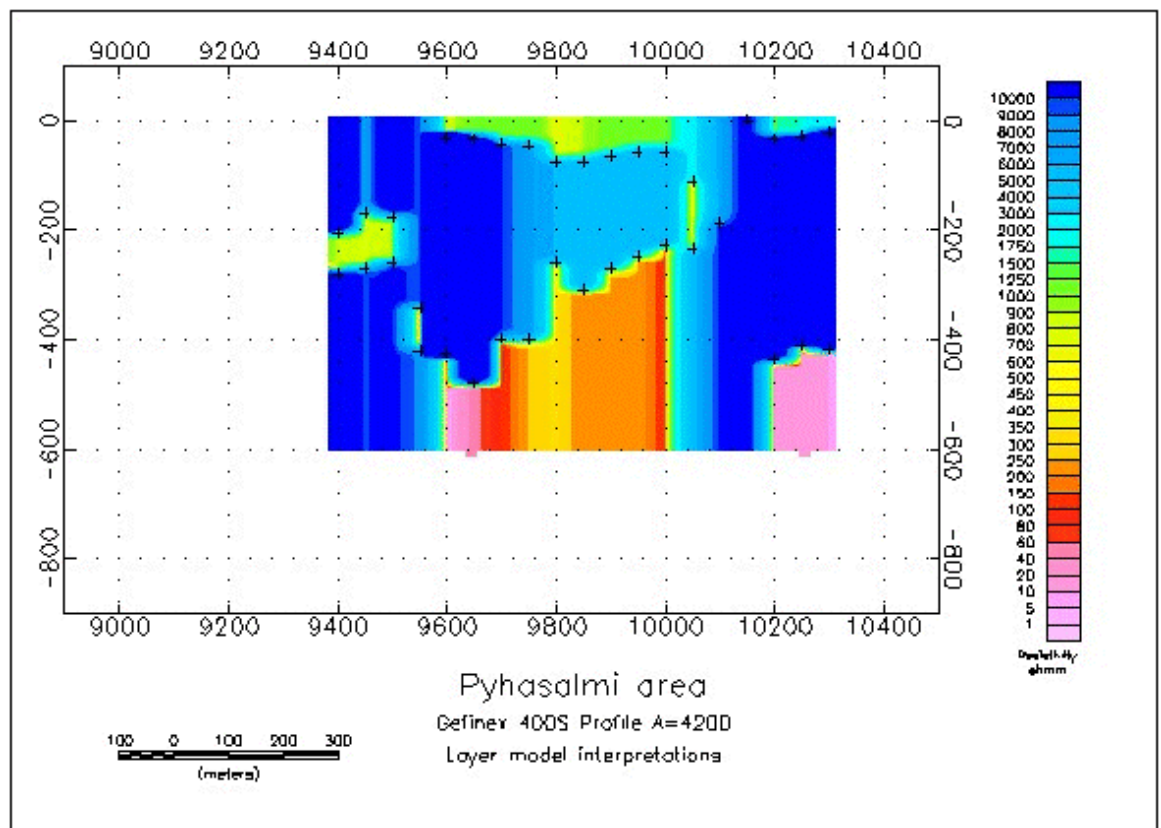


Figure D22.

The Gefinex 400S interpretation sections are presented in the geophysics directory of the attached project CD-ROM in Geosoft Oasis Montaj map format.

D 5.3 DOWNHOLE EM INTERPRETATIONS IN THE RUOTANEN AREA

Protem downhole EM data were roughly interpreted to confirm that there really exist near-hole conductors as suggested by Gefinex 400S interpretations.

In the Lehto area, a survey in drillhole PYS-107 (continued during the project) showed that there really exists a conductor outside the hole. However, this conductor was not intersected in a new test hole (PYS-118) drilled further southeast. Only a very weak Protem anomaly was detected there.

Protem measurements in drillhole PYS-119, located in an area between Kettuperä and the Pyhäsalmi mine, showed two conductors (Fig. D23). One of them was intersected in drillhole (the upper layer), the other is off-hole. This result fits the Gefinex 400S interpretation discussed above. Downhole EM survey in drillhole PYS-113, located southwest of PYS-119, showed that both of the conductors are outside this hole.

Heikki Puustjärvi (ed.)

01.05.1999

Confidential

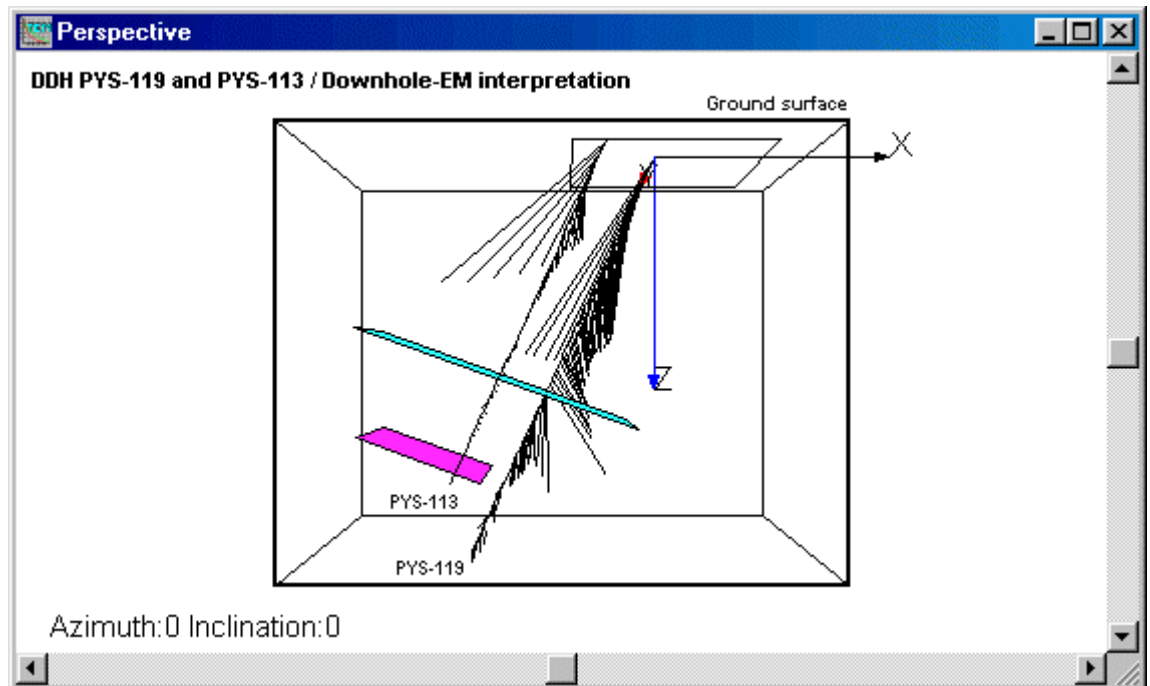


Figure D23.

D 5.4 GRAVITY INTERPRETATIONS IN THE MULLIKKORÄME AREA

A three-dimensional geological model was created for the Mullikkoräme area using gravity interpretations. The results are presented in Fig. D24 as a block model.

A 200-meter spacing between interpreted lines was mostly used.

An interpretation of the granite area east of the Mullikkoräme deposit showed that the dimensions of this granite couldn't be as big as drawn on geological cross sections and maps. Interpretation (profile X=66600) is exemplified in Fig. D25 and shows that high-density rock must exist below the granite. This means that, if the volcanites continue east below the granite, it is possible that also the mineralized zone continues east.

High-density rock exists also at the eastern end of the profile. However, as these rocks seem to continue outside the survey area, it was not possible to interpret their dimensions and density values reliably. Therefore these bodies are presented as unidentified rocks in Fig. D26.

Heikki Puustjärvi (ed.)

01.05.1999

Confidential

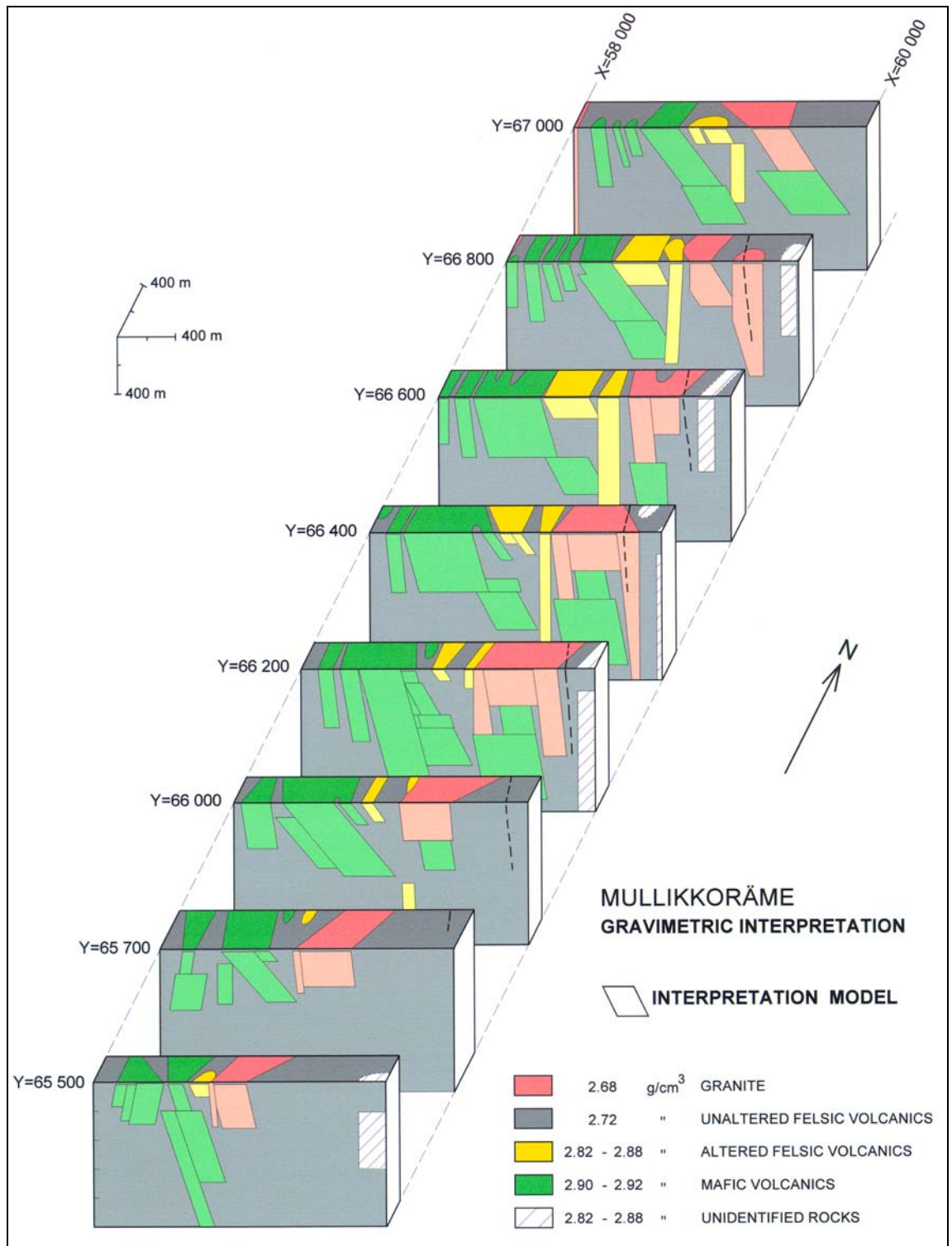


Figure D24.

Heikki Puustjärvi (ed.)

01.05.1999

Confidential

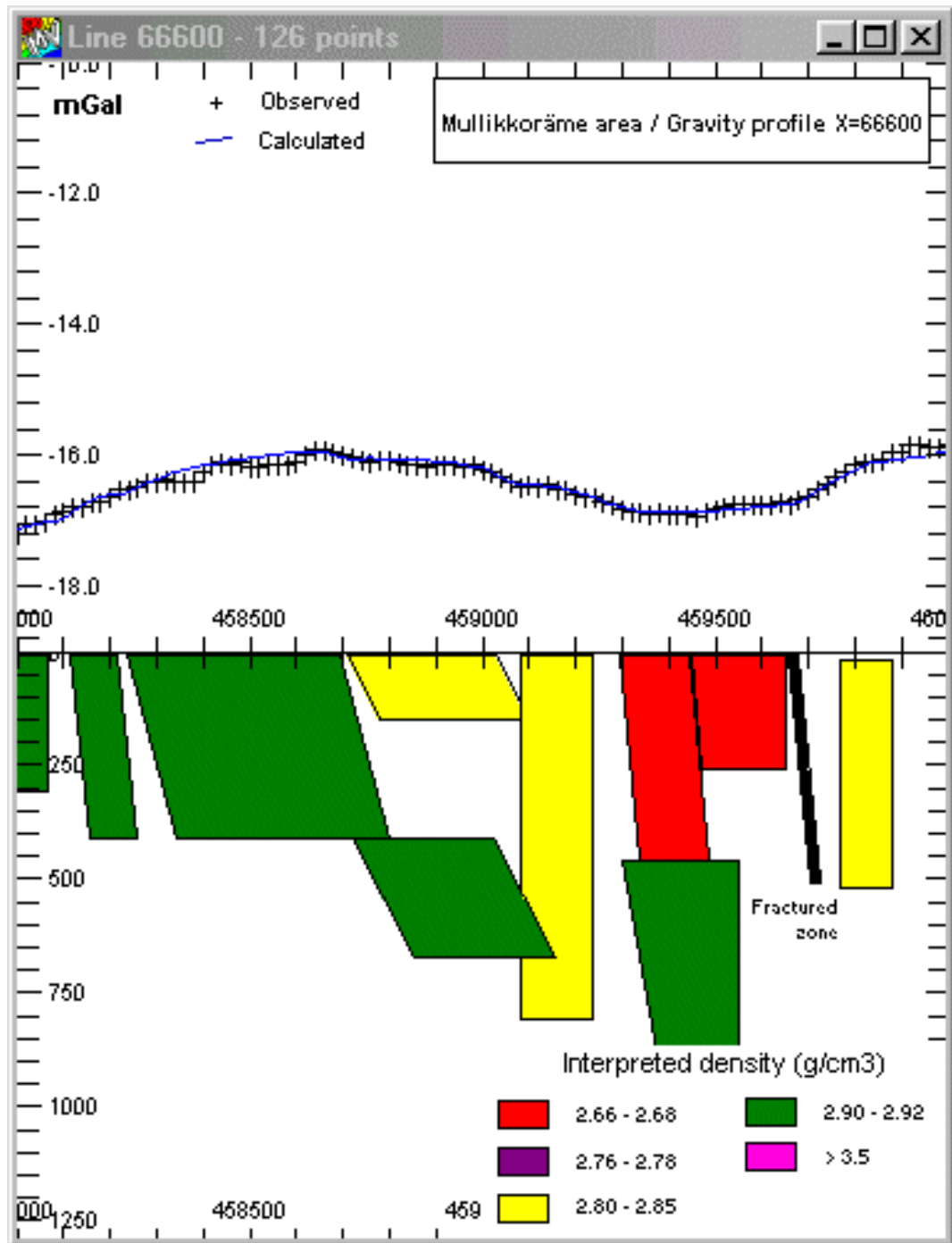


Figure D25.

According to the interpretations, deep-seated mineralisation may extent south, further than known so far. E.g. on line X=66100 the zone of altered felsic volcanites (with possible mineralisation) may be located below the eastern granite (Fig. D26).

Heikki Puustjärvi (ed.)

01.05.1999

Confidential

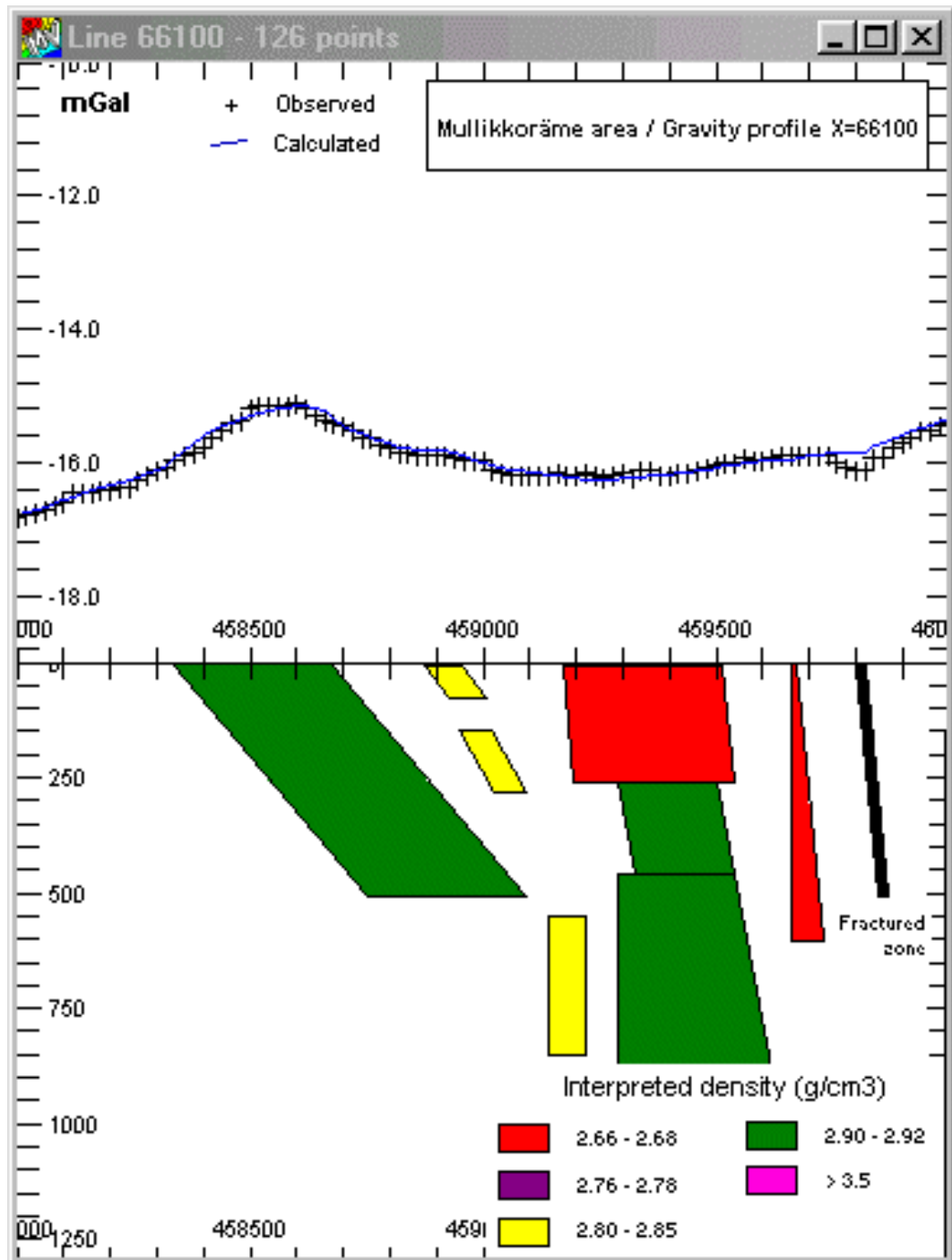


Figure D26.

The three-dimensional model created during the interpretations is saved in ModelVision session format and filed in the project geophysics directory (CD-ROM).

Heikki Puustjärvi (ed.)

01.05.1999

Confidential

D5.5 GEFINEX 400S INTERPRETATIONS IN THE MULLIKKORÄME AREA

A total of 1230 measured Gefinex 400S stations were examined on 37 lines in the Mullikkoräme area. Most of these stations were interpreted and the interpretation results were plotted as cross sections.

The western parts of the profiles were measured using 400 m coil separation and the eastern parts using that of 800 m. Figs. D27 (a=400 m) and D28 (a=800 m) exemplify the interpretation results on Profile X=66400.

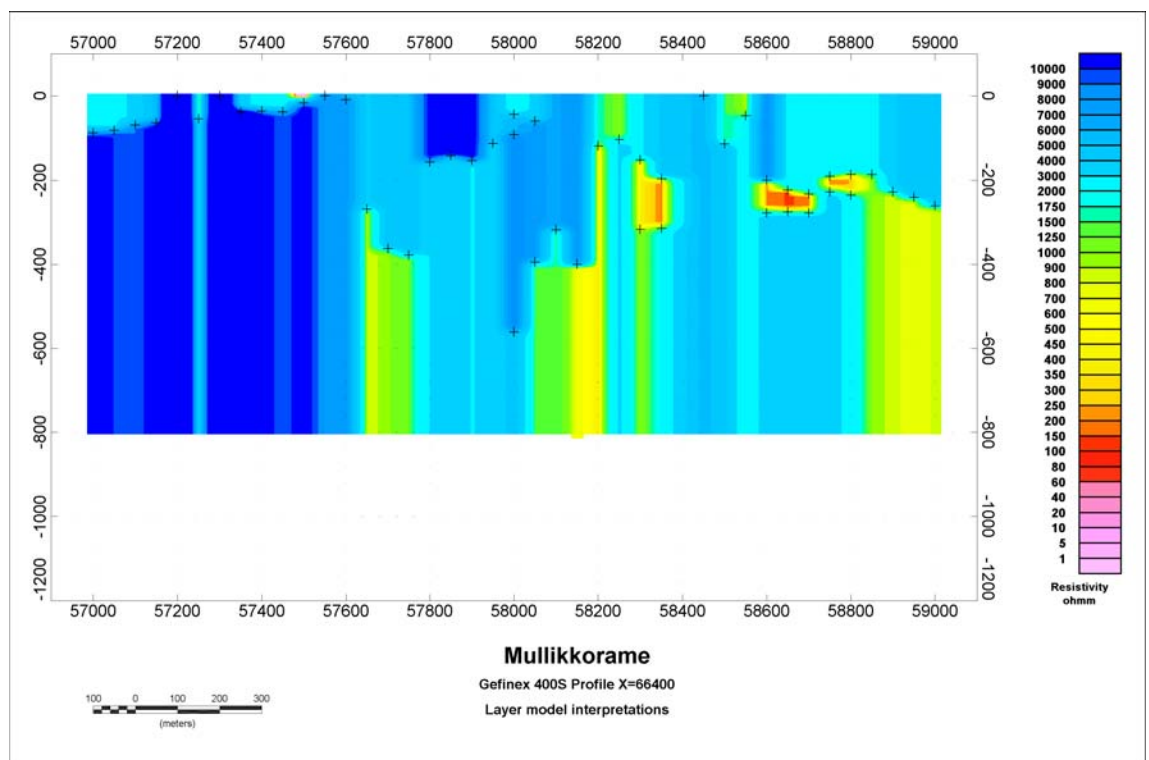


Figure D27.

Conductors west of co-ordinate Y=59000 (Fig. D28) are mostly caused by weakly mineralized mafic volcanites. The “terrace” with lower resistivity values around co-ordinate Y=59100 fits known ore. East of co-ordinate Y=59200 there are two conductors, one at c. 200 m depth, the other clearly deeper. The upper conductor seems to be a low-resistivity layer inside granite and the deep-seated one is either granite contact or a mineralized layer in volcanites. According to the gravity interpretations the latter alternative is more probable.

On line Y=66000 (Figs. D29 and D30) the situation resembles that on line Y=66400. There the western conductors are mineralized mafic volcanites while the eastern one is either granite contact or located in volcanites underneath granite. Between the eastern and western conductors there again exists a narrow terrace with lower resistivity values around co-ordinate Y=59100. According to the gravity interpretations this may be the southern continuation of the deep-seated “ore zone”.

Heikki Puustjärvi (ed.)

01.05.1999

Confidential

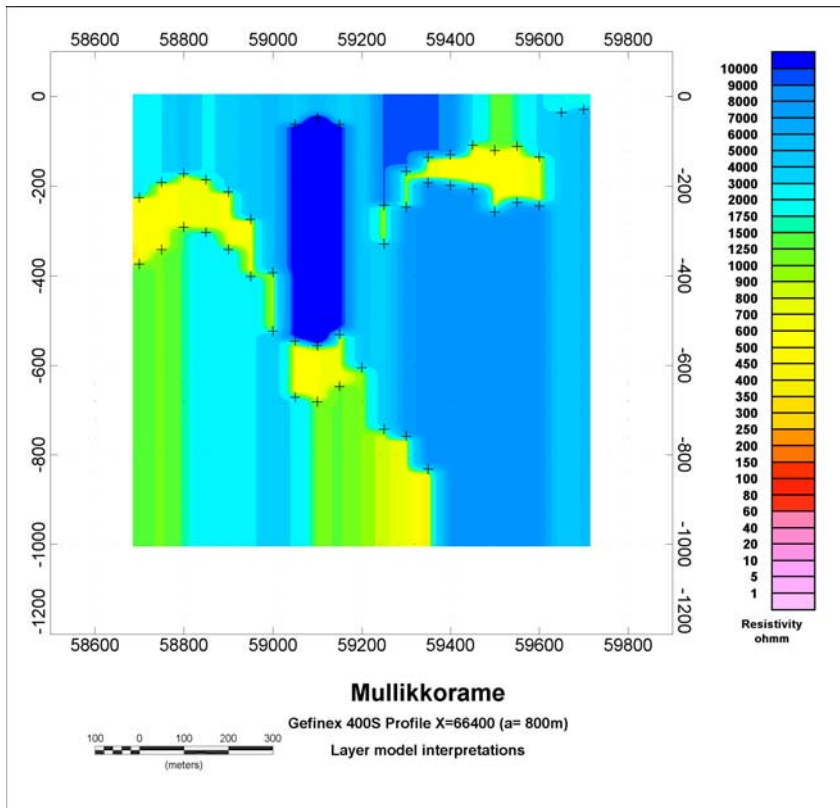


Figure D28.

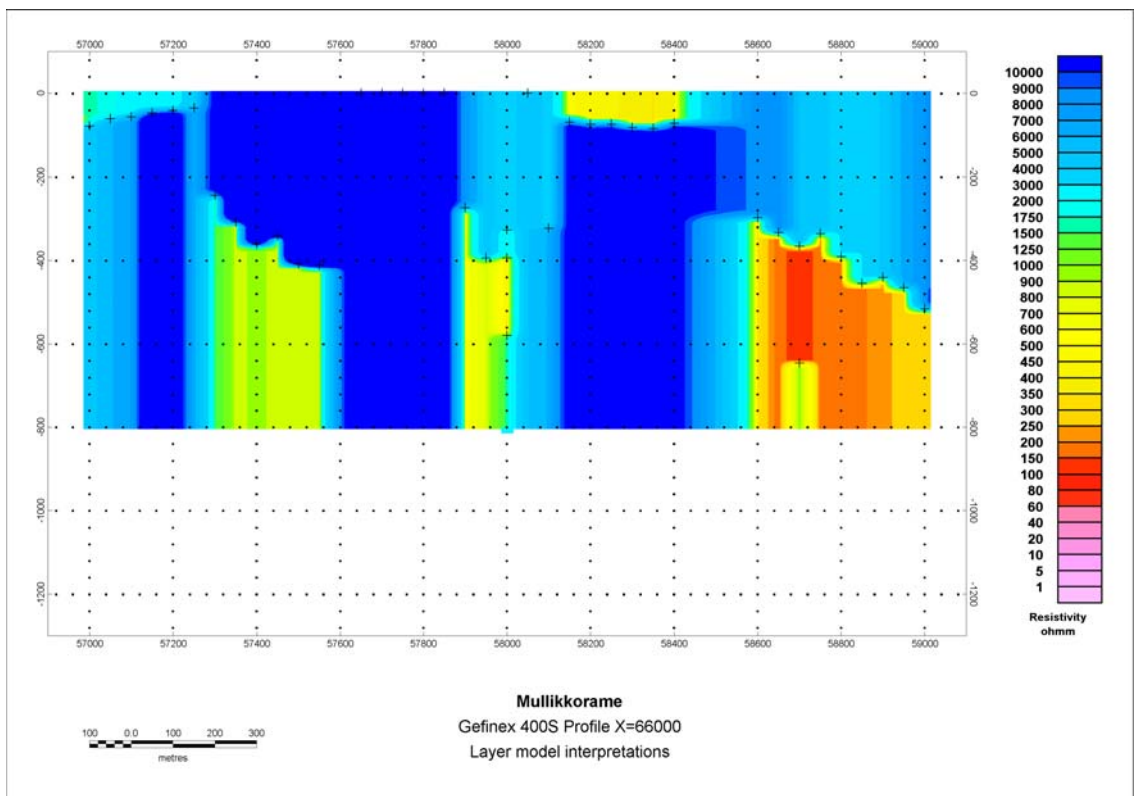


Figure D29.

Heikki Puustjärvi (ed.)

01.05.1999

Confidential

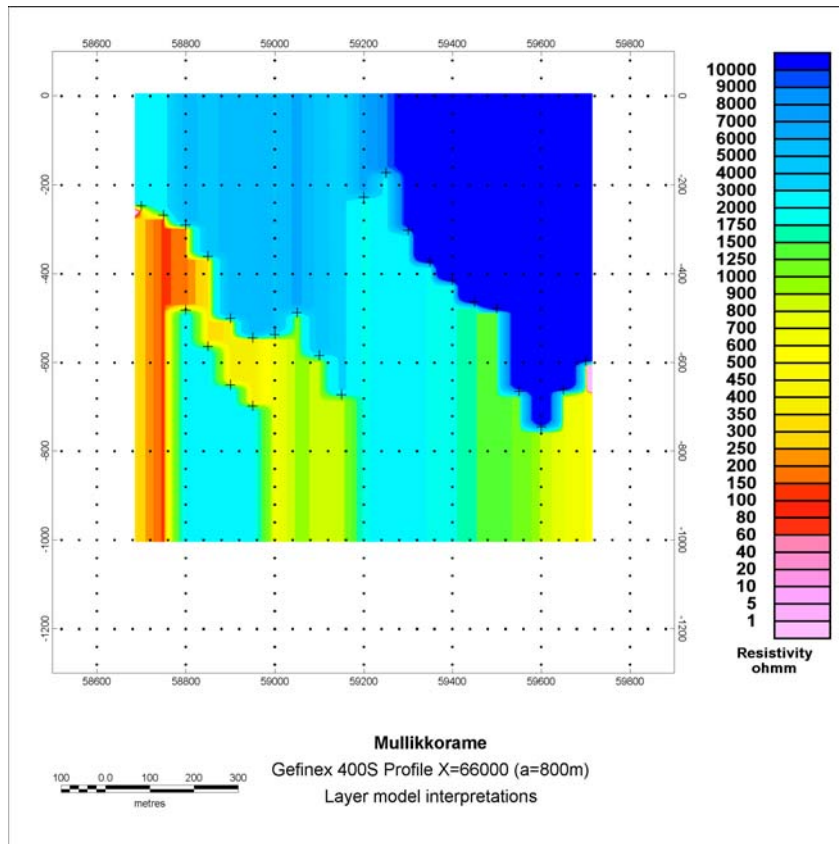


Figure D30.

D 5.6 DOWNHOLE EM INTERPRETATIONS IN THE MULLIKKORÄME AREA

A Protem Downhole EM survey was carried out in the Mullikkoräme area. Hole MU-152 drilled on line X=66100 was measured to find out the location of the deep-seated conductor detected in Gefinex 400S survey.

Figure D31 shows the Z-component of the measured EM data.

Rough interpretation showed that, in addition to conductive zones intersected at the eastern contact of the mafic volcanites, there seems to exist a conductor deeper and ahead of the drillhole (Fig. D32). This conductor fits that detected in Gefinex 400S survey and also the possible continuation of the deep “ore horizon” detected in gravity interpretations.

Heikki Puustjärvi (ed.)

01.05.1999

Confidential

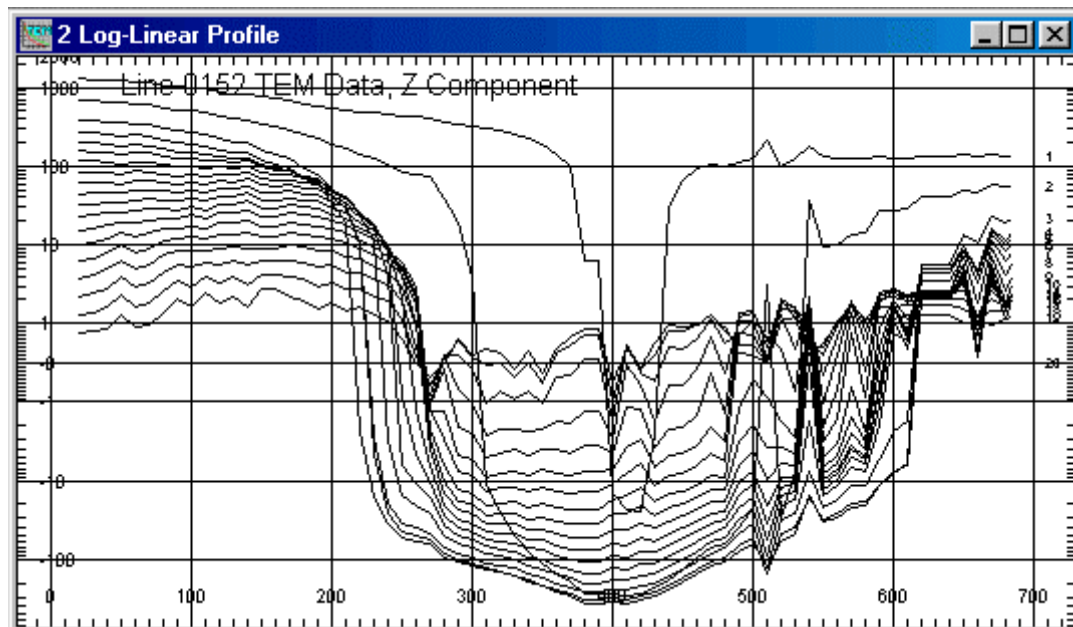


Figure D31.

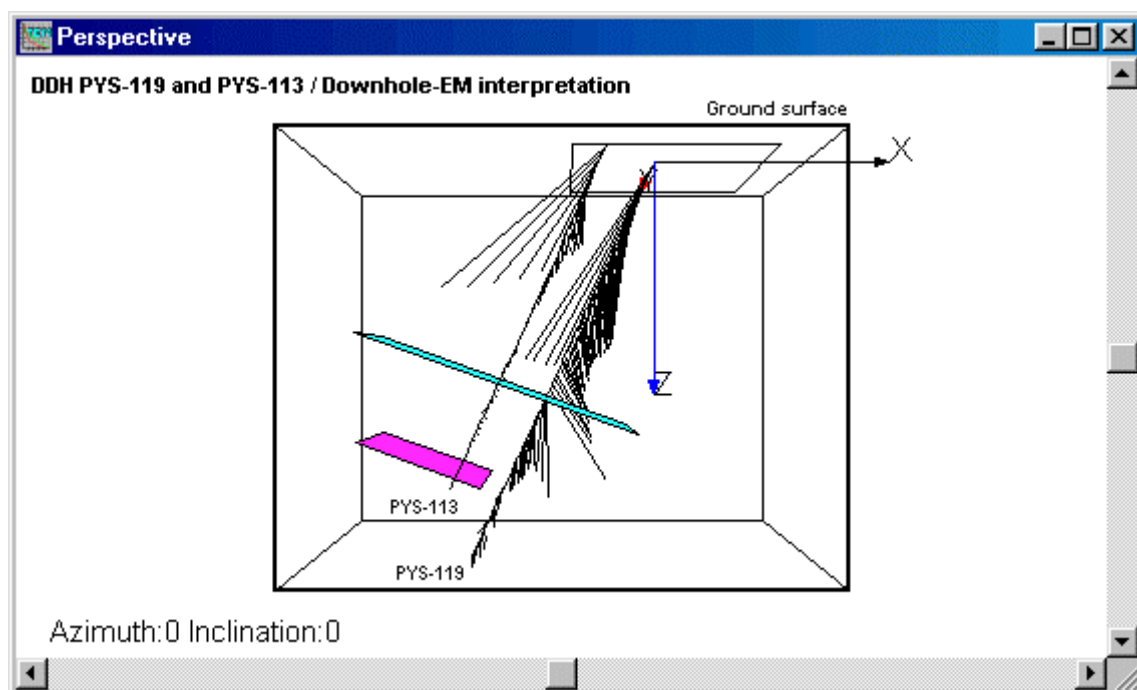


Figure D32.

Heikki Puustjärvi (ed.)

01.05.1999

Confidential

D 5.7 CONCLUSIONS AND RECOMMENDATIONS

The petrophysical property determinations of various rock types suggest that the gravity and EM methods are the most useful geophysical exploration tools in the Pyhäsalmi area.

Gravity interpretations showed that it is possible to create a 3-dimensional structural model of the geology in this area and to test geological ideas.

Under favorable circumstances it is also possible to detect ore deposits by gravity surveying as the Pyhäsalmi case has shown earlier.

Mineralisations are the best and almost the only conductors in the project area. Because of this fact it was possible to detect the Pyhäsalmi ore deposit in the earlier HLEM surveys. Also the results of the Gefinex 400S surveys carried out during last ten years (mostly interpreted during this project) have been useful, for instance showing the deep-seated ore lens in the Mullikkoräme area.

Because of the vast amount of data and limited time the interpretations carried out during this project are rather rough. Consequently it is recommended that interpretation be continue in co-operation with geologists at the most promising parts of the area examined.

New Gefinex 400S profiles are recommended as well as downhole EM after new drilling, however there already exist enough data for detailed interpretations. Such interpretations will save time and money as drilling can be directed to the most interesting targets; thus first-phase-drilling costs will be reduced. Since data files and interpretation models do exist it is easy to continue modeling as needed.

SECTION E

STATISTICS AND 3D-MODELING

E STATISTICS AND 3D-MODELING

E 1 DATA MANAGEMENT

General data collection, management and transfers to subproject researchers has been described in section A.

E 2 DATA STRUCTURE ANALYSIS (I.Suppala)

E 2.1 METHODS

E 2.1.1 Multivariate data structure

The *multivariate data structure* of the lithogeochemical data set was investigated using two unsupervised classification methods: (1) Partition Around Medoids (PAM) and (2) Kohonen's self-organizing map. Both methods unravel possible groupings in multivariate data.

PAM is a partitioning clustering algorithm where representative objects called *medoids* are extracted (Kaufmann & Rousseuw, 1990). Such medoids define the clusters and each object is assigned to its nearest medoid. The medoids are obtained by minimizing the sum of dissimilarities in all objects to their nearest medoid. The dissimilarity employed here was the Manhattan distance (the sum of element-wise absolute differences).

Kohonen's Self-Organizing Map (SOM) algorithm, also called Kohonen feature map, is an artificial neural network algorithm. It is based on unsupervised learning.

E 2.1.2 Spatial data structure

The *spatial structure* of the data, related to the distances between samples and their nearest ore samples, was also investigated by modeling the contents as a function of distance.

E 2.1.3 The association of the contents in lithogeochemical assays with distance to ore

Lithogeochemical data sets are analysed statistically to describe associations between the assayed element contents and the distances of respective samples to ore. Ore-forming and other geological processes are not considered here. Probably some elements have anomalous contents due to ore, but any causalities between the ore and the contents in its vicinity are not intended to be proposed. Whatever the geological history is, it would be beneficial to know how the element contents in assays can be associated to nearness with an orebody.

A multivariate sample in a lithogeochemical data set can be localized with the coordinates of the sample centre. Every sample was classified according to rock

type by a geologist. We used the coordinates of the classified ore samples to present the ore bodies and calculated distances from every other sample to these samples. Minimum distance represents the distance from a (host rock) sample to ore. Most of the ore samples contain information on the ore type (Cu, Zn, or S). This classification is not generally used. We did not find significant differences in correlation when we used separately the minimum distances to samples from different ore types.

Ore sample coordinates do not exactly describe the true 3-D orebodies. Errors in the calculated distances are obviously greater in the vicinity of a true orebody than farther away. The aim was only to describe qualitatively the effect of “nearness of the ore”. If a robust model for the “apparent distance” could be found, it should be used to highlight outliers of that model. It would provide a different way to explore this large spatial multivariate data set.

Samples from different rock types have to be analysed separately. Felsic volcanites form the largest and most interesting subset in the lithochemical data set. This subset can be divided to altered and unaltered volcanites. Here this is done using the Hashimoto index which is calculated using the measured contents for MgO, K₂O, Na₂O and CaO $((\text{MgO}+\text{K}_2\text{O})/(\text{MgO}+\text{K}_2\text{O}+\text{Na}_2\text{O}+\text{CaO}))$. Felsic volcanites are said to be altered if the Hashimoto alteration index is more than 0.5.

First we tested whether the calculated distances and measured contents of assays are uncorrelated. This was done using the Spearman's rank correlation coefficient. Samples nearer than 200 m were used in calculations. Correlations were verified by 2-D scatter plots. Data from Pyhäsalmi and Mullikkoräme were separately examined. Samples from Pyhäsalmi used for the calculations and in visual “modelling” originate from between $x=7062000$ m and $x=7062750$ m. The Mullikkoräme samples were from below $z=-200$ m. Samples marked to be located in the ore zone were not used. Calculated models for felsic volcanites were then tested in summary fashion using all felsic samples from these two areas. Original sampling was not done for this kind of analysis. Presumably the subsets used were not statistically representative.

E 2.2 RESULTS

Tables E2.1 and E2.2 show the calculated Spearman's values that rank correlation between minimum distance to ore and contents in each assay. The samples were altered and unaltered felsic volcanites from Pyhäsalmi (Table E2.1) and Mullikkoräme (Table E2.2). Altered samples (index>0.5) are on the left, unaltered ones on the right. In the column, p shows the p-value (probability) under the null hypothesis when the correlation between x and y is zero. Calculated rank correlations in the Pyhäsalmi samples differ from those originating from Mullikkoräme. One of the causes is different sampling. In the Mullikkoräme data set, correlations are better when using samples from deeper than level $z=200$ m. Also in the Pyhäsalmi data, correlations between distance and contents vary as the function of depth.

In general, association patterns in altered felsic volcanites differ from those in unaltered ones. In altered volcanites, many of the assays display “nearness of ore” effect. In the subset of altered felsic volcanites, calculated correlations are relatively weaker or, commonly, there is no statistical correlation. In some subset cases the numeric values of ρ show only tendencies of association. For example, one can visually see that the contents of TiO_2 display similar trends both at



Pyhäsalmi altered				Pyhäsalmi unaltered			
assay	ρ	p	number	assay	ρ	p	number
SiO_2	0.28	0	951	SiO_2	0.03	0.43	535
TiO_2	0.07	0.04	951	TiO_2	-0.19	0	535
Al_2O_3	0.14	0	951	Al_2O_3	-0.02	0.68	535
Fe_2O_3	-0.42	0	951	Fe_2O_3	-0.11	0.01	535
MnO	0.43	0	951	MnO	-0.14	0	535
MgO	0.15	0	951	MgO	-0.11	0.01	535
CaO	0.21	0	951	CaO	-0.3	0	535
Na_2O	0.37	0	951	Na_2O	0.29	0	535
K_2O	0.11	0	951	K_2O	-0.05	0.27	535
P_2O_3	0.27	0	951	P_2O_3	-0.11	0.01	535
CO_2	-0.07	0.1	472	CO_2	0.12	0.04	300
Zr	0.24	0	951	Zr	0.12	0.02	535
Cr	0.01	0.65	951	Cr	0.12	0.01	535
V	0.29	0	533	V	-0.05	0.42	308
Rb	0.35	0	533	Rb	-0.16	0	308
Sr	0.18	0	951	Sr	0.01	0.73	535
Ba	-0.31	0	951	Ba	-0.07	0.13	535
Cu	-0.35	0	944	Cu	-0.33	0	530
Zn	0.15	0	944	Zn	0	0.97	530
Pb	-0.19	0	944	Pb	-0.07	0.09	530
Ni	0.13	0	933	Ni	0.06	0.14	529
S	-0.56	0	944	S	-0.16	0	530
Co	-0.18	0	473	Co	0.06	0.37	229
Ag	-0.31	0	485	Ag	-0.2	0	230

Table 1. Spearman's rank correlations (ρ) between the minimum distance and contents from Pyhäsalmi

Mullikoräme altered				Mullikoräme unaltered			
assay	ρ	p	number	assay	ρ	p	number
SiO ₂	0.27	0.00	280	SiO ₂	0.00	0.96	610
TiO ₂	0.28	0.00	280	TiO ₂	0.11	0.01	610
Al ₂ O ₃	0.23	0.00	280	Al ₂ O ₃	0.12	0.00	610
Fe ₂ O ₃	-0.09	0.13	280	Fe ₂ O ₃	0.05	0.23	610
MnO	0.22	0.00	280	MnO	0.09	0.00	610
MgO	-0.20	0.00	280	MgO	-0.11	0.01	610
CaO	-0.43	0.00	280	CaO	-0.11	0.01	610
Na ₂ O	0.29	0.00	280	Na ₂ O	0.34	0.00	610
K ₂ O	0.07	0.25	280	K ₂ O	-0.25	0.00	610
P ₂ O ₃	0.04	0.51	280	P ₂ O ₃	0.14	0.00	610
CO ₂	-0.01	0.96	114	CO ₂	0.05	0.37	362
Zr	0.04	0.46	280	Zr	-0.20	0.00	610
Cr	-0.07	0.26	280	Cr	0.12	0.01	610
V	-0.07	0.21	280	V	-0.00	0.94	610
Rb	0.06	0.35	280	Rb	-0.16	0.00	610
Sr	-0.35	0.00	280	Sr	0.01	0.80	610
Ba	-0.61	0.00	280	Ba	-0.45	0.00	610
Cu	-0.63	0.00	279	Cu	-0.41	0.00	610
Zn	-0.55	0.00	279	Zn	-0.40	0.00	610
Pb	-0.72	0.00	279	Pb	-0.48	0.00	610
Ni	-0.22	0.00	279	Ni	-0.07	0.07	610
S	-0.35	0.00	263	S	-0.26	0.00	593
Co	-0.11	0.17	165	Co	-0.20	0.00	248
Ag	-0.65	0.00	161	Ag	-0.47	0.00	232

Table 2. Spearman's rank correlations (ρ) between the minimum distance and contents from Mullikoräme

Pyhäsalmi and Mullikkoräme. The weak negative correlation in Pyhäsalmi data is probably caused by noise (a greater variance in measured values).

The nature of associations can be verified using scatter plots of calculated distances and measured contents. Figure E2.1 is a scatter plot of distances to the nearest ore sample and Zn contents at Pyhäsalmi. To emphasize possible dependencies the measured contents are also smoothed by means of running medians. The median and 0.75 and 0.9 quantiles at a distance d_i are calculated using contents the distances of which are greater than $d_i - 8.5$ m and less than $d_i + 8.5$ m. The vertical straight line is the estimated maximum background composition for unaltered felsic volcanites. The other line is a fit through 0.9 quantiles which were calculated using altered and unaltered samples.

As was expected the variances of measured contents increase near the ore. In altered felsic volcanites from Pyhäsalmi (Fig. E2.1a) Zn contents partly appear to increase when distance to nearest ore sample decrease. Surprisingly, near the ore there seems to be another population which displays low (lowered?) Zn concentration. The calculated $r = 0.15$ (Table E2.1) means weak positive correlation between calculated distances and contents. Such low concentrations appear to exist near all of the ore types (Cu, Zn, and S ores). Between the Zn contents and alteration indexes there is a weak positive correlation ($r = 0.33$). When the alteration index exceeds 0.8 there are also (a population of?) low measured Zn contents. In the Pyhäsalmi deposit, the contents seems to have increased variance in a wider area than at Mullikkoräme (Fig. E2.2).

Figures E2.3 and E2.4 display scatterplots between distances to the nearest ore sample and Ba contents. The running 0.5, 0.75, and 0.9 quantiles and fitted lines are calculated as described above. In figure E2.4, the dotted vertical line is an estimated maximum background composition for unaltered felsic volcanites. The solid vertical line is the background used for visualisation. In these plots, Ba contents in Pyhäsalmi samples seem to be more heterogeneous than in those from Mullikkoräme. At Pyhäsalmi, anomalous values and the nearness of ore correlate in altered felsic volcanites but not in unaltered ones. At Mullikkoräme, Ba contents and distances to the nearest ore sample correlate in altered and unaltered felsic volcanites.

It was expected that distances to the orebody and at least some assay contents would correlate. Assuming that there is an outlying model for anomalous values as a function of the distance to the ore, the solid lines or curves are drawn in Figures E2.1-4 to visualize such hypothetical models. They roughly outline samples which have high-enough contents and appear to locate nearer to the ore than the distances to the nearest ore sample indicate. Figures E2.5 and E2.6 display the ore samples (brown) plotted for Pyhäsalmi and Mullikkoräme; also are shown anomalous samples and apparent distances which were calculated using these simple models.

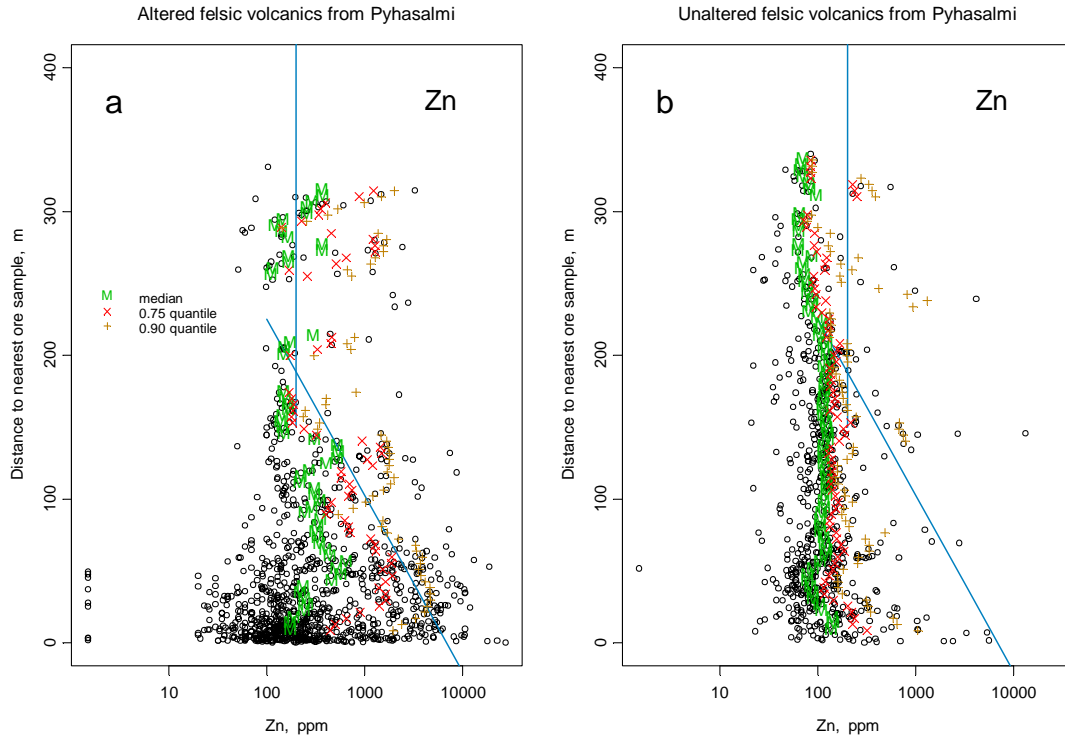


Figure E 2.1. Scatter plot of distances to the nearest ore sample and Zn content at Pyhäsalmi.

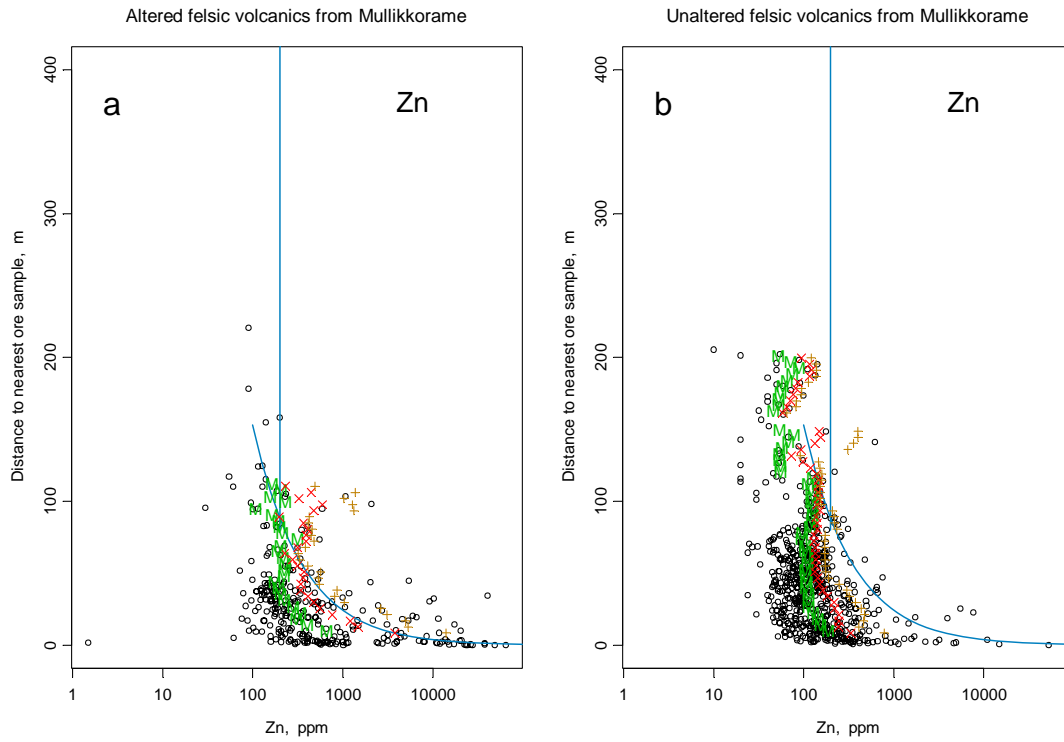


Figure E2.2. Scatter plot of distances to the nearest ore sample and Zn contents at Mullikkoräme.

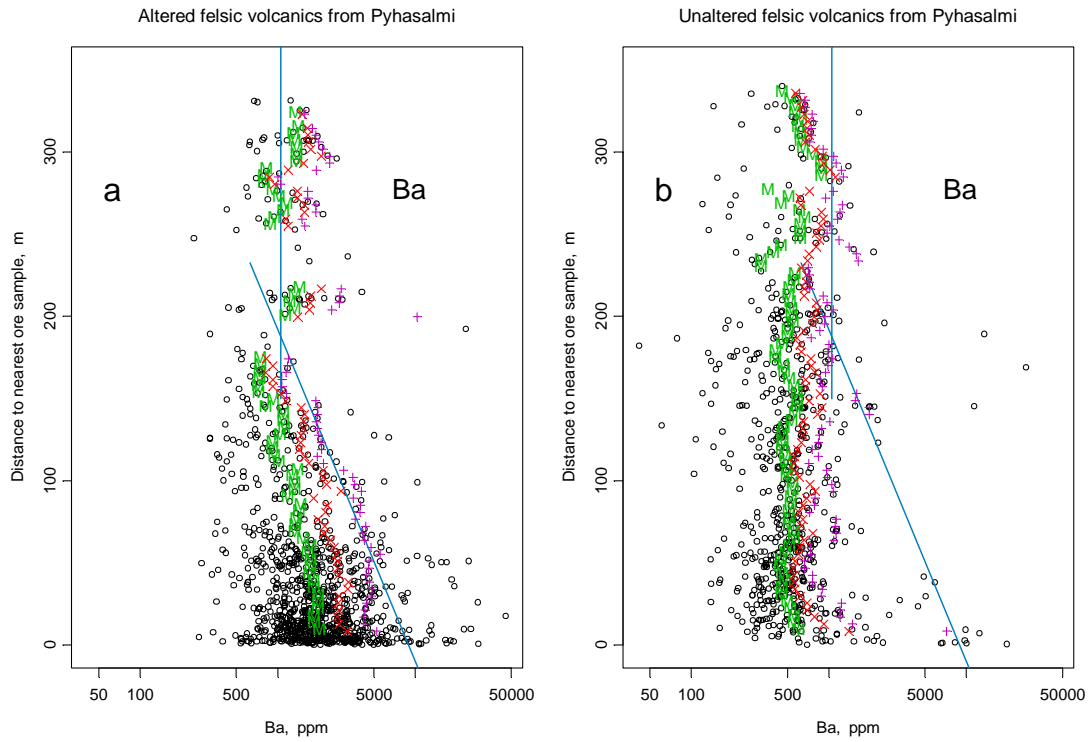


Figure E 2.3. Scatter plot of distances to the nearest ore sample and Ba contents at Pyhäsalmi.

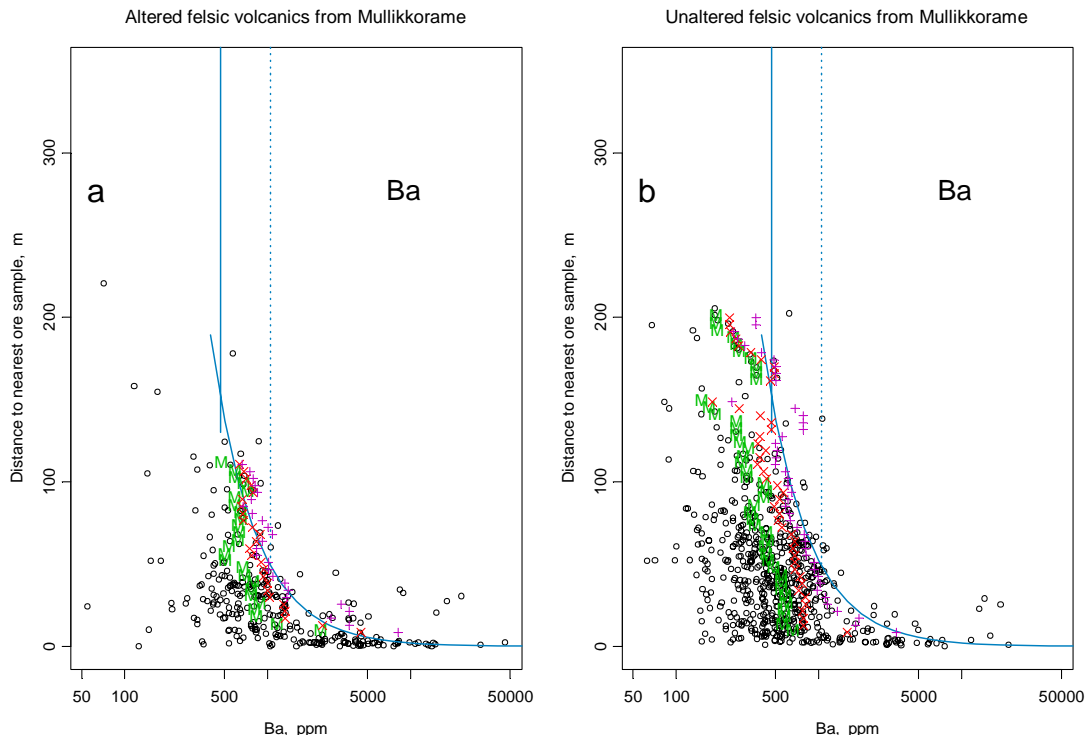


Figure E 2.4. Scatter plot of distances to the nearest ore sample and Ba contents at Mullikkoräme. The dotted line is an estimated maximum background content.

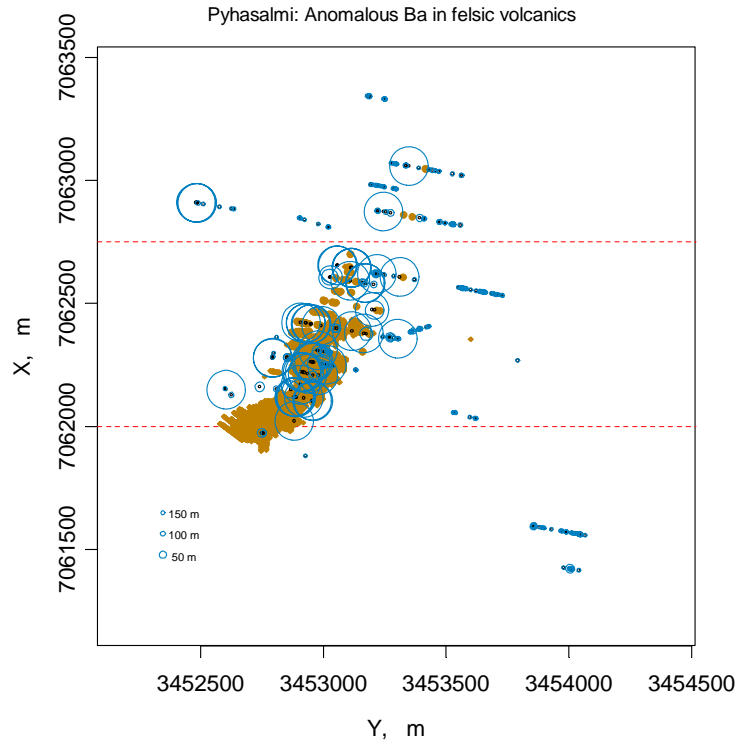


Figure E 2.5. Ore samples (brown) and the anomalous samples which are on the right side of lines in figure E2.3. The circle radius is a function of the modelled distance.

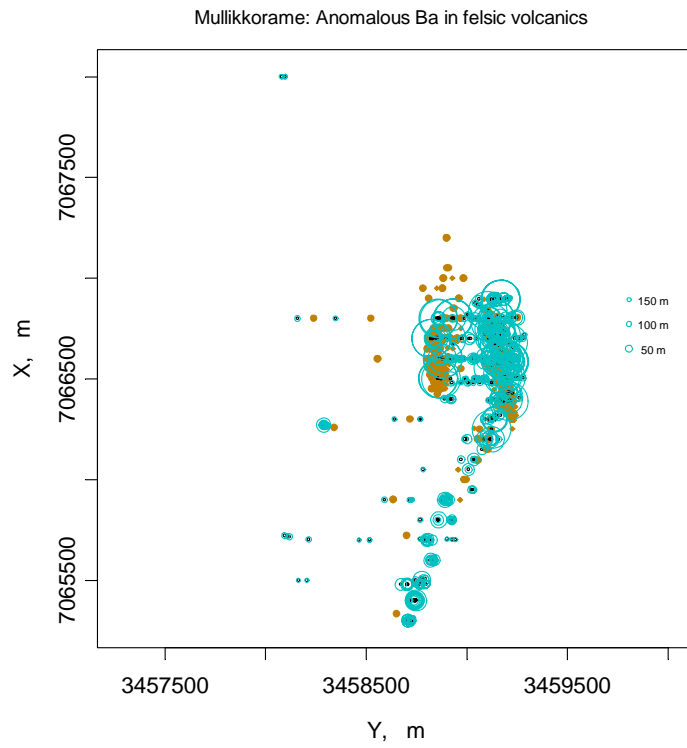


Figure E 2.6. Ore samples (brown) and the anomalous samples from Mullikkoräme indicated as in the previous figure.

E 3 STATISTICAL CLASSIFICATION OF LITHOLOGICAL SAMPLES (N. Gustavsson)

E 3.1 METHOD

In this study the objects to be classified are lithochemical samples from drillholes. In general a pattern is the vector of values of variables observed for each object. A classifier attempts to assign patterns (corresponding to objects) into previously defined (supervised method) or undefined (unsupervised method) classes. The particular method employed here is the Empirical Discriminant Analysis (EmpDA) which is a supervised method classifying unknown objects into given classes (bedrock type, type of ore, etc.) defined by user. The given classes are defined by training data representing geochemical assays for each class.

EmpDa is a nonparametric and nonlinear method based on Bayes classification rule where prior probabilities are involved and misclassification is penalized with a loss value for each class. The Bayes rule minimizes the expected overall loss and is optimal in that sense. The conditional probability density of a class is estimated from the training data by the kernel method (Parzen's window).

Early descriptions of EmpDA, also called Kernel Classifier, Potential Function Method, or Parzen's Classifier, were reported by Specht (1967). Applications in the geosciences are reported by Howarth (1971 and 1973), Gustavsson & Björklund (1976), Gustavsson (1983), Sinding-Larsen et al. (1988), and Gustavsson & Kontio (1990). A thorough theoretical description of this and other statistical pattern recognition methods can be found in Fukunaga (1990) and its relation to neural networks was described by Specht (1990).

The only assumption for EmpDA is that the variables must be numeric and scaled on the ratio scale permitting arithmetics of the values. Because EmpDA is nonparametric nothing is assumed about the conditional density and normality, for example, is not required even if the kernels may be Gaussian. The conditional density distributions may be even multimodal.

Nothing is assumed about the shapes of the classes or if they form connected clusters. This means that that classes can be folded in each other and may consist of multiple subgroups scattered anywhere in the variable space. This is not true for the classical linear discriminant analysis, for example.

To avoid spurious results due to unequal scales of variables all variables were standardized.

E 3.1.1 Bayes decision rule

Consider L classes of patterns (objects, samples) and denote them Σ_k , $k = 1, \dots, L$. A pattern is a vector of features (variables) in a p -dimensional pattern space. Let P_i denote the *prior* probability of class i , and $p_i(\mathbf{x})$ the *conditional density function* (or class density) for class i and \mathbf{x} a p -dimensional random vector, then the *mixture density function* for L classes is

$$p(\mathbf{x}) \hat{=} \prod_{i=1}^L P_i p_i(\mathbf{x}) \quad (1)$$

Using the Bayes theorem and (1) the posterior probability for class i becomes

$$q_i(\mathbf{x}) \hat{=} \frac{P_i p_i(\mathbf{x})}{p(\mathbf{x})} \quad (2)$$

A loss (penalty) value λ_{ij} can be introduced for incorrectly classifying a pattern belonging to class i into class $j \neq i$. The loss is zero for a correct decision. A high loss value for one class increases the correct decisions for that class on the expense of recognition of other classes. If all classes are equally important to be correctly recognized then they should have equal losses, which was assumed here. The expected loss when T_s is decided is the *conditional risk*

$$R(\omega_s | \mathbf{x}) \hat{=} \sum_{j=1}^L \lambda_{sj} q_j(\mathbf{x}) P(\omega_j | \mathbf{x}) \quad (3)$$

For every \mathbf{x} the decision function $\forall(\mathbf{x})$ gets one of the L values $\forall_1 \dots \forall_L$. The *overall risk* is given by

$$R \hat{=} \int R(\omega_s | \mathbf{x}) p(\mathbf{x}) d\mathbf{x} \quad (4)$$

where $d\mathbf{x}$ is the p -dimensional volume element. Then the *Bayes decision rule* for minimizing the overall risk is to compute the conditional risks (3) for all classes and choose the class for which $R(\forall_i | \mathbf{x})$ is minimum:

Bayes rule is optimal in the sense that it achieves a minimum overall risk (*Bayes*

$$\text{Decide } \mathbf{x} \in \omega_s \hat{=} \text{Arg} \min_{1 \leq s \leq L} R(\omega_s | \mathbf{x}) \quad (5)$$

risk), which is less than under any other rule.

E 3.1.2 Estimating prior probabilities

The prior probabilities can be known from earlier experience, assumed equal, or estimated as simple proportions $P_i = n_i / n$ where n_i is the number of training patterns in class i and n the total number of training patterns. In this study all prior probabilities were equal.

E 3.1.3 Estimating the conditional densities

The kernel method is chosen for estimating the conditional density functions from training patterns. A kernel density is centred at each training pattern with a given spread or uncertainty. In this program the only kernel density is the Gaussian with a standard deviation Φ (smoothing coefficient) indicating the spread around training patterns. The conditional density is then achieved by taking the average of the frequencies from the kernels at desired points. Φ can be considered the known measurement error or can be estimated from the training data. The estimate of the class density is then

$$p_k(\mathbf{x}) \hat{=} \frac{1}{(2\pi)^{p/2} \sigma^p} \frac{1}{L} \sum_{i=1}^{n_k} \exp[-\|\mathbf{x} - \mathbf{y}_{ki}\|^2 / 2\sigma^2] \quad , \quad (k \hat{=} 1, \dots, L) \quad (6)$$

where $\|\mathbf{x} - \mathbf{y}_{ki}\|^2$ is the Euclidean norm (distance) between the unknown pattern \mathbf{x} and \mathbf{y}_{ik} , the i th training pattern in the k th class, and n_k is the number of training patterns in class k .

Two ways of determining the smoothing coefficient Φ which is mandatory in (6) are provided:

- (1) Φ is entered by the user (knowing the uncertainty of the data);
- (2) Φ is derived through an iterative procedure where the classifier is applied repeatedly on the test set or the unknown set and the percentage of unclassified is retained; at every step Φ is increased until the number of unclassified is less than a given percentage.

Here the same value of Φ is valid for all classes and variables. Since the data are standardized it is justified to assign the same Φ to all variables.

Classifying a pattern means that (6) must be computed over all training patterns and the decision is made following the rule expressed in (5). If the unknown pattern is far away from any training patterns the posterior probability (2) may become very small indicating that none of the classes are probable. For this reason a threshold is built in to avoid spurious decisions. Patterns which are distant from any training patterns and with a posterior probability falling below the

threshold are not classified but kept as unknowns. The threshold chosen here was a very small value depending on the dimension of the data.

E 3.1.4 Estimating the performance of the classifier

The performance of the classifier is here tested using the training set by the *leave-one-out method* (Fukunaga, 1990). In the leave-one-out method the classifier is designed using $n-1$ of the n training patterns and the one left out is classified. Each training pattern is left out in turn and the average classification rates are presented in the *confusion matrix*. Also the total *error rate* is reported. The confusion matrix shows how the misclassified patterns are distributed and which classes are more confused than others.

Another matrix showing the confusion between the decision by EmpDA and the class of the nearest training pattern is also generated with the final classification of the unknown set.

E 3.2 DATA SET AND CLASSIFICATION SETTINGS

The data included was a selected set of lithogeochemical analyses from drillhole samples: SiO₂, TiO₂, Al₂O₃, Fe₂O₃, MnO, MgO, CaO, NaO, K₂O, P₂O₅, Zr, Rb, Sr, Ba, S, Cu, Zn, Pb, and Ni. They were gathered from the areas Pyhäsalmi, Mullikkoräme and Kettuperä. Only samples with all selected elements analysed were accepted for the classification. Thus, the problem of missing data was avoided.

Two separate supervised classifications were done using EmpDA:

1. classifier trained by two classes: unaltered and altered rocks,
2. classifier trained by four classes: felsic unaltered volcanites in Pyhäsalmi and Kettuperä areas (class 1), felsic unaltered volcanites in the Mullikkoräme area (class 2), mafic unaltered volcanites in the Pyhäsalmi and Kettuperä areas (class 3) and mafic unaltered volcanites in the Mullikkoräme area (class 4).

In the first classification the training samples were collected using the alteration index as a criteria. The unaltered class was trained by samples with index < 30%, altered with index > 90%.

In the second classification the training data set was generated using attributes for alteration state, area and rock type stored in the data base.

E 3.3 RESULTS FROM THE FIRST CLASSIFICATION

The performance of the classification as measured by the leave-one-out method was very convincing showing that none of the training samples were outliers and the training data were homogenous within classes (Fig. E3.1). The misclassification rate was almost nil implying that if the training data are representative for the classes then the classification result can be expected reliable.

The box plot in Fig. E3.2 shows how the level of Na₂O varies within and between

```

Variables                16
Classes (incl. unknown)  3

A priori probabilities and loss matrix
  Class Nr  Name          A Priori Prob.    Loss Value
    1      class 1          0.50             1.00
    2      class 2          0.50             1.00

The smoothing parameter for normal base densities is      0.30000
The smallest probability for assigning a pattern to a class is 0.10000-199

Relative frequencies of training patterns per class
Classes      # of training samples (%)
1...class 1 1918   93.97
2...class 2  123    6.03

The confusion matrix based on the leave-one-out method:

Fractions(%) for actual (rows) versus assigned (columns) classes

          class 1    class 2    Unknown
1 class 1    99.06     0.00     0.94
2 class 2     0.00    92.68     7.32
The misclassification rate:      0.00%

RELATIVE FREQUENCIES OF PATTERNS ON CLASSES:
Class  Name          Number of items    Percentage
  1    class 1          4558             57.60
  2    class 2          2622             33.14
  3    Unknown           733             9.26

Number of underflows causing 0 probability:      604

```

Figure E3.1. Computer output from the first classification.

the classes. The resultant classes were shown as interactive 3D-plots as colored dots generated with the program Gemcom for Windows. In general the strongly altered samples were gathered at or close to locations known as ore-bearing. The classification results were all stored and integrated to the data base for further interpretation.

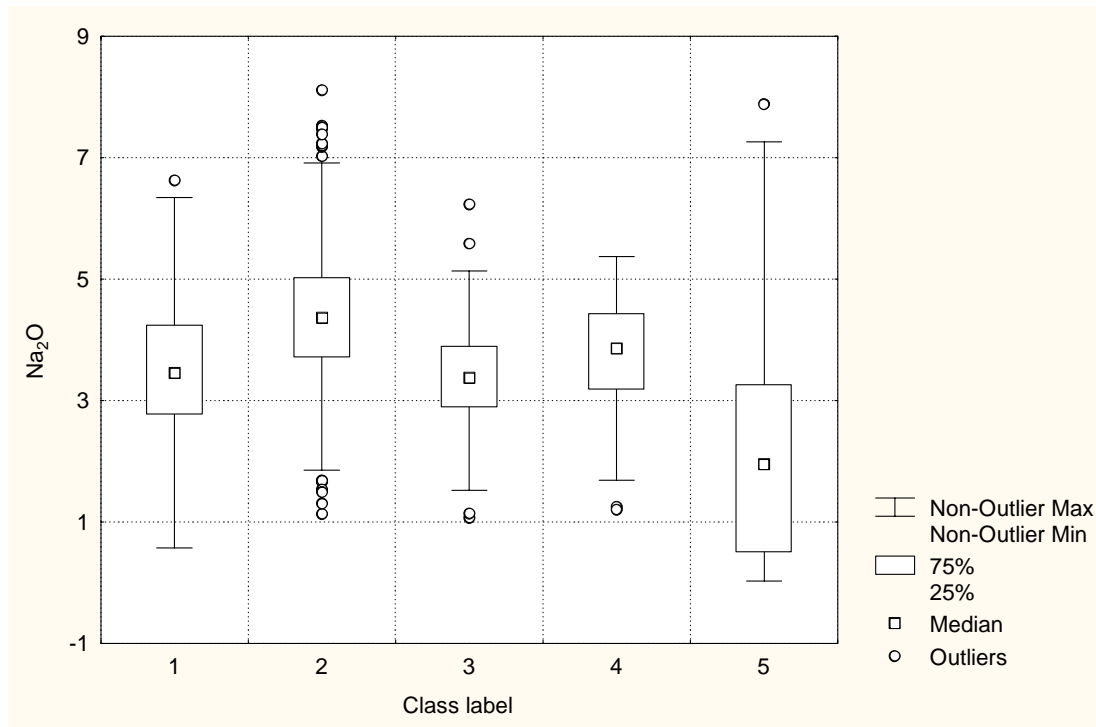


Figure E3.2. Box plot showing the variation between and within classes (5 is the unknown class).

E 3.4 RESULTS FROM THE SECOND CLASSIFICATION

Also the second training data set appeared to be very homogenous. The computer output in Fig. E3.3 shows that the confusion between classes is low for training data and the misclassification rate not more than 3.89%. If the training data is representative this indicates that the classification result is reliable.

The frequency matrix of classified objects versus distance to nearest training sample from objects confirm that the classification may be reliable: most classified samples are rather close to training samples in the multivariate space.

Fig. E3.4 shows the distribution of class labels. The distribution between and within classes is shown as an example in Fig. E3.5.

In addition to class labels each classified sample was equipped with posterior probabilities for each class. Both labels and probabilities were displayed as 3D-plots (Gemcom). All classification results were stored for further interpretation.

Variables 19
Classes (incl. unknown) 5

A priori probabilities and loss matrix

Class Nr	Name	A Priori Prob.	Loss Value
1	Class 1	0.25	1.00
2	Class 2	0.25	1.00
3	Class 3	0.25	1.00
4	Class 4	0.25	1.00

The smoothing parameter for normal base densities is 0.40000
The smallest probability for assigning a pattern to a class is 0.10000-199

Relative frequencies of training patterns per class

Classes, # of training samples (%)			
1...Class 1	91	29.35	
2...Class 2	92	29.68	
3...Class 3	86	27.74	
4...Class 4	41	13.23	

The confusion matrix based on the leave-one-out method:

Fractions(%) for actual (rows) versus assigned (columns) classes

		Class 1	Class 2	Class 3	Class 4	Unknown
1 Class 1	87.91	8.79	0.00	0.00	3.30	
2 Class 2	3.26	92.39	0.00	0.00	4.35	
3 Class 3	0.00	0.00	94.19	0.00	5.81	
4 Class 4	0.00	0.00	2.44	82.93	14.63	

The misclassification rate: 3.87%

RELATIVE FREQUENCIES OF PATTERNS ON CLASSES:

Class	Name	Number of items	Percentage
1	Class 1	623	9.47
2	Class 2	1323	20.10
3	Class 3	367	5.58
4	Class 4	87	1.32
5	Unknown	4182	63.54

Number of underflows causing 0 probability: 0

EmpDA (rows)/ Euclidean distance (columns) to nearest neighbour
in % excl. unknowns, rows are Emp.Discr. Anal. and cols Eucl.Dist:

	Class 1	Class 2	Class 3	Class 4
1 Class 1	98.88	1.12	0.00	0.00
2 Class 2	0.91	99.09	0.00	0.00
3 Class 3	0.00	0.00	100.00	0.00
4 Class 4	0.00	0.00	3.45	96.55
5 Unknown	10.76	32.07	33.21	23.96

Figure E3.3. Summary report from the second classification. The confusion matrix shows outstandingly high rates on diagonal which indicates that the classes are distinct in the training data and no confusion occurs.

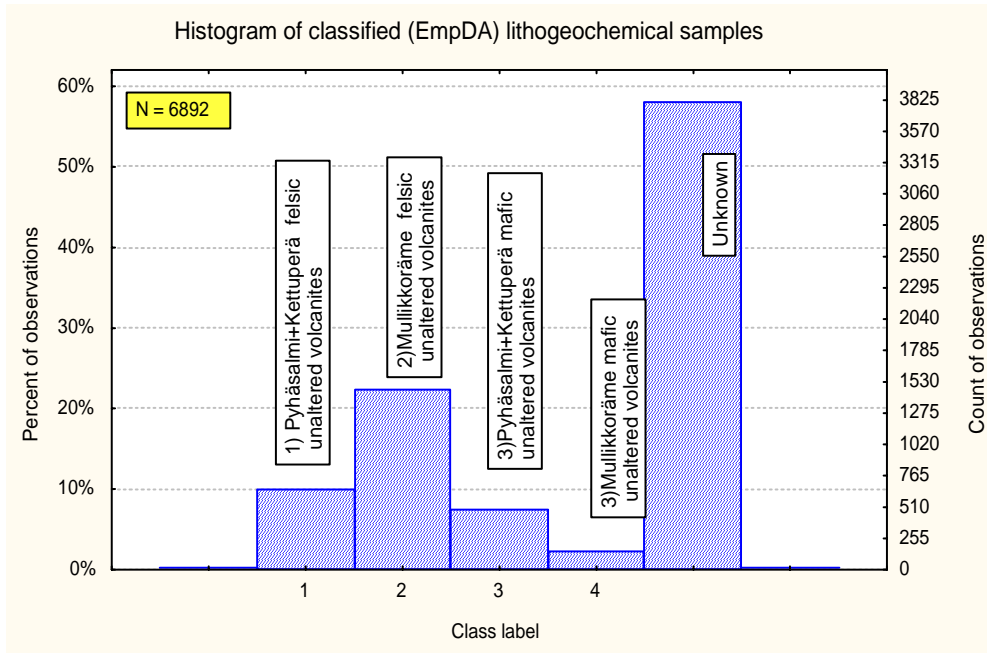


Figure E3.4. distribution of class labels in the second classification

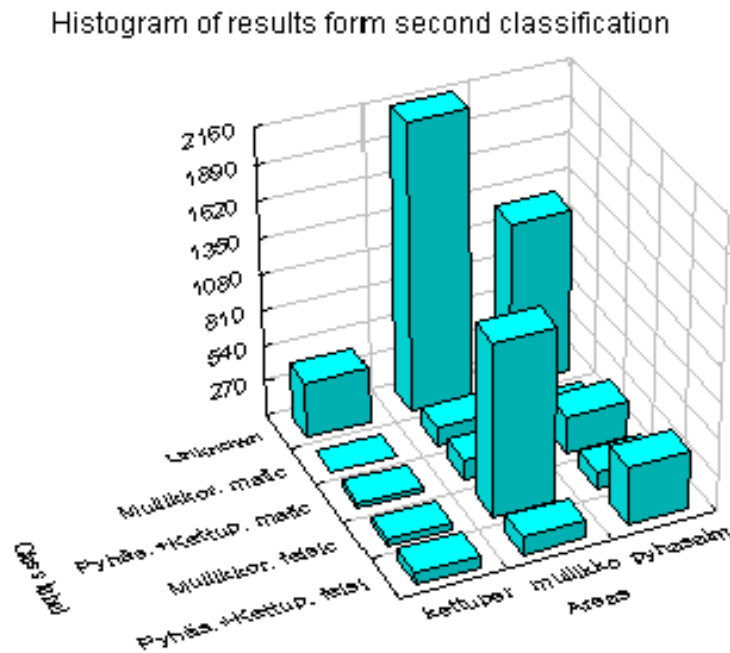


Figure E3.5. Distribution of class labels over areas in the second classification.

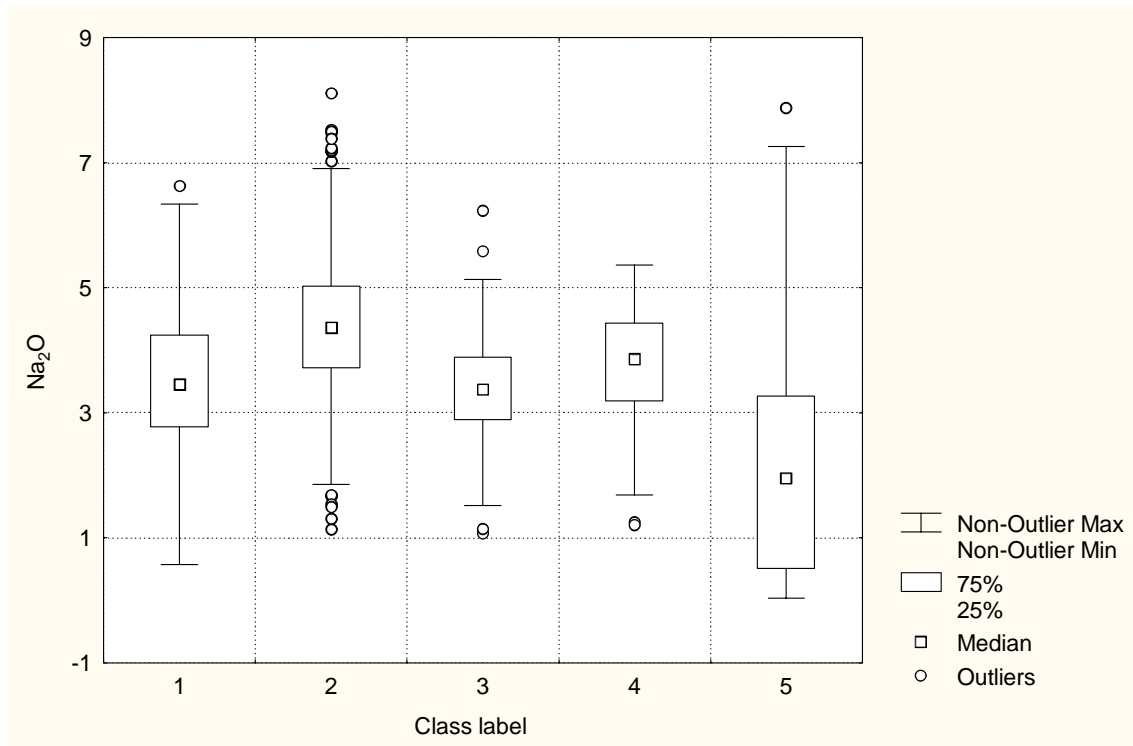


Figure E3.6. Box plot showing the spread of contents in and between classes in the second classification (5 is the unknown class).

E 4 3D-MODELING

E 4 SUMMARY

A statistical and geostatistical study on core sample assays originating from 2518 drillholes was performed to model spatial distribution patterns for copper, zinc and sulfur in bedrock of the Pyhäsalmi District. The resulting parameters were estimated to characterize grade anisotropy features of these elements in the Pyhäsalmi, Kettuperä and Mullikkoräme subareas; similarities and differences between subareas were recorded and discussed. 3D solid models for the distribution of the above-mentioned elements, and for silver and lead at Mullikkoräme, were created. Metal zoning trends intended for the detection of feeder systems were studied.

E 4.1 INTRODUCTION

E 4.1.1 Objective

The objective of this subproject was to prepare a three-dimensional (3D) description for the spatial distribution of copper, zinc, sulfur, lead and silver as well as the respective ore types in the Pyhäsalmi District. Also mathematical parameters measuring the behaviour of the above-mentioned elements were to be estimated. These results were to be used to create a geomathematical model for the Pyhäsalmi type of ore deposits to serve exploration for similar deposits in the future.

E 4.1.2 Material

A total of 34 522 core samples from 2 518 drillholes were analyzed for copper, zinc and sulfur and also for lead and silver at Mullikkoräme (Table E4.1). The results of analyses were used in this modeling. The lengths of single core samples varied from 0.02 m to 66.60 m averaging 2.37 m.

Data from the Pyhäsalmi District drill core sample material were handled both collectively for the area and also divided into three geographical subareas: Pyhäsalmi, Kettuperä and Mullikkoräme (Fig. E4.1).

Figure E 4.1. Pyhäsalmi District divided into Pyhäsalmi, Kettuperä and Mullikkoräme Areas.

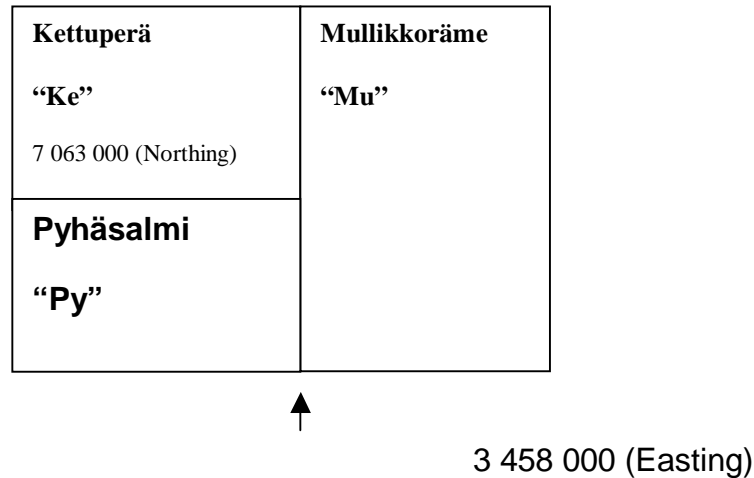


Table E4.1. Origin of sample material for this study.

Location	Drill holes	Original assays	3-m composites
Pyhäsalmi	1 776	23 794	19 644
Kettuperä	61	2 297	3 140
Mullikkoräme	681	8 431	8 135
Total	2 518	34 522	30 919

E 4.1.3 Methods

Integrity and representativity classical and spatial statistics were used for the check-up of data faultlessness. Especially the check-up of coordinate validity proved to be necessary.

Classical statistics and geostatistics were used to describe the distribution, anisotropy and spatial properties of Cu, Zn, S, Pb and Ag. Inverse Distance (ID2) was used for 2D interpolations with anisotropy parameters calculated by variogram analysis. 3D modeling was based on sectional or plan polygons. Gemcom's GEM98W software was used in all of the processes.

Details of this work are given in Appendix E4.1 (in Finnish).

E 4.2 SPATIAL STATISTICS

E 4.2.1 Pyhäsalmi District and subareas, classical statistics

Classical statistics were applied to each of the sampling subareas discussed earlier. The effect of samples combined into 2, 3 and 5-m composites with and without background values was studied (Appendix and Figs. E4.2-3, Table E4.2). Based on the results of this analysis data from the original uncombined samples and 3-m composites without background value were used in advanced statistical analyses.

All of the elements, except sulfur, are roughly lognormally and bimodally distributed; the distribution of sulfur is bimodal and extremely skewed (Figs. E4.2A-D). A comparison of metals with sulfur revealed that background values of 0.001% for metals and of 0.01% for sulfur are appropriate. These same values can be used as general cutoff grades for the statistical treatment of assays.

The bimodality in element distribution indicates the presence of at least two generations of sulfide material in the region, one with low sulfur (0.001 – 5%, maximum peak at 1.1%), low copper (maximum peak at 0.01%) and low zinc (maximum peak at 0.01%), the other with high sulfur, 'high' copper (maximum peak at 1%) and a wide variability in zinc content (0.01 – 10%).

Moreover, low correlation between all these elements (Table E4.2) indicates the presence of four different types of sulfide material characterized by 1) Low sulfur and low Zn & Cu, 2) High S and low Zn & Cu, 3) High Zn, 4) High Cu.

Figure E4.2. Pyhäsalmi District frequency distribution histograms for copper (A-B), zinc (C) and sulfur (D). A: original samples, B–D: 3-m composites.

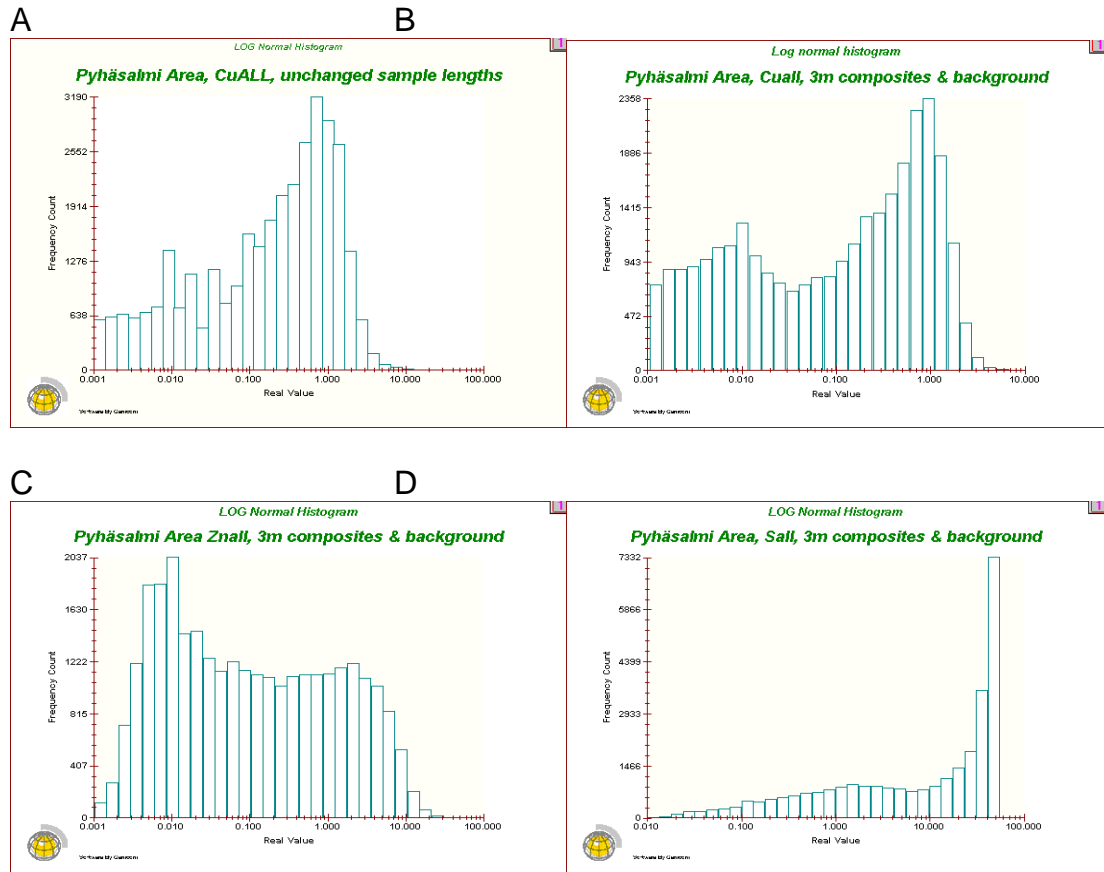


Figure E4.3. Pyhäsalmi District subareas, frequency distribution histograms for copper: A-B: Pyhäsalmi, C-D: Kettuperä, E-F: Mullikkoräme. A, C and E: original samples; B, D and F: 3-m composites.

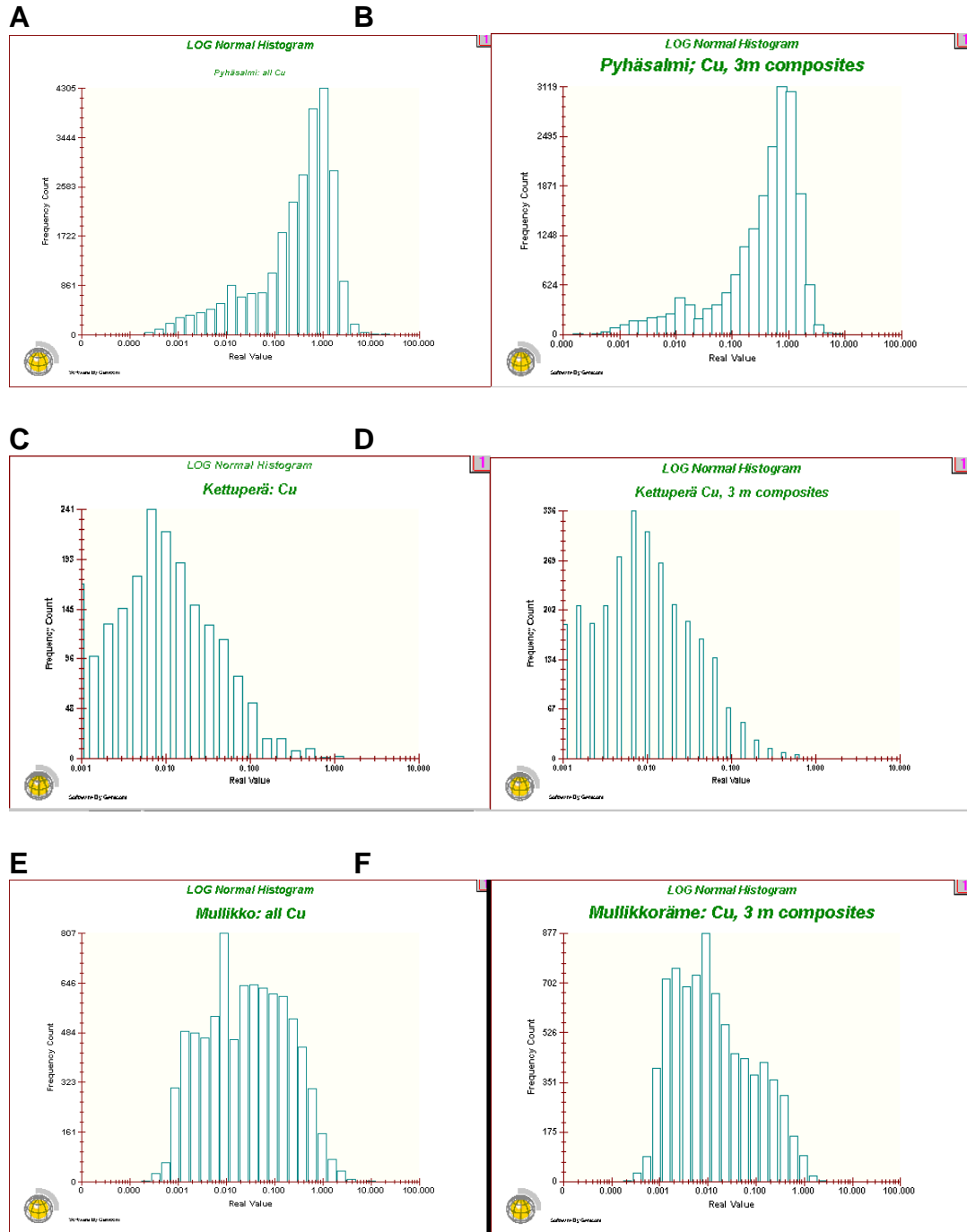
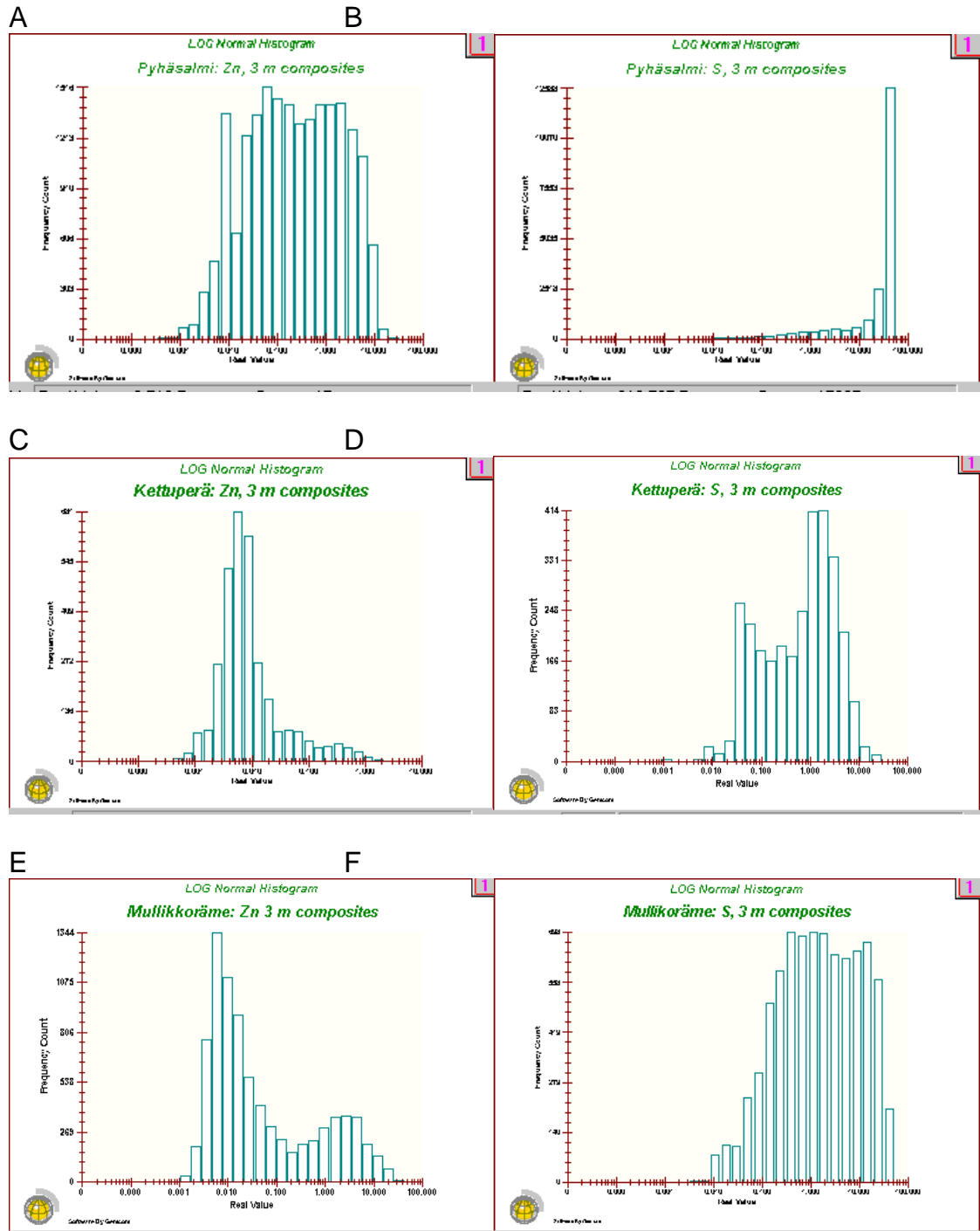


Figure E4.4. Frequency distribution histograms for subareas in the Pyhäsalmi District. A-B: Pyhäsalmi, C-D: Kettuperä, E-F: Mullikkoräme. A, C and E: zinc assays; B, D and F: sulfur assays, 3-m composites.



E4.2.2 Pyhäsalmi District geostatistics

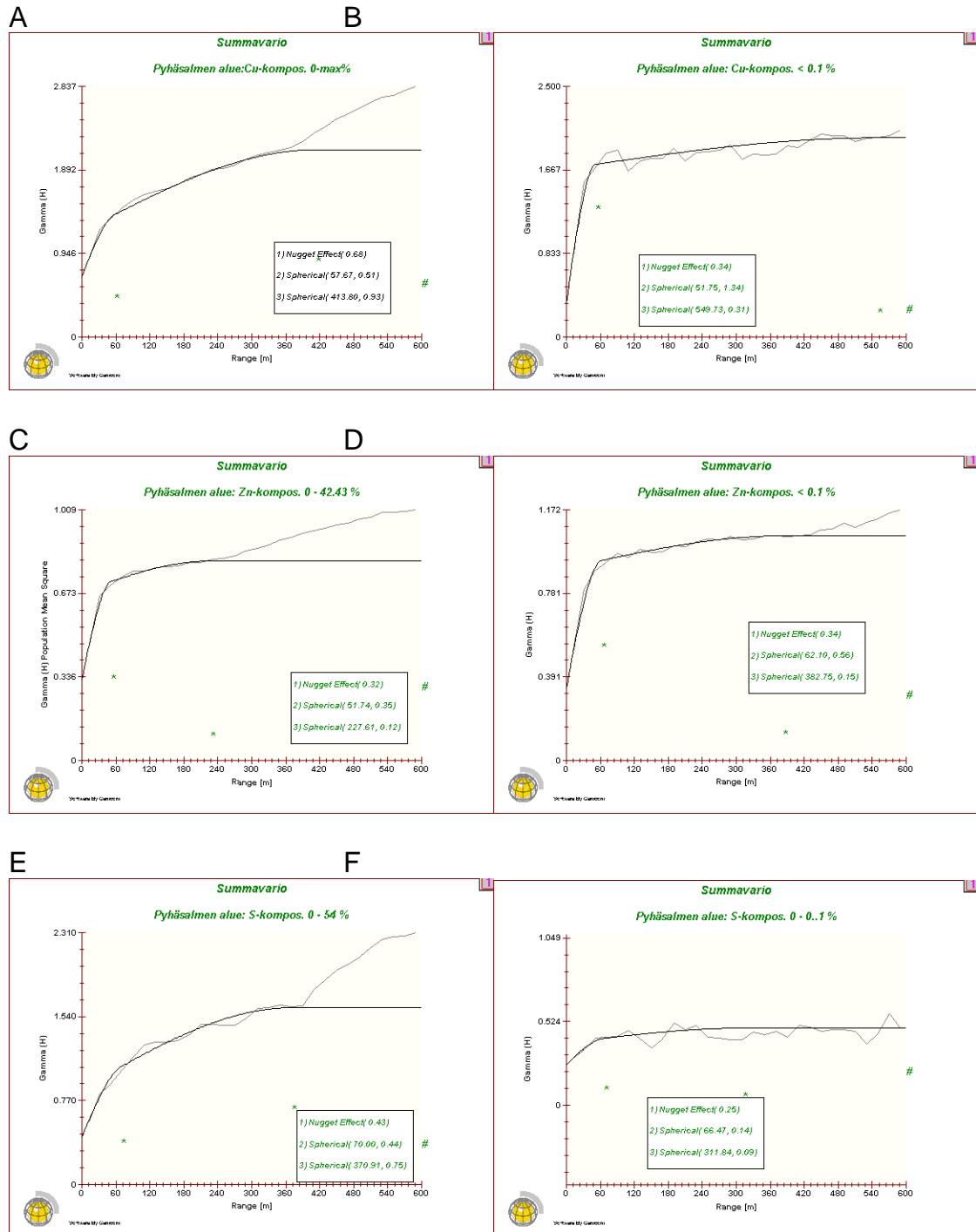
Diagrams in Fig. E4.5 show average ranges of grade continuity for all and the low-grade assays of Cu, Zn and S. Parameters based on spherical semivariogram models are given in Table E4.3. Range 1 may roughly indicate the lateral continuity class (40–70 m) of high-grade mineralization while Range 2 shows overall extensions of low-grade halos (300–500 m).

Different ranges for Cu, Zn and S indicate the presence of three different types of mineralization: iron sulfidic, sphaleritic and chalcopyritic. There are at least two range classes for each of them. The low relative nugget (Table E4.3) indicates that even low-grade values of Cu and Zn are useful (representative and reliable) unlike those of S. Therefore the cutoff grade for Cu and Zn should be chosen small enough (in this study: 0.001%).

Table E4.3. Pyhäsalmi District geostatistical parameters for models in Fig. E4.5 (+ parameters for high-grade values). Semivariance = nugget + sill 1 + sill 2. Relative nugget = 100 x nugget / (sill 1 + sill 2).

		Cu	Zn	S	
All data		A	A	A	0 - max
< 0.1(Cu, S)		B	B	B	< 0.2 (Zn)
0.1-max (Cu, S)		C	C	C	0.2 – max (ZN)
Nugget		0.68	1.47	0.43	
		0.34	0.24	0.25	
		0.41	1.06	0.37	
Sill 1		0.51	1.78	0.44	
		1.34	0.34	0.14	
		0.18	0.34	0.41	
Range 1	1	58	41	70	
		52	47	66	
		49	43	84	
Sill 2		0.93	0.69	0.75	
		0.31	0.17	0.09	
		0.03	0.20	0.48	
Range 2	2	414	140	371	
		550	303	312	
		344	229	312	
Relative Nugget		47	60	36	
		21	47	109	
		195	196	42	
Semi-variance		2.09	3.94	1.62	
		1.99	0.75	0.48	
		0.62	1.60	1.26	

Figure E4.5. Pyhäsalmi District non-directional (summary) semivariograms and models for Cu (A all, B 0 – 0.1%), Zn (A all, B 0 - 0.2%), and S (A all, B 0 – 0.1%) 3 m composites; logarithmic transformation. Lag = 20 m.



E 4.2.3 Spatial grade anisotropy

Anisotropy directions in Table E4.4 and Fig. E4.6 are derived from anisotropy roses in Figs. E4.7 – E4.13 for spatial grade distributions in the Pyhäsalmi, Kettuperä and Mullikkoräme areas. These roses are based on the modeling of directional variograms at 20 degrees azimuthal and 30 degrees dip intervals. First anisotropy ranges using a lag of 20 m and a spherical model were calculated for directions 000, 020, 040, 060, 080, 100, 120, 140 and 180. In the direction of maximum lateral range, anisotropy ranges for dips 00, 30, 60, 90, 120 and 150 (or 020 / 00-90 and 200 / 00-90) were then calculated.

The diagram in Fig. E4.7A shows several preferred anisotropy directions that result from the twisted structure of the ore body. To get results comparable to those at the other areas, another rose was constructed for the Pyhäsalmi data above the level –200 m bsl. This rose (Fig. E4.7B) shows a maximum range at 020/200 (NNE). The rounded ‘fat’ appearance of the rose also indicates minor twisting or a relative broad halo around the orebody. When anisotropy at various dips toward 020 and 200 were calculated, the result (Fig. E4.7C) shows a clear maximum at 60 degrees to 020. A conclusion is that in the surficial part (350 m deep) of the Pyhäsalmi orebody there is a strong copper grade lineation of 020/60. Data for other elements (Cu, S, Pb) and from other subareas (Kettuperä, Mullikkoräme) was treated similarly.

Table E4.4. Grade anisotropy lineation at Pyhäsalmi, Kettuperä and Mullikkoräme for Cu, S and Pb (Pb for Mullikkoräme only). Long ranges (2) and short ranges (1).

	Range 2 & (Range 1)		
	Pyhäsalmi	Kettuperä	Mullikko
Cu	020/60 120/30 (120/00)	020/70 140/60 (140/30) (040/00)	180/30 (100/40)
S	080/00 080/90 (280/30)	160/60 (160/90)	220/30-50 (120/30)
Pb			200/00 (020/00-30)

Figure E4.6. Pyhäsalmi, Kettuperä and Mullikkoräme grade anisotropy interpretations after table E 4.4. A. Long ranges (2). B. Short ranges (1).

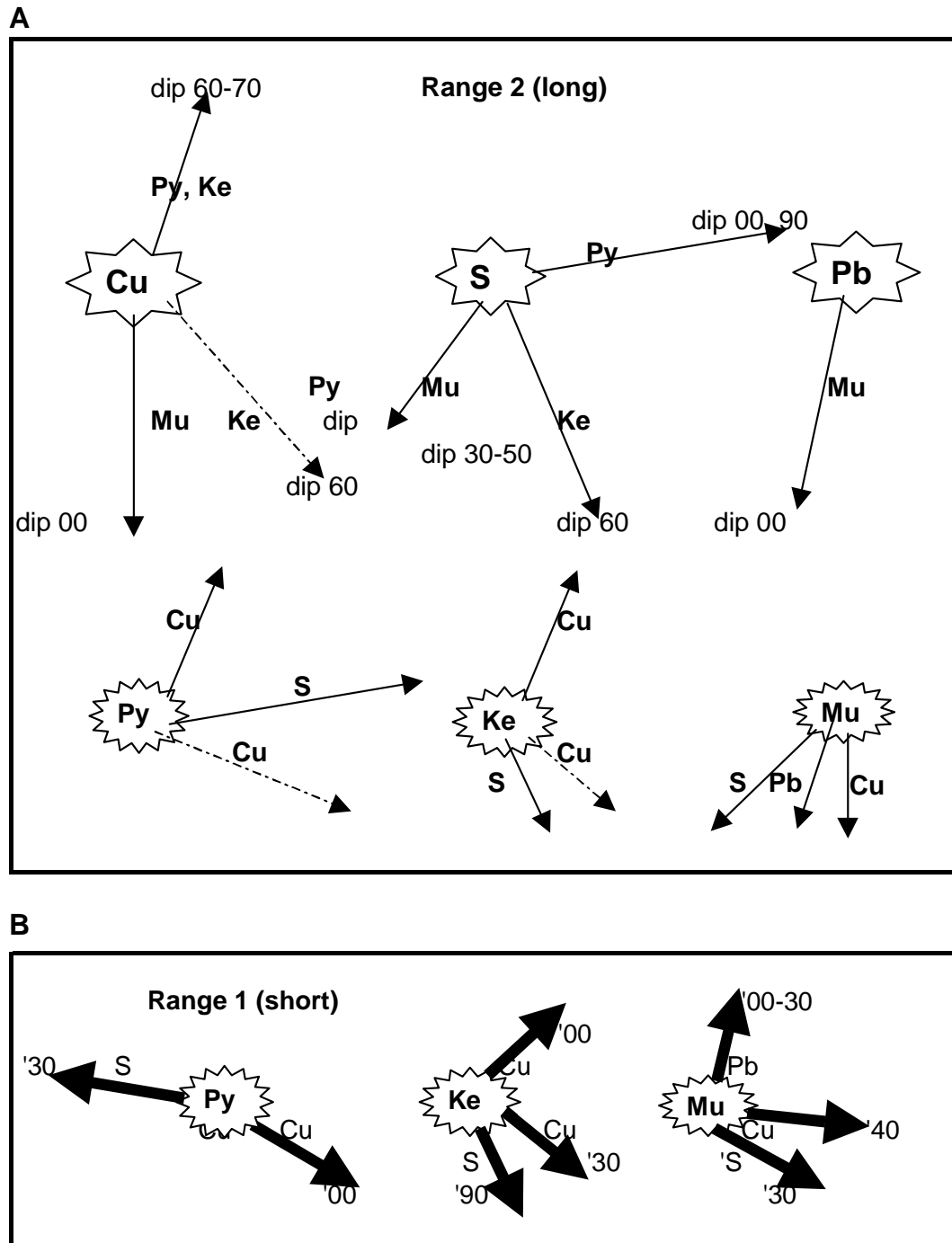


Figure E4.7. Pyhäsalmi area rose diagrams showing azimuthal ranges of Cu grade anisotropy. A. All Pyhäsalmi data, dips 00; B. Surface data down to -200 m bsl, dips 00; C. Surface data down to -200 m bsl, direction 020/200, dips 00, 30, 60, 90.

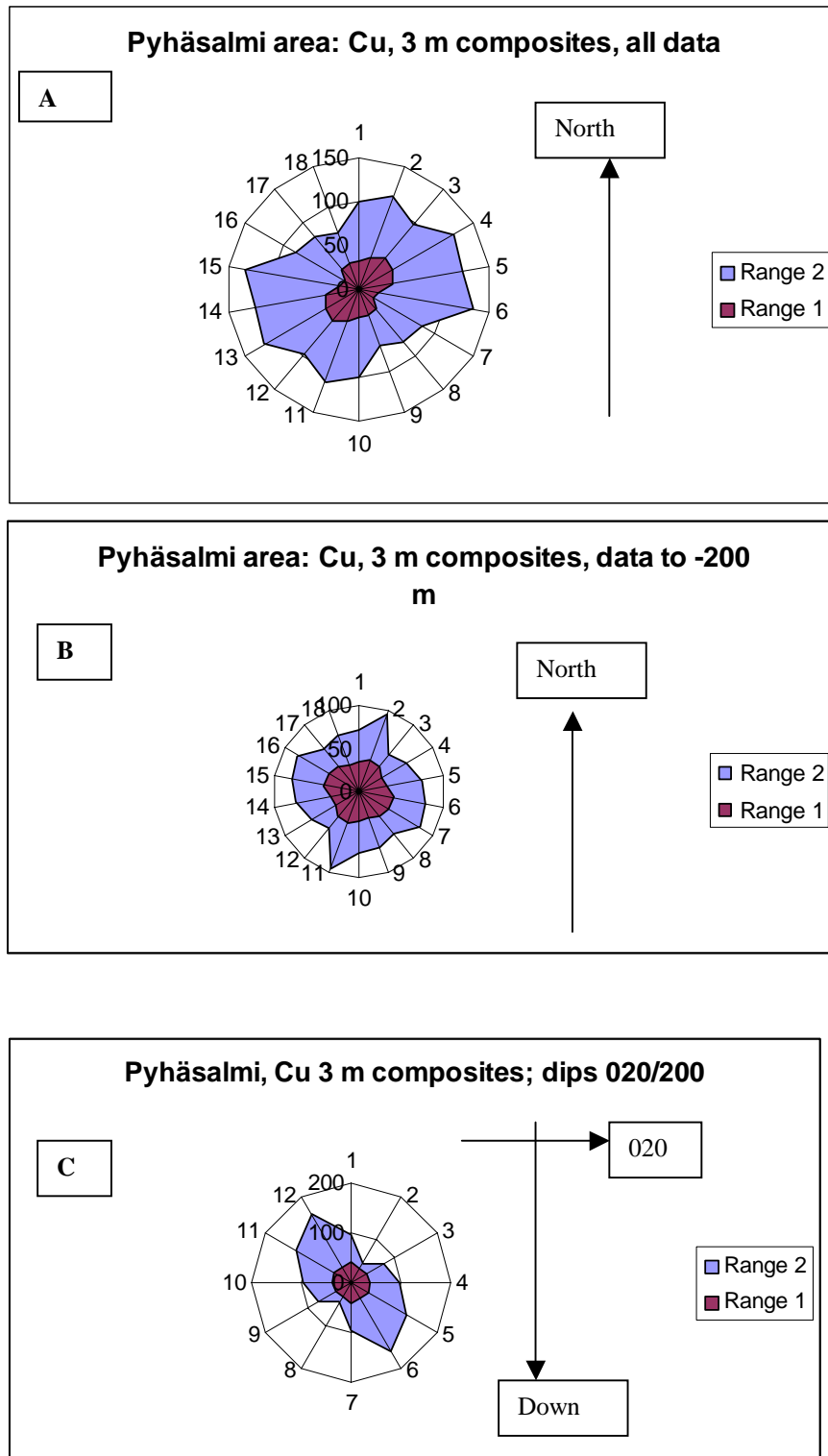


Figure E4.8. Pyhäsalmi area rose diagrams showing azimuthal ranges of S grade anisotropy. A. All Pyhäsalmi data, dips 00; B. Surface data down to -200 m bsl, dips 00; C. Surface data down to -200 m bsl, direction 080/260, dips 00, 30, 60, 90.

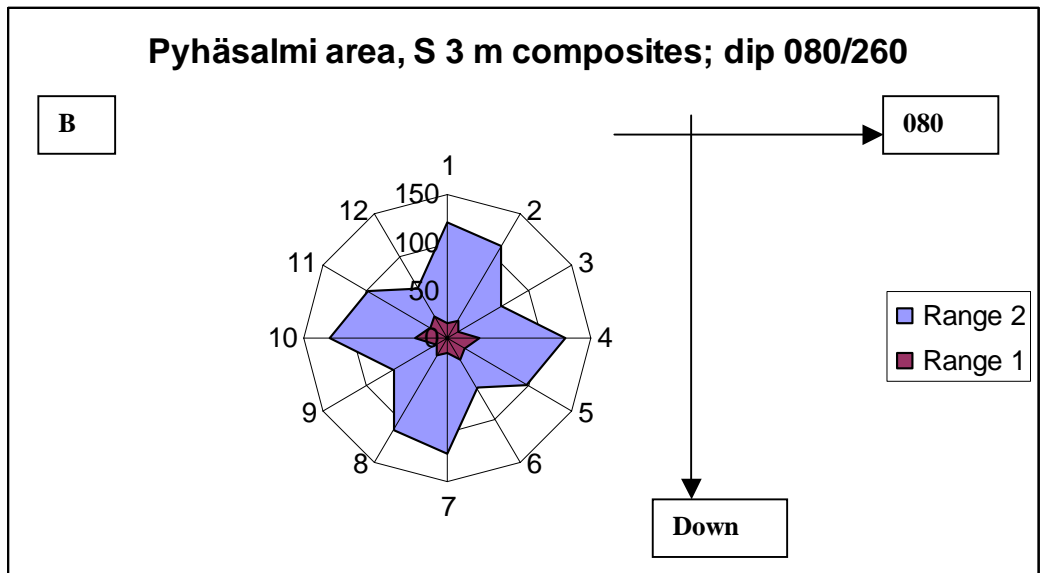
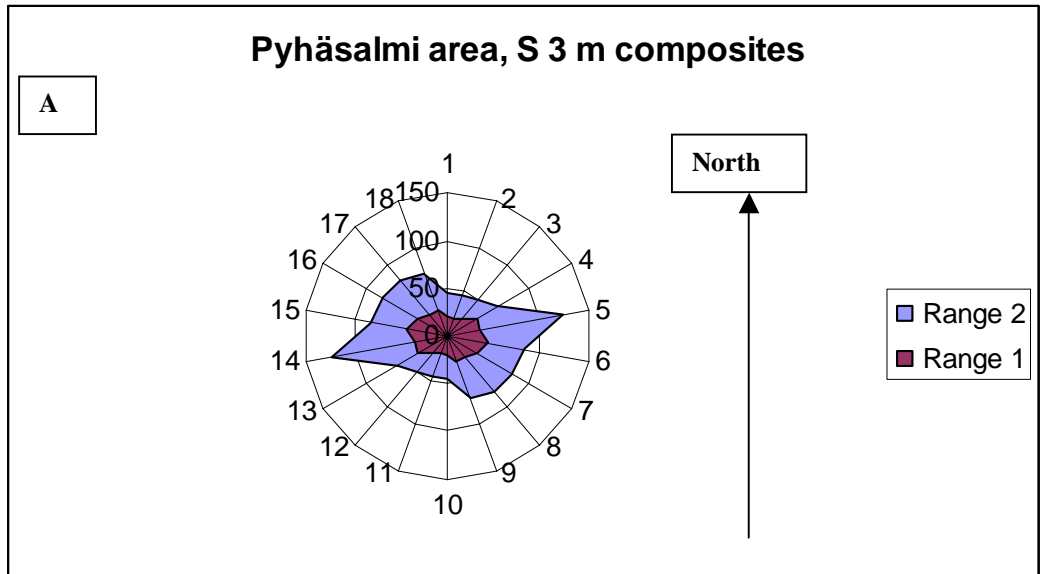


Figure E4.9. Kettuperä area rose diagrams showing azimuthal ranges of Cu grade anisotropy. A. All Kettuperä data, dips 00; B. All Kettuperä data, direction 020/200, dips 00 – 90. C. All Kettuperä data, direction 320/140.

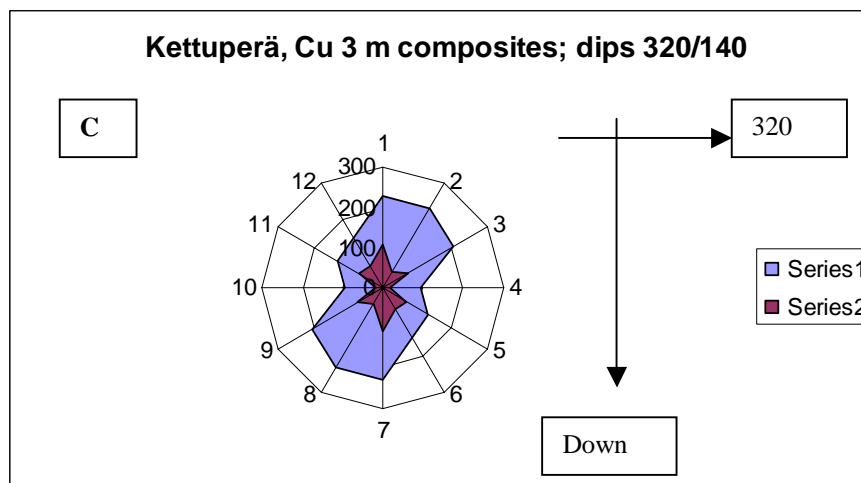
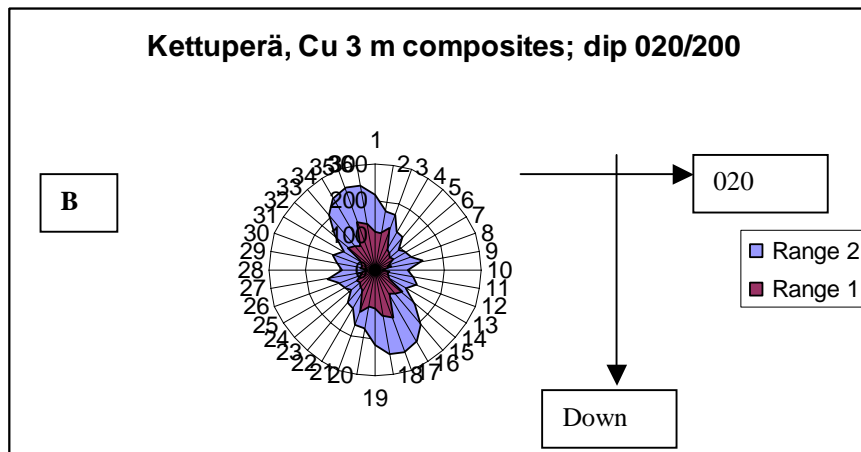
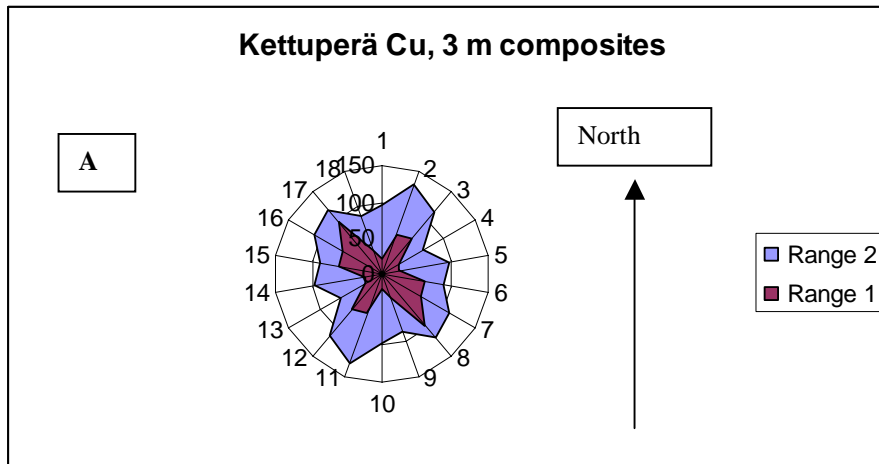


Figure E4.10. Kettuperä area rose diagrams showing azimuthal ranges of S grade anisotropy. A. All Kettuperä data, dips 00; B. All Kettuperä data, direction 160/340, dips 00, 30, 60, 90.

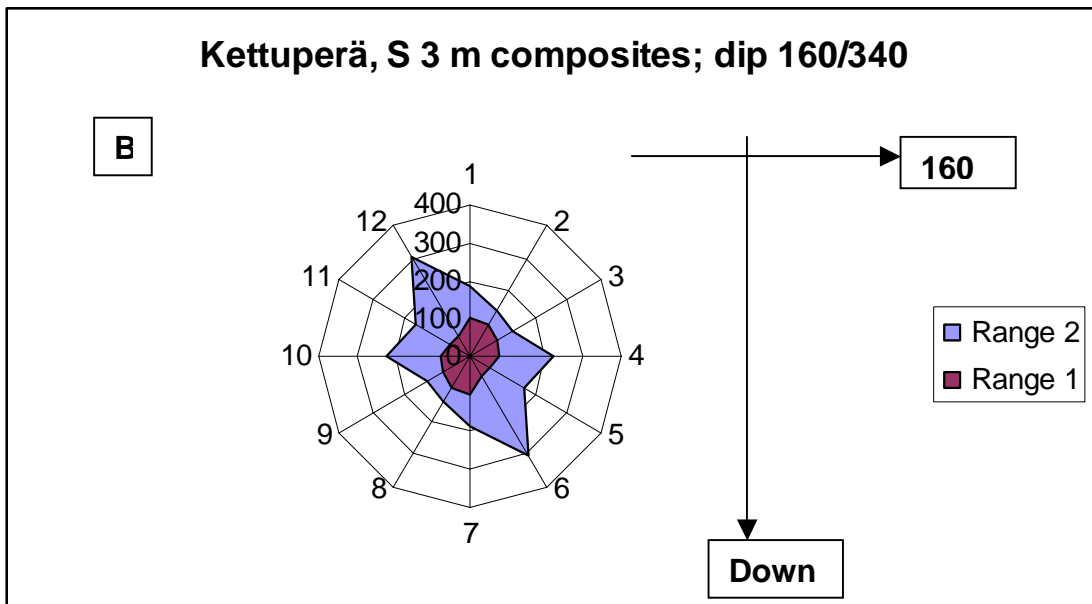
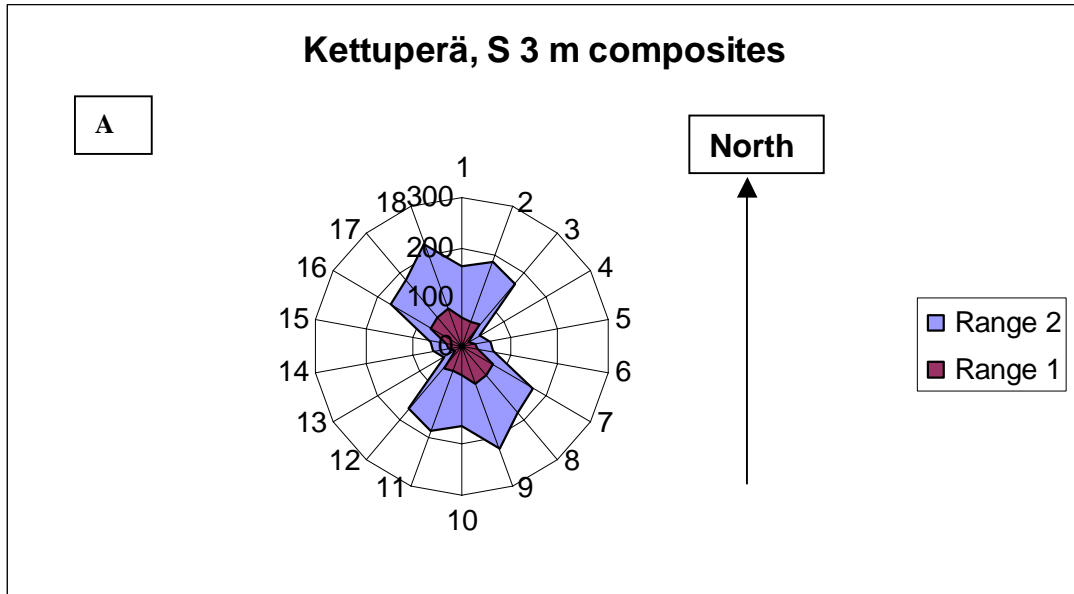


Figure E4.11. Mullikkoräme area rose diagrams showing azimuthal ranges of Cu grade anisotropy. A. All Mullikkoräme data, dips 00; B. All Mullikkoräme data, direction 020/200, dips 00 – 90.

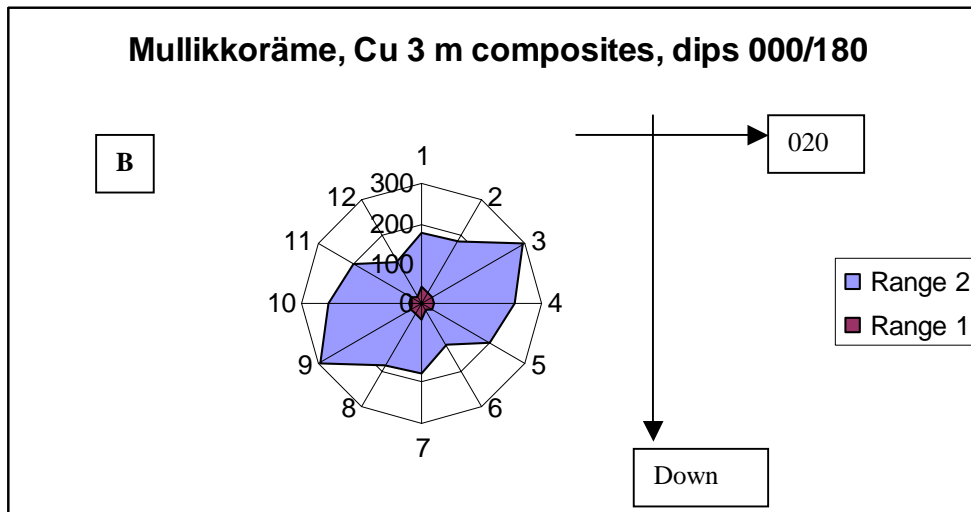
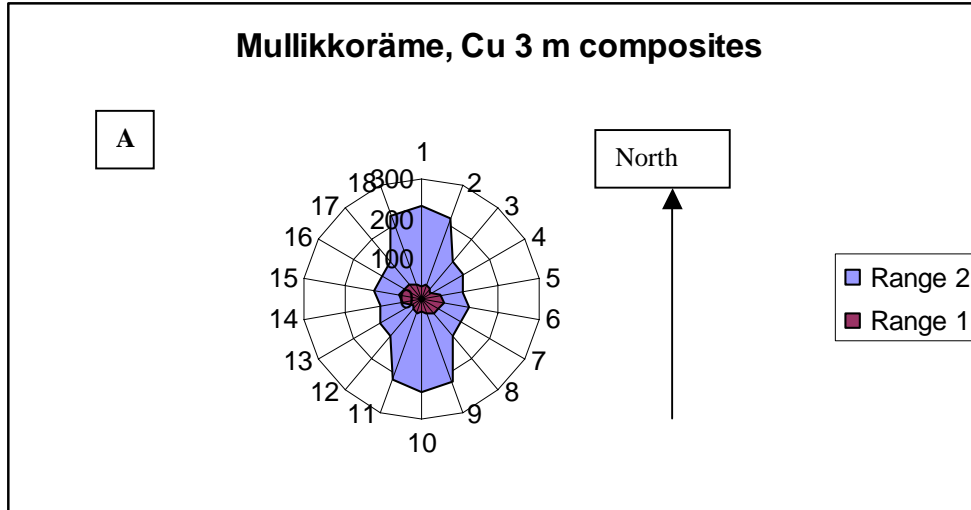


Figure E4.12. Mullikkoräme area rose diagrams showing azimuthal ranges of S grade anisotropy. A. All Mullikkoräme data, dips 00; B. All Mullikkoräme data, direction 040/220, dips 00 – 90.

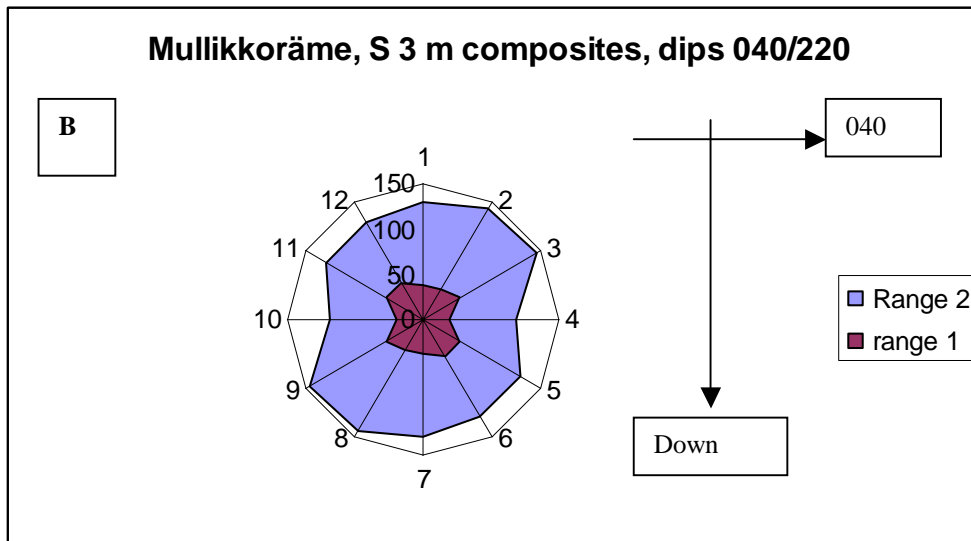
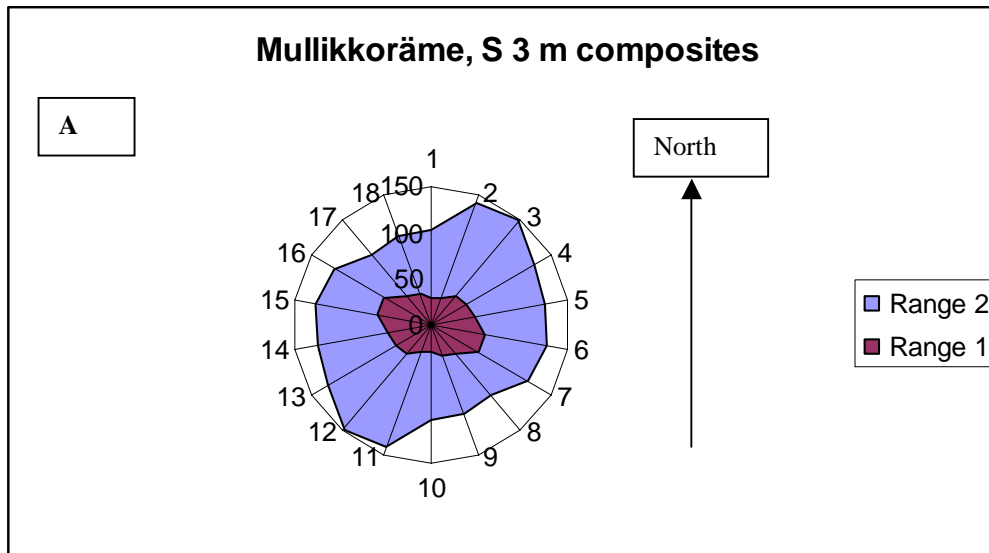
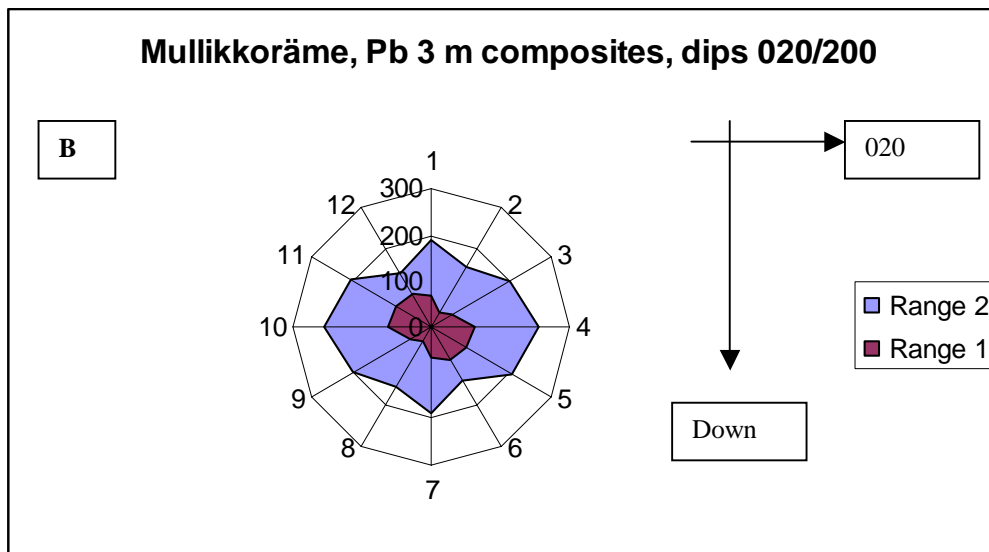
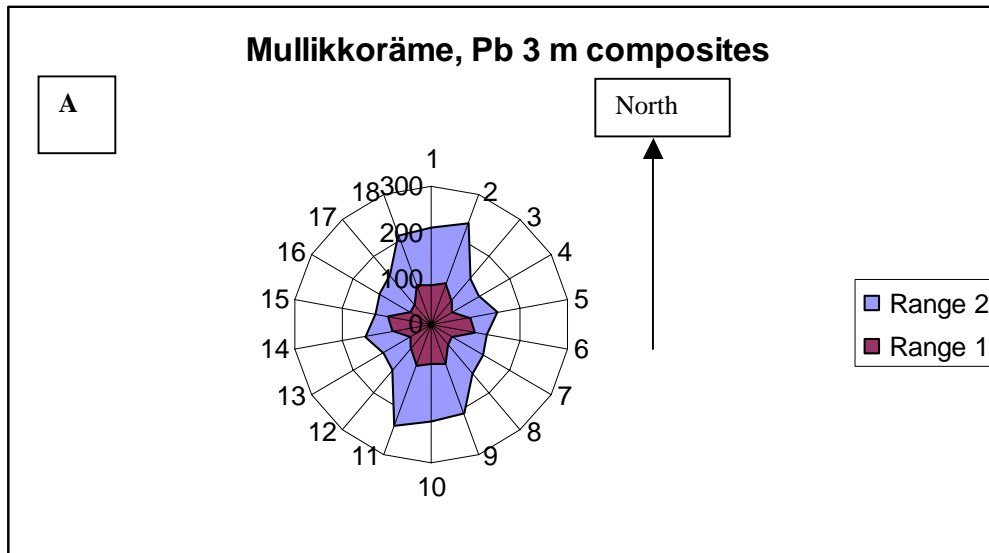


Figure E4.13. Mullikkoräme area rose diagrams showing azimuthal ranges of Pb grade anisotropy. A. All Mullikkoräme data, dips 00; B. All Mullikkoräme data, direction 020/200, dips 00 – 90.



E 4.2.4 Mulliköräme special features

The shapes of histograms in Figs. E4.9A for Pb and E4.9B for Ag resemble those in Figs. E4.4E for Zn and E4.3F for Cu, respectively. Also the correlation coefficients between Pb and Zn and between Ag and Cu are relatively high, as are those between Pb and Ag (Table E4.4). At least three ore types (or mineralization phases) are indicated by this analysis: iron sulfides, Cu-Ag sulfides and Zn-Pb-Ag sulfides. Also geostatistical analysis shows differences in the shape and orientation of these three types represented by Cu (Fig. E4.8), Pb (Fig. E4.10) and S (Fig. E4.11). Their grade lineations are the following.

	Mulliköräme	Kettuperä	Pyhäsalmi (to -200 m)
Cu	180 / 30	020 / 70	020 / 60
Pb	200 / 00		
S	220 / 30 (-50)		

Figure E4.14. Mulliköräme area frequency distribution histograms for lead (A) and silver (B). 3-m composite samples.

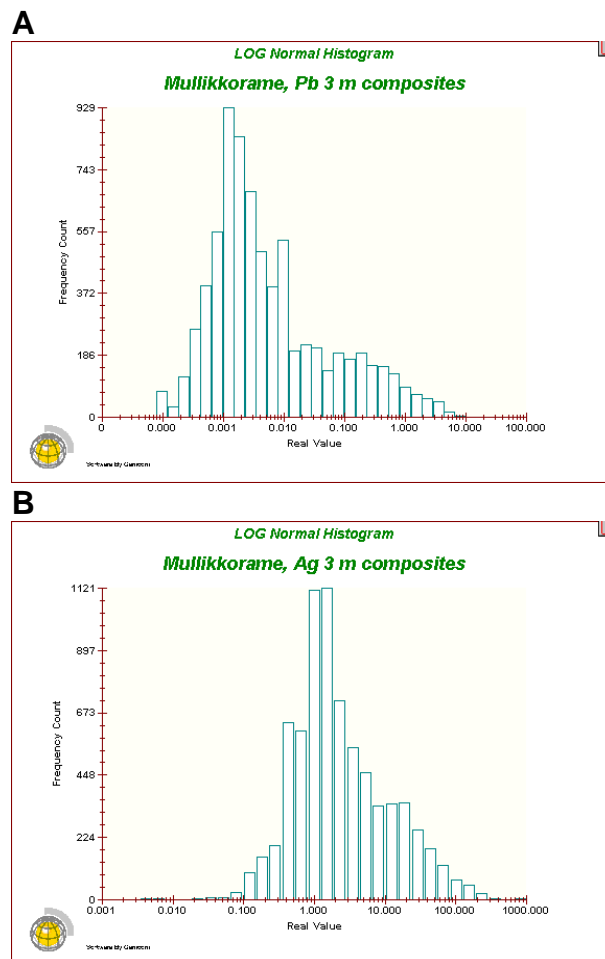


Table E4.5. Statistical parameters for Cu, Zn, Pb, Ag and S at Mullikkoräme. Original samples.

Mullikkoräme 8431 original samples						
Field name	CU	ZN	PB	S	AG	
Data Set Minimum Value	0	0	0	0	0	
Data Set Maximum Value	12.17	55.5	22.6	61.95	1574	
Mean	0.1271	2.0085	0.21717	9.70779	14.82222	
Geometric Mean	0.02509	0.13288	0.01329	2.70163	4.04852	
Natural LOG of Mean	-3.68519	-2.0183	-4.32081	0.99385	1.39835	
Variance	0.10367	19.39644	0.67136	156.4004	1629.939	
LOG Variance	3.90941	7.57561	6.10111	4.09262	2.79158	
Standard Deviation	0.32198	4.40414	0.81936	12.50601	40.37251	
Coefficient of Variation	2.53331	2.19275	3.77285	1.28824	2.72378	
Correlation Coefficient Table						
	CU	ZN	PB	S	AG	
CU	1	0.16458	0.10744	0.27927	0.45060	
ZN	0.16458	1	0.5916	0.58535	0.48146	
PB	0.10744	0.5916	1	0.22544	0.68125	
S	0.27927	0.58535	0.22544	1.00000	0.25134	
AG	0.4506	0.48146	0.68125	0.25134	1.00000	

E 4.3 SPATIAL MODELING

E 4.3.1 Grade value interpolation on planes

Grade value interpolation on vertical and horizontal sections helps in recognizing grade continuity, structural patterns and optimal cutoff grades for ore type delineation. Inverse square distance (ID2) was used for grade estimates on 3x3-m grids as default. Variogram analysis was used to determine the search ellipse orientation and axial lengths.

In the case of the Pyhäsalmi area and orebody the dominating axial direction (of grade anisotropy lineation, see Fig. E4.2.2.1 and Appendix 1.41) is nearly vertical and directed to SSW. However, secondary axes show the following average clockwise rotation for the following depth zones:

depth zones, m	clockwise rotation, degrees
+180 → -50	20
- 100 → -400	40
- 440 → -810	60
- 860 → -1015	80
- 1015 → -1240	100.

Therefore the orientation of the search ellipse for each zone must be different. Axial ratios (X:Y:Z) estimated for the Pyhäsalmi area were 1:2:3 and 1:2:4 (easting-northing-vertical). In practice the corresponding axial lengths were 6:12:20 m and 8:16:20 m.

Parameters for Kettuperä are similar to those of the near-surface area at Pyhäsalmi whereas they are different from the parameters for Mullikkoräme where horizontal to subhorizontal grade anisotropy to S-SW dominates. For Mullikkoräme, axial ratios (X:Y:Z) were 2:4:3. An example of grade interpolation is shown in Fig. E4.17.

E 4.3.2 Mineralization type delineation on planes

Pyhäsalmi area delineations were done on horizontal planes and with the help of existing mine maps, geological profiles constructed by Jouni Luukas, on the above interpolations and on drillhole data. Three ore types were clearly distinguished with a characteristic cutoff grade for each: **Copper ore, cutoff grade 0.8% Cu; Zinc ore, cutoff grade 2.0% Zn; Sulfur ore, cutoff grade 43.0% S {iron sulfides *} .** These criteria were prioritized in importance so that $Cu > Zn > S$. Thus “mixed” types were named “Copper ore” if $Cu > 0.8\%$ regardless the assays for Zn and S. For Kettuperä mineralization type delineation was not done because the present sampling density was considered too low for proper interpolations.

*) $S\{\text{iron sulfides}\} = [S] \times (S/(S) - 2 \times Cu/[Cu] - Zn/[Zn])$. Let $S = 48.0\%$, $Cu = 2.0\%$ and $Zn = 1.0\%$. Then $S\{\text{iron sulfides}\} = 32.06 \times (48/32.06 - 2 \times 2/63.546 - 1/65.38) = 45.5\%$. This ore, however, is copper type because $Cu > 0.8\%$.

For Mullikkoräme, delineations were based on geological profiles constructed by Jouni Luukas, on the above interpolations and on drill hole data on vertical

planes. Five mineralization types were defined according to characteristic cutoff grades but without any weighting. Thus Mullikkoräme delineations are in some cases overlapping. Cutoff grades: Copper type, 0.5% Cu, Zinc type, 1.0% Zn, Silver type, 1 ppm Ag; Lead type, 0.3% Pb, Sulfur type, 20% S.

E 4.3.3 3D solid modeling

The corresponding ore type delineations (technically “polygons”) on successive planes were connected and solid “wireline” models created. Rendered solids are shown in Figs. E4.17-23.

E 4.3.4 “Hot spots” and metal zoning

Gemmel and Large (1992) and Huston & Large (1987) traced feeder systems of volcanic-hosted massive sulfide deposits by identifying metal zoning. According to them iron and copper are concentrated in the cores of the feeders with zinc and lead, silver, gold and arsenic and barium becoming increasingly dispersed away from the centers of hydrothermal activity. To describe metal zoning they used “Zn ratio” and “Cu ratio” , or $\{100 \times \text{Zn} / (\text{Zn} + \text{Pb})\}$ and $\{100 \times \text{Cu} / (\text{Cu} + \text{Zn})\}$, respectively. Accordingly high Zn ratio values (>67) outline margin feeders (temperatures less than 200° C) whereas low Zn ratio values (<61 mark the central feeder (temperatures 240° to 300°). High Cu ratio values (>5) highlight the central feeder system, but low Cu ratio values (<3) outline secondary systems. Here also a Ni ratio $\{100 \times \text{Ni} / (\text{Cu} + \text{Zn})\}$ has been studied for zonality description.

Only the Cu ratio criterium can be applied to the entire Pyhäsalmi area because of incomplete lead assay coverage. Statistical parameters are as follows:

	Samples	average ratio	STD
Pyhäsalmi, Cu ratio	25 453	57	31
Mullikkoräme, Cu ratio	7 735	27	23
Mullikkoräme, Zn ratio	6 738	84	14
Huston&Large, typical Zn ratio		64 – 77	<15

Distribution histograms for Cu ratios at Pyhäsalmi and Mullikkoräme, and for Zn and Ni ratios at Mullikkoräme, are shown in Figs. E4.16 A-D. Cu ratio interpolations on vertical and horizontal projections are shown in Figs. E4.24 and E4.25 (Pyhäsalmi and Kettuperä areas) and in Figs. E4.26 A-D (Mullikkoräme area). It seems that “hot spots” can be localized at Pyhäsalmi and Kettuperä whereas Mullikkoräme represents a “cool “ area as based on Zn ratio and an extremely “hot” area as based on Cu ratio.

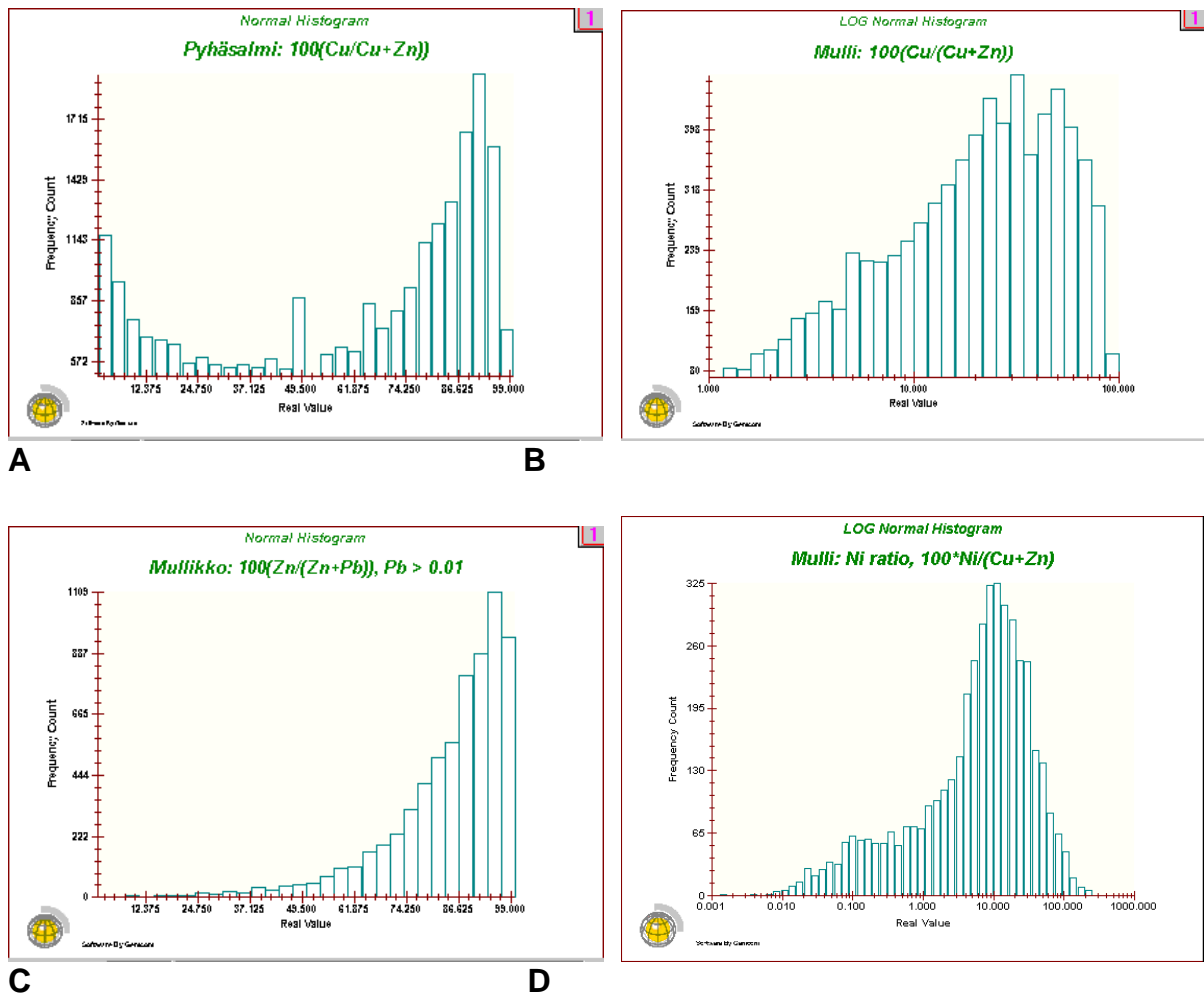


Figure E 4.16A-D. Frequency distribution histograms for the Pyhäsalmi and Mullikkoräme areas.

- A. Pyhäsalmi: frequency distribution histograms for Cu ratios.
- B. Mullikkoräme: frequency distribution histograms for Cu ratios.
- C. Mullikkoräme: frequency distribution histograms for Zn ratios.
- D. Mullikkoräme: frequency distribution histograms for Ni ratios.

Metal zoning in the Pyhäsalmi case is rather obvious as shown in Figs. E4.17-18. A platy core rich in Zn and enveloped by chalcopyritic material is twisted or screwed like a dishcloth around a subvertical axis and together with a separate iron sulfidic "layer" outside the envelope.

Metal zoning in the Mullikkoräme case is much less obvious. On one hand solids shown in Figs. E4.19 – 23 indicate that different metals may exhibit different patterns, and especially iron sulfidic zones may crosscut other mineralized zones. On the other hand, as shown in Figs. E4.27 and E4.28, copper, zinc, lead, silver and sulfur follow a similar pattern while nickel follows a different one. To further illustrate this possible zonality, also Ni ratio $\{100 \times \text{Ni} / (\text{Cu} + \text{Zn})\}$ was calculated. It shows maximum values in between and around known orebodies. Whether Ni

assays tell about silicate nickel or sulfidic nickel is not known. Therefore this observation may not be relevant.

E 4.4 CONCLUSIONS AND RECOMMENDATIONS

The Pyhäsalmi and Mullikkoräme ore types are qualitatively and structurally two different species. While at Pyhäsalmi three different ore types can be differentiated on a chemical and a mineralogical as well as on a spatial basis, this kind of separation does not work at Mullikkoräme where ore type differences are not that explicit. Further, at Mullikkoräme orebody boundaries seem more diffuse than they are at Pyhäsalmi. Certain structural features like the folding and twisting of plates around a steeply dipping axis (and folding with more gentle axes as related to faults) is typical to Pyhäsalmi while at Mullikkoräme subhorizontal linear features dominate on the small-sized ore lenses that may be fragments of a faulted ore layer.

Kettuperä resembles Pyhäsalmi as was known already. Sampling density, especially the lack of deep holes makes it difficult to apply to Kettuperä what has been learnt from Pyhäsalmi.

This report is based on a superficial and tentative study. The study can be deepened and improved a lot. A remarkable step would be the integration of different studies, done for this modeling project, to be followed by a "second phase iteration". The second phase might give verifiable results, possibly drill hole targets.

E4 EXPLANATIONS FOR FIGURES E4.17-28.**Fig. E4.17A-E.**

Pyhäsalmi area: A
 B C D E

- A. Mine level –990 bsl, drillholes and grade histograms for Cu (red) and S (yellow).
- B. Mine level –990 bsl, samples (circles), interpolation for Zn (cyan above cutoff) and ore type delineation: cyan Zn type, red Cu type, yellow S type).
- C. 3D solid rendered models for zinc type (cyan) and sulfur type (yellow) from south.
- D. 3D solid rendered models for zinc type, copper type (red) and sulfur type from south.
- E. 3D solid rendered models for zinc type, copper type and sulfur type from west.

Fig. E4.18A-F.

Pyhäsalmi area: A C
 B D E F

- A. Mine level –990 bsl, 3D “wireline” model of ore types, colours as in Fig. 16.
- B. Mine level –990 bsl, 3D rendered solid model of ore types, colours as above.
- C. Mine level –200 bsl, interpolation of
- D. Mine level –500 bsl, interpolation
- E. Vertical section 7062025 with drill hole intercepts and a “wireline” ore type model.

Fig. E4.19.

Mullikkoräme.

A 3D rendered solid model of copper mineralizations. At the background geological profile, section 7066800 by Jouni Luukas.

Fig. E4.20.

Mullikkoräme.

A 3D rendered solid model of sulfide mineralizations. At the background geological profile, section 7066800 by Jouni Luukas.

Fig. E4.21.

Mullikkoräme.

A 3D rendered solid model of zinc mineralizations. At the background geological profile, section 7066800 by Jouni Luukas.

Fig. E4.22.

Mullikkoräme.

A 3D rendered solid model of silver mineralizations. At the background geological profile, section 7066800 by Jouni Luukas.

Fig. E4.23.

Mullikkoräme.

A 3D rendered solid model of lead mineralizations. At the background geological profile, section 7066800 by Jouni Luukas.

Fig. E4.24.

Pyhäsalmi orebody: A C E G
 B D F H / I / J

Interpolation for Cu ratio: < 10 green, 10 to 85 grey, > 85 red (“hot spots”).

A – D: SW-NE vertical sections to NW, thickness 10 m and slicing the ore body from back (A) to forth (D). E: Projection of all Cu ratios interpolated on a vertical SW-NE section.

F – J: Cu ratio interpolations on planes +100, -200, -600, -990, and -1110; plane thickness 50 m.

Fig. E4.25.

Pyhäsalmi and Kettuperä areas.

Level 180 asl, thickness 200 m.

Interpolation for Cu ratio: < 10 blue, 10 – 50 green, 50 – 85 grey, > 85 red.

Fig. E4.26.

Mullikkoräme area.

Level 180 asl, thickness 200 m.

Interpolation for Cu ratio: < 10 blue, 10 – 50 green, 50 – 85 grey, > 85 red.

Fig. E4.27.

Mullikkoräme area: A B C
 D E F.

2D ID interpolations of metal assays as projected on the surface. Grid 5 x 5 m, anisotropy axes for search ellipse: X = 20 m, Y = 40 m.

A. Cu grades 0.0001-0.01-0.2-max%, grey-blue-magenta.

B. Zn grades 0.0001-0.01-2-max%, grey-cyan-red.

C. Pb grades 0.001-0.01-0.3-max%, grey-blue-red.

D. S grades 0.001-1-15-max%, grey-yellow-magenta.

E. Ag grades 0.01-1-10-max ppm, grey-green-red.

F. Ni grades 0.0001-0.0015-0.003-max, grey-green-red.

Fig. E4.28.

Mullikkoräme area: A B C
 D

2D ID interpolations of metal ratios as projected on the surface. Grid 5 x 5 m, anisotropy axes for search ellipse: X = 20 m, Y = 40 m.

A. Cu ratio $100 \times \text{Cu} / (\text{Cu} + \text{Zn})$, -20-50-100 grey-blue-red.

B. Zn grades as in Fig. E4.27B.

C. Ni ratio $100 \times \text{Ni} / (\text{Cu} + \text{Zn})$, -5-16-250 grey-cyan-red.

D. Zn ratio $100 \times \text{Zn} / (\text{Pb} + \text{Zn})$ -75-92-100 grey-green-magenta.

Figure E4.17A-E

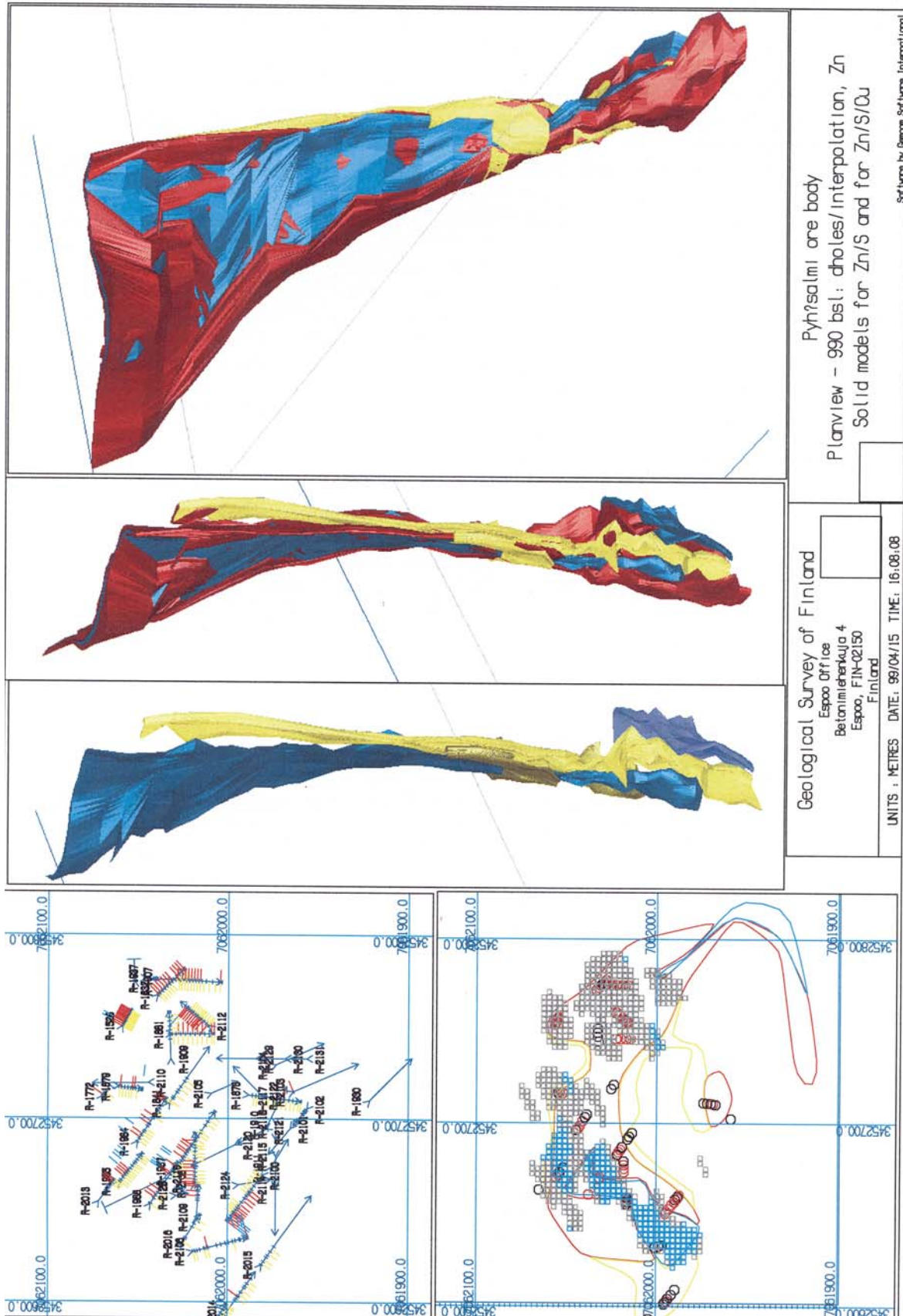


Figure E4.18A-F

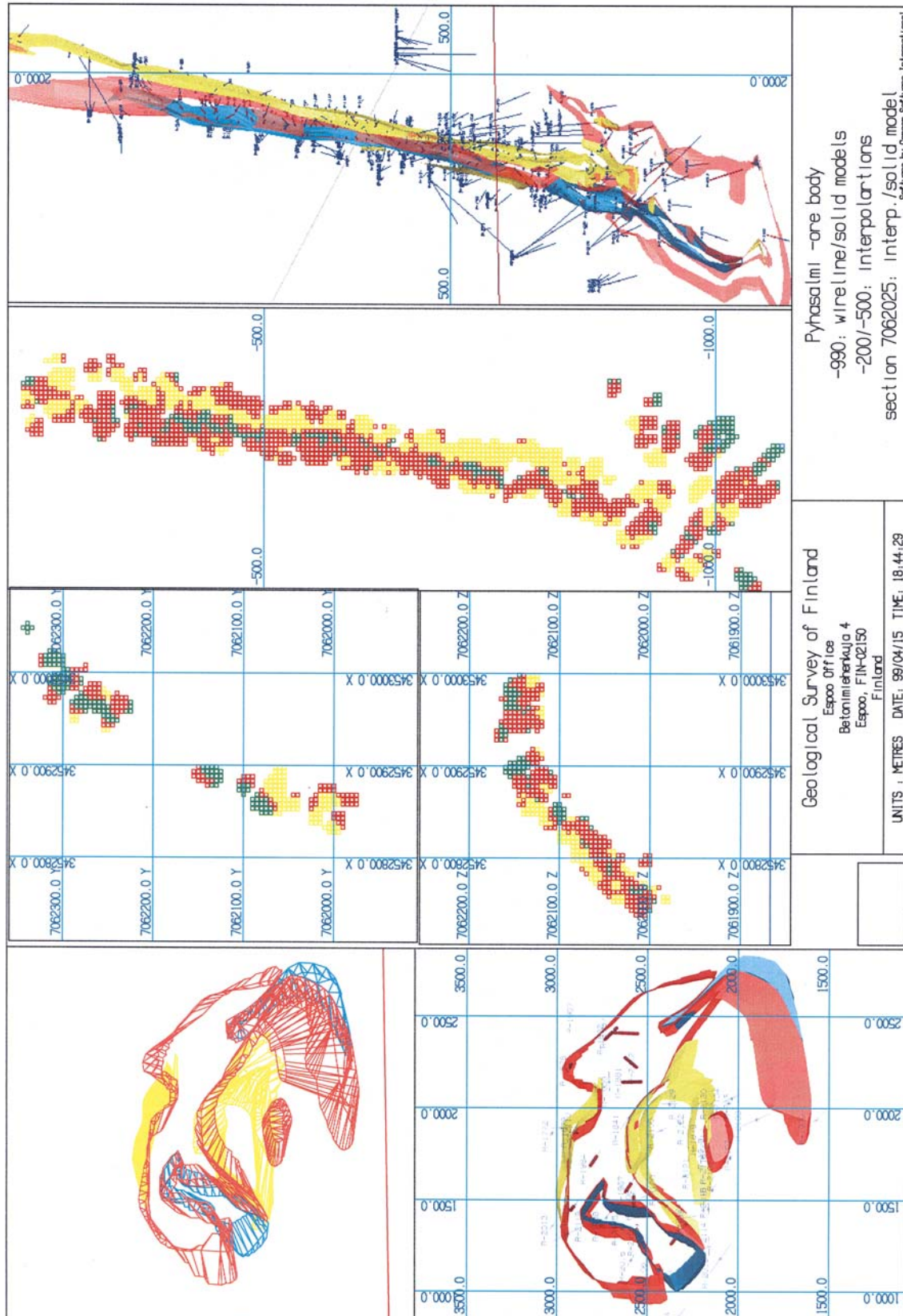


Figure E4.19

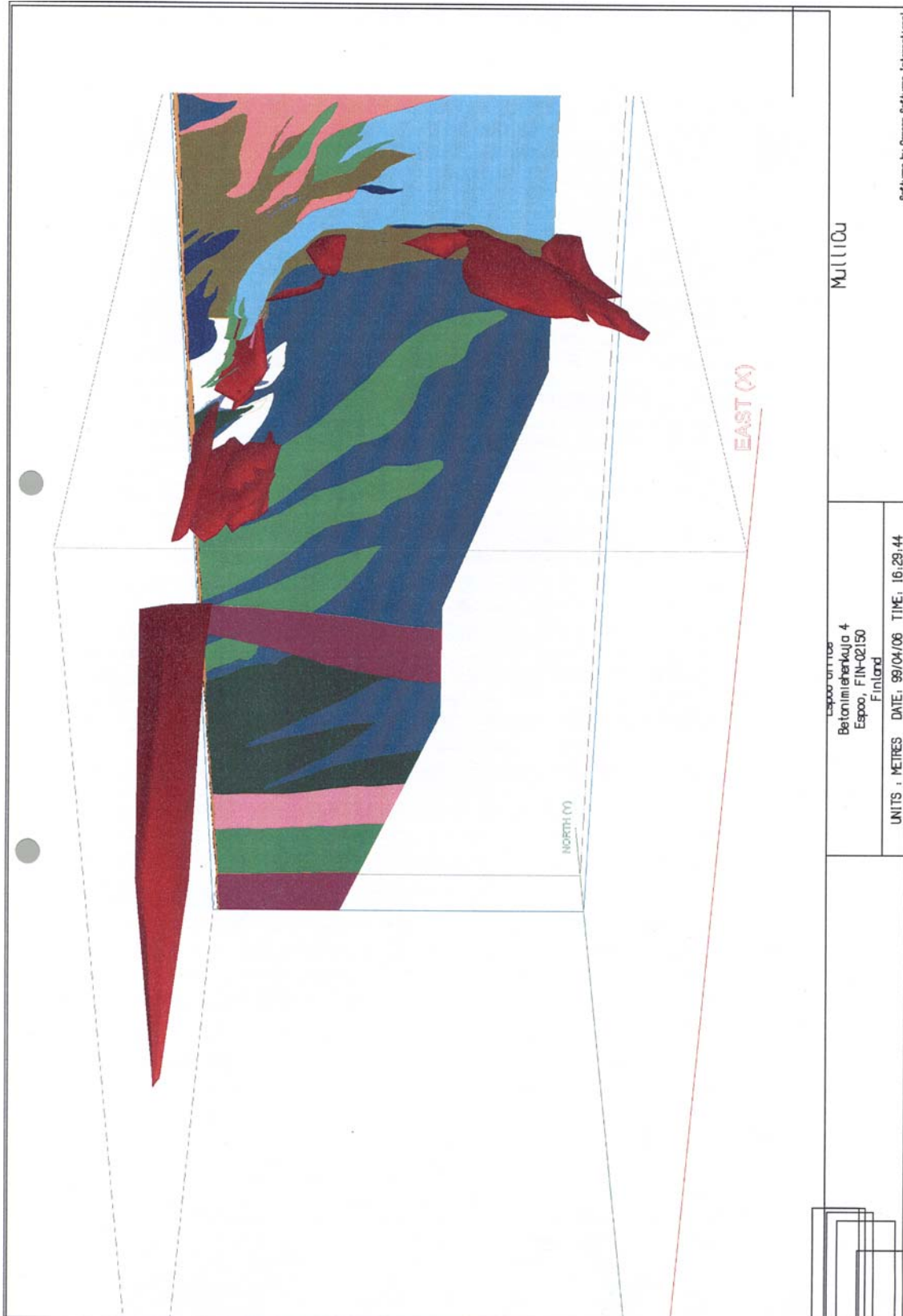


Figure E4.20

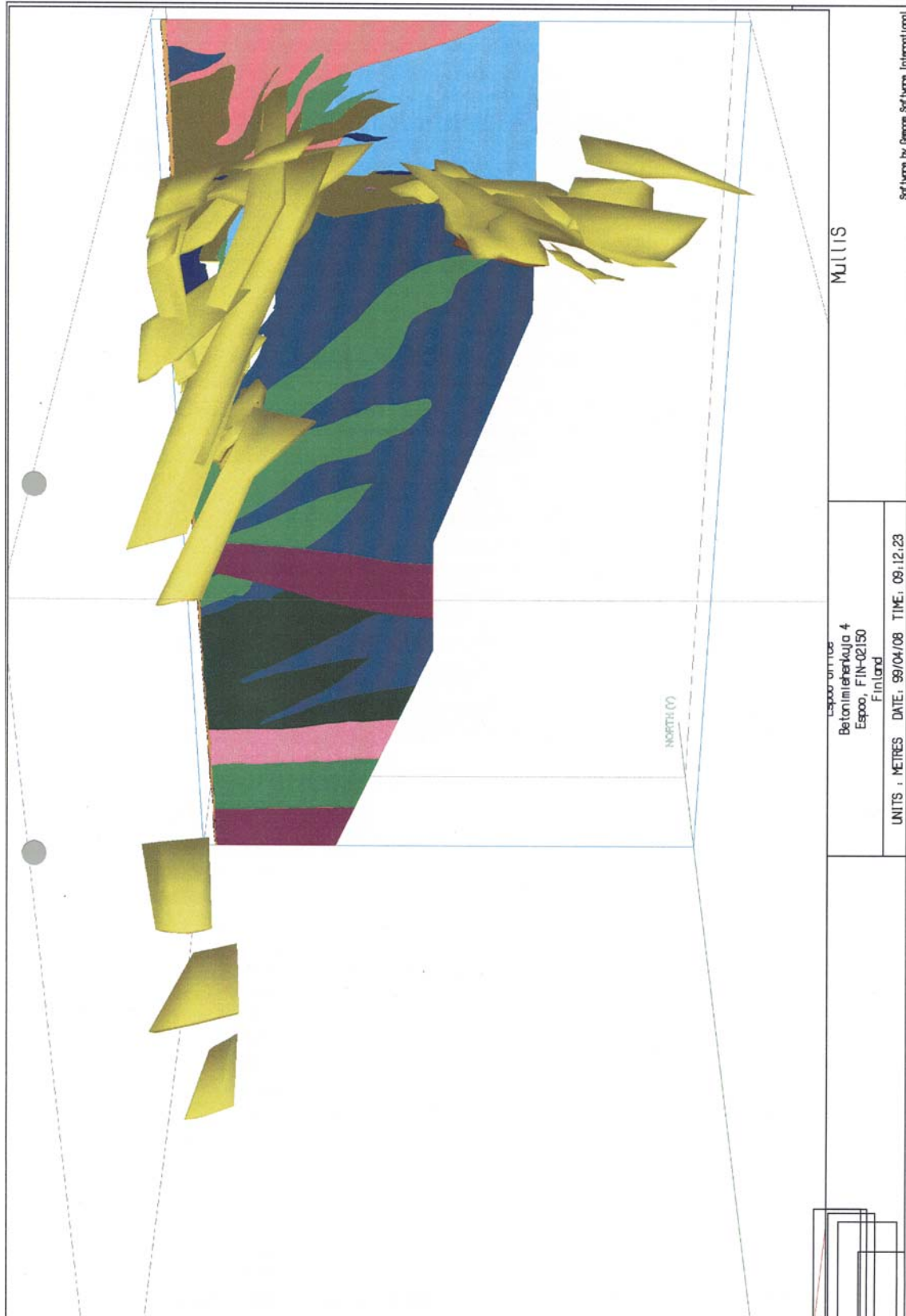


Fig. E4.21

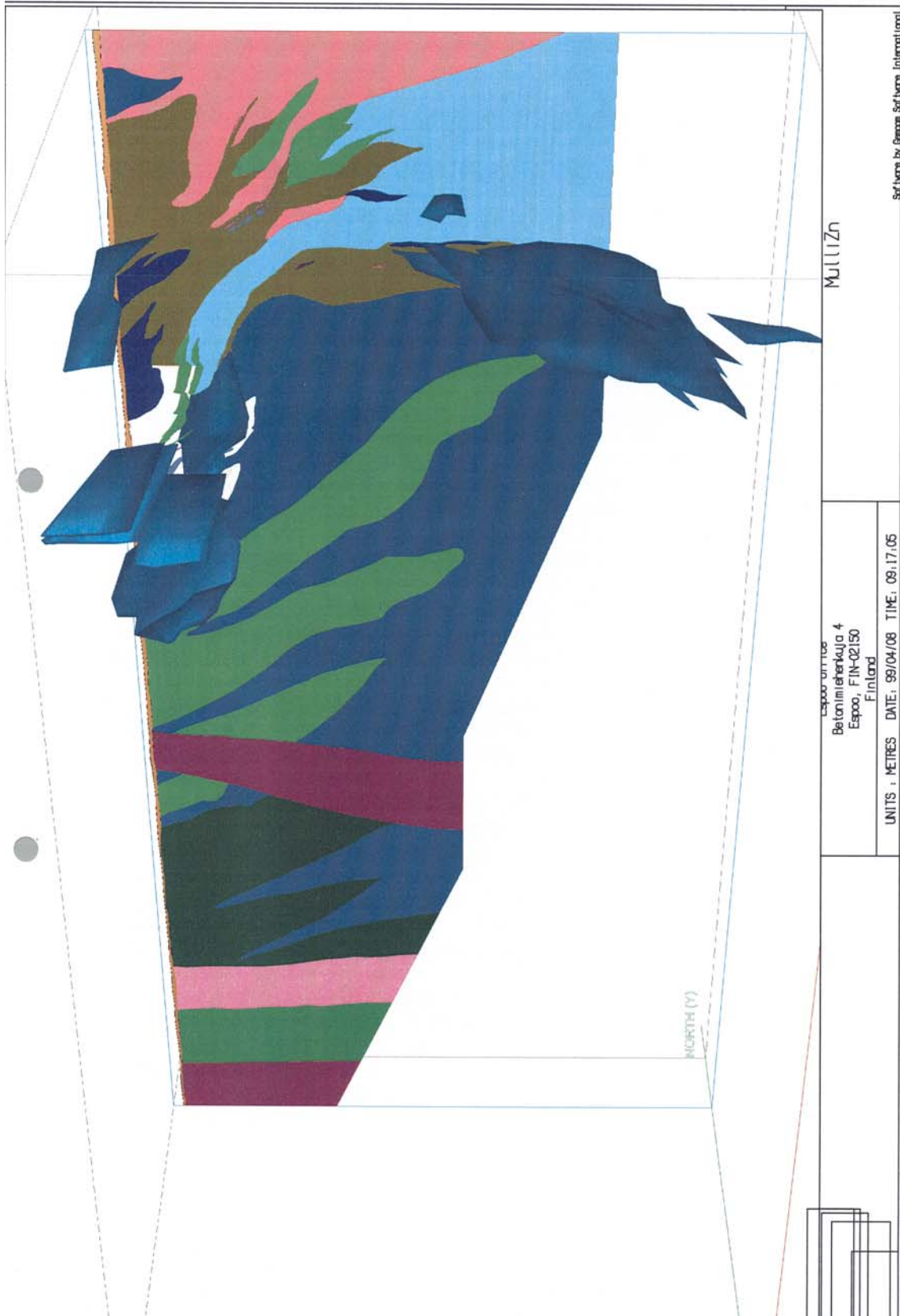


Fig. E4.22

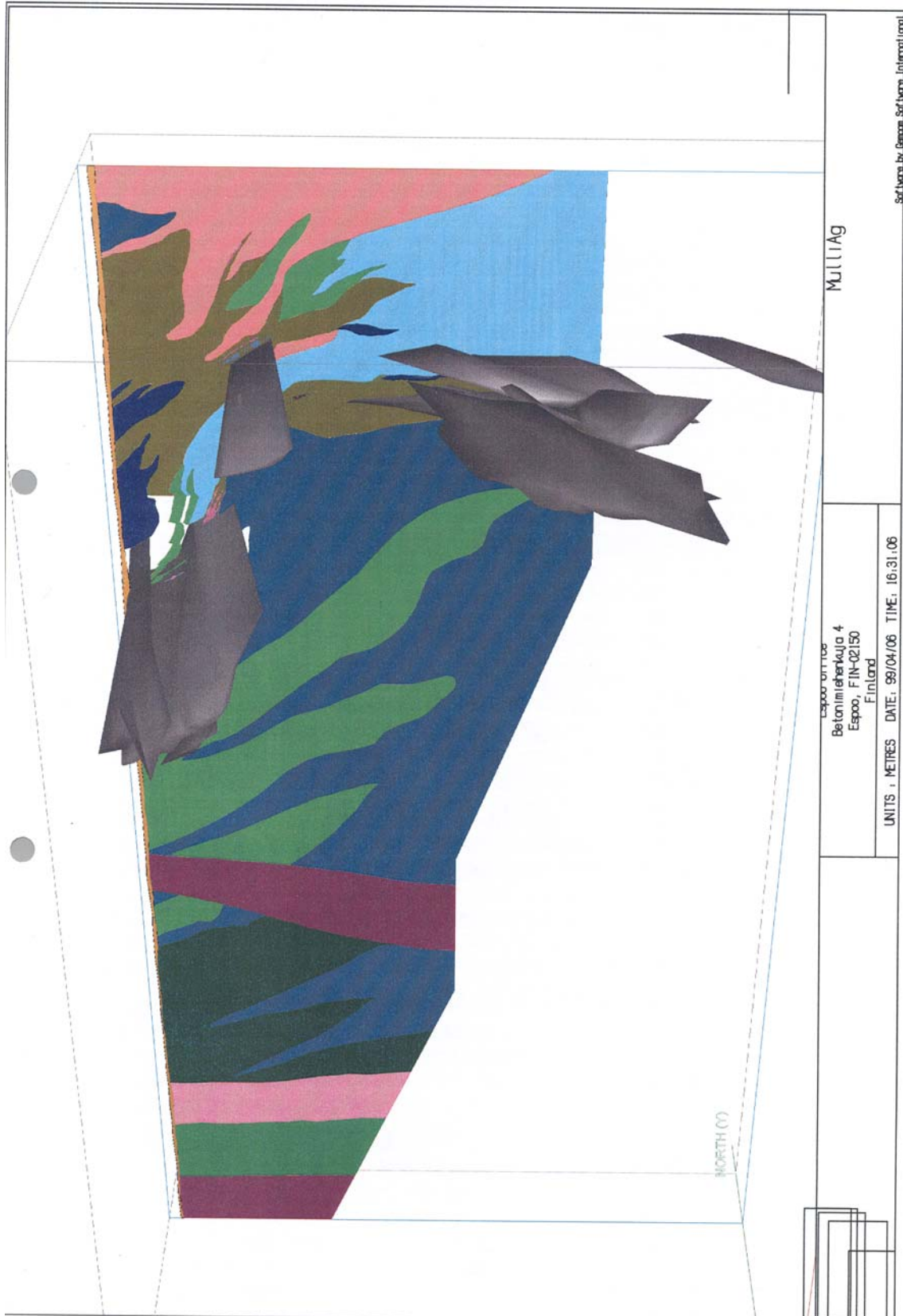
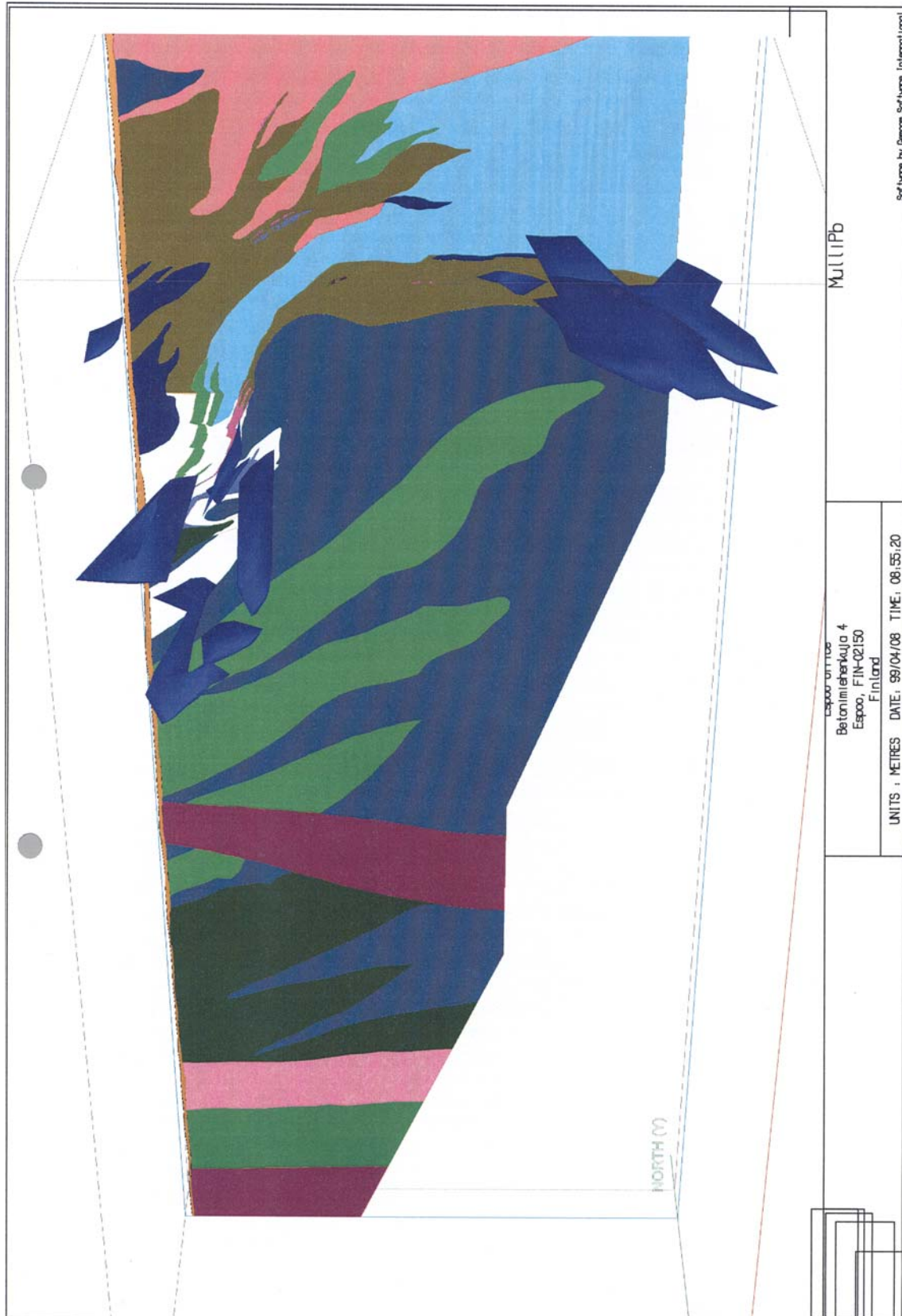


Fig. E.23



Software by Geomac Software International

Fig. E4.24A-J

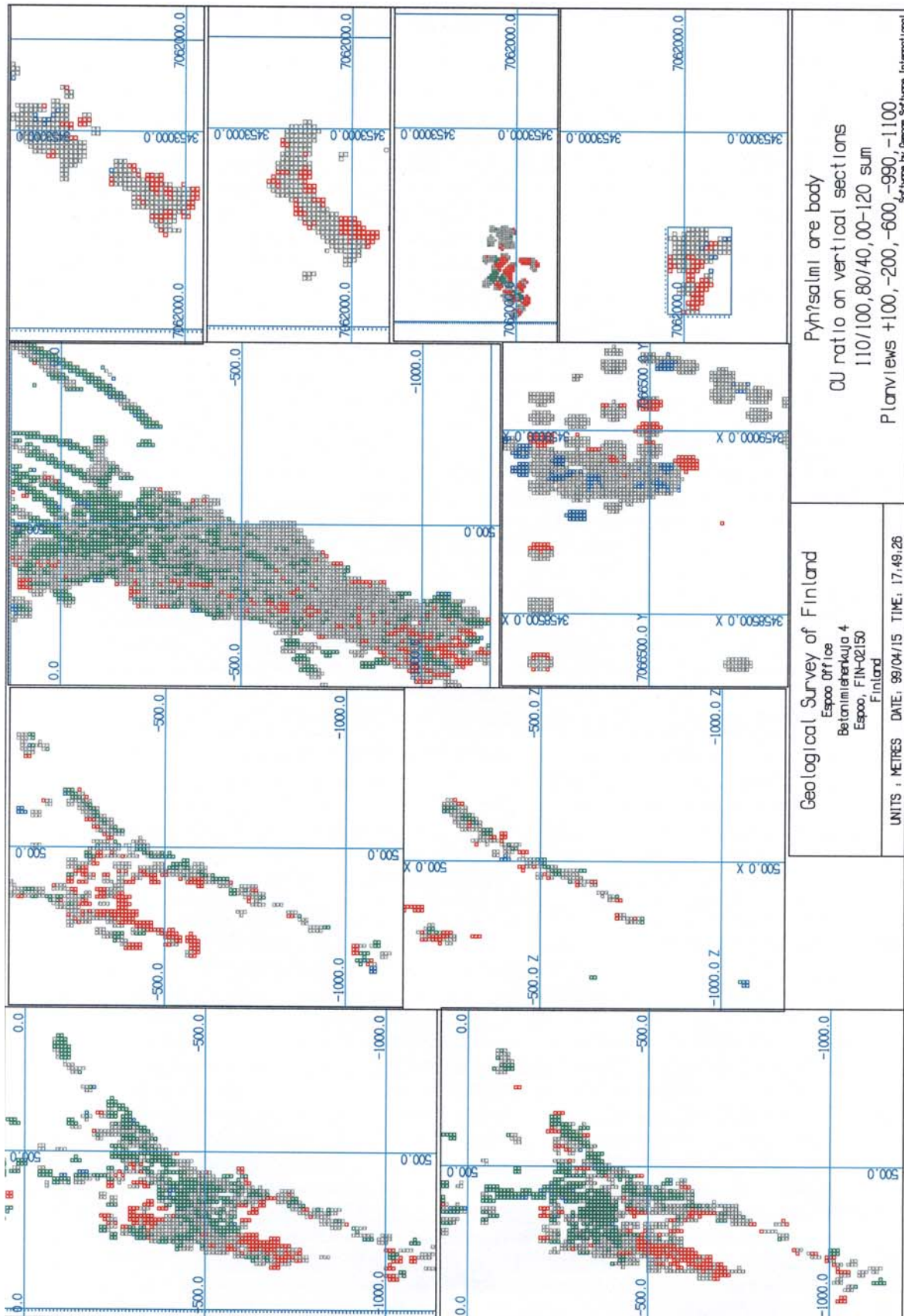


Fig. E4.25

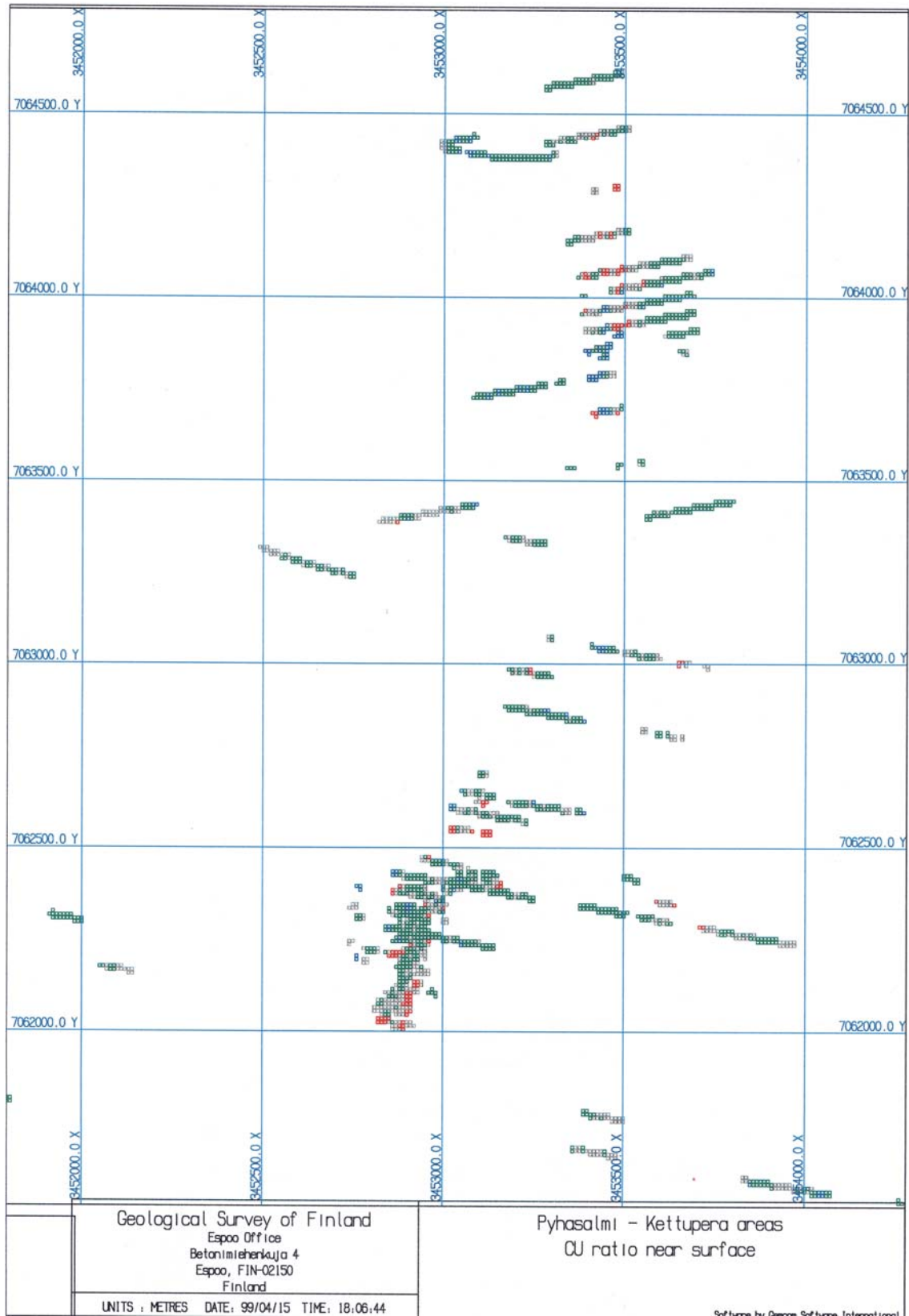


Fig. E4.26A-F

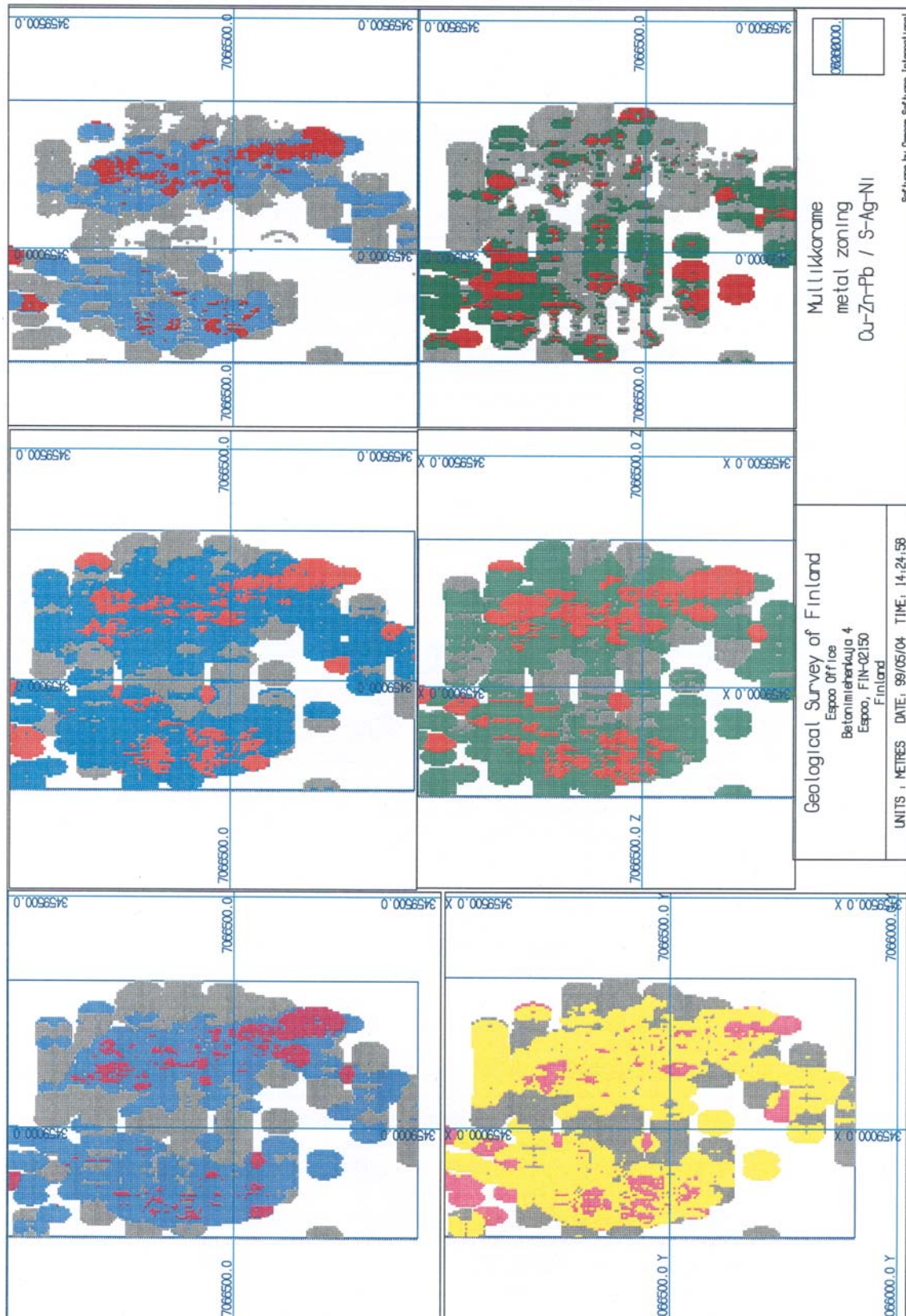


Fig. E27.A-F

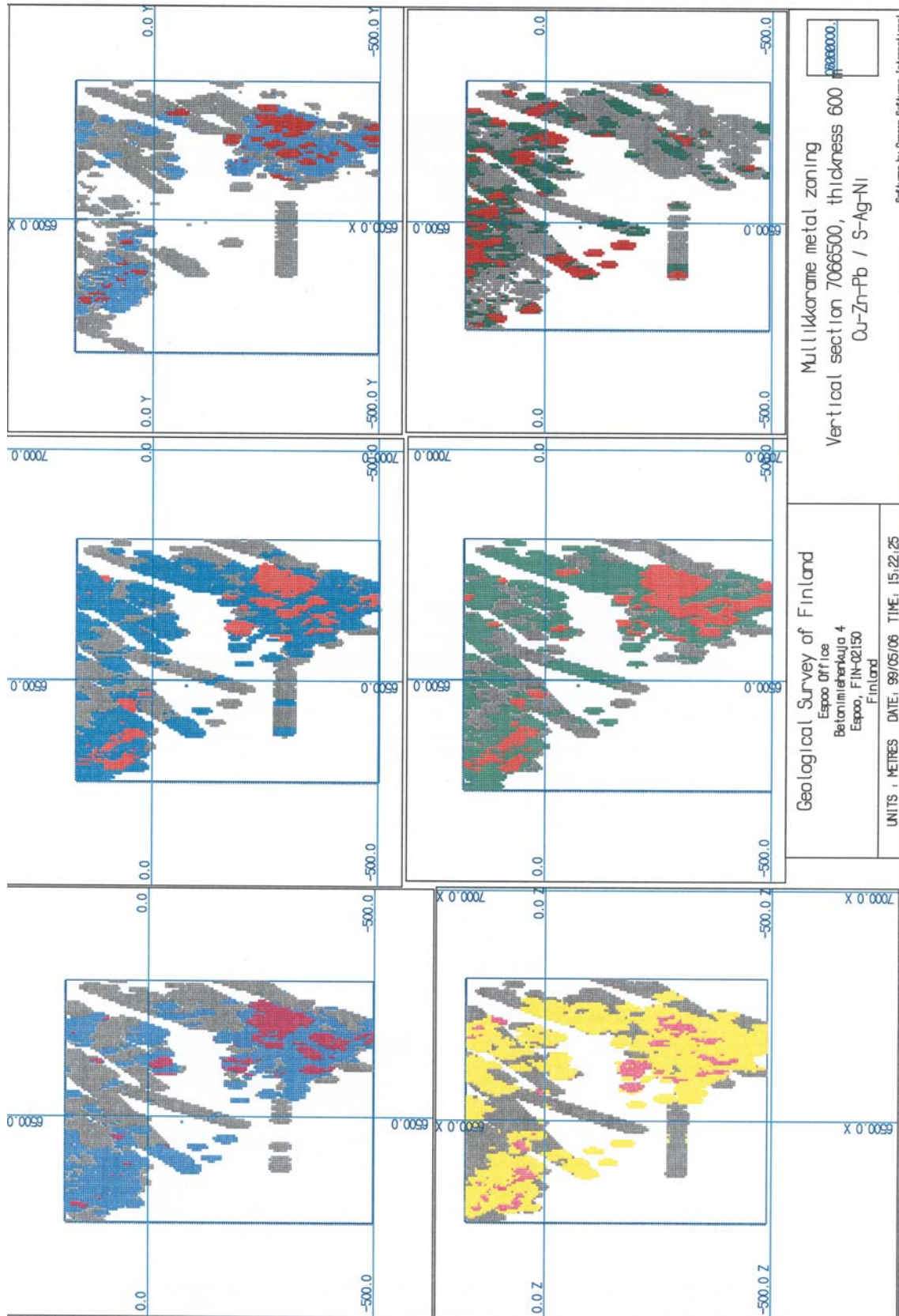


Fig. E4.28A-D

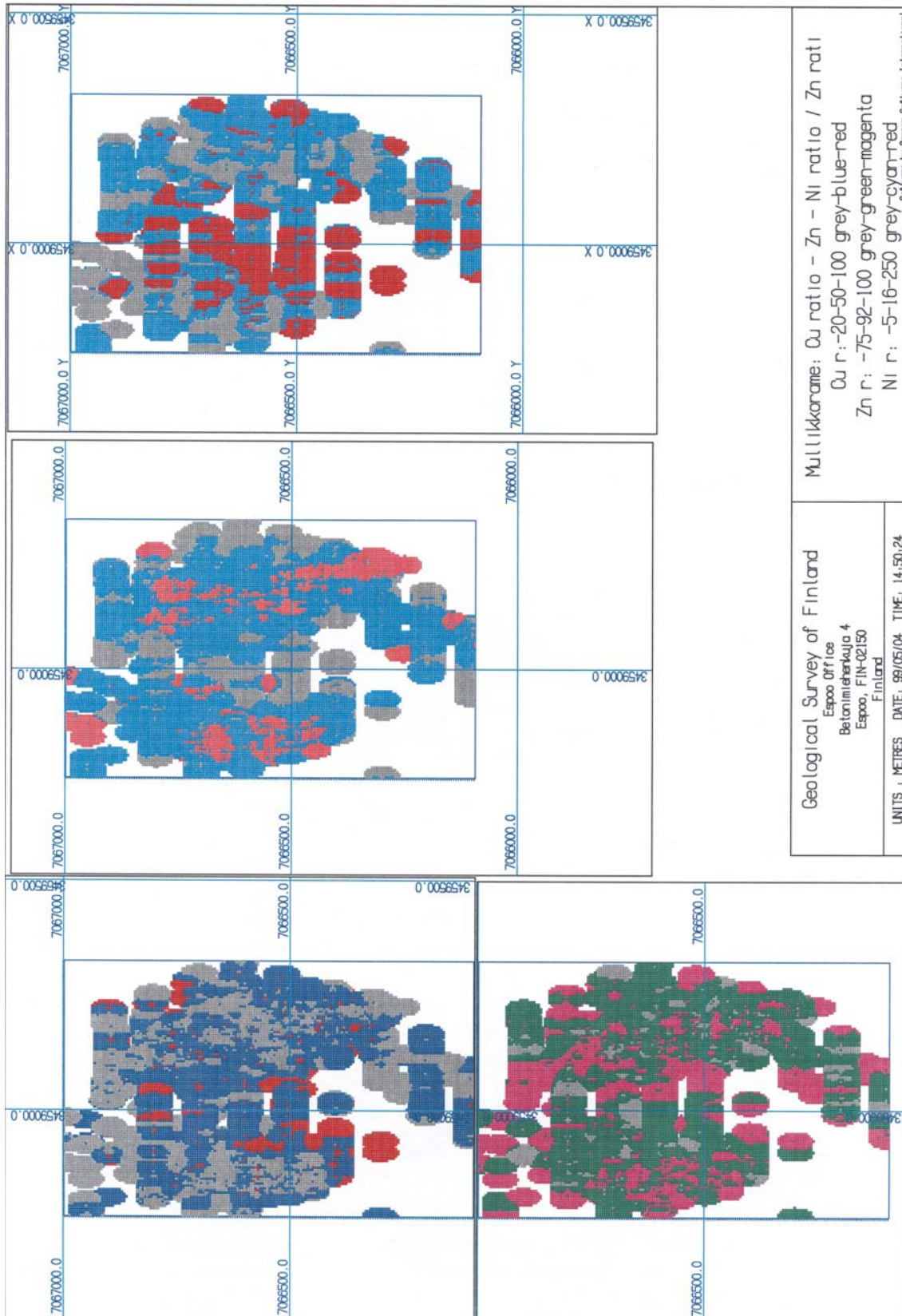
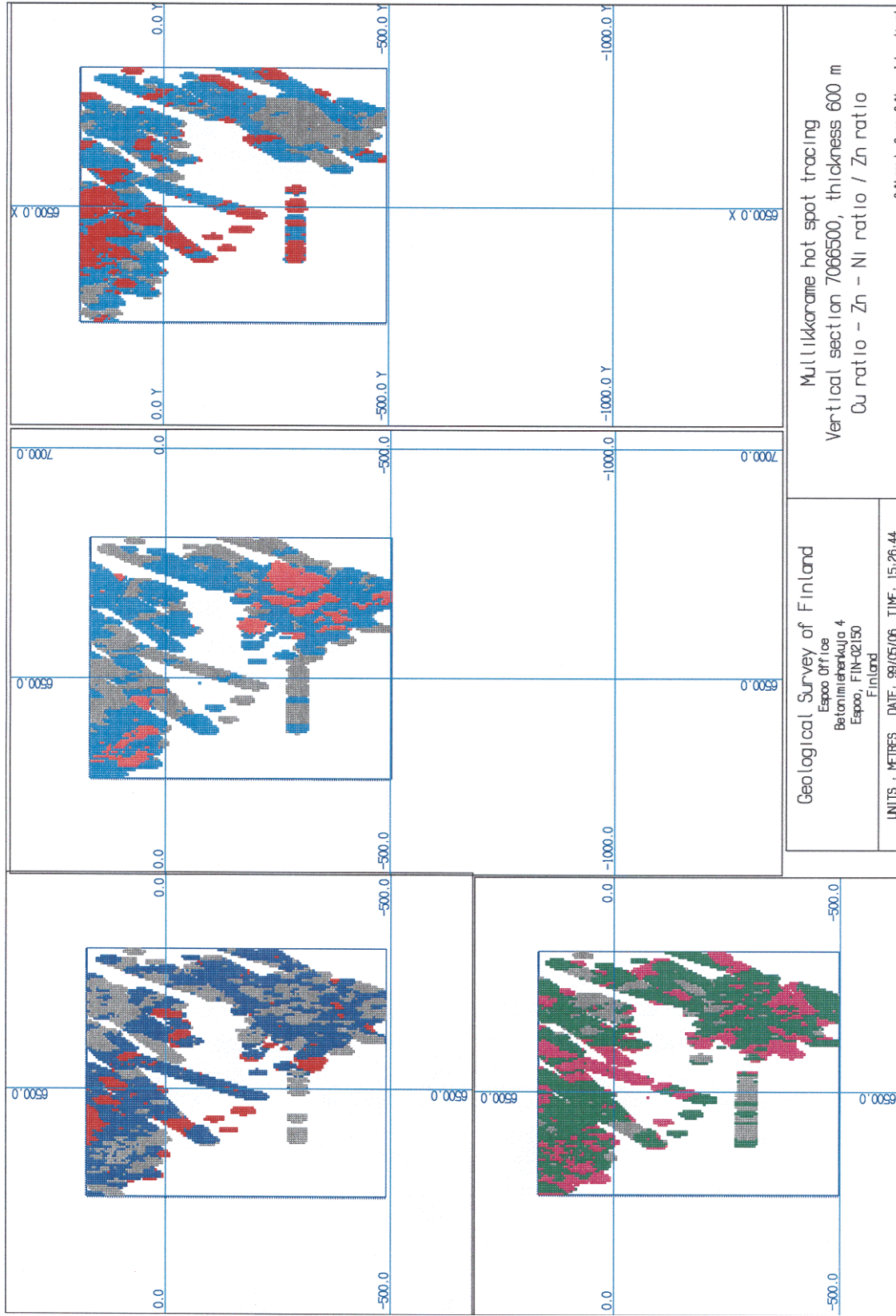


Fig. E4.29A-D



E REFERENCES

- Fukunaga, K., 1990.** Introduction to Statistical Pattern Recognition. Second Edition. Academic Press, Inc.. 1990.
- Gemmel, J.B. and Large, R.R.1992.** Stringer System and Alteration Zones Underlying the Hellyer Volcanic Hosted Massive Sulfide Deposit, Tasmania, Australia. Economic Geology, Vol. 87, 1992, 620-649.
- Gustavsson, N. 1983.** Use of pattern classification methods in till geochemistry. In: ed. R. J. Howarth Handbook of Exploration Geochemistry. Volume 2: Statistics and Data Analysis in Geochemical Prospecting, p. 303-309. Amsterdam: Elsevier.
- Gustavsson, N., Björklund, A. 1976.** Lithological classification of tills by discriminant analysis. Journal of Geochemical Exploration 5 (3), p. 393-395.
- Gustavsson, N.; Kontio, M. 1990.** Statistical classification of regional geochemical samples using local characteristic models and data of the Geochemical Atlas of Finland and from the Nordkalott Project. In: G. Gaál, D. F. Merriam (eds.) Computer applications in resource estimation: prediction and assessment for metals and petroleum, p. 23-41. Oxford: Pergamon Press.
- Howarth, R.J., 1971.** An Empirical Discriminant Method Applied to Sedimentary-Rock Classification from Major-Element Geochemistry. Math. Geol. Vol 3., No. 1, 1971.
- Howarth, R.J., 1973.** FORTRAN IV Programs for Empirical Discriminant Classification of Spatial Data. Geocom Bull., 6: 1-31.
- Huston, D.L. and Large, R.R.1987.** Genetic and Exploration Significance of the Zinc Ratio ($100 \text{ Zn}/(\text{Zn}+\text{Pb})$) in Massive Sulfide Systems. Economic Geology, Vol. 82, 1987, 1521-1539.
- Kaufmann, L. and Rousseuw, P.J. 1990.** Finding Groups in Data: An Introduction to Cluster Analysis, John Wiley & Sons, Inc., New York.
- Sinding-Larsen, R., Strand, G., Berner, H., Nilsson, G., Gustavsson, N. & Tontti, M., 1988.** An Assessment of the Mineral Resource Potential of the Northern Fennoscandia, using Quantitative Data Integration Techniques. Geol. Jb. A 104, pp. 175-186.
- Specht, D.F., 1967.** Generation of polynomial discriminant functions for pattern recognition: IEEE Trans. Electr. Computers, Vol. 16, p. 308-319.
- Specht, D.F., 1990.** Probabilistic neural networks. Neural Networks. Vol 3, 109-118.

SECTION F

EXPLORATION MODEL

Heikki Puustjärvi (ed.)

10.11.2006

Confidential

F EXPLORATION MODEL (H. Puustjärvi)

An effective exploration model combines the critical features and deposit models with geological, geochemical and geophysical criteria that are useful for exploration. Specific models can be developed for particular volcanic belts and deposit types. It is important that exploration models are not too constrained; they need to be flexible enough to cover the range of ore deposit styles that are known or predicted to exist in a specific volcanic province.

Exploration for volcanogenic massive sulphide (VMS) deposits requires a multidisciplinary approach incorporating the best available geological, geochemical and geophysical techniques. In general, a combination of detailed mapping of volcanite domains, alteration recording, rock-chip and drillhole lithogeochemistry, volcanic facies mapping (paleovolcanology) and systematically-used surface and downhole geophysics can be used to successfully locate deposits of the VMS type. Numerous examples of this kind of an approach exist in Canadian and Australian archaean-proterozoic environments, one even within the current project area – at Mullikkoräme.

F 1 PYHÄSALMI EXPLORATION MODEL

Figure F1.1 schematically incorporates the above-mentioned critical features and criteria to be studied in order to formulate a working exploration model. The figure also clearly illustrates that an exploration model is a path of procedures to be tested in a target area that has been estimated to be ore-potential.

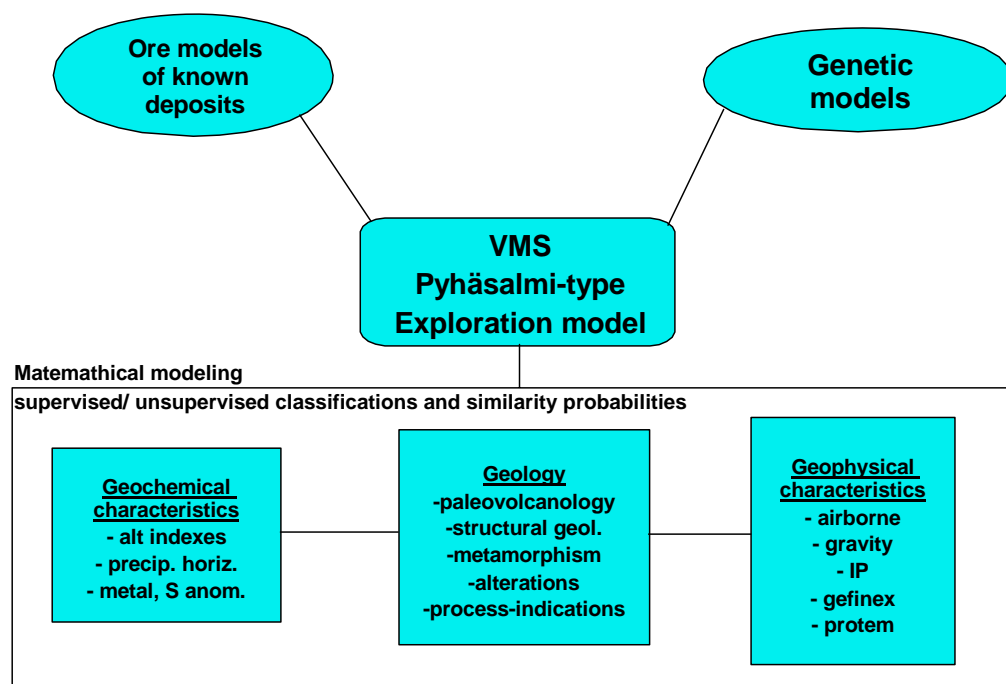


Figure F1. Diagram incorporating general criteria for the exploration of VMS deposits of the Pyhäsalmi type.

Heikki Puustjärvi (ed.)

10.11.2006

Confidential

F 1.1 DEPOSIT ENVIRONMENTS AT PYHÄSALMI AND MULLIKKORÄME

One of the first things in constructing an exploration model is to study known deposits within the area to be explored. The identification of critical, typical and variable characteristics of known ore deposits enables one to construct a genetic model. In this project it was possible to take advantage of the knowledge gathered previously on the Pyhäsalmi and Mullikkoräme ore deposits.

The following list presents characteristics found important for the Pyhäsalmi and Mullikkoräme deposits and their environments.

- Coherent domain of bimodal subaqueous volcanism indicating rifting environment. Felsic quartz-feldspar porphyries and breccias. Mafic pillow lavas and breccias.
- Sodium-rich felsic volcanites of heterogeneous affinity (thol-trans-calcalk) and rift/arc-related origin.
- Intrusive complexes closely connected to the volcanites (composition, timing). Even younger intrusives can be signs of reactivated magma pathways or domed parts of an older magma chamber (Kokkokangas granodiorite).
- VMS-typical alteration (K+Mg enrichment and Na+Ca depletion) halo around the deposits leading to sericite-, cordierite- and antophyllite-bearing metamorphic lithologies.
- Abundant pyrite (with or without pyrrhotite) dissemination within altered rocks.
- Extensive Ba-anomalies within the altered volcanites. Exhalite within ores and on their extensions – i.e. barite and carbonate horizons, sometimes rich in gold at the ore margins.
- Sulphides occurring as massive/semimassive tabular (high to medium aspect ratio) bodies.
- Metal zonation within lenses and occasionally richness in magnetite.
- Ore lens clusters can be highly variable in base metals content and closely connected to totally barren massive pyrite.
- Dikes rich in Au-Cu-Pb and Au anomalies around the ore (Pyhäsalmi).

F 1.2 GENETIC MODEL

The construction of a genetic model according to factors presented above is still fairly conceptual because there are not enough studies concerning ore fluid source rocks, ore fluid transport systems or trapping mechanisms. However, during this project it became obvious that one of the most important factors, which control ore location could be the intrusion of hot rift related rhyolites (Fig. F2, also see C2.2.3 and this section later). The problem of metals source region was briefly looked at by modeling approximately the volumes of source rock regions. This was done by calculating the volumes of ore fluid needed to form the Pyhäsalmi and Mullikkoräme deposits and assuming that all of the metals were leached from the least-altered type of felsic volcanite (see CD-ROM's spreadsheet files okpHVsource.xls and okmuHVsource.xls).

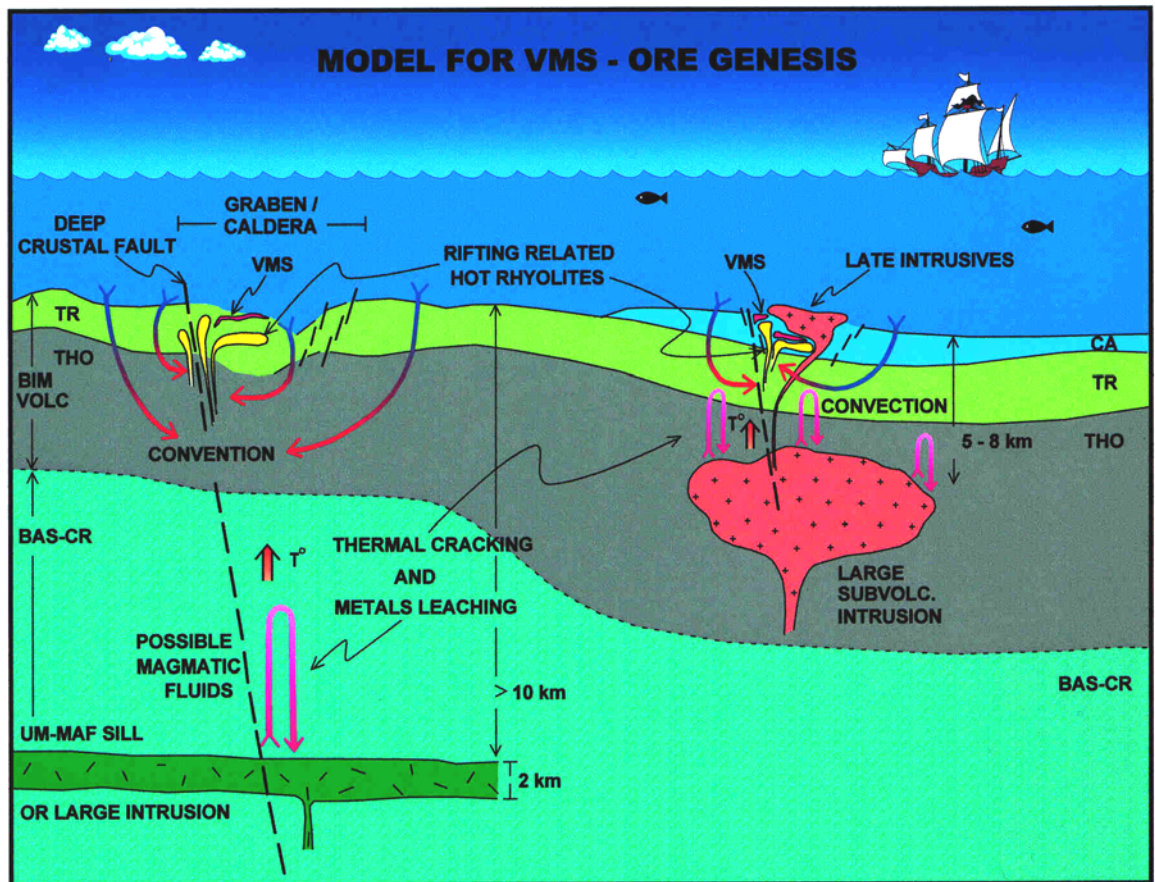


Figure F2. A schematic genetic model for VMS deposits (including Pyhäsalmi) enhancing the role of hot rhyolite injections that control the location of ore deposit.

The calculation was based on the assumption that 50% of the source rock metals content (totalling 100 ppm Cu+Zn+Pb) was leached and redeposited at a 90% level. Then the source rock volume for the 62-Mt Pyhäsalmi deposit would be 17.8 km³ and 1.2 km³ would be needed for the total 2 Mt of ore in the Mullikkoräme deposit and mineralizations. Also the volumes of convective heat-driving subvolcanic intrusives were estimated at two different temperatures (700°C and 1300°C) resulting in intrusion sizes between 79.4 and 3.3 km³. Although the calculation is rough, it is surprising to notice how small volumes of rock rather low in base metals content are needed to produce ore deposits of decent size provided that the leaching-convecting-precipitating process is present.

F 1.3 GEOLOGICAL CHARACTERISTICS

In VMS exploration it is important to look for characteristics that indicate the presence of synvolcanic ore-forming hydrothermal processes. Paleovolcanological features such as mafic pillow lavas, coherent felsic quartz–(feldspar)-phyric lavas, breccias and other permeable units (pumiceous layers) and coarse volcanic conglomerates are important features in bimodal volcanic complex. They, together with felsic cryptodomes, indicate subaqueous environment and unstable tectonic conditions where heat flow affected volcanic sequences.

Heikki Puustjärvi (ed.)

10.11.2006

Confidential

The understanding of structural geology in connection with geophysical images is crucial in connecting few surface observations into continuous or discontinuous geological trends to be followed as exploration proceeds. The mapping of synvolcanic faults, which act as fluid pathways in VMS genesis, is difficult in polydeformed paleoproterozoic environments. All mappable faults are important because they might be regenerated fossil synvolcanic faults. Major geological discontinuities may be helpful in this kind of interpretation.

Altered lithologies are the most important indications of hydration and element enrichment/depletion processes. Fault-related alteration and the effects of metamorphism cause complexities into this and have to be solved by detailed geological observations (mapping, thin sections, metamorphic studies etc.) and lithogeochemistry. Unmetamorphosed and low-grade metamorphic assemblages can differ from alteration mineralogies affected e.g. by amphibolite facies metamorphism, and it is not always possible to tell the protolith without lithogeochemistry. The following list is an example from T.J.Barret & W.H.McLean (1994),

<u>Alteration assemblage</u>		<u>Amphibolite facies</u>
Mg-chlorite+qtz	>>>	cordierite+anthophyllite
Fe>Mg-chlorite+qtz	>>>	staurolite in the paragen.
Fe-chlorite+qtz	>>>	almandine in the paragen.
Sericite>Mg-chlor.+qtz	>>>	biotite+sillimanite
Sericite<Mg-chlor.+qtz	>>>	biotite+cordierite+anthophyllite
Sericite<Fe-chlor.+qtz	>>>	biotite (staur.-gedr.-almand.)

F 1.4 LITHOGEOCHEMICAL CHARACTERISTICS

Deposits of the VMS type usually lodge within altered rocks. In VMS exploration an important task is to look for lithogeochemical base metals and sulphur anomalies. Important features also include the existence of exhalite horizons (baryte, carbonates, Fe/Mn-horizons), distal/proximal polarity indications and even negative base metals anomalies in unaltered rocks (source regions). It is important to categorize volcanites (affinity, arc/rift relation, hot rhyolites) to see if the necessary heterogeneity is present. All this has to be done by careful sampling and proper analysing (preferably ICP-MS and XRF) of samples from outcrops and first-phase drillholes to be able to carry out lithogeochemical classification and modeling. Lithogeochemical assays are easy to manipulate into necessary indices (see section C.2.2.3) that make above-mentioned comparisons possible.

F 1.4.1 Hot rhyolites

An idea for the importance of “hot rhyolites” in VMS exploration originates from studies in the Flin Flon and Kidd Creek areas, Canada (E.C.Syme, 1998 and C.T.Barrie, 1995). Syme (op. Cit.) found out that high Zr/TiO₂ ratios (>0.13) in rhyolites best indicate the rifting episode and related high heat flow pathways.

Heikki Puustjärvi (ed.)

10.11.2006

Confidential

Barrie (op. cit.) noticed that high-silica, high-temperature rhyolites are commonly found near Cu-Zn deposits of the VMS type in the Archean Abitibi subprovince.

Similar features do occur in the Pyhäsalmi and Mulliköräme areas. There are at least three populations of felsic volcanites as shown in Zr/TiO₂ scatter plots (ref. C2). One of the populations clearly represents high Zr/TiO₂ ratio rift-related felsic volcanites. This population includes both unaltered and altered samples and is more abundant at Pyhäsalmi than at Mulliköräme. Most of the hot rhyolite samples are located close to the ore deposits. One could even conclude that the more hot rhyolites are present the bigger is the mineralization.

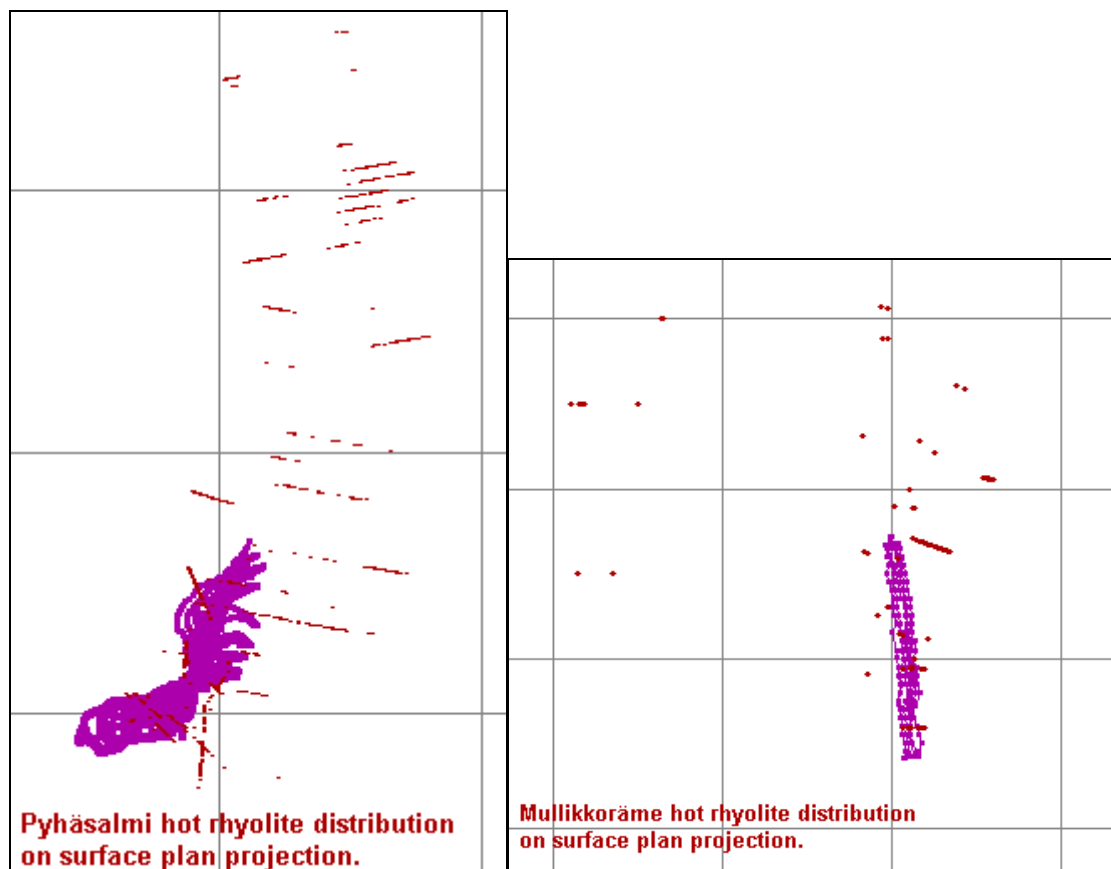


Figure F3. Locations of hot rhyolites on surface plan projections at Pyhäsalmi and Mulliköräme. Grid size the left is 1 km and 200 m on the right. Magenta-coloured lines indicate Pyhäsalmi and Siperia (Mulliköräme deep ore) ore outlines on different levels. Red dots indicate hot rhyolite sample sites.

F 1.5 GEOPHYSICAL CHARACTERISTICS

VMS deposits are in rather simple geophysical targets being massive/semimassive sulphide bodies. Usually they are conductive and occasionally contain strongly magnetized parts, and usually they are located within a sulphide-disseminated alteration halo. Consequently a range of ground and borehole geophysics should work in the exploration of VMS deposits. The Pyhäsalmi and Mulliköräme deposits are detectable by gravity, electric and electromagnetic methods (see Section D).

Heikki Puustjärvi (ed.)

10.11.2006

Confidential

The following list is presented as a general geophysical path for the exploration of VMS deposits of the Pyhäsalmi type.

- Airborne data image processing to evaluate geological formations and to detect potential features (discontinuities, blocks, thickness variations in strata, faults). Interesting features should be interpreted/modeled from the original data.
- Magnetic, IP (with several n values for better penetration) and gravity line surveys to look for alteration halos (pyrite/pyrrhotite dissemination) and possible subsurface ore bodies (dense massive deposits).
- Systematic outcrop sample petrophysics.
- Drillhole in-situ logging (res-susc-dens) and downhole Protem surveys. Possibly 3d-magnetometry if geological features so require.
- Gefinex EM line surveys should be used after the positive indications of alteration zone and some 3d knowledge of geology.

F 1.6 GEOMATHEMATICS

Geomathematics was brought into this project in order to check the validity of rock classification and to see if there are important yet unobserved correlations in the analytical data.

The results reported in E3 indicate that rock classification was generally good and that the tested XRF database did not contain surprises. Now that we have a fair knowledge of lithogeochemical characteristics for the Pyhäsalmi and Mullikkoräme areas, it is possible to test sample sets from other bimodal volcanite domains by supervised and unsupervised classification methods for their exploration potentiality.

An test to analyse the material was done by calculating the distance of each sample to the nearest ore sample (see E2). Zinc and barium distribution graphs were then graphically presented against the distance values in unaltered and altered felsic volcanite samples separately for Pyhäsalmi and Mullikkoräme. Element halo distances were clearly showed.

Approach of this sort can indicate new correlation but one has to be aware of the material features. This is clearly a methodology that should be tested in greater detail than was done in this project.

F CONCLUSIONS AND RECOMMENDATIONS

Certain geological factors control ore-forming processes, consequently they must be taken into consideration in exploration for VMS deposits of the Pyhäsalmi type.

Heikki Puustjärvi (ed.)

10.11.2006

Confidential

Such important factors include high heat flow regime, fluid transport system, and metal trap horizons.

High heat flow regime – Subaqueous bimodal volcanism is a large-scale indicator for tensional crustal processes, often related to early continental margin back arc rifting. Thick tholeiitic low-K pillow lava, and coherent quartz(-feldspar)-phyric flows and related autobreccias/hyaloclastites (“high-level cryptodomes” and high Zr/TiO₂-ratio “hot rhyolites”), point to focused high-temperature “spots” within bimodal sequences. Such features are commonly associated with widespread spilitic background alteration resulting in high Na contents in felsic volcanites. Quartz-epidote alteration in mafic volcanites indicates high heat flow and hydrothermal activity of low water/rock ratio, features related to volcanic centers (Santaguida, F. et al., 1998).

Fluid transport system – Second-stage alteration in “splitized” volcanites is a major indicator for hydrothermal processes. Depletion in Na and Ca, and enrichment in K and Mg, delineate fluid convection (recharge-discharge) domains that are most potential for ore-forming processes. Epidote-alteration in felsic volcanites delineates venting areas with high fluid flow within deep alteration zones (Santaguida, F. op. cit.). Vectors that point to locations potential of ore precipitation can be evaluated within alteration zones by studying alteration intensities as well as barium, base metals and sulphur anomaly gradients.

Metal trap horizons – Direct indications for ore-potential horizons are recognized as baryte-carbonate-bearing layers that have high base metals, sulphur and gold contents, and high Fe/Mn ratio, and are related to strong Mg-K-alteration (talc-bearing associations). Stratigraphic and proximity/distality features within ore-potential trap areas can be evaluated from spatial variations in the following associations: baryte-gold-pyrite (precipitation top), pyrite-chert (proximal top), pyrite-gold (distal), and copper-gold (stringer zone).

The above-mentioned features are important factors in modelling regional and deposit-scale exploration for VMS deposits of the Pyhäsalmi type. The said features are common to VMS deposits worldwide. Consequently it is recommended that, along with the planning and execution of exploration activities in Finland and elsewhere, ore-potential bimodal volcanic domains are classified according to the criteria developed in the Pyhäsalmi Modeling Project. However, one should bear in mind that all models require testing as well as further development and refinement.

F REFERENCES

Sanatguida, F. et. al., 1998. Semi-conformable epidote-quartz hydrothermal alteration in the Central Noranda Complex, Canada: Relationship to volcanic activity and VMS mineralization. In: Camiro Project 94E07 third annual report, September 1998, pp.139-179. CAMIRO-Exploration Division, Canadian Mining Industry Research Organization.

SECTION G
TEST DRILLING

Heikki Puustjärvi (ed.)

10.11.2006

Confidential

G TEST DRILLING (H. Puustjärvi)

The test drilling phase originally had two main objectives. The first one was to test targets generated during the project thus obtaining indications for new ore deposits – to make a discovery hole. The second one was to launch into Finland a previously untested directional drilling method.

Test drilling was included in OM's part of the joint project from planning through execution to reporting. The original budget included 2000 m of normal test drilling and 1000 m of directional drilling as well as all necessary geophysical drillhole surveys.

The test drilling phase was planned to start at the beginning of November 1998 and to last for five months.

G 1 DRILLING CAMPAIGN

Suomen Malmi Oy (SMOY) was chosen to contract the test drilling. The directional drilling phase was subcontracted by SMOY to Liwinstone AB (LIW) from Sweden. LIW provided the necessary equipment and consultants to instruct working procedures but SMOY was the operator. The LIW method was chosen, as it was previously untested in Finland and their offer was cheaper than that of competitors. LIW also presented good references from Sweden (Zinkgruvan) and was close enough for fast support.

The drilling campaign started on November 9, 1998, with one drilling rig and ended on March 21, 1999. Most of the time there were two rigs (Diamec 1000 and Diamec 700/ Diamec 264) in operation. During the said period, five test holes were drilled. One of them was wedged and directionally drilled. Normal test drilling totalled 2794.65 metres. Additional 211.8 metres were directionally drilled with the Liw-In-Stone method. Prior to the main campaign, in June 1998, one short hole was drilled and an old one continued; they total 468.2 m (Table G1, Fig. G1).

Table G1. Header data for the test drill holes.

Hole-id	Y(nat)	X(nat)	Z(nat)	length	azimuth	dip
PYS107cnt	3453172.1	7061764.3	-182.53	210.60	99.4	-54.7
PYS116	3452968	7061698	153	257.60	10	-80
PYS117	3451434	7062197	141	526.10	102	-70.3
PYS118	3453443	7061435	148.5	825.85	232.4	-80.8
PYS119	3453765	7063680	154.5	745.90	300	-65
PYS119a	3453610.3	7063778.8	-202.95	211.80	306.7	-56.1
MU152	3458825	7066100	182	696.80	90	-65.5

The cost of the two-phase drilling campaign totalled approximately 2220 TFIM. Costs per metre were 600 FIM for conventional and 1215 FIM for directional drilling. Included are all costs except drillhole in situ logging and Protem soundings.

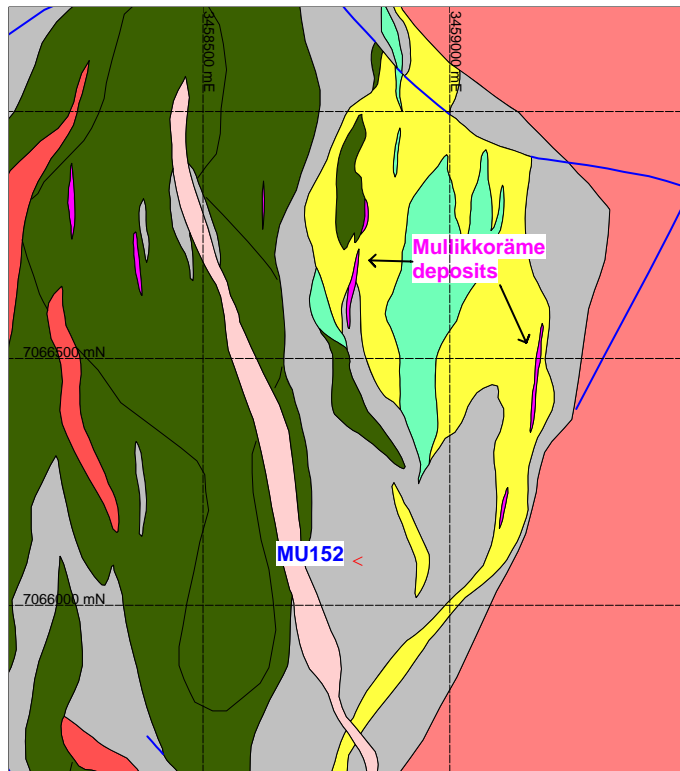
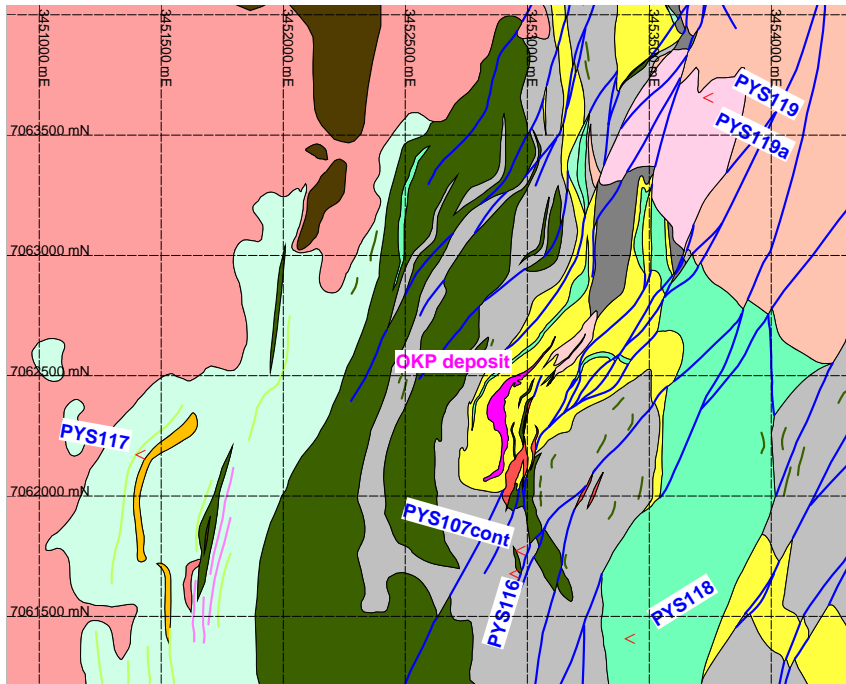


Figure G1. The location of the test drillholes shown on geological maps for the Pyhäsalmi and Mullikkoräme areas.

Heikki Puustjärvi (ed.)

10.11.2006

Confidential

G 2 TEST DRILLHOLES

G 2.1 PYS-107 CONTINUATION

PYS-107 was an old hole drilled to the depth of 382 m. The continuation of the hole became necessary because the upper edge of the deep-seated Gefinex-400S EM anomaly at Lehto extended close to the end of this hole.

The hole was first tested by downhole 3-component (xyz) Protem survey to see if there would be indications for ore near the deep anomaly. The result was negative. Then the hole was continued to 592.60 m where it was stopped in a thick pegmatite dike. At the downhole-depth of c. 465 m the hole intersected a brecciated, slightly quartz-phyric rhyolite with some pyrite dissemination occurring as stripes and fracture fillings in weak stringer-type sericite alteration. Later analyses showed a weak Ba anomaly in this section. Protem surveys did not respond to possible near-hole conductors. Hole deviation measurements showed later that the true distance (c. 150 m) to the interpreted deep anomaly at Lehto was too long for any response, especially when the resistivity values in the said anomaly were low at just less than 100 ohmm.

The felsic volcanite intersected at 465 m, anomalous in pyrite, Ba and sericite, remains an unsolved indicator for possible ore. Investigations in that area may be warranted in future.

G 2.2 PYS-116

PYS-116 was collared 100 m south of PYS-107 and directed to NNE. The purpose was to test a 150-m long Gefinex-EM anomaly interpreted to exist in an antiform structure on an E-W-striking section $x=14850$, 150-250 m below surface.

The hole was drilled to 257.6 metres. It intersected mainly mafic volcanites with some felsic and skarned layers. Sulphides were scarce. Sections in the hole had abundant fractures with weak pyrite dissemination.

Protem-EM downhole logging did not show signs for missed conductors. Reinterpretation of the original Gefinex-EM anomaly indicated the possibility of a pseudoanomaly caused by the measurement configuration combined with infrastructure disturbances (powerlines, vicinity of mine).

G 2.3 PYS-117

PYS-117 was collared 1.5 km west of the Pyhäsalmi mine, close to the Lake Pyhäjärvi shoreline. The hole was planned to test a Gefinex-EM and a gravity anomaly within the Pellonpää member (felsic tuffites and skarn with graphite- and pyrrhotite-bearing layers). The interpreted conductor on line $X=15000$ (Pyhäsalmi mine area geophysical co-ordinate system) forms a 300 m long, E-W trending and 30° west dipping layer. Its thickness was not possible to interpret. The anomaly lies

Heikki Puustjärvi (ed.)

10.11.2006

Confidential

250-425 m below surface correlating with a remarkable “gravity bench” on a local gradient.

The hole, 526.1 m deep, intersected a thick sequence of Pellonpää-member skarns and amphibolites, and possibly thin interlayers of the Lippikylä member and/or Lepikko lithodeme. The sequence was underlain by a unit of qtz-fsp-(bt)-gneisses and graphitic schists of unknown stratigraphic position (possibly basal formation(s) for the Pyhäsalmi volcanic complex).

The Gefinex-EM anomaly was caused by the combination of a heavily pyrrhotite-disseminated layer, 4.2 m thick, and underlying, minimum 70-m thick sequence of graphitic schists. The “gravity bench” was due to the skarn rocks.

The pyrrhotite-rich layer was analysed and graded 0.11% Zn. Enclosing felsic-intermediate gneisses were slightly chlorite-sericite-altered but did not indicate mineralisation of the Pyhäsalmi type in the area.

G 2.4 PYS-118

PYS-118 was collared in the Lippikylä area 900 m SE of the Pyhäsalmi mine. This hole was targeted to a deep Gefinex-EM anomaly 500-900 m below surface. The anomaly was first interpreted according to Gefinex results on line X=14850 (800 m T-R separation). Because of the widespread and heterogeneous nature of the anomaly it was reinterpreted on the basis of new Gefinex results (800 m T-R separation) on lines Y=40600-41200 (200 m spacing, geophysical mine area coordinates) and on lines A=20400-20800 (200 m spacing, a local geophysical coordinate system). All of the interpretations were modeled. The drilling target was selected to test an area, which overlapped best-overlapping in different interpretations, c. 700 m below surface.

The purpose was to test if this anomaly was caused by Pyhäsalmi-analogous altered and mineralized felsic volcanite sequence along an initial “depression corridor” on a NW-SE trend and passing through the mine area.

This 825.85-m deep hole intersected surprisingly deep-sited (550 m in vertical depth) altered mafic volcanites in the western contact zone of the Lehto lithodeme. In depth followed weakly altered felsic volcanites and a fairly thick sequence of mafic volcanites/dikes of the Lepikko lithodeme. Next, alternating felsic volcanite layers were intersected; they probably represent the unaltered volcanites of the Lippikylä member.

At the targeted depth interval, explanation for the wide Gefinex-EM anomaly was not gained, nor were mineralised lithologies of the Pyhäsalmi type encountered. A possible, at least partial, reason for the anomaly was fractures with iron sulphide dissemination.

The hole was later probed twice with Protem downhole-EM using different frequencies. It was surveyed with 3d-magnetometry and in-situ logged for

Heikki Puustjärvi (ed.)

10.11.2006

Confidential

susceptibility and resistivity. The only piece of information given by these measurements was a very weak but interpretable conductor, still hiding in front and furthers NW of the hole. An additional explanation for the original widespread nature of the anomaly is that all fractures within the locally intensive D4-shear zone contain sulphide dissemination and are filled with salt water (brine); such conductors could explain the recorded Gefinex-EM results. Russian geophysicists who consulted in the Pyhäsalmi-Mullikkoräme area lately on a semiregional CP-survey, reported similar findings.

The results of the drilling remain problematically open and warrant further investigations.

G 2.5 PYS-119

PYS-119 was collared 1.5 km NE of the Pyhäsalmi mine just north of the Ruotanen mine village. The drilling direction was perpendicular to the SE contact zone of the Kettuperä alteration domain. The test target was a combination of a lithogeochemical base metal anomaly, old geophysical indications on a Gefinex-EM line A=4200 (a local geophysical grid) and a previously untested downhole EM anomaly (PYS-96 and PYS-97, on section line K=11000, another local diagonal grid system).

The hole is located c. 100 m SW of holes PYS-96 and PYS-97 drilled previously. It was targeted into the NE hinge zone of a SW-plunging conductor (Gefinex interpretation on the line A=4200) coinciding at 350-m level with the trend of a strong base metal anomaly at an alteration zone contact.

The 745.9-m deep hole intersected a 350-m thick alteration zone with consistent pyrite dissemination. At the contact of the alteration zone there was a 13 m long intersection (360-373 m in downhole depth) of heavily pyritized, sphalerite-bearing sericite-cordierite-altered felsic volcanites which included a 3-m interval of 2% Zn. As drilling continued through the alteration zone, another mineralized and weakly chalcopyrite-bearing horizon was intersected at 610-620 m.

Downhole Protem-EM logging showed that the upper mineralized layer was intersected at the reachable range of the Protem method and that the method just sniffed the deeper anomaly at its southwestern corner.

The Zn-anomalous layer should be further drilled along plunge and depth in order to locate economical units within the base metal-potential alteration contact zone.

G 2.6 PYS-119a

Heikki Puustjärvi (ed.)

10.11.2006

Confidential

Since the results in PYS-119 were not satisfactory, a wedged and directed hole was decided to be drilled, with PYS-119 as “mother hole”, towards a more interesting sector of the inferred conductor.

The off-hole wedging was started at 400 m hole depth and steering at 415 m. It was planned to steer the hole c. 50 m up and 75 m to the right of the original PYS-119 conductor intersection.

Steering was done for 211.8 metres. The new intersection was obtained c. 75 m up from the original one but only 5 m to the right. The hole intersected mineralisation analogous to the previous one but richer in pyrrhotite, which feature explained the increase in conductivity.

As a whole, the steered drilling was a failure. The course of action taken during that exercise is explained in paragraph G2.7.

G 2.7 MU-152

Mu-152 was collared 400 m SE of the Mullikkoräme mine portal. The target was Gefinex-EM anomaly on Mullikkoräme deep ore (Siperia) trend c. 200 m south of the known ore at 550m level. It was known that the ore-potential zone (Reijusneva lithodeme) is located within the Riitavuori felsic volcanites that form a narrow synform between the Korvenkallio granite and mafic volcanites of the Tetrinmäki member, features interpreted from the Gefinex-EM section results (X=66100, E-W line in the national grid system).

The hole was drilled to 696.8 m. It intersected the contact zone between the Tetrinmäki member mafic and Riitavuori member felsic volcanites. At the target level, before entering into the ore-potential altered Reijusneva felsic volcanites, the hole intersected 10 m (at 627-637 m downhole depth) of heavy pyrrhotite-pyrite-magnetite dissemination within an altered mafic volcanite contact. The iron sulphides did not contain economical quantities of base metals. Thereafter the hole intersected a cutting intermediate dike and a possible fault before reaching felsic volcanites without ore-potential alteration.

Subsequent downhole Protem-EM logging and its interpretation indicated a weak conductor that was not reached. It is upwards and in front of the hole's toe. A geological interpretation for the situation is that the dikes and coinciding fault had displaced the potential zone up and eastwards out of the reach of the drilled hole. Gefinex reinterpretation of the section showed a weak response further to the east, previously interpreted to be insignificant.

It is concluded that the southern continuation of the Mullikkoräme deep trend (Siperia) is still open and should be drilled for new orebodies. The first trial could be a hole wedged from Mu-152.

G 2.8 DIRECTIONAL DRILLING

As previously mentioned, SMOY subcontracted the directional drilling to LIW, a Swedish company.

Mr. Lars Liw developed the drilling method used. Figure G2. displays the main components of the Liw-In-Stone deviation equipment.

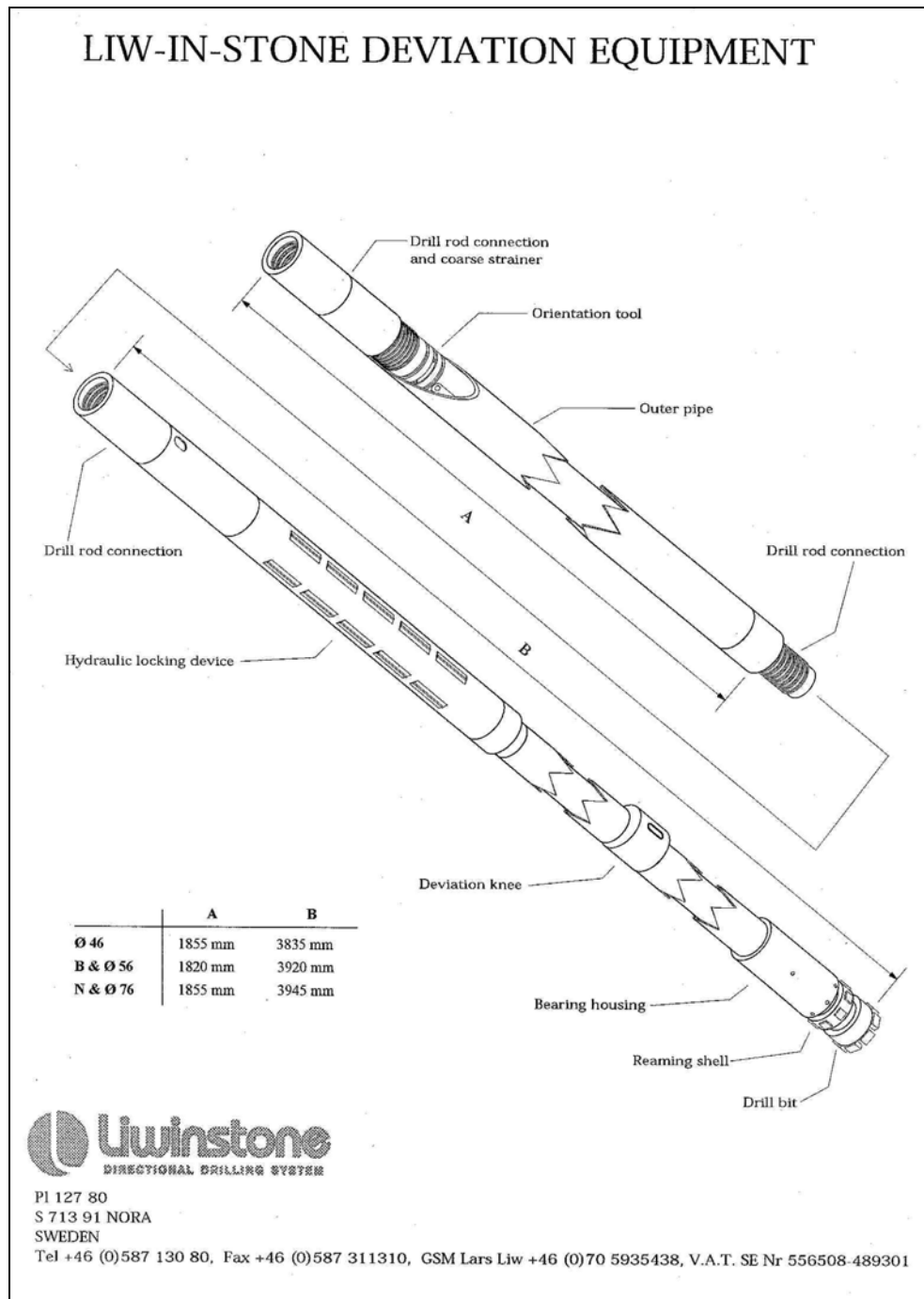


Figure G2. Liw-In-Stone deviation drilling equipment. Advantages of the Liw-In-Stone system include that drilling can be steered continuously and a continuous core sample is recovered along the deviated section. Core diameter for the 56-mm diameter equipment used is 28 mm. It is also claimed

Heikki Puustjärvi (ed.)

10.11.2006

Confidential

to be cheaper to operate than Navidrill, the world market leader. The basic construction idea is that the Liw-In-Stone deviation equipment is hydraulically pressed against drillhole wall and sledged down along the deepening hole without rotation. Only the drill bit and the reaming shell are rotating with the inner 3-m-long core barrel. The locking takes place with a hydraulic locking device. An orientation tool and a deviation knee control the steering (see Fig.G2).

G 2.8.1 Steering test in hole PYS-119a

A branched hole from the mother hole PYS-119 was started from 400 m downhole depth. The target was described above at G 2.5.

Work started on March 12, 1998, with cementing, plugging and steel wedge mounting. The wedge was planned in a position which would “shoot” the new daughter hole into the right direction from start. The wedge face should have been at 325° (geographical azimuth). As known from many previous wedge mounting trials in other drilling campaigns, failure was possible and that’s what happened. The final wedge face azimuth remained at its original direction and did not deviate the planned 20°. However, the problem was not serious, and it was planned to be corrected by the deviation instrument properties during directional drilling.

Table G2. summarises the drilling phase results showing actual downhole depths for drilling methods, azimuth and dip variations, drilled lengths and cumulative up/right deviations reached from the start position.

Table G2. Directional drilling summary.

Depth	Azimuth(degr.)	Dip(down degr.)	To right(m)	Up(m)	Notes	Length(m)
399.7	306.26	-57.52	0.2	0.91	wedge top	
401.7	306.75	-55.74	0.23	1.12	wedge toe	2
414.6	307.14	-54.54	0.41	2.37	dir.drilling start	12.9
497.65	302.97	-34.14	4.36	24.33	norm.drilling start	83.05
550.5	304.89	-30.61	3.05	49.32	dir.drilling start	52.85
576.3	308.17	-32.86	4.05	62.16	norm.drilling start	25.85
611.5	307.24	-32.17	5.2	78	end of hole	35.15
						211.8

At the start of the steered drilling campaign LIW’s representative instructed SMOY crew into the methodology and equipment handling. The Liw-In-Stone system is easy to understand and the basics are fast learned.

As shown in table G2, drilling started with reaming and traditional drilling. The purpose was to pass the wedge sufficiently to start directional drilling at 414.6 m. First, directional drilling was done for 83.05 m. The interval down to 474 m (59.4 m of directional drilling) resulted in 0.25 ° /m (0.18 ° up and 0.07° to the right) deviation, values less than expected (0.3 ° /m).

Already at the start of the directional drilling there were problems in getting a proper signal for the deviation tool locking via the crucial water pressure readings.

Heikki Puustjärvi (ed.)

10.11.2006

Confidential

Equipment malfunction was later understood to be caused by high natural water pressure downhole.

After the Swedish consultant left, problems started with water pressure and valves, and there was a serious drawback especially with azimuth deviation to the right. Consequently it was decided to drill traditionally for c. 50 m with high torque pressures in order to trend the hole back to the right track.

This trial helped a little and the directional drilling was resumed under the supervision of Mr. Lars Liw himself. He made mechanical adjustments into the deviation equipment (turbulent airbubble release in holes) to overcome the problems in downhole water pressure. Directional drilling was restarted at 550.5 m. This second phase was drilled for 25.85 m to the depth of 576.35 m. The first 13.5 m (550.5-564 m) were the only moments during the whole campaign when most things went right. Then deviation even exceeded the supposed 0.34° /m. Dip remained stable, as planned, and all of the deviation was to the right.

After Mr. Liw left the problems at drilling site started again. Equipment gaskets failed and sludge influx made the pressure release holes stuck. SMOY crew could not meet the situation, consequently the last 12.35 m of the second directional drilling phase did not return the same kind of positive results as previously. At this point the target depth was already so close that the hole was finished with traditional drilling. The hole ended at the depth of 611.5 m on April 21, 1999, 40 days after start.

G 2.8.2 Conclusions on directional drilling

As a whole, the directional drilling failed mainly due to mechanical problems in equipment. High downhole natural water pressure caused uncertainties in the hydraulic locking device that anchors against drillhole wall. High tool water pressures used resulted in disruptions in the mechanics of valves and gaskets, which then led to serious sludge influx into the deviation tool. Experience is needed to understand and correct the causes of equipment malfunction.

The Liw-In-Stone system is rather rock-sensitive. It is possible that the drillhole wall in fairly soft altered rocks did not support enough the pushing effect of the deviation knee to get a maximum bending of the deviation equipment. Fractures, and broken rock in general, cause hydraulic locking device (the sledge) rotation which should not happen at all.

Winter conditions are not favourable for the said system because of the easy freezing of the sensitive water pressure-operated valve systems. Probably this is the reason for good experiences and references obtained by the Liw-In-Stone method under non-freezing mine conditions.

The duration of 40 days for a campaign resulting in 211.8 m drilling was too long. This was mainly caused by many equipment malfunction periods, instruction sessions, Maxibor deviation measurements performed at 10 m intervals, and off-

Heikki Puustjärvi (ed.)

10.11.2006

Confidential

duty days. The per-metre costs of the deviation drilling campaign were 1215 FIM including all site costs, equipment rent, consultants and deviation measurements.

As its best (total 13.5 m in this drilling), the Liw-In-Stone method seems to perform well, drilling rate is quite fast (6 m/8-hour shift) and core (28 mm in diameter) recovery is 100%. It appears to be effective to carry out separately dip- and azimuth-related steering and not to try and do them coeval.

The results of this test drilling indicate that the Liw-In-Stone method and equipment have not yet been enough tested under variable conditions. There is place for additional developed before the method can be brought into routine use in exploration drilling.

APPENDIX 1

Heikki Puustjärvi

17.06.1997

Confidential

PYHÄSALMI MODELING

TEKSTIEN KIRJOITUSVASTUUT
(lisätty 21.12.98)

PROJEKTIAIKATAULU

A. Tiedon keruu ja käsittely

(Puustjärvi)

- A1. Projektin aloituskokouksessa päätettiin olla luomatta varsinaista omaa tietokantaa, koska iso osa tiedoista on jo OMEXia palvelevassa TIKUn Ingress tietokannassa. Poikkeuksen muodostaa tietysti OKPn kairausmateriaali, joka on kaivoksen omassa Minenet kannassa. Tiedonsiirtorutiinit TIKUn ja OKPn välillä ovat olemassa ja aineistojen siirto tutkijoiden käyttämiin ohjelmiin onnistuu (ArcView, PC-XPLOR, Geosoft, Systat, AutoCad, G-Pick). Alkuvaiheessa on suurin työmäärä aineiston käyttökelpoisuuden määrittelyssä ja kivilajinimistön yksinkertaistamisessa. Tiedon siirrosta eri tutkijoille vastaa H.Puustjärvi (TIKU/J.Parviainen ja OMEX/E.Sotka) yhdessä osa-alueiden vastaavien kanssa. Käyttökelpoisuuden arvioinnin tekee kukin osa-alueen tutkija. Kivilajinimistön yksinkertaistamisen tekee H.Puustjärvi. Tämä työ on valmiina -97 elokuun loppuun mennessä.
- A2. Vanhojen kairareikien uudelleenraportointia tehdään tarkoin valituilta profiileilta ja kohteista, jotka parhaiten palvelevat rakennegeologista, geofysikaalista ja litogeokemiallista tulkintaa. Lisänäytteiden määräksi on arvioitu n.3000kpl (XRF). Näytteenotto tehdään ns. litonäytteenottona (kivilajikontaktien rajaamista yksiköistä 10cm/m max. 5m komposiitteina). Tämän lisäksi tarvitaan joitakin kymmeniä erikoisanalyysijä (ICP) litogeokemiallisia ja paleovulkanologisia tulkintoja varten. Vanhojen reikien raportoinnin tekee H.Puustjärvi syyskuun loppuun mennessä. Lisänäytteenotoksi luetaan myös Pyhäsalmen kaivoksesta tehtävä lisäkairaus (yht.n. 1300m tasoilta +400 ja +810-850). Tämä on välttämätöntä näyteverkon saattamiseksi edes välttäväksi malmin syvemmistä osista. Kairaus on valmiina syyskuun loppuun mennessä.
- A3. Kohdan A2 tuottaman näyteaineiston analysoinnista vastaa GTKn laboratorio ja yhdyshenkilönä toimii K.Rasilainen. Analysoinnin tulisi olla valmiina -98 tammikuun lopussa. Vanhan analyysiaineiston kelpoisuuden testausta varten on analysoitavana 49 näytettä, joista saadaan tulokset kesäkuun aikana.

Geofysikaalisia tulkintoja varten kerätään tarpeellinen määrä uusia täydennysnäytteitä eri kivilajityypeistä petrofysiikan määrittelyyn (suskis, omv, tiheys), jotka tehdään OMEXn toimesta Outokummussa. Tämän työn tekevät T.Ahokas ja H.Puustjärvi.

Heikki Puustjärvi

17.06.1997

Confidential

B. Geologia

(Luukas, Kilpeläinen, Kousa, Puustjärvi, Tapio)

Tämän osa-alueen tavoitteena on selvittää Pyhäsalmi-Mullikkoräme muodostumien geologinen evoluutio - magmatotektoninen miljöö, rakenne, malminmuodostumisprosessi.

B1. Tämä käsittää kaiken geologisen pintatiedon ja geofysikaalisten pintakarttojen siirron ArcView ohjelmistoon muokattavaksi ja tulkittavaksi (J.Luukas, H.Puustjärvi). Myöhemmässä vaiheessa tietoja täydennetään uusilla pintatiedoilla.

Tässä yhteydessä siirretään myös yhtenäistetty reikägeologia ja uudelleen raportoidut reikätiiedot käsiteltäväksi PC-XPLOR ohjelmalla (J.Parkkinen, H.Puustjärvi).

B2. Pintageologian uudistamisesta, lisäkartoituksista ja apuna käytettävästä kaivuroinnista vastaa J.Luukas (S.Penninkilampi).

B3. Geologisten profiilien ja tasojen konstruointi tehdään yhteistyönä J.Luukas-H.Puustjärvi-J.Parkkinen käyttäen pääasiassa PC-XPLOR ohjelmistoa. Työ koostuu yksinkertaistetun litologian ja muuttumisilmiöiden tulkinnasta profiili/ tasokartoille ja digitoinnista.

B4. Rakenne- ja deformaatiomallinnuksesta vastaa J.Luukas tehden yhteistyötä T.Kilpeläisen (Turun Yliopisto) kanssa. Työssä selvitetään muodostumien rakennepiirteet alueelliseen suurrakenteeseen ja yhdistyminen metamorfiseen kehitykseen.

B5. Paleovulkanologian tulkinnasta vastaa J.Kousa (yhteistyössä J. Luukkaan kanssa). Työ koostuu uudistetun pintageologian tulkinnoista ja lisäanalyysistä. Tämä työ palvelee malminetsintämallin luomista malminmuodostusprosessien määrittelyssä.

C. Litogeokemia

(Rasilainen, Puustjärvi)

Tavoitteena on ymmärtää malminmuodostuksen kemiallinen kehitys. Tästä työstä vastaa K.Rasilainen.

C1. Kaiken vanhan analyysitiedon ja kohdan A tuottaman aineiston siirto ja käsittely.

C2. Karakterisointi käsittää malmin ja sivukivien koostumuksen kuvauksen. Palvelee osaltaan paleovulkanologista tulkintaa.

C3. Malminmuodostuksen tektonisen miljööön tulkinta, muuttumisen kvantifiointi, muuttumisvektorit ja tehokkaimmat "pathfinder"-alkuaineet ja alkuaineyhdistelmät.

Heikki Puustjärvi

17.06.1997

Confidential

D. Geofysiikka

(Ahokas)

Geofysikaalisen mallinnuksen tavoitteena on tunnistaa ne parametrit/parametrikombinaatiot, jotka parhaiten karakterisoivat malmia ja sen välittömiä kiviä ja ovat tulkinnallisesti tunnistettavia kemiallisesti muuttuneissa ja kompleksisesti tektonisoituneissa ympäristöissä. Tästä työstä vastaa T.Ahokas.

- D1. Projektialueen kaikki vanha geofysiikan tutkimusmateriaali, täydentävät petrofysiikan määritykset ja mahdollisesti tarvittavat uudet mittaukset siirretään käsiteltäväksi Geosoft ohjelmalla. Ennen tiedonsiirtoa on OKPn materiaalille tehtävä koordinaatiston muunnos (valtakunnan 3-kaistaan).
- D2. Reikämateriaalista tehtyä petrofysiikkaa käytetään hyväksi litologisten yksiköiden karakterisoinnissa ja luokittelussa.
- D3. Kivilajiyksiköiden tunnistaminen ja vaihteluiden karakterisointi. Profiilitulkinnat.
- D4. Malmin, muuttumisvyöhykkeiden ja sivukivien karakterisointi sekä tulkinat.
- D5. Malmikriittisten parametrikombinaatioiden tunnistaminen, mallintaminen ja tulkinta. Tässä vaiheessa yhteys rakennegeologiaan on erityisen tärkeitä.

E. Matemaattinen mallinnus

(Gustavsson, Parkkinen, Suppala)

Tästä osa-alueesta vastaa N.Gustavsson. Mallinnuksen tavoitteena on kuvata moniulotteista aineistoa pelkistämällä sitä ohjaamattomilla ja ohjatuilla luokittelumenetelmillä.

- E1. Kairareikien vanha ja uusi analyysiaineisto, petrofysiikka ja numeeristettu litologia.
- E2. Aineiston testaus eri menetelmin ja malmikriittistä yksikköä parhaiten karakterisoivan luokittelumenetelmän valinta.
- E3. Kriittisten parametrien tunnistus ja aineiston luokittelu.
- E4. 3D-mallinnus koostuu matemaattisesta ja geologisesta osasta sekä näiden yhdistelmänä paikallisesta rakennemallista edustaen yksityiskohtaa alueellisessa rakennemallissa. Geologisten yksiköitten kuvaus, hahmotus ja rajaus kaivosten (OKP, OKMU) lähiympäristöissä.

F. Malminetsintämalli

(Puustjärvi)

Osa-alueiden synteesi, jossa määritellään testikairauksen kohteet ja uusilla tutkimusalueilla käytettävä toimintamalli Pyhäsalmi-Mullikkoräme tyyppisten malmien löytämiseksi.

Heikki Puustjärvi

17.06.1997

Confidential

G. Testikairaus

(Puustjärvi)

Projektiohjelmaan sisältyy testikairausta 3000m, josta osa on uutta Suomessa kokeilematonta ohjattua kairausta. Testikairauksen yhteydessä tehdään myös reikien geofysikaalisia mittauksia (mm. 3-komp. EM). Työstä vastaa H.Puustjärvi yhteistyössä kairausurakoitsijan kanssa.

H. Raportointi

(Puustjärvi)

Projektin tarkistuspisteinä ovat projektikokoukset -97 syyskuussa, -98 huhtikuussa ja lokakuussa sekä loppukokous -99 toukokuussa loppuraportin valmistuttua. Projektin sisäinen raportointi tapahtuu kunkin tutkijan toimesta kuukausittain projektipäällikölle (H.Puustjärvi) ja edelleen projektin johtajalle (K.Mäkelä). Väli- ja lopulliset raportit TEKESille toimitetaan ohjeiden mukaisesti.

APPENDIX A1

Heikki Puustjärvi

10.11.2006

Confidential

Explanation to drill hole data sets collected from Ingres (exploration) data base and Minenet (Pyhäsalmi mine) data base and imported into the GEM4WIN software Gcdbmp.mdb data base:

Workspace **Drillhole_A** includes **564 holes** which consists of all surficial exploration and resource drilling holes in OKP (Pyhäsalmi mine) and OKMU (Mullikkoräme mine).

These include **480 holes** of which 454 (PyO*, Pys*, PysLi*, Mu*, MuLi*, Kat*, Par* holes) are surficial and 26 from OKP mine (R*-holes) and most of these have XRF-assays.

Additionally there are litho-logged (combining 10cm samples each meter not crossing lithological boundaries and not exceeding 5m) and XRF assayed drill holes (old relogged ones and some new ones) with a prefix M* (modeling-project) comprising 20 holes from OKP underground (MR*), 22 holes from surface exploration drilling (MPYS*, MPYO*), 16 from OKMU underground (MMUR*), 19 new drill holes (MR*, MPYS*, MKAT*, MMUR*) and 7 test drill holes (MPYS*, MMU*) totaling **84 holes** which are listed in the Appendix A3.

Then there are two separate workspaces **R-Holes-OKP** and **Drillhole-MU** which include only assay data (AAS-assays) of the underground holes from Pyhäsalmi mine (OKP) and Mullikkoräme mine (OKMU). R-Holes-OKP has 1595 holes with Cu, Zn, S data and Drillhole_MU has 363 holes with Cu, Zn, Pb, Ag, S and some Au data. These data sets have been used to model ore body metal distributions and in Mullikkoräme mineralization boundaries.

APPENDIX A2

Hole-id	Location	Length	Assays	Ass#f	Ass#t	AdAss#f	AdAss#t	Geologist	Notes	Laboratory	meters	Holes	XRFasstot
PYO-50	X2800	295.70	54	9712147	9712200			HOP	OKP-deposit	GTK			
PYO-39	X2800	360.65	71	9712076	9712146			HOP	OKP-deposit	GTK			
PYO-22	X2800	151.26	43	9712033	9712075			HOP	OKP-deposit	GTK			
PYO-16	X2800	110.96	32	9712001	9712032			HOP	OKP-deposit	GTK			
PYO-4	X2600	189.00	32	9711797	9711828			HOP	OKP-deposit	GTK			
PYO-11	X2600	224.01	43	9711829	9711871			HOP	OKP-deposit	GTK			
PYO-5	X2500	130.31	25	9712254	9712278			HOP	OKP-deposit	GTK			
PYO-18	X2500	255.43	53	9712201	9712253			HOP	OKP-deposit	GTK			
PYO-53	X2400	214.70	23	9712334	9712356			HOP	OKP-deposit	GTK			
PYO-6	X2400	155.17	17	9711780	9711796			HOP	OKP-deposit	GTK			
PYO-25	X2300	265.81	31	9711900	9711930			HOP	OKP-deposit	GTK			
PYO-10	X2300	144.71	28	9711872	9711899			HOP	OKP-deposit	GTK	2497.71	12	452
PYS-10	X3650	152.64	30	9711751	9711779	9713000		HOP	OKP-vicinity	GTK			
PYS-75	X3400	310.40	72	9730011	9730082			HOP	OKP-vicinity	GTK			
PYS-9	X3300	158.02	34	9711977	9712000	9730001	9730010	HOP	OKP-vicinity	GTK			
PYS-94	X2950	473.30	119	9730083	9730201			HOP	OKP-vicinity	GTK	1094.36	4	255
PYS-24	A4550	264.25	60	9730214	9730250	9730501	9730523	HOP	Kettuperä	GTK			
PYS-82	A4300	71.10	12	9730202	9730213			HOP	Kettuperä	GTK			
PYS-29	A4300	430.30	64	9730637	9730700			HOP	Kettuperä	GTK			
PYS-20	A4250	505.35	100	9730701	9730800			HOP	Kettuperä	GTK			
PYS-90	A4200	321.50	54	9730524	9730577			HOP	Kettuperä	GTK			
PYS-28	A4200	283.90	59	9730578	9730636			HOP	Kettuperä	GTK	1876.40	6	349
R-104	T300	173.64	34	9712399	9712432			HOP	OKP-mine	GTK			
R-110	T400	116.00	20	9712433	9712452			HOP	OKP-mine	GTK			
R-123	T100	147.00	24	9712357	9712380			HOP	OKP-mine	GTK			
R-176	T210	108.25	18	9712381	9712398			HOP	OKP-mine	GTK			
R-199	T300	181.60	30	9712279	9712308			HOP	OKP-mine	GTK			
R-233	T500	170.05	25	9712309	9712333			HOP	OKP-mine	GTK			
R-246	T500	146.60	18	9712453	9712470			HOP	OKP-mine	GTK			
R-603	E1,608/0	200.70	40	9712898	9712937			HOP	OKP-mine	GTK			
R-975	E8,774/60	136.75	10	9712503	9712512			HOP	OKP-mine	GTK			
R-977	E8,771/1-60	135.15	18	9712513	9712530			HOP	OKP-mine	GTK			
R-981	E7,770/21	189.15	33	9712666	9712698			HOP	OKP-mine	GTK			
R-1515	E8,831/47	224.15	9	9712553	9712561			HOP	OKP-mine	GTK			
R-1579	C1,810/10	157.35	29	9712699	9712727			HOP	OKP-mine	GTK			
R-1580	E8,831/63	251.60	22	9712531	9712552			HOP	OKP-mine	GTK			
R-1585	C6,806/1	188.70	23	9712728	9712750			HOP	OKP-mine	GTK			
R-1587	C4,806/1	334.50	62	9712938	9712999			HOP	OKP-mine	GTK			
R-1657	T400,394/0	309.60	67	9712751	9712817			HOP	OKP-mine	GTK			
R-1667	E8,831/29	233.30	43	9712562	9712604			HOP	OKP-mine	GTK			
R-1716	T800,812/1	188.45	35	9712818	9712852			HOP	OKP-mine	GTK			
R-1726	Surface/E	143.00	32	9712471	9712502			HOP	OKP-mine	GTK	3735.54	20	592
MUR-283	X66320	110.20	31	9729064	9729094			HOP	OKMU-mine	GTK			
MUR-326	X66380	156.35	52	9710892	9710943			HOP	OKMU-mine	GTK			
MUR-144	X66395	201.90	47	9729271	9729317			HOP	OKMU-mine	GTK			
MUR-298	X66400	137.85	37	9730955	9730991			HOP	OKMU-mine	GTK			
MUR-223	X66480	116.00	26	9710786	9710811			HOP	OKMU-mine	GTK			
MUR-293	X66480	163.00	41	9729095	9729135			HOP	OKMU-mine	GTK			
MUR-294	X66480	151.95	40	9729136	9729175			HOP	OKMU-mine	GTK			
MUR-218	X66480	140.85	30	9729176	9729205			HOP	OKMU-mine	GTK			
MUR-206	X66600	160.75	40	9730871	9730910			HOP	OKMU-mine	GTK			
MUR-314	X66600	344.25	80	9710812	9710891			HOP	OKMU-mine	GTK			
MUR-273	X66600	180.80	59	9710976	9711000	9729001	9729034	HOP	OKMU-mine	GTK			
MUR-166	X66680	177.65	40	9729318	9729357			HOP	OKMU-mine	GTK			
MUR-318	X66700	291.95	65	9729206	9729270			HOP	OKMU-mine	GTK			
MUR-264	X66720	120.20	29	9729035	9729063			HOP	OKMU-mine	GTK			
MUR-246	X66780	111.50	32	9710944	9710975			HOP	OKMU-mine	GTK			
MUR-201	X66800	190.35	44	9730911	9730954			HOP	OKMU-mine	GTK	2755.55	16	693
R-1962	E9,T1000	296.50	43	9730251	9730293			TVM	OKP-mine	GTK			
R-1981	T810,30 SW	150.90	31	9712605	9712635			HOP	OKP-mine	GTK			
R-1989	T1030,30 S	200.60	30	9712636	9712665			HOP	OKP-mine	GTK			
R-1991	T400/0 SSE	249.40	45	9712853	9712897			HOP	OKP-mine	GTK			
R-1992	T400/0 SW	199.40	46	9711931	9711976			HOP	OKP-mine	GTK			
R-1993	T400/10 NW	350.20	70	9730801	9730870			HOP	OKP-mine	GTK	1447.00	6	265
PYS-109	X3600	364.10	90	9730294	9730383			PVH	OKP-vicinity	GTK			
PYS-110	X3100	267.40	69	9729687	9729755			PVH	OKP-vicinity	GTK			
PYS-111	X3100	287.30	55	9729551	9729606			PVH	OKP-vicinity	GTK			
PYS-112	X3100	343.20	84	9730384	9730467			PVH	OKP-vicinity	GTK	1262.00	4	298
PYS-113	A3950	621.30	85	9821193	9821197	9823528	9823607	PVH	Kettuperä	VTT			
PYS-114	A4850	457.90	113	9821001	9821113			PVH	Kettuperä	VTT			
PYS-115	A3950	395.10	108	9729790	9729897			PVH	Kettuperä	VTT	1474.30	3	306
KAT-22	X65700	500.10	81	9730470	9730500	9729501	9729550	KaP	OKMU-vicini.	VTT			
KAT-23	X65700	293.80	81	9729606	9729686			KaP	OKMU-vicini.	VTT			
KAT-24	X65700	500.70	no assays					KaP	OKMU-vicini.	VTT			
KAT-25	X65700	395.00	79	9721114	9721192			KaP	OKMU-vicini.	VTT			
MU-149	X66254	351.20	80	9721198	9721250	9723501	9723527	KaP	OKMU-vicini.	VTT	2040.80	5	321
MUR-353	X66680/+484	200.15	34	9729756	9729789			KaP	OKMU-mine	VTT	200.15	1	34
PYS-107cont	X2100	210.60	7	9815550	9815556			HOP	OKP-vicinity	VTT			
PYS-116	Y40400	257.60	no assays					HOP	OKP-vicinity	VTT			
PYS-117	X2200	526.10	55	9819385	9819439			HOP	OKP-vicinity	VTT			
PYS-118	A20600	825.85	24	9819440	9819447	9910401	9910418	HOP	OKP-vicinity	VTT	1820.15	4	86
PYS-119	L10900	745.90	107	9910251	9910337	9910339	9910358	HOP	Kettuperä	VTT			
PYS-119a	L10900	211.80						HOP	Kettuperä	VTT	957.70	2	107
MU-152	X66100	696.80	59	9910419	9910477			HOP	OKMU-vicini.	VTT	696.80	1	59
										SUM	21858.46	84	3817
													GTK 2904
													VTT 913

Note! In the GCDBMP data base all the above holes have a M* (modeling) prefix e.g. MU-152 = MMU152 as a hole-id.

APPENDIX C1

K. Rasilainen

20.4.1999

Confidential

All sampled diamond drill holes at Pyhäsalmi

Count	Cum Count	Pct	Cum Pct	DHOLE\$
44.	44.	0.7	0.7	PYO1
42.	86.	0.6	1.3	PYO10
83.	169.	1.2	2.5	PYO11
11.	180.	0.2	2.7	PYO12
37.	217.	0.5	3.2	PYO13
41.	258.	0.6	3.8	PYO14
41.	299.	0.6	4.4	PYO16
15.	314.	0.2	4.7	PYO17
127.	441.	1.9	6.5	PYO18
39.	480.	0.6	7.1	PYO19
72.	552.	1.1	8.2	PYO2
22.	574.	0.3	8.5	PYO21
60.	634.	0.9	9.4	PYO22
37.	671.	0.5	9.9	PYO23
53.	724.	0.8	10.7	PYO25
53.	777.	0.8	11.5	PYO27
75.	852.	1.1	12.6	PYO28
19.	871.	0.3	12.9	PYO29
58.	929.	0.9	13.8	PYO3
27.	956.	0.4	14.2	PYO31
47.	1003.	0.7	14.9	PYO32
9.	1012.	0.1	15.0	PYO33
12.	1024.	0.2	15.2	PYO34
25.	1049.	0.4	15.5	PYO36
50.	1099.	0.7	16.3	PYO37
116.	1215.	1.7	18.0	PYO38
115.	1330.	1.7	19.7	PYO39
93.	1423.	1.4	21.1	PYO4
122.	1545.	1.8	22.9	PYO40
13.	1558.	0.2	23.1	PYO41
29.	1587.	0.4	23.5	PYO42
134.	1721.	2.0	25.5	PYO43
38.	1759.	0.6	26.1	PYO44
59.	1818.	0.9	26.9	PYO45
146.	1964.	2.2	29.1	PYO47
43.	2007.	0.6	29.7	PYO5
80.	2087.	1.2	30.9	PYO50
66.	2153.	1.0	31.9	PYO53
162.	2315.	2.4	34.3	PYO54
47.	2362.	0.7	35.0	PYO6
23.	2385.	0.3	35.3	PYO7
195.	2580.	2.9	38.2	PYO84
46.	2626.	0.7	38.9	PYO9
31.	2657.	0.5	39.4	PYS1
45.	2702.	0.7	40.0	PYS10
3.	2705.	0.0	40.1	PYS100
5.	2710.	0.1	40.1	PYS101
2.	2712.	0.0	40.2	PYS102
3.	2715.	0.0	40.2	PYS103
3.	2718.	0.0	40.3	PYS104
6.	2724.	0.1	40.3	PYS105
30.	2754.	0.4	40.8	PYS106
5.	2759.	0.1	40.9	PYS107
26.	2785.	0.4	41.3	PYS108
126.	2911.	1.9	43.1	PYS109
133.	3044.	2.0	45.1	PYS110
88.	3132.	1.3	46.4	PYS111

K. Rasilainen

20.4.1999

Confidential

114.	3246.	1.7	48.1	PYS112
134.	3380.	2.0	50.1	PYS115
21.	3401.	0.3	50.4	PYS2
74.	3475.	1.1	51.5	PYS31
66.	3541.	1.0	52.5	PYS38
38.	3579.	0.6	53.0	PYS40
4.	3583.	0.1	53.1	PYS41
26.	3609.	0.4	53.5	PYS42
75.	3684.	1.1	54.6	PYS43
80.	3764.	1.2	55.8	PYS44
36.	3800.	0.5	56.3	PYS45
54.	3854.	0.8	57.1	PYS46
104.	3958.	1.5	58.6	PYS47
2.	3960.	0.0	58.7	PYS48
14.	3974.	0.2	58.9	PYS49
55.	4029.	0.8	59.7	PYS5
15.	4044.	0.2	59.9	PYS50
12.	4056.	0.2	60.1	PYS51
25.	4081.	0.4	60.5	PYS52
12.	4093.	0.2	60.6	PYS53
40.	4133.	0.6	61.2	PYS54
55.	4188.	0.8	62.0	PYS55
42.	4230.	0.6	62.7	PYS56
10.	4240.	0.1	62.8	PYS57
7.	4247.	0.1	62.9	PYS58
1.	4248.	0.0	62.9	PYS59
11.	4259.	0.2	63.1	PYS60
44.	4303.	0.7	63.7	PYS62
65.	4368.	1.0	64.7	PYS63
15.	4383.	0.2	64.9	PYS64
2.	4385.	0.0	65.0	PYS68
8.	4393.	0.1	65.1	PYS69
60.	4453.	0.9	66.0	PYS7
56.	4509.	0.8	66.8	PYS71
37.	4546.	0.5	67.3	PYS72
52.	4598.	0.8	68.1	PYS73
102.	4700.	1.5	69.6	PYS75
49.	4749.	0.7	70.3	PYS76
33.	4782.	0.5	70.8	PYS8
42.	4824.	0.6	71.5	PYS9
167.	4991.	2.5	73.9	PYS94
1.	4992.	0.0	73.9	PYS99
57.	5049.	0.8	74.8	R104
42.	5091.	0.6	75.4	R110
58.	5149.	0.9	76.3	R113
39.	5188.	0.6	76.8	R123
28.	5216.	0.4	77.3	R136
12.	5228.	0.2	77.4	R140
73.	5301.	1.1	78.5	R1515
62.	5363.	0.9	79.4	R1579
93.	5456.	1.4	80.8	R1580
56.	5512.	0.8	81.6	R1585
93.	5605.	1.4	83.0	R1587
90.	5695.	1.3	84.4	R1657
69.	5764.	1.0	85.4	R1667
72.	5836.	1.1	86.4	R1716
45.	5881.	0.7	87.1	R1726
29.	5910.	0.4	87.5	R176
47.	5957.	0.7	88.2	R1981
97.	6054.	1.4	89.7	R1982
52.	6106.	0.8	90.4	R1989
49.	6155.	0.7	91.2	R199

K. Rasilainen

20.4.1999

Confidential

80.	6235.	1.2	92.4	R1991
54.	6289.	0.8	93.2	R1992
86.	6375.	1.3	94.4	R1993
20.	6395.	0.3	94.7	R210
53.	6448.	0.8	95.5	R233
35.	6483.	0.5	96.0	R246
64.	6547.	0.9	97.0	R603
45.	6592.	0.7	97.6	R814
46.	6638.	0.7	98.3	R975
61.	6699.	0.9	99.2	R977
52.	6751.	0.8	100.0	R981

K. Rasilainen

20.4.1999

Confidential

All sampled diamond drill holes at Kettuperä

Count	Cum Count	Pct	Cum Pct	DHOLE\$
37.	37.	1.7	1.7	PYS11
150.	187.	6.9	8.6	PYS113
161.	348.	7.4	16.0	PYS114
49.	397.	2.3	18.3	PYS12
86.	483.	4.0	22.2	PYS17
98.	581.	4.5	26.7	PYS18
81.	662.	3.7	30.4	PYS19
129.	791.	5.9	36.4	PYS20
71.	862.	3.3	39.6	PYS21
65.	927.	3.0	42.6	PYS22
87.	1014.	4.0	46.6	PYS23
78.	1092.	3.6	50.2	PYS24
78.	1170.	3.6	53.8	PYS25
64.	1234.	2.9	56.7	PYS26
75.	1309.	3.4	60.2	PYS27
79.	1388.	3.6	63.8	PYS28
114.	1502.	5.2	69.1	PYS29
64.	1566.	2.9	72.0	PYS30
58.	1624.	2.7	74.7	PYS32
35.	1659.	1.6	76.3	PYS33
3.	1662.	0.1	76.4	PYS34
35.	1697.	1.6	78.0	PYS35
72.	1769.	3.3	81.3	PYS36
26.	1795.	1.2	82.5	PYS37
71.	1866.	3.3	85.8	PYS39
37.	1903.	1.7	87.5	PYS61
18.	1921.	0.8	88.3	PYS74
43.	1964.	2.0	90.3	PYS77
14.	1978.	0.6	90.9	PYS78
13.	1991.	0.6	91.5	PYS81
14.	2005.	0.6	92.2	PYS82
2.	2007.	0.1	92.3	PYS84
12.	2019.	0.6	92.8	PYS85
9.	2028.	0.4	93.2	PYS86
7.	2035.	0.3	93.6	PYS87
4.	2039.	0.2	93.7	PYS88
24.	2063.	1.1	94.9	PYS89
65.	2128.	3.0	97.8	PYS90
25.	2153.	1.1	99.0	PYS95
10.	2163.	0.5	99.4	PYS96
12.	2175.	0.6	100.0	PYS97

K. Rasilainen

20.4.1999

Confidential

All sampled diamond drill holes at Mullikkoräme

Count	Cum Count	Pct	Cum Pct	DHOLE\$
51.	51.	0.9	0.9	KAT1
6.	57.	0.1	1.0	KAT10
22.	79.	0.4	1.3	KAT11
21.	100.	0.3	1.7	KAT12
21.	121.	0.3	2.0	KAT13
19.	140.	0.3	2.3	KAT15
5.	145.	0.1	2.4	KAT16
9.	154.	0.2	2.6	KAT17
1.	155.	0.0	2.6	KAT18
2.	157.	0.0	2.6	KAT19
20.	177.	0.3	2.9	KAT2
5.	182.	0.1	3.0	KAT20
7.	189.	0.1	3.1	KAT21
157.	346.	2.6	5.8	KAT22
85.	431.	1.4	7.2	KAT23
122.	553.	2.0	9.2	KAT25
14.	567.	0.2	9.4	KAT3
11.	578.	0.2	9.6	KAT4
27.	605.	0.4	10.1	KAT5
19.	624.	0.3	10.4	KAT6
10.	634.	0.2	10.6	KAT7
5.	639.	0.1	10.6	KAT8
2.	641.	0.0	10.7	KAT9
74.	715.	1.2	11.9	MU1
63.	778.	1.0	13.0	MU10
11.	789.	0.2	13.2	MU100
16.	805.	0.3	13.4	MU101
67.	872.	1.1	14.5	MU102
13.	885.	0.2	14.8	MU103
9.	894.	0.2	14.9	MU104
14.	908.	0.2	15.1	MU105
5.	913.	0.1	15.2	MU106
121.	1034.	2.0	17.2	MU108
73.	1107.	1.2	18.5	MU109
20.	1127.	0.3	18.8	MU11
32.	1159.	0.5	19.3	MU110
7.	1166.	0.1	19.4	MU111
20.	1186.	0.3	19.8	MU112
89.	1275.	1.5	21.3	MU113
79.	1354.	1.3	22.6	MU114
53.	1407.	0.9	23.5	MU115
68.	1475.	1.1	24.6	MU116
107.	1582.	1.8	26.4	MU117
33.	1615.	0.6	26.9	MU118
6.	1621.	0.1	27.0	MU119
17.	1638.	0.3	27.3	MU12
79.	1717.	1.3	28.6	MU120
11.	1728.	0.2	28.8	MU121
42.	1770.	0.7	29.5	MU122
5.	1775.	0.1	29.6	MU123
12.	1787.	0.2	29.8	MU124
1.	1788.	0.0	29.8	MU125
11.	1799.	0.2	30.0	MU126
13.	1812.	0.2	30.2	MU127
14.	1826.	0.2	30.4	MU128
5.	1831.	0.1	30.5	MU129
25.	1856.	0.4	30.9	MU13

K. Rasilainen

20.4.1999

Confidential

2.	1858.	0.0	31.0	MU131
9.	1867.	0.2	31.1	MU132
10.	1877.	0.2	31.3	MU133
14.	1891.	0.2	31.5	MU133B
11.	1902.	0.2	31.7	MU134
30.	1932.	0.5	32.2	MU135
25.	1957.	0.4	32.6	MU135B
7.	1964.	0.1	32.7	MU137
4.	1968.	0.1	32.8	MU138
62.	2030.	1.0	33.8	MU14
8.	2038.	0.1	34.0	MU141
6.	2044.	0.1	34.1	MU142
9.	2053.	0.2	34.2	MU144
1.	2054.	0.0	34.2	MU148
109.	2163.	1.8	36.0	MU149
15.	2178.	0.3	36.3	MU15
21.	2199.	0.3	36.6	MU16
14.	2213.	0.2	36.9	MU17
9.	2222.	0.2	37.0	MU18
7.	2229.	0.1	37.1	MU19
29.	2258.	0.5	37.6	MU2
13.	2271.	0.2	37.8	MU21
30.	2301.	0.5	38.3	MU22
7.	2308.	0.1	38.5	MU23
12.	2320.	0.2	38.7	MU24
13.	2333.	0.2	38.9	MU25
3.	2336.	0.1	38.9	MU26
3.	2339.	0.1	39.0	MU27
5.	2344.	0.1	39.1	MU28
26.	2370.	0.4	39.5	MU29
29.	2399.	0.5	40.0	MU3
7.	2406.	0.1	40.1	MU30
2.	2408.	0.0	40.1	MU31
47.	2455.	0.8	40.9	MU32
1.	2456.	0.0	40.9	MU33
12.	2468.	0.2	41.1	MU34
30.	2498.	0.5	41.6	MU35
18.	2516.	0.3	41.9	MU37
21.	2537.	0.3	42.3	MU38
6.	2543.	0.1	42.4	MU39
39.	2582.	0.6	43.0	MU4
6.	2588.	0.1	43.1	MU40
1.	2589.	0.0	43.1	MU41
6.	2595.	0.1	43.2	MU42
2.	2597.	0.0	43.3	MU44
7.	2604.	0.1	43.4	MU47
4.	2608.	0.1	43.5	MU48
16.	2624.	0.3	43.7	MU49
30.	2654.	0.5	44.2	MU5
45.	2699.	0.8	45.0	MU50
18.	2717.	0.3	45.3	MU51
47.	2764.	0.8	46.1	MU52
42.	2806.	0.7	46.8	MU53
24.	2830.	0.4	47.2	MU54
1.	2831.	0.0	47.2	MU55
31.	2862.	0.5	47.7	MU56
65.	2927.	1.1	48.8	MU57
28.	2955.	0.5	49.2	MU58
1.	2956.	0.0	49.3	MU59
43.	2999.	0.7	50.0	MU6
14.	3013.	0.2	50.2	MU60
42.	3055.	0.7	50.9	MU61

K. Rasilainen

20.4.1999

Confidential

33.	3088.	0.6	51.5	MU62
11.	3099.	0.2	51.6	MU63
4.	3103.	0.1	51.7	MU65
6.	3109.	0.1	51.8	MU66
2.	3111.	0.0	51.8	MU69
27.	3138.	0.4	52.3	MU7
5.	3143.	0.1	52.4	MU70
1.	3144.	0.0	52.4	MU71
3.	3147.	0.1	52.4	MU72
3.	3150.	0.1	52.5	MU73
5.	3155.	0.1	52.6	MU74
7.	3162.	0.1	52.7	MU76
3.	3165.	0.1	52.7	MU77
2.	3167.	0.0	52.8	MU79
35.	3202.	0.6	53.4	MU8
1.	3203.	0.0	53.4	MU80
16.	3219.	0.3	53.6	MU81
50.	3269.	0.8	54.5	MU82
8.	3277.	0.1	54.6	MU83
15.	3292.	0.3	54.9	MU84
42.	3334.	0.7	55.6	MU85
42.	3376.	0.7	56.3	MU86
45.	3421.	0.8	57.0	MU87
42.	3463.	0.7	57.7	MU88
41.	3504.	0.7	58.4	MU89
45.	3549.	0.8	59.1	MU9
25.	3574.	0.4	59.6	MU90
73.	3647.	1.2	60.8	MU91
22.	3669.	0.4	61.1	MU92
48.	3717.	0.8	61.9	MU93
36.	3753.	0.6	62.5	MU94
26.	3779.	0.4	63.0	MU95
30.	3809.	0.5	63.5	MU96
21.	3830.	0.3	63.8	MU98
97.	3927.	1.6	65.4	MU99
37.	3964.	0.6	66.1	MUR1
31.	3995.	0.5	66.6	MUR10
59.	4054.	1.0	67.6	MUR11
48.	4102.	0.8	68.4	MUR12
10.	4112.	0.2	68.5	MUR13
3.	4115.	0.1	68.6	MUR14
65.	4180.	1.1	69.7	MUR144
2.	4182.	0.0	69.7	MUR15
20.	4202.	0.3	70.0	MUR16
53.	4255.	0.9	70.9	MUR166
39.	4294.	0.6	71.6	MUR17
4.	4298.	0.1	71.6	MUR18
8.	4306.	0.1	71.8	MUR19
39.	4345.	0.6	72.4	MUR2
3.	4348.	0.1	72.5	MUR20
62.	4410.	1.0	73.5	MUR201
43.	4453.	0.7	74.2	MUR206
17.	4470.	0.3	74.5	MUR21
34.	4504.	0.6	75.1	MUR218
11.	4515.	0.2	75.2	MUR22
40.	4555.	0.7	75.9	MUR223
13.	4568.	0.2	76.1	MUR23
16.	4584.	0.3	76.4	MUR24
36.	4620.	0.6	77.0	MUR246
7.	4627.	0.1	77.1	MUR25
19.	4646.	0.3	77.4	MUR26
37.	4683.	0.6	78.0	MUR264

K. Rasilainen

20.4.1999

Confidential

14.	4697.	0.2	78.3	MUR27
67.	4764.	1.1	79.4	MUR273
5.	4769.	0.1	79.5	MUR28
37.	4806.	0.6	80.1	MUR283
17.	4823.	0.3	80.4	MUR29
44.	4867.	0.7	81.1	MUR293
48.	4915.	0.8	81.9	MUR294
43.	4958.	0.7	82.6	MUR298
37.	4995.	0.6	83.2	MUR3
11.	5006.	0.2	83.4	MUR30
17.	5023.	0.3	83.7	MUR31
94.	5117.	1.6	85.3	MUR314
67.	5184.	1.1	86.4	MUR318
7.	5191.	0.1	86.5	MUR32
59.	5250.	1.0	87.5	MUR326
9.	5259.	0.2	87.6	MUR33
15.	5274.	0.3	87.9	MUR34
14.	5288.	0.2	88.1	MUR35
53.	5341.	0.9	89.0	MUR353
21.	5362.	0.3	89.4	MUR36
20.	5382.	0.3	89.7	MUR37
9.	5391.	0.2	89.8	MUR38
24.	5415.	0.4	90.2	MUR39
16.	5431.	0.3	90.5	MUR4
23.	5454.	0.4	90.9	MUR40
11.	5465.	0.2	91.1	MUR41
16.	5481.	0.3	91.3	MUR42
12.	5493.	0.2	91.5	MUR43
19.	5512.	0.3	91.9	MUR44
16.	5528.	0.3	92.1	MUR45
5.	5533.	0.1	92.2	MUR46
22.	5555.	0.4	92.6	MUR48
11.	5566.	0.2	92.8	MUR49
4.	5570.	0.1	92.8	MUR5
16.	5586.	0.3	93.1	MUR50
17.	5603.	0.3	93.4	MUR51
19.	5622.	0.3	93.7	MUR52
19.	5641.	0.3	94.0	MUR53
9.	5650.	0.2	94.2	MUR54
7.	5657.	0.1	94.3	MUR55
12.	5669.	0.2	94.5	MUR56
6.	5675.	0.1	94.6	MUR57
12.	5687.	0.2	94.8	MUR58
14.	5701.	0.2	95.0	MUR59
10.	5711.	0.2	95.2	MUR6
10.	5721.	0.2	95.3	MUR60
2.	5723.	0.0	95.4	MUR61
7.	5730.	0.1	95.5	MUR64
14.	5744.	0.2	95.7	MUR65
8.	5752.	0.1	95.9	MUR66
6.	5758.	0.1	96.0	MUR67
7.	5765.	0.1	96.1	MUR69
19.	5784.	0.3	96.4	MUR7
7.	5791.	0.1	96.5	MUR70
3.	5794.	0.1	96.6	MUR72
5.	5799.	0.1	96.6	MUR73
11.	5810.	0.2	96.8	MUR74
10.	5820.	0.2	97.0	MUR75
4.	5824.	0.1	97.1	MUR76
18.	5842.	0.3	97.4	MUR77
14.	5856.	0.2	97.6	MUR78
3.	5859.	0.1	97.6	MUR79

K. Rasilainen

20.4.1999

Confidential

9.	5868.	0.2	97.8	MUR8
45.	5913.	0.8	98.5	MUR84
40.	5953.	0.7	99.2	MUR86
11.	5964.	0.2	99.4	MUR88
27.	5991.	0.4	99.8	MUR9
7.	5998.	0.1	100.0	PAR1
2.	6000.	0.0	100.0	PAR

K. Rasilainen

20.4.1999

Confidential

APPENDIX C2

K. Rasilainen

20.4.1999

Confidential

Regression equations

The regression equations used in calibrating the old OKU chemical analyses are of the following form:

$$\text{element}_{\text{new}} = a + b \times \text{element}_{\text{old}}$$

where $\text{element}_{\text{new}}$ and $\text{element}_{\text{old}}$ are the concentrations of the element in the new and old chemical analysis, respectively, and a and b are constants. The constants were solved iteratively and were then used to calculate the calibrated concentrations by the following equation:

$$\text{element}_{\text{cal}} = a + b \times \text{element}_{\text{old}}$$

In cases where the regression was performed separately for certain years, the constants for each year are given in the following table.

Table of regression coefficients

Element	a	b
SiO ₂	0.7202	0.9856
TiO ₂	0.0052	1.0698
Al ₂ O ₃ (year < 1986)	-1.1734	1.0566
Al ₂ O ₃ (year = 1986)	-0.2731	0.8963
Al ₂ O ₃ (year >1986)	0.3759	0.9524
Fe ₂ O ₃ (year < >1986)	0.4815	0.9946
Fe ₂ O ₃ (year = 1986)	1.0007	1.0203
MnO	0.0029	0.9972
MgO	0.0303	0.9894
CaO	0.022	0.9833
Na ₂ O (year < 1987,1988)	-0.0536	1.0742
Na ₂ O (year = 1987,1989)	0.1387	0.9028
Na ₂ O (year >1989)	0.0074	0.9776
K ₂ O (year = 1984,1985)	0.0602	1.0668
K ₂ O (year = 1983,1988,1990,1995)	0.0037	0.9908
K ₂ O (year = 1986,1987,1989,1991,1993)	0.0713	0.8476
P ₂ O ₅ (year = 1984)	0.0071	1.0853
P ₂ O ₅ (year = 1987,1988,1993,1995)	-0.0012	0.9766
P ₂ O ₅ (year = 1983,1985,1986,1989-1991)	0.0099	0.852
Zr (year < 1986)	-8.4464	1.0349
Zr (year = 1986)	-24.8824	1.3077
Zr (year = 1988)	4.3079	1.0361

K. Rasilainen

20.4.1999

Confidential

Zr (year = 1987, 1989-1995)	11.8434	1.1403
-----------------------------	---------	--------

Table of regression coefficients (continued)

Element	a	b
Cr	17.68	0.849
V	6.3314	0.9586
Rb	4.6772	0.8958
Sr (year < 1987)	-3.8382	0.9387
Sr (year > 1986)	0.054	1.1458
Ba (year < 1987)	-256.43	1.1954
Ba (year > 1986)	3.346	1.0053
Cu (year < 1991)	3.8231	1.1759
Cu (year > 1990)	10.2078	0.9922
Zn	64.9042	1.1521
Pb	27.2264	1.4735
Ni	1.5242	0.975
S	0.1496	0.8058

APPENDIX C3

K. Rasilainen

20.4.1999

Confidential

Subgroup classification criteria for the volcanic rocks

The felsic volcanics were classified into nine subgroups according to the value of Zr/TiO_2 . The classes and their limits are as follows:

Felsic subgroup	Range of Zr/TiO_2 values
1	0.000 - 0.035
2	0.035 - 0.040
3	0.040 - 0.048
4	0.048 - 0.059
5	0.059 - 0.075
6	0.075 - 0.095
7	0.095 - 0.125
8	0.125 - 0.200
9	0.200 -

The mafic volcanics were classified into two subgroups according to the value of Zr/TiO_2 . A small number of mafic samples with Zr/TiO_2 values greater than 0.02 were discarded as probably misclassified altered felsic volcanics. The classes and their limits are as follows:

Mafic subgroup	Range of Zr/TiO_2 values
1	0.0000 - 0.0085
2	0.0085 - 0.0200

Background compositions of the volcanic rocks

The following pages contain the background concentrations of the elements for the felsic and mafic volcanic rocks by area and Zr/TiO_2 subgroup. For each of S, Cu, Zn, Pb, Ni, Co, Ag and Au, the same value was used as the background concentration for all the felsic volcanic subgroups. These values were derived from the combined set of the least altered felsic volcanics. A similar procedure was followed for the mafic volcanics. For Au, 0.001 ppm was used as the background concentration for all volcanic rocks. For Pb, 37.5 ppm was used as the background concentration for all mafic volcanic rocks.

GEOCHEMISTRY REPORT
Appendix C3

2

K. Rasilainen

20.4.1999

Confidential

Least altered felsic volcanic rocks

Elements for which these values were used as background concentrations regardless of the Zr/Ti₂ subgroup are bolded

	SIO2	TIO2	AL2O3	FE2O3	MNO
N of cases	1033	1033	1033	1033	1033
Minimum	59.20000	0.06700	7.63000	0.73365	0.00300
Maximum	84.80000	0.85034	17.70000	11.53735	0.30100
Median	74.90000	0.25981	12.70000	3.19026	0.05700
Mean	74.49167	0.25464	12.70478	3.31184	0.06416
Standard Dev	3.16921	0.10354	1.22118	1.17017	0.03289
	MGO	CAO	NA2O	K2O	P2O5
N of cases	1033	1033	1033	1033	1033
Minimum	0.01000	0.38300	2.42278	0.09300	0.00300
Maximum	5.76000	7.20000	8.11000	3.71000	0.27572
Median	1.22000	1.57000	4.50000	0.97600	0.05250
Mean	1.34661	1.76402	4.48456	1.12505	0.05484
Standard Dev	0.91606	0.93407	0.89516	0.64211	0.03751
	LOI	CO2	ZR	CR	V
N of cases	247	247	1033	1033	828
Minimum	0.10000	0.01832	59.20000	10.00000	10.00000
Maximum	2.54000	0.32967	439.00000	743.57500	159.00000
Median	0.51000	0.01832	172.16958	10.00000	19.36836
Mean	0.61053	0.04642	181.72373	55.47036	24.36111
Standard Dev	0.36328	0.05942	49.12123	88.57260	18.35562
	RB	SR	BA	CU	ZN
N of cases	828	1033	1033	986	986
Minimum	3.00000	38.07000	10.00000	0.50000	1.50000
Maximum	111.11616	639.00000	996.73163	50.00000	199.69990
Median	21.05242	107.34143	412.16000	21.46160	107.53190
Mean	25.03364	121.49482	431.07143	21.73381	103.97366
Standard Dev	14.06609	64.49584	204.74868	12.68245	41.11978
	PB	NI	S	CO	AG
N of cases	985	985	981	740	657
Minimum	0.50000	0.50000	0.00500	0.50000	0.05000
Maximum	96.48090	78.54920	0.49609	140.00000	4.60000
Median	34.59390	5.42420	0.18989	13.00000	0.50000
Mean	30.01152	6.84269	0.20281	24.41757	0.66317
Standard Dev	22.85724	7.94524	0.12271	22.16542	0.61596
	AU	CL	SC	GA	AS
N of cases	31	330	247	247	247
Minimum	0.00050	20.00000	15.00000	10.00000	15.00000
Maximum	0.70000	170.00000	15.00000	32.00000	15.00000
Median	0.02500	70.00000	15.00000	22.00000	15.00000
Mean	0.06818	65.63636	15.00000	20.05668	15.00000
Standard Dev	0.16005	32.74273	0.00000	6.74302	0.00000
	Y	NB	MO	SB	LA
N of cases	330	330	247	247	247
Minimum	1.50000	2.50000	5.00000	10.00000	15.00000
Maximum	55.00000	32.00000	24.00000	32.00000	60.00000
Median	29.00000	11.00000	5.00000	10.00000	15.00000
Mean	29.73182	10.76515	5.07692	10.08907	18.17004
Standard Dev	7.36964	8.06707	1.20894	1.39983	8.09769
	CE	BI	TH	U	W
N of cases	330	247	247	330	83
Minimum	15.00000	15.00000	5.00000	2.00000	10.00000
Maximum	120.00000	15.00000	5.00000	2.00000	440.00000
Median	60.00000	15.00000	5.00000	2.00000	120.00000
Mean	59.22424	15.00000	5.00000	2.00000	135.42169
Standard Dev	16.15008	0.00000	0.00000	0.00000	111.48992

K. Rasilainen

20.4.1999

Confidential

Least altered felsic volcanic rocks
Area=Pyhäsalmi-Kettuperä and Zr/TiO₂ subgroup=1

	SIO2	TIO2	AL2O3	FE2O3	MNO
N of cases	18	18	18	18	18
Minimum	59.90000	0.23400	7.80000	1.81189	0.01900
Maximum	79.70000	0.85034	17.70000	9.91536	0.16400
Median	67.95000	0.47050	14.28000	5.35462	0.07800
Mean	67.79444	0.45309	14.19722	5.27576	0.08472
Standard Dev	5.28989	0.15575	2.23548	2.04756	0.04064
	MGO	CAO	NA2O	K2O	P2O5
N of cases	18	18	18	18	18
Minimum	0.33000	0.76000	3.04010	0.26000	0.06600
Maximum	4.19000	5.71000	5.63000	2.47000	0.27572
Median	1.90500	3.07000	4.14000	1.48500	0.12220
Mean	2.04500	3.15167	4.14775	1.45870	0.13100
Standard Dev	0.89553	1.26182	0.78389	0.62703	0.05446
	LOI	CO2	ZR	CR	V
N of cases	7	7	18	18	12
Minimum	0.20000	0.01832	59.20000	10.00000	33.32000
Maximum	0.80000	0.14652	229.40000	259.92000	159.00000
Median	0.59000	0.01832	123.00000	40.00000	70.38000
Mean	0.54143	0.04971	129.51111	70.18395	77.53667
Standard Dev	0.19836	0.05465	50.95143	73.35542	39.20831
	RB	SR	BA	CU	ZN
N of cases	12	18	18	16	16
Minimum	16.00000	76.00000	10.00000	0.50000	20.00000
Maximum	50.00000	527.00000	969.00000	49.00000	144.39910
Median	32.03800	181.83000	442.52000	28.50000	96.50000
Mean	33.81667	218.05676	486.29179	26.06802	88.61307
Standard Dev	10.37039	136.64042	242.12026	15.18920	37.62923
	PB	NI	S	CO	AG
N of cases	16	16	16	9	6
Minimum	0.50000	0.50000	0.03700	0.50000	0.05000
Maximum	47.85540	30.00000	0.29400	80.00000	3.20000
Median	12.25000	2.75000	0.13633	15.00000	0.67500
Mean	18.72620	7.66704	0.13035	22.05556	1.10833
Standard Dev	20.10799	9.87267	0.07902	23.46333	1.30898
	AU	CL	SC	GA	AS
N of cases	0	10	7	7	7
Minimum	.	50.00000	15.00000	10.00000	15.00000
Maximum	.	120.00000	15.00000	31.00000	15.00000
Median	.	80.00000	15.00000	23.00000	15.00000
Mean	.	86.00000	15.00000	22.28571	15.00000
Standard Dev	.	21.70509	0.00000	9.10521	0.00000
	Y	NB	MO	SB	LA
N of cases	10	10	7	7	7
Minimum	1.50000	2.50000	5.00000	10.00000	15.00000
Maximum	32.00000	20.00000	5.00000	32.00000	15.00000
Median	23.00000	2.50000	5.00000	10.00000	15.00000
Mean	20.55000	8.50000	5.00000	13.14286	15.00000
Standard Dev	10.45214	7.93725	0.00000	8.31522	0.00000
	CE	BI	TH	U	W
N of cases	10	7	7	10	3
Minimum	30.00000	15.00000	5.00000	2.00000	10.00000
Maximum	67.00000	15.00000	5.00000	2.00000	10.00000
Median	48.50000	15.00000	5.00000	2.00000	10.00000
Mean	47.90000	15.00000	5.00000	2.00000	10.00000
Standard Dev	9.85957	0.00000	0.00000	0.00000	0.00000

GEOCHEMISTRY REPORT
Appendix C3

4

K. Rasilainen

20.4.1999

Confidential

Least altered felsic volcanic rocks
Area=Pyhäsalmi-Kettuperä and Zr/TiO₂ subgroup=2

	SiO2	TiO2	Al2O3	Fe2O3	MNO
N of cases	5	5	5	5	5
Minimum	64.60000	0.31100	11.40000	4.45055	0.04100
Maximum	72.90000	0.50052	14.90000	6.88000	0.19600
Median	69.10000	0.40100	13.70000	5.03549	0.06100
Mean	68.96000	0.40416	13.53400	5.42155	0.08420
Standard Dev	3.02457	0.07055	1.32355	1.07763	0.06324

	MGO	CAO	NA2O	K2O	P2O5
N of cases	5	5	5	5	5
Minimum	0.98000	1.04000	3.33013	0.96000	0.07330
Maximum	1.80000	5.37000	5.24221	2.40000	0.16800
Median	1.45000	2.49000	4.26000	1.33000	0.13600
Mean	1.42200	2.94400	4.19647	1.50340	0.12046
Standard Dev	0.30557	1.66811	0.70670	0.54254	0.04377

	LOI	CO2	ZR	CR	V
N of cases	1	1	5	5	1
Minimum	0.30000	0.01832	111.00000	40.90864	135.00000
Maximum	0.30000	0.01832	199.80000	212.04000	135.00000
Median	0.30000	0.01832	148.00000	177.84000	135.00000
Mean	0.30000	0.01832	150.64000	133.93669	135.00000
Standard Dev	.	.	32.22248	83.06470	.

	RB	SR	BA	CU	ZN
N of cases	1	5	5	5	5
Minimum	19.00000	133.00000	421.12000	6.00000	38.00000
Maximum	19.00000	279.18000	750.38360	34.00000	169.00000
Median	19.00000	210.57965	564.48000	26.16520	119.05290
Mean	19.00000	203.02962	595.23030	22.18464	117.58166
Standard Dev	.	62.61807	132.90197	10.96195	49.77092

	PB	NI	S	CO	AG
N of cases	5	5	5	4	4
Minimum	0.50000	2.49920	0.06700	3.00000	0.05000
Maximum	64.06390	30.00000	0.37522	12.00000	1.00000
Median	20.00000	8.00000	0.10000	7.00000	0.42500
Mean	28.09446	13.50468	0.16242	7.25000	0.47500
Standard Dev	25.96009	11.57995	0.12829	4.42531	0.49749

	AU	CL	SC	GA	AS
N of cases	0	1	1	1	1
Minimum	.	170.00000	15.00000	22.00000	15.00000
Maximum	.	170.00000	15.00000	22.00000	15.00000
Median	.	170.00000	15.00000	22.00000	15.00000
Mean	.	170.00000	15.00000	22.00000	15.00000
Standard Dev

	Y	NB	MO	SB	LA
N of cases	1	1	1	1	1
Minimum	28.00000	2.50000	5.00000	10.00000	15.00000
Maximum	28.00000	2.50000	5.00000	10.00000	15.00000
Median	28.00000	2.50000	5.00000	10.00000	15.00000
Mean	28.00000	2.50000	5.00000	10.00000	15.00000
Standard Dev

	CE	BI	TH	U	W
N of cases	1	1	1	1	0
Minimum	58.00000	15.00000	5.00000	2.00000	.
Maximum	58.00000	15.00000	5.00000	2.00000	.
Median	58.00000	15.00000	5.00000	2.00000	.
Mean	58.00000	15.00000	5.00000	2.00000	.
Standard Dev

K. Rasilainen

20.4.1999

Confidential

Least altered felsic volcanic rocks
Area=Pyhäsalmi-Kettuperä and Zr/TiO₂ subgroup=3

	SIO2	TIO2	AL2O3	FE2O3	MNO
N of cases	17	17	17	17	17
Minimum	61.60000	0.21400	12.40000	2.81232	0.04200
Maximum	73.80000	0.56200	16.30000	6.72511	0.30100
Median	69.30000	0.33791	13.81000	4.95912	0.07800
Mean	69.48235	0.35727	13.94294	4.93604	0.09029
Standard Dev	3.07332	0.10911	1.03127	1.11304	0.06023
	MGO	CAO	NA2O	K2O	P2O5
N of cases	17	17	17	17	17
Minimum	0.48000	1.71000	2.92000	0.19888	0.04183
Maximum	2.58000	4.91000	5.65000	3.26000	0.27000
Median	1.61000	3.32000	4.27000	0.90000	0.12500
Mean	1.54412	3.25588	4.31883	1.09937	0.14104
Standard Dev	0.65000	0.95257	0.79956	0.66253	0.07972
	LOI	CO2	ZR	CR	V
N of cases	1	1	17	17	6
Minimum	0.50000	0.01832	96.20000	10.00000	27.20000
Maximum	0.50000	0.01832	251.60000	287.28000	91.00000
Median	0.50000	0.01832	148.00000	81.55876	34.68000
Mean	0.50000	0.01832	154.59147	126.58696	46.10654
Standard Dev	.	.	45.64514	107.77340	24.61086
	RB	SR	BA	CU	ZN
N of cases	6	17	17	14	14
Minimum	17.00000	67.68000	170.24000	0.50000	40.00000
Maximum	85.91600	496.47013	922.88000	47.00000	123.66130
Median	19.66621	221.00000	643.27576	22.50000	66.00000
Mean	32.54340	230.70911	592.84563	24.04255	71.43931
Standard Dev	26.95906	140.98897	225.06129	14.53923	26.61532
	PB	NI	S	CO	AG
N of cases	14	14	14	13	11
Minimum	0.50000	0.50000	0.01600	0.50000	0.05000
Maximum	67.01090	34.00000	0.28659	24.00000	1.10000
Median	26.00000	4.44920	0.12900	17.00000	0.90000
Mean	28.47547	10.98376	0.13009	13.46154	0.64545
Standard Dev	19.11443	12.42737	0.08690	8.58648	0.47511
	AU	CL	SC	GA	AS
N of cases	0	3	1	1	1
Minimum	.	60.00000	15.00000	29.00000	15.00000
Maximum	.	100.00000	15.00000	29.00000	15.00000
Median	.	80.00000	15.00000	29.00000	15.00000
Mean	.	80.00000	15.00000	29.00000	15.00000
Standard Dev	.	20.00000	.	.	.
	Y	NB	MO	SB	LA
N of cases	3	3	1	1	1
Minimum	18.00000	15.00000	5.00000	10.00000	15.00000
Maximum	27.00000	21.00000	5.00000	10.00000	15.00000
Median	18.00000	19.00000	5.00000	10.00000	15.00000
Mean	21.00000	18.33333	5.00000	10.00000	15.00000
Standard Dev	5.19615	3.05505	.	.	.
	CE	BI	TH	U	W
N of cases	3	1	1	3	2
Minimum	15.00000	15.00000	5.00000	2.00000	230.00000
Maximum	60.00000	15.00000	5.00000	2.00000	250.00000
Median	50.00000	15.00000	5.00000	2.00000	240.00000
Mean	41.66667	15.00000	5.00000	2.00000	240.00000
Standard Dev	23.62908	.	.	0.00000	14.14214

GEOCHEMISTRY REPORT
Appendix C3

6

K. Rasilainen

20.4.1999

Confidential

Least altered felsic volcanic rocks
Area=Pyhäsalmi-Kettuperä and Zr/TiO₂ subgroup=4

	SiO ₂	TiO ₂	Al ₂ O ₃	Fe ₂ O ₃	MnO
N of cases	32	32	32	32	32
Minimum	67.40000	0.24100	11.20000	1.04000	0.02000
Maximum	79.50000	0.38500	16.60000	5.44558	0.13800
Median	73.70000	0.27250	12.60000	3.78000	0.08200
Mean	73.33125	0.29187	12.80938	3.76487	0.07447
Standard Dev	2.82665	0.04144	1.06267	0.97558	0.02836

	MgO	CaO	Na ₂ O	K ₂ O	P ₂ O ₅
N of cases	32	32	32	32	32
Minimum	0.16000	1.11000	2.81000	0.20400	0.03200
Maximum	3.48000	5.88000	6.15000	3.33000	0.11200
Median	1.10000	2.31500	3.99270	1.57000	0.06250
Mean	1.20812	2.29937	4.16813	1.59727	0.06765
Standard Dev	0.82396	0.90232	0.86950	0.87500	0.01799

	LOI	CO ₂	Zr	CR	V
N of cases	16	16	32	32	22
Minimum	0.20000	0.01832	129.00000	10.00000	10.00000
Maximum	1.35000	0.32967	207.20000	163.00000	108.00000
Median	0.44500	0.01832	155.34657	10.00000	18.86418
Mean	0.54000	0.08814	159.13640	29.82589	25.53569
Standard Dev	0.33359	0.09534	19.45821	38.88166	23.16479

	RB	SR	BA	CU	ZN
N of cases	22	32	32	29	29
Minimum	3.00000	51.75161	108.00000	0.50000	26.00000
Maximum	77.00000	496.47013	930.00000	45.00000	185.87470
Median	27.21000	110.00000	485.30700	22.00000	86.00000
Mean	29.56086	130.38333	464.82380	21.13429	95.37086
Standard Dev	17.08192	83.54358	192.79124	10.43428	41.38489

	PB	NI	S	CO	AG
N of cases	29	29	29	13	10
Minimum	0.50000	0.50000	0.00500	0.50000	0.05000
Maximum	71.43140	46.00000	0.38800	30.00000	1.60000
Median	0.50000	0.50000	0.10400	1.00000	0.90000
Mean	21.53519	5.58079	0.14680	6.26923	0.81000
Standard Dev	26.52224	11.35063	0.11598	8.61833	0.53790

	AU	CL	SC	GA	AS
N of cases	2	19	16	16	16
Minimum	0.02500	20.00000	15.00000	10.00000	15.00000
Maximum	0.02500	110.00000	15.00000	27.00000	15.00000
Median	0.02500	80.00000	15.00000	21.50000	15.00000
Mean	0.02500	72.10526	15.00000	18.75000	15.00000
Standard Dev	0.00000	30.47384	0.00000	6.36134	0.00000

	Y	NB	MO	SB	LA
N of cases	19	19	16	16	16
Minimum	20.00000	2.50000	5.00000	10.00000	15.00000
Maximum	43.00000	24.00000	5.00000	10.00000	33.00000
Median	31.00000	2.50000	5.00000	10.00000	15.00000
Mean	31.21053	7.44737	5.00000	10.00000	17.06250
Standard Dev	6.05144	7.98765	0.00000	0.00000	5.66238

	CE	BI	TH	U	W
N of cases	19	16	16	19	3
Minimum	48.00000	15.00000	5.00000	2.00000	10.00000
Maximum	81.00000	15.00000	5.00000	2.00000	110.00000
Median	52.00000	15.00000	5.00000	2.00000	100.00000
Mean	55.42105	15.00000	5.00000	2.00000	73.33333
Standard Dev	8.63659	0.00000	0.00000	0.00000	55.07571

K. Rasilainen

20.4.1999

Confidential

Least altered felsic volcanic rocks
Area=Pyhäsalmi-Kettuperä and Zr/TiO₂ subgroup=5

	SIO2	TIO2	AL2O3	FE2O3	MNO
N of cases	66	66	66	66	66
Minimum	67.50000	0.13300	9.27000	1.13382	0.01400
Maximum	82.70000	0.68600	14.50000	6.23000	0.13200
Median	75.30000	0.23100	12.50000	3.17401	0.05750
Mean	74.73333	0.24568	12.49318	3.07809	0.06298
Standard Dev	2.69057	0.10493	1.05274	1.14938	0.02813

	MGO	CAO	NA2O	K2O	P2O5
N of cases	66	66	66	66	66
Minimum	0.01000	0.47000	2.72000	0.16800	0.02121
Maximum	2.75000	6.06000	6.49000	3.54000	0.21100
Median	0.67500	1.83500	4.45500	1.33500	0.05050
Mean	0.77455	2.12941	4.38884	1.37367	0.06423
Standard Dev	0.58076	1.00342	0.95654	0.78902	0.04207

	LOI	CO2	ZR	CR	V
N of cases	31	31	66	66	48
Minimum	0.10000	0.01832	96.20000	10.00000	10.00000
Maximum	0.89000	0.25641	439.00000	218.88000	65.00000
Median	0.30000	0.01832	155.20000	10.00000	10.00000
Mean	0.39097	0.05613	162.77432	46.99740	16.82317
Standard Dev	0.19504	0.06619	68.49468	65.45454	13.86846

	RB	SR	BA	CU	ZN
N of cases	48	66	66	60	60
Minimum	3.00000	44.00000	61.00000	0.50000	20.00000
Maximum	105.11000	639.00000	940.80000	47.00000	180.11420
Median	26.75300	98.76801	497.28000	18.55490	59.50000
Mean	29.23515	130.88198	473.73739	15.83878	70.78601
Standard Dev	22.47371	96.41220	229.69260	13.98911	39.26236

	PB	NI	S	CO	AG
N of cases	60	60	60	29	18
Minimum	0.50000	0.50000	0.01500	0.50000	0.05000
Maximum	84.69290	20.00000	0.45000	120.00000	2.00000
Median	0.50000	0.50000	0.10000	6.00000	0.85000
Mean	16.70752	1.71160	0.14229	12.20690	0.82222
Standard Dev	20.52123	3.20283	0.11383	22.72055	0.62596

	AU	CL	SC	GA	AS
N of cases	3	42	31	31	31
Minimum	0.00050	20.00000	15.00000	10.00000	15.00000
Maximum	0.00050	170.00000	15.00000	32.00000	15.00000
Median	0.00050	70.00000	15.00000	21.00000	15.00000
Mean	0.00050	65.71429	15.00000	18.61290	15.00000
Standard Dev	0.00000	35.14034	0.00000	7.32884	0.00000

	Y	NB	MO	SB	LA
N of cases	42	42	31	31	31
Minimum	16.00000	2.50000	5.00000	10.00000	15.00000
Maximum	45.00000	28.00000	5.00000	10.00000	42.00000
Median	29.00000	2.50000	5.00000	10.00000	15.00000
Mean	28.61905	9.84524	5.00000	10.00000	17.22581
Standard Dev	5.48146	8.85485	0.00000	0.00000	6.96998

	CE	BI	TH	U	W
N of cases	42	31	31	42	11
Minimum	15.00000	15.00000	5.00000	2.00000	10.00000
Maximum	102.00000	15.00000	5.00000	2.00000	280.00000
Median	55.00000	15.00000	5.00000	2.00000	180.00000
Mean	56.61905	15.00000	5.00000	2.00000	150.00000
Standard Dev	17.08937	0.00000	0.00000	0.00000	110.54411

GEOCHEMISTRY REPORT
Appendix C3

8

K. Rasilainen

20.4.1999

Confidential

Least altered felsic volcanic rocks
Area=Pyhäsalmi-Kettuperä and Zr/TiO₂ subgroup=6

	SiO2	TiO2	Al2O3	Fe2O3	MNO
N of cases	42	42	42	42	42
Minimum	67.70000	0.07600	7.63000	1.03378	0.01700
Maximum	84.80000	0.38400	14.05000	6.35216	0.12300
Median	76.25000	0.19150	12.20000	2.86500	0.05550
Mean	75.97857	0.19597	11.97905	2.92087	0.05736
Standard Dev	3.13591	0.05502	1.43000	1.05656	0.02531

	MGO	CAO	NA2O	K2O	P2O5
N of cases	42	42	42	42	42
Minimum	0.01000	0.51400	2.63000	0.25000	0.01600
Maximum	1.94000	3.91000	5.81153	3.12000	0.16700
Median	0.55500	1.84500	4.09500	1.34500	0.03250
Mean	0.63024	1.91176	4.06252	1.41103	0.04391
Standard Dev	0.42336	0.78823	0.83311	0.72064	0.03687

	LOI	CO2	ZR	CR	V
N of cases	17	17	42	42	30
Minimum	0.10000	0.01832	66.60000	10.00000	10.00000
Maximum	0.79000	0.07326	333.00000	369.36000	38.92380
Median	0.49000	0.01832	161.00000	12.18200	10.00000
Mean	0.44941	0.03771	164.44743	59.27516	15.14987
Standard Dev	0.16342	0.02463	46.48726	87.23188	7.88489

	RB	SR	BA	CU	ZN
N of cases	30	42	42	34	34
Minimum	10.05400	38.82787	35.84000	0.50000	10.00000
Maximum	110.00000	313.02000	994.56000	44.00000	180.00000
Median	37.42765	104.00000	465.50000	21.00000	65.50000
Mean	37.15116	117.50325	495.76265	17.93493	78.58776
Standard Dev	19.60703	61.08661	252.06887	14.69773	48.71470

	PB	NI	S	CO	AG
N of cases	34	34	34	17	12
Minimum	0.50000	0.50000	0.00500	0.50000	0.05000
Maximum	95.00740	27.84920	0.46386	17.00000	1.80000
Median	6.00000	0.50000	0.10000	4.00000	0.80000
Mean	18.22059	3.66539	0.14989	5.26471	0.70833
Standard Dev	22.30509	6.94380	0.13435	4.96902	0.58147

	AU	CL	SC	GA	AS
N of cases	7	22	17	17	17
Minimum	0.00050	20.00000	15.00000	10.00000	15.00000
Maximum	0.70000	110.00000	15.00000	31.00000	15.00000
Median	0.02500	70.00000	15.00000	23.00000	15.00000
Mean	0.23236	59.54545	15.00000	20.23529	15.00000
Standard Dev	0.29515	28.19613	0.00000	7.34447	0.00000

	Y	NB	MO	SB	LA
N of cases	22	22	17	17	17
Minimum	14.00000	2.50000	5.00000	10.00000	15.00000
Maximum	44.00000	21.00000	5.00000	10.00000	32.00000
Median	29.50000	6.25000	5.00000	10.00000	15.00000
Mean	29.72727	9.15909	5.00000	10.00000	16.00000
Standard Dev	7.51622	7.28728	0.00000	0.00000	4.12311

	CE	BI	TH	U	W
N of cases	22	17	17	22	5
Minimum	40.00000	15.00000	5.00000	2.00000	10.00000
Maximum	75.00000	15.00000	5.00000	2.00000	440.00000
Median	56.00000	15.00000	5.00000	2.00000	110.00000
Mean	56.50000	15.00000	5.00000	2.00000	178.00000
Standard Dev	9.96064	0.00000	0.00000	0.00000	166.04216

K. Rasilainen

20.4.1999

Confidential

Least altered felsic volcanic rocks
Area=Pyhäsalmi-Kettuperä and Zr/TiO₂ subgroup=7

	SIO2	TIO2	AL2O3	FE2O3	MNO
N of cases	65	65	65	65	65
Minimum	71.20000	0.06700	7.83000	0.90039	0.00800
Maximum	80.70000	0.19990	13.60000	5.32182	0.10600
Median	76.90000	0.15711	11.90000	2.93000	0.05800
Mean	76.54000	0.15034	11.74377	2.86278	0.05748
Standard Dev	1.94613	0.02987	1.07786	0.81066	0.02125
	MGO	CAO	NA2O	K2O	P2O5
N of cases	65	65	65	65	65
Minimum	0.01000	0.65000	2.46000	0.26000	0.00300
Maximum	2.22000	2.93000	5.65040	2.95000	0.12100
Median	0.40000	1.48000	4.32914	1.49000	0.01900
Mean	0.57508	1.57678	4.25513	1.48566	0.02405
Standard Dev	0.46794	0.58729	0.74129	0.51778	0.02041
	LOI	CO2	ZR	CR	V
N of cases	22	22	65	65	30
Minimum	0.10000	0.01832	81.40000	10.00000	10.00000
Maximum	0.70000	0.29304	217.04210	328.32000	10.00000
Median	0.40000	0.01832	170.20000	10.00000	10.00000
Mean	0.44273	0.06161	167.13477	63.44787	10.00000
Standard Dev	0.16281	0.07381	32.00765	71.83615	0.00000
	RB	SR	BA	CU	ZN
N of cases	30	65	65	63	63
Minimum	16.00000	38.07000	10.00000	0.50000	30.00000
Maximum	92.00000	270.72000	860.16000	50.00000	184.72260
Median	33.00000	105.00000	493.32478	21.00000	102.92350
Mean	36.49920	106.86609	474.17980	19.95174	100.51978
Standard Dev	17.27376	44.67236	182.53204	13.84263	41.68011
	PB	NI	S	CO	AG
N of cases	63	63	63	41	33
Minimum	0.50000	0.50000	0.00500	0.50000	0.05000
Maximum	83.00000	37.59920	0.41300	30.00000	1.60000
Median	34.59390	0.50000	0.15766	5.00000	0.70000
Mean	28.81007	5.55604	0.15228	6.58537	0.61818
Standard Dev	25.53186	9.32071	0.09028	6.88649	0.40016
	AU	CL	SC	GA	AS
N of cases	1	30	22	22	22
Minimum	0.02500	20.00000	15.00000	10.00000	15.00000
Maximum	0.02500	120.00000	15.00000	28.00000	15.00000
Median	0.02500	60.00000	15.00000	21.50000	15.00000
Mean	0.02500	64.00000	15.00000	19.18182	15.00000
Standard Dev	.	26.47054	0.00000	6.75162	0.00000
	Y	NB	MO	SB	LA
N of cases	30	30	22	22	22
Minimum	20.00000	2.50000	5.00000	10.00000	15.00000
Maximum	44.00000	26.00000	5.00000	10.00000	34.00000
Median	33.00000	10.50000	5.00000	10.00000	15.00000
Mean	31.26667	9.50000	5.00000	10.00000	16.63636
Standard Dev	6.02829	7.52925	0.00000	0.00000	5.30539
	CE	BI	TH	U	W
N of cases	30	22	22	30	8
Minimum	15.00000	15.00000	5.00000	2.00000	10.00000
Maximum	77.00000	15.00000	5.00000	2.00000	280.00000
Median	61.50000	15.00000	5.00000	2.00000	160.00000
Mean	55.80000	15.00000	5.00000	2.00000	145.00000
Standard Dev	15.47724	0.00000	0.00000	0.00000	106.77078

K. Rasilainen

20.4.1999

Confidential

Least altered felsic volcanic rocks
Area=Pyhäsalmi-Kettuperä and Zr/TiO₂ subgroup=8

	SiO2	TiO2	Al2O3	Fe2O3	MNO
N of cases	176	176	176	176	176
Minimum	71.30000	0.08116	9.06000	0.73365	0.00300
Maximum	83.80000	0.24900	14.46000	4.47121	0.16300
Median	77.40000	0.11800	11.70000	2.39155	0.04100
Mean	77.16136	0.12069	11.71918	2.42972	0.04590
Standard Dev	1.92006	0.02105	0.94989	0.68401	0.02191

	MGO	CAO	NA2O	K2O	P2O5
N of cases	176	176	176	176	176
Minimum	0.01000	0.39000	2.59967	0.39600	0.00300
Maximum	2.21000	5.54000	6.18000	3.71000	0.11400
Median	0.38500	1.56500	4.07566	1.44500	0.00300
Mean	0.45057	1.67721	4.21689	1.55548	0.01088
Standard Dev	0.30641	0.70004	0.93421	0.77940	0.01620

	LOI	CO2	ZR	CR	V
N of cases	81	81	176	176	98
Minimum	0.10000	0.01832	114.00000	10.00000	10.00000
Maximum	1.30000	0.32967	370.00000	266.76000	33.00000
Median	0.50000	0.01832	197.34407	10.00000	10.00000
Mean	0.50926	0.04613	194.05416	64.56166	10.77919
Standard Dev	0.22462	0.06144	31.39443	71.65330	3.32587

	RB	SR	BA	CU	ZN
N of cases	98	176	176	153	153
Minimum	3.00000	45.00000	53.76000	0.50000	1.50000
Maximum	111.00000	270.72000	996.73163	50.00000	198.54780
Median	26.00000	91.45862	478.74700	23.00000	87.00000
Mean	27.63460	98.61838	491.43970	22.36187	90.46050
Standard Dev	16.78770	37.87590	204.84654	12.40665	45.35700

	PB	NI	S	CO	AG
N of cases	152	152	152	71	66
Minimum	0.50000	0.50000	0.00500	0.50000	0.05000
Maximum	83.21940	30.00000	0.49100	70.00000	2.20000
Median	0.50000	0.50000	0.16572	6.00000	0.50000
Mean	20.75615	2.86850	0.15611	8.69014	0.51591
Standard Dev	23.11804	4.33456	0.10759	10.52085	0.43784

	AU	CL	SC	GA	AS
N of cases	10	86	81	81	81
Minimum	0.02500	20.00000	15.00000	10.00000	15.00000
Maximum	0.02500	120.00000	15.00000	28.00000	15.00000
Median	0.02500	60.00000	15.00000	22.00000	15.00000
Mean	0.02500	52.79070	15.00000	18.07407	15.00000
Standard Dev	0.00000	30.27914	0.00000	6.55320	0.00000

	Y	NB	MO	SB	LA
N of cases	86	86	81	81	81
Minimum	16.00000	2.50000	5.00000	10.00000	15.00000
Maximum	48.00000	27.00000	5.00000	10.00000	39.00000
Median	35.00000	10.00000	5.00000	10.00000	15.00000
Mean	34.15116	8.24419	5.00000	10.00000	17.82716
Standard Dev	5.15071	5.35490	0.00000	0.00000	6.58937

	CE	BI	TH	U	W
N of cases	86	81	81	86	5
Minimum	15.00000	15.00000	5.00000	2.00000	10.00000
Maximum	90.00000	15.00000	5.00000	2.00000	240.00000
Median	64.00000	15.00000	5.00000	2.00000	160.00000
Mean	63.10465	15.00000	5.00000	2.00000	152.00000
Standard Dev	12.17329	0.00000	0.00000	0.00000	88.71302

K. Rasilainen

20.4.1999

Confidential

Least altered felsic volcanic rocks
Area=Pyhäsalmi-Kettuperä and Zr/TiO₂ subgroup=9

	SIO2	TIO2	AL2O3	FE2O3	MNO
N of cases	5	5	5	5	5
Minimum	75.60000	0.08116	10.60000	2.27255	0.03300
Maximum	79.50000	0.10148	13.30000	3.56608	0.08800
Median	76.10000	0.09078	11.40000	2.54894	0.04400
Mean	77.32000	0.09100	11.72000	2.76343	0.04960
Standard Dev	1.99800	0.00754	1.19038	0.53422	0.02221

	MGO	CAO	NA2O	K2O	P2O5
N of cases	5	5	5	5	5
Minimum	0.04000	0.97000	2.88971	0.58000	0.00300
Maximum	0.55000	3.45000	4.96291	3.18000	0.02268
Median	0.06000	2.16000	3.93168	1.11000	0.00300
Mean	0.22000	2.21800	4.00043	1.42000	0.01036
Standard Dev	0.23885	0.88638	0.77739	1.05847	0.01012

	LOI	CO2	ZR	CR	V
N of cases	0	0	5	5	0
Minimum	.	.	177.60000	151.24468	.
Maximum	.	.	214.60000	267.38788	.
Median	.	.	192.40000	186.08764	.
Mean	.	.	192.40000	193.05623	.
Standard Dev	.	.	13.84413	48.30775	.

	RB	SR	BA	CU	ZN
N of cases	0	5	5	5	5
Minimum	.	99.40003	139.86891	9.70260	115.59660
Maximum	.	139.10704	793.22673	41.45190	170.89740
Median	.	115.28283	311.24145	32.04470	137.48650
Mean	.	118.45939	379.79047	28.28182	139.56028
Standard Dev	.	16.46764	252.62469	13.13118	24.43158

	PB	NI	S	CO	AG
N of cases	5	5	5	5	5
Minimum	46.38190	2.49920	0.18183	3.00000	0.05000
Maximum	96.48090	20.04920	0.27853	9.00000	0.20000
Median	81.74590	8.34920	0.23824	6.00000	0.05000
Mean	75.26250	10.10420	0.23985	6.40000	0.08000
Standard Dev	18.94465	7.37399	0.04085	2.30217	0.06708

	AU	CL	SC	GA	AS
N of cases	5	0	0	0	0
Minimum	0.02500
Maximum	0.02500
Median	0.02500
Mean	0.02500
Standard Dev	0.00000

	Y	NB	MO	SB	LA
N of cases	0	0	0	0	0
Minimum
Maximum
Median
Mean
Standard Dev

	CE	BI	TH	U	W
N of cases	0	0	0	0	0
Minimum
Maximum
Median
Mean
Standard Dev

K. Rasilainen

20.4.1999

Confidential

Least altered felsic volcanic rocks
Area=Mullikkoräme and Zr/TiO₂ subgroup=1

	SiO2	TiO2	Al2O3	Fe2O3	MNO
N of cases	10	10	10	10	10
Minimum	65.40000	0.29200	12.70000	0.96708	0.03500
Maximum	74.00000	0.70164	16.10000	7.66781	0.18800
Median	68.40000	0.42361	15.05000	4.45365	0.07550
Mean	68.69000	0.41927	14.89000	4.41978	0.09080
Standard Dev	2.61298	0.12380	1.16280	1.93690	0.04487

	MGO	CAO	NA2O	K2O	P2O5
N of cases	10	10	10	10	10
Minimum	1.63000	2.13000	3.12000	0.33100	0.06900
Maximum	3.67000	5.32000	6.47000	1.67326	0.20700
Median	2.54000	3.48000	4.41500	0.64300	0.10409
Mean	2.60100	3.36000	4.47766	0.75606	0.11175
Standard Dev	0.72960	0.88559	0.82108	0.39934	0.04286

	LOI	CO2	ZR	CR	V
N of cases	1	1	10	10	10
Minimum	1.40000	0.10989	74.00000	10.00000	29.24000
Maximum	1.40000	0.10989	180.60780	104.78740	151.64000
Median	1.40000	0.10989	115.75102	31.57274	86.67582
Mean	1.40000	0.10989	121.77432	42.85798	87.45883
Standard Dev	.	.	29.83585	31.44358	41.51557

	RB	SR	BA	CU	ZN
N of cases	10	10	10	10	10
Minimum	12.86481	104.90400	80.64000	0.50000	10.00000
Maximum	37.42765	533.19474	564.48000	41.95820	170.89740
Median	18.29521	223.83200	282.24000	24.84645	100.35335
Mean	20.86409	261.73709	297.05600	20.30646	92.26452
Standard Dev	8.55460	153.03458	173.61559	16.82634	46.71553

	PB	NI	S	CO	AG
N of cases	10	10	10	9	5
Minimum	0.50000	0.50000	0.00500	0.50000	0.05000
Maximum	52.27590	41.00000	0.41200	140.00000	1.60000
Median	31.64690	12.64960	0.20250	20.00000	0.50000
Mean	27.90046	13.91718	0.17758	34.66667	0.72000
Standard Dev	18.33000	14.48381	0.14576	43.30344	0.73875

	AU	CL	SC	GA	AS
N of cases	0	5	1	1	1
Minimum	.	60.00000	15.00000	24.00000	15.00000
Maximum	.	150.00000	15.00000	24.00000	15.00000
Median	.	80.00000	15.00000	24.00000	15.00000
Mean	.	94.00000	15.00000	24.00000	15.00000
Standard Dev	.	34.35113	.	.	.

	Y	NB	MO	SB	LA
N of cases	5	5	1	1	1
Minimum	18.00000	2.50000	5.00000	10.00000	15.00000
Maximum	29.00000	25.00000	5.00000	10.00000	15.00000
Median	22.00000	21.00000	5.00000	10.00000	15.00000
Mean	22.40000	18.30000	5.00000	10.00000	15.00000
Standard Dev	4.03733	9.03881	.	.	.

	CE	BI	TH	U	W
N of cases	5	1	1	5	4
Minimum	50.00000	15.00000	5.00000	2.00000	10.00000
Maximum	60.00000	15.00000	5.00000	2.00000	120.00000
Median	50.00000	15.00000	5.00000	2.00000	20.00000
Mean	52.80000	15.00000	5.00000	2.00000	42.50000
Standard Dev	4.38178	.	.	0.00000	52.51984

K. Rasilainen

20.4.1999

Confidential

Least altered felsic volcanic rocks
Area=Mullikkoräme and Zr/TiO₂ subgroup=2

	SIO2	TIO2	AL2O3	FE2O3	MNO
N of cases	21	21	21	21	21
Minimum	66.60000	0.23800	12.10000	2.61223	0.04600
Maximum	75.20000	0.44061	15.00000	5.46769	0.16900
Median	72.10000	0.35200	13.60000	4.38000	0.07700
Mean	71.97619	0.34065	13.58571	4.21451	0.08605
Standard Dev	1.87774	0.06849	0.77090	0.73945	0.03485
	MGO	CAO	NA2O	K2O	P2O5
N of cases	21	21	21	21	21
Minimum	0.80000	0.54700	2.99000	0.20300	0.04300
Maximum	5.38000	6.93000	6.61000	1.89000	0.14400
Median	2.14000	1.82000	4.55000	0.84100	0.07636
Mean	2.26762	2.00605	4.48066	0.86203	0.08471
Standard Dev	1.04666	1.29128	0.98102	0.40417	0.02642
	LOI	CO2	ZR	CR	V
N of cases	2	2	21	21	21
Minimum	0.88000	0.01832	88.80000	10.00000	10.00000
Maximum	1.46000	0.29304	172.16958	331.26664	97.59012
Median	1.17000	0.15568	140.60000	10.00000	23.80000
Mean	1.17000	0.15568	130.59636	33.13590	31.97043
Standard Dev	0.41012	0.19426	27.30069	70.96110	22.99403
	RB	SR	BA	CU	ZN
N of cases	21	21	21	21	21
Minimum	10.05400	53.29800	143.36000	0.50000	30.00000
Maximum	45.61526	319.93844	689.92000	43.94260	170.00000
Median	21.05242	118.44000	313.60000	17.93390	85.00000
Mean	22.65270	129.37447	338.16952	15.97091	89.84960
Standard Dev	9.19226	62.40658	147.88415	15.58903	45.26300
	PB	NI	S	CO	AG
N of cases	21	21	21	19	9
Minimum	0.50000	0.50000	0.06200	0.50000	0.20000
Maximum	81.74590	26.87420	0.48500	56.00000	1.40000
Median	30.00000	0.50000	0.28000	27.00000	0.70000
Mean	32.01686	5.81394	0.27937	21.36842	0.80000
Standard Dev	22.74731	7.84172	0.12527	20.65917	0.45826
	AU	CL	SC	GA	AS
N of cases	0	12	2	2	2
Minimum	.	20.00000	15.00000	26.00000	15.00000
Maximum	.	90.00000	15.00000	26.00000	15.00000
Median	.	70.00000	15.00000	26.00000	15.00000
Mean	.	62.50000	15.00000	26.00000	15.00000
Standard Dev	.	21.79449	0.00000	0.00000	0.00000
	Y	NB	MO	SB	LA
N of cases	12	12	2	2	2
Minimum	18.00000	2.50000	5.00000	10.00000	15.00000
Maximum	33.00000	26.00000	5.00000	10.00000	15.00000
Median	21.50000	19.00000	5.00000	10.00000	15.00000
Mean	22.66667	18.20833	5.00000	10.00000	15.00000
Standard Dev	4.51932	6.17715	0.00000	0.00000	0.00000
	CE	BI	TH	U	W
N of cases	12	2	2	12	10
Minimum	30.00000	15.00000	5.00000	2.00000	10.00000
Maximum	76.00000	15.00000	5.00000	2.00000	360.00000
Median	50.00000	15.00000	5.00000	2.00000	40.00000
Mean	53.08333	15.00000	5.00000	2.00000	129.00000
Standard Dev	13.69445	0.00000	0.00000	0.00000	141.84890

GEOCHEMISTRY REPORT
Appendix C3

14

K. Rasilainen

20.4.1999

Confidential

Least altered felsic volcanic rocks
Area=Mullikkoräme and Zr/TiO₂ subgroup=3

	SIO2	TIO2	AL2O3	FE2O3	MNO
N of cases	105	105	105	105	105
Minimum	61.70000	0.20400	11.70000	0.73365	0.01900
Maximum	76.10000	0.48126	15.00000	6.35216	0.17000
Median	72.90000	0.34754	13.50000	4.12993	0.08000
Mean	72.57714	0.34019	13.45810	3.96364	0.08570
Standard Dev	2.22621	0.04193	0.59964	1.00406	0.03520
	MGO	CAO	NA2O	K2O	P2O5
N of cases	105	105	105	105	105
Minimum	0.38000	0.38300	2.94000	0.21000	0.05200
Maximum	3.49000	4.10000	8.11000	1.92000	0.16922
Median	1.84000	1.33000	4.85000	0.75300	0.07976
Mean	1.81476	1.61562	4.87590	0.78915	0.08304
Standard Dev	0.66510	0.82847	0.86054	0.32663	0.01721
	LOI	CO2	ZR	CR	V
N of cases	19	19	105	105	102
Minimum	0.50000	0.01832	96.20000	10.00000	10.00000
Maximum	2.54000	0.07326	214.36068	563.55304	64.99772
Median	0.90000	0.01832	155.29314	10.00000	19.36836
Mean	1.02211	0.02603	152.68808	53.11059	24.09143
Standard Dev	0.51854	0.01761	19.64659	102.23700	13.96948
	RB	SR	BA	CU	ZN
N of cases	102	105	105	105	105
Minimum	3.00000	55.00000	62.72000	0.50000	10.00000
Maximum	63.00000	620.43595	959.00000	49.68320	199.69990
Median	21.05242	116.37562	349.44000	21.12200	112.14030
Mean	20.96959	127.69403	373.24152	20.65436	106.75176
Standard Dev	8.27784	77.61500	181.72859	14.51497	39.15997
	PB	NI	S	CO	AG
N of cases	105	105	105	86	70
Minimum	0.50000	0.50000	0.00500	0.50000	0.05000
Maximum	75.85190	70.00000	0.49609	72.00000	3.00000
Median	34.59390	6.39920	0.24630	15.00000	0.60000
Mean	29.31261	7.90831	0.26309	24.45349	0.70000
Standard Dev	21.14587	9.33800	0.13599	20.00686	0.65464
	AU	CL	SC	GA	AS
N of cases	1	35	19	19	19
Minimum	0.02500	20.00000	15.00000	22.00000	15.00000
Maximum	0.02500	150.00000	15.00000	30.00000	15.00000
Median	0.02500	80.00000	15.00000	25.00000	15.00000
Mean	0.02500	81.14286	15.00000	25.52632	15.00000
Standard Dev	.	31.13268	0.00000	2.85518	0.00000
	Y	NB	MO	SB	LA
N of cases	35	35	19	19	19
Minimum	15.00000	2.50000	5.00000	10.00000	15.00000
Maximum	32.00000	24.00000	5.00000	10.00000	33.00000
Median	26.00000	12.00000	5.00000	10.00000	15.00000
Mean	24.97143	13.70000	5.00000	10.00000	16.78947
Standard Dev	4.37564	7.33365	0.00000	0.00000	5.37048
	CE	BI	TH	U	W
N of cases	35	19	19	35	16
Minimum	15.00000	15.00000	5.00000	2.00000	10.00000
Maximum	76.00000	15.00000	5.00000	2.00000	220.00000
Median	55.00000	15.00000	5.00000	2.00000	120.00000
Mean	53.20000	15.00000	5.00000	2.00000	120.00000
Standard Dev	14.39935	0.00000	0.00000	0.00000	59.44185

K. Rasilainen

20.4.1999

Confidential

Least altered felsic volcanic rocks
Area=Mullikkoräme and Zr/TiO₂ subgroup=4

	SIO2	TIO2	AL2O3	FE2O3	MNO
N of cases	222	222	222	222	222
Minimum	62.80000	0.17900	10.70000	1.84137	0.02600
Maximum	78.40000	0.52298	17.30000	7.51302	0.21700
Median	73.80000	0.31437	13.00000	3.55503	0.06750
Mean	73.77793	0.31871	13.09685	3.68054	0.07472
Standard Dev	2.30418	0.04466	1.01898	0.91161	0.03371

	MGO	CAO	NA2O	K2O	P2O5
N of cases	222	222	222	222	222
Minimum	0.01000	0.44700	2.63000	0.11400	0.03500
Maximum	5.52000	5.22000	7.18000	2.01230	0.10106
Median	1.66000	1.29500	4.61500	0.87059	0.06329
Mean	1.68766	1.52631	4.60569	0.89024	0.06527
Standard Dev	0.70477	0.76638	0.78643	0.36727	0.01375

	LOI	CO2	ZR	CR	V
N of cases	33	33	222	222	215
Minimum	0.38000	0.01832	96.20000	10.00000	10.00000
Maximum	2.52000	0.07326	256.55178	424.18120	71.51620
Median	0.80000	0.01832	164.50000	10.00000	25.88684
Mean	0.85364	0.02720	171.33470	64.45959	27.62389
Standard Dev	0.41145	0.01838	23.71776	100.76283	13.01452

	RB	SR	BA	CU	ZN
N of cases	215	222	222	222	222
Minimum	3.00000	44.00000	62.72000	0.50000	20.00000
Maximum	53.80287	252.08417	944.00000	49.68320	196.24360
Median	21.05242	116.37562	394.24000	24.09860	114.44450
Mean	21.60873	118.94438	411.77712	25.03157	116.82927
Standard Dev	8.33791	33.33693	196.36692	11.81154	34.45027

	PB	NI	S	CO	AG
N of cases	222	222	221	189	186
Minimum	0.50000	0.50000	0.00500	0.50000	0.05000
Maximum	96.48090	24.92420	0.49609	114.00000	4.60000
Median	37.54090	8.34920	0.23824	19.00000	0.70000
Mean	34.38126	8.45186	0.24537	29.47884	0.78683
Standard Dev	23.04807	5.92740	0.11914	23.61182	0.68296

	AU	CL	SC	GA	AS
N of cases	1	36	33	33	33
Minimum	0.01000	20.00000	15.00000	10.00000	15.00000
Maximum	0.01000	130.00000	15.00000	29.00000	15.00000
Median	0.01000	80.00000	15.00000	23.00000	15.00000
Mean	0.01000	71.94444	15.00000	22.33333	15.00000
Standard Dev	.	32.32155	0.00000	5.21217	0.00000

	Y	NB	MO	SB	LA
N of cases	36	36	33	33	33
Minimum	14.00000	2.50000	5.00000	10.00000	15.00000
Maximum	34.00000	19.00000	5.00000	10.00000	34.00000
Median	29.00000	10.00000	5.00000	10.00000	15.00000
Mean	28.02778	7.48611	5.00000	10.00000	17.09091
Standard Dev	4.29941	5.15958	0.00000	0.00000	5.73565

	CE	BI	TH	U	W
N of cases	36	33	33	36	3
Minimum	15.00000	15.00000	5.00000	2.00000	280.00000
Maximum	76.00000	15.00000	5.00000	2.00000	400.00000
Median	63.50000	15.00000	5.00000	2.00000	330.00000
Mean	59.61111	15.00000	5.00000	2.00000	336.66667
Standard Dev	12.17322	0.00000	0.00000	0.00000	60.27714

K. Rasilainen

20.4.1999

Confidential

Least altered felsic volcanic rocks
Area=Mullikkoräme and Zr/TiO₂ subgroup=5

	SiO2	TiO2	Al2O3	Fe2O3	MNO
N of cases	92	92	92	92	92
Minimum	59.20000	0.18000	11.00000	1.60920	0.01400
Maximum	78.50000	0.45131	16.00000	11.53735	0.24700
Median	74.00000	0.28602	12.90000	3.33944	0.06350
Mean	73.73370	0.29417	13.01196	3.49963	0.06728
Standard Dev	2.92640	0.04629	0.99888	1.25871	0.03219

	MGO	CAO	NA2O	K2O	P2O5
N of cases	92	92	92	92	92
Minimum	0.46000	0.60000	2.42278	0.21539	0.02800
Maximum	5.40000	7.20000	7.38000	2.33439	0.12600
Median	1.74000	1.32000	4.56475	0.75950	0.06102
Mean	1.93533	1.66772	4.60281	0.85483	0.06204
Standard Dev	0.89692	1.15267	1.03225	0.45315	0.01597

	LOI	CO2	ZR	CR	V
N of cases	4	4	92	92	78
Minimum	0.91000	0.01832	133.20000	10.00000	10.00000
Maximum	1.19000	0.01832	290.30466	743.57500	97.59012
Median	0.99000	0.01832	180.60780	10.00000	25.88684
Mean	1.02000	0.01832	187.76806	62.85746	29.23714
Standard Dev	0.11972	0.00000	28.60590	136.87542	14.19668

	RB	SR	BA	CU	ZN
N of cases	78	92	92	92	92
Minimum	12.86481	58.21481	89.60000	0.50000	20.00000
Maximum	70.17810	232.69723	985.60000	49.89580	185.87470
Median	21.05242	126.06908	340.48000	21.29180	120.78105
Mean	23.42286	124.25443	405.23522	23.26126	126.01676
Standard Dev	10.02061	35.21048	207.05489	10.46154	31.49791

	PB	NI	S	CO	AG
N of cases	92	92	90	88	85
Minimum	0.50000	0.50000	0.00500	0.50000	0.05000
Maximum	83.21940	46.37420	0.48000	87.00000	4.20000
Median	37.54090	9.32420	0.21406	32.00000	0.60000
Mean	38.89342	10.10256	0.23650	29.63636	0.69588
Standard Dev	18.21024	7.50052	0.10106	21.61812	0.71590

	AU	CL	SC	GA	AS
N of cases	1	7	4	4	4
Minimum	0.00050	20.00000	15.00000	10.00000	15.00000
Maximum	0.00050	160.00000	15.00000	25.00000	15.00000
Median	0.00050	80.00000	15.00000	23.00000	15.00000
Mean	0.00050	84.28571	15.00000	20.25000	15.00000
Standard Dev	.	54.72877	0.00000	7.08872	0.00000

	Y	NB	MO	SB	LA
N of cases	7	7	4	4	4
Minimum	25.00000	2.50000	5.00000	10.00000	15.00000
Maximum	34.00000	22.00000	5.00000	10.00000	39.00000
Median	26.00000	18.00000	5.00000	10.00000	15.00000
Mean	27.28571	14.28571	5.00000	10.00000	21.00000
Standard Dev	3.25137	8.35592	0.00000	0.00000	12.00000

	CE	BI	TH	U	W
N of cases	7	4	4	7	3
Minimum	40.00000	15.00000	5.00000	2.00000	10.00000
Maximum	120.00000	15.00000	5.00000	2.00000	330.00000
Median	70.00000	15.00000	5.00000	2.00000	170.00000
Mean	75.42857	15.00000	5.00000	2.00000	170.00000
Standard Dev	26.30499	0.00000	0.00000	0.00000	160.00000

K. Rasilainen

20.4.1999

Confidential

Least altered felsic volcanic rocks
Area=Mullikkoräme and Zr/TiO₂ subgroup=6

	SIO2	TIO2	AL2O3	FE2O3	MNO
N of cases	102	102	102	102	102
Minimum	68.30000	0.14600	10.50000	1.26721	0.01800
Maximum	80.60000	0.45559	15.10000	5.56719	0.14000
Median	74.70000	0.23895	13.00000	2.75901	0.04150
Mean	74.71863	0.26022	12.86961	2.92743	0.04638
Standard Dev	2.24899	0.07273	0.81055	0.93932	0.02025

	MGO	CAO	NA2O	K2O	P2O5
N of cases	102	102	102	102	102
Minimum	0.51000	0.62000	2.85000	0.09300	0.02500
Maximum	5.76000	5.46000	6.54000	2.18000	0.11470
Median	1.83000	1.92500	4.44500	0.80800	0.04739
Mean	1.93451	1.96328	4.46959	0.84593	0.05490
Standard Dev	0.92764	0.78626	0.79807	0.39806	0.02159

	LOI	CO2	ZR	CR	V
N of cases	5	5	102	102	102
Minimum	0.50000	0.01832	111.00000	10.00000	10.00000
Maximum	1.89000	0.01832	400.00152	459.02416	51.00000
Median	0.69000	0.01832	205.92246	10.00000	19.36836
Mean	0.97400	0.01832	221.47610	24.22843	23.70673
Standard Dev	0.57683	0.00000	61.18630	53.22294	9.76700

	RB	SR	BA	CU	ZN
N of cases	102	102	102	102	102
Minimum	3.00000	52.00000	80.64000	0.50000	10.00000
Maximum	102.92854	252.08417	994.56000	46.15550	180.11420
Median	21.05242	135.76255	322.56000	18.03965	104.65165
Mean	22.81720	129.55109	379.47255	19.12774	103.54441
Standard Dev	12.93285	34.91614	190.82422	10.24071	32.77707

	PB	NI	S	CO	AG
N of cases	102	102	102	99	89
Minimum	0.50000	0.50000	0.00500	0.50000	0.05000
Maximum	86.16640	78.54920	0.46386	74.00000	3.00000
Median	37.54090	6.39920	0.18989	30.00000	0.40000
Mean	36.86939	8.88537	0.21593	31.59596	0.50281
Standard Dev	17.11857	10.25288	0.10500	19.50754	0.53286

	AU	CL	SC	GA	AS
N of cases	0	15	5	5	5
Minimum	.	20.00000	15.00000	10.00000	15.00000
Maximum	.	100.00000	15.00000	31.00000	15.00000
Median	.	60.00000	15.00000	10.00000	15.00000
Mean	.	58.66667	15.00000	16.20000	15.00000
Standard Dev	.	28.99918	0.00000	9.33809	0.00000

	Y	NB	MO	SB	LA
N of cases	15	15	5	5	5
Minimum	20.00000	2.50000	5.00000	10.00000	15.00000
Maximum	53.00000	31.00000	24.00000	10.00000	35.00000
Median	24.00000	21.00000	5.00000	10.00000	15.00000
Mean	25.53333	20.03333	8.80000	10.00000	22.00000
Standard Dev	7.98093	8.00996	8.49706	0.00000	9.74679

	CE	BI	TH	U	W
N of cases	15	5	5	15	10
Minimum	30.00000	15.00000	5.00000	2.00000	10.00000
Maximum	112.00000	15.00000	5.00000	2.00000	280.00000
Median	60.00000	15.00000	5.00000	2.00000	70.00000
Mean	61.66667	15.00000	5.00000	2.00000	115.00000
Standard Dev	20.63861	0.00000	0.00000	0.00000	108.65337

K. Rasilainen

20.4.1999

Confidential

Least altered felsic volcanic rocks
Area=Mullikoräme and Zr/TiO₂ subgroup=7

	SiO2	TiO2	Al2O3	Fe2O3	MNO
N of cases	13	13	13	13	13
Minimum	65.00000	0.16800	12.00000	1.07824	0.02300
Maximum	78.70000	0.35182	17.50000	4.82645	0.09100
Median	75.60000	0.22237	12.70000	2.77006	0.04400
Mean	74.42308	0.23679	13.13077	2.74682	0.04492
Standard Dev	4.06861	0.04336	1.43026	1.09283	0.01745

	MGO	CAO	NA2O	K2O	P2O5
N of cases	13	13	13	13	13
Minimum	0.77000	0.63000	2.82904	0.30500	0.02600
Maximum	3.83000	2.99000	6.63000	2.20000	0.07976
Median	1.21000	1.39000	5.26000	0.81400	0.03887
Mean	1.86923	1.49808	4.87727	0.89353	0.04212
Standard Dev	1.14287	0.76175	1.19499	0.57404	0.01392

	LOI	CO2	ZR	CR	V
N of cases	0	0	13	13	11
Minimum	.	.	177.60000	10.00000	13.60000
Maximum	.	.	366.24864	58.33012	38.92380
Median	.	.	239.67534	10.00000	25.88684
Mean	.	.	252.42585	17.35122	27.73280
Standard Dev	.	.	51.64089	16.05198	7.04201

	RB	SR	BA	CU	ZN
N of cases	11	13	13	13	13
Minimum	9.14000	58.21481	98.56000	13.00000	71.00000
Maximum	111.11616	184.22989	582.40000	41.95820	166.28900
Median	21.05242	96.98868	295.68000	22.63750	130.57390
Mean	28.15709	108.25077	330.14154	24.19645	127.76375
Standard Dev	29.15920	46.54155	137.24925	8.51538	24.41364

	PB	NI	S	CO	AG
N of cases	13	13	13	13	13
Minimum	16.00000	2.00000	0.00500	2.00000	0.05000
Maximum	69.95790	11.27420	0.42000	64.00000	1.10000
Median	43.43490	8.34920	0.18989	33.00000	0.60000
Mean	43.13806	7.78580	0.20639	30.76923	0.50385
Standard Dev	14.05716	2.71524	0.09749	22.46165	0.34548

	AU	CL	SC	GA	AS
N of cases	0	0	0	0	0
Minimum
Maximum
Median
Mean
Standard Dev

	Y	NB	MO	SB	LA
N of cases	0	0	0	0	0
Minimum
Maximum
Median
Mean
Standard Dev

	CE	BI	TH	U	W
N of cases	0	0	0	0	0
Minimum
Maximum
Median
Mean
Standard Dev

K. Rasilainen

20.4.1999

Confidential

Least altered felsic volcanic rocks
Area=Mullikkoräme and Zr/TiO₂ subgroup=8

	SIO2	TIO2	AL2O3	FE2O3	MNO
N of cases	41	41	41	41	41
Minimum	74.80000	0.13251	10.50000	1.68659	0.02800
Maximum	79.90000	0.25981	12.60000	3.76509	0.07200
Median	76.50000	0.15900	12.20000	2.93590	0.04700
Mean	76.64634	0.16907	12.05854	2.86967	0.04785
Standard Dev	0.97675	0.02823	0.46205	0.43065	0.01069
	MGO	CAO	NA2O	K2O	P2O5
N of cases	41	41	41	41	41
Minimum	0.20000	0.42000	3.68000	0.36500	0.01800
Maximum	2.50000	1.28000	6.23000	2.27506	0.05420
Median	1.17000	0.79000	5.07000	1.04604	0.03631
Mean	1.15268	0.82483	5.11439	1.17206	0.03795
Standard Dev	0.54111	0.20118	0.59461	0.53110	0.00768
	LOI	CO2	ZR	CR	V
N of cases	7	7	41	41	41
Minimum	0.70000	0.01832	248.11356	10.00000	10.00000
Maximum	1.39000	0.10989	338.00000	40.90864	32.40532
Median	0.83000	0.01832	290.30466	10.00000	19.36836
Mean	0.93429	0.03140	289.54505	17.48841	16.89484
Standard Dev	0.29131	0.03461	22.03629	11.81857	5.92783
	RB	SR	BA	CU	ZN
N of cases	41	41	41	41	41
Minimum	3.00000	38.82787	134.40000	0.50000	39.00000
Maximum	61.99048	87.29521	689.92000	42.95040	189.33100
Median	29.24004	67.90828	376.32000	20.28570	122.50920
Mean	29.03445	65.93301	395.19317	21.59131	123.94304
Standard Dev	13.04302	12.64460	147.07362	10.93095	31.85697
	PB	NI	S	CO	AG
N of cases	41	41	40	34	34
Minimum	0.50000	0.50000	0.00500	23.00000	0.10000
Maximum	91.00000	11.27420	0.49609	71.00000	1.80000
Median	39.01440	7.37420	0.16975	48.00000	0.35000
Mean	37.19326	6.22314	0.15823	48.08824	0.49118
Standard Dev	18.55590	3.27942	0.12329	9.05662	0.40629
	AU	CL	SC	GA	AS
N of cases	0	7	7	7	7
Minimum	.	20.00000	15.00000	22.00000	15.00000
Maximum	.	90.00000	15.00000	29.00000	15.00000
Median	.	60.00000	15.00000	26.00000	15.00000
Mean	.	52.85714	15.00000	25.71429	15.00000
Standard Dev	.	32.51373	0.00000	2.13809	0.00000
	Y	NB	MO	SB	LA
N of cases	7	7	7	7	7
Minimum	48.00000	27.00000	5.00000	10.00000	39.00000
Maximum	55.00000	32.00000	5.00000	10.00000	60.00000
Median	49.00000	28.00000	5.00000	10.00000	49.00000
Mean	50.00000	28.57143	5.00000	10.00000	48.85714
Standard Dev	2.44949	1.90238	0.00000	0.00000	8.07111
	CE	BI	TH	U	W
N of cases	7	7	7	7	0
Minimum	100.00000	15.00000	5.00000	2.00000	.
Maximum	118.00000	15.00000	5.00000	2.00000	.
Median	102.00000	15.00000	5.00000	2.00000	.
Mean	106.42857	15.00000	5.00000	2.00000	.
Standard Dev	7.61265	0.00000	0.00000	0.00000	.

K. Rasilainen

20.4.1999

Confidential

Least altered felsic volcanic rocks
Area=Mullikoräme and Zr/TiO₂ subgroup=9

	SiO2	TiO2	Al2O3	Fe2O3	MNO
N of cases	1	1	1	1	1
Minimum	78.90000	0.09934	12.00000	1.42125	0.02000
Maximum	78.90000	0.09934	12.00000	1.42125	0.02000
Median	78.90000	0.09934	12.00000	1.42125	0.02000
Mean	78.90000	0.09934	12.00000	1.42125	0.02000
Standard Dev

	MGO	CAO	NA2O	K2O	P2O5
N of cases	1	1	1	1	1
Minimum	1.08000	1.06000	5.31000	0.48662	0.00300
Maximum	1.08000	1.06000	5.31000	0.48662	0.00300
Median	1.08000	1.06000	5.31000	0.48662	0.00300
Mean	1.08000	1.06000	5.31000	0.48662	0.00300
Standard Dev

	LOI	CO2	ZR	CR	V
N of cases	0	0	1	1	1
Minimum	.	.	239.67534	10.00000	10.00000
Maximum	.	.	239.67534	10.00000	10.00000
Median	.	.	239.67534	10.00000	10.00000
Mean	.	.	239.67534	10.00000	10.00000
Standard Dev

	RB	SR	BA	CU	ZN
N of cases	1	1	1	1	1
Minimum	12.86481	96.98868	152.32000	17.15320	104.07560
Maximum	12.86481	96.98868	152.32000	17.15320	104.07560
Median	12.86481	96.98868	152.32000	17.15320	104.07560
Mean	12.86481	96.98868	152.32000	17.15320	104.07560
Standard Dev

	PB	NI	S	CO	AG
N of cases	1	1	1	1	1
Minimum	43.43490	10.29920	0.00500	59.00000	0.50000
Maximum	43.43490	10.29920	0.00500	59.00000	0.50000
Median	43.43490	10.29920	0.00500	59.00000	0.50000
Mean	43.43490	10.29920	0.00500	59.00000	0.50000
Standard Dev

	AU	CL	SC	GA	AS
N of cases	0	0	0	0	0
Minimum
Maximum
Median
Mean
Standard Dev

	Y	NB	MO	SB	LA
N of cases	0	0	0	0	0
Minimum
Maximum
Median
Mean
Standard Dev

	CE	BI	TH	U	W
N of cases	0	0	0	0	0
Minimum
Maximum
Median
Mean
Standard Dev

K. Rasilainen

20.4.1999

Confidential

Least altered mafic volcanic rocks

Elements for which these values were used as background concentrations regardless of the Zr/TiO₂ subgroup are bolded

	SIO2	TIO2	AL2O3	FE2O3	MNO
N of cases	375	375	375	375	375
Minimum	45.10000	0.29512	11.80000	6.07576	0.10200
Maximum	64.20000	1.84000	20.70000	15.62802	0.43600
Median	51.50000	0.53700	15.90000	10.60000	0.18000
Mean	52.00240	0.60991	15.88026	10.68421	0.18940
Standard Dev	3.22087	0.22330	1.58606	1.74676	0.04941

	MGO	CAO	NA2O	K2O	P2O5
N of cases	375	375	375	375	375
Minimum	1.92000	4.01000	1.62832	0.06900	0.03300
Maximum	8.51000	19.50000	6.63867	2.76000	0.58100
Median	5.55000	8.96000	3.53000	0.62800	0.10362
Mean	5.39445	9.07597	3.59112	0.71289	0.12919
Standard Dev	1.37042	2.43506	0.79954	0.43273	0.08624

	LOI	CO2	ZR	CR	V
N of cases	150	150	375	375	242
Minimum	0.20000	0.01832	5.00000	10.00000	82.28000
Maximum	2.71000	2.16117	248.11356	1128.00000	376.00000
Median	0.70000	0.01832	49.00000	116.40172	258.40000
Mean	0.76633	0.08669	52.28555	158.05528	251.54572
Standard Dev	0.33199	0.22037	34.89459	135.12267	51.58307

	RB	SR	BA	CU	ZN
N of cases	242	375	375	363	363
Minimum	3.00000	57.52800	22.05028	0.50000	14.00000
Maximum	123.00000	561.00000	986.02084	195.49480	198.00000
Median	15.53800	203.00000	286.72000	72.02530	109.00000
Mean	19.11703	214.98426	307.51969	75.01105	112.15564
Standard Dev	16.83597	94.82901	178.51665	43.88860	32.27434

	PB	NI	S	CO	AG
N of cases	363	363	363	214	165
Minimum	0.50000	0.50000	0.00500	0.50000	0.05000
Maximum	97.95440	242.00000	0.49300	70.00000	5.90000
Median	0.50000	34.00000	0.16700	20.00000	1.00000
Mean	19.21560	36.83410	0.17250	23.53505	1.27576
Standard Dev	24.45217	29.29820	0.13019	13.81135	1.08095

	AU	CL	SC	GA	AS
N of cases	18	198	150	150	150
Minimum	0.00050	20.00000	15.00000	10.00000	15.00000
Maximum	0.07000	290.00000	51.00000	32.00000	15.00000
Median	0.02500	100.00000	41.00000	23.00000	15.00000
Mean	0.02617	100.75758	37.88667	21.76000	15.00000
Standard Dev	0.01500	35.93468	10.18654	6.09178	0.00000

	Y	NB	MO	SB	LA
N of cases	198	198	150	150	150
Minimum	1.50000	2.50000	5.00000	10.00000	15.00000
Maximum	30.00000	27.00000	5.00000	28.00000	45.00000
Median	10.00000	2.50000	5.00000	10.00000	15.00000
Mean	9.69949	6.34091	5.00000	10.12000	15.20000
Standard Dev	7.55836	6.48025	0.00000	1.46969	2.44949

	CE	BI	TH	U	W
N of cases	198	150	150	198	48
Minimum	15.00000	15.00000	5.00000	2.00000	10.00000
Maximum	112.00000	15.00000	5.00000	15.00000	140.00000
Median	15.00000	15.00000	5.00000	2.00000	10.00000
Mean	22.69697	15.00000	5.00000	3.12626	13.54167
Standard Dev	13.80242	0.00000	0.00000	2.86573	19.18439

K. Rasilainen

20.4.1999

Confidential

Least altered mafic volcanic rocks
Area=Pyhäsalmi-Kettuperä and Zr/TiO₂ subgroup=1

	SiO ₂	TiO ₂	Al ₂ O ₃	Fe ₂ O ₃	MnO
N of cases	177	177	177	177	177
Minimum	46.40000	0.30200	12.43000	7.99232	0.10200
Maximum	60.30000	1.84000	20.70000	15.62802	0.31300
Median	50.90000	0.47800	16.30000	10.70000	0.17700
Mean	51.36723	0.55145	16.34376	10.94918	0.18025
Standard Dev	1.94354	0.19458	1.29763	1.34972	0.02801

	MgO	CaO	Na ₂ O	K ₂ O	P ₂ O ₅
N of cases	177	177	177	177	177
Minimum	3.00000	4.55000	2.02000	0.11354	0.03300
Maximum	8.16000	14.60000	6.23000	2.20000	0.40600
Median	5.90000	9.34000	3.52000	0.59800	0.08416
Mean	5.94814	9.36808	3.54122	0.64225	0.10299
Standard Dev	1.08759	1.74546	0.72445	0.36145	0.06490

	LOI	CO ₂	Zr	CR	V
N of cases	123	123	177	177	158
Minimum	0.20000	0.01832	5.00000	10.00000	116.00000
Maximum	2.71000	2.16117	122.00000	1128.00000	376.00000
Median	0.69000	0.01832	24.00000	101.00000	272.00000
Mean	0.75593	0.09038	28.30120	154.20484	271.30703
Standard Dev	0.34713	0.23393	17.60704	146.65004	34.94213

	RB	SR	BA	CU	ZN
N of cases	158	177	177	172	172
Minimum	3.00000	57.52800	22.05028	0.50000	14.00000
Maximum	98.00000	556.00000	794.00000	191.00000	198.00000
Median	15.53800	178.81405	201.00000	82.50000	108.84200
Mean	16.98994	192.49362	231.47447	82.75720	110.23555
Standard Dev	14.51629	84.38427	142.61938	43.07716	32.85063

	PB	NI	S	CO	AG
N of cases	172	172	172	49	17
Minimum	0.50000	0.50000	0.00500	0.50000	0.60000
Maximum	68.48440	242.00000	0.48000	70.00000	2.70000
Median	0.50000	42.00000	0.10150	37.00000	1.00000
Mean	3.75049	45.51447	0.14263	34.64286	1.30000
Standard Dev	11.36135	28.66592	0.12602	17.76291	0.55453

	AU	CL	SC	GA	AS
N of cases	2	154	123	123	123
Minimum	0.00050	20.00000	15.00000	10.00000	15.00000
Maximum	0.02500	160.00000	51.00000	32.00000	15.00000
Median	0.01275	95.00000	42.00000	22.00000	15.00000
Mean	0.01275	95.58442	41.21951	21.21138	15.00000
Standard Dev	0.01732	29.77008	6.40509	6.13142	0.00000

	Y	NB	MO	SB	LA
N of cases	154	154	123	123	123
Minimum	1.50000	2.50000	5.00000	10.00000	15.00000
Maximum	24.00000	22.00000	5.00000	10.00000	15.00000
Median	5.50000	2.50000	5.00000	10.00000	15.00000
Mean	7.23701	5.24026	5.00000	10.00000	15.00000
Standard Dev	6.20700	5.49843	0.00000	0.00000	0.00000

	CE	BI	TH	U	W
N of cases	154	123	123	154	31
Minimum	15.00000	15.00000	5.00000	2.00000	10.00000
Maximum	49.00000	15.00000	5.00000	15.00000	10.00000
Median	15.00000	15.00000	5.00000	2.00000	10.00000
Mean	18.28571	15.00000	5.00000	2.88312	10.00000
Standard Dev	7.75584	0.00000	0.00000	2.57425	0.00000

K. Rasilainen

20.4.1999

Confidential

Least altered mafic volcanic rocks
Area=Pyhäsalmi-Kettuperä and Zr/TiO₂ subgroup=2

	SIO2	TIO2	AL2O3	FE2O3	MNO
N of cases	141	141	141	141	141
Minimum	45.50000	0.29512	11.80000	6.11000	0.10200
Maximum	64.20000	1.69548	18.10000	14.85411	0.37900
Median	52.20000	0.56257	14.70000	10.65289	0.17000
Mean	52.61773	0.62673	14.70958	10.84417	0.17662
Standard Dev	4.22968	0.24133	1.11976	1.87861	0.04026

	MGO	CAO	NA2O	K2O	P2O5
N of cases	141	141	141	141	141
Minimum	1.92000	4.01000	2.01961	0.15621	0.03546
Maximum	8.51000	16.80000	6.63867	2.76000	0.58100
Median	5.25000	8.38000	3.45000	0.81763	0.11129
Mean	5.09085	8.46014	3.50197	0.90970	0.15011
Standard Dev	1.28559	2.23995	0.74201	0.48016	0.10133

	LOI	CO2	ZR	CR	V
N of cases	25	25	141	141	34
Minimum	0.49000	0.01832	37.00000	10.00000	82.28000
Maximum	1.22000	0.32967	248.11356	528.71008	257.00000
Median	0.70000	0.01832	66.60000	128.01604	177.50000
Mean	0.77920	0.04469	76.93258	153.59635	174.15076
Standard Dev	0.21662	0.07700	35.23080	111.52344	52.61828

	RB	SR	BA	CU	ZN
N of cases	34	141	141	134	134
Minimum	3.00000	91.45862	107.52000	0.50000	21.00000
Maximum	123.00000	561.00000	986.02084	195.49480	191.63520
Median	29.70500	218.52106	383.00000	59.04520	107.26595
Mean	34.92943	232.48389	413.35560	64.12949	110.86627
Standard Dev	25.40849	110.60159	166.89536	42.47783	28.93839

	PB	NI	S	CO	AG
N of cases	134	134	134	109	101
Minimum	0.50000	0.50000	0.00500	0.50000	0.05000
Maximum	96.48090	220.00000	0.49300	51.00000	3.20000
Median	37.54090	18.09920	0.18745	18.00000	0.90000
Mean	32.26103	24.70915	0.19467	18.17431	0.87129
Standard Dev	22.34782	26.93613	0.13041	9.21462	0.59613

	AU	CL	SC	GA	AS
N of cases	12	33	25	25	25
Minimum	0.02500	20.00000	15.00000	10.00000	15.00000
Maximum	0.07000	180.00000	42.00000	32.00000	15.00000
Median	0.02500	100.00000	15.00000	25.00000	15.00000
Mean	0.02875	106.66667	22.28000	24.36000	15.00000
Standard Dev	0.01299	28.57738	10.13870	5.52178	0.00000

	Y	NB	MO	SB	LA
N of cases	33	33	25	25	25
Minimum	11.00000	2.50000	5.00000	10.00000	15.00000
Maximum	30.00000	22.00000	5.00000	28.00000	45.00000
Median	18.00000	2.50000	5.00000	10.00000	15.00000
Mean	19.06061	8.18182	5.00000	10.72000	16.20000
Standard Dev	5.42528	7.76190	0.00000	3.60000	6.00000

	CE	BI	TH	U	W
N of cases	33	25	25	33	8
Minimum	15.00000	15.00000	5.00000	2.00000	10.00000
Maximum	112.00000	15.00000	5.00000	12.00000	140.00000
Median	40.00000	15.00000	5.00000	2.00000	10.00000
Mean	39.33333	15.00000	5.00000	3.48485	31.25000
Standard Dev	20.17837	0.00000	0.00000	3.23188	45.17822

K. Rasilainen

20.4.1999

Confidential

Least altered mafic volcanic rocks
Area=Mullikkoräme and Zr/TiO₂ subgroup=1

	SiO2	TiO2	Al2O3	Fe2O3	MNO
N of cases	20	20	20	20	20
Minimum	49.10000	0.43200	15.20000	6.29159	0.13100
Maximum	59.40000	1.56000	20.30000	12.72033	0.43600
Median	52.80000	0.73534	17.25000	10.80767	0.24450
Mean	52.83000	0.80155	17.60000	10.21585	0.26525
Standard Dev	2.92918	0.30667	1.33061	2.04681	0.09153

	MGO	CAO	NA2O	K2O	P2O5
N of cases	20	20	20	20	20
Minimum	3.34000	4.10000	1.82694	0.06900	0.06400
Maximum	8.22000	10.40000	5.72000	0.93400	0.44900
Median	6.27500	7.69500	4.16919	0.38850	0.13961
Mean	5.88250	7.23050	4.05020	0.44440	0.19935
Standard Dev	1.19045	2.08092	1.15170	0.22919	0.12109

	LOI	CO2	ZR	CR	V
N of cases	2	2	20	20	20
Minimum	1.00000	0.07326	5.00000	10.00000	186.32000
Maximum	1.49000	0.69597	99.00000	916.56000	338.77388
Median	1.24500	0.38462	38.57903	76.26600	283.36680
Mean	1.24500	0.38462	43.24914	151.47579	278.35213
Standard Dev	0.34648	0.44032	22.49019	201.04018	36.88505

	RB	SR	BA	CU	ZN
N of cases	20	20	20	20	20
Minimum	3.00000	138.74400	44.80000	0.50000	40.00000
Maximum	30.16200	543.00000	385.28000	180.20810	192.78730
Median	14.16700	200.07900	183.12000	40.00000	117.11385
Mean	15.88810	230.25857	201.62400	51.07679	119.93889
Standard Dev	6.57450	87.22070	110.14879	48.78081	52.65920

	PB	NI	S	CO	AG
N of cases	20	20	20	19	10
Minimum	0.50000	0.50000	0.00500	16.00000	0.05000
Maximum	97.95440	157.00000	0.43969	50.00000	5.50000
Median	0.50000	39.79960	0.16539	33.00000	0.90000
Mean	18.37199	44.34472	0.18779	35.63158	1.67500
Standard Dev	30.35351	39.26100	0.14408	10.95552	1.87012

	AU	CL	SC	GA	AS
N of cases	1	11	2	2	2
Minimum	0.00050	70.00000	15.00000	22.00000	15.00000
Maximum	0.00050	290.00000	41.00000	24.00000	15.00000
Median	0.00050	120.00000	28.00000	23.00000	15.00000
Mean	0.00050	155.45455	28.00000	23.00000	15.00000
Standard Dev	.	73.80564	18.38478	1.41421	0.00000

	Y	NB	MO	SB	LA
N of cases	11	11	2	2	2
Minimum	9.00000	2.50000	5.00000	10.00000	15.00000
Maximum	22.00000	27.00000	5.00000	10.00000	15.00000
Median	17.00000	18.00000	5.00000	10.00000	15.00000
Mean	16.09091	16.22727	5.00000	10.00000	15.00000
Standard Dev	3.78033	5.87947	0.00000	0.00000	0.00000

	CE	BI	TH	U	W
N of cases	11	2	2	11	9
Minimum	15.00000	15.00000	5.00000	2.00000	10.00000
Maximum	50.00000	15.00000	5.00000	13.00000	10.00000
Median	30.00000	15.00000	5.00000	2.00000	10.00000
Mean	34.54545	15.00000	5.00000	5.45455	10.00000
Standard Dev	12.73863	0.00000	0.00000	4.43539	0.00000

K. Rasilainen

20.4.1999

Confidential

Least altered mafic volcanic rocks
Area=Mullikkoräme and Zr/TiO₂ subgroup=2

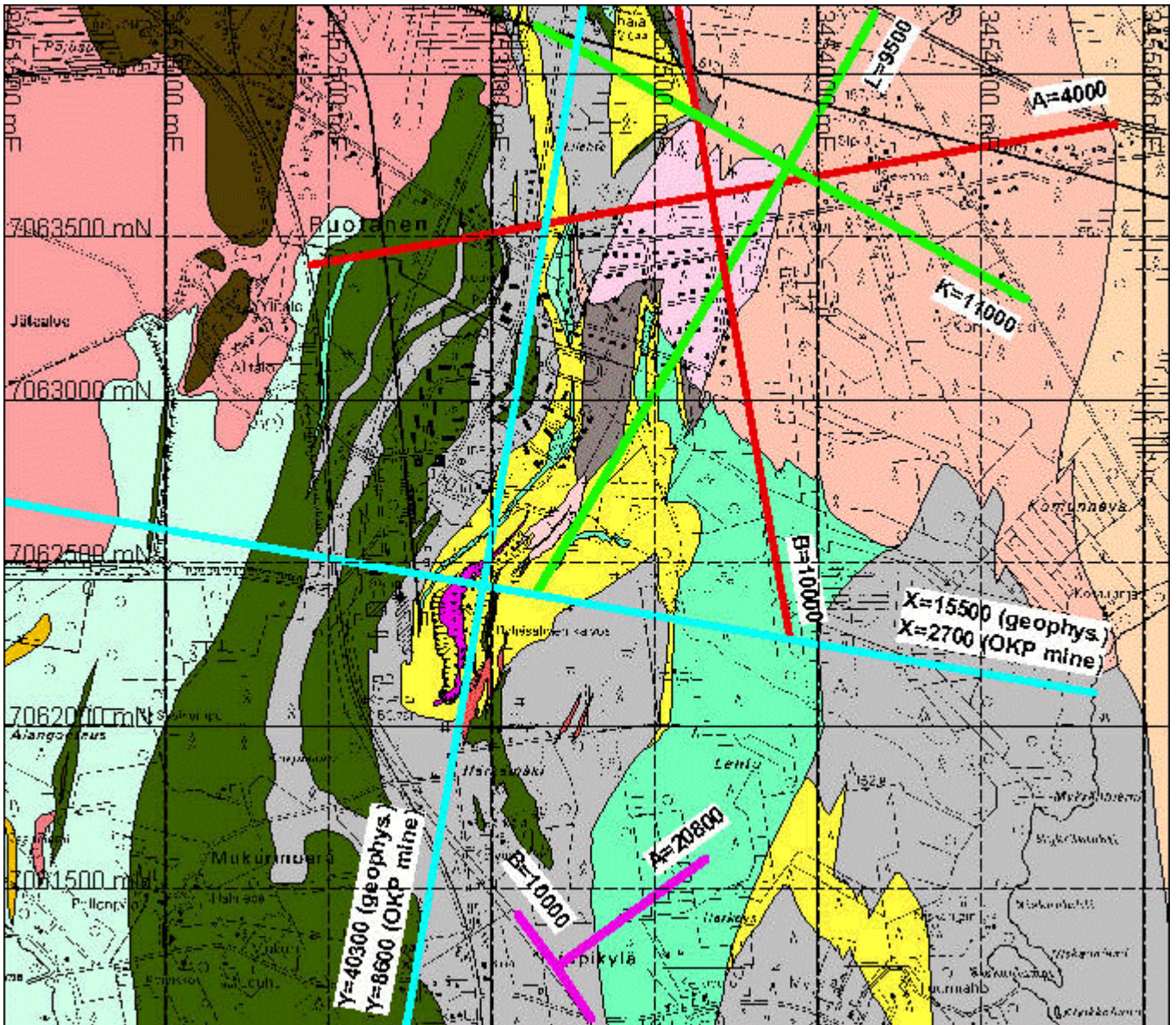
	SIO2	TIO2	AL2O3	FE2O3	MNO
N of cases	37	37	37	37	37
Minimum	45.10000	0.55187	14.50000	6.07576	0.15900
Maximum	58.80000	0.86960	19.50000	13.19573	0.39600
Median	53.30000	0.73052	16.90000	9.12718	0.22700
Mean	52.24865	0.72185	17.19459	9.06025	0.24086
Standard Dev	3.36102	0.07469	1.49962	1.89165	0.06191
	MGO	CAO	NA2O	K2O	P2O5
N of cases	37	37	37	37	37
Minimum	1.95000	6.00000	1.62832	0.15400	0.09680
Maximum	6.30000	19.50000	5.49230	1.68174	0.22460
Median	3.57000	10.40000	4.22000	0.34253	0.12151
Mean	3.63892	11.02297	3.92140	0.44597	0.13690
Standard Dev	1.17672	4.14921	0.98061	0.30466	0.03346
	LOI	CO2	ZR	CR	V
N of cases	0	0	37	37	30
Minimum	.	.	62.47272	10.00000	175.81188
Maximum	.	.	96.22560	424.18120	306.18148
Median	.	.	79.34916	220.93060	214.92276
Mean	.	.	77.98080	197.02354	217.31287
Standard Dev	.	.	10.43248	114.47881	24.53865
	RB	SR	BA	CU	ZN
N of cases	30	37	37	37	37
Minimum	3.00000	174.53642	71.68000	17.93390	81.03360
Maximum	61.99048	397.48619	869.12000	160.21780	183.57050
Median	12.86481	242.39070	295.68000	93.19150	114.44450
Mean	14.55163	247.63041	325.22378	91.34820	121.54393
Standard Dev	10.25942	45.95714	195.07146	36.23259	25.35276
	PB	NI	S	CO	AG
N of cases	37	37	37	37	37
Minimum	0.50000	3.47420	0.00500	10.00000	0.05000
Maximum	90.58690	87.32420	0.47192	34.00000	5.90000
Median	44.90840	36.62420	0.19795	17.00000	2.50000
Mean	44.31788	36.33434	0.22281	18.40541	2.26081
Standard Dev	25.36992	17.18796	0.11138	5.82838	1.35057
	AU	CL	SC	GA	AS
N of cases	3	0	0	0	0
Minimum	0.02500
Maximum	0.05000
Median	0.02500
Mean	0.03333
Standard Dev	0.01443
	Y	NB	MO	SB	LA
N of cases	0	0	0	0	0
Minimum
Maximum
Median
Mean
Standard Dev
	CE	BI	TH	U	W
N of cases	0	0	0	0	0
Minimum
Maximum
Median
Mean
Standard Dev

APPENDIX D1

Turo Ahokas

10.11.2006

Confidential



Pyhäsalmi area grid system for geophysics and drilling. The original mine area co-ordinate grid is two-fold, mine XY and geophysics XY , both numbered differently (blue). Kettuperä AB co-ordinate grid (red). Mine village KL co-ordinate grid (green). Lippikylä co-ordinate grid (magenta). Respectively Mullikkoräme geophysics and drilling is based on national XY (north/south) co-ordinate grid and is not therefore presented at all.

APPENDIX E1

Pyhäsalmi Modeling Project

Appendix E1

Sisälllys

Lyhennelmä

1. Näytteiden ja malmityyppien tilastollinen tarkastelu

1.1 Paikkatietojen tarkkuus

1.2 Näytealueet ja näytekoot

1.3 Alkuperäiset näytteet ja näytesyhdistelmät: vertailu

1.4 Geostatistinen tarkastelu

1.4.1 Alueelliset rakennepuitteet

1.4.2 Vertailu: Cu, Zn, S, alkuperäiset ja yhdistelmänäytteet

1.5 Anisotropiasuuntien määrittäminen

1.5.1 Pyhäsalmen kaivosalue

1.5.2 Kettuperä

1.5.3 Mullikkoräme

1.5.3.1 Pitoisuusjakaumat

1.5.3.2 Variogrammianalyysi

1.6 Interpoloinnin parametrit

1.7 Käytännön interpolointi

(**Malmityyppien spatiaalinen rajaus**

ei lisätietoa raporttiin

Metallijakaumien integrointi litologiaan

Jää puuttumaan – iterointikierroksen aiheita)

2. “Kuumat alueet”, rakenneanalyysi

2.1 Yleiskuvaus

2.2 “Kuumat alueet”, tulokanavien jäljitys

Lyhennelmä

Liitteessä selostetaan E4-osaprojektin ongelmia, työmenetelmiä ja taustoja eräin osin yksityiskohtaisemmin kuin varsinaisessa raportissa. Osittain asiat menevät limittäin.

Heterogeenisen aineiston valmistelu varsinaista tutkimusta varten vaatii runsaasti työläitä porrastettuja testejä, joista tässä annetaan kuvausta. Sitä on etukäteen vaikea mitoittaa. Tässä on painopisteenä ollut geostatistinen tarkastelu, joka on osa valmistelua. Soveltaminen on vielä edessä.

1. Näytteiden ja malmityyppien tilastollinen tarkastelu

1.1 Paikkatietojen tarkkuus

Paikkatietojen käsittelyssä tuli esille useita virhe- ja epämääräisyystekijöitä, joiden vaikutukset tulisi tutkia ennen muita toimenpiteitä järkevien tavoitteiden määrittämiseksi. Eniten ongelmia aiheuttaa aineiston heterogeenisuus: tietoja on koottu eri aikajaksoina, eri tarkoituksiin, erilaisin menetelmin ja erilaisin vaatimuksin niin havaintopisteiden määrittystarkkuuden kuin havaintoarvojenkin lukuisuuden, laadun ja määrittystarkkuuksien suhteen. Esimerkkejä:

1. Koordinaatistomuunnokset

Jatkokäsittelyä varten kaikki tieto on kytkettävä samaan, tässä tapauksessa valtakunnan koordinaatistoon. Koordinaatistomuunnosten toimivuus tulee esille vasta vertailtaessa samoista kohteista eri koordinaatistoihin tehtyjä havaintoja. Tässä projektissa kesällä 1999 havaittiin että muunnoskaavassa Pyhäsalmen kaivostietojen siirtämisessä valtakunnankoordinaatistoon oli kulmamerkkivirhe, mikä aiheutti määrältään vaihtelevia (0 – 40 m) siirtymiä havaintopisteisiin. Vasta korjauksen jälkeen voitiin Pyhäsalmen kaivokselta havaittu materiaali (kairanreiät, tasokartat) yhdistää muuhun materiaaliin eli valtakunnan koordinaatistoon sidottuun pintakairaukseen, geofysiikkaan ja pintakartoitukseen.

2 Reikien suuntamittaus

Reikien kaateen suuntainen taipuma on perinteellisesti mitattu pitkistä (yli 50 m:n) rei'istä. Sivutaipumaa mitataan vieläkin vain erikoistapauksissa menetelmien kalleuden takia. Mullikkorämeeseen kairatuista pintarei'istä on mitattu sivutaipumakin. Tuloksia havainnollistaa kuva 1. Siinä näkyy miten kaateen suuntainen taipuminen on vähäistä. Eräät reiät näyttävät lisäksi kaateltaan paikoin jyrkkenevän kun niiden säännönmukaisesti pitäisi loiveta. Mutta sivutaipuma on eräissä rei'issä uskomattoman suuri. Yleisintä näyttää olevan taipuminen myötöpäivään mutta senkin suuruus, suunta ja tasaisuus vaihtelevat. Tämän perusteella voimme olettaa, että niissä rei'issä joiden sivutaipumaa ei ole mitattu, saattaa esiintyä oikealle vievää taipumista jopa 50 m jokaista 100 m:n kairausta kohti kuitenkin niin että ensimmäiset ja viimeiset 50 m ovat melko suoria.

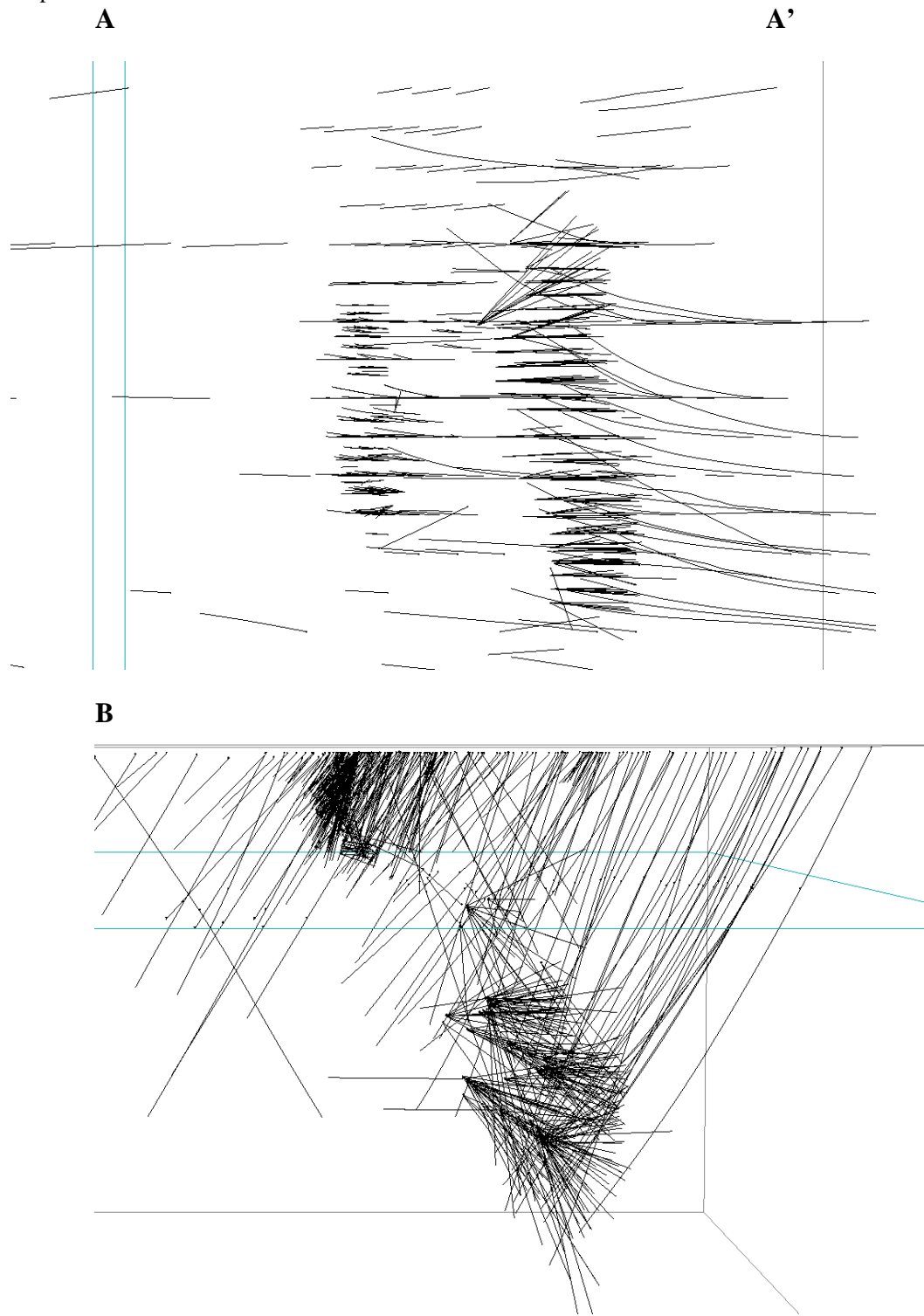
3 Näytteiden koko

Näytepituudet vaihtelevat tavalla jota kuvataan erikseen kohdassa 1.2. Useat tilastomenetelmät edellyttävät aineiston tasausta, tässä tapauksessa näytekoon muuntamista, jota selvitetään kohdassa 1.3. Epätarkkuutta luonnollisesti aiheuttaa sekä 60 m:n näyteen pilkkominen 3 m:n paloiksi että havainnon kohdistaminen tuon 60 m:n näyteen keskipisteeseen, jonka ohjelmat laskevat ottamatta taipumia huomioon. Toinen epätarkkuuslähde on näyteen osittaminen joko halkaisemalla (tai kvadroittamalla) tai pätkittämällä.

Yllä mainitut epätarkkuuslähteet vaikuttavat kaikkiin paikkatiedon tilastotuloksiin virhemarginaalia lisäten. Vaikutukset ovat niin monimutkaisia että virhearvioita ei ainakaan tässä yhteydessä yritetä liittää tuloksiin, jotka onneksi ovatkin luonteeltaan kvalitatiivisia ja suuntaa antavia.

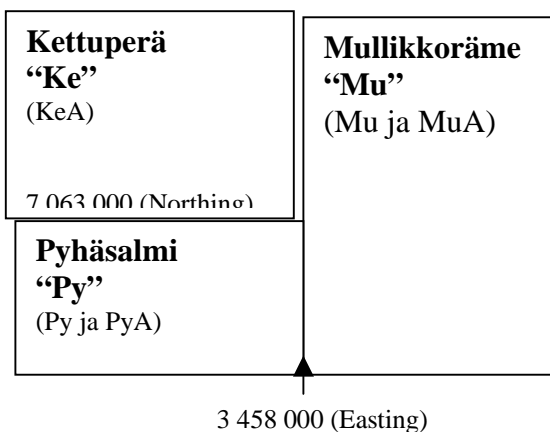
Kuva 1A-B.

Mullikkoräme, pintaprojektio ja pystyprojektiio. (Väli A..A' on noin 700 m).
Kairanreikien sivutaipuma. Huom! Kaikista rei'istä sitä ei ole mitattu.



1.2 Näytealueet ja näytekoot

Koko näytemäärä on 34 522, kairanreikien luku 2518. Näytteistä 10 836 on pinnalta kairatuista malminetsinnän (Sarja A, 553 reikää), 20 681 Pyhäsalmen kaivoksen (Sarja Py, 1596 reikää) ja 3 005 Mullikkorämeen (Sarja Mu, 369 reikää) sydämistä. Analyysitulosten tarkastelussa näytekatat yhdistettiin ja jaettiin uudelleen alaluokkiin PyA (Pyhäsalmi), MuA (Mullikko) ja KeA (Kettuperä) oheisen kaavion mukaan.



Näytteiden pituudet vaihtelevat rajoissa 0.02 – 66.60 m. Kuvassa 2 ovat eriteltyinä malminetsinnän ja kaivosten kairausnäytteiden pituusjakaumien histogrammit.

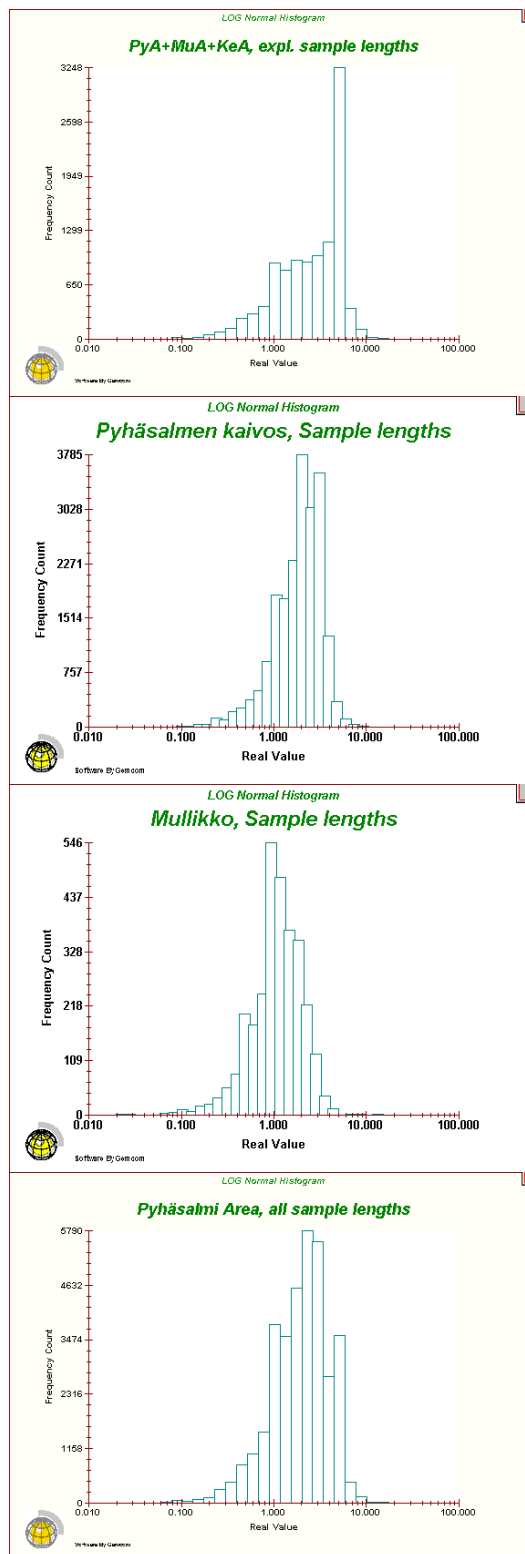
Taulukko 1.
Näytepituuksien vertailu.

Sarja	A	Py	Mu	Yht.
Reikiä kpl	560	1595	369	2524
Näytteitä Kpl	10836	20681	3005	34522
Pituus				
Min. m	0.03	0.05	0.02	0.02
Max. m	66.60	15.55	14.68	66.60
K.arvo m	3.19	2.10	1.26	2.37

Kuva 2A-D.

Näytepituuksien vertailu histogrammein:

- Pyhäsalmen alueen malminetsintäkairaus,
- Pyhäsalmen kaivoksen kairaus,
- Mullikkorämeen kaivoksen kairaus,
- Malminetsintä- ja kaivoskairaus yhdistettynä.



1.3 Alkuperäiset näytteet ja näyteyhdistelmät: vertailu

Suuri hajonta näytekoossa johtaa virheisiin kaikessa statistiikassa, mistä puuttuu pitoisuuksien painotus näytekoolla. Yksi osaratkaisu näihin pulmiin on tasavälisten yhdistelmien, tässä 2m, 3m ja 5m pitkien näytteiden konstruointi. Yhdistelmiä lyhemmät näytteet ja tyhjat välitilat voidaan korvata valituilla tausta-arvoilla, tässä arvolla 0.001 % kuparille ja sinkille sekä arvolla 0.01 % rikille. Kuvassa 3 on esitetty kuparipitoisuuden jakautuminen alkuperäisissä ja yhdistelmänäytteissä ilman tausta-arvoja.

Taulukossa 2 on esitetty sekä alkuperäiset painottamattomat analyysitiedot että komposiittitiedot ilman tausta-arvoja ja vielä komposiittitiedot 3m:n näytteille tausta-arvojen kanssa (3mB). Tarkasteluun on hyväksytty Cu- ja Zn-pitoisuudet 0.001 %:n ja S-pitoisuudet 0.01 %:n cutoffilla, jolloin pelkän tausta-arvon antavat näytteet jäävät tarkastelusta pois.

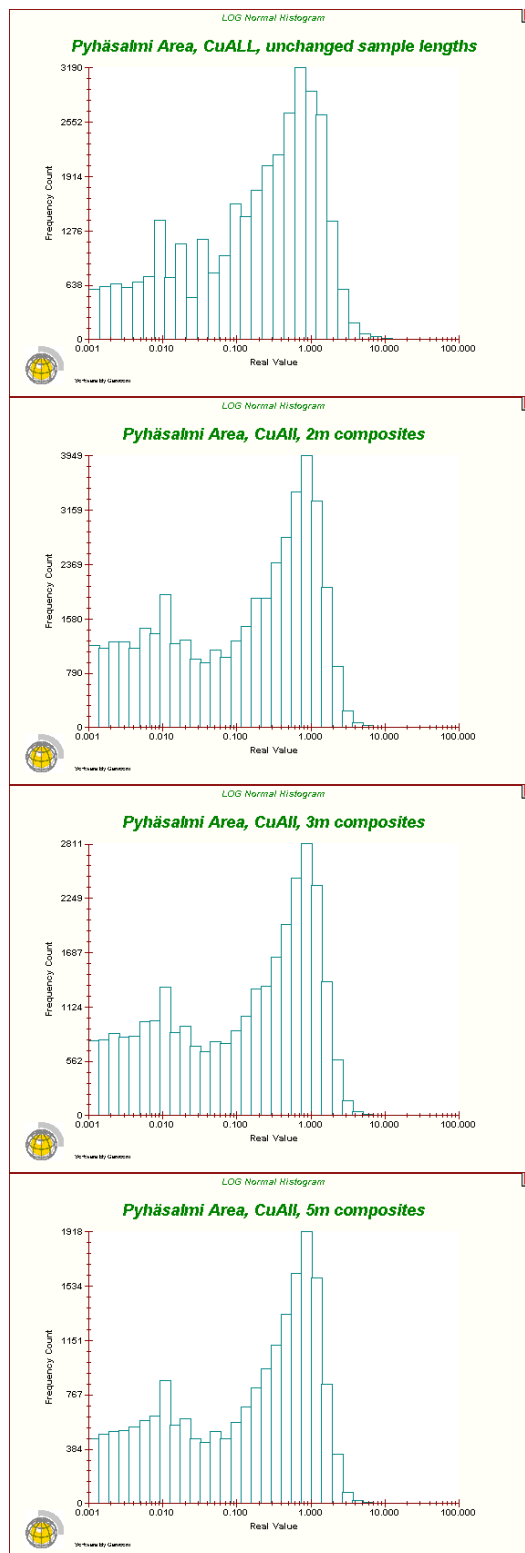
Taulukko 2A,B,C.
Cu-,Zn- ja S-pitoisuuksien statistiikkaa alkuperäisin ja yhdistelmänäyttein.

A				
Analyytit: Cu				
Koko	Lkm	Mean	Median	Var
Alkup.	34 522	0.524	0.380	0.622
2m	45 283	0.436	0.330	0.376
3m	31 592	0.433	0.332	0.356
3mB	29 715	0.407	0.250	0.308
5m	20 448	0.432	0.336	0.334

B				
Analyytit: Zn				
Koko	Lkm	Mean	Median	Var
Alkup.	34 522	1.436	1.153	10.112
2m	45 283	1.035	0.880	5.503
3m	31 592	1.022	0.879	5.088
3mB	29 715	0.987	0.875	4.676
5m	20 448	1.012	0.854	4.514

C				
Analyytit: S				
Koko	Lkm	Mean	Median	Var
Alkup.	34 522	24.957	27.177	389.410
2m	45 283	21.938	18.491	398.723
3m	31 592	21.901	19.198	388.588
3mB	29 265	20.610	15.616	361.452
5m	20 448	21.986	20.695	375.119

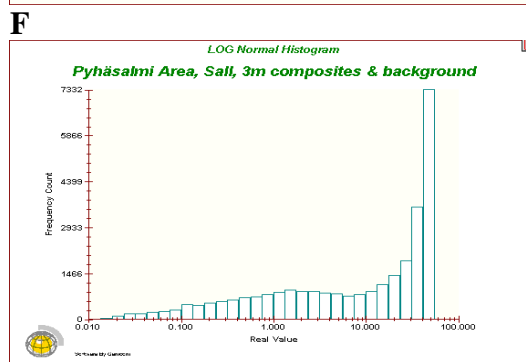
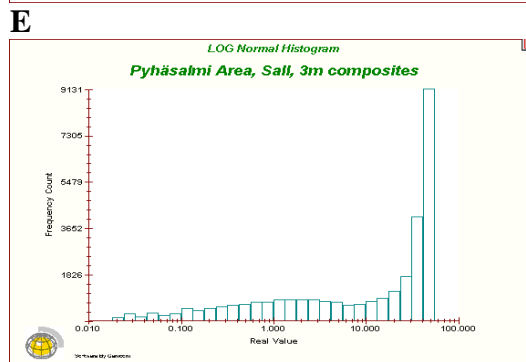
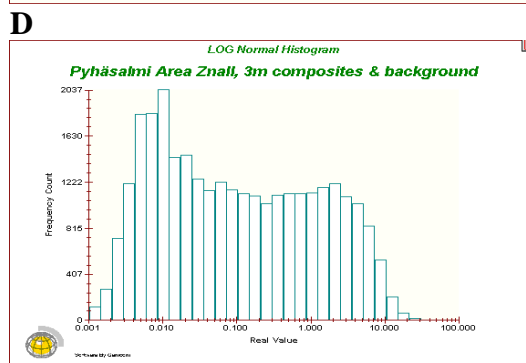
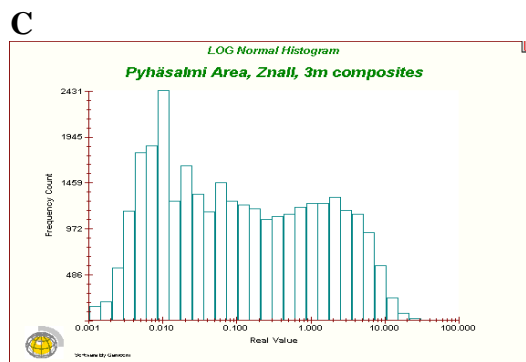
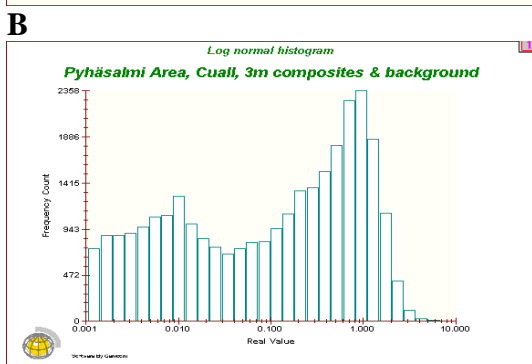
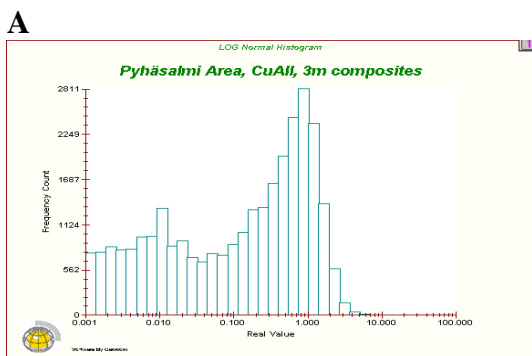
Kuva 3A-D.
Kuparipitoisuuden jakautuminen alkuperäisissä (A) ja yhdistelmänäytteissä (C-D), ilman tausta-arvoja.



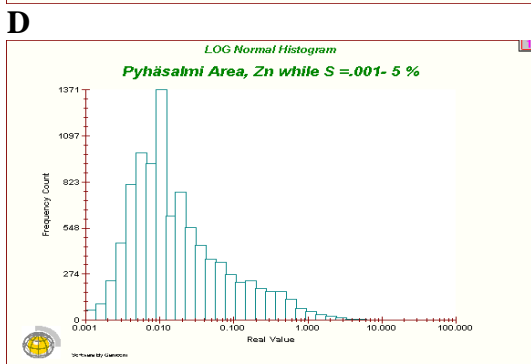
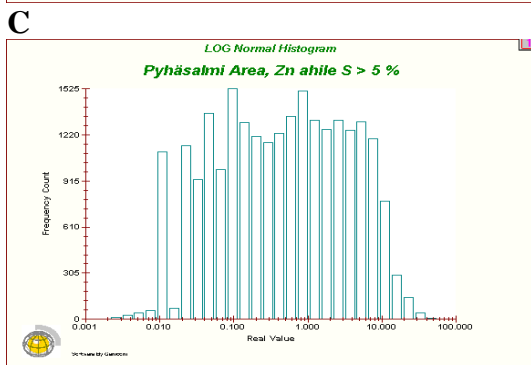
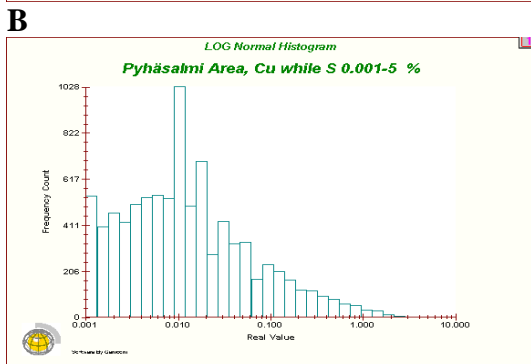
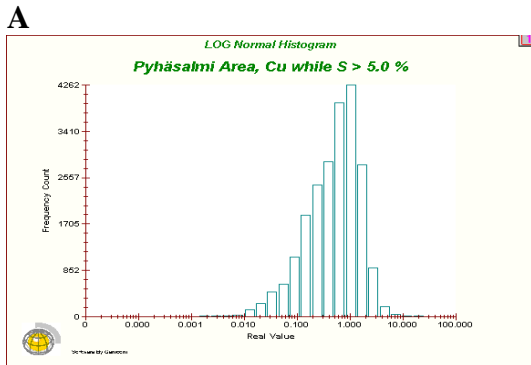
Kuvissa 4A-F ovat Cu-, Zn- ja S- jakaumahistogrammit 3m:n yhdistelmistä sekä ilman tausta-arvoja että näiden kanssa. Tämän tarkastelun perusteella voidaan jatkoanalyysiin valita soveltuva aineisto.

Kaikki jakaumat ovat kaksihuippuisia, ja rikin jakauma lisäksi äärimmäisen vino. Alkuperäisessä aineistossa rikin korrelaatiokerroin sinkin suhteen on 0.2 ja kuparin suhteen 0.4. Tilannetta havainnollistaa kuva 5A-D, jossa on esitetty kuparin ja sinkin jakaumahistogrammit rikin pitoisuusalueilla 0 - 5 % S ja 5 - max % S.

Kuva 4A-F.
Cu (A-B), Zn-(C-D) ja S-(E-F)pitoisuuksien jakautuminen 3m:n yhdistelmänäytteissä, tausta-arvoina 0.001 % (Cu ja Zn) ja 0.01 (S).



Kuva 5A-D
Kuparin (A, B) ja sinkin (C,D)
pitoisuusjakaumien histogrammit rikin
pitoisuusalueilla 5 – max % (A,C)
ja 0 – 5 % (B, D).

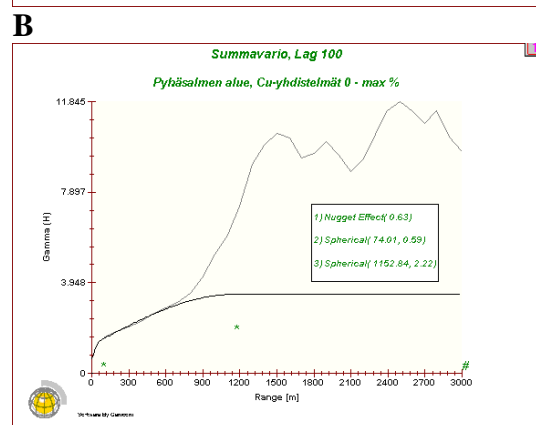
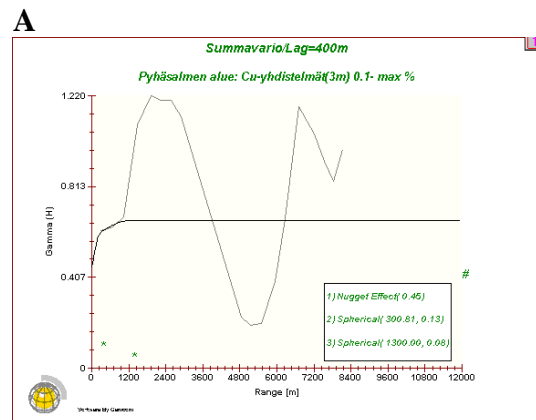


1.4 Geostatistinen tarkastelu
1.4.1 Alueelliset rakennepuitteet

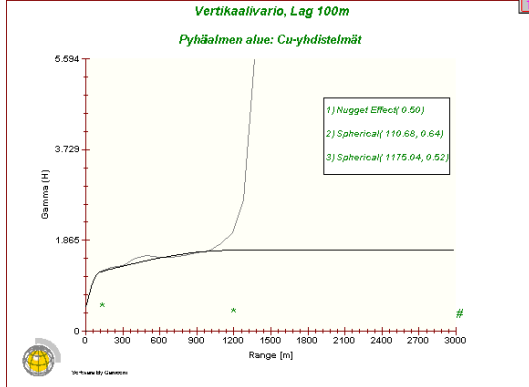
Geologisissa rakenteissa saattaa olla piirteitä kuten lineaarisuutta ja vyöhykkeisyyttä, jotka voidaan todeta ja määrittellä numeerisesti visuaalisen (geologisen) havaitsemisen lisäksi geostatistisen rakenne-analyysin eli variogrammanalyysin avulla. Geostatistinen summavariogrammi, jossa varianssin muutos näytteiden välisen kasvavan etäisyyden funktiona on laskettu kaikkien 3D-suuntien keskiarvona, antaa yleiskuvan näytekoon, näytetiheyden ja pitoisuusrajausten sopivuudesta geostatistiseen tarkasteluun sekä pitoisuuksien jatkuvuudesta.

Kuvat 6A-F
Variogrammit Pyhäsalmen alueen kaikista Cu-analyyseistä. 3m:n yhdistelmänäytteet (paitsi F), logaritminen muunnos.

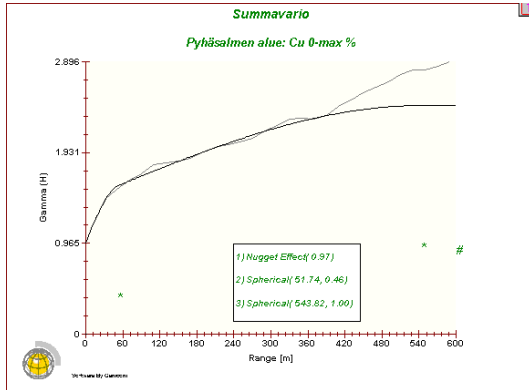
- A. Lag = 400m.
- B. Lag = 100m.
- C. Lag = 100m, vertikaalisuunta, angle = 20°.
- D. Lag = 20m.
- E. Lag = 5m.
- F. Lag = 2m, alkuperäisanalyysit.



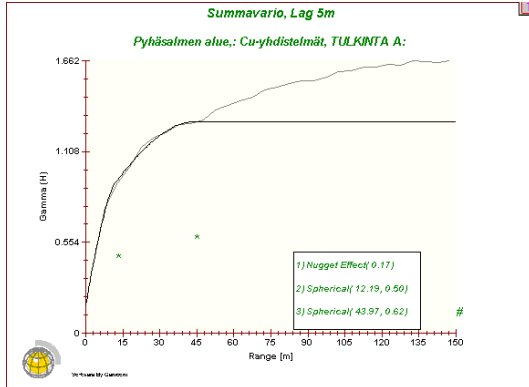
C



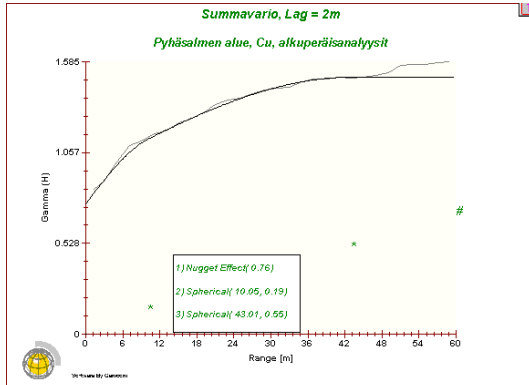
D



E



F



Kuvissa 6A-G on tarkasteltu eri suuruusluokkien pitoisuusrakenteita kuparianalyyseistä. Karkeimmassa esityksessä (A) näkyy ns. Hole-efekti: varianssi kohoaa maksimiin ja putoaa minimiin noin 5 km:n välein. Tämä kertoo joko analyysitiedon tai malmimuodostumien esiintymistäajuuksista alueella. Tässä tapauksessa se kuvaa Pyhäsalmen ja Mullikkorämeen välistä karkeaa etäisyyttä. Mallinnus antaa kaksi pitoisuuden jatkuvuusrakennetta: 300m ja 1300m.

Kuvissa 6B-F malli tarkentuu: Erilaisia rakennekoluokkia erottuu: 10-12m, n. 50m, n. 120m, n. 1200m. Näiden summamallien merkitys täsmentyy lisää, kun analyysiä edelleen laajennetaan koskemaan muita alkuaineita ja tarkennetaan pienemmille alueille ja rajattuihin suuntiin. Jatkossa näyttäisi lag = 20m olevan sopivin yleisvertailuun.

1.4.2 Vertailu: Cu, Zn, S, alkuperäiset ja yhdistelmänäytteet; pitoisuusalueet

Oheen on mallinnettu semivariogrammeja Cu-pitoisuuksille näyte-etäisyysluokille (lag) 50m ja 5m (Kuvat 7A-F) ja 20m (Kuvat 8 A-C) pitoisuusalueille A 0-max %, B 0.1-max % ja C 0 – 0.1 %. Kuviiin 9A-F on käytetty alkuperäisiä Cu-analyysiarvoja ja kuviiin 6A-C ja 8A-C on käytetty 3m:n yhdistelmänäytteitä ilman taustatarvoja. Summavariogrammeissa hakukulma on 90 astetta.

Kuvissa 10A-C ja 10D-F on vastaavat variogrammimallit sinkin ja rikin yhdistelmänäytteille. Näiden summavariogrammien mallinnuksesta saadut alueelliset alkuainekohtaiset parametrit on kerätty taulukkoon 3.

Kuvien B-osien malleista näkyy miten pienten pitoisuusarvojen (< 0.1 %) leikkaaminen aineistosta aiheuttaa nugget-osuuden voimistumisen varianssissa. Sama näkyy taulukossa 3 (relative nugget). Tämä osoittaa, että mikään interpolointimenetelmä suurten pitoisuuksien kohdalla ei ole luotettava Pyhäsalmen alueella nyt käytetyllä resoluutiolla (Lag = 20m). Eli havaintotiheys on liian pieni. Jos alhaiset pitoisuudet kelpaavat edustamaan mineralisointia, sitten materiaalia on kylliksi ja se on tilastisesti käyttökelpoista. Poikkeus tästä säännöstä on rikki.

Kuvat 7A-C

Variogrammit Pyhäsalmen alueen kaikista

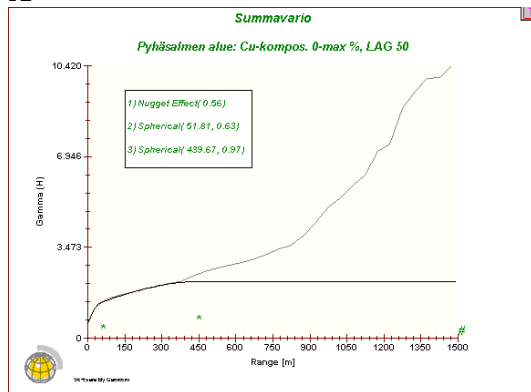
Cu-analyyseistä. Logaritminen muunnos.

A. Kaikki Cu-analyysit 0- 24 %. Lag 50.

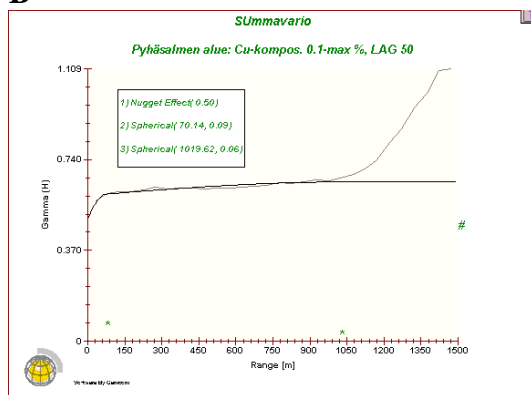
B. Cu-analyysit 0.1 – 24 %. Lag 50.

C. Cu-analyysit 0 – 0.1 %. Lag 50

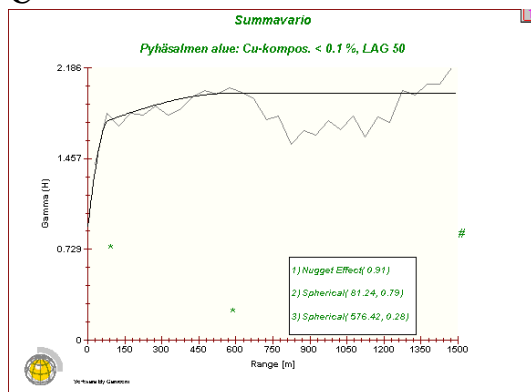
A



B



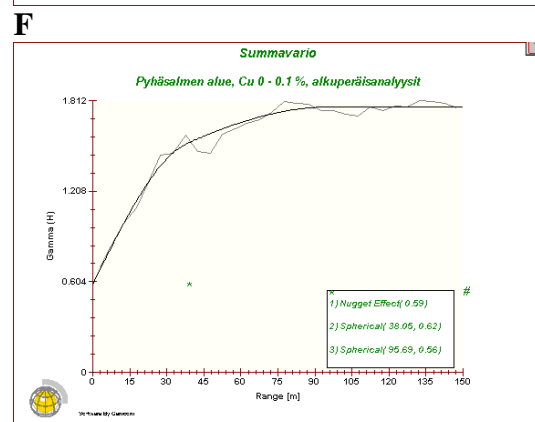
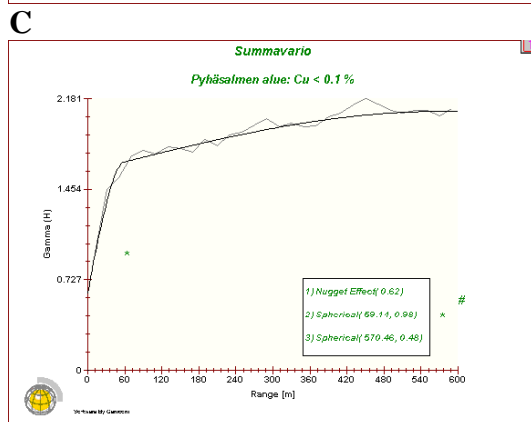
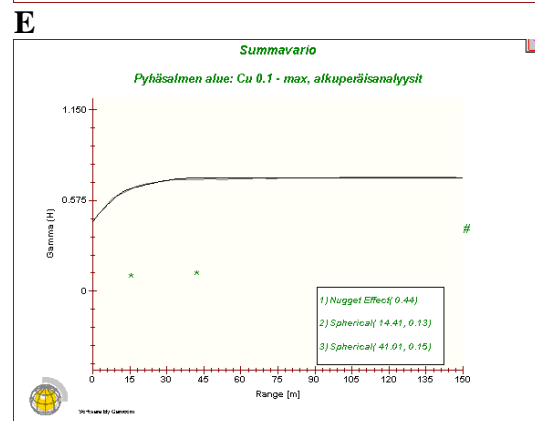
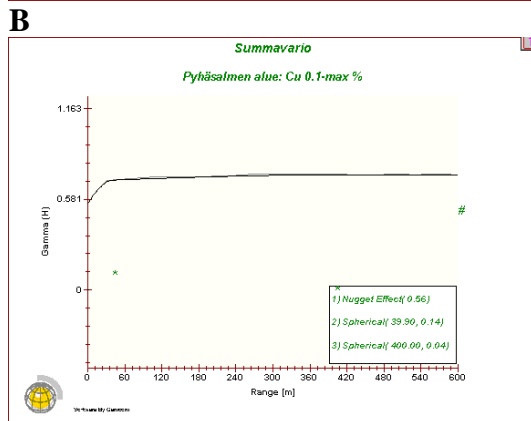
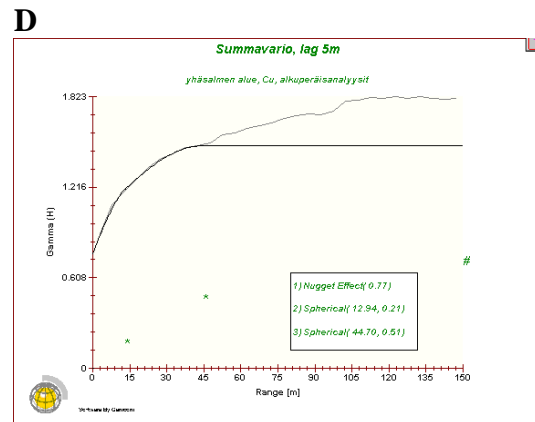
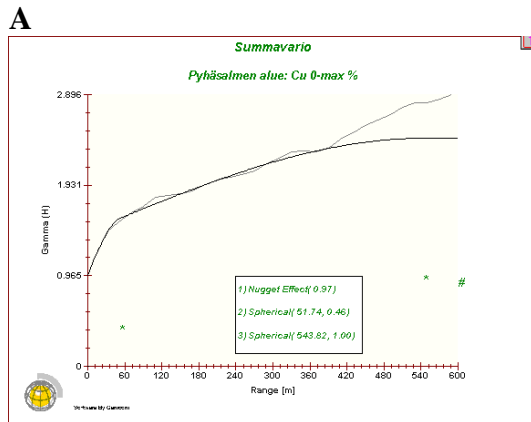
C



Kuvat 8A-C

Variogrammit Pyhäsalmen alueen Cu-analyyseistä. Logaritminen muunnos.

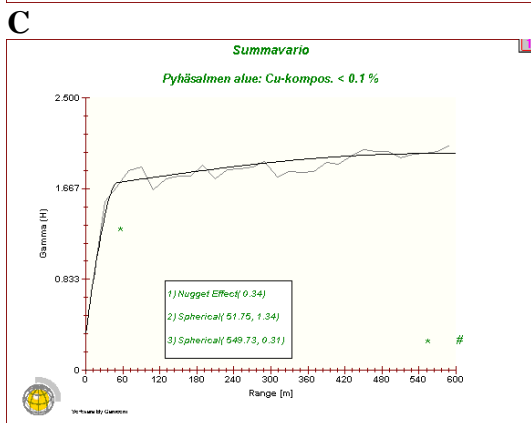
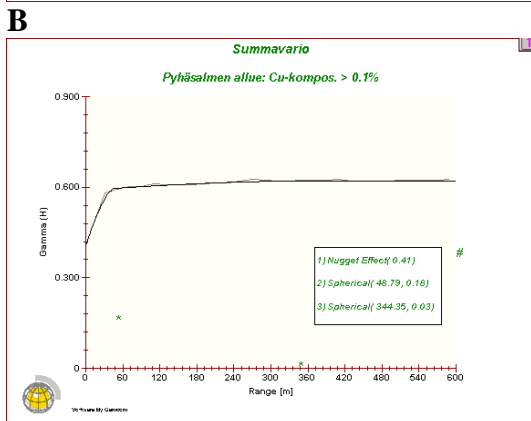
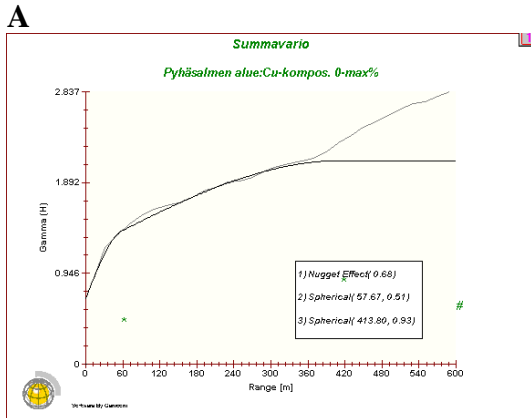
- A. Kaikki Cu-analyysit 0 - max %. Lag = 20m.
- B. Cu-analyysit 0.1 - max%. Lag = 20m.
- C. Cu-analyysit 0 - 0.1 %. Lag = 20m.
- D. Cu-analyysit 0 - max %. Lag 5m.
- E. Cu-analyysit 0.1 -max %. Lag 5m.
- F. Cu-analyysit 0 - 0.1 %. Lag 5m.



Kuvat 9A-C

Variogrammit Pyhäsalmen alueen Cu-analyysien yhdistelmästä /3m. Logaritminen muunnos. Lag = 20m.

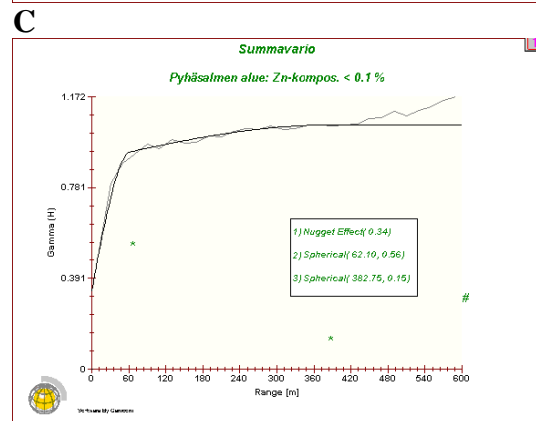
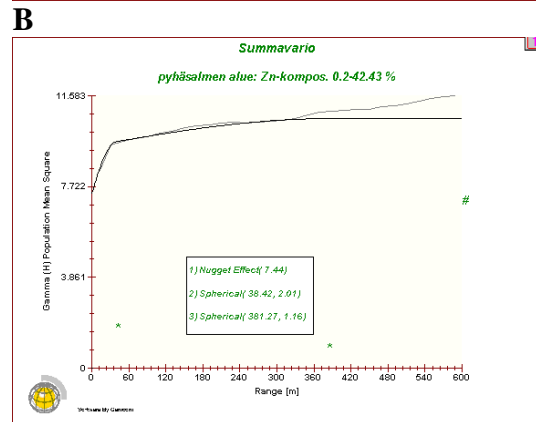
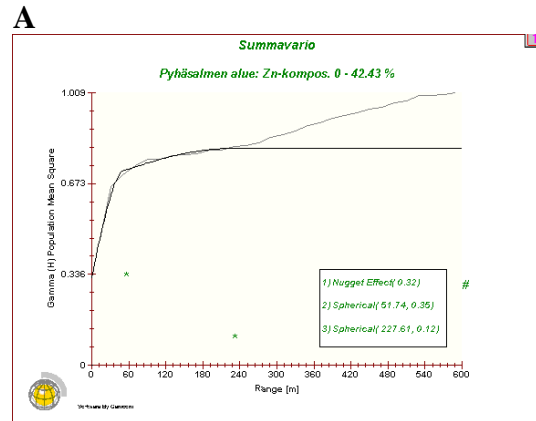
- A. Kaikki Cu-analyysit 0 - max%.
- B. Cu-analyysit 0.1 - max%.
- C. Cu-analyysit 0 - 0.1 %.



Kuvat 10A-C

Variogrammit Pyhäsalmen alueen Zn-analyysien yhdistelmästä /3m. Logaritminen muunnos. Lag = 20m.

- A. Kaikki Zn-analyysit 0 - %.
- B. Zn-analyysit 0.2 - %.
- C. Zn-analyysit 0 - 0.2 %.



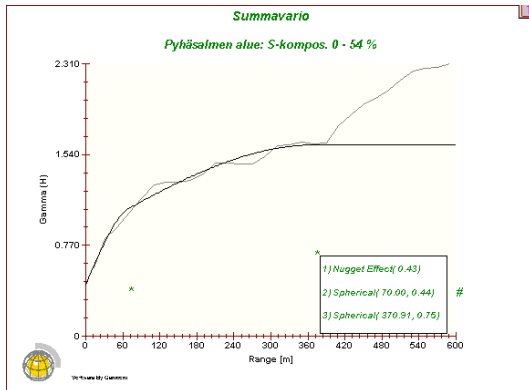
Kuvat 10 D -F

Variogrammit Pyhäsalmen alueen S-analyysien yhdistelmistä /3m.

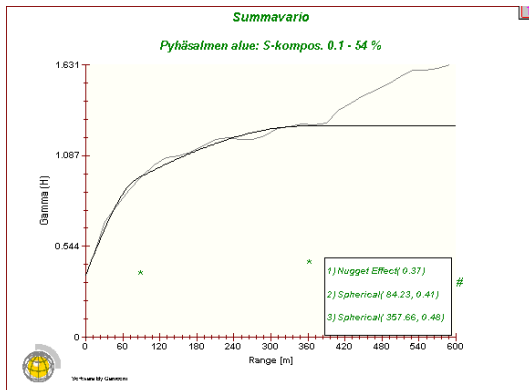
Logaritminen muunnos. Lag = 20m.

- D. Kaikki S-analyysit 0- %.
- E. S-analyysit 0.1 - %.
- F. S-analyysit 0 - 0.1 %.

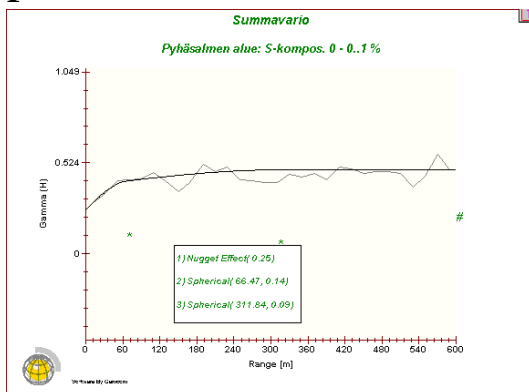
D



E



F



Taulukko 3.

Yhteenveto kuvien 6-10 parametreista.

Numerointi kuten kuvissa.

	6A	7A	8A	9A	10A
	6B	7B	8B	9B	10B
	6C	7C	8C	9C	10C
	Cu	Cu	Cu	Zn	S
Nugget	0.56	0.97	0.68	1.47	0.43
	0.50	0.56	0.41	1.06	0.37
	0.91	0.62	0.34	0.24	0.25
Sill 1	0.66	0.46	0.51	1.78	0.44
	0.09	0.14	0.18	0.34	0.41
	0.79	0.62	1.34	0.34	0.14
Range1	52	52	58	41	70
	70	40	49	43	84
	81	59	52	47	66
Sill 2	1.25	1.00	0.93	0.69	0.75
	0.06	0.04	0.03	0.20	0.48
	0.28	0.48	0.31	0.17	0.09
Range2	646	544	414	140	371
	1020	400	344	229	357
	576	570	550	303	312
Relative Nugget	29	66	47	60	36
	333	311	195	196	42
	85	56	21	47	109
Semi-variance	2.47	2.43	2.09	3.94	1.62
	0.64	0.74	0.62	1.60	1.26
	1.98	1.72	1.99	0.75	0.48

Taulukosta voidaan päätellä:

- Komposiittien käyttö pienentää nuggetia, suhteellista nuggetia ja semivarianssia.
- Pitoisuuksien vaikutusmatka (range) jakautuu täällä lag-välillä (20 m) pääsääntöisesti kolmeen komponenttiin: n. 50m, n. 300m ja n. 550m. Rikki käyttäytyy tasaisimmin.
- Pienten pitoisuuksien leikkaaminen näkyy kohonneissa nugget-arvoissa (relative nugget). Suhteellinen nugget (tässä tapauksessa $100 * \text{nugget} / (\text{sill1} + \text{sill2})$) kuvastaa aineiston käyttökelpoisuutta. Suhteellisen korkea nugget-arvo ($> 100\%$) kuvastaa ei-geologisista tekijöistä kuten analyysivirheistä ja näyteresoluutiosta koostuvaa osavarianssia Pienten pitoisuuksien leikkaaminen (kuvat 7B - 10B) tekee aineiston käyttökelpoisuuden kyseenalaiseksi, poikkeuksena rikki (kuva 10).

Jatkotarkasteluissa tulee tämän mukaan pääsääntöisesti käyttää 3 m:n yhdistelmä-näytteistä koottua aineistoa kuitenkin siten, että kontrolloidaan tätä valintaa testein 'raakadatan' avulla. Pitoisuusalueiden leikkaamista erityisesti alapäästä pitää varoa.

1.5 Anisotropiasuuntien määrittäminen osa-alueittain

1.5.1 Pyhäsalmen kaivosalue

Taustamateriaalia raportin anisotropiatarkastelulle: taulukot 4 – 7 ja kuvat 11A-K.

Taulukko 4.
Anisotropia valituissa suunnissa.

Range	R I R II Cu	R I R II Zn	R I R II S
Azim.			
340	55 132	36/38 140/219	64 191
000	42 239	38/65 183/229	55 223
020	43 264	35/41 234/308	42 279
045	47 226	46 194	37 248
090	54 124	35 194	64 200
110	60/- 100/177	35 58	80 170
135	72 112	50 123	71 130
pysty	67 485	56/74 198/585	40 519
All	59 439	46/46 231/585	52/67 248/437

Taulukko 5.

Vaikutusmatkojen vertailu vertikaalisuunnassa: Cu, Zn, S

Range m.	R I R II Cu	R I R II Zn	R I R II S
H.kulma astetta			
20	70 709	92/96 713/1437	67 923
10	74 296	115/129 421/1467	59 857

Taulukko 6.
Pyhäsalmen kaivoksen alue: anisotropia-akselit kuparille, sinkille ja rikille.

Range	R I R II Cu	R I R II Zn	R I R II S
Azim.			
All	47 291	44 563	58 389
010	41 171	37 101	38 169
100	46 115	41 98	51 139
pysty	75 300	56/87 145/594	40 188

Taulukko 7.
Pisimmät anisotropia-akselit

	Akseli	Suunta	Pituus
Cu	Z	pysty	300
	X	010	171
	Y	100	115
Zn	Z	pysty	145
	X	010	101
	Y	100	98
S	Z	pysty	188
	X	000	169
	Y	90	139

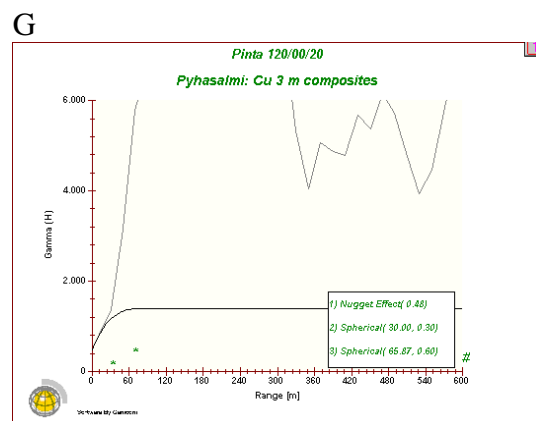
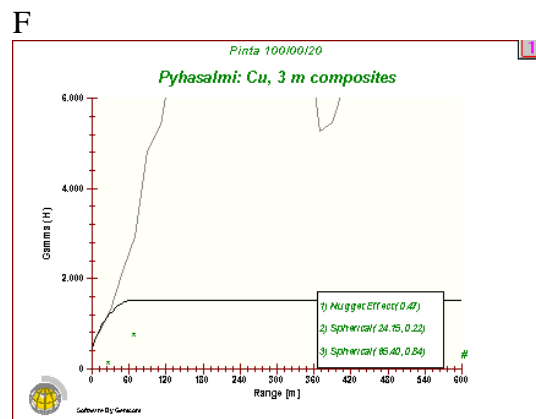
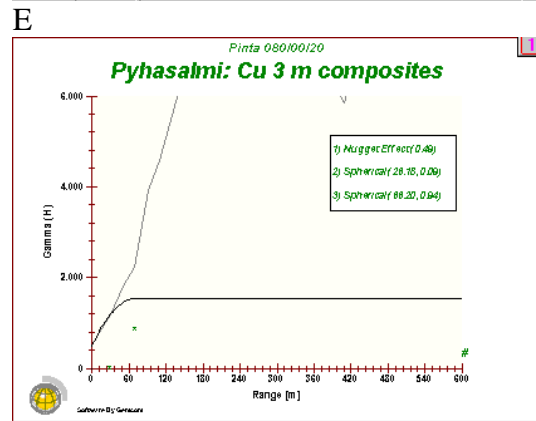
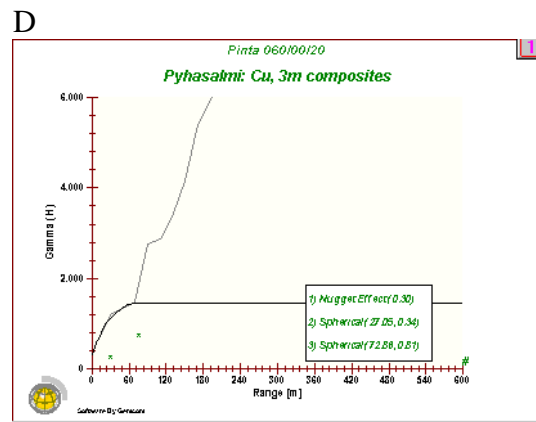
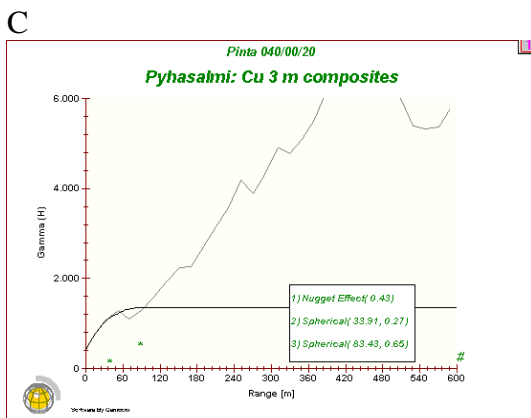
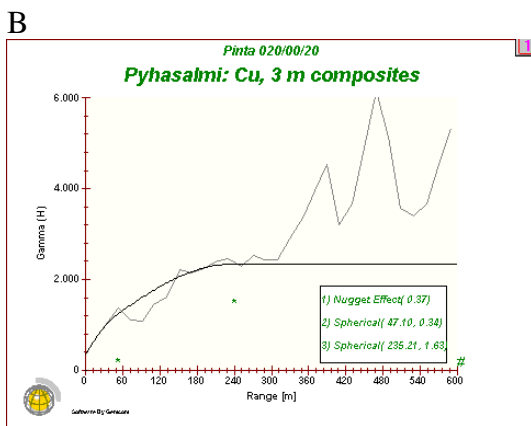
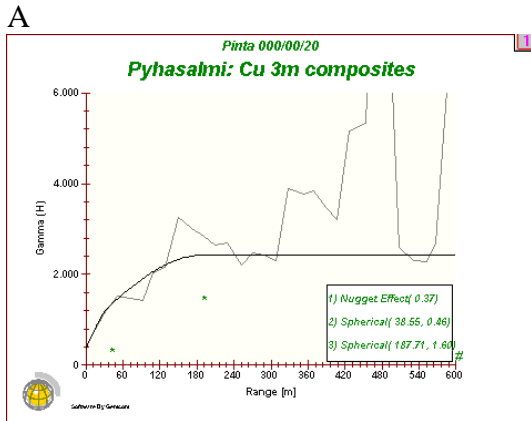
Kuva 11 A-K

Suunnatut semivariogrammit

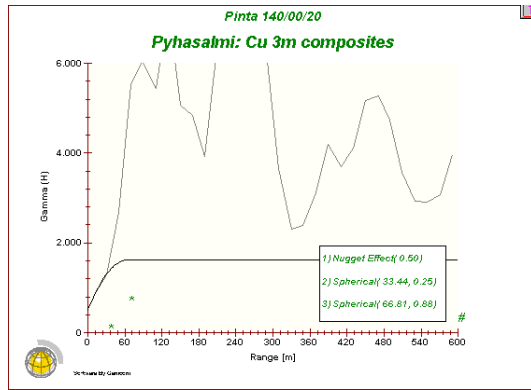
Pyhäsalmen kaivosalueen pintaosalle:

+150 - -100 m. Suunnat:

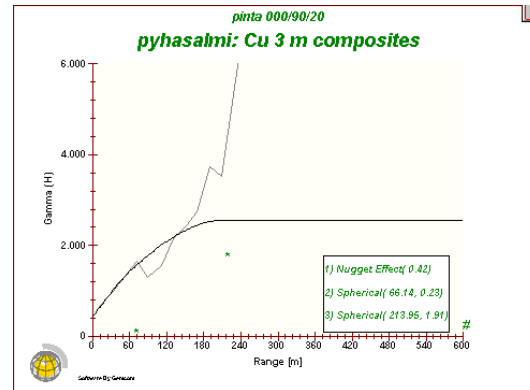
A 000	E 080	I 160
B 020	F 100	J pysty
C 040	G 120	K kaikki
D 060	H 140	



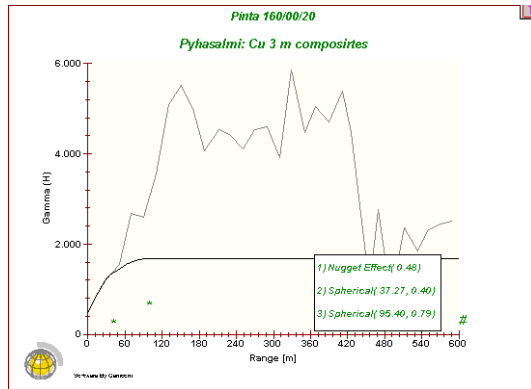
H



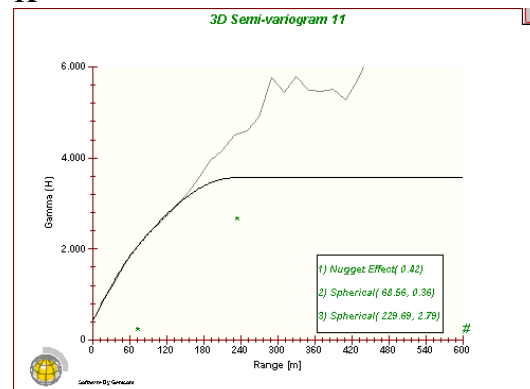
J



I



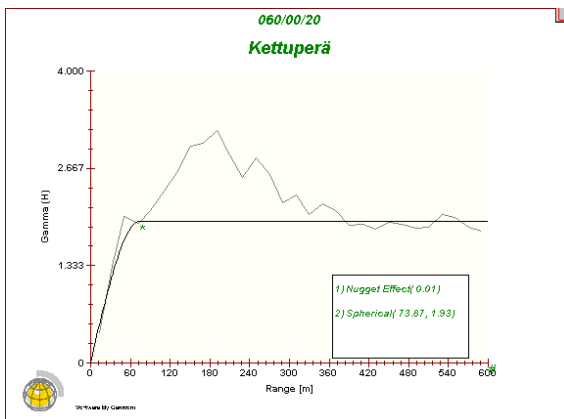
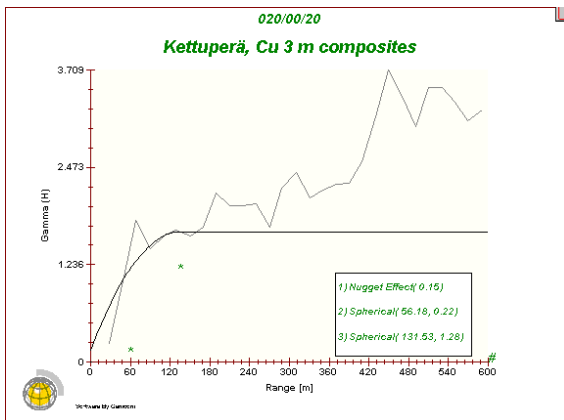
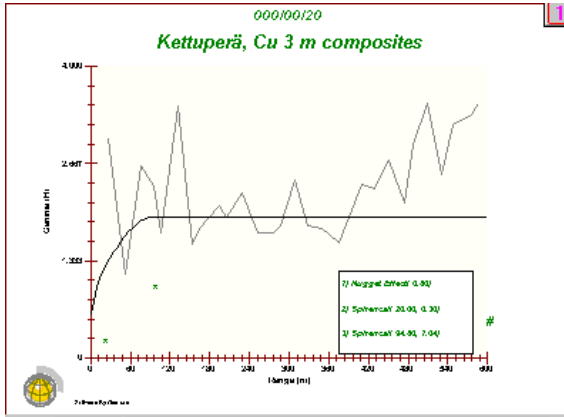
K



1.5.2 Kettuperä

Dokumentteja Kettuperän semivariogrammeista:

Kuva 12 A-C



1.5.3 Mullikkoräme

1.5.3.1 Pitoisuusjakaumat: S, Cu, Zn, Pb, Ag

Logaritmisten jakaumahistogrammien mukaan (Kuva 20) kupari ja hopea ovat ‘hyvin käyttäytyviä’, sen sijaan rikin jakauma on oikealle ja lyijyn vasemmalle vino; sinkin jakauma on kaksihuippuinen. Spatiaalinen mallinnus onkin syytä aloittaa kuparista ja hopeasta, joiden käyttäytyminen antaa pohjaa päätelmille muista alkuaineista.

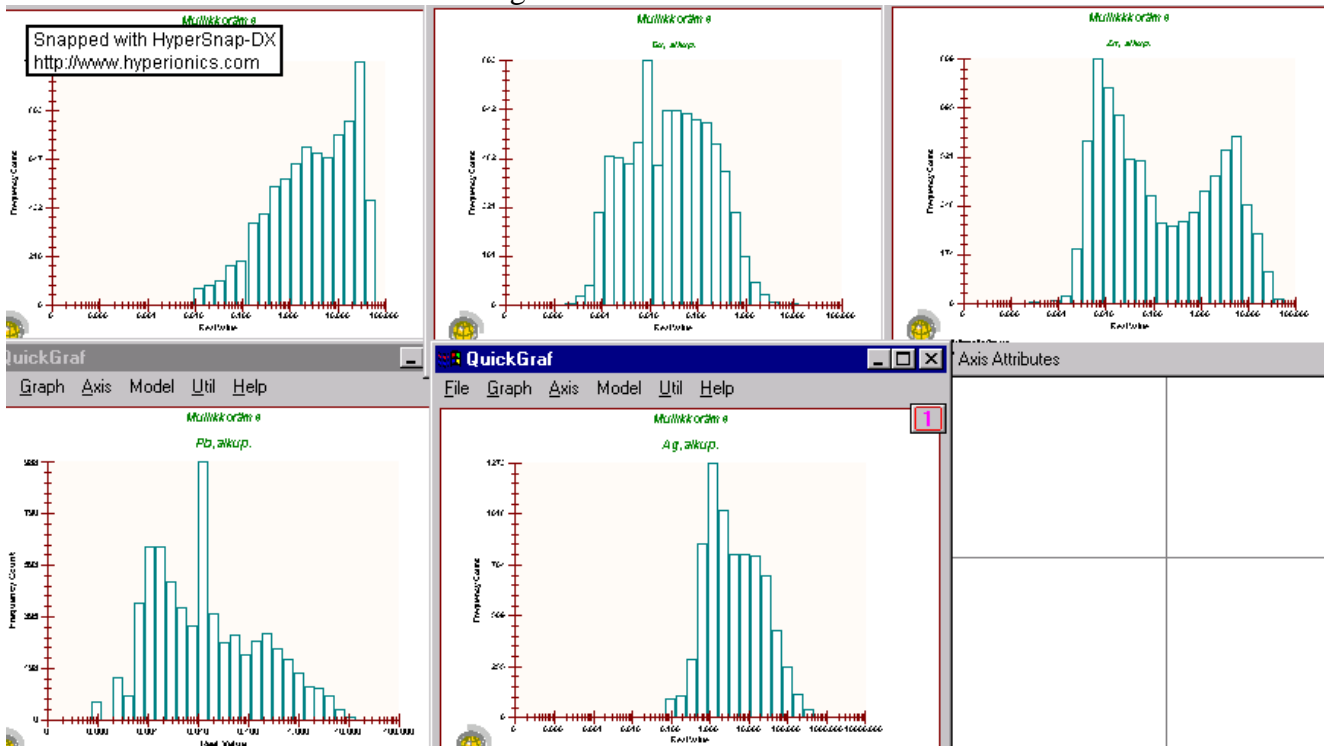
Kuva 13

Logaritmiset jakaumat, alkuperäiset analyysit:

S
 Pb

Cu
 Ag

Zn



1.5.3.2 Variogrammanalyysi

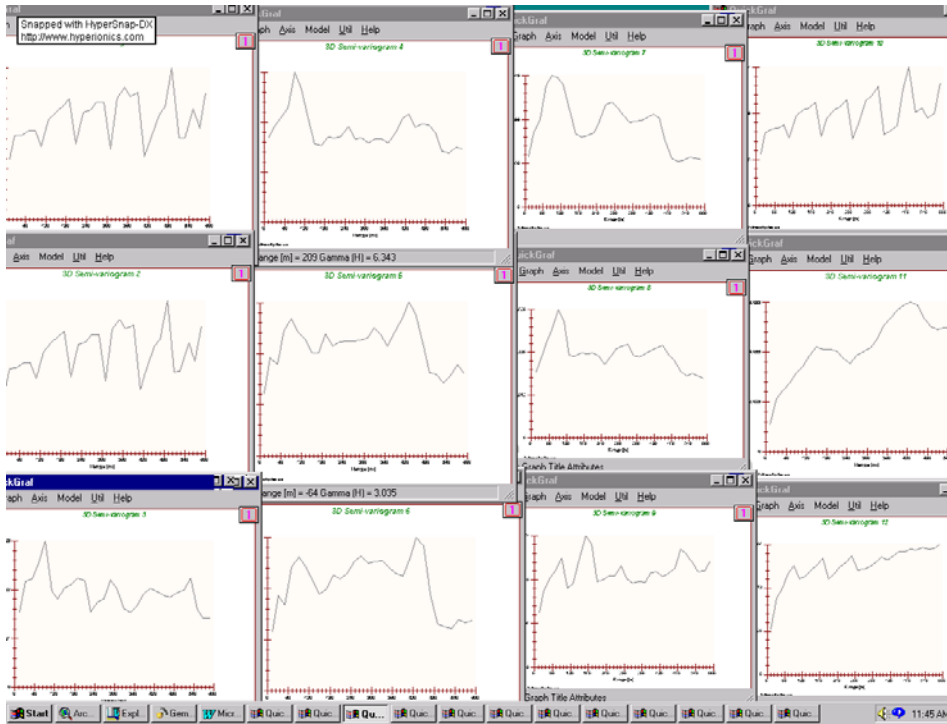
Suunnatuilla variogrammeilla on tarkoitus etsiä pitoisuusanisotropioille suuntaa, määrää ja varianssia osoittavat parametrit käytettäväksi alueen rakenteen tarkastelussa ja interpolointien perustana. Suuria rakenteita tarkastellaan käyttämällä 20 m:n lag-luokitusta ja 3 m:n yhdistelmäanalyysejä, pieniä rakenteita tarkastellaan käyttämällä 5 m:n lageja ja alkuperäisanalyysejä.

Kuvassa 14 on alustava kokoelma variogrammeja kuparille. Niistä näkyy anisotropian pieneneminen suunnasta 000 (pohjoinen) suuntaan 090 (itä) ja jälleen kasvu suuntaan 170. Niistä näkyy myös ns. Hole-efekti eli (tässä tapauksessa) säännöllisin välein toistuvat kuopat, jotka ovat tulkittavissa johtuviksi itä läntisistä kairausleikkauksista 100 m:n välein. Kuvassa 15. ovat vastaavat variogrammit hopealle.

Kuva 14

Variogrammit kuparille, lag = 20m, angle = 20°, kaade 00, suunnat:

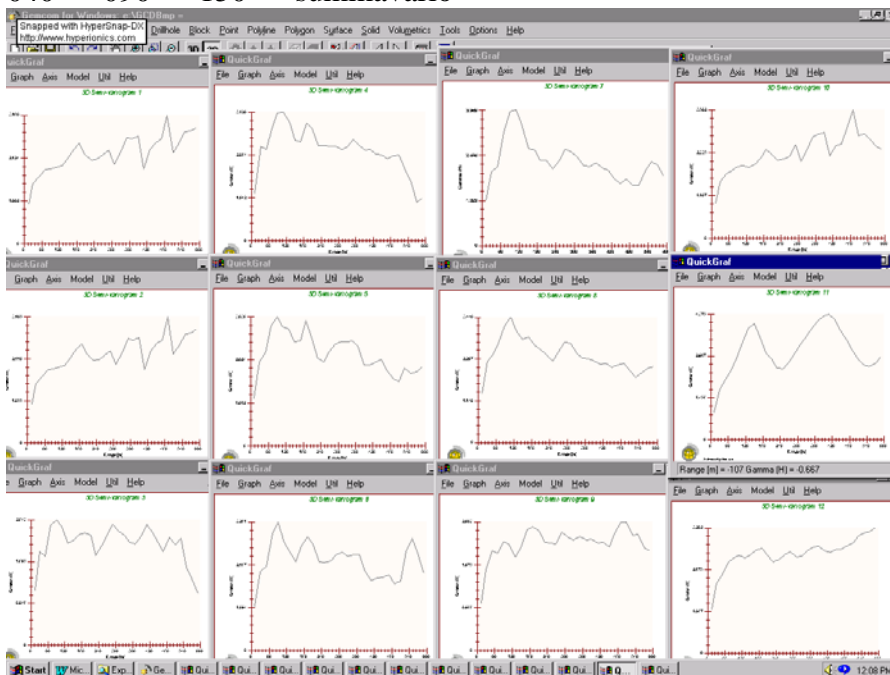
- 000 060 110 170
- 020 080 130 kaade 90 (vertikaali)
- 040 090 150 summavario



Kuva 15

Variogrammit hopealle, lag = 20m, angle = 20°, kaade 00, suunnat:

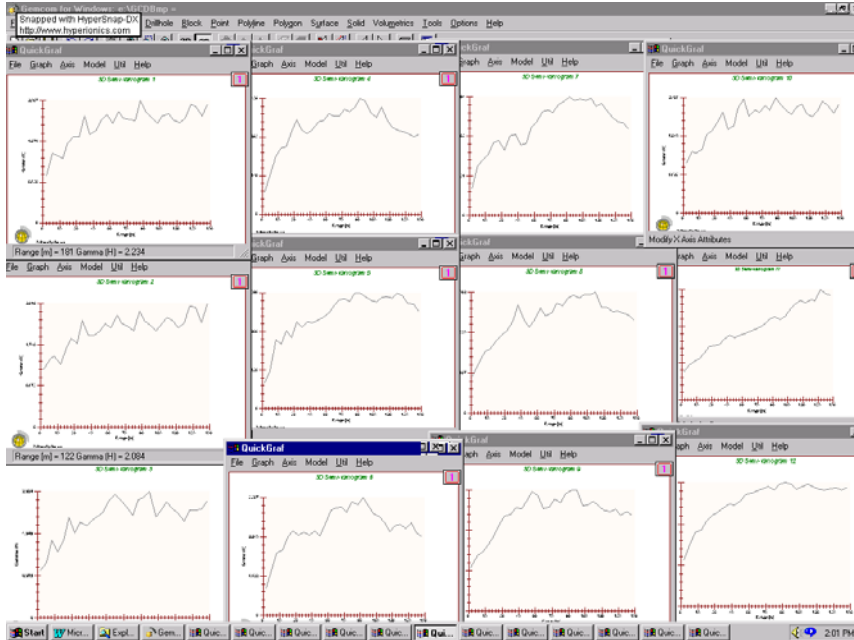
- 000 060 110 170
- 020 080 130 kaade 90 (vertikaali)
- 040 090 150 summavario



Kuva 16

Variogrammit hopealle, lag = 5m, angle = 20°, kaade 00, suunnat:

000	050	110	170
010	070	130	kaade 90 (vertikaali)
030	090	150	summavario

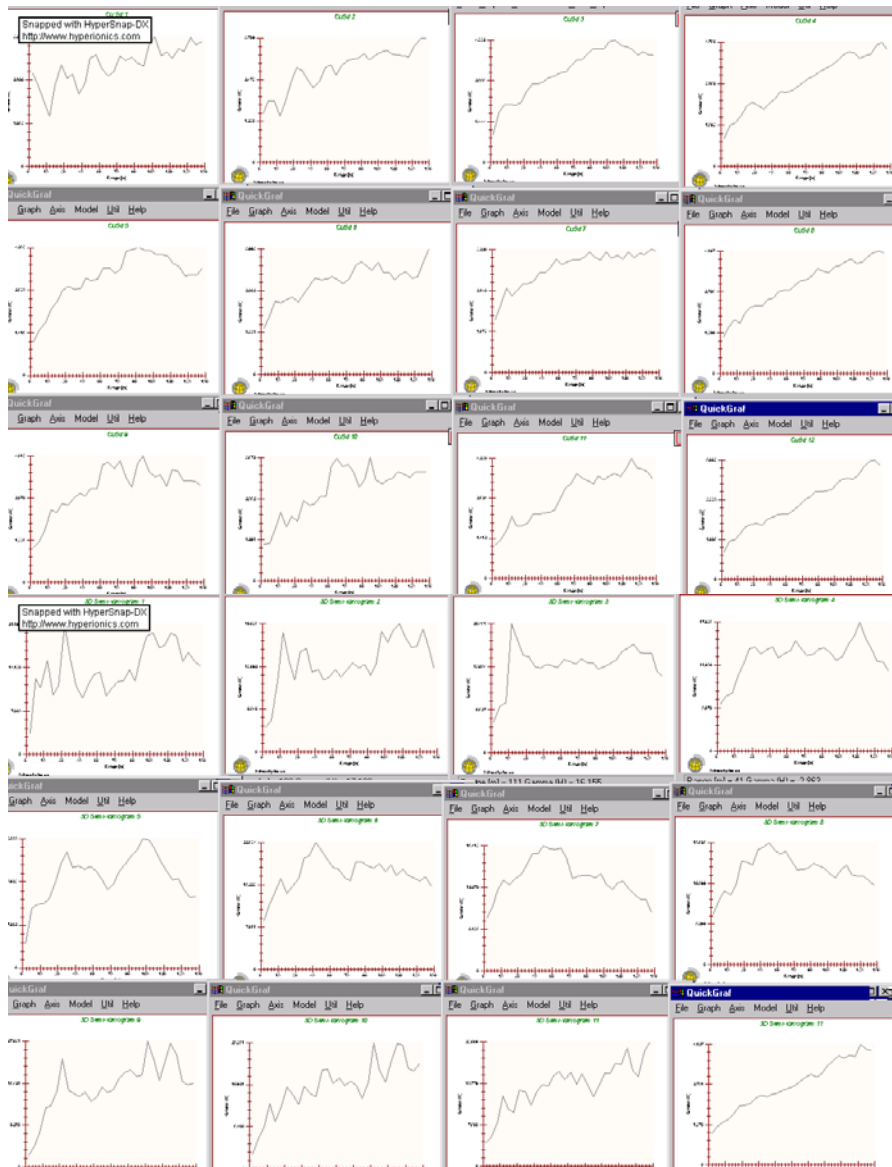


Anisotropiamaksimin tarkentamiseksi on kuvaan 16 hieman muutettu suuntavalintoja. Näyttää kuitenkin siltä että Mullikkorämeen alueella parhaat anisotropiasuunnat ovat 000/00 eli vaaka N-S ja 000/90 eli pysty. Sen varmistamiseksi on kuparille ja hopealle laskettu variogrammit pääsuunnissa eri kaateille, Kuva 17. Kuvissa näkyy anisotropian vähittäinen kasvu kohti pystysuuntaa.

Kuva 17

Variogrammit kuparille ja hopealle, suunnat 000, 090 ja 270, kaateet 20-80, lag = 5 m.

Cu,	suunta 000, kaade:	20	40	60	80
	suunta 090, kaade:	20	40	60	80
	suunta 270, kaade:	20	40	60	90
Ag,	suunta 000, kaade:	20	40	60	80
	suunta 090, kaade:	20	40	60	80
	suunta 270, kaade:	20	40	60	90

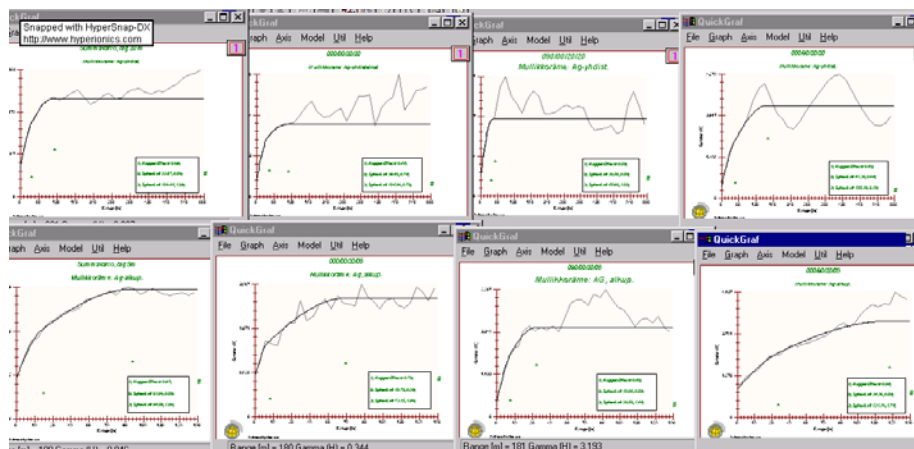


Anisotropiaparametrien laskemiseksi mallinnettiin valitut semivariogrammit kuvan 18 osoittamalla tavalla. Tulokset on esitetty Taulukossa 11. Lag 5:n mallinnus on uudelleen tehtynä, vähän tarkennettuna kuvassa ja tiedot taulukossa 12.

Kuva 18

Variogrammit hopealle, summa, anisotropiamaksimi (000), -minimi (090) ja pystysuunta.

		Pohjoiseen	itään	alas
Yläriivi, lag = 20 m:	summavario	000/00/20	090/00/20	000/90/20
Alarivi, lag = 5 m:	summavario	000/00/20	090/00/20	000/90/20



Taulukko 11

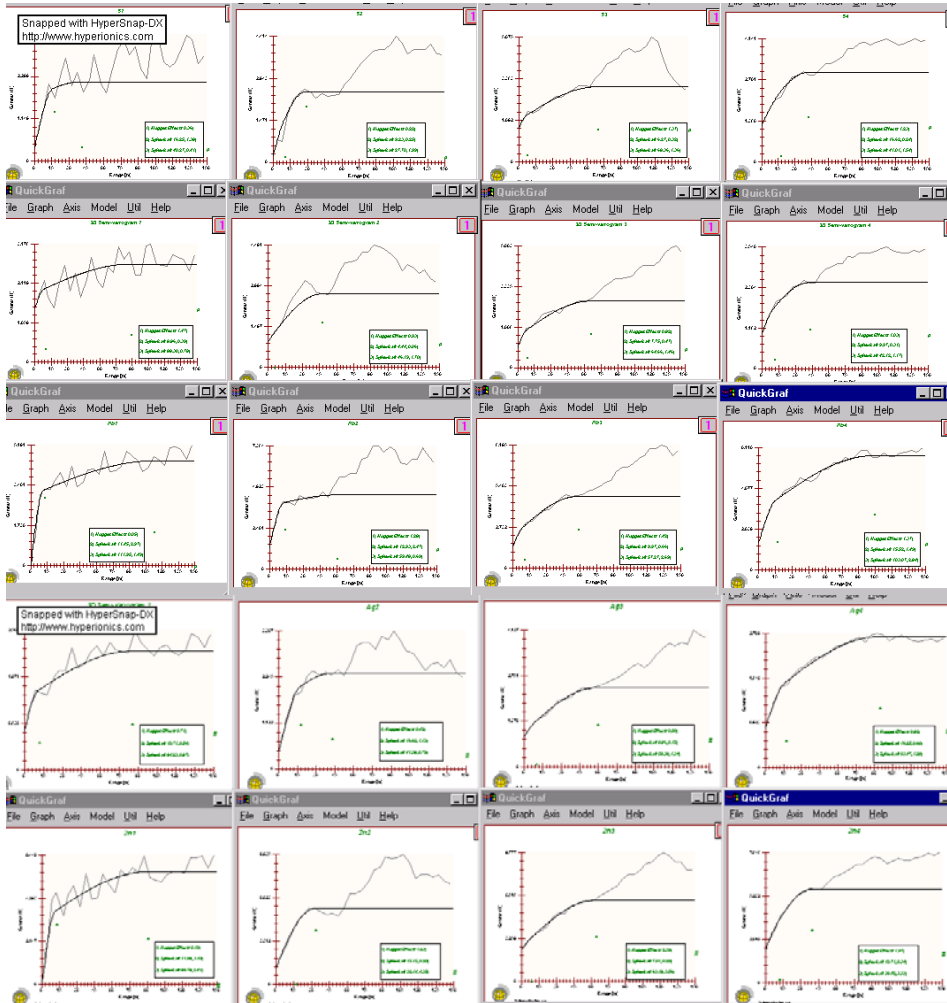
Kuvan 18 variogrammeista mallinnetut parametrit, järjestys kuten kuvassa 18.

Nugget	0.72	0.48	0.59	0.50
	0.84	0.69	0.40	0.94
Sill 1	0.69	0.56	0.46	0.44
	0.64	0.65	0.90	0.39
Range 1	49	33	35	37
	18	13	14	25
Sill 2	1.13	0.80	1.06	2.14
	1.20	0.85	1.06	1.84
Range 2	115	86	43	133
	92	82	41	125
Relative Nugget	40	35	39	19
	46	46	20	42
Semi-Variance	1.82	1.36	1.52	2.58
	1.84	1.50	1.96	2.23

Kuva 19

Suunnatut (lag = 5 m) ja summavariogrammit alkuperäisin analyysiarvoin.
 Variogrammien järjestys:

	Pohjoiseen	itään	alas	summavario
S	000/00/20	090/00/20	000/90/20	000/00/90
Cu	000/00/20	090/00/20	000/90/20	000/00/90
Pb	000/00/20	090/00/20	000/90/20	000/00/90
Ag	000/00/20	090/00/20	000/90/20	000/00/90
Zn	000/00/20	090/00/20	000/90/20	000/00/90



Kuvan 19 variogrammeista lasketut parametrit on summeerattu taulukkoon 12. Sen mukaan kohtuullisen luotettava interpolointi voidaan suorittaa mainituille alkuaineille Range 2:n osoittamalle etäisyydelle saakka. Ainoastaan kuparille osoittaa Relative Nugget epäluotettavuutta N-S-suunnassa. Katsottaessa kuvaa 19 voidaan kuitenkin todeta että mallikäyrän sovituksessa Nuggetin osuutta on saatettu liioitella. Taulukosta voidaan edelleen arvioida että anisotropiaellipsoidin pääakselien pituudet suhtautuvat kuten (000/00) : 1.5 (000/90) : 1 (090/00) karkeasti laskien kaikilla a.o. aineilla. Tämä voidaan ottaa 3D-interpoloinnin perustaksi.

Taulukko 12

Kuvan 19 variogrammeista mallinnetut parametrit, järjestys kuten kuvassa 19.

Nugget	0.36	0.22	1.37	1.23
	1.47	0.93	0.82	1.03
	0.04	0.28	1.42	1.37
	0.71	0.42	0.90	0.82
	0.1	1.23	2.39	1.97
Sill 1	1.38	0.25	0.32	0.24
	0.39	0.06	0.57	0.31
	2.97	2.47	0.66	1.49
	0.54	1.30	0.15	0.60
	3.1	0.2	0.2	0.34
Range 1	11	9	6	17
	9	4	8	10
	11	13	10	16
	11	17	9	16
	11	15	7	11
Sill 2	0.41	1.99	1.36	1.54
	0.78	1.7	1.46	1.17
	1.49	0.69	2.69	2.84
	0.87	0.79	1.34	1.28
	2.41	4.35	3.56	3.33
Range 2	40	28	68	41
	88	46	65	42
	112	59	57	93
	84	41	58	93
	90	32	63	78
Relative Nugget	20	10	81	69
	126	53	40	70
	1	9	42	40
	50	20	60	44
	2	27	64	54
Semi-variance	2.15	2.46	3.05	3.01

2. “Kuumat alueet”, rakenneanalyysi

2.1 Yleiskuvaus

Pyhäsalmi

Malmi muodostuu dominoivasta kuparikiisuvaltaisesta levystä, jonka keskelle mutta lähelle NW-reunaa jää ohut sinkkivälkerikas “kerros”. Pyriittivaltainen malminosa asettuu pääosin levyn SE-puolella yläosastaan levystä irrallaan ja levyä kapeampana “tappina”.

Kuparikiisuvaltainen levy on kiertynyt poimulle karkeasti akselin **210/80** ympärille siten että kiertymän intensiteetti kasvaa alaspäin. Sinkkivaltainen malminosa ei ole yhtenäinen vaan katkonainen ja jakaantuu kahteen osaan esiintymän alapäässä. Pyriitti näyttää puuttuvan lähellä pintaa.

2.2 “Kuumat alueet”, tulokanavien jäljitys

Gemmel and Large (1992) ja Huston and Large (1987) ovat soveltaneet nk. Cu-suhteen ja Zn-suhteen vaihtelua kiteytymislämpötilojen määrittämiseen massiivisissa sulfidimalmeissa. Cu-suhde: $100 * Cu / (Cu + Zn)$, Zn-suhde: $100 * Zn / (Zn + Pb)$. Valitettavasti Pyhäsalmen ympäristöstä ei ole systemaattisesti analysoitu lyijyä, joten seuraavassa rajoitutaan pääosin Cu-suhteen tarkasteluun. Kuvassa 20 A,B,C on jakaumahistogrammit Pyhäsalmen ja Mullikkorämeen Cu-suhteelle ja Mullikkorämeen Zn-suhteelle.

Yhteenveto Cu- ja Zn-suhteista:

Cu/Pyhäsalmi: average 57, näytteitä 25453
STD 31

Cu/Mullikko: average: 27, näytteitä 7735
STD 23

ZN/ Mullikko: average: 84, näytteitä 6738
STD 14

Referenssien mukaan rauta ja kupari konsentroituvat tulokanaviin ja sinkin, lyijyn, hopean, kullan ja arseenin konsentroitumien voimistuessa siirtytessä hydrotermisen aktiviteetin keskuksista pois päin. Korkea kuparisuhde ja alhainen sinkkisuhde näin ollen indikoisivat tulokanavaa tai sen läheisyyttä. Referensseissä tutkituissa tilanteissa (Cu.-suhde > 5) kuvaa keskustulokanavaa ja (Cu-suhde > 3) kuvaa sekundaarikanaavia. Vastaavasti (Zn-suhde > 67) kuvaa sivukanavia ja (Zn-suhde < 61) kuvaa keskuskanavaa.

Hustonin ja Largen (1992) mukaan volkanogeenisille sulfidiesiintymille on tyypillistä sinkkisuhteen normaalisuus, keskiarvon sijoittuminen välille 64 ja 77 sekä STD alle 15. Tässä mielessä Mullikkorämeen sinkkisuhde ei ole tyypillinen muistuttaen eniten devonista Stirling Valley:n monimseetaaliusta juoniesiintymää. Huomattakoon, että referenssien teoreettiset lukuarvot perustuvat kymmeneen näytteeseen, kun tässä käsitellään tuhansia.

Pyhäsalmeelle ja Mullikkorämeelle ei suoraan voida soveltaa kirjallisuuden antamia parametreja mutta analogian perusteella voidaan otaksua, että korkeimmat Cu –suhteet ovat lähinnä keskustulokanavia ja korkeimmat Zn suhteet lähimpänä marginaalikanavia. Tällöin Pyhäsalmen malmin kuuma alue sijoittuu malmin itäiselle-eteläiselle nurkalle ja voimistuu alimpiin osiin mentäessä. Mullikon malmien kohdalla analogisia vastaavuuksiakin on vaikea löytää.

Kuva 20.

- A. Pyhäsalmen ympäristön Cu-suhteet.**
- B. Mullikkorämeen ympäristön Cu-suhteet.**
- C. Mullikkorämeen ympäristön Zn-suhteet.**

